Meixiang Wan

Conducting Polymers with Micro or Nanometer Structure

Meixiang Wan

Conducting Polymers with Micro or Nanometer Structure

Meixiang Wan

Conducting Polymers with Micro or Nanometer Structure

With 106 figures

TSINGHUA UNIVERSITY PRESS

Springer

AUTHOR:

Prof. Meixiang Wan
Institute of Chemistry, Chinese Academy
of Sciences Beijing, P. R. China, 100080
E-mail: wanmx@iccas.ac.cn

To my teacher and friend, Prof. Alan G. MacDiarmid at the University of Pennsylvania, USA, who had passed away in 2007.
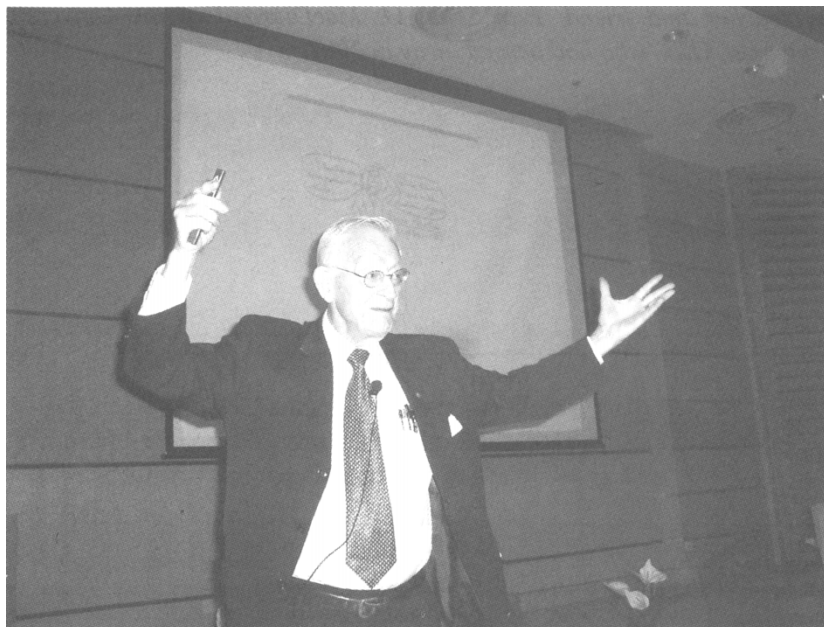
Prof. MacDiarmid gave a report when he visited Institute of Chemistry, Chinese Academy of Sciences in 2004.

Author visited Professor MacDiarmid at his office, University of Pennsylvania, USA in 2004.

About Author

Meixiang Wan was born in Jiangxi Province, China, in 1940 and graduated from Department of Physics at University of Science and Technology of China in 1965. She joined the Institute of Chemistry, Chinese Academy of Sciences in 1972 in the Laboratory of Organic Solid State established by Prof. Renyuan Qian, an academy member of Chinese Academy of Sciences, to study electrical properties of organic solid states including organic photo-conductor, conductor and conducting polymers. In 1985, as a post-doctor she was fortunately recommended by Professor Qian to further pursure advanced studies on conducting polymers (e. g. polyacetylene and polyaniline) under Prof. Alan MacDiarmid', who was awarded the Nobel Prize for Chemistry in 2000, at the University of Pennsylvania, Philadelphia, USA.

Since returning to China in 1988, she has studied conducting polymers in Japan, France and the United States for a short time (3 – 6 months) as a visiting professor and often attends a variety of international conferences in the world. In 1992, she became a professor and leaded a group to study conducting polymers of polyaniline with regard to the mechanism of proton doping, electrical, optic and magnetic properties and related mechanism as well as application of electro-magnetic functionalized materials such as the microwave absorbing materials. In addition, she studied the origin of intrinsic ferromagnetic properties of organic ferromagnets. In 1988, she discovered that conductive nanotubes of polyaniline could be synthesized by in-situ doping polymerization in the presence of β-naphthlene surfonaic acid as a dopant, without using any membrane as a hard-template. This novel method is referred to as the template-free method due to the absence of a membrane as a template. Since discovery of the new method, her research has focused on nanostructures of conducting polymers, especially synthesized by a template-free method. So far, more than 200 papers have been published in Advanced Materials, Chemical Materials, Micromolecules, Langmuir, and some of them have been cited for more than 2000 times. Moreover, eight books chapters written in Chinese have been published, including "Conducting Polymer

Nanotubes" which was selected as a chapter in *Encyclopedia of Nanoscience and Nanotechnology* edited by H. S. Nalwa, America Scientific Publisher in 2004. In addition, ten Chinese patents were granted and several prizes, such as the Prize of the National Natural Sciences of China (second degree, 1988), the Prize of Advanced Technology of the Chinese Academy of Sciences (second degree, 1989), the Prize of Natural Sciences of the Chineses Academy of Sciences (first degree, 1995), Outstanding Younger Scientists of Chinese Academy of Sciences (1996) and Excellent Doctoral Teachers of the Chinese Academy of Sciences (2005) were awarded.

Preface

A traditional idea is that organic polymer is regarded as an excellent insulator because of its saturated macromolecule. However, a breakthrough of organic polymer imitating a metal was coming-out in the 1960s—1970s. It implied electrons in polymers need to be free to move and not bound to the atoms. The breakthrough was realized by awarders of Nobel Chemistry Prizes in 2000, who were Alan J. Heeger at the University of California at Santa Barbara, USA, Alan G. MacDiarmid at the University of Pennsylvania, Philadelphia, USA, and Hideki Shirakawa at the University of Tsukuba, Japan. In 1977, actually, they accidentally discovered that room-temperature conductivity of conjugated polyacetylene doped with iodine was as high as 10^3 S/cm, which was enhanced by 10^{10} times compared with original insulating polyacetylene. The change of the electrical properties from insulator to conductor was subsequently ascribed to "doping", but completely different from the doping concept as applied in inorganic semiconductors. The unexpected discovery not only shattered a traditional idea that organic polymers are insulators, but also established a new filed of conducting polymers or "synthetic metals".

Since discovery of the first conducting polymer (i.e. polyacetylene), conducting polymers have been received considerable attention because of their unique properties such as highly-conjugated chain structure, covering whole insulator-semiconductor-metal region of electrical properties, a reversible doping/de-doping process, an unusual conducting mechanism and the control of physical properties by the doping/de-doping process. The unique properties not only lead to promising applications in technology, but also hold an important position in material sciences. Up to date, the potential applications of conducting polymers include electronic devices (e.g. Schottky rectifier, field-effect transistor, light emitting diode and solar cell), electromagnetic interference shielding and microwave absorbing materials, rechargeable batteries and supercapacitors, electrochromic devices, sensors (e.g. gas, chemical and biochemical sensors) and artificial muscles. As a result, research on conducting polymers has spread rapidly from the United States.

Moreover, the significant progress on conducting polymer synthesis, new materials, conducting and transport mechanisms, processability, structure-property relationship and related mechanisms as well as applications have been achieved. After 23 years, conducting polymers, awarded the 2000 Nobel Prize in Chemistry, have affirmed contributions of the above-mentioned three scientists for the discovery and development of conductive polymers, and also for further promoting the development of conducting polymers.

Proferssor Renyuan Qian as an academy member of the Chinese Academy of Sciences, for the first time, established a laboratory of entilted organic solid state at the Institue of Chemistry, Chinese Academy of Sciences in the early 1980s. The research has covered synthetic method, structureal characterization, and the optical, electrical and magnetic properties and related mechanisms of organic solid states photoconductors, conductors, superconductors and ferromagnets as well as conducting polymers.

I was fortunate to enter the laboratory recommended by Professor Qian, to study electrical properties of organic photoconductors, conductors and conducting polymers. In 1985, I was again recommended by Professor Qian to pursure advanced studing on conducting polymers under Professor MacDiarmid as a post-doctor. In USA, I studied photo-electro-chemistry of polyaniline, which was discovered by Professor MacDiarmid in 1985 for the first time. Compared with other conducting polymers, polyaniline is advantageous of simple and low cost synthesis, high conductivity and stability, special proton doping mechanism and controlling physical properties by both oxidation and protonation state, resulting in a special position in the field of conducting polymers. These novel physical properties and promising potential applications in technology therefore promissed me to study continuously polyaniline when I came back from USA to China in 1988.

Since discovery of carbon nanotube in 1991, nanoscience and nanotechnology have become some of the fastest growing and most dynamic areas of research in the 20th centrury. Scientifically, "nano" is a scale unite that means 1 nanomerter, one billionth of a meter (10^{-9} m). Generally speaking, therefore, the nanomaterials are defined structural features in the range of 1 – 100 nm. Based on the definition, it is understood that nanotechnology deals with atomic and molecular scale functional structures. With nano-scaled features but large surface area, nanomaterials offer unique and entirely different properties compared with their bulk materials. Thereby, the unique properties of nanomaterials result in nanomateials and nanotechnology rapidly spreading to academic institutes and industries around the world.

In the 1990s, I accidentally found that nanotubes of polyaniline could be prepared by a conventional *in-situ* doping polymerization in the presence of nanphthalene surfonic acid as the dopant without using any membrane as the template. The created method was latterly called as template-free method because of omitting membrane as a template. Especially, further studies demonstrated that

essency of the method belongs to self-assembly process because the micelles composed of dopnat, dopant/monomer salt or supermolecules even monomer itself are served as the soft-templates in the formation of the template-free synthesized nanostructures of conducting polymers. Compared with the template-synthesis method, which was commonly used, the efficient and controlled approach to prepare conducting polymer nanostructures is simple and inexpensive because of the lack of template and the post-treatment of template removal. However, many questions dealing with this method were completely un-understood at that time. For instance, how about the universality of the method to nanostructures of conducting polymers? What is formation mechanism of the self-assembled nanostructures by the method? How about controllability of the morphology and size for the template-free synthesized nanostructures? Do the electrical properties of the template-free synthesized nanostructures differ from the bulk materials? Is it possible to fabricate multi-functionalized nanostructures of conducting polymers based on template-free method? Can we identify applications for the template-free synthesized nanostructures? All above-mentioned issues promised me to systematically and significantly study nanostructures of conducting polymers by a template-free method.

In fact, the significant progress on conducting polymer nanostructures by the method has been achieved. In 2006, Tsingua University Press in Beijing and Springer-Verlag GmbH in Berlin invited me to write a book about conducting polymers and related nanostructures. Although a lot of good books and excellent reviews on conducting polymers and corresponding nanostructures have been widely published in the world, I was eager to share my knowledge and experience on studying conducting polymers and their nanostructures with other scientists, teachers and students who are interested in conducting polymers. I therefore was pleased to accept the invitation to write up this book.

The book consists of five chapters. The first chapter briefly introduces basic knowledge of conducting polymers, such as doping item, conducting mechanism, structural characteristics and physical properties of conducting polymers. The second chapter further considers structural characteristic, doping mechanism, processability and structure-property relationship of conducting polymers using polyaniline as an example. The third chapter mainly reviews physical properties and corresponding potential application of conducting polymers in technology. The fourth chapter summarizes progress and developing directions in conducting polymer nanostructures, dealing with synthesis method, unique properties and fabricating technology of nano-arrays, patents, and potential application in technology. The fifth chapter mainly reviews results on template-free synthesized conducting polymer micro/nanostructures focusing on the universality, controllability and formation mechanism of the method, multifunctional nanostructure based on template-free method associated with other approaches, electrical and transport properties of the self-assembled nanostructures, especially electrical and transport properties of a single nano-tube or hollow sphere, as measured by a four-probe

method, and applications as microwave absorbing materials and gas sensors guided by reversible wettability. I hope this book is able to provide some basic and essential reference information for those studying conducting polymers and their nanostructures.

Contents

Chapter 1   Introduction of Conducting Polymers

According to electrical properties, materials can be divided into four-types: insulator, semiconductor, conductor and superconductor. In general, a material with a conductivity less than 10^{-7} S/cm is regarded as an insulator. A material with conductivity larger than 10^3 S/cm is called as a metal whereas the conductivity of a semiconductor is in a range of $10^{-4} - 10$ S/cm depending upon doping degree. Organic polymers usually are described by σ (sigma) bonds and π bonds. The σ bonds are fixed and immobile due to forming the covalent bonds between the carbon atoms. On the other hand, the π-electrons in a conjugated polymers are relatively localised, unlike the σ electrons. Plastics are typical organic polymers with saturated macromolecules and are generally used as excellent electrical insulators. Since discovery of conductive polyacelene (PA) doped with iodine [1], a new field of conducting polymers, which is also called as "synthetic metals", has been established and earned the Nobel Prize in Chemistry in 2000 [2]. Nowadays, conducting polymers as functionalized materials hold a special and an important position in the field of material sciences. In this Chapter, discovery, doping concept, structural characteristics, charge transport and conducting mechanism for the conducting polymers will be brief discussed.

1.1   Discovery of Conducting Polymers

In the 1960s—1970s, a breakthrough, polymer becoming electrically conductive, was coming-out. The breakthrough implied that a polymer has to imitate a metal, which means that electrons in polymers need to be free to move and not bound to the atoms. In principle, an oxidation or reduction process is often accommpanied with adding or withdrawing of electrons, suggesting an electron can be removed from a material through oxidation or introduced into a material through reduction. Above idea implies that a polymer might be electrically conductive by withdrawing electron through oxidation (i.e. a "hole") or by adding electron through reduction, which process was latterly described by an item of "doping". The breakthrough was realized by three awarders of Chemistry Nobel Prize in 2000, who were Alan J. Heeger at the University of California at Santa Barbara, USA, Alan G. MacDiarmid at the University of Pennsylvania, Philadelphia, USA, and Hideki Shirakawa at the University of Tsukuba, Japan [2]. In 1977, they accidentally discovered that insulating π-conjugated PA could become conductor with a

conductivity of 10^3 S/cm by iodine doping [1]. The unexpected discovery not only broken a traditional concept, which organic polymers were only regarded as the insulators, but also establishing a new filed of conducting polymers, which also called as "Synthetic Metals". According to a report of the Royal Swedish Academy of Sciences in 2000 [2], there was an interesting story about discovery of the conducting polymers. Since accidental discovery in science often happens, author would like to briefly introduce the story to share with readers. Based on above idea of polymer imitating a metal, scientists thought that PA could be regarded as an excellent candidate of polymers to be imitating a metal, because it has alternating double and single bonds, as called conjugated double bonds. From Fig. 1.1, one can see, PA is a flat molecule with an angle of 120° between the bonds and hence exists in two different forms, the isomers *cis*-polyacetylene and *trans*-polyacetylene [2].
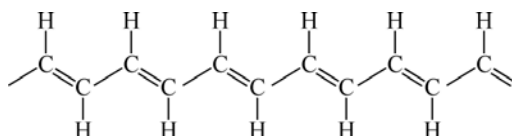
Figure 1.1   Molecular structure of polyacetylene [1, 2]

Thereby, synthesis of PA received great of attention at that time. At the beginning of the 1970s, Hedeki Shirakawa at Tokyo Institute of Technology, Japan, was studying the polymerization of acetylene into plastics by using catalyst created by Ziegler-Natta, who was awarded the 1963 Nobel Prize of Chemistry for a technique of polymerizing ethylene or propylene into plastics. Usually, only the form of black powder could be synthesized by using the conventional polymerization method. A visiting scientist in Shirakawa's group tried to synthesize PA in the usual way. However, a beautifully lustrous silver colored film, rather than the black powder synthesized by the conventional method, was obtained. The unexpected results promised Shirakawa to check the polymerization conditions again and again, and Shirakawa finally found that the catalyst concentration used was enhanced by 10^3 times! Shirakawa was stimulated by the accidental discovery and further found the molecular structure of the resulting PA was affected by reaction temerature, for instance, the silvery film was *trans*-polyacetylene whereas copper-colored film was almost pure *cis*-polyacetylene.

In another part of the world, chemister Alan G. MacDiarmid and physicist Alan J. Heeger at University of Pennsylvania, Philadephia, USA were studing the first metal-like inorganic polymer sulphur nitride $((SN)_x)$, which is the first example of a covalent polymer without metal atoms [3]. In 1975, Prof. MacDiarmid visited Tokyo Institute of Technology and gave a talk on $(SN)_x$. After his lecture, MacDiarmid met Shirakawa at a coffee break and showed a sample of the golden $(SN)_x$ to Shirakawa. Consequently, Shirakawa also showed MacDiarmid a sample

of the silvery $(CH)_x$. The beautiful silvery film caught the eyes of MacDiarmid and he immediately invited Shirakawa to the University of Pennsylvania in Philadelphia to further study PA. Since MacDiarmid and Heeger had found previously that the conductivity of $(SN)_x$ could be increased by 10 times after adding bromine to the golden $(SN)_x$ material, which is called as "doping" item in inorganic semiconductor. Therefore, they decided to add some bromine to the silvery $(CH)_x$ films to see what was happen. Miracle took place on November 23, 1976! At that day, Shirakawa worked with Dr. C.K. Chiang, a postdoctoral fellow under Professor Heeger, for measuring the electrical conductivity of PA by a four-probe method. Surprise to them, the conductivity of PA was ten million times higher than before adding bromine. This day was marked as the first time observed the "doping" effect in conducting polymers. In the summer of 1977, Heeger, MacDiarmid, and Shirakawa co-published their discovery in the article entitled "Synthesis of electrically conducting organic polymers: Halogen derivatives of polyacetylene $(CH)_n$" in *The Journal of Chemical Society, Chemical Communications* [1].

After discovery of the conductive PA, fundamental researches dealing with synthesis of new materials, structural characterization, solubility and processability, structure-properties relationship and conducting mechanism of conducting polymers as well as their applications in technology have been widely studied and significant progress have been achieved. After 23 years, The Royal Swedish Academy of Sciences has decided to award the Nobel Prize in Chemistry for 2000 jointly to Alan J. Heeger at University of California at Santa Barbara, USA, Alan G. MacDiarmid at University of Pennsylvania, Philadelphia, USA, and Hideki Shirakawa at University of Tsukuba, Japan *"for the discovery and development of conductive polymers"* [2]. Photograph of the three scientists are shown as Fig. 1.2. Nowadays, the field of conducting polymers had been well established

Figure 1.2　Photograph of three awardees of the Nobel Chemistry Prize in 2000

Alan G. MacDiarmid (left)　Prof. at the Univ. of Pennsylvania, USA

Hideki Shirakawa (middle)　Prof. Emeritus, Univ. of Tsukuba, Japan

Alan J. Heeger (right)　Prof. at the Univ. of California at Santa Barbara, USA

and conducting polymers as functional materials hold an important position in the field of material sciences. Up to date, a large number of articles, reviews and books dealing with conducting polymers has been published. Among these books, "Handbook of Conducting Polymers" (Ed. T. A. Skotheim), Marcel Dekker, New York, 1986 and which re-published in 1998 [4] is a good and basically reference book for scientists and students studying conducting polymers. In this Chapter, therefore, only basic knowledge and concepts, such as doping, characteristic of molecular structure, conducting mechanism and electrical and transport properties of conducting polymers, are briefly discussed.

1.2 Structural Characteristics and Doping Concept

Since discovery of conductive PA by iodine doping [1], other π-conjugated polymers, such as polypyrrole (PPy), polyaniline (PANI), polythiophenes (PTH), poly(*p*-phenylene)(PPP), poly(*p*-phenylenevinylene)(PPV), and poly(2,5-thienyl-enevinylene)(PTV) have been reported as conducting polymers [5], which molecular structure is shown in Fig. 1.3. Usually the ground states of conjugated polymers are divided into degenerate and non-degenerate. The prototype of degenerate polymers is *trans*-polyacetylene, which has alternating C—C and C═C bonds as shown in Fig. 1.1. The total energy curve of *trans*-polyacetylene has two equal minima, where the alternating C—C and C═C bonds are reversed [1]. On the other hand, a non-degenerate polymer has no two identical structures in the ground state. Most conjugated polymers, such as PPy and PANI belong to non-degenerate. The band gaps of conjugated polymers are estimated to be typically in the range between 1 and 3 eV from their electronic absorption spectra [4]. These observations are consistent with their insulator or semiconductor electrical properties [6]. From molecular structure as shown in Fig. 1.3, moreover, the polymer backbone in conducting polymers consists of π-conjugated chain, where are the π-electrons of the carbon atoms and the overlap of their wave function. The wave overlap is called conjugation, because it leads to a sequence of alternating double and single bonds, resulting in unpaired electrons delocalized along the polymeric chain [4].

As above-mentioned, PA is the simplest model system for conjugated polymers and is also the first sample for a polymer being conducting polymers [2], indicating π-conjugated polymer chain is a basic requirement for a polymer becoming conducting polymer. The delocalization of π-bonded electrons over the polymeric backbone, co-existing with unusual low ionization potentials, and high electron affinities lead to special electrical properties of conducting polymers [7]. On the other hand, π-conjugated chain of conducting polymers leads to insoluble and poor mechanical properties of conducting polymers, limiting their application in technology. Thereby continue effort to improve solubility and to enhance mechanic strength of conducting polymers is needed.

(a) PA   (b) PPy   (c) PTH

(d) PPP   (e) PPV

(f) PANI
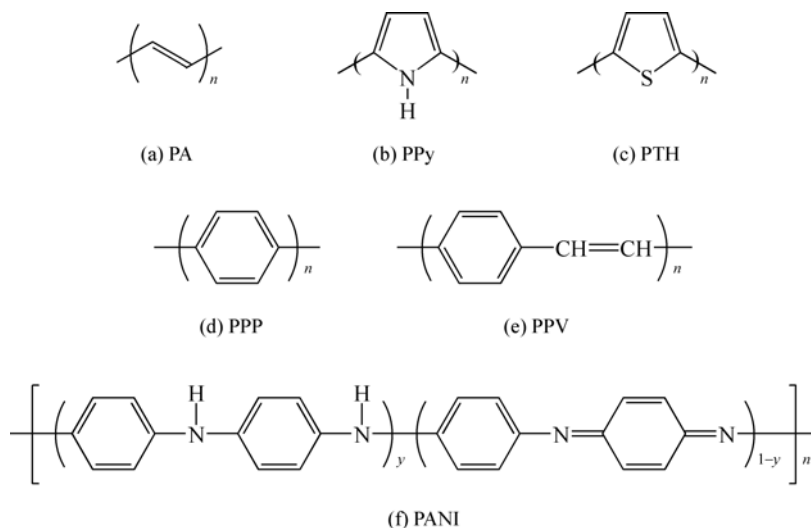
Figure 1.3   Molecular structure of typical conducting polymers
(a) *trans*-polyacetylene; (b) polythiophenes; (c) poly(*p*-phenylene); (d) polypyrrole;
(e) poly (*p*-phenylenevinylene); (f) poly(2, 5-thienylenevinylene) [5]

As above described, the transition of π-conjugated polymer from insulator to metal is carried out by a "doping" process. However, the "doping" item used in conducting polymers differs significantly from traditional inorganic semiconductor [5]. Differences in "doping" item between inorganic semiconductors and conducting polymers are shown as follows:

(1) Intrinsic of doping item in conducting polymers is an oxidation (*p*-type doping) or reduction (*n*-type doping) process, rather than atom replacement in inorganic semiconductors. Using PA as a sample, for instance, the reaction of *p*- and *n*-doping is written as:

Oxidation with halogen (*p*-doping): $[CH]_n + 3x/2I_2 \rightarrow [CH]_n^{x+} + xI_3^-$ (1.1)

Reduction with alkali metal (*n*-doping): $[CH]_n + xNa \rightarrow [CH]_n^{x-} + xNa^+$ (1.2)
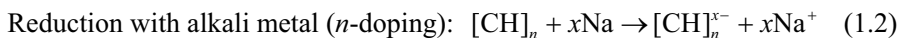
(2) *p*-doping (withdrawing electron from polymeric chain) or *n*-doping (adding electron into polymeric chain) in conducting polymers can be acquired and consequently accompanied with incoppration of couterion, such as cation for *p*-doping or anion for *n*-doping, into polymer chain to satisfy electrical nature. In the case of oxidation, taking PA as a sample again, the iodine molecule attracts an electron from the PA chain and becomes I_3^-. The PA molecule, now positively charged, is termed a radical cation [1]. Based on above description, therefore, conducting polymers not only consist of π-conjugated chain, but also containing counter-ions caused by doping. This differs from conventional inorganic semiconductors, where the counterions are absent. The special chain structure of

conducting polymers results in their electrical properties being affected by both structure of polymeric chain (i.e. π-conjugated length) and dopant nature. Doping process can be completed through chemical or electrochemical method [4]. Except for chemical or electrochemical doping, other doping methods, such as "photo-doipng" and "charge-injection doping", are also possible [8]. For instance solar cells is based on "photo-doping" whereas light emitting diodes (LEDs) results from "charge-injection doping", respectively, that are further discussed in Chapter 3. Besides, "proton doping" discovered in PANI is an unusual and efficient doping method in conducting polymers [9]. The proton doping does not involve a change in the number of electrons associated with the polymer chain [10] that is different from redox doping (e.g. oxidation or reduction doping) where the partial addition (reduction) or removal (oxidation) of electrons to or from the π system of the polymer backbone took place [4,11].

(3) The insulating π-conjugated polymers can be converted to conducting polymers by a chemical or electrochemical doping and which can be consequently recombacked to insulate state by de-doping. This suggests that not only de-doping can take place in conducting polymers, but also reversible doping/de-doping process, which is different from inorganic semiconductor where de-doping can't take place [5]. As a result, conductivity of the conducting polymers at room temperature covers whole insulator-semiconductor-metal region by changing doping degree as shown in Fig. 1.4. On the contrary, those processes are impossible to take place in inorganic semiconductors!
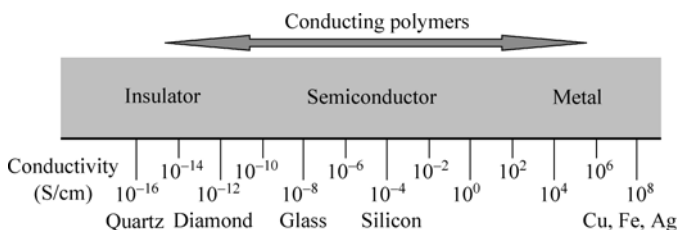
Figure 1.4   Conductivity of conducting polymers can cover whole insulator-semiconductor-metal region by changing doping degree [5]

(4) The doping degree in inorganic semiconductor is very low (~ tenth of thousand) whereas doping degree in conducting polymers can be achieved as high as 50% [5]. So electron density in a conducting polymer is higher than that of inorganic semiconductor; however, the mobility of charge carriers is lower than that of inorganic semiconductor due to defects or poor crystalline.

(5) Conducting polymers mostly composed of C, H, O and N elements and their chain structure can be modified by adding substituted groups along the chain or as the side chains that result in conducting polymers reserving light-weight and flexibility of conventional polymers. Based on above descriptions, conducting polymers are intrinsic rather than conducting plasters prepared by a

physical mixture of insulating polymers with conducting fillers (e.g. carbon or meter) [11]. The differences of the conducting plastics from conducting polymers also exhibit as follows: one is the conductivity of conducting plasters increases suddenly at a percolation threshold, at which the conductive phase dispersed in the non-conductive matrix becomes continuous, while conductivity of the conducting polymers increases with increase of the doping degree. Another is the conductivity of the conducting plastics is lower than that the doped conducting polymers, for instance, their conductivity of the conducting plastics above percolation threshold is only $0.1 - 0.5$ S/cm at 10 wt% $-$ 40 wt% fractions of the conductive filler. In addition, the position of the percolation threshold is affected by particle size and shape of filler [12].

1.3　Charge Carriers and Conducting Mechanism

As is well known, conductivity (σ), as measured by a four-probe method, is an important property for evaluation of conducting polymers. Usually σ is expressed as $ne\mu$, where e is charge of electron, n and μ are density and mobility of charge carriers, respectively. The doping concept in the conducting polymers completely differs from inorganic semiconductors, as above-described, leading to a significant difference in electrical properties between conducting polymers and inorganic semiconductors, which are summarized as follows:

(1) Inorganic semiconductor process few charge carriers, but these carries have high mobility due to the high crystalline degree and purity presented by these materials. On the contrary, conducting polymers have a high number of charge carriers due to a large doping degree (>50%), but a low mobility attributed to structural defects.

(2) A free-electron is regarded as a charge carrier in a metal; and temperature dependence of the conductivity for a metal increases with decreasing temperature. On the other hand, electron or hole is assigned as a charge carrier in an inorganic semiconductor and the electrical properties of semiconductors are generally dominated by minion charge carrier (electron or hole) produced by n- or p-type doping. Charge transport in a semiconductor is described by a band model, which the electrical properties are dominated by the width of the energy gap, which is defined as a difference in energy between the valence band and conducting band, as presented by E_{g}. The charge transport in semiconductor can be therefore expressed by following equation,

$$\sigma(T) = \sigma_0 \left(-\frac{\Delta E}{\kappa T} \right) \tag{1.3}$$

where σ_0 is a constant, ΔE the activation energy, κ the Borthman constant, T the temperature, respectively. For a conducting polymer, solitons [13], polarons [14]

and bipolarons [14b, 15] are proposed to interpret enhancement of conductivity of π-conjugated polymers from insulator to metal regime via a doping process. Usually, soliton is served as the charge carrier for a degenerated conducting polymer (e.g. PA) whereas polaron or bipolaron is used as charge carrier in a non-degenerated conducting polymer (e.g. PPy and PANI) [4]. The model assumed that soliton can move along the PA backbone carrying charge but no spin (spinless), and if an electron is added to the action or taken away from the anion, a neutral radical soliton is again established [16]. In a mechanism involving solitons, electron conduction involves only fully occupied bands in the ground state and leads to formation of a half-occupied electronic level (one electron) within the gap. Theoretical models also demonstrate that two radical ions (polarons) react exothermically to produce a dication or dianion (bipolaron). The polaron is thermodynamically more stable than two polarons due to electronic repulsion exhibited by two charges confined in the same site and cause strong lattice distortions. Meanwhile, polaron is spin whereas bipolaron is spinless. As a result, polaron and bipolaron can be distinguished by means of electron spin response (ESR). Schematic positive polaron and bipolaron as two positive polarons in PTH are as shown in Fig. 1.5. The chemical term, charge and spin for soliton, polaron and bipolaron are also given in Table 1.1.

Thus charge carrier (i.e. soliton, polaron and bipolaron) in conducting polymers is different from either free-electron in a metal or electron/hole in an inorganic semiconductor. It should point out that the item of soliton, polaron and bipolaron is only used to interpret the electronic motion along the segment of polymeric chain [4]. As above-mentioned, the polymeric chain of the doped conducting polymers composes of π-conjugated length and counter-ions, depending upon

(a)

(b)

(c)
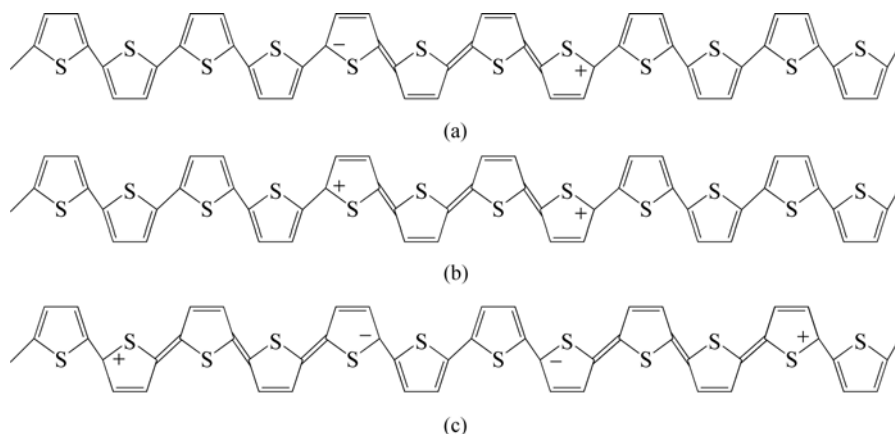
Figure 1.5   Schematic structure of (a) a positive polaron, (b) a positive bipolaron, and (c) two positive bipolarons in polythiophenes [16]

8

Table 1.1   Chemical term, charge and spin of soliton, polaron and bipolaron in conducting polymers

Carrier nature	Chemical term	Charge	Spin
Positive soliton	Cation	+e	0
Negative soliton	Anion	−e	0
Neutral soliton	Neutral radical	0	1/2
Positive polaron (hole polaron)	Radical cation	+e	1/2
Negative polaron (electron polaron)	Radical anion	−e	1/2
Positive bipolaron	Dication	+2e	0
Negative bipoloron	Dianion	−2e	0

doping fashion (e.g. cation for *n*-doping whereas anion for *p*-doping). Obviously, conductivity of the conducting polymers is also affected by parameters as follows:

(1) Chain structure includes π-conjugated structure and length, crystalline and substituted grounds and bounded fashion to the polymeric chain. Regarding polymeric chain structure, for instance, the maximum value of the conductivity in iodine-doped PA was on the order of 10^3 S/cm [1, 17]. On the other hand, the maximum conductivity for the doped PPy [4] and PTH [4, 18] were below 200 S/cm. Regarding π-conjugated length, it is found that high number of conjugated length for a high electrically conductive polymer is unnecessary, because the conductivity of oligomers is comparable with its long-conjugated polymers as shown in Chapter 3. Regarding crystalline, in general, the electrical conductivity at room temperature is proportional to the crystalline degree because of closer intermolecular distance in crystalline phase [19]. Therefore, the conducting polymers with a branched chain have a low conductivity at room temperature is expected due to less crystalline.

(2) Dopant structure and doping degree are keys to realize an insulating π-conjugated polymer to become a conducting polymer. Molecular structure of dopants not only affects electrical properties, but also solubility in organic solvent or water. For example camphorsulfonic acid (CSA) doped PANI not only has high conductivity (200 S/cm), but also can soluble in *m*-cresol [20], which will be discussed in Chapter 3 in detail. As shown in Chapter 5, moreover, morphology and diameter of conducting polymer nanostructures prepared by either hard- and soft-template method are strongly affected by dopant nature and dopant degree. Regarding doping degree, in general, room-temperature conductivity of the conducting polymers, as measured by four-probe method, is a function of the doping degree, showing the conductivity increases with increase of the doping degree undergoing from insulator to metal through a semiconductor.

(3) Polymerization conditions including concentration of monomer, dopant and oxidant, the molar ratio of dopant and oxidant to monomer and polymerization temperature and time are other important parameters affect the conductivity, because these are contributed to chain conformation, morphology and crystalline of

the final product. In Chapter 5, the influences of these parameters on morphology, diameter and electrical properties are discussed by using sufficient samples. Above-mentioned parameters should keep in mind as one studies conducting polymers even though their nanostructures!

In principle, temperature dependence of the conductivity, as measured by four-probe method, can be used to describe characteristic of charge transport for a material. Temperature dependence of conductivity can be expressed by a logarithmic derivative, $\alpha = \Delta \ln \sigma / \Delta \ln T$. Metal has a positive temperature coefficient of α and a finite dc conductivity as $T \to 0$ is observed. On the contrary, α for insulator or semiconductor is a negative coefficient. The symbol of α is therefore can be used to distinguish between metal and semiconductor or insulator. Metallic-like conductivity of conducting polymers at room temperature ($\sigma \sim 10^2 - 10^3$ S/cm) has been observed [21]. Moreover, the metallic properties of the doped conducting polymers (e. g. PA) have been revealed by their optical properties [22], thermo-electrical power [23] and magnetic susceptibility [24]. Similarly, heavily doped PTH also shows metallic properties, such as Pauli spin susceptibility [25] and a linear temperature dependence of the thermoelectric power have been observed [26]. Based on the one-electron band theory, Furukawa [16] suggested that the interaction between polarons in the polaron lattice leads to the formation of a half-filled band responsible for the metallic properties, because the electronic wave function of each polaron in the polaron lattice is overlapped, indicating the electronic states are not localized. However, the metallic temperature dependence of the conductivity is not observed instead of a thermally activated conduction characteristic of a semiconductor, in other word, a negative α coefficient was observed. Moreover, finite dc conductivity as $T \to 0$ was also not observed [27]. This is attributed to the inter-contact resistance in the inter-febrile, inter-granular or inter-crystallinity regions of conducting polymers. Similar problem has been encountered in the measurement of the temperature dependence of conductivity of polycrystalline powder compactions, as measured by four-probe method. Coleman [28] proposed a voltage shorted compaction (VSC) method could effectively short circuit the inter-crystallinity contact resistance, showing true temperature dependence of conductivity. VSC method is similar to four-probe method, for instance, four metallic wires with a same distance are used as the probes. However, the specimen between two voltage terminals is shorted by a thin layer of silver paste [29]. Author proved the validity of VSC method by comparison of temperature dependence of conductivity of Qn(TCNQ)$_2$ polycrystalline powder measured by VSC method with that of single crystal measured by four-probe method [30]. It showed that temperature dependence of conductivity of Qn(TCNQ)$_2$ poly-crystalline powder, as measured by VSC method, was in agreement with the results obtained from its single crystal, suggesting the intrinsic properties of temperature dependence of the tested materials can be qualitatively determined by VSC method due to eliminate the

inter-crystalline contact resistance. However, the specific conductivity, as measured by VSC, is meaningless, because the measured conductivity involves resistance of the silver paste. Besides, author also proposed a simple physical model to interpret why VSC method can qualitatively be used to determine the intrinsic properties of temperature dependence of conductivity of the test materials [31]. The model was assumed that the measured resistance is dominated by resistance of three layers: resistance of the silver paste itself (presented by A layer), resistance of the particles of conducting polymers or organic poly-crystals immersed in the silver layer (represented by B layer) and the resistance of the tested materials (presented by C layer). Obviously, the inter-particle contact resistance in the layer B is completely shorted by silver paste. Moreover, the resistance of the layer B can be considered as the resistance of the test material and silver paste in series. The resistance between voltage terminals of VSC device, therefore, consists of the resistance of A, B and C layers in parallel.

According to mathematical analysis of this model, it is found that the layer B is a technical key for preparing VSC device and its thickness should be thinner as possible in order to have successful VSC measurement [31]. Author, for the first time, successfully observed the metallic temperature dependence of conductivity of highly-doped PA by VSC method [29], i.e., the conductivity increased with decreasing temperature from 300 to 77 K, exhibiting a metallic behavior. Moreover, metal-semiconductor transition for PPy [32] and PTH [33] was also observed by VSC method.

The substantial progress in developing new conducting polymers and in enhancement of conductivity were obviously for the last thirty years. In 1987, for example, Naarmann et al. [34] reported that the conductivity of doped PA was as high as of 10^4 S/cm comparable to those of traditional metals (e.g. lead), showing the onset of a new generation of conducting polymers. After that, the conductivity of doped PA continually increased to 10^5 S/cm reported by Tsukomoto [35]. In addition, conductivity of doped PPV on order of 10^4 S/cm was also reported [36]. Moreover, the PF$_6$-doped PPy synthesized by electrochemical polymerization at a lower temperature showed a high conductivity ($\sim 10^3$ S/cm) and, for the first time, a positive temperature coefficient of resistivity (TCR) was observed at temperature below 20 K [37]. Meanwhile the conductivity of CSA doped PANI was as high as $300 - 400$ S/cm [20] and a significant positive TCR in the temperature range $160 - 300$ K [38] was also observed. Although a great progress has been made in enhancement of room-temperature conductivity of the conducting polymers, as above-mentioned, it is necessary to reduce the microscopic and macroscopic disorder and thereby bring out the intrinsic metallic features of conducting polymers.

Up to date, various models have been proposed to interpret charge transport of conducting polymers. For instance a model considered charge transport by inter-chain hopping has been proposed by Matveeva [39]. This model suggested

that single chain or intra-molecular transport, across inter-chain transport and inter-particle contact contribute to the overall conductivity of the conducting polymers, as measured by four-probe method. It implies that these elements comprise a complicated resistive network, which determines the effective mobility of the carriers in the conducting polymers. This model also indicated that the mobility and the conductivity of conducting polymers are dominated by both microscopic (intra-chain and inter-chain) and macroscopic (inter-particles) level [40]. Although room-temperature conductivity of the conducting polymers shows a metal-like behavior, charge transport across inter-chain and inter-particles in conducting polymers, as presented by temperature dependence of conductivity, only exhibits a semiconductor behavior and obeys a Variable Range Hopping (VRH) model proposed by Mott and Davis [41], which is expressed as

$$\sigma = \sigma_0 T^{-1/(n+1)} \exp[-(T_0/T)^{1/(n+1)}] \tag{1.4}$$

where σ_0 and T_0 are constants and $n = 1, 2$, and 3 for 3D, 2D and 1D conduction, respectively. The value of "n" is defined as the dimensionality of the conduction, which can be obtained from the plot of log σ against to $T^{1/(n+1)}$. The Mott parameter (T_0) is directly proportional to the density of state at Fermi level and is inversely proportional to the location length [41]. It is found that the dimensionality (n) is affected by the diameter of nanostructure, for instance, 3D-electronic conduction in PANI or PPy nanotubes with a 400 nm is often observed [42] whereas 1D-conduction is occurring for small diameter tubules owing to the large proportion of the ordered material [43].

Sheng and Klasfter's fluctuation induced tunneling (FIT) model has been also widely used to interpret temperature dependence of conductivity of conducting polymers (e.g. high conducting PA) [44]. However, some argues on the FIT model were arisen [45] and modification on the FIT model was also proposed [46]. Baughman and Shacklette [47] proposed a random resistor net-work model with a wide distribution of activation energies to interpret temperature dependence of conductivity for conducting polymers. A similar correction between the conjugation length, conductivity, and the exponential temperature dependence of $\sigma(T)$ was reported by Roth [48]. Epstein et al. [49] also proposed a "metallic islands" model, which is a composite model consisting of high conductivity crystalline regions surrounded by insulating amorphous regions, to interpret the transport properties of PANI protonated by common acids (e.g. HCl and H_2SO_4). Besides, some other models, such as random dimmer model with a set of delocalized conducting states [50] and polaron/bipolaron model involving correlated hopping and multi-phonon process [51] have been also proposed for explaining the exponential temperature dependence of conductivity observed in conducting polymers.

Based on above-discussions, in summary, conducting polymers not only have semiconductor and metal properties, but also maintain many advantages of

conventional polymers, such as light weight, flexible chain and processability. The unique properties resulted from delocalized π-conjugated structure and unusual doping concept and reversible doping/dedoping process, and conducting mechanism completely differs from either inorganic semiconductors or metals. Moreover, it should be noted that the conducting polymers are intrinsic and differ from conducting plastics blended by conductive carbon or metallic materials as the fillers.

References

[1] H. Shirakawa, E. J. Louis, A. G. MacDiarmid, C. K. Chiang, A. J. Heeger. J. Chem. Soc. Chem. Commun., 1977, 578

[2] www.nobel.se/chemistry/laureaters/2000/idex.html

[3] a) V. V. Walatka, M. M. Labes and J. H. Perlstein. Phys. Rev. Lett., 1973, 31: 1139; b) C. M. Mikulsk, P. J. Russo, M. S. Saran, A. G. MacDiamid, A. F. Garito, A. J. Heeger. J. Am. Chem. Soc., 1975, 97: 6358

[4] Handbook of Conducting Polymers (Ed. T. A. Skotheim). Marcel Dekker, New York, 1986 and 1998

[5] Encyclopedia of Nanoscience and Nanotechnology (Ed. H. S. Nalwa). 2004, 2: 153 – 169

[6] Yukio Furukawa. J. Phys. Chem., 1996, 100: 15644

[7] J. D. Stenger-Smith. Progr. Polym. Sci., 1998, 23: 57

[8] A. G. MacDiarmid. Angew. Chem. Int. Ed., 2001, 40: 2581

[9] J. C. Chiang, A. G. MacDiarmid. Synth. Met., 1986, 13: 193

[10] A. G. MacDiarmid, A. J. Epstein. Faraday Discuss. Chem. Soc., 1989, 88: 317

[11] Conductive Polymers (Ed. R.B. Seymour). New York: Plenum Press, 1981, 23 – 47

[12] Joseph Jagur-Grodzinski. Polym. Adv. Technol., 2002, 13: 615

[13] W. P. Su, J. R. Schrieffer, A. J. Heeger. Phys. Rev. Lett., 1979, 42: 1698; Phys. Rev. B, 1980, 22: 2099

[14] a) S. A. Brazovski, N. N. Kirova. Sov. Phys. JETP Lett., 1981, 33: 4; b) A. R. Bishop, D. Campbell, K. Fesser. Mol. Cryst. Liq. Cryst., 1981, 77: 253; c) J. L. Bredas, R. R. Chance and R. Silbey. Phys. Rev. B, 1982, 26: 58431; d) H. Kaufman, N. Colaneri, J. C. Scott, and G. B. Street. Phys. Rev. Lett., 1984, 53: 1005; e) S. Stafstrom, J. L. Bredas, A. J. Epstein, H. S. Woo, D. B. Tanner, W. S. Huang, and A. G. MacDiarmid. Phys. Rev. Lett., 1987, 59: 1464

[15] S. A. Brazovski, N. N. Kirova. Sov. Phys. JETP Lett., 1981, 33: 4; J. L. Briad, R. R. Chance, R. Silbey. Mol. Cryst. Liq. Cryst., 1981, 77: 319

[16] Yukio Furukawa. J. Phys. Chem., 1996, 100: 15644

[17] a) C. K. Chiang, C. R. Fincher, Y. W. Park, A. J. Heeger, H. Shirakawa, E. J. Louis, S. C. Gua, and A. G. MacDairmid. Phys. Rev. Lett., 1977, 39: 1098; b) C. K. Chiang, M. A. Druy, S. C. Gua, A. J. Heeger, H. Shirakawa, E. J. Louis, A. G. MacDairmid, and Y. W. Park, J. Am. Chem. Soc., 1978, 100

[18] A. O. Patil, A. J. Heeger and F. Wudl. Chem. Rew., 1988, 88: 183; J. Roncali. Chem. Rev., 1992, 92: 711

[19] A. G. MacDiarmid, A. J. Epstein. in Proceedings of the 2nd ; Brazilian Polymer Congress, Sao Paulo, 1993, p.544

[20] a) Y. Cao, P. Smith and A. J. Heeger. Synth. Met., 1992, 48: 91; b) Y. Cao and A. J. Heeger. Synth. Met., 1992, 52: 195; c) Y. Cao, J. J. Qiu, and P. Smith. Synth. Met., 1995, 69: 167

[21] A. B. Kaiser. Phys. Rev. B, 1989, 40: 2806

[22] C. R. Fincher, D. L. Peebles, A. J. Heeger, M. A. Druy, Y. Matsumura, A. G. MacDiarmid, H. Shirakawa and Ikeda. Solid State Commun., 1978, 27: 489

[23] Y. W. Park, A. Denenstein, C. K. Chiang, A. J. Heeger and A. G. MacDiarmid. Solid State Commun., 1979, 29: 747

[24] B. Rr. Weinberger, J. Kaufer, A. J. Heeger, A. G. MacDiamid. Physical Review B, 1979, 20: 233

[25] S. Musubuchi, S. Kazama. Synth. Met., 1987, 18: 195; and 1995, 69: 315

[26] K. Kaneto, S. Hayashi, S. Ura, K. Yoshino. J. Phys. Soc. Jpn., 1985, 54: 1146

[27] C. M. Gould, D. M. Bates, H. M. Bozler, A. J. Heeger, M. A. Dury, and A. G. MacDiarmid. Phys. Rev. B, 1980, 23: 6820

[28] L. B. Coleman. Review of Scientific Instrumentation, 1978, 49: 58

[29] M. X. Wan, P. Wang, Y. Cao and R.Y. Qian, F. S. Wang, X. J. Zhao and Z. Gong. Solid State Commun., 1983, 47: 759

[30] M. X. Wan, D. B. Zhu, M. Z. Li, R. Y. Qian. Science Bulletin, 1982, 24: 1495 (in Chinese); M. X. Wan and P. Wan. Acta Physica Sinica, 1986, 35: 82

[31] M. X. Wan. Chinese J. Polymer Science, 1989, 7: 330

[32] a) P. Wang, M. X. Wan, X. T. Bi, Y. X. Yao, R. Y. Qian. Acta Physica Sinica, 1984, 33: 1771; b) X. T. Bi, Y. X. Yao, M. X. Wan, P. Wang, K. Xiao, Q. Y. Yang and R. Y. Qian. Makromol. Chem., 1985, 186: 1101

[33] Y. Cao, P. Wang and R. Y. Qian. Makromol. Chem., 1985, 186: 1093

[34] a) H. Naamann and N. Theophilou. Synth. Met., 1987, 22: 1; b) N. Basescu, Z. X. Liu, D. Moses, A. J. Heeger, H. Naamann, and Theophiou. Nature, 1987, 327: 403; c) Th. Schimmel, D. Glaser, M. Schwoerer, and H. Naamann. in Conjugated Polymers (J. L. Bredas and R. Silbey, Eds). Dordrecht: Kluwer Academic, 1991, p.49

[35] J. Tsukamoto. Adv. Phys., 1992, 41: 509

[36] a) I. Murase, T. Ohnishi, T. Noguchi, and M. Hirooka. Synth. Met., 1984, 17: 639; b) F. E. Karaz, J. D. Capistran, D. R. Gagnon, and R. W. Lenz. Mol. Cryst. Liq. Crys., 1985, 118: 327; c) T. Ohnishi, T. Noguchi, T. Nakano, M. Hirooka, and I. Murase. Synth. Met., 1991, 41 − 43: 309

[37] a) T. Hagiwara, M. Hirasaka, K. Sato, and M. Tamaura. Synth. Met., 1990, 36: 241; b) K. Sato, M. Yamaura, T. Hagiwara, K. Murata, and M. Tokumoto. Synth. Met., 1991, 40: 35

[38] a) Y. W. Park, C. Park, Y. S. Lee, C. O. Yoon, H. Shirakawa, Y. Suezaki, and K. Akagi. Solid State Commun., 1988, 65: 147; b) M. Reghu, Y. Cao, D. Moses, and A. J. Heeger. Phys. Rev. B, 1993, 48: 17685

[39] E. S. Matveeva. Synth. Met., 1996, 79: 127

[40] J. I. Kroschwitz. Encyclopedia of polymers: Science and Engineering. 1986, 5: 462. New York: Wiley

[41] N. F. Mott and E. A. Davis. Electronic Processes in Noncrystalline Solid (2nd Ed). Oxford: Clarendon Press, 1979, p.32

[42] J. P. Spatz, B. Lorenz, K. Weishaupt, H. D. Hochheimer, V. P. Menon, R. V. Parthasarathy, C. R. Martin, J. Bechtold, and P. H. Hor. Phys. Rev. Lett., 1994, 50: 888

[43] M. L. Knotek, M. Pollak, T. M. Donovan and H. Kurtzman. Phys. Rev. Lett., 1973, 30: 853

[44] P. Sheng and J. Klasfter. Phys. Rev. B, 1983, 27: 2583

[45] a) J. Voit and H. Buttner. Solid State Commun., 1988, 67: 1233; b) E. M. Conwell and H. A. Mizes. Synth. Met., 1990, 38: 319

[46] a) A. B. Kaiser and S. C. Graham. Synth. Met., 1990, 36: 367; b) G. Paasch. Synth. Met., 1992, 51: 7

[47] a) R. H. Baughman and L. W. Shacklette. Phys. Rev. B, 1989,39: 5872; b) R. H. Baughman and L. W. Shacklette. J. Chem. Phys., 1989, 90: 7492

[48] S. Roth. in Hopping Transport in Solids (M. Pollak and B. Shklovskii eds.) North-Holland, Amsterdam, 1991, p.377

[49] a) A. J. Epstei, J. M. Ginder, F. Zho, H. S. Woo, D. B. Tanner, A. F. Richter, M. Angeloupolos, W. S. Huang, and A. G. MacDiarmid. Synth. Met., 1987, 21: 63; b) A. G. MacDiarmid and A. J. Epstein. Synth. Met., 1994, 65: 103; c) Z. Wang, A. Ray, A. G. MacDiarmid and A. J. Epstein, Phys. Rev., 1991, 43: 4373

[50] a) P. Phillips and H. L. Wu. Science, 1991, 252: 1805; b) D. H. Dunlap, H. L. Wu, and P. Phillips. Phys. Rev. Letter, 1990, 65: 88

[51] a) L. Zuppiroli, M. N. Bussac, S. Paschen, O. Chauvet and L. Forro. Phys. Rev. B, 1994, 50: 5196; b) M. N. Bussac and L. Zuppiroli. Phys. Rev. B, 1994, 49: 5876; c) O. Chauvet, S. Paschen, L. Forro, L. Zuppiroli, P. Bujard, K. Kai, and W. Wernet. Synth. Met., 1994, 63: 1159

Chapter 2 Polyaniline as A Promising Conducting Polymer

As mentioned in Chapter 1, the discovery of the conducting polymers was attributed to MacDiarmid et al. who exposed free standing films of PA to vapors of chlorine, bromine and iodine, resulting in increasing 12 orders of magnitude in conductivity at room temperature [1]. In fact, the first work describing the synthesis of what is now recognized as a conducting polymer was "Aniline black" published in 1862 [2]. "Aniline black" was prepared from the anodic oxidation of aniline and accompanied a color change upon switching potential, which latterly was called as electrochromism [3]. However, it was regret that the electrical properties were not measured at that time! In 1985, MacDiarmid, for the first time, found that aniline monomer in an acid aqueous solution (e.g.1.0 mol/L HCl) can be chemically oxidized by ammonium peroxydisulfate (APS) to obtain green powder of PANI with a conductivity of as high as 3 S/cm, as measured by four-probe method, which results were published in 1986 [4].This was the first sample of the conducting polymers doped by proton, which latterly was called "proton doping". Compared with other conducting polymers, PANI is advantageous of easy synthesis, low-cost, structure complex and special proton doping mechanism, as well as physical properties controlled by both oxidation and protonation state. These unique properties result in PANI holding an important position in the field of conducting polymers. At that time, author was pursure advanced studying on conducting polymers under Prof. MacDiarmid at University of Pennsylvania, the United States of America as a post-doctor. As a result, author was fascinated by the novel properties and promising application of PANI to further study PANI when came back to China from USA in 1988. The research objects included synthesis method, doping mechanism, solubility, and physical properties of PANI. In this chapter, therefore, author would like to further introduce character of molecular structure, synthesis method, doping concept and associated conducting mechanism and processability of conducting polymers by using PANI as a promising sample.

2.1 Molecular Structure and Proton Doping

Compared with other conducting polymers, PANI has a complex molecular structure dominated by its oxidation and protonation state. MacDiarmid et al. [5], for the first time, proposed that the base form of PANI has a general formula [6]

as shown Fig. 2.1. They assumed that the base form of PANI consists of alternating reduce and oxidized repeat unit chain and can be divided into three states based on the oxidation state [4, 7] as shown in Fig. 2.1. The completely reduced form and oxidized form are assigned as "leucoemeraldine" base form ($y = 1$, LEB) and "pernigraniline" form ($y = 0$, PEN), respectively. The "half-oxidized" form is called as "emeraldine base" form ($y = 0.5$, EB). The general molecular formula of the base form of PANI proposed by MacDiarmid has been firstly conformed by the analysis of the ^{13}C-NMR spectra [8].

reduced   oxidized

(a)

(b)

(c)

(d)
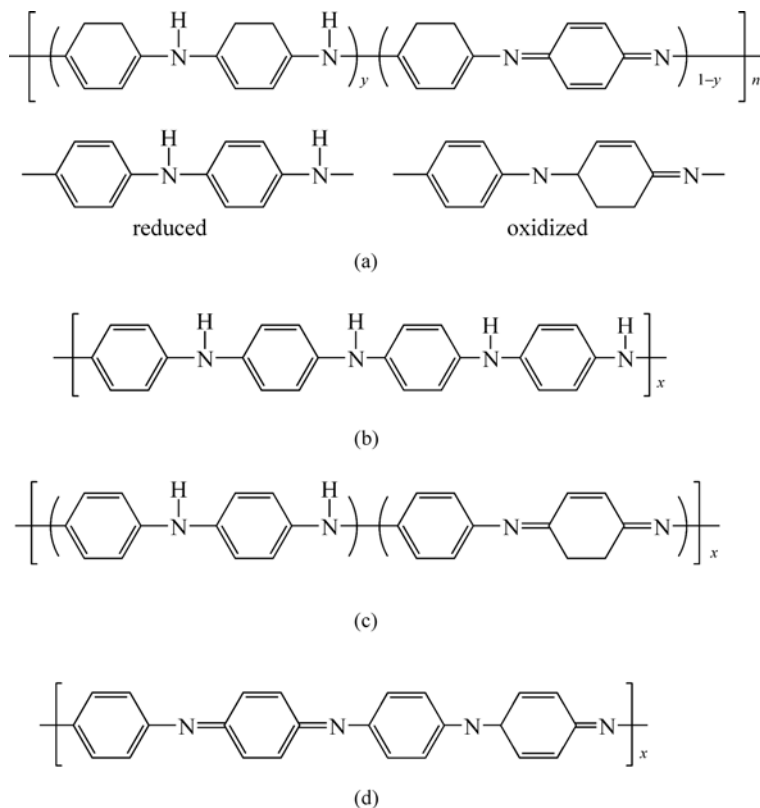
Figure 2.1   (a) Generalized composition of PANI indicating the reduced and oxidized repeat units; (b) completely reduced polymer; (c) half-oxidized polymer; (d) fully oxidized polymer [6]

As above-mentioned, PANI was the first sample of a doping conjugated polymer to a highly conducting regime by a proton doping [4]. Proton doping means that the emeraldine base form (EB, $y = 0.5$) is doped with a protonic acid (e.g. 1.0 mol/L HCl) to produce a protonated emeraldine base form with a high conductivity (~ 3 S/cm), which is called as the emeraldine salt form (ES) [4, 7b]. As shown in Fig. 2.2, the proton doping dose not involve a change of the number

of electrons associated with the polymer backbone during the proton doping [4, 7b]. This significantly differs from redox doping (e.g. oxidation or deduction) where involves the partial addition (reduction) or removal (oxidation) of electrons to or from the polymer backbone [9]. Thus proton doping is major characteristics of PANI differing from other conducting polymers.
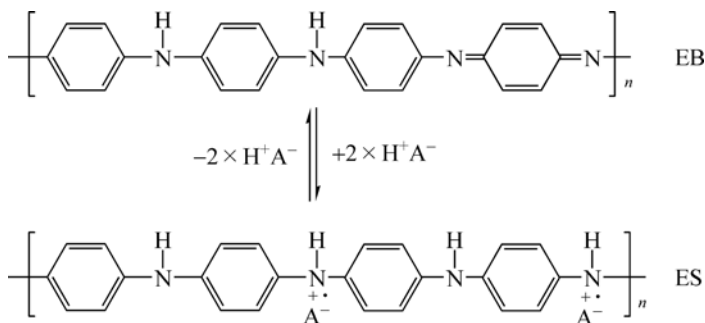
Figure 2.2   Scheme of proton doping in PANI [6]

In principle, the imine nitrogen atom on the polymeric chain of PANI can be protonated in whole or in part to obtain the corresponding salts and the protonation degree on the polymeric base, depending on its oxidation state and the pH value of the aqueous acid [4]. MacDiarmid et al. [5], for the first time, proposed that proton doping only took place on the imine segment of the emeraldine base form to form a bipolaron. However, this was contradictory with both theoretical calculation and ESR, because theoretical calculation rules out the presence of a bipolaron lattice (spinless) in the emeraldine salt form [10] and a strong ESR signal rather than spinless was observed [11]. In order to solve above contradictory, Epstein et al. [11, 12] and Wnek [13] suggested that spinless bipolaron can convert to two spinning protons due to instability of bipolaron. MacDiarmid et al. [7b] also proposed the polaron is of semiquinone form as shown in Fig. 2.2. It means that the complete protonation of the imine nitrogen atom in the emeraldine base by proton doping results in the formation of a delocalized poly-semiquinone radical cation [4, 7b, 9a]. Author also studied mechanism of proton doping in PANI by means of UV-visible and fluorescence spectra as well as *in situ* UV-visible and ESR spectra [14]. The main results are summarized as follows:

(1) Further proved MacDiarmid suggestion [4] that the protonation process only takes place on the imine segment of the poly-emeraldine chain.

(2) Proposed that the protonation process consists of a chemical reaction of proton with nitrogen on the imine segment and a diffusion process of counter-irons from aqueous solution to polymers. The first process is fast whereas the later is a slow process.

(3) Suggested that the protonation state (i.e. the emeraldine salt form, ES) should be considered in molecular structure of a partial protonated state. This

implies molecular structure of the protonated PANI should be determined by both oxidation and protonation state. This was further conformed by UV-visible spectral of thin film of PANI with different protonation state (i.e. different pH) [15]. As shown in Fig. 2.3, VU-visible spectra for the emeraldine base form show two peaks at 325 and 630 nm (Fig. 2.3) which are assigned as the excitation of the amine and imine segment on the polyemeraldine chain, respectively [10, 16]. This is consistent with that the molecular structure of the emeraldine base form of PANI consists of an amine and imine segment on the polyemeraldine chain [5]. For fully protonated emeraldine base form, on the other hand, the peak at 630 nm disappeared, whereas a new peak at 950 nm occurred that is assigned as proton band produced by proton doping [7b, 10 – 12]. In addition, the position of the peak at 325 nm does not change with its protonation state although the intensity of this peak decreases with its protonation state (Fig. 2.3) [15]. These indicated that the protonation process only takes place on the imine segment of the emeraldine chain, which was also consistent with Huang's suggestion [4]. That was also conformed by fluorescence excitation and emission spectra of PANI [14]. It noted that the intensity of peaks at 630 and 950 nm are strongly affected by the protonation state [15]. As shown in Fig. 2.4, the intensity of the peak at 630 nm decreases with increase of the protonation state (i.e. reduced pH value).On the contrary, the intensity of the peak at 950 nm increases with increase of the protonation state; however, the peak at 630 nm is still observed in a partially protonated PANI (e.g. at pH = 2 – 6), indicating the quinoid segment on the polyemeraldine chain is present in partially protonated PANI. Based on above results, author modified the general molecular formula of PANI by adding a parameter of the protonation state (x) as shown in Fig. 2.5 [15]. Above-described molecular structure and protonated state of APNI are also supported by its FTIR spectra. For example, the C═C stretching deformation of quinoid (1570 cm^{-1}) and benzenoid rings (1494 cm^{-1}), the C—N stretching of
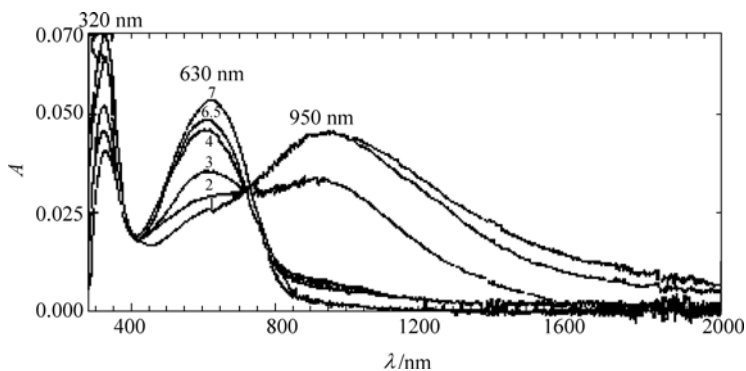
Figure 2.3   Absorption of the emeraldine base form of PANI files with different protonation state (i.e. pH) [15]
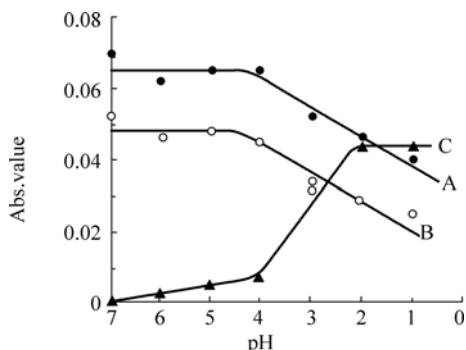
Figure 2.4 Intensity of the peak at 630 and 950 nm as a function of the protonation state [15]
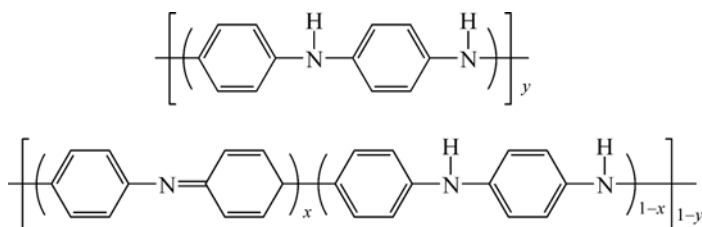
Figure 2.5 Modified molecular structure of the protonated PANI by adding protonation parameter (x) [15]

secondary aromatic amine (1300 cm^{-1}), the aromatic C—H in-plane bending (1141 cm^{-1}), and the out-of-plane deformation of C—H in the 1,4-disubstituted benzene ring (821 cm^{-1} and 505 cm^{-1}), and the aromatic C—H in-plane band at 1141 cm^{-1} related to proton doping PANI are observed [17]. Similar to other conducting polymers, the emeraldine salt form of PANI (i.e. conducting state) can be converted to its emeraldine base form (i.e. insulating state) by a base (e.g. NaOH or ammonium), consequently, which can be re-doping by acids to form the emeraldine salt form, showing a reversible protonation/de-protonation process [7b].

Except for proton doping, PANI is also able to be p-doped by charge transfer with an oxidation agent, achieving conductivity up to about 1.0 S/cm [4, 7b, 18]. In particular, Chen et al. [19] reported a novel soluble n-doped PANI in dimethyl suffixed (DMSO) synthesized by doping the emeraldine base of PANI with a strong reductant (KH or NaH). The room-temperature conductivity, spin density and magnetic susceptibility of the n-doped PANI were comparable with self-doping PANI [19]. However, stability of the conductivity is poor, for instance, the conductivity decreases rapidly by $6-7$ orders of magnitude within 90 s as exposed to air. In addition, they also suggested that the n-doping can be considered as a direct doping on the full oxidized form of PANI (i.e. PEN) by using the alkali metals K and Na [19]. Besides, n-doped and 100% sulfonated PANI, which is soluble in both organic and aqueous solvent, has been also synthesized

by electrochemical polymerization in an acetoneeitrile-water mixture (4:1) [20]. In particular, PANI can be doped by a photo-induced doping. In this method, photo-acid generators, which can release protons under light excitation, are required. In other words, the proton released by photo-acid generators under light excitation is served as a dopant. Based on above mechanism, Marier et al. [21] extensively studied on structure-property relationship of the PANI doped by photo-acid generators. Author also obtained a conducting PANI film by using a copolymer of vinylidene chloride and methyl acrylate (VCMAC) as a photo-acid generator [22]. Moreover, Lee et al. [23] reported a soluble PANI synthesized by modifying with a photo-labile, acid-labile, and thermo-labile *tert*-butoxycarbonyl (*t*-BOC) group. The resultant PANI (*t*-BOC) is highly soluble and thermody-namically stable in low-boiling solvents (e.g. THF, dioxane, and $CHCl_3$) and suggested the PANI (*t*-BOC) can be used as conductive matrix polymers for negative type photo-imaging or printing materials or for novel solution-processed applications in various microelectronic devices, which more discussions are given in Chapter 3.

PANI prepared by MacDiarmid method is mostly amorphous [7b], as measured by X-ray diffraction (XRD). Usually, the XRD of the doped PANI shows a broad peak centered at $2\theta = 18°$ and $25°$ that are attributed to the periodicity perpen-dicular and parallel to the polymer chain, respectively [24]. Except for the long-chain PANI, in addition, it also has its oligo-aniline, which electrical properties are as same as its long-chain [25]. The oligo-aniline is generally divided into three groups according to their terminal groups, which include amino-capped, phenyl-capped and amino/phenyl-capped [26], as synthesized by a simple oxidative coupling reaction [27].

2.2   Synthesis Method

Like other conducting polymers, PANI is generally synthesized by both chemical and electrochemical methods [9a]. But mechanochemical route has been recently reported to prepare conducting PANI. These methods to PANI will be briefly discussed below.

2.2.1   Chemical Method

In general, the emeraldine salt form of PANI (i.e. its conducting state) is prepared by oxidative polymerization of aniline in a strong acidic medium [4,5, 18a]. The scheme of chemical polymerization of aniline can be described as follows:

$$\text{Aniline} + \text{Dopant} \xrightarrow[0-25℃]{\text{Oxidant}} \begin{array}{c} \text{PANI} \\ \text{(BS)} \end{array} \xrightarrow[NH_3]{NH_4OH} \begin{array}{c} \text{PANI} \\ \text{(EB)} \end{array}$$
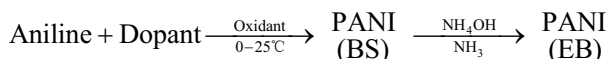
Typical chemical polymerization of PANI is as follows [9a]: APS of 10 mL (e.g. of 2.5 mol/L) as an oxidant is added with stirring to 100 mL solution of a mixture of aniline monomer (e.g. 0.55 mol/L) and 1.0 mol/L HCl at room temperature or in an ice/water bath $(0-5℃)$ and the polymerization is continued for pre-desired time. The precipitate is then filtered, washed with small amounts of 0.5 mol/L HCl solution, then with methanol until colorless, and finally diethyl ether until color-less. It is finally dried at ca. $60-70℃$ in air for ca. 24 h. The product so obtained is the emeraldine salt form with conductivity of ~ 10 S/cm, depending preparation conditions. The resultant emeraldine salt form can be converted to its emeraldine base form by NH_4OH or NH_3, which process is called as de-doping. From above scheme of polymerization of aniline, one can see, the reaction system of aniline polymerization is very simple, only including monomer, dopant and oxidant and water. Among these reagents, dopant is the most important reagent, because it is mainly attributed to electrical properties of PANI. Speaking generally, inorganic acids (e.g. HCl, H_2SO_4, H_3PO_4 and HF) and organic acids are widely used as dopants for doping PANI. Dopant feature includes molecular structure and acidity, strongly affect the properties of the doped PANI [9a]. Except for dopant, oxidant is another important reagent for chemical polymerization of PANI. Up to date various oxidants such as APS [4], tetrabutylammonium persulfate (TBAP) [28], hydrogen peroxide (H_2O_2) [29], benzoyl peroxide [30], ferric chloride ($FeCl_3$) [31] and chloroaurate acid ($HAuCl_4$) [32], have been used to synthesize PANI. However, most previous reported results mainly emphasized the effect of oxidants on the polymerization yield, and APS was regarded as the optimal oxidant for PANI because of its high yield [33]. Interestingly, author found that the diameter of PANI nanotubes synthesized by template-free method is directly related to the redox potential of oxidant [34] that will be discussed in Chapter 5 in more detail. In addition, reaction temperature, polymerization time as well as stirring fashion and speed also affect the structure and physical properties of the final PANI product. Reaction temperature is more important because it affects the crystallinity of PANI, showing a low reaction temperature is favorable for preparing high crystalline PANI [9a]. A low reaction temperature can be achieved by freezing the reaction bath (e.g. ice/salt bath with $T<4℃$) or by addition of inorganic salts (e.g. NaCl) in the reaction solution, resulting in the polymerization is proceed in the solid state [35].

2.2.2 Electro-Chemical Method

Electrochemical polymerization is another major tool to prepare conductive PANI. In an electrochemical method, a PANI film or layer is formed on a work electrode surface in an acidic medium (e.g. 1.0 mol/L HCl) including high concentrations of aniline monomer [9a]. The electrochemical method has some advantages over

chemical procedures to prepare PANI as follows: ① Electrochemical method is easy to be controlled by changing current quantity passed through between the work and counter electrodes, applied voltage and polymerization time. Moreover, the oxidation and electrically conducting form of PANI is reversibly transformed into the reduced, isolating form by changing its electrochemical potential to negative values. On the other hand, the chemical method is difficult to ensure a same micro-environment for preparing PANI, insulting in disorder of the product. ② A small amount reagent is required in an electrochemical method. On the contrary, a large amount of reactive chemical reagents in the chemical method is required, which could cause environment pollution. ③The quantum of the product prepared by electrochemical method is limited by size of the work electrode; however, large amount of product is easily synthesized by a chemical method. It has been demonstrated that the electrochemical polymerization of aniline is as a bimolecular reaction involving a radical cation intermediate and a two-electron-transfer process for each step of polymerization [36]. Based on the assumption that the oxidation of PANI follows Faraday's law, the electrochemical polymerization of aniline can be monitored by PANI deposition on the work electrode and doping charges [37]. In some strong acids such as HC1 or H_2SO_4, the deposition charge was found to increase proportionally to the second powers of the cycle number [36]. When potentiostatic techniques was used to electro-chemically polymerize aniline, moreover, the initial formation (or nucleation) of PANI on the surface of the electrode is slow, but the initially formed PANI accelerated the polymer growth greatly and the current increased proportionally with the second power, which is called as "self-catalyzing" or "auto-acceleration" process in the electrochemical polymerization of aniline [38]. Wei et al. [36] employed the anodic peek current instead of charges to monitor the electrochemical polymerization process of aniline in aqueous HCl solution using cyclic potential sweep techniques. This method was more sensitive to the presence of irreversible side reaction [39]. By using this method, the cyclic voltammograms of aniline polymerization showed three peaks [36], which are associated with three oxidation states suggested by MacDiarmid [6]. Wei et al. [40] also investigated effect of the additives, such as paminodiphenylamine, benzidine, and phenoxyaniline, on the rate of electrochemical polymerization of aniline. They found all of these additives have lower oxidation potentials than the aniline monomers and at least one satirically accessible aromatic amino group incorporated into polymer chains as a part of the structural backbones [40].

2.2.3   Mechano-Chemical Route

Since the liquid monomer aniline forms solid salts with doping acids (e.g. HCl, H_2SO_4 and CSA) through an acid/base reaction, room-temperature solid-state polymerization of aniline is possible using a solid anilinium salt as the precursor.

Kaner et al. [41] recently describe a solvent-free mechanochemical route to PANI in which the reaction is induced by ball-milling an aniline salt and an oxidant under ambient conditions. According to the report of Kaner et al. [41], the typical synthesis procedure of mechanochemical route to PANI is shown as: firstly a salt of aniline and CSA was prepared by the reaction between aniline and CSA in water followed by evaporation that was served as the precursor. Then a mixture of an anilinium salt (e.g. aniline/CSA) and APS as an oxidant were loaded into a stainless steel grinding bowl and which was then sealed and spun at 600 r/min in a planetary micro-mill for 1 h [41]. Once the spinning stopped, the product was transferred into a beaker and washed with water for several times. A yield of up to 65% based on aniline can be achieved using a 1:1 molar ratio of anilinium salt to oxidant and typical sample of the PANI powder prepared by this method is shown in Fig. 2.6. Spectroscopic studies indicate that the resultant PANI is identical to the emeraldine salt form of PANI with a conductivity of 10^{-2} S/cm [41]. This method opens a sample and solvent-free method to prepare a large amount of the conducting PANI.

Figure 2.6   Powder of PANI prepared by mechanochemical method for 1 h [41]

2.3   Physical Properties

Like other conducting polymers, PANI has unique physical properties including optical, electrical and magnetic properties and corresponding effects (Schottky and thermo-chromic effect and photo-emission effect) which will be briefly discussed below.

2.3.1   Nonlinear Optical (NLO)

Nonlinear optical (NLO) effect is defined that when a light passes through a nonlinear optic-active medium, the frequency, phase, amplitude or transmission

of the coming out of light are changed [42]. The NLO phenomena therefore are expected to provide hey functions necessary for the photonic technology of optical switching, frequency modulation, wave-guiding, and eventually practical all-optical computing [43]. Compared with inorganic or organic NLO materials, NLO polymers are of somewhat advantageous as follows: ① The design, synthesis and fabrication of NLO polymers are more flexible, facile and cost-effective than those of inorganics [44]. ② The lower dielectric constant of polymers make it easier to design traveling wave electro-optic (EO) modulators due to the close match of velocity between the microwave and optic wave. ③ Processing polymers in conjunction with thin films technologies offers the unique opportunity for them to be used in inter-grated optic and EO application. As a result, organic and polymeric NLO materials have been received great attention in NLO materials and their applications in technology.

Generally speaking, the NLO phenomena can be described at both the molecular and bulk lever. The molecular polarization in an intense electric field is field-dependent and is usually described by equation [45]:

$$\mu(E) = \mu_0 + \alpha E + \beta E^2 + \gamma E^3 \tag{2.1}$$

where μ is the molecular dipole moment, μ_0 is the intrinsic dipole moment of the molecule, and E is the electric field vector. The α, β and γ coefficient represents the polarizability, hyperpolarizability and the second hyperpolarizability of the molecules, respectively. The bulk polarization of a material can be described in a similar equation:

$$P(E) = P_0 + \chi^{(1)} E + \chi^{(2)} E^2 + \chi^{(3)} E^3 \tag{2.2}$$

in which $\chi^{(1)}, \chi^{(2)}$ and $\chi^{(3)}$ are assigned as the first-, second- and third-order susceptibilities and P represents the bulk polarization of the medium. P_0 is the permanent polarization of the material. Therefore, nonlinear responses in bulk media are usually described by $\chi^{(2)}$ and $\chi^{(3)}$, respectively. According to above Eq. (2.2), all materials including gases, liquids and solids can show third-order NLO effects, but second-order NLO materials require a noncentrosymmetric alignment of NLO molecules [45].

Bulk and molecular nonlinear optical properties can be measured by laser optical techniques such as second and third harmonic generation (SHG and THG), electric-induced second harmonic generation (EFISH), and degenerate four-wave mixing (DFWM), while molecular NLO responses are calculated by quantum-mechanic methods [46].

Conducting polymers are regarded as excellent third-order NLO materials due to highly polarizability electrons in their polymeric chain. It was predicted that $\chi^{(3)}$ is proportional to the reciprocal of the band gap raised to the sixth power [47],

indicating any structural changes result in a shift in oscillator strength, leading to change $\chi^{(3)}$. In other words, decreasing band gap for conducting polymeric NLO materials is efficient approach for enhancing $\chi^{(3)}$. Based on above assumption, one method of enhancing $\gamma^{(3)}$ is simply to increase the length of the conjugation sequence. However, experimental results showed that γ/N, where N is the number of repeat units, does not increase continuously and will eventually level off with increasing N [48], indicating very long conjugation sequences may not be required to maximize third-order NLO response. Detail review is given by Reference [49]. Since the nitrogen atom between phenyl rings on the chain of PANI exist different oxidation and protonation states, as above-mentioned, PANI not only has three different bases: emeraldine, leucoemeraldine and pernigraniline [50], but also doping and un-doping state through acidic /base reaction. The protonation doping process allows protons to nitrogen atoms on the chain and results in a displacement of electrons [51]. These electrons are responsible for the high optical nonlinearities of PANI, because the relatively weak binding allows the necessary electronic mobility for the nonlinear response [52]. Optical nonlinearities of PANI have already been studied [53].

In general, it is difficult to understand effect of the polymer chain length on the physical and chemical properties of PANI because their structure, crystallinity and aggregation morphology are sensitive to synthesis conditions. Therefore, it seems worthwhile to investigate its corresponding oligomers instead of PANI itself. MacDiarmid et al. [54] observed geometrical (*cis* and *trans*) and positional isomers of phenyl/—NH$_2$ end-capped tetra-aniline that allowed the observation of dichroism of aniline tetramers in polymeric films [55]. Franzen et al. [56], for instance, reported the nonlinear optical properties of phenyl/—NH$_2$ end-capped tetra-aniline in dimethyl sulfoxide solutions are as a function of the tetra-aniline concentration for both doped and undoped samples, as measured by the single beam Z-scan technique with 70 ps duration pulses at 532 nm. Their results suggested that optical nonlinearities of PANI do not depend on the electronic mobility because the addition of protons during the doping process produced a modest variation in the optical nonlinearities due to decrease of the absorption coefficient. Moreover, the optical properties of tetra-aniline are comparable to those of the much longer PANI [56].

The refractive index and optical band gap are the fundamental parameters of an optical material, because it is a key parameter for device design such as switches, filters, and modulators [57]. Arslan et al. [58] investigated the optical properties of the poly (*N*-benzylaniline) thin film. They reported that the refractive index (6.37 to 5.71) and the optical band E_g (2.089 to 2.046 eV) of the film, as measured by the transmittance and reflectance spectra that were affected by the thermal annealing.

Photovoltaic effect, which means that electrons and holes produced by light irradiation are collected at electrodes when an optical material is illuminated, has

been attracted much attention in photovoltaic devices. The photoelectric conversion properties of a novel self-assembled multilayer film of the self-doped PANI (SPAN) containing diazoresin (DR) were measured by a conventional three-electrode photoelectrochemical cell in a 0.5 mol/L KCl solution as the supporting electrolyte [59]. It reported that the photocurrent spectroscopy responses coincide with the absorption spectrum of the self-assembly film, indicating the SPAN/DR film is responsible for the photocurrent generation [59].

2.3.2   Electrical and Charge Transport Properties

Highly conducting form (ES) of PANI is controlled by two completely different processes: protonic acid doping and oxidative doping, while other conductive polymers are affected by their oxidation state alone [60], resulting in it has a special position in the field of conducting polymers.

As mentioned before, the insulate state of PANI (the emeraldine base form, EB) can be doped by proton doping (e.g. 1 mol/L HCl) to conducting state of PANI (the emeraldine salt form, ES) [4, 5]. As shown in Fig. 2.7, the protonation is accompanied by a 9 to 10 order of magnitude increase in conductivity achieving about 10 S/cm, showing the conductivity is strongly affected by the protonation state (i.e. pH value of reaction) and undergone a change from insulator to metal through semiconductor [6]. A lot of papers dealing with PANI electrical properties have been reported [4, 5, 61]. Moreover, the doped PANI can be obtained by chemical oxidation (*p*-doping) of the full-reduced form of PANI (i.e. leucoemeraldine base) [7a].
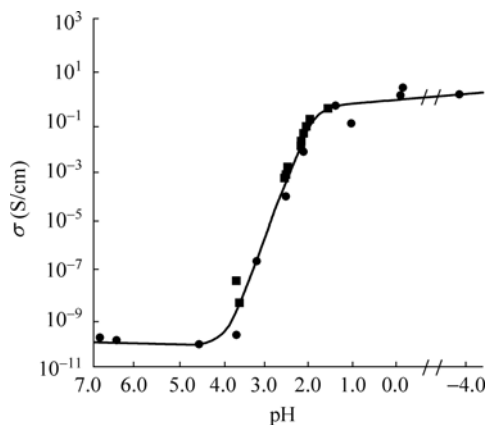
Figure 2.7   Conductivity of emeraldine base as a function of the pH of the HCl dopant solution as it undergoes protonic acid doping (● and ■ represent two independent series of experiments) [6]

Charge transport of PANI showed that the localized conductivity of PANI is affected by the localized variations in the thickness, stoichiometry, defects, or even substrates [62]. For intermediate protonation levels (e.g. the emeraldine salt form of PANI), for instance, magnetic and optical experiments supported the phase segregation between highly conducting regions and the insulating background [63]. The charge conduction was proposed via charging energy- limited tunneling among the small granular polymeric grains [64], assuming the conductivity of the "conducting island" in PANI could be up to 10^3 S/cm [11]. Moreover, difference in charge transport between PANI-H_3PO_4 [65] and PANI-H_2SO_4 [66] has been also observed, implying that the dopants have a large impact on the charge transport properties of doped PANI in bulk. Furthermore, effect of synthesis conditions on morphology and conductivity of PANI has been also reported due to the difference in formation mechanism in different polymerization media [67]. Therefore it will be interesting to the charge transport properties of PANI films in nano-scale. Atomic force microscopy (AFM) with a conducting tip (C-AFM) or current-sensing atomic force microscopy (CS-AFM), which is an excellent tool for measuring the local conductivity and current-voltage (*I-V*) characteristics of conducting polymers, has found its applications in many areas including organic materials [68]. The method has some advantageous as follows: ① The contact in CS-AFM can be made between the conducting tip and the substrate with a certain confidence by maintaining a prescribed load force. ② Topographical and current images could be obtained simultaneously which provide information on the conductivity in nano-scale domains that is not provided by other methods. ③ The current-voltage (*I-V*) traces can provide the relations between structural features and electrical properties of the materials on the nanometer scale [69]. Thereby a lot of papers dealing with electrical properties and charge transport of PANI measured by C-AFM or CS-AFM have been reported [70]. For instance, Wu et al. [71] reported current images of the fully doped PANI (i.e. emeraldine salt form) thin films recorded in air demonstrate, showing the electric conductivity of the highest conducting regions is 10^5 times higher than that of the lowest conducting regions. The large spatial variations in the film conductivity on topographically featureless regions were tentatively attributed to the presence of nano-scale crystallites of polaron lattice [71].

Sulfonated polyaniline (SPAN) is the first reported self-doped water soluble conducting PANI derivative and a prime model for dopant and secondary dopant induced processability [72]. It has high water solubility and a novel pH-dependent conductivity that is of interest for fundamental science and also for applications in technology such as rechargeable batteries with a higher charge density [73] as compared to that obtainable utilizing the parent PANI [74], hetero-structure light emitting diode devices [75], electrolyte acidity and enzyme activity [76] resist on a wafer [77]. Epstein and coworkers extensively studied synthesis and physical properties of SPAN with different sulfur-to-nitrogen (S/N) ratios (represented as S/N with 0.5 – 0.75). The physical properties including the pH dependence of the

conductivity and electrochemical properties of SPAN with a high S/N ratio of 0.75 (i.e. LEB-SPAN) were extensively studied [78].

2.3.3   Magnetic Properties

Since the magnetic properties can provide important details of charge carrying species and unpaired spins, magnetic properties of PANI have been extensively studied [79]. Usually the total static magnetic susceptibilities of the doped PANI could be separated into three components: atomic core diamagnetism, local-moment Curie-law paramagnetic and temperature-independent Pauli paramagnetic. It is generally observed that the magnetic susceptibility changes from a Curie-like to a Pauli-like behavior as the temperature increases [80]. Moreover, the magnetic properties of PANI are affected by doping structure and degree, chain structure as well as synthesis conditions. For instance, Jinder et al. [11] found that the Pauli susceptibility of HCl-doped PANI is approximately linearly proportional to the degree of protonation. In addition, the magnetic properties of PANI and its derivatives (e.g. poly-alkyl-aniline) have a nearly linear $\chi(T)$ dependence on T attributed to disorder-induced localized polaron pairs [81]. Although a lot of efforts have been done on the magnetic properties of APNI through different methods such as static magnetic measurements, electron paramagnetic resonance (EPR) and NMR spectroscopy [82], some of the results are still contradictory possibly, particular focused on the nature of the temperature-independent susceptibility, due to the complexity of polymeric materials caused by synthesis and doping conditions [83].

2.3.4   Other Properties

Rannom et al. [84] recently reported diesters of 4-sulfophthalic acid doped PANI exhibits strong thermo-chromic effect in the UV-visible -NIR spectra and improved mechanical properties. It was suggested that the diesters of 4-sulfophthalic acid play a double role: one is sufficiently strong acids rendering PANI conductive; another results in lower glass transition temperature (T_g) due to containing strongly plasticizing groups. In addition, the thermo-chromic effect of PANI dissolved in N-methylpyrrolidone (NMP) solution of three principal forms of neutral (i.e., insulating) PANI, namely, leucoemeraldine, emeraldine, and pernigraniline [85] as well as in films plasticized with NMP [86] has been observed. In addition, it has also been reported for optically active doped PANI, i.e., PANI protonated with (+) - camphor-10-sulfonic acid; however, the effect was observed at a relatively elevated temperature of 413 K at which slow decomposition of doped PANI takes place [87]. Since spectral changes in poly-conjugated systems are caused by changes in the polymer chain conformation,

which are not only thermally induced, but also caused by interactions with solvents used, therefore, thermo-chromic polymers frequently exhibit solvate-chromium, which is consistent with observations of solvent-induced conformational changes in protonated PANI with CSA [88].

Solution processing of PANI into fibers is extraordinarily difficult because of following reasons: ① Poor solubility in solvents compared with normal engineering plastics. ② Very rapid polymer gelatin times at low total solids content. ③ Strong aggregation tendency due to inter-chain attractive forces. There were a few reports [89] regarding the subject of reproducible fiber spinning of PANI. However, Mattes et al. [90] reported the development of PANI fiber production techniques that have been used to create commercial fibers (PANION). The techniques hold good promise for further significant advances in the field of solid-state electrochemical devices [91].

It is well known that water present in the PANI matrix affects the conductivity of PANI in its emeraldine salt oxidation state due to de-doping process taking place [92]. Only a few studies have been performed on the mechanism of water adsorption by PANI. The earliest work indicated that there existed two forms of water adsorbed by the materials weakly bonded water molecules that possess activation energy of de-sorption of about 5 kcal/mol and strongly bonded water molecules that are only desorbed during simultaneous decomposition of the polymer backbone [93]. It has been suggested that these water molecules form hydrogen bonds with the acid sites in the emeraldine salt form of PANI [94]. More recent work suggested that reversibly absorbed water consists of two forms, that is, the hydrogen bonded water (as found in previous studies with a de-sorption energy of 5 kcal/mol) and another form with a de-sorption energy of 15 – 18 kcal/mol [95]. This energy for de-sorption of the water molecules exceeds that of a single hydrogen bond and could correspond to the formation of a chemical bond with the polymer backbone. Pellegrino et al. [96] studied the water sorption kinetics and mass uptake of the PANI with respect to the dopant anion. The PANI-ES solid fibers adsorbed as much water as many hydrophilic polymers and the electronic conductivity of these fibers is proportional to the relative humidity in a reproducible fashion [97]. These attributes can provide the possibility for advanced humidity control and sensing applications [97].

2.4   Solubility and Processability

As above-described, PANI is very popular conductive polymer and has great scientific and industrial interest because of its high conductivity, environmental stability, simple and cheap synthesis method as well as technological applications in electrical devices [98]. PANI has also great interest as an organic magnet due to the potentially strong exchange interactions occurring through the conjugated

backbone [99]. However, for such applications, PANI must be processability including soluble in common solvents or melt process below the glass transition temperature [100].

2.4.1   Solubility

The EB form of PANI is soluble in NMP, which can be used to fabricate a free-standing film of the EB form. However its doped form (i.e. ES form) is insoluble in organic solvent or aqueous solution. Therefore, to synthesize soluble conducting PANI (i.e. the protonated state, ES form) is a key for realizing commissural application of PANI in technology. To solve solubility and processability of PANI therefore is not only necessary for commercial application, but also fundamental research (e.g. structural characterizations). Great effort for improving solubility in solvent and processability of PANI has been reported [101]. For instance, sulfonation or incorporation of *N*-alkyl-sulfonic acid pendant groups [102], dopant-inducted [103], self-doping polymer [104], micro-emulsion polymerization [105], and controlled relative molecular mass [106], have been reported for improvement of solubility and processability of PANI. In the next, above-mentioned methods for improving solubility and processability of PANI will be briefly discussed.

1. Substitution onto Backbone

Alkyl- and aryl-substitution attached on the polymer chain is a common tool to synthesize soluble PANI dissolved in organic solvent or aqueous solution [107]. A lot of papers dealing with alkyl- [108], alkoxy-ring-substituted [109] and alkyl-*N*-substituted [110] PANI had been reported. Although these derivatives of PANI retain their electrochromic properties, their conductivity decreases dramatically to values between 10^{-3} and 10^{-7} S/cm. Moreover, the alkyl- and alkoxy-ring-substituted PANI after acid-doping have a moderate conductivity of $10^{-1} – 10^{-3}$ S/cm, but their molecular weights are usually low (on the order of 10^{3}). Han et al. [111] reported a method to reduce PANI backbones from the emeraldine base form to the leucoemeraldine form and simultaneously derivative the backbones to form functionalized PANI by various functional alkanethiols. This method provided a novel way to control the degree of substitution of PANI. In fact, the most successful approach to a conductive PANI with solubility in aqueous solutions is introduced by sulfuric acid groups. This can be achieved by treating the polymer with the appropriate reagents after the polymerization or by polymerizing the substituted aniline derivatives. An example of the approach is the sulfonation of the emeraldine base with fuming sulfuric acid to produce a soluble PANI in aqueous alkaline solutions [112].

2. Self-Doping PANI (SPAN)

Another successful approach toward soluble conductive PANI is to introduce sulfuric acid groups on PANI chains. Sulfonated polyaniline (SPAN) is the first reported self-doped water soluble conducting PANI derivative, which molecular structure with different degree of sulfonation defined as the sulfur-to-nitrogen (S/N) ratio is shown in Fig. 2.8 [113]. Usually, EB and PNB forms of PANI have been used as starting materials for the preparation of SPAN, which defined as EB-SPAN and PNB-SPAN, respectively. Fuming sulfuric acid, chlorosulfonic acid, and sulfur trioxide/triethyl phosphate complex were also used as sulfonation agents in the synthesis of SPAN [113]. Although Genies et al. [114] have attempted to synthesize a self-doped SPAN by reaction of the EB form directly with propane- or butanesultone, the product has a very poor solubility and low conductivity (10^{-9} S/cm) at room temperature. Usually the doping degree for the SPAN is assigned as the S/N ratio and all of these earlier methods resulted in the
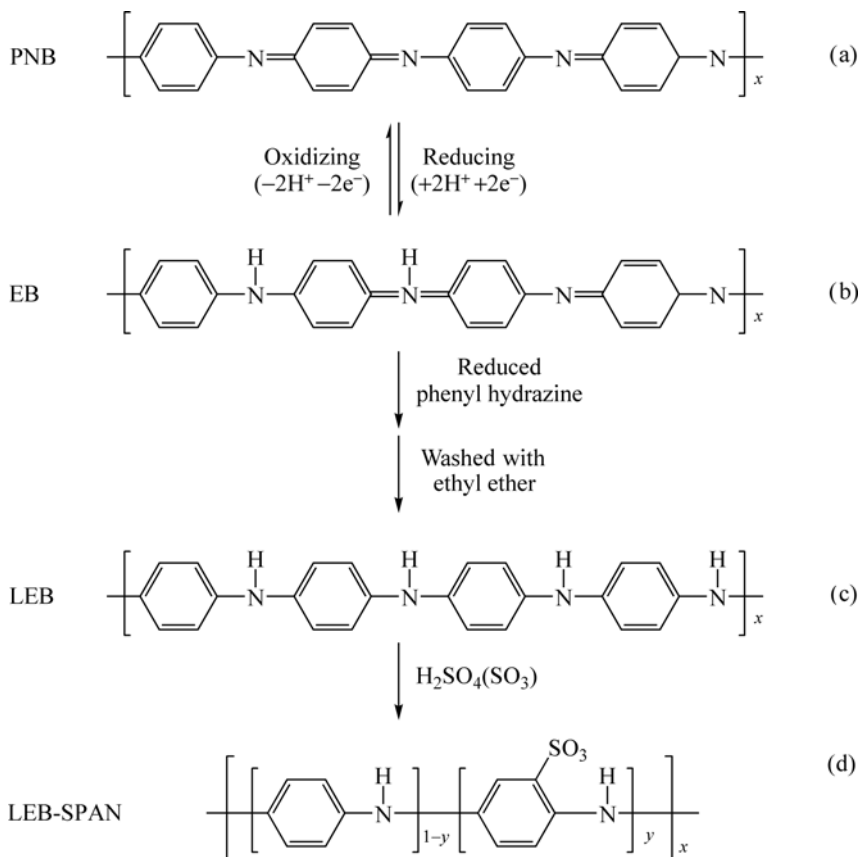
Figure 2.8   Molecular structure of SPAN [113]

S/N ratio of 0.5 [113, 115]. However, Epstein et al. [104] reported an S/N ratio as high as 0.75 could be synthesized by using the full reduced LEB as the starting material, which final product is termed LEB-SPAN. Bergeron et al. [116] have also synthesized a water-soluble PANI by reaction of LEB with propanesulfonic.

The S/N ratio is a key to control the physical properties of the self-doped SPAN. The conductivity of SPAN with S/N ratio of 0.5 is about 10^{-1} S/cm, for instance, the conductivity of LEB-SPAN (S/N ratio of 0.75) is enhanced by one order of magnitude to be about 1.0 S/cm [104]. Moreover, the conductivity of LEB-SPAN is unaffected by pH over the range 0<pH<14 whereas EB-SPAN becomes insulating at pH>3 and pH>7.5, respectively [104]. In addition, the thermal stability of SPAN is better than PANI doped with HCl [117].

3. Water soluble PANI

Water soluble PANI is of interesting because of its low cost and friend-environment. It is noted that the above-mentioned SPAN is only soluble in aqueous alkaline solution (NH_4OH) and NaOH rather than in pure water. To obtain an aqueous solution of SPAN, it is therefore necessary to follow the treatment with an H^+ type ion-exchange resin [118]. Thus, an efficient approach toward water soluble conductive PANI is substituted aniline co-monomer to produce copolymers [119]. The copolymers are advantageous of the electrical conductivity and solubility of the copolymer being varied by adjustment of the monomer ratio in the copolymer. For instance to polymerize protonic-acid moiety containing aniline derivatives, such as aminobenzylphosphoric acid to give poly (o-aminobenzylphosphoric acid) (PABPA) [120] or to copolymerize aniline with similar monomers, such as N-(4-sulfophenyl) aniline and o-anthranilic acid to yield poly (aniline-co-N-(4-sulfophenyl) aniline) (PASPA) [121], and poly(aniline-co-o-anthranilic acid) (PAAA) [122] have been reported. However, the above two copolymers are also partially soluble in water, while the homo-polymer PABPA is only soluble in alkaline aqueous solution. Therefore, a new water-soluble self-doped PANI has been proposed by grafting PANI onto a water-soluble polymer having pendant aniline dimers and sulfonic acid groups to obtain poly(aniline-co-2-acrylamido-2-methyl-1-propanesulfonic acid) (PAMPANI) [123]. Bhavana et al. [124] also reported a novel approach to the creation of a substituted PANI can be controlled via complication between boronic acid groups along the backbone with D-fructose in the presence of fluoride. Nguyen et al. [121] also report copolymers of poly (N-(4-sulfophenyl) aniline) and the poly-(aniline-co-N-(4-sulfophenyl)) aniline. They found that their conductivities are range between 3.5×10^{-4} S/cm and 5.2 S/cm for home-polymer of poly (N-(4-sulfophenylhniline)) and PANI, respectively. Although the conductivity of homo-polymer poly (N-(Gsulfopheny1) aniliie) is 10^3 times less conductive than PANI, it is still 10^6 times more conductive than other PANI polymers with sulfonated groups. These copolymers are soluble in aqueous NH_4OH, but not in aqueous HCl solutions. In addition, poly (aniline-co-N-propanesulfonic acid aniline) (PAPSAH) with a conductivity of 10^{-2} S/cm

without external doping could be cast into free-standing film directly from its aqueous solution [125]. Chan et al. [126] also reported a novel conducting PANI synthesized by persulfate oxidative coupling of *o*-aminobenzylphosphonic acid in an acidic medium. The resultant PANI is water-soluble in its conducting form. However, it does not exhibit any conductivity dependence on pH below 6, in marked contrast to the HCl-doped PANI. The lower conductivity (10^{-3} S/cm) obtained is attributed to the decrease in conjugation resulted from a large steric effect of the bulky PO_3H_2 and a significant hydrogen bond interaction between $PO_2 (OH)^-$ and NH^+ [126]. In addition, water-soluble copolymers of poly-(aniline-*co-N*-(4-sulfophenyl) aniline (PAPSA) was synthesized directly from aniline and sodium diphenylamine-4-sulfonate salt by a chemical polymerization [121].The monomer composition of the copolymers (PAPSA) can be controlled by varying the molar ratio of the monomers in the reaction mixture. The copolymers have a monotonic variation in their molecular weight, solubility in aqueous NH_4OH, and electrical conductivity with the monomer composition. Besides, Liu et al. [127] reported oxidizing aniline in the presence of aniline-formaldehyde condensates (AFC) through a cation radical mechanism to synthesize conductive PANI/AFC copolymer with high molecular weight and solubility. AFC acts as a terminating agent in the polymerization process and by terminating many PANI chains, resulting in branchlike structural copolymers. The conductivity (~ 10 S/cm), average molecular weight (~ of 10^6), and solubility of the copolymer are controlled by the ratio of AFC to aniline monomer prior to chemical polymerization [127].

As above-mentioned, grafted polymer is one way to produce soluble conducting polymers. Poly (ethylene glycol) (PEG) has many unique physical and biochemical properties, such as non-toxicity, biocompatibility, and miscibility with many solvents [128]. These unique properties lead to their promising application in biomedical and industrial applications [129]. Wang et al. [130] reported that PEG-grafted PANI copolymers were prepared by incorporating a chlorine end-capped methoxy PEG (mPEGCl) onto the LEB form of PANI via *N*-alkylation. The graft concentration (degree of *N*-alkylation) can be controlled by adjusting the molar feed ratio of mPEGCl to the number of repeat units of PANI. The mPEG-*g*-PANI copolymers enhanced solubility in common organic solvents and water [130]. In addition, the enzyme horseradish peroxidase (HRP) has been also extensively used for the oxidative polymerization of phenols and anilines in the presence of hydrogen peroxide [131]. Aniline monomers containing hydrophilic substituent [132] or photodynamic azobenzene groups [133], and HRP-catalyzed polymerization of aniline [134] have been polymerized to yield a wide range of soluble PANI. In these cases, the polyelectrolyte provides a preferential local environment for coupling of the monomer, the counter-ions for doping the PANI, and imparting water solubility. Recently, Roy et al. [135] reported that the biomimetic polymerization of aniline in the presence of lignosulfonate (LGS) to yield a conducting, water-soluble PANI, where LGS was used as either dopant or polymeric template. The LGS-PANI complex provided a

unique combination of properties for the PANI including electrical conductivity, processability, corrosion protection, and biodegradability [136].

4. Emulsion Polymerization and Colloidal Suspension

Emulsion polymerization processes have been used to prepare soluble PANI salts [137]. The reagents in this method consist of aniline, a protonic acid and an oxidant combined with a mixture of water, and a non-polar or weakly polar solvent (e.g. xylene, chloroform, or toluene). For instance, the PANI with high molecular weight ($M_w > 22,000$) and high conductive ($\sim 10^{-5}$ S/cm) synthesized by emulsion polymerization process in the presence of dinonylnaphthalenesulfonic acid (DNNSA) was soluble in xylene and toluene [138]. The method yields a direct approach to prepare truly soluble and conducting emeraldine salt without the need for a post-doping process step.

Dispersion polymerization or colloidal suspension is also employed to produce soluble PANI. The dispersion polymerization of PANI is carried out in an aqueous mixture, which contains aniline monomers, dopant, oxidant and steric stabilizer, to produce soluble PANI colloidal particles [139]. Stejskal et al. [140] suggested formation of the colloidal particles underwent process as follows: the aniline oligomers adsorbs firstly at the stabilizer chains and produces PANI nucleus. By the auto-acceleration mechanism, the formation of new oligomers and polymerization proceeds in the close vicinity, and the PANI particle then grows. Occasionally, other stabilizer chains become entrapped in the growing particle, producing a particle shell that prevents the particles from aggregating due to the auto-acceleration mechanism close to the nucleus. Based on above-formation, the colloidal particles of PANI have been mostly produced by a process referred to dispersion polymerization. The colloids prepared from dispersion polymerization usually have a "core-shell" structure, where the core is mainly composed of insoluble APNI whereas the shell is constructed with either water soluble polymeric or colloidal stable ultra-fine inorganic steric stabilizers. Li et al. [141] demonstrated the PANI colloids with a size of about 100 nm have excellent processability when applied electrophoretically. They reported the electrophoretic deposition of PANI colloids can be controlled with great flexibility by adjusting various process parameters such as the duration of the deposition, the colloid concentration, or the applied voltage. In particular, pattern of PANI on macroscopic substrate from its colloidal suspension can be electrophoretically fabricated [141].

5. Ionic Liquids

Ionic liquids (ILs) are organic salts with a low melting point (<100℃) that has chemical stability, low flammability, negligible vapor pressure, high ionic conductivity and wide electrochemical window [142]. Especially, the ionic liquids are expected to be stable and excellent electrolyte solutions [143] and are

considered as prospective environmentally friendly solvents for chemical or electrochemical reactions [144]. The electrochemical syntheses of conducting polymers such as PPy [145], PTH [146] and PANI [147] have been prepared in the presence of moisture-sensitive chloroaluminate ionic liquids. However, the hydrolysis of the ionic liquids results in the formation of highly corrosive products such as HCl [148], which leads to decomposition of the polymer films [149]. Moreover, the chloroaluminate ionic liquids are intractable materials, and their treatment requires special equipment such as a glove box. Imidazolium ionic liquid with counter-anion (e.g. $CF_3SO_3^-$) exhibits air and moisture stability [150]. Thus, the breakthrough for the above problem should be achieved by using an imidazolium ionic liquid having a stable counter-anion such as $CF_3SO_3^-$, which has been developed recently and exhibits air and moisture stability [151]. Yakuphanoglu et al. [152] recently reported polymerization of aniline monomer by using dibenzoyl peroxide (BP) as the oxidant in ionic liquid. Compared with APS as the oxidant, there are some advantageous of using benzyl peroxide (BP) oxidizing agent as follows [152]: ① Good stability. ② The reaction can be controlled in the presence of surfactant and thereby acid as well as surfactant group can be incorporated in the PANI salt as dopants. ③ Reaction can be carried out at $25-40\,^{\circ}\text{C}$. ④ Process PANI salt can be prepared due to the solubility of BP in most of the organic solvents.

2.4.2 Processability

Most applications for electronic devices of conducting polymers, such as transistors [153], and light-emitting diodes (LEDs) [154], require in the formation of thin film or patterned conducting polymers with feature sizes less than 100 nm. Soluble PANI is easy to prepare its thin film by spinning coating. Besides, various other approaches, such as photolithographic techniques based on photo-induced doping/de-doping [155], photochemical reaction [156], chemical implication [157] and non-photolithographic methods [158], ink-jet [159], screen printing [160] and electrochemical dip-pen nano-lithography [161] have been used to prepare thin film of conducting polymers. Some typical methods to prepare thin films or patents of PANI are briefly introduced as follows:

1. Adsorption Polymerization

In 1989, MacDiarmid et al. [162] actually noted that "PANI may also be deposited by *in-situ* adsorption polymerization as strongly adhering films on a variety of substrates". This indicated that PANI film coated on any substrate can be prepared by placing a substrate into reaction solution, indicating it is the simplest approach to prepare PANI films. Based on above concept, aniline oligomers anchored on the surface stimulate the growth of PANI chains in a perpendicular

direction to the support has been reported [163, 164]. Similar concepts have been also suggested for electrochemically produced films [165]. The growth of the films prepared by this method undergone three processes [166]: ① The oxidation of aniline in an acidic aqueous medium at the initial state of polymerization produces aniline oligomers. ② Those oligomers have a tendency to separate from the aqueous medium by adsorbing themselves at available surfaces in contact with aqueous reaction mixture because of their hydrophobic than the original anilinium cations. ③ The adsorbed oligomers on the surface of substrate have a higher reactivity toward initiating the growth of PANI chains followed by growth of PANI film along the substrate via an auto-accelerating polymerization.

2. Layer-By-Layer

A layer-by-layer is a common and controlling self-assembly technique to prepare thin and oriented films through anion/cation or electrostatic and hydrogen bonding interactions. The method is advantageous of simple in procedure, easy to control and friendly to environment [167]. The method also introduced into fabrication of PANI fibers and films since 1990s, but ionic self-assembled films are not stable in the high ionic strength of the electrolyte solution because they can be easily scaled off [168]. It therefore is a challenge for chemistry to fabricate a much more stable the assembled PANI film. Chen et al. [169] proposed a novel way to fabricate covalently attached multilayer films by the ionic or hydrogen-bonding self-assembly technique associated with the photoreaction. By using this method, ultra-thin film is fabricated with diazoresin as poly-cation and SPAN as poly-anion via self-assembly electrostatic process. And then the resulting films are exposed under UV irradiation to undergo photoreaction between diazonium and sulfonate, and finally convert the ionic bonds between the layers into covalent [169]. Interestingly, the covalent attached films are very stable toward polar solvents and high ionic strength of the electrolyte solution [170]. In addition, PANI can be self-assembled with a number of different nonionic, water-soluble polymers, such as poly (vinylpyrrolidone), poly (vinyl alcohol), poly (acrylamide) and poly (ethylene oxide) [171]. Each of these polymers contains functional groups that are capable of forming hydrogen bonds with PANI. The ability to fabricate multilayer thin films and thin film hetero-structures containing nonionic polymers opens up new possibilities for self-assembled films of conjugated polymers. Since poly (ethylene oxide) (PEO) is an ion-conducting polymer, for instance, it is possible to create multilayer thin films that are both electronically and ironically conductive. These films may be of use in thin film devices that are based on electrochemical processes such as the light-emitting devices [172]. Stockton et al. [173] demonstrated that hydrogen-bonding interactions can be used to assemble multilayer thin films of PANI by a layer-by-layer manner. The multi-layers prepared by a layer-by-layer through hydrogen bonding interactions are more thickness than that of films made by electrostatic interaction due to the

tendency of the hydrogen-bonding polymers to adsorb with a high segmental density of loops and tails [173]. The PANI films formed via hydrogen-bonding self-assembly also exhibit conductivities about one order of magnitude larger than that of films assembled via electrostatic interactions [173].

3. Photolithography Technique Associated with Photo-Acid Generation Processes

As above-mentioned, PANI can be doped by photon-acid generators due to proton released under light irradiation. It has been showed that the PANI modified with a thermo-labile and acid-labile *tert*-butoxycarbonyl (t-BOC) group is highly soluble and thermodynamically stable in low-boiling solvents (e.g. THF, dioxane, and $CHCl_3$) and which is converted to the insoluble and electrically conductive emeraldine salts upon photodoping with photo-acid generators (e.g. *N*-(tosyloxy)- or (camphorsulfonyloxy) norborneneimide or -onium salts [174a]. As a result of this solubility difference, conducting patterns of high resolution were produced by conventional photolithography process. Upon removal of the t-BOC groups in PANI (t-BOC) by acid doping, no obvious morphology change of the films was observed, and such conversion recovered the original conductivity level of the doped PANI [174b]. Since the t-BOC protecting groups are easily removed in doping or acid-catalyzed reaction by chemical amplification or thermal bake, the PANI (t-BOC) can be used as conductive matrix polymers for negative type photo-imaging or printing materials or for novel solution-processed applications in various microelectronic devices [174b].

In summary, PANI still holds important position in the field of conducting polymers at the present time because of its unique properties such as easy and low-cost synthesis, high conductivity and stable in air as well as physical and electrochemical properties controlled by both oxidation and protonation state, leading to potential applications in technology. However, large-mass synthesis, high solubility in organic or water and high stability of physical properties of PANI are still required to realize its commercial applications.

References

[1] H. Shirakawa, E. J. Louis, A. G. MacDiarmid, C. K. Chiang, and A. J. Heeger. J. Chem. Soc. Chem. Commun., 1977, 578

[2] H. Letheby. J. Chem. Soc., 224, 161: 1862

[3] M. F. Goppelsroder. Compt. Rend., 82, 331: 1876

[4] J. C. Chiang, A. G. MacDiarmid. Synth. Met., 1986, 13: 193

[5] W. S. Huang, B. D. Humphrey, and A. G. MacDiarmid. J. Chem. Soc. Commun. Faraday Trans., 1986, 82: 2385

[6] A. G. MacDiarmid. Angew. Chem. Int. Ed., 2001, 40: 2581

[7] a) A. G. MacDiarmid, A. J. Epstein. Faraday Discuss. Chem. Soc., 1989, 88: 317; b) A. G. MacDiarmid, J. C. Chiang, A. F. Richter, A. J. Epstein. Snyth. Met., 1987, 18: 285

[8] T. Hagiwara, M. Yamaura, and K. Iwata. Synth. Met., 1988, 26: 185

[9] a) A. G. MacDiarmid, A. J. Heeger. Synth. Met., 1879/80, 1: 101; Handbook of Conducting Polymers, Vol.1 &2 (Ed. T. A. Skotheim), Marcel Dekker, New York, 1986; b) M. G. Kanatzidis. Chem. Eng. News, 1990, 68: 36

[10] S. Stafström, J. L. Bredas, A. J. Epstein, et al. Phys. Rev. Lett., 1987, 59: 1464

[11] J. M. Ginder, A. F. Richter, A. G. MacDiarmid and A. J. Epstein. Solid State Commun., 1987, 63: 97

[12] A. J. Epstein, J. M. Ginder, F. Zuo et al. Synth. Met., 1987, 18: 303

[13] G. Wnek. Synth. Met., 1986, 16: 213

[14] M. X. Wan and J. P. Yang. J. Appl. Polym. Sci., 1995, 55: 399

[15] M. X. Wan. J. Polym. Sci. Part A. Chemistry of Polymers, 1992, 30: 543

[16] a) M. X. Wan. Synth. Met., 1989, 31: 51; b) P. M. M. McManus, S. C. Yang, and R. J. Cushman. J. Chem. Soc. Chem. Commun., 1985, 1556

[17] a) S. A. Chen, H. T. Lee. Macromolecules, 1995, 28: 2858; b) S. G. Kim, J. W. Kim, H. J. Choi, M. S. Suh, M. J. Shin, M. S. Jhon. Colloid. Polym. Sci., 2000, 278: 894; c) I. Sapurina, M. Mokeev, V. Lavrentev, V. Zgonnik, M. Trchová, D. Hlavatá, J. Stejskal. Eur. Polym. J., 2000, 36: 2321; d) G. E. Asturias, A. G. MacDiarmid, R. P. McCall, A. J. Epstein. Synth. Met., 1989, 29: 157

[18] a) A. G. MacDiarmid, J. C. Chiang, M. Halpern, W. S. Huang, S. L. Mu, N. L. D. Somasiri, W. Wu, S. I. Yaniger. Mol. Cryst. Liq. Cryst., 1985, 121: 173; b) H. Naarmann. Adv. Mater., 1990, 2: 345

[19] M. Y. Hua, G. W. Hwang, Y. H. Chuang, and S. A. Chen. Macromolecules, 2000, 33: 6235

[20] K. Krishnamoorthy, A. Q. Contractor and Ani Kumar. Chem. Commun., 2002, 240

[21] M. Angelopoulos, J. M. Shaw, K. L. Lee, et al. Polym. Eng. Sci., 1992, 32: 1535

[22] S. Z. Lei, M. X. Wan. Chinese J. Poly. Sc., 1997, 15: 108

[23] C. W. Lee, Y. H. Seo, and S. H. Lee. Macromolecules, 2004, 37: 4070

[24] J. P. Pouget, M. E. Jozefowicz, A. J. Epstein, X. Tang, A. G. MacDiarmid. Macromolecules, 1991, 24: 779

[25] A. G. El-Shekeil, S. A. M. K. Hamid, D. A. Ali. Angewandte Makromolekulare Chemie, 1997, 253: 99

[26] A. G. MacDiarmid, Y. Zhao, J. Feng. Synth. Met., 1999, 100: 131

[27] a) C. N. Liang, Y. H. Yu, H. P. Mao, X. F. Lu, W. J. Zhang, Y. Wei. Materials Letters, 2005, 59: 2446; b) L. Chen, Y. H. Yu, H. P. Mao, X. F. Lu, W. J. Zhang, Y. Wei. Synth. Met., 2005, 149: 129; c) J. B. Gao, W. J. Zhang, K. Li, C. Wang, Zh. W. Wu, Y. P. Ji. Macromol. Rapid Commun., 1999, 20: 463; d) Y. Wei, Ch. C. Yang, G. Wei, G. Zh. Feng. Synth. Met., 1997, 84: 289

[28] I. Kogan, L. Fokeeva, I. Shunina, Y. Estrin, L. Kasumova, M. Kaplunov, G. Davidova, E. Knerelman. Synth. Met., 1999, 100: 303

[29] a) Z. Sun, Y. Geng, J. Li, X. Wang, X. Jing, F. Wang. J. Appl. Polm. Sci., 1999, 72: 1077; b) B. K. Kim, Y. H. Kim, K. Won, H. Chang, Y. Choi, K. Kong, B. W. Rhyu, J. J. Kim, J. O. Lee. Nanotechnology, 2005, 16: 1177

[30] a) S. Palaniappan. Polym. Adv. Technol., 2004, 15: 111; b) P. S. Rao, D. N. Sathyanarayana, S. Palaniappan. Macromolecules, 2002, 35: 4988

[31] A. Yasuda, T. Shimidzu. Polym. J., 1993, 4: 329

[32] Y. Wang, Z. Liu, B. Han, Z. Sun, Y. Huang, G. Yang. Langmuir, 2005, 21: 833

[33] a) A. Pron, F. Genoud, C. Menardo, M. Nechtschein. Synth. Met., 1988, 24: 193; b) Y. Cao, A. Andreatta, A. J. Heeger, P. Smith. Polymer, 1989, 30: 2305; c) S. Tan, J. H. Tieu, D. Belanger. J. Phys. Chem. B, 2005, 109: 14085; d) E. Erdem, M. Karakisla, M. Sacak. Europ. Polym. J., 2004, 40: 785

[34] H. J. Ding, M. X. Wan, Y. Wei. Adv. Mater., 2007, 19: 465

[35] a) H. Gong, X. J. Cui, Z. W. Xie, S. G. Wang, L. Y. Qu. Synth. Met., 2002, 129: 187; b) J. Stejskal, A. Riede, D. Hlavata, J. Prokes, M. Helmstedt, P. Holler. Synth. Met., 1998, 96: 55

[36] Y. Wei, Y. Sun, and X. Tang. J. Phys. Chem., 1989, 93: 4878

[37] a) A. Kitani, J. Izumi, J. Yano, Y. Hiromoto, K. Sasaki. Bull. Chem. SOC. Jpn., 1984, 57: 2254; b) G. Zotti, S. Cattarin, N. Comisso. J. Electroanal. Chem., 1987, 235: 259; c) G. Zotti, S. Cattarin, N. Comisso. J. Electroanal. Chem., 1988, 239: 387

[38] a) K. Sasaki, M. Kaya, J. Yano, A. Kitani, A. Kunai. J. Elecrroanal. Chem., 1986, 215: 401; b) A. Thyssen, A. Borgerding, J. W. Schultze. Makromol. Chem., Macromol. Symp., 1987, 8: 143

[39] U. Kenig, J. W. Schultze. J. Electroanal. Chem., 1988, 242: 243

[40] Y. Wei, G. W. Jaag, C. C. Chan, K. F. Hsueh, R. Hariharan, S. A. Patel, and C. K. Whitecar. J. Phys. Chem., 1990, 94, 7716

[41] J. Huang, J. A. Moore, J. H. Acquaye, and R. B. Kaner. Macromolecules, 2005, 38: 317

[42] M. Thakur and S. Tripathy. in Encycloedia of Polymer Science and Engineering (J. I. Kroschwitz Ed., 2nd ed.). New York: John Wiley and Sons Ltd., 1986, Vol.5, p.756 – 771

[43] D. F. Eaton. Science, 1991, 253: 281; D. F. Eaton. Chemtech., 1992, 22: 308

[44] Nonilinear Optics: Fundamentals, Materials and Devices (Ed. S. Miyata). New York: Elsevier, 1992

[45] P. N. Prasad and D. J. Williams. Introduction to Nonlinear Optical Effects in Molecules and Polymers (Ed. J. Zyss). New York: Wiley, 1991; Molecular Nonlinear Optics: Materials, Physics, and Devices. San Diego: Academic Press, 1994

[46] Handbook of Conducting Polymers (Ed. Tepje A. Skotheim). New York, Bashi, Hong Kong, 1986, p.765-822

[47] C. Sauteret, J. P. Herman, R. Frey, F. Pradere, J. Ducuing, R. H. Baughman, and R. R. Chance. Phys. Rev. Lett., 1976, 36: 956

[48] D. N. Beratan, J. N. Onuchic, and J. W. Perry. J. Phys. Chem., 1987, 91: 2696

[49] Handbook of Conducting polymers (Ed. Tepje A. Skotheim et al.). New York, Basel and Hong Kong, 1986, p.727 – 821

[50] J. Libert, J. L. Brédas, A. J. Epstein. Phys. Rev. B, 1995, 51: 5711; J. Libert, J. Cornil, D. A. Dos Santos, J. L. Brédas. Phys. Rev. B, 1997, 56: 8638

[51] a) F. Zuo, R. P. Mccall, J. M. Ginder, M. G. Roe, J. M. Leng, A. J. Epstein, G. E. Asturias, S. P. Ermer, A. Ray, A. G. Macdiarmid. Synth. Met., 1989, 29: E445; b) O. Kwon, O. M. L. McKee. J. Phys. Chem. B, 2000, 104: 1686

[52] P. N. Prasad, D. J. Williams. Introduction to Nonlinear Optical Effects in Molecules and Polymers. New York: Wiley, 1991

[53] a) A. S. L. Petrov, C. B. Gomes, J. M. de Araújo, W. M. de Souza, J. V. de Azevedo, de Melo, F. B. Diniz. Opt. Lett., 1995, 20: 554; b) A. Samoc, B. Luther-Davies, J. Swiatkiewicz, C. Q. Jin, J. W. White. Opt. Lett., 1995, 20: 2478; c) G. S. Maciel, A. G. B. Jr. Nikifor Rakov, C. B. de Araújo, A. S. L. Gomes. J. Opt. Soc. Am. B, 2001, 18: 1099

[54] G. A. MacDiarmid, Y. Zhou, J. Feng. Synth. Met., 1999, 100: 131

[55] C. R. Mendoncüa, D. S. Santos, L. De Boni, D. T. Balogh, O. N. Oliveira, S. C. Zilio. Adv. Mater., 2000, 12: 1126

[56] P. L. Franzen, L. De Boni, D. S. Santos, Jr. C. R. Mendoncüa, and S. C. Zílio. J. Phys. Chem. B, 2004, 108: 19180

[57] H. Neumann, W. Horig, E. Reccius, H. Sobotta, K. B. Schumann. Thin Solid Films, 1979, 61: 13

[58] M. Arslan, H. Duymusü, and F. Yakuphanoglu. J. Phys. Chem. B, 2006, 110: 276

[59] T. Cao, L. Wei, S. Yang, M. Zhang, C. Huang, and W. Cao. Langmuir, 2002, 18: 750

[60] Handbook of Organic Conductive Molecules and Polymers (Ed. H. S. Nalwa). Chichester: John Wiley & Sons Ltd., England, 1997, Vol.2

[61] a) D.E. Stilwell, S. M. Park. J. Electrochem. Soc., 1988, 135: 2254; b) G. Zotti, S. Cattarin. J. Electroanal. Chem., 1988, 239: 387; c) A. F. Diaz, J. A. Logan. J. Electroanal. Chem., 1980, 111: 111; d) E. M. Genies, E. Vieil. Synth. Met., 1987, 20: 97; e) H. Pingsheng, Q. Xiaohua, L. Chune. Synth. Met., 1993, 57: 5008

[62] a) S. B. Basame, H. S. White. J. Phys. Chem., 1995, 99: 16430; b) S. B. Basame, H. S. White. J. Phys. Chem. B, 1998, 102: 9812; c) C. J. Boxley, H. S. White, C. E. Gardner, J. V. Macpherson. J. Phys. Chem. B, 2003, 107: 9677

[63] H. Y. Choi, E. Mele. J. Phys. Rev. Lett., 1987, 59: 2188

[64] B. Abeles, P. Sheng, M. D. Coutts, Y. Arie. Adv. Phys., 1975, 24: 407

[65] A. M. Elamin, Z. L. Liu, K. I. Yao. Acta Phys. Sin (Overseas ed.), 1997, 7: 458

[66] V. Luthra, R. Singh, S. K. Gupta, A. Mansingh. Curr. Appl. Phys., 2003, 3: 219

[67] a) Z. M. Zhang, Z. X. Wei, M. X. Wan. Macromolecules, 2002, 35: 5937; b) R. Cordova, M. A. Valle, A. Arratia, H. Gomez, R. Schrebler. J. Electroanal. Chem., 1994, 377: 75; c) S. J. Choi, S. M. Park. J. Electrochem. Soc., 2002, 149: E26

[68] a) T. W. Kelley, E. L. Granstrom, C. D. Frisbie. Adv. Mater., 1999, 11: 261; b) C. E. Gardner, J. V. Macpherson. Anal. Chem., 2002, 74: 576A

[69] a) J. Planes, F. Houze, P. Chretien, O. Schneegans. Appl. Phys. Lett., 2001, 79: 2993; b) M. Gadenne, O. Schneegans, F. Houze, P. Chretien, C. Desmarest, J. Sztern, P. Gadenne. Physica B, 2000, 279: 94; c) J. V. Macpherson, J. P. G. De Mussy, J. L. Delplancke. J. Electrochem. Soc., 2002, 149: B306

[70] a) C.G. Wu, S. S. Chang. J. Phys. Chem. B, 2005, 109: 825; b) C. G. Wu, H. T. Hsiao, Y. R. Yen. J. Mater. Chem., 2001, 11: 2287

[71] S. S. Chang and C. G. Wu. J. Phys. Chem. B, 2005, 109: 18275

[72] a) A.G. MacDiarmid, A. J. Epstein. Synth. Met., 1994, 65: 103; b) A. G. MacDiarmid, A. J. Epstein. Trans. 2nd Congresso Brazileiro de Polimeros, 1993, 5 – 8: 544; c) Y. Min, A. G. MacDiarmid, A. J. Epstein. Polym. Prepr., 1993, 231 – 2; d) A. G. MacDiarmid, A. J.

Epstein. Synth. Met., 1995, 69: 85; e) Y. Cao, P. Smith, A. J. Heeger. Synth. Met., 1992, 48: 91; f) Y. Cao, A. J. Heeger. Synth. Met., 1993, 52: 193; g) Y. Cao, G. M. Treacy, P. Smith, A. J. Heeger. Appl. Phys. Lett., 1992, 60: 2711; h) Y. Cao, P. Smith. Polymer, 1993, 34: 3139

[73] a) C. Barbero, M. C. Miras, B. Schnyder, O. Haas, R. Koetz. J. Mat. Chem., 1994, 4: 1775; b) C. Barbero, M. C. Miras, R. Kotz, O.Haas. Lithium Batteries. In Proc. Electrochem. Soc., 1994, 94-4: 281; c) C. Barbero, M.C. Miras, R. Koetz, O. Haas. Synth. Met., 1993, 55: 1539

[74] a) H. Tsutsumi, S. Fukuzawa, M. Ishikawa, Y. Morita. J. Electrochem. Soc., 1995, 142: L168; b) K. Hwang, J.S. Kim, M. Kong. Synth. Met., 1995, 71: 2201; c) N. Oyama, T. Tatsuma, T. Sato, T. Sotomura. Nature, 1995, 373: 598; d) M. Morita, S. Miyazaki, M. Ishikawa, Y. Matsuda, H. Tajima, K. Adachi, F. Anan. J. Electrochem. Soc., 1995, 142: L3

[75] a) M. Onoda, K. Yoshino. J. Appl. Phys., 1995, 78: 4456; b) M. Onoda, K. Yoshino. Jpn. J. Appl. Phys., Part 2, 1995, 34: L260; c) M. Ferreira, M. F. Rubner. Macromolecules, 1995, 28: 7107

[76] J. Yue, A. J. Epstein. J. Chem. Soc., Chem. Commun., 1992, 21: 1540

[77] a) T. Namiki, E. Yano, K. Watabe, Y. Igarashi, Y. Kuramitsu, T. Maruyama, K. Yano, T. Nakamura, S. Shimizu, T. Saito. Patent, JP 07179754 A2 950718; b) K. Watable, Y. Yoneda, T. Maruyama, K.Yano, T. Nakamura, S. Shimizu, T.Saito. Patent, JP 06003813 A2 940114

[78] X. L. Wei, Y. Z. Wang, S. M. Long, C. Bobeczko and A. J. Epstein. J. Am. Chem. Soc., 1996, 118: 2545

[79] a) Y. Long, J. Luo, J. Xu, Z. Chen, L. Zhang, J. Li, M. Wan. J. Phys.: Condens. Matter, 2004, 16: 1123; b) Y. Cao, A. J. Heeger. Synth. Met., 1992, 52: 193; N. S. Sariciftci, A. J. Heeger, Y. Cao. Phys. Rev. B, 1994, 49: 5988; c) A. Raghunathan, T. S. Natarajan, G. Rangarajan, S. K. Dhawan, D. C. Trivedi. Phys. Rev. B, 1993, 47: 13189; d) P. K. Kahol, J. C. Ho, Y. Y. Chen, C. R. Wang, S. Neeleshwar, C. B. Tsai, B. Wessling. Synth. Met., 2005, 151: 65; e) A. Raghunathan, P. K. Kahol, J. C. Ho, Y. Y. Chen, Y. D. Yao, Y. S. Lin, B. Wessling. Phys. Rev. B, 1998, 58: R15955; f) P. K. Kahol, B. McCormick. J. Phys. Rev. B, 1993, 47: 14588; J. Fan, M. Wan, D. Zhu. Solid State Commun., 1999, 110: 57

[80] B. R. Weinberger, J. Kaufer, A. J. Heeger, A. Pron, A. G. MacDiarmid. Phys. Rev. B, 1979, 20: 223

[81] a) P. K. Kahol, A. Raghunathan, B. J. McCormick. Synth. Met., 2004, 140: 261; b) P. K. Kahol, J. C. Ho, Y. Y. Chen, C. R. Wang, S. Neeleshwar, C. B. Tsai, B. Wessling. Synth. Met., 2005, 151: 65; c) A. Raghunathan, P. K. Kahol, J. C. Ho, Y. Y. Chen, Y. D. Yao, Y. S. Lin, B. Wessling. Phys. Rev. B, 1998, 58: R15955; d) P. K. Kahol, B. J. McCormick. Phys. Rev. B, 1993, 47: 14588; e) P. K. Kahol, A. Raghunathan, B. J. McCormick, A. J. Epstein. Synth. Met., 1999, 101: 815; f) N. J. Pinto, P. K. Kahol. Synth. Met., 2001, 119: 317

[82] Y. Z. Long, Z. J. Chen, J. Y. Shen, Z. M. Zhang, L. J. Zhang, H. M. Xiao, M. X. Wan, and J. L. Duvail. J. Phys. Chem. B, 2006, 110: 23228

[83] a) D. C. Trivedi. Phys. Rev. B, 1993, 47: 13189; b) S. M. Yang, C. P. Li. Synth. Met., 1993, 55: 636; c) F. Genoud, M. Nechtschein, C. Santier. Synth. Met., 1993, 55: 642; d) P. K. Kahol, A. Raghunathan, B. J. McCormick. Synth. Met., 2004, 140: 261

[84] P. Rannou, B. Dufour, J. P. Travers, and A. Pron. J. Phys. Chem. B, 2002, 106: 10553

[85] J. G. Masters, J. M. Ginder, A. G. MacDiarmid, A. J. Epstein. J. Chem. Phys., 1992, 96: 4768

[86] H. T. Lee, K. R. Chuang, S. A. Chen, P. K. Wei, J. H. Hsu, W. Fann. Macromolecules, 1995, 28: 7645

[87] I. D. Norris, L. A. P. Kane-Maguire, G. G. Wallace. Macromolecules, 1998, 31: 6529

[88] Y. Xia, J. M. Wiesinger, A. G. MacDiarmid. Chem. Mater., 1995, 7: 443

[89] a) A. Andreatta, A. J. Heeger, P. J. Smith. Polym. Commun., 1990, 31: 275; b) E. M. Sherr, A. G. MacDiarmid, S. K. Manohar, J. G. Masters, J. G. Sun, Y. X. Tang, M. A. Druy, P. J. Glatkowski, V. P. Cajipe, J. E. Fisher, K. R. Cromack, M. E. Ginder, R. P. Macall, A. J. Epstein. Synth. Met., 1991, 41: 735; c) C. H. Hsu, J. D. Cohen, R. F. Tietz. Synth. Met., 1993, 59: 37; d) J. Rajiv, R. V. Gregory. Synth. Met., 1995, 74: 263; e) C. H. Hsu, A. J. Epstein. Synth. Met., 1997, 84: 51; f) S. J. Pomfret, P. N. Adams, N. P. Comfort, A. P. Monkman. Adv. Mater., 1998, 10: 1351; g) K. Eaiprasersak, R. V. Gregory. ANTEC '98. 1998, 2: 1263; h) S. J. Pomfret, P. N. Adams, A. P. Monkman, N. P. Comfort. Synth. Met., 1999, 101: 24; i) S. J. Pomfret, P. N. Adams, N. P. Comfort, A. P. Monkman. Polymer, 2000, 41: 2265

[90] B. R. Mattes, P. N. Adams, D. Yang, L. A. Brown, A. G. Fadeev, I. D. Norris, Spinning, PCT WO 2004/042743, 2004

[91] W. Lu, A. G. Fadeev, B. Qi, E. Smela, B. R. Mattes, J. Ding, G. M. Spinks, J. Mazurkiewicz, D. Zhou, G. G. Wallace, D. R. MacFarlane, S. A. Forsyth, M. Forsyth. Science, 2002, 287: 983

[92] a) M. Nechtschein, C. Santier, J. P. Travers, J. Chroboczek, A. Alix, M. Ripert. Synth. Met., 1987, 18: 311; b) T. Taka. Synth. Met., 1993, 55 – 57: 5014

[93] B. Lubentsov, O. Timofeeva, S. Saratovskikh, V. Krinichnyi, A. Pelekh, V. Dmitrenko, M. Khidekel. Synth. Met., 1992, 47: 187

[94] A. Alix, V. Lemoine, M. Nechtschein, J. P. Travers, C. Menardo. Synth. Met., 1989, 29: 457

[95] E. S. Matveeva, R. Diaz Calleja, V. P. Parkhutik. Synth. Met., 1995, 72: 105

[96] M. M. Ostwal, J. Pellegrino, I. Norris, T. T. Tsotsis, M. Sahimi, B. R. Mattes. Ind. Eng. Chem. Res., 2005, 44: 7860

[97] B. Qi, B. R. Mattes. U.S. Patent Application 2005/0062486, 2005

[98] a) V. George, D. Young. J. Polym. Commun., 2002, 43: 4073; b) M. G. Mikheal, A. B. Padias, H. K. Hall. J. Polym. Sci. Polym. Chem., 1997, 35: 1673

[99] N. A. Zaidi, S. R. Giblin, I. Terry, A. P. Monkman. Polymer, 2004, 45: 5683

[100] a) H. Goto, M. Okuda, T. Oohazama, K. Akagi. Synth. Met., 1999, 102: 1293; b) A. Gök, B. Sarl, M. Talu. Synth. Met., 2004, 142: 41

[101] a) M. Leclerc, J. Guay, L. H. Dao, Macromolecules, 1982, 22: 649; b) Y. Wei, W. W. Focke, G. E. Wnek, A. Ray, A. G. MacDiarmid. J. Phys. Chem., 1989, 93: 495; c) D. Jr. MaCinnes, B. L. Funt. Synth. Met., 1989, 25: 235; d) L. H. C. Mattoso, S. V. Mello, A. Jr. Riul, O. N. Jr. Oliverira, R. M. Faria. Thin Solid Film, 1994, 244: 714

[102] a) J. Yue, A. J. Epstein. J. Am. Chem. Soc., 1990, 112: 2800; b) J. Yue, Z. F. Wang, K. R. Cromack, A. J. Epstein, A. G. MacDiarmid. J. Am. Chem. Soc., 1991, 113: 2665; c) S. A. Chen, G. W. Hwang. J. Am. Chem. Soc., 1994, 116: 7939

[103] Y. Cao, P. Smith, A. J. Heeger. Synth. Met., 1992, 48: 91

[104] J. Yue, G. Gordon, A. J. Epstein. Polymer, 1992, 33: 4409

[105] H. S. O. Chan, L. M. Gan, C. H. Chew, L. Ma, S. H. Seow. J. Muter. Chem., 1993, 3: 1109

[106] R. E. Cameron, S. K. Clement. U.S. Patent 5,008,041, 1991

[107] A. F. Dim, A. Logan. J. Electroanal. Chem., 1980, 111: 111

[108] M. Leclerc, J. Guay, L. H. Dao. Macromolecules, 1989, 22: 649

[109] D. Macinnes, B. L. Funt. Synth. Met., 1988, 25: 235

[110] S. K. Manohar, A. G. MacDiarmid, K. R. Cromack, J. M. Ginder, A. J. Epstein. Synth. Met., 1989, 29: E349

[111] C. C. Han, W. D. Hseih, J. Y. Yeh, S. P. Hong. Chem. Mater., 1999, 11: 480

[112] a) J. Yue, H. Wang, K. R. Cromack, A. J. Epetein, A. G. MacDiarmid. J. Am. Chem. Soc., 1991,113: 2665; b) E.T. Kang, K. G. Neoh, K. L. Tan, H. K. Wong. Synth. Met., 1992, 48: 231

[113] X. L. Wei, Y. Z. Wang, S. M. Long, C. Bobeczko, and A. J. Epstein. J. Am. Chem. Soc., 1996, 118: 2545

[114] P. Hany, E. M. Genies, C. Santier. Synth. Met., 1989, 31: 369

[115] a) J. Yue, A. J. Epstein. J. Am. Chem. Soc., 1990, 112: 2800; b) J. Yue, Z. H. Wang, K. R. Cromack, A. J. Epstein, A. G. MacDiannid. J. Am. Chem. Soc., 1991, 113: 2665; c) J. Yue, A. J. Epstein. J. Chem. Soc., Chem. Commun., 1992, 1540

[116] J. Y. Bergeron, J. W. Chevalier, L. H. Dao. J. Chem. Soc., Chem. Commun., 1990, 180

[117] a) J. Yue, A. J. Epstein, Z. Zhong, P. K. Gallagher, A. G. MacDiamid. Synth. Met., 1991, 41: 765; b) T. C. Tsai, D. A. Tree, M. S. High. Ind. Eng. Chem. Res., 1994, 33: 2600

[118] S. A. Chen, G. W. Hwang. Macromolecules, 1996, 29: 3950

[119] a) L. H. Dao, M. T. Nguyen, T. D. Do. Polym. Prep. (Am. Chem. Soc., Diu. Polym. Chem.), 1992, 33: 408; b) J. Y. Bergeron, L. D. Dao. Macromolecules, 1992, 25: 3332; c) Y. Wei, R. Harihara, S. A. Patel. Macromolecules, 1990, 23: 758

[120] H. S. O. Chan, P. K. H. Ho, S. C. Ng, K. L. Tan. J. Am. Chem. Soc., 1995, 117: 8517

[121] M. T. Nguyen, P. Kasai, J .L. Miller, A. F. Diaz. Macromolecules, 1994, 27: 3625

[122] M. T. Nguyen, A. F. Diaz. Macromolecules, 1995, 28: 3411

[123] W. Yin, E. Ruckenstein. Macromolecules, 2000, 33: 1129

[124] B. A. Deore, I. Yu, and M. S. Freund. J. Am. Chem. Soc., 2004, 126: 52

[125] S. A. Chen, G. W. Hwang. J. Am. Chem. Soc., 1994, 116: 7939

[126] H. S. O. Chan, P. K. H. Ho, S. C. Ng, B. T. G. Tan, K. L. Tan. J. Am. Chem. Soc., 1995, 117: 8517

[127] G. Liu, M. S. Freund. Macromolecules, 1997, 30: 5660

[128] J. H. Lee, H. B. Lee, J. D. Andrade. Prog. Polym. Sci., 1995, 20: 1043

[129] a) J. M. Harris. J. Macromol. Sci. RMCP, 1983, C25: 325; b) P. Novak, K. Müller, K. S. V. Santhanam, O. Haas. Chem. Rev., 1997, 97: 207

[130] P. Wang and K. L. Tan. Chem. Mater., 2001, 13: 581

[131] J. A. Akkara, K. J. Senecal, D. L. Kaplan. J. Polym. Sci., Polym. Chem., 1991, 29: 1561

[132] a) K. S. Alva, J. Kumar, K. A. Marx, S. K. Tripathy. Macromol. Rapid Commun., 1996, 17: 859; b) K. S. Alva, J. Kumar, K. A. Marx, S. K. Tripathy. Macromolecules, 1997, 30: 4024

[133] K. S. Alva, T. S. Lee, J. Kumar, S. Tripathy. Chem. Mater., 1998, 10: 1270

[134] a) L. Samuelson, A. Anagnostopoulos, K. S. Alva, J. Kumar, S. K. Tripathy. Macromolecules, 1998, 31: 4376; b) W. Liu, A. Cholli, R. Nagarajan, J. Kumar, S. Tripathy, F. F. Bruno, L. Samuelson. J. Am. Chem. Soc., 1999, 121: 11345; c) W. Liu, J. Kumar, S. Tripathy, K. Senecal, L. Samuelson. J. Am. Chem. Soc., 1999, 121: 71

[135] S. Roy; J. M. Fortier, R. Nagarajan, S. Tripathy, J. Kumar, L. A. Samuelson, and F. F. Bruno; Biomacromolecules 2002, 3, 937

[136] a) K. Underhill-Shanks, T. Viswanathan. Polym. Prep. (Am. Chem. Soc; Div. Polym. Chem.), 1996, 37: 508; b) M. Sudhakar, A. D. Toland, T. Viswanathan. Polym. Prep. (Am. Chem. Soc.; Div. Polym. Chem.), 1998, 39: 125; c) B. Berry, A. Shaikh, T. Viswanathan, Polym. Prep. (Am. Chem. Soc.; Div. Polym. Chem.), 2000, 41: 327; d) B. Berry, D. Lindquist, J. P. Smith, T. Viswanathan. Polym. Prep. (Am. Chem. Soc.; Div. Polym. Chem.), 2000, 41: 1110

[137] a) Y. Cao, P. Smith, A. J. Heeger. U.S. Patent 5,232,631, 1993; b) Y. Cao, J. E. Osterholm. International Patent Application (PCT) WO94/03528, 1994; c) Y. Cao, J. E. Osterholm. U.S. Patent No. 5,324,453, 1994; d) J. E. Osterholm, Y. Cao, F. Klavetter, P. Smith. Synth. Met., 1993, 55: 1034; e) J. E. Osterholm, Y. Cao, F. Klavetter, P. Smith. Polymer, 1994, 35: 2902

[138] P. J. Kinlen, J. Liu, Y. Ding, C. R. Graham, E. E. Remsen. Macromolecules, 1998, 31: 1735

[139] J. Stejskal. J. Polym. Mater., 2001, 18: 225

[140] J. Stejskal, I. Sapurina. Pure Appl. Chem., 2005, 77: 815

[141] G. Li, C. Martinez, and S. Semancik. J. Am. Chem. Soc., 2005, 127: 4903

[142] V. R. Koch, C. Nanjundiah, G. B. Appetecchi, B. Scrosati. J. Electrochem. Soc., 1995, 142: L116

[143] A. Noda, A. B. H. Susan, K. Kudo Md, S. Mitsushima, K. Hayamizu, M. Watanabe. J. Phys. Chem. B, 2003, 107: 4024

[144] T. Welton. Chem. Rev., 1999, 99: 2071

[145] a) P. G. Pickup, R. A. Osteryoung. J. Am. Chem. Soc., 1984, 106: 2294; b) P. G. Pickup, R. A. Osteryoung. J. Electroanal. Chem., 1985, 195: 271; c) A. T. Zawodzinski, L. Jr. Janiszewska, R. A. Osteryoung. J. Electroanal. Chem., 1988, 255: 111

[146] L. Janiszewska, R. A. Osteryoung. J. Electrochem. Soc., 1987, 134: 2787

[147] a) N. Koura, H. Ejiri, K. Takeishi, D. Kagaku. Electrochemistry, 1991, 59: 74; b) M. Sairam, S. Palaniappan. J. Mater. Sci., 2004, 39: 3069

[148] K. Sekigucki, M. Atobe, T. Fuchigami. J. Electroanal. Chem., 2003, 557: 1

[149] N. Koura, H. Ejiri, K. Takeishi. J. Electrochem. Soc., 1993, 140: 602

[150] a) R. Hagiwara. Electrochemistry, 2002, 70: 130; b) W. Lu, A. G. Fadeev, B. Qi, E. Smela, B. R. Mattes, J. Ding, G. M. Spinks, J. Mazurkiewicz, D. Zhou, G. G. Wallace, D. R. MacFarlane, S. A. Forsyth, M. Forsyth. Science, 2002, 297: 983

[151] M. Sairam, S. Palaniappan. J. Mater. Sci., 2004, 39: 3069

[152] F. Yakuphanoglu, B. F. Sü enkal. J. Phys. Chem. C, 2007, 111: 1840

[153] a) Y. Yang, A. J. Heeger. Nature, 1994, 372: 344; b) A. R. Brown, A. Pomp, C. M. Hart, D. M. Leeuw. Science, 1995, 270: 972

[154] a) H. Sirringhaus, N. Ztessler, R. H. Friend. Science, 1998, 280: 1741; b) M. Berggren, A. Dodabalapur, R. E. Slusher, Z. Bao. Nature, 1997, 389: 466; c) F. Hide, M. A. Diaz-Garcia, B. L. Schwartz, A. J. Heeger. Acc. Chem. Res., 1997, 30: 430 – 435; d) M. Granstrom, M. Berggren, O. Inganas. Science, 1995, 267: 1479

[155] M. Angelopoulos, J. M. Shaw. Polym. Eng. Sci., 1992, 32: 153

[156] Handbook of Organic Conductive Molecules and Polymers (Ed. H. S. Nalwa). Chichester: John Wiley & Sons, 1997, Vol. 4

[157] a) J. Yu, M. Abley, C. Yang, S. Holdcroft. Chem. Commun., 1998, 1503 – 1504; b) J. Lowe, S. Holdcroft. Synth. Met., 1997, 85: 1427 – 1431; c) J. Yu, S. Holdcroft. Chem. Commun., 2001, 1274 – 1275

[158] W. S. Beh, I. T. Kim. D. In Xia, G. M. Whitesides. Adv. Mater., 1999, 11: 1038

[159] a) L. F. Rozsnyi, M. S. Wrighton. J. Am. Chem. Soc., 1994, 116: 5993; b) T. R. Hebner, J. C. Sturn. Appl. Phys. Lett., 1998, 73: 1775

[160] Z. Bao, Y. Feng, A. Dodabalapur, A. Lovinger. Chem. Mater., 1997, 9: 1299

[161] R. D. Piner, J. Zhu, F. Xu, S. H. Hong, C. A. Mirkin. Science, 1999, 283: 661

[162] A. G. MacDiarmid and A. J. Epstein. Faraday Discuss. Chem. Soc., 1989, 88: 317

[163] a) A. G. MacDiarmid. Synth. Met., 1997, 84: 27; b) R. V. Gregory, W. C. Kimbrell, H. H. Kuhn. Synth. Met., 1989, 28: C823

[164] a) I. Sapurina, A. Riede, J. Stejskal. Synth. Met., 2001, 123: 503; b) I. Sapurina, A. Yu. Osadchev, B. Z. Volchek, M. Trchová, A. Riede, J. Stejskal. Synth. Met., 2002, 129: 29

[165] H. Okamoto, M. Okamoto, T. Kotaka. Polymer, 1998, 39: 4359; G. Láng, M. Ujvári; G. Inzelt. Electrochim. Acta, 2001, 46: 4159

[166] J. Stejskal, I. Sapurina. Pure Appl. Chem., 2005, 77: 815

[167] a) G. Decher. Science, 1997, 277: 1232; b) N. Sarkar, M. K. Ram, A. Sarkar, R. Narizzano, S. Paddeu, C. Nicolini. Nanotechnology, 2000, 11: 30

[168] G. Mao, Y. Tsao, M. Tirrell, H. T. Davis, V. Hessel, H. Ringsdorf. Langmuir, 1995, 11: 942

[169] a) J. Y. Chen, L. Huang, L. M. Ying, G. B. Luo, X. S. Zhao, W. X. Cao. Langmuir, 1999, 15: 7208; b) T. B. Cao, S. M. Yang, Y. L. Yang, C. H. Huang, W. X. Cao. Langmuir, 2001, 17: 6034; c) T. B. Cao, J. Y. Chen, C. H. Yang, W. X. Cao. Macromol. Rapid Commun., 2001, 22: 181

[170] T. B. Cao, L. H. Wei, S. M. Yang, M. F. Zhang, C. H. Huang, W. X. Cao. Langmuir, 2002, 18: 750

[171] W. B. Stockton, M. F. Rubner. Mater. Res. Soc. Symp. Proc., 1994, 369: 587

[172] Q. Pei, G. Yu, C. Zhang, Y. Yang, A. J. Heeger. Science, 1995, 269: 1086

[173] G. F. Li, C. Martinez, and S. Semancik. J. Am. Chem. Soc., 2005, 127: 4903

[174] a) C. W. Lee, Y. H. Seo, S. H. Lee. Macromolecules, 2004, 37: 4070; b) X. Zhang, J. P. Sadighi, T. W. Mackewitz, S. L. Buchwald. J. Am. Chem. Soc., 2000, 122: 7606

Chapter 3   Physical Properties and Associated Applications of Conducting Polymers

A great number of articles, reviews, and books about conducting polymers and their applications are available in the literature [1]. As mentioned in Chapter 1, the intrinsically conductive nature of the conducting polymers arises from a unique bonding structure along the polymer backbone, consisting of alternating double (π) and single (π) bonds. If an electron is added to the conjugated polymer backbone (via reduction, n-type doping) or removed from it (via oxidation, p-type doping) during the chemical or electrochemical doping process, then the charge can freely travel down these conjugation paths when an electrical potential is applied. The electrical conductivity covers whole insulator ($<10^{-7}$ S/cm)-semiconductor (10^{-5} to 10^{-1} S/cm)-metal (10^{2} to 10^{5} S/cm) range depending on the doping degree. The conductivity achieved depends strongly on the type of dopant, the polymer characteristics (such as specific repeat unit and molecular mass, chain defects such as branching and chemical heterogeneity), and how the polymer was processed. For example, stretching doped conducting polymer films can increase their conductivity by two orders of magnitude as a result of the anisotropic alignment of the polymer chains [2].

Moreover, highly conjugated polymer chain, special doping, reversible doping/ de-doping process and electrical redox reversibility, result in unique properties of conducting polymers, such as high nonlinear optical properties and the electrical properties inherent to metal or semiconductors, while retaining mechanical properties close to those observed for conventional polymers. These properties open new possibilities of conducting polymers for technological application. Obviously, all promising applications in technology are corresponding to their properties. Regarding their semiconducting behavior, for instance, conducting polymer-based electronic devices (e.g. Schottky rectifier, field-effect resistor, light emitting diode (LED) and solar cell) can be made as same as inorganic semiconductors. In the metal-conducting region, conducting polymers are excellent candidates as electromagnetic interference (EMI) shielding and microwave absorbing materials as well as conductive textiles. The metal-like conductivity of conducting polymers combined with the reversible redox behavior lead to be used in rechargeable batteries and supercapacitors. Color change of the conducting polymers induced by the electrochemical doping/de-doping enables use in the manufacture of multi-chromic displays or electrochromic windows. Sensitive conductivity of the conducting polymers with reversible doping/de-doping process can be used to fabricate drug-releasing agents, gas separation membrane and

chemical or biochemical sensors. Above-all applications and corresponding properties of the conducting polymers are summarized in Fig. 3.1. In this chapter, these potential applications of the conducting polymers in technology are briefly discussed following an order of electronic devices, EMI shielding and microwave absorbing materials, rechargeable batteries and supercapacitors, sensors, electrochromic devices and artificial muscles as well as others.
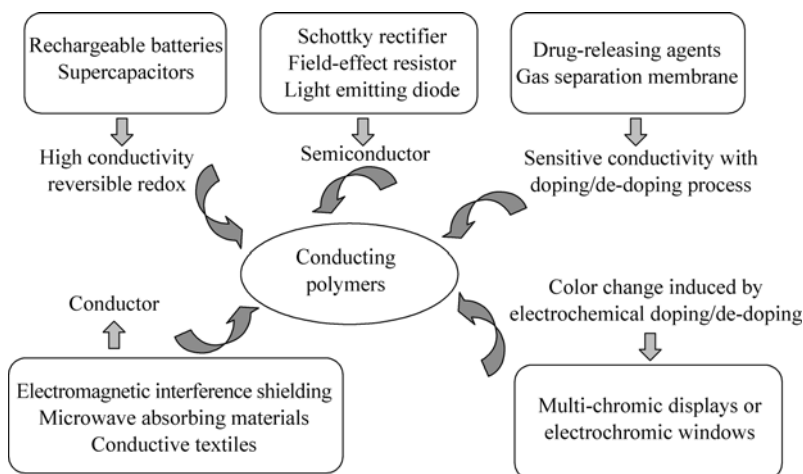
Figure 3.1 Potential applications and corresponding physical properties of conducting polymers

3.1 Electronic Devices

Like inorganic semiconductors, conducting polymers in a semiconductor range can be used to fabricate electronic devices, such as LEDs, solar cells, field emitting diodes (FED), Schottky diodes. Among these electronic devices, LEDs and solar cells have attracted attention as green energy sources. Moreover, development of LEDs and solar cells is recently greater than that of other electronic devices. Thus, discussion on conducting polymer-based electronic devices will focus on concept and method of the electronic devices and issues associated with application in technology.

3.1.1 Light Emitting Diodes (LEDs)

LEDs is one of important electronic devices that is the electromagnetic radiation emitted from a solid when the thin film of a suitable optic solid is sandwiched between two electrodes and an electric field is applied that drives a current through the solid.

In 1990, Friend et al. [3], for the first time, reported the conjugated polymer PPV sandwiched two electrodes could emit green-yellow light. The polymer LED (PLED) is basically associated with injection, recombination and separation of charge carriers. Scheme for a typical PLED divide with single layer is shown in Fig. 3.2.
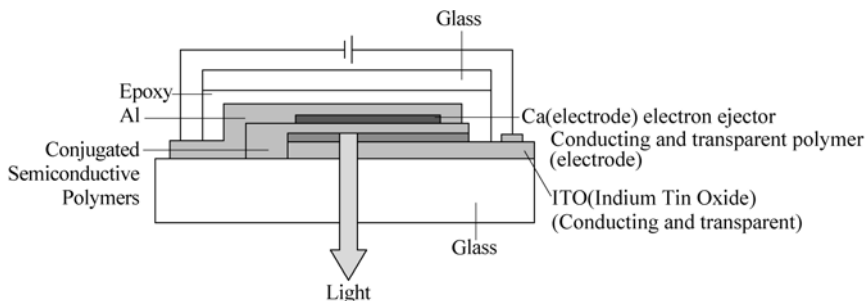
Figure 3.2   Scheme of structure of polymeric light emitting diodes
(www.nobel.se/chemistry/laureaters/2000/idex.html)

So far PPPs [4], PPVs [5], polyalkyflorences [6] and PTH [7] as well as their derivatives or oligomers are widely used as electroluminescence polymers in PLEDs. The emission characteristic of the electroluminescence polymers is affected by the chemical constitution and length of the molecules which dominated an energetic difference between the highest occupied molecular orbital (HOMO) and the lowest unoccupied molecular orbital (LUMO), and defects that disturb the perfect arrangement and therefore break conjugation [1b]. Moreover, the optical properties of materials are also determined by the so-called dielectric function. The imaginary part of the dielectric function, which is proportional to the optical absorption coefficient, is on the orientation parallel and perpendicular to the chain axis. As a result, the optical absorption in the visible and ultraviolet range is mainly determined by the dielectric function parallel to the polymer chain [1b]. That is why the photoluminescence (PL) and electroluminescence (EL) emission spectra are used to characterize the electroluminescence properties of the polymers in LEDs [1b].

Moreover, the light emission process in LEDs consists of charge injection, separation and transport of the injected charges and radiative decay of single exciton. Thus co-ordination effect of molecular structure of light emission polymers, balancing injection of electron and hole within the emission layer, and the recombination process to form single or triplet excitions as well as the radiative decay of single exciton or triplets will dominate emission color, photoluminescence quantum yield and lifetime of the LEDs [1b]. Some basically and important parameters to affect feature of the LEDs are briefly summarized as follows:

(1) Metal/semiconductor interact and charge carrier injection related to metal/ semiconductor interact is important parameter for high performance of LEDs. As

shown in Fig. 3.2, the optical polymers are sandwiched between metal and transparent electrode so that charge carrier injunction is related to work function of metal electrode and band structure of the active polymers. Usually the interface between semiconductor and metal divides into either an Ohmic or rectifying Schottky contact, which not only determined by the work function, ϕ, which is the energetic difference between the Fermi level and the vacuum level of the semiconductor relative to the metal [8], but also nature of charge carriers (*n*- or *p*-type) of semiconductor. The work function for semiconductor and metal is usually assigned as ϕ_s and ϕ_m, respectively, and nature of semiconductor is divided into *n*- and *p*-type. In principle, a rectifying contact, which is also called as Schottky contact, between a metal and a *p*-type semiconductor is formed if $\phi_s > \phi_m$ [8]. The contact results in that electrons flow from the metal into the semiconductor until the Fermi level of the two materials are equal, and spontaneously a build-in potential ($V_{bi} = \phi_s - \phi_m$) in between the metal and the semiconductor is created. The electrons, which are the minority carriers in a *p*-type semiconductor, recombine with the holes in the semiconductor, so that a negative space-charge region is created in the semiconductor at the interface with metal. When the external bias voltage is applied, the voltage drops over this high resistance region assigned as depletion region [8]. The depletion width (W) of free charge carriers is reduced when the semiconductor is made positive with respect to the metal. On the contrary, the depletion width increases when the semiconductor is negative to the metal [8]. The width of charge carrier depletion at the rectifying contact, which forms a Schottky barrier, can be calculated [8]. When a metal and *p*-type semiconductor where $\phi_s < \phi_m$ are electrically connected, on the other hand, electrons flow from the semiconductor into the metal until the Fermi level of the two materials are again equal. In this case a charge depletion region is formed, but the number of free positive carriers in the semiconductor is even increased. This contact is Ohmic, and the resistance of this junction is independent of the applied voltage [8]. Above-discussion suggests that rectifying or Schottky contact between semiconductor and metal therefore is a basic requirement for designing and fabricating LEDs.

(2) To increase mobility of charge carries in polymer is a key in application of LEDs. As well known, the electrical conductivity is a product of carrier concentration and carrier mobility. In general, the charge carrier concentration in organic semiconductor used as active layer in LED consists of intrinsic carrier concentration produced by thermal excitation across the band gap, injected carrier and carrier resulted from ionized defects [1b]. The intrinsic carrier concentration in conducting polymers is related to π-conjugation length and doping degree whereas the injected carrier depends on the properties of the polymer/metal interface [1b]. Mobility of charge carriers in conducting polymers is generally affected by crystalline and morphology of conducting polymers and charge transport is a bulk property [1b]. In organic electroluminescent devices,

thus, both interface and bulk properties are essential for the performance of LEDs, especially enhancement of mobility of charge carries is very important for high performance of LEDs. To increase mobility of charge carries in polymer used as LEDs is therefore a challenge issue in application of LEDs.

(3) Purity of emission color for the PLEDs is required to be improved. Since each wavelength of light corresponds to a certain emission color, the light emission of conjugated polymers is spectrally distributed over more than 100 nm, so a relation to a certain pure color is difficult for polymeric LEDs [1b]. The emission process is determined by the probability for the radioactive transition from the excited state to the ground state so that the emission color then depends on the shape and the energetic position of the emission spectral. Although the emission colors of the most common conjugated polymers (e.g. PPP, PPV and PHT) used in LED range from blue to red so that the realization of any emission color with LEDs is possible by chemical modifications on polymer chain [1b], high purity of emission color for polymeric LEDs is still required.

(4) Photoluminescence quantum efficiency is one important parameter in the electroluminescence process. The photoluminescence quantum yield, $\eta\Phi$, can be expressed by a simple equation [9] as

$$\eta\Phi = \gamma\,\Phi_r\eta_r \tag{3.1}$$

where γ is a double charge injected factor (maximal value is 1 if a balanced charge injection that number of injected positive carriers are equal to number of injected negative carriers); η_r, quantifies efficiency of the formation of a singlet exciton from a positive and a negative polaron; and Φ_r is the photoluminescence quantum efficiency. Above equation gives a good qualitative picture of the emitting light device functions and optimization.

(5) Stability or lifetime is a key for practical application and completion with inorganic LEDs. Although the lifetime for the polymeric LEDs has significantly improved through understanding of the physical process operating in LEDs and fabrication techniques, there is a large distance from the requirement for practical applications. It is believed that great progress in basically fundamental research of the polymeric LEDs and a high level of industrial interest and activity in these devices will speed up the process of commercialization of the polymeric LEDs [10].

3.1.2   Solar Cells

Solar cells are able to directly convert sunlight into electric power so that it is a cheap and friendly environment energy source. Inorganic semiconductor-based solar cells have been widely used as common solar cells. Although these solar cells are advantageous of high efficient, their application is still limited by complex fabrication technique and high cost. As a result, various other solar cells, such as

organic molecules [11], stacked discostic liquid crystals [12], self-assembling organic semiconductors [13], and conjugated polymer [1b, 11, 14] have been also explored as new solar cells.

Similar to LEDs, solar cells are optic specie as optic-absorber is sandwiched between two electrodes, where one electrode is metallic electrode (Cesium or Aluminum) and another electrode is indium-tin-oxide (ITO) coated on transparence glass substrate [1b]. In principle, the convertion of sunlight into electric power for solar cells is mainly based on photovoltaic effect. The process of photovoltaic energy conversion is divided into two steps [15]. One is related to generation of electron/hole pairs photo-induced by absorbing sunlight, and another is separation process of electro/hole pairs into free electron and hole generated by photoexcitation before recombination processes took place by electrical contact. Moreover, it is expected that the number of electro/hole pairs photo-induced by sunlight is affected by absorption characteristics of the absorbers in the range of absorption spectrum of sunlight. Thereby an optimal optic spectrum match between the absorber and sunlight is necessary to enhance the efficiency of the solar cells [1b]. Usually, feature of solar cells are evaluated by open circuit voltage, V_c, short-circuit current density (I_{sc}), and overall solar-to-electrical energy conversion efficiency (η_e).

π-conjugated polymer photovoltaic devices offer great as a renewable, alternative source of electric energy technological potential because of their mechanical flexibility, lightweight, easy thin-film and large-area coating by spin-coating technique[1b, 16]. However, energy conversion efficiencies of photon-voltaic cells made with pure conjugated polymers were typically 10^{-3}% to 10^{-2}% [1b], which is too low to be used in application. So improvement of energy conversion efficiencies for π-conjugated polymer-based solar cells is a key for realizing their commercial application in technologies. Various approaches such as bulk-heterojuction concept [17], dye-sensitized cells [18] and post-annealing treatment under external applied voltage [19] have been provided for improving energy conversion efficiency of π-conjugated polymer-based solar cells. A brief discussion about those approaches is described below.

1. Bulk-Hetero-Junction

Generally speaking, the stabilization of the photoexcitation electron-hole in conjugated polymers can be achieved by blending the polymer with an acceptor molecule. The acceptor molecule should be satisfied following conditions [1b]: One is that the electron affinity of the acceptor is larger than the electron affinity of the polymer, but still smaller than its ionization potential. Another is that the HOMO of the acceptor should be lower than the HOMO of the conjugated polymer. Under these conditions it is energetically favorable for the photoexcited conjugated polymer to transfer an electron to the acceptor molecule. The bulk-hetero-junction concept actually means that π-conjugated polymer as a donor with acceptor (e.g. fullerence) together form a three-dimensional photoactive

matrix with a large charge generation interface to ensure charge creation throughout the whole bulk of the photoactive layer [19]. This concept has been widely used to design π-conjugated polymer solar cells. By using this concept, for instance, power conversion efficiency as high as 2.5% [20] and high-efficiency photovoltaic conversion for composites of conducting polymers as donors and buckminsterfullerene (C_{60}) as acceptors have been reported [14b]. High energy conversion efficiency of the solar cells maybe resulting from following reasons: one is that the time scale for photo-induced charge transfer is subpicosecond, usually, more than 1000 times faster than the radiative or nonradiative decay of photo excitations [16b]. Thereby, the quantum efficiency of charge separation from donor to acceptor thus can be close to unity. Another is that photo-induced charge transfer across a donor-acceptor interface provides an effective way to overcome early time-carrier recombination in composites, enhancing their optoelectronic response. For instance, the photoconductivity increases by an order of magnitude over that of pure MEH-PPY by addition of only 1% C_{60} [11]. It is reasonable that interpenetrating phase-separated donor (D)/acceptor (A) network composites would be appear to be ideal photovoltaic materials because a D/A interface in the composite is a few nanometer, so that, such a composite can be regarded as a "bulk D/A hetero-junction" materials [21]. Moreover, the interfacial potential barrier is dominated by the built-in potential in the D/A hetero-junction diode so that ultra-fast photo-induced charge transfer and charge separation will occur with quantum efficiency approaching unity, leaving hole in the donor phase and electrons in the acceptor phase. Such a bi-continuous D/A network material are promising for use in thin-film solar cells. Heeger and coworkers [17] reported photovoltaic cells made with MEH-PPV: C_{60} composites sandwiched between metal (CA or Al) and transparent ITO electrodes. They reported that the energy conversion efficiencies of the solar cells was of about 29% of electrons per photon, which is better by more than two orders of magnitude than those devices made with pure MEH-PPV. In these types of devices, the photoactive layer is a solution processed mixture of an electron donor phase (i.e. π-conjugated polymers) and an electron acceptor phase (e.g. TiO_2 nano-crystals or C_{60}). Feature of such devices is affected by the blending morphology of the mixture [22]. A number of methods have been pursued to obtain a favorable three-dimensional interpenetrating network in polymer photocells [23]; however, fabrication of intimate nano-composites of conjugated polymers and semiconductor nano-crystals in hybrid solar cells is still needed.

2. End-Functional Conjugated Polymers

Although organic surfactant can facilitate the dispersion of inorganic nano-crystal in polymers, it is disadvantageous of reducing the device efficiency by impeding the transfer of charges between nano-crystal and polymer, and the transport of electrons between adjacent nano-crystals [24]. Moreover, surfactants can be stripped from the nano-crystals during film processing to afford direct

contact between the nano-crystals and the polymer. However, it is difficult to control the morphology and dispersion of nano-crystals within the polymer [24, 25]. To solve this problem, Liu et al. [26] fabricated an end-functional P3HT/CdSe solar cell without introducing insulating surfactant that can effectively disperse CdSe nano-crystals to afford intimate nano-composites with favorable morphology. Thereby using end-functional conjugated polymers could provide a general tool to control morphology and optimize efficiency in polymer/nano-particle photovoltaic devices.

3. Dye-Sensitized Solar Cell

As one knows, the light absorption and charge carrier generation for a p-n junction solar cell occurs in the bulk semiconductor. In other words, photo-generation electrons and hole must move a substantial distance through a high concentration of oppositely charged carriers without recombining and contribute to the photocurrent [27]. The dye-sensitized solar cell (DSSC) is an efficient approach to ensure the interfacial charge recombination after initial charge separation [27]. Usually, a DSSC consists of a nano-crystalline, mesoporous network of a wide band gap semiconductor (e.g.TiO_2), which is covered with a mono-dye of dye molecules (e.g. Ru dye) [28]. The TiO_2 pose are filled with a redox electrolyte (e.g. I^- / I_3^-) that acts as a conductor and that is electrically connected to a metallic electrode (e.g. Pt or Al). The concept of dye-sensitized solar cells is that upon illumination, electrons are injected from the photoexcited dye into the semiconductor and move toward the transparent conductive oxide electrode (e.g. ITO), while the electrolyte reduces the oxidized dye and transports the positive charge to the metallic electrode, resulting in formation of high-surface-area interface between the semiconductor and the electrolyte solution [28]. The high-surface-area interface between the semiconductor and the electrolyte solution allows the use of inexpensive and lower quality materials in these devices. Such cell structure can reach solar to electric conversion efficiencies of about 10% [29]. Recently, Tan et al. [30] also reported that influence of conductivity and pore filling of conducting polymers (e.g. PANI) on the photovoltaic behaviors of polymers in dye-sensitized solar cells. They reported that the photovoltaic behaviors of the devices are as the function of the conductivity and morphology of PANI. A detail review on DSSC can be found in references [28, 29].

High mobility of charge carrier is necessary for enhancement of energy conversion efficiency of π-conjugated polymer-based solar cells. By improving the purity and crystallinity of the photoactive materials is one way to enhance energy conversion efficiency of polymeric solar cells. In addition, post-production treatment of the solar cells is another tool to enhance mobility of charge carriers inside of photoactive matrix materials. The post-production treatment is that the polymeric cells are annealed to a temperature higher than its glass-transition temperature of the photoactive polymers at applied external voltage [31]. This approach is based on two facts: one is that the crystallization of the π-conjugated

polymers was enhanced by annealing at a temperature higher than its glass-transition temperature, and another is that the enhanced crystallization resulted in increase of hole conductivity dramatically. By using this approach, Padinger et al. [31] fabricated solar cells based on poly (3-hexylthiophene) (P3HT) and (6,6)-phenyl C_{61}-butyric acid methyl ester (PCBM) as the photoactive matrix and reported the short-circuit current density is enhanced to $8.5 \, mA/cm^2$ under illumination with white light at an illumination intensity of $800 \, W/m^2$. Above-discussion on solar cells indicated that π-conjugated polymer solar cells have received great attention in application of energy conversion from sunlight to electric power owing to their unique properties, and remarkable progresses on their investigations have been developed. However, realization of the π-conjugated polymer solar cells with high energy conversion efficiency and high stability still needs deeply understanding fundamental principle of the devices, and solving technique problems in fabricating devices.

3.2   EMI Shielding and Microwave Absorbing Materials

3.2.1   EMI Shielding Materials

Electromagnetic wave contains components with frequencies ranging from the lower power frequencies (e.g. 50, 60 and 400 Hz) to the microwave region (e.g. 2 – 18 GHz) [32]. Therefore shielding of electromagnetic interference (EMI) is of critical issue because of not only concerning its interference with other electronic devices, but also the dangerousness of electromagnetic field on health as exposure to electromagnetic wave. In general, metal exhibits as an excellent EMI shielding material due to skin effect, which means the current conducts only along the surface of the metal and the skin depth is defined as:

$$\delta = (\pi f \mu \sigma)^{-1/2} \qquad (3.2)$$

where f is the frequency in Hz, μ is the magnetic permeability and equal to μ_0 μ_r, μ_0 is the absolute permeability of free space (air), $\mu_0 = 4\pi \times 10^{-7}$ and σ is the electrical conductivity in S/cm. Therefore, metallic materials are usually employed as traditional EMI shielding materials because of their excellent shielding effectiveness resulted from their high conductivity and dielectric constant [33]. Although metals have good EMI shielding efficiency (SE) and mechanical properties, metallic materials as SEM shielding materials are limited by their heavy weight, easy corrosion, and poor processability. In order to overcome above-problem, the metallic EMI shielding materials are replaced by various types of conductive fillers (e.g. metal fibers, metal powder, carbon-black and carbon-fibers) that are blended with insulating plastic or coated on the surface of

insulating polymers. However, high conductivity for those composites is difficult to achieve because their maximum conductivity of those composites is limited by contents of conductive fillers in the composites and their mechanical properties will be destroyed at a high loading fraction of fillers in the composites. Carbon powders are used in EMI shielding applications, mainly as conductive fillers (fibers, particles, powders, filaments tubes) in composite materials due to their electrical conductivity, chemical resistance and low density. With the exclusive use of carbon fillers, however, the conductivity and resulting EMI shielding performance not only is not good enough, but also damage the electronic devices. Since metal-like conductivity for the highly doped conducting polymers can be obtained, as mentioned in Chapter 1, conducting polymer-based SMI shielding materials have been received great of attention owing to their low density, high and controlling conductivity as well as good processability and hard corrosion, exhibiting preferred in military applications like camouflage and stealth technology [1b, 34]. Among those conducting polymers, PANI or PPy has been used as an excellent EMI shielding conducting polymer due to its high conductivity, easy of preparation and stability in air. It is found that the SE of PANI is affected by the frequency applied it, for example, it is as high as $30 - 40$ dB at the frequency of $100 - 1000$ MHz whereas it decreased to $3 - 11$ dB at $8 - 12$ GHz [35]. An excellent review paper is recommended [36]. On the other hand, it is still difficult to achieve an extremely high level of shielding SE by using conducting polymers only. Thereby the synthesis of conducting polymer/metal complexes has been proposed [37]. Besides, the homogeneous coating of conductive PANI or PPy samples on the insulating woven or non-woven fabrics is a promising candidate to prepare mechanically strong, flexible, and conducting fabrics. SE of HCl-doped PANI composites made from silicone rubber (SR) with different loading in the low frequency rang from 3 to 1500 MHz were reported, showing SE of the composites are from 16 to 19.3 dB at 100 mass ratio loading of the PANI-HCl [38]. Author also studied the EMI characteristics of free standing films of PANI doped with CSA and DBSA as co-dopant containing multi-walled carbon nanotubes (MCNTs), which will discuss in Chapter 5.

Usually one often confuses concept of SMI shielding and microwave absorbing. As a result, it is necessary to understand what is happen when an electromagnetic wave is incident on shielding material. It is well known that electromagnetic energy usually consists of a magnetic (H-field) and electric (E-field) component perpendicular to each other. The ratio of E to H is defined as the wave impedance (Z_W in ohms) that depends on the type of source and the distance from the source. Far from the source, the ratio of E to H remains constant and equal to 377Ω, which is defined as the intrinsic impedance of free space [1b]. Thereby the near field and far field region for EMI shielding are needed to be considered. The far field region is defined that the distance between the radiation source and the shield material is larger than $\lambda/(2\pi)$, where λ is the wavelength

of the source [1b]. The electromagnetic plane wave theory is generally applied for EMI shielding in this region. When the distance is less than $\lambda/(2\pi)$, it is in the near field shielding and the theory based on the contribution of electric and magnetic dipoles is used for EMI shielding [1b]. *SE* is a main parameter for evaluating feature of EMI shielding materials and definite as the ratio of the power of incoming and outgoing wave in dB unit, which can be expressed as

$$SE = 10\lg(P_i/P_o) = 20\lg(E_i/E_o) \tag{3.3}$$

where P_i and P_o are the power (electric field) of incoming and outgoing waves, respectively. According to Collaneri-Shacklette expressions [39] value of *SE* at near-field and far-field for electrically thin samples (thickness < skin depth) can be expressed as

At near-field: $SE\,(\mathrm{dB}) = 20\lg[cZ_0\sigma d/(2\omega r)] \tag{3.4}$

At far-field: $SE\,(\mathrm{dB}) = 20\lg[1 + Z_0\sigma d/2] \tag{3.5}$

Where $c = 2.998 \times 10^8$ m/s is the velocity of light, $Z_0 = 377\,\Omega$ is the free space impedance, $r = 3.95 \times 10^{-2}$ m is the source-to-shield distance, ω is the angular frequency, σ and d are the conductivity and the thickness of the sample, respectively. If the thickness of the films (or layers) and conductivity of the EMI shielding materials are known, the *SE* at the near-field and far-field can be calculated based on above equations.

In principle, absorption and multiple reflections are observed when the plan wave is incident on shielding material. Therefore, the *SE* can be also described as [40]

$$SE = SE_A + SE_R + SE_M \tag{3.6}$$

where SE_A, SE_R, and SE_M are the *SE* due to absorption, reflection and multiple reflection, respectively. Reflection loss SE_R is the result of interaction between conducting particles in the conducting material and electro-magnetic field, and it has relationship with the value of σ_r/μ_r, where σ_r is the electrical conductivity of the shield relative to copper and μ_r is the magnetic permeability of the shield relative to free space. Therefore, the large conductivity of the material is, the smaller magnetic permeability is, and then the larger reflection loss will be. On the other hand, absorption loss, SE_A, is caused by the heat loss under the action between electric dipole and/or magnetic dipole in the shielding material and the electromagnetic field so that the absorption loss is a function of the product $\sigma_r\mu_r$. Multiple reflection loss SE_M is the loss resulted from the constantly touch to the wave surface of the shielding material that is very low [40] and can be neglected when the distance between the reflecting surfaces or interfaces is large compared to skin depth.

3.2.2 Microwave Absorption Materials (Stealth Materials)

Stealth technology is essentially the shape of the target and the nature of the radar-absorbing material (RAM) or microwave absorbing material (MAM). MAM or RAM is made with compounds having a high loss energy, which enables them to absorb the incident radiation in synchronized frequencies and dissipate in the form of heat [41]. Therefore, MAM or RAM materials play an important role in the field of stealth materials and technologies. The manufacture of RAM or MAM materials basically involves the use of compounds capable of generating dielectric and /or magnetic loss when impinged by an electromagnetic wave [42]. In principle, RAM or MAM materials are complex composites that compose of conductive additives or magnetic fillers into an insulating binder or matrix. Those conductive additives with a dielectric loss or magnetic fillers are generally called absorbers in microwave absorbing materials. The absorber is an important component of microwave absorbing materials because they dominate microwave absorbing characteristics of materials at the microwave frequency. According to feature of microwave absorbers, thus, microwave absorbing materials divides into electrical and magnetic loss microwave absorbing materials, respectively [1b, 43]. In principle, the absorption loss is a function of the product $\sigma\mu$, where σ and μ are the electrical conductivity and the magnetic permeability of materials, respectively. The dielectric loss is mainly related to the conductivity (σ) of materials whereas the magnetic loss not only results from electrical conductivity (σ), but also magnetic permeability (μ) [44]. The magnetic loss materials, therefore, have a characteristic of high absorption efficiency and width broadband compared to that of dielectric loss materials.

Carbonyl irons and ferrites are excellent and commercial magnetic loss microwave absorbing materials, however, their application is limited by their heavy mass. Carbon materials are usually served as the dielectric loss microwave absorbing materials. Compared to the magnetic loss absorbers, the dielectric loss microwave absorbers are advantageous of light-weight; however, their practical application is limited by their low absorbing efficiency and narrow bandwidth. Although much promise offered by carbon nanotubes used as a fiber filler in the development of microwave absorbing materials owing to its high conductivity ($1 - 10^3$ S/cm), lightweight and larger special surface, carbon nanotubes still belong to dielectric loss microwave absorbing materials. Therefore microwave absorbing materials with an abroad bandwidth, high absorption coefficient and thinner coating layer are required in order to satisfy direction of developing new type microwave absorbing materials. Thus design and preparation of such materials at the microwave frequency region ($1 - 18$ GHz) become a hot objective field in material sciences.

Conducting polymers have also evinced much attention in potential application as broadband microwave absorbers due to their unique properties of high

conductivity combined with very light weight, flexibility, reasonably facile processability and controllable electromagnetic properties by doping nature and degree, main polymeric chain as well as synthesis method and conditions [1b, 44, 45]. Compared to metals, moreover, conducting polymers do not only reflect but also selectively absorb electromagnetic radiation [46] that has made conducting polymers useful in microwave absorbing materials applied to military and civil purposes such as in stealth technology [47]. Especially, conducting polymers appear to be one of the few materials capable of switchable microwave absorption, which are called as "intelligence stealth materials", due to their reversible electrical properties of conducting polymers by doping/de-doping processes.

PANI, PPy and PTH, for creating microwave absorbing materials, have been noticed in 1989 [48]. However, conducting polymers obtained at that time only exhibited a dielectric loss without magnetic loss. Incorporation of fillers with a magnetic loss into conducting polymers thus is basically way to expend the bandwidth of the absorption response for the conducting polymers as the microwave absorbers. For instance, Abbas et al.[49] reported that PANI containing $BaTiO_3$ composites having a maximum reflection loss of -15 dB at 10 GHz with a bandwidth of 3 GHz in a sample thickness of less than 3.0 mm have been achieved and found that the absorption properties of the composites are greatly improved with increasing content of PANI in the composites. In addition, their theoretic calculation suggested that the matching frequency decreases with increase in the absorber thickness. However, the surface mass of the composites containing inorganic magnetic loss materials is still limited by loading inorganic materials. Another way to expand bandwidth of conducting polymers at the microwave frequency is to combine with organic dielectric loss absorbers because different absorbers correspond to different absorption response with frequency. Carbon nanotubes (CNTs) are not only typical carbon materials, but also unique nanostructures with low specific mass and excellent electrical, thermal and mechanism properties[50]. The high aspect ratio of CNTs allows small amounts to be dispersed in polymer materials to yield composite materials with superior properties [51]. Darren et al. [52] reported the microwave absorption properties of conductive thermoplastic composites containing both multi-wall carbon nanotubes and PANI doped with para-toluene sulfonic acid (*p*-TSA) at X-band frequency (8 – 12 GHz) that indicated that the microwave absorption properties is affected by synthesis and post-synthesis processing conditions for doped PANI.

Besides, a shortcoming of conducting polymers as the microwave absorbing materials is their relatively low strength. A common method used to overcome the poor mechanical properties is blending the conducting polymers with an insulating polymer. This implies that it is necessary to dilute the conductive phase to obtain an appropriate surface electrical resistance because of metal-like conductivity ($1 - 10^2$ S/cm) of the conducting polymers by various methods [53].

Among those methods, mechanical mixing is the simplest method for large scale processing that lead to wide range of absorbing material properties. Faez et al. [53] reported that the microwave absorption behavior in the 8 − 12 GHz range for the blends of ethylene-propylene-diene monomer (EPDM) and PANI doped with dodecylbenzene sulfonic acid (DBSA) prepared by anical mixing method. It is found that the microwave absorption behavior was affected by the processing time and blending composition, suggesting broadband behavior with microwave radiation absorption of up to 90% is possible. Moreover, the relative electrical permittivity (ε) and permeability (μ) of PANI and derivatives at 1 − 18 GHz are affected by structure of dopant and polymeric chain as well as synthesis conditions [54]. Author also studied electromagnetic characteristics of conducting polymers (e.g. PANI and PPy) and their micro/nanostructures prepared by template-free method in the microwave frequency (1 − 18 GHz), which will discuss in Chapter 5.

It is practice to characterize the absorbability of electromagnetic wave absorbers by the reflection coefficient R for a plane monochromatic electromagnetic wave normally incident on a plane infinite sheet of the absorbing materials [55]. The normalized input impedance (Z) with respect to the impedance in free space, and reflection loss (R) are given by [55]

$$Z = (\mu_r / \varepsilon_r)^{1/2} \tanh\left[-j(2\pi/c)((\mu_r/\varepsilon_r)^{1/2} fd\right) \qquad (3.7)$$

$$R(\text{dB}) = -20\lg[(Z-1)/(Z+1)] \qquad (3.8)$$

where μ_r and ε_r are the relative complex permeability and permittivity of the absorber medium, f and c are the frequency of microwave in free space and the velocity of light, respectively, and d is the sample thickness. The μ_r and ε_r are expressed as

$$\varepsilon_r = \varepsilon' - j\varepsilon'' \qquad (3.9)$$

$$\mu_r = \mu' - j\mu'' \qquad (3.10)$$

$$\tan\delta_e = \varepsilon''/\varepsilon' \qquad (3.11)$$

$$\tan\delta_\mu = \mu''/\mu' \qquad (3.12)$$

where ε_r and μ_r are the relative permittivity and permeability, and $j = (-1)^{1/2}$, "$'$" and "$''$"denote the real and imaginary parts, respectively. Based on above-equations, design of a microwave absorbing material is required to be accorded following parameters: ① Since the $\tan\delta_e$ and $\tan\delta_\mu$ are defined as angle of the dielectric and magnetic loss, respectively, the microwave absorbing properties are dominated by the imaginary parts of the relative permittivity and permeability, indicating increase of the imaginary of the relative permittivity and permeability is one way to improve absorption efficiency at the microwave frequency.

② Actually, the reflection loss is determined by the six parameters, ε_r', ε_r'', μ_r', μ_r'', f and d. According to designed requirements, one can change those parameters depending on what one prefer. If the reduction of weight is more important, for instance, it is appropriate to use the dielectric loss absorbing materials. On the contrary, if it is more important to reduce the thickness, it is preferable to use both dielectric and magnetic loss microwave absorbing materials. However, the radar characteristics of newly developed absorbing materials must be provided under the condition that their thickness and weight are minimal. ③ Two fundamental conditions, such as the matching to free space (i.e. attaining a negligibly small reflection from the external surface, $Z = 1$) and the total absorption of the energy of the wave transmitted into the materials, must be satisfied. In general, choosing close values of ε_r and μ_r are efficient way to achieve dielectric matching to space, while inhomogeneous absorbing microwave materials, where quantities ε_r and μ_r vary smoothly (gradient materials) or stepwise (multilayer structures) from about unity on the external surface to the value providing the required absorption, are usually considered to ensure the total absorption of wave energy transmitted into the inside of materials [56].

Although conducting polymer-based microwave absorbing materials have received great attention in the stealth materials owing to their high conductivity, controlling electro-magnetic properties and lightweight, their commercial application at current time is still limited by their narrow bandwidth due to only having dielectric loss and poor strength. Investigations for conducting polymer-based microwave absorbing materials should forward to enhancing their absorbing efficiency, expending bandwidth and improving mechanical properties. Hybrid conducting polymers with a magnetic loss or development of nanostructure conducting polymers might be an approach to fabricate conducting polymer-based microwave materials to satisfy requirements for developing new type microwave absorbing materials.

3.3   Rechargeable Batteries and Supercapacitors

3.3.1   Rechargeable Batteries

Rechargeable batteries, sometimes are called as secondary batteries, can be restored to its original charged condition by an electric current flowing in the direction opposite to the flow of current when the cell was discharged. Electrical energy in battery is generated by conversion of chemical energy via redox reactions at the anode and cathode. As reactions at the anode usually take place at lower electrode potentials than at the cathode, which means the more negative electrode is designated the anode, whereas the cathode is the more positive one.

Based on above definition, electro-active species are a key component of the batteries. The terms, such as "specific energy" expressed in watt-hours per kilogram (Wh/kg), "energy density" in watt-hours per liter (Wh/L) and rechargeable times, are generally used to evaluate the properties of rechargeable batteries.

According to unique properties of conducting polymers described in Chapter 1, it is reasonable for conducting polymers being used as electrode materials in rechargeable batteries. The reasons are summarized as follows: ① Reversible change in conductivity can be realized by a doping/de-doping process. The insulator-to-metal transition in conductivity actually relates to extensive delocalization of the electronic charge along the polymer backbone. The charging results in the appearance of positively charged electronic species (polarons or bipolarons) on the polymer chain, accompanied by insertion of charge compensating ions (anions in p-doping case or cations in n-doping case) from the electrolyte solutions to maintain the polymer bulk electroneutrality. ② Conductivity of conducting polymers at room temperature is about $10 - 10^3$ S/cm that basically satisfies requirement of electrical properties used as electrode materials. ③ Conducting polymers are easily produced in the form of films grafted onto the surface of metallic or semiconductor electrodes by either chemically or electrochemically oxidation of suitable monomer species [57]. Up to date, rechargeable batteries made of PA [58], PPy [57a], PANI [59], PTH [60] and PPP [61] as well as their derivatives have been reported. A comprehensive and detailed review on the application of a large variety of conducting polymers for rechargeable batteries has been reported [62].

PANI or PPy is generally used as cathode (positive electrode, p-doping with anions); however, PPP and PTH and their derivatives can be used as either cathode or the anode (negative electrode, n-doping with cations). For instance, the films of PTH derivatives (e.g. 3,3-dialkylsulfanyl-2,2'-bithiophenes) undergo electrochemical p- and n-doping under the electrochemical system Bu_4NBF_4-CH_3CN-Pt [63]. At the beginning of the 1990s, Li/PANI and Li/PPy cells were attempted for commercialization [62a]. In both these batteries, however, the bulk electrolyte salt concentration is changed during cycling of the batteries, resulting in decreasing the practical specific capacity and energy density. Novak et al. thought [62a] that might result from two factors: one is both the cation and the anion are involved in the charging-discharging process, and another is existing excess of the salt in the solution in order to ensure stable conductivity throughout the charge-discharge process. An alternative concept has been therefore developed at approximately over the same period, which was called as the Li-rocking-chair rechargeable battery [62a]. This system generally consists of a lithiated carbon anode and a transition metal oxide cathode. Such batteries showed high-energy density performance due to a small atomic weight of Li^+ ion compared with that of a variety of the commonly used insertion anions, and no change in the solution composition during charge-discharge cyclic. Ryu et al. [64] reported PANI doped with nucleophilic dimethyl sulfate (DMS) can be used as electrode in a lithium

rechargeable battery that optimized performance of more than 80A · h/g after 50 cycles were obtained.

All-solid-state rechargeable batteries are developing direction of rechargeable batteries at the present time. Poly (ethylene oxide) (PEO) is a typical and common solid electrolyte. However, the PEO-based solid electrolytes are disadvantageous of low conductivity at room temperature and poor mechanical properties. Gu et al. [65] recently reported that all-solid-state rechargeable battery composed of lithium and PANI /polyether polyurethaneneurea (PEUU) bi-layer, where lithium is used as anode; the PANI/PEUU bi-layer is used as a cathode and an electrolyte, respectively. The bi-layer films have good redox stability, reversibility and high electrochemical activity in the solid state at room temperature. Carbon black in such batteries is as a bridge for electrical contact between the insulating lithium cobalt oxide particles and the aluminum cathode. Since conducting polymers have similar conductivity to carbon black so that carbon black replaced by conducting polymers is reasonable. One considers its application as replacement for carbon black; however, the redox potential of the polymer needs to be adjusted in order to doing not interfere with the electrode reactions of the battery as charging or discharging. Thus polymer structure should simultaneously contain structural elements required for ion and electron conduction [66] that is one approach to reducing the number of components in the batteries. PPy with oligo (oxyethylene) side chains end capped by a methyl group grafted or associated with the backbone reported by Costantini et al. [67] is a typical sample, which has both ionic and electronic conduction.

In addition, hybrid approach, which is combination of organic and inorganic species to form novel and functional hybrid materials, has been recently received considerable attention in the field of material sciences [68]. This concept has been also employed in fabricating conducting polymer-based rechargeable batteries. Hexacyanoferrate (HCF) is commonly used in rechargeable lithium batteries (e.g. $LiCoO_2$ or $LiMn_2O_4$) due to its electro-active that able to reversibly cycle one electron per metal atom, but could not be used as the basis for electrode materials due to its molecular nature and solubility. Gloria et al. [69] reported that PANI/HCF hybrid used as cathodes in lithium rechargeable batteries showed high specific charges up to 140 Ah/kg, an apparent diffusion coefficient of $5 \times 10^{-8} \, cm^2$/s and an activation energy of 15.5 kJ/mol (0.16 eV). By using hybrid approach, PPy/$PMo_{12}O_{40}$ [70], PANI/ $PMo_{12}O_{40}$ [71], hybrid as the cathode in rechargeable lithium batteries have been also reported.

Organic disulfide electrode materials possess highly desirable features, such as low cost, low toxicity, good cyclability, and high energy density. It was found that the formation of S—S bonds takes place when the organic disulfide is electrochemically oxidized to a disulfide polymer, and the scission of S—S bonds occurs when the polymer is electrochemically reduced to monomer unit. This electrochemical process is accompanied by the movement of cations (Li^+) into (upon reduction) and out (upon oxidation) of the polymer matrix [72]. However,

the redox kinetics of these materials is rather slow, leading to significantly lower power density and rate capability of an electrochemical energy conversion [73]. Therefore, conducting polymers, such as PANI [74] and PPy [72] have been also used as electro-catalyst for organic disulfides to improving feature of rechargeable batteries.

As above-mentioned, the promising application of conducting polymers as electrode materials in rechargeable batteries and lithium or solid-state rechargeable batteries has been still received considerable attention; and that still becomes one of major objects in the field of conducting polymers although their commercial application is not realized. However, practical application of rechargeable batteries made of only conducting polymers is more difficult. Combination of conducting polymers especially their nanostructures with other electrode materials might be a good approach for developing new type of conducting polymer-based rechargeable batteries.

3.3.2   Supercapacitors

A growing interest in the development of electrochemical supercapacitors has been arisen because of their possible potential application in electrical equipment, medical devices and electrical vehicles [75]. Supercapacitor is a device that stores electrical energy in the electrical double layer formed at the interface between an electrolytic solution and an electronic conductor [76]. The configuration of supercapacitors is almost similar to that of batteries, where the energy-providing in supercapacitors take also place at the phase boundary of the electrode/electrolyte interface. However, there are some differences between batteries and supercapacitors. In batteries, for example, energy is generated by conversion of chemical energy via redox reaction at the anode and cathode. On the other hand, the energy-delivering process in supercapacitors is performed via electrical double layers formed and released by orientation of electrolyte ions at the electrolyte/electrolyte interface, resulting in a parallel movement of electrons in the external wire [76].

According to the charge storage mechanism of electrode materials, supercapacitors are classified as electrical double-layer capacitors and redox supercapacitors, respectively. Carbon or other similar materials are used as blocking electrodes in the electrical double-layer capacitors whereas electro-active materials called as insertion type compounds (e.g. RuO_2, NiO) for redox supercapacitors are required [77]. The charge storage mechanism in electrical double-layer capacitors is electrostatic in origin, which involves the formation of an electrical double layer due to charge separation at the electrode/electrolyte interfaces. In redox supercapacitors based on insertion compounds (e.g. RuO_2-type electrode materials), on the other hand, a faradic charge transfer process takes place, leading to the pseudocapacitance at the interface. Activated carbon is usually considered to be typical electrical double-layer capacitors, especially which in

the form of fibers are most attractive because of their large surface area (e.g. 1,000 – 2,500 m^2/g), which correspond to very high specific capacitance value of 200 – 500 F/g [77]. RuO$_2$-type electrode material is regarded as a good redox supercapacitor that the highest value of specific capacitance is as high as 840 F/g [78]. Compared to battery or fuel, supercapacitor is considered to be high-power system [76].Therefore, characteristics of supercapacitors are generally evaluated by the terms of "specific power" (in W/kg) and "power density" (per kilogram). Nowadays, much research on electrochemical capacitors is aimed at increasing power and energy density as well as lowering fabrication costs while using environmentally friendly materials.

Conducting polymers, such as PANI, PPy and PTH, represent an attractive class of materials for use as electrodes in electro-chemical capacitors because of advantageous properties:

(1) High specific capacitance due to involvement of the whole polymer mass in the charging process.

(2) High conductivity in the doped state and charging process.

(3) Fast charge/discharge electro-transfer kinetics [79]. Conducting polymers are usually regarded as electrodes in redox supercapacitors that can be divided into three types, depending on the component of two electrode materials [80]. Among those conducting polymers, PANI has been considered as one of the most promising materials for electrode materials in redox supercapacitors because of its low cost, ease of synthesis, and relatively high conductivity. However, its capacitance is much less than that of RuO$_2$ [81].

Therefore, various tools for improving performance of PANI or other conducting polymer-based supercapacitors have been reported. The basic idea of the methods is summarized as follows:

(1) Porous electrode is a variable approach to improve characteristics of the supercapacitors. Electrode materials in supercapacitors essentially involve processes at the interface between an electrode and an electrolyte solution. This is reasonable to be believed that the larger area of the interface, the larger will be the rate of the process. Porous electrode materials with high surface-area electrodes, especially with structure elements down to nanometer scale have been received considered attention [82].

(2) By changing dopant structure might be another tool to adjust performance of conducting polymer-based supercapacitors, because conductivity and morphology of conducting polymers is affected by dopant structure. PANI is usually doped by protons (e.g. HCl) [83]; however, Ryu et al. recently reported [64] that PANI doped by the nucleophilic addition of dimethyl sulfate (DMS) can be used as electrode in the redox supercapacitors, which specific capacitance is about 115 F/g initially and $\sim$ 95 F/g after 5,000 cycles at a current density of 2.5 mA/cm^2. Moreover, they proposed that the nucleophilic addition of DMS into PANI concurrently resulted in an increase of the charge transport properties (e.g. electrical conductivity) and enhanced the processability (e.g. lowing of the

melting point). In particular, the porous behavior of the resultant PANI-DMS is contributed to improve the capacitance of redox supercapacitors [64].

(3) Using the electrode materials composed nanostructured conducting polymers is an efficient way to increase the power density and specific capacitance. Since the capacitance in the redox supercapacitors is mainly produced by the fast faradic reaction occurring near a solid electrode surface at an appropriate potential [84], a relatively short diffusion path can be provided by nanostructured materials to improve the power density of supercapacitors. Therefore, electrode materials composed of nanostructured conducting polymers have been recently received consideration in supercapacitors. Gupta and Miura [85] reported a specific capacitance of 724 F/g of the redox supercapacitors could be obtained from PANI nanowires. Wang et al. [86] also reported that the specific capacitance of the PANI/mesoporous carbon composite is as high as 900 F/g at a charge/ discharge current density of 0.5 A/g (or 1221 F/g for PANI based on the pure PANI in the composite) that is even higher than that of amorphous hydrated RuO_2 (840 F/g).

(4) Since CNTs are of high surface area, high conductivity and chemical stability [87], combination of conducting polymers with CTNs (as electron acceptors) is also efficient approach to increase the capacitance of the composite, resulting from redox contribution of the conducting polymers [88]. By this way, capacitance values from 20 to 180 F/g have been reported depending on carbon nanotubes purity and electrolyte [89]. In particular, Zhou et al. [87] recently reported that supercapacitor electrodes based on pyrrole treated-functionalized single wall carbon nanotubes that exhibited high value of capacitance (350 F/g), power density (4.8 kW/kg), and energy density (3.3 kJ/kg) were obtained in 6 mol/L KOH, showing the macrospores make a significant contribution to the capacitance performance of these materials. Besides, a lot of other studies dealing with conducting polymer/carbon nanotube composite in the electrochemical capacitor application have been also reported [90].

(5) Hybrid conducting polymer-inorganic nanocomposite are being considered another approach to improve properties of electrode materials. Since polyoxometalates (POMs) can be electrochemically reduce to form blue species, POM-doped PANI can be applied in energy storage [91]. Based on this line, Karina et al. [92] recently reported that the molecular hybrid PANI/$H_4SiW_{12}O_{40}$ and PANI/$H_3PW_{12}O_{40}$ prepared by electrochemically on platinum or carbon substrates showed the specific capacitance of 120 F/g and good cyclability beyond 1,000 cycles.

As above-discussion, current research on conducting polymer-based redox supercapacitors still emphasis on the development of new electrode materials with high specific capacitance and high energy density. Nanostructures of conducting polymers and hybrid of conducting polymer-inorganic nanocomposite might be playing an important role in the field of conducting polymer-based electrochemical redox supercapacitors.

3.4   Sensors

As mentioned in Chapter 1, the molecular arrangement of alternating single and double bonds along the chain for conducting polymers results in delocalization electronic states [93]. The bond alternation combined with the consequent restriction on the extent of delocalization leads to the formation of a large energy gap. Most conducting polymers, such as PANI and PPy are p-type semiconductors, and unstable in the undoped state [44]. Based on doping concept in conducting polymers described in Chapter 1, the doping process actually is that the primary dopants (anions), introduced during the chemical or electrochemical polymerization, maintain charge neutrality and generally increase the electrical conductivity. The charge localization along the chain and the lattice bond distortion results in more easily oxidized due to gaining elastic energy of the system, lower the ionization energy of the distorted chain and decreasing electron affinity. Therefore, introduction of an electrically neutral gas into a primary-doped conducting polymer can be regarded as adding an "inert" secondary dopant that induces further changes in its electronic, optical or magnetic properties [94]. The effects of secondary doping are based primarily on a change in molecular conformation of the conducting polymers from compact to expanded coil that is principle of conducting polymer-based sensors. Changes in the electronic properties induced by "inert" doping are related to changes of electronic coupling between redox sites in the matrix that define a physical electron transfer pathway in the conducting polymers recognized in conductivity and work function. In general, the electron transfer pathway relies on the premise that covalent bonds, hydrogen bonds and Van der Waals contacts between atoms all modulate electronic coupling differently. The magnitude of the electronic coupling depends on the extent of these chemical interactions [95].

Conducting polymers used as sensors can be generally divided into two kinds: one is in electronic [96], optoelectronic [97] or electromechanical devices [98] and another is in chemical sensors based on electronic, optical or mechanical transduction mechanism [98]. The most common sensors using conducting polymers are chemical sensors because of relative easy and inexpensive fabrication. The simplest chemical sensors consist of a pair of electrodes contacted to conducting polymers deposited on an insulating substrate. When a constant current is applied, the resulting potential change (i.e. difference) at the electrodes is defined as a response signal. However, it is seldom known what is taking place between the two contact electrodes. When the chemical sensors are exposed to detected gas the conductivity increases as the conducting polymer interacts with gaseous species acting as an electron donor (p-type). On the contrary, it decreases when the conducting polymers serve as electron acceptors (n-type). Thus the sensitivity of the sensors can be expressed by following equation:

$$S = \frac{R_{\mathrm{t}} - R_0}{R_0} \times 100\% \tag{3.13}$$

where R_0 and R_t are resistance before and after sensors exposed to gas, respectively. The characteristics of sensors can be evaluated by sensitivity, response time and cyclic stability. From Eq. (3.13), as one can see, the sensitivity of sensors is determined by the difference in resistance before and after exposed to gas. Therefore, increasing specific surface area of the conducting polymer interacts with gaseous specious is a key to enhance sensitivity of the sensors. Nanostructures, such as nanofibers or nanotubes, are expected to be the excellent candidates for sensors because of their having large specific surface area [99], which will be discussed in Chapter 4.

As one knows, the number of charge carries for the conducting polymers are related to doping degree, but mobility of charge carries is affected by the dopant structure and conformation of the polymer backbone. Moreover, both the number and mobility of charge carries are changed by gas secondary doping that are attributed to the overall change of conductivity. Therefore, the response originating in the bulk of the conducting polymers is relative long time constant (tens of seconds to minutes) due to slow penetration of gases into the conducting polymers, and often is accompanied by hysteresis. This is the most disadvantageous of conducting polymers as the gas sensors [100]. Besides, other facts affected the characteristics of sensors should be also concerned as follows:

(1) The chemical sensor device can be regarded as equivalent capacitor. When a direct current is used in measurement, the equivalent capacitors in parallel with the resistors can be ignored. However, it plays an important role when the sensor is excited with alternating current or when the transient signal is concerned [100].

(2) Change of the conductivity at the electrode/conducting polymer contact also can be attributed to modulation of the height of the Schottky barrier that is determined by the difference in work function of the conducting polymer and electrode, where work function is defined as the work needed to bring an electron from the bulk of the material up to the surface dipole layer (chemical potential), and the energy of extraction of an electro through the surface dipole layer up to the vacuum level [100]. In this contact, thus, a space-charge region is created at the conducting polymer and metal interface that leads to the effective resistance depending on the bias voltage applied during the measurement [100].

(3) The interface between the conducting polymer and the insulating substrate is another location that maybe attributed to the overall conductivity. Glass, quartz and sapphire are commonly used as substrate in the chemical sensors made of conducting polymers. Those substrates are generally oxides and which surface conductivity is affected by the degree of hydration [101].

As a result, water vapour becomes the most common interface for chemiresistors operated at room temperature. This problem can be solved by using the substrate with a hydrophobic surface before deposition of the conducting polymers [102]. Outperforming of conducting polymer-based chemical sensors can be achieved by carefully choosing above-factors.

Among those conducting polymers, PANI has received great attention as a gas sensor because its conductivity is not only dependent ability of charge carriers along the polymer backbone controlled by its proton and oxidation state, but also charge carries hopping across the polymer chain. Thus PANI is generally used as the selective layer in a chemical-vapor sensor (e.g., resistance-type detectors) due to its temperature sensitivity, the ease of deposition on a wide variety of substrates and the rich chemistry of structural modification. However, poor diffusion of gas in the bulk of PANI degrades sensitivity [103]. Some approaches, such as producing monolayer [104], increasing the surface area by coating layer on porous supports [105] or nanostructures (nanofibers, nanowires and nanotubes) [106], have been provided to improve the sensitivity. Among those approaches, conducting polymer nanostructures (e.g. nanowires, nanofibers and nanotubes) have received great attentions due to large surface area per unit mass and light weight that will discussed in Chapter 4. Since conductivity of PANI depends on the proton doping, moreover, hydrochloric-acid-doped PANI films can be used as base sensors. In other works, when fully HCl-doped PANI is exposed to ammonia vapor, a drop in conductivity is observed. Kaner et al. [107] also reported that nanofibers film outperforms a conventional PANI film without thickness-dependence. However, there are only few papers on nanostructured conducting polymer sensors probably due to the lack of facile and reliable methods for fabricating high quality conducting polymer nanostructures [108].

Besides, optical sensors and biosensors made of conducting polymers have recently received attention in application of DNA, proteins, and drugs. For instance, the sequence-specific detection of DNA is of central importance for genetic analysis to diagnose infections and various genetic diseases. When DNA binding with targets (e.g. ions, proteins and drugs) takes place the oligonucleotide probe often undergoes a conformational transition [109]. Based on conformational modifications of the conjugated backbone of a cationic poly (3-alkoxy-4-methylthiophene) when mixed with single-stranded DNA, Ho et al. [109] provided a new, sensitive and versatile electrostatic approach for identification of target nucleic acids, proteins and other biologic molecules. This methodology does not require any chemical modification of the probe or the analytes. Among those conducting polymers, PPy recently has emerged as promising materials in the development of planar electrochemical biosensors because of its high electronic conducting, environmental stability, easy and controlled processing by electrochemical polymerization, and biocompatibility [110]. Moreover, biomolecules can be incorporated into conductive PPy in a simple step during polymer synthesis rather than the multiple steps needed for synthesis of surface-modified silicon nanowires and carbon nanotubes [111]. Ramanathan et al. [112] recently reported a simple, bimolecular friendly, single-step protocol for the fabrication of a PPy nanowire biosensor of controlled dimension and composition, large aspect ratio used as label-free bioaffinity sensing.

In summary, conducting polymer-based chemical or biochemical sensors have

received great attention in application. Research on conducting polymer sensors should forward to developing nanostructure conducting polymer-based sensors owing to large surface area of nanostructures. Facile and reliable methods for fabricating high quality conducting polymer nanostructures are necessary.

3.5   Electrochromic Devices and Artificial Muscles

As shown in Chapter 1, doping/dedoping process in conducting polymers not only results in change of conductivity, but also accompanied color variation, which is called as electrochromic effect. Based on the electrochromic effect, conducting polymers can be developed a series electrochromic devices such as displays, smart windows, and electronic paper [113]. Moreover, the doping process allows counter-ions to penetrate into the polymeric chain, resulting in volume expansion. On the contrary, the de-doping process promotes counter-ions removing from the polymeric chain, leading to volume reduction. In other words, the doping/ dedoping process in conducting polymers is always accompanies a physical process of volume expansion (doping)/reduction (dedoping). Conducting polymer-based artificial muscles are based on the volume change through doping/dedoping process. Electrochromic devices and artificial muscles are briefly discussed below.

3.5.1   Electrochromic Devices

Electrochromic effect, which has been known for many years, is based on the fact that certain materials change color by means of redox reaction [114]. In other words, the electro-active species exhibit various colors, in accompaniment with an electron-transfer reaction (reduction or oxidation) due to an applied voltage in a suitable device. A primary advantageous of electrochromic materials is that a single electrochromic electrode can in theory display different colors at difference applied potential. The simplest electrochromic devices are usually made of an electrochromic material sandwiched between metal electrode (e.g. Au) and transparent electrode (e.g. ITO); and their electrochemical performance is carried out in liquate or solid electrolyte under applied suitable voltage. Various electrochromic materials including inorganic transition metallic materials (e.g.WO_3) [115], and organic liquid crystal materials [116] have been reported. Among those materials, WO_3 is the earliest electrochromic materials as "smart windows" [117]. However, WO_3 electro-chromic material films are usually prepared by cost-intensive sputtering process under high vacuum. Moreover, transition metal oxide films exhibit slow response times for obtaining their full contrast. [118]. Liquid crystal material displays are practical electrochromic devices; however, they generally provide angle-dependent viewing, and often require a backlight that insults in adding-weight and costing energy. As discussed in

Chapters 1 and 2, one feature of π-conjugated polymers is that the color changes accompanied by a chemical or electrochemical doping and dedoping process are reversible and present true optical contrast that can be used for developing new electrochromic materials. Compared to other electrochromic materials, π-conjugated polymer-based electrochromic materials provide reasonable contrast without angle dependence, backlights or extensive materials synthesis [119]. Moreover, the conducting polymer-based electrochromic materials exhibit fast switching times and high contrast ratios in the visible and near inference range, straightforward device integration, and mechanical flexibility [120].

Various novel electrochromic conducting polymers with high contrast and coloration efficiency have been synthesized [121]. Among those conducting polymers, PANI is excellent electrochromic materials, as shown in Chapter 2, because the color of PANI is changed by both of the oxidation state and proton state. For instance, the color changes from colorless at the full reduced form (i.e. LEB, $y = 1$) to a deep cyan at full oxidation state (PEN, $y = 0$) when PANI is oxidized from its full reduced form to its full oxidized form. Moreover, the color also changes from blue to green when the emeraldine base (EB, $y = 0.5$) is doped with a proton (e.g. HCl acid as a dopant) [122]. As a result, PANI is regarded as an excellent electrochromic material and a lot of papers on electrochromic materials made of PANI have been reported [123]. Except for PANI, PTH and its derivatives or composites are also excellent π-conjugated polymer-based electrochromic materials. Heuer et al. [124] reported a conductive polymeric complex of poly(3,4-ethylenedioxythiophene) and poly (styrenesulfonate) (PEDT/PSS) complex as an electrochromic materials. Moreover, feature of the electrochromic devices can be improved by incorporation of ions (e.g. NiO_x, or CeO_2/TiO_2) in the complex by a sol-gel process[124].

Fast switching speed, high color contrast and stability for the electrochromic devices are basic requirements in order for commercial application in technology (e.g. as smart window and display). There are some approaches to improve color contrast and stability of conducting polymer-based electrochromic materials, which are summarized as follows: ① In order to obtain a high degree of contrast during the switching process [125], a low band (cathodically coloring) polymer needs matching with a high band gap (anodically coloring) polymer. Thus band gap control is an important strategic key in the construction of polymer-based electrochromic devices. Reynolds et al. [126] recently reported that the switching speed of the electrochromic devices of poly (3,4-alkylnedioxythiophene) (PXDOT) and their derivatives can be improved by gold-patterned porous electrodes prepared by means of a shutter mask during the metal vapor deposition process. By using this approach, these polymers yield reflective contrast values of up to 90% in the near inference regions and ~ 60% in the visible regions; and the electrochromic devices were switched repetitively 180,000 times with less than 10% contrast loss [126]. ② Electro-active polymer film with low-roughness and high conductivity is required that can be fabricated using layer by layer (LBL) assembly technique

[127]. In LBL assembly, a thin film is to grown up from a substrate by alternating its exposure to aqueous solutions containing species with opposite multivalent attractive affinities [128]. In general, electrostatic interaction in LBL assembly technique is employed to fabricate a film combined a polycation and a poly-anion [129]. The method is simple and inexpensive, and allows the incorporation of different functional materials within a single film at a full range of composition without phase separation [130] as well as creates low-roughness and high conductivity electro-active polymer films. Longchamp and Hammond [130] reported a fully functional switchable electrochromic devices made of PANI/PEDOT by LBL technique. The devices have been shown to undergo over 35,000 cycles without failure utilizing a PAMPS/H$_2$O ion transport medium that make them good candidates for smart windows or large area, long term for electronic paper and lightweight displays. Moreover, Delongchamp and Hammond [131] also reported a multiply colored electrochromic electrode of a polycation PANI combined with anionic nano-particle dispersion of iron (III) hexacyanoferrate (II) by LBL assembly technique.

Moreover, V$_2$O$_5$/PANI nano-composites prepared by LBL technique recently promote new electrochromic effects [132]. Kim et al. [133] also studied an LBL assembled electrochromic devices fabricated by using poly (aniline-*N*-bulylsulfonate) (PANIBS) as an electrochromic anionic polymer, and acid-doped PANI and vinylbenzyldimethyl-*n*-octadecylammonium salt (VBOD) as a polycation. These results showed the conjugated polymer-based electrochromic devices become one of interesting objects in the field of conducting polymers. However, its development is slower compared with that of organic light emitting diodes. Therefore, depth investigations on both materials and devices are required for their practical applications in technology.

3.5.2   Conducting Polymer-Based Artificial Muscles

Gel fibers [131] and piezoelectric polymers [132] are already known as artificial muscles. Gel fibers as artificial muscles results from contraction and expansion of gel fibers proving a means of converting chemical energy into mechanic energy [131]. On the other hand, piezoelectric polymers as artificial muscles are based on fast and reversible charge polarization process (no chemical reaction occurs) [133]. Gel artificial muscles are of disadvantageous of low actuation rates, high working potentials and lower mechanical stresses [133].

As discussed in Chapters 1 and 2, when a neutral conducting polymer film is electrochemically oxidized after being submitted to sufficient anodic potential in an electrolytic medium, positive charges are generated along the polymeric backbone and solvated counter-ions are forced to enter the polymer from the solution to maintain the electro-neutrality of the solid [134]. It implies that a physical process occurs during oxidation, in which volume expansion due to the

opening of the polymeric structure allowing counter-ions to penetrate into the solid. The opposite process occurs during reduction: counter-ions are expelled from the solid, and conformational changes promote the closing of the polymer network, resulting in the polymer recovering its neutral state and decreasing the volume of the film. Thus volume change of a conducting polymer during its redox process is thought to be achieved by electrolyte ion transport into/out of the polymer, solvent transport into/out of polymer, polymer chain configuration change, and electrostatic expulsion between polymer chains [135]. Above-described properties of conducting polymers have attracted attention as new electrochemical actuators [136]. The availability of redox properties of conducting polymers opening new possibilities for development of artificial muscles was firstly reported by Baughman et al [137]. After that, a series artificial muscles dealing with PPy [138], PANI [138b, 139] and poly (3-alkylthiophene) [138b, 140] has been reported. However, the electrochemimechanical actuators made by conducting polymers will be only regarding as secondary machines because no direct transformation of electric energy to mechanical work due to existence of an intermediate electrochemical process, resulting in a flow of electrons and ions through the polymer and conformational changes along the polymeric chain. Moreover, conducting polymer-based artificial muscles also undergo some problems as follows: ① A high applied potential at the electrode to achieve a desired oxidation level might damage the material closer to the electrode. ② Oxygen reduction reactions further limit the electrochemical potentials in a resistive film [141]. ③ Since conductivity of most conducting polymers is typically 100 S/cm or less used in an actuator [142], a metal layer needs for electrical contact. The metal maybe corroded by reacting in the electrolyte or cracking. ④ Most conducting polymer actuators were carried out in aqueous electrolytes, which have a narrow electrochemical window, and some conducting polymers degrade in aqueous media. Therefore, a nonaqueous electrolyte with a wide electrochemical window, a high boiling point, and a high ionic conductivity can be advantageous.

In recent years, there has been an effort to create nanometer-sized devices capable of carrying out mechanical work. For instance, Mattes et al. [143] reported highly electrically conductive (400 – 1,000 S/cm) fibers of PANI doped with 2-acrylamido-2-methyl-1-propanesulfonic acid (AMPSA) as electrochemical actuators. The high conductivity of the fibers ensures well-defined electro-activity and actuation without a metal backing. They also found that in propylene carbonate (PC) used as an electrolyte, the electrochemical and actuation behavior of the fibers was influenced by the dopant solubility and size, electrolyte anions. In particular, electrochemical linear actuators with a unique solid-in-hollow configuration were developed using a PANI solid fiber in a PANI hollow fiber with a gel electrolyte. In terms of stress generation, these actuators behaved better than skeletal muscle [143]. In addition, nanorobotic devices capable of operating in a fluid environment, for instance, could be used in biomedical

sciences and in health care, allowing small-scale manipulation of flows and particles. A series of papers, such as nanoelectromechanical actuators with ultraviolet or electron-beam lithography and scanning probe-microscopy manipulation by top-down fabrication approach, and molecular machines and DNA motors as well as harvesting natural biomotors by bottom-up chemical synthesis, have been reported [144].

Moreover, "artificial-muscle materials" composed of conducting and ionic polymers, dielectric elastomers and other materials can expand or contract upon application of an electric field or a pH change. Nanowires of PPy doped with dodecylbenzenesulfonate anions (DBS) electrochemical polymerized by using alumina membrane (200 nm in diameter and 60 mm in thickness) as the template showed that the nanowires expanded /contracted by approximately 3% of their original length under applied voltage [144d]. Those nanoactuators are suitable for operation in a wide variety of environments, such as blood plasma or salt water, with potential applications in micro- and nanofluidics for medicine, biosciences, and environmental monitoring because of the electrochemical actuation requiring only the presence of small, positively charged ions in the fluid [144d].

Obviously, the conducting polymer-based artificial muscles are different from nature muscles. Firstly the driving power in nature muscles is chemical energy that is differs from the conducting polymer based-artificial muscles, where the driving force results from the consumed electric charge with redox reaction. Moreover, natural muscles work only under contraction owing to the irreversibility of chemical reactions whereas conducting polymer-based artificial muscles work under both contraction and expansion due to reversal of the electrochemical reactions. From a practical point of review, new devices of microrobotics and micromachinery can be constructed by conducting polymer-based actuators and artificial muscles. In order to realize above applications, somewhat difficulties related to material synthesis and device fabrication have to be overcome.

3.6   Others

Except for above-mentioned applications of the conducting polymers, conducting polymers as new corrosion and electrostatic dissipation materials as well as separated membranes and conducting textiles have also received attention. Concept, method and feature of these applications are briefly discussed as below.

3.6.1   Corrosion Materials

Corrosion, which is essentially an electrochemical process, is the destructive result of chemical reactions between a metal or metal alloy and its environment. Corrosion generally divides to corrosion science and engineering. Corrosion science

is studying chemical and metallurgical process occurring during the corrosion process, whereas corrosion engineering involves design and application of methods to prevent corrosion. Both above-investigations are necessary to develop useful methods and materials for the prevention and control of corrosion [145]. In principle, if a perfect barrier layer is applied to the surface of a metal exposed to a corrosive environment, then neither oxygen nor water can reach its surface and corrosion will be prevented. Most coatings, however, are not perfect barriers due to either existing pinholes in the coating or diffusion of oxygen and water. An impervious coating layer, such as paint cover surface of metal is the most common approach to prevent a metal from corrosion. Besides, common efficient methods for corrosion protection involve both chemical and electrochemical techniques, such as chemical inhibitors, cathodic protection, and anodic protection [145a].

As discussed in Chapter 1, a reversible change in oxidation/reduction of conducting polymers is accrued by chemical or electrochemical reaction. Therefore, conducting polymers are capable of providing all above-three types of corrosion inhibitors for iron. Pyrrole and its derivatives were found to be effective corrosion inhibitors for iron and aluminum allays in both hydrochloric and sulfuric acid solution [146]. In 1985, DeBerry [147] found that PANI electrochemically deposited on ferrite stainless steels provided a form of anodic protection that significantly reduced corrosion rate in sulfuric acids solution. After that, MacDiarmid et al. [148] used potentiostatic techniques to measure anodic current from a corroding iron surface. Although their results indicated the cell current was reduced when the iron was coated with PANI, no definitive conclusion could be reached about quantitative corrosion protection by conducting polymers because the influence of surface coverage at the anode was neglected [148]. The results indicated that the electrochemical deposition of PANI was preceded by the formation of a passive oxide layer on the steel surface, in other words, the doped PANI layer in electrochemical contact with the steel established the passive oxide layer against dissolution and reduction. Thus the electron transfer exchange with the metal may be partially responsible for the ability of PANI to maintain the passivity of the stainless steel. Moreover, aniline for corrosion protection of metal in different electrolytes was also reported [149]. Other conducting polymers, such as PTH, polyacylamide, polyphenylene oxide, and their derivatives were also studied as the corrosion inhibition. Detail review on the corrosion subject was given [1b]. However, corrosion mechanism of the conducting polymer-based corrosion materials is not clear. Moreover, searching efficient conducting polymers and their derivatives as the corrosion inhibition for metal still need.

3.6.2   Electrostatic Dissipation Materials

As well known, charge is easily accumulated on the surface of insulator materials and accumulation of electrostatic charge on the surface of materials often results

in discharge suddenly, which will damage to electronic devices or human health. With the rapid advancement in electronic data processing and communication systems, moreover, electronic components have become increasingly smaller and are inherently more sensitive to electrostatic discharge. Thereby electrostatic dissipation has received great deal attention in protecting damage of electronic devices or packaging materials. The ideal situation of discharge protection is that the surface resistance of the electrostatic dissipation materials should be less than about $1 \times 10^{10} \, \Omega/\square$, preferably between 10^5 and $10^{10} \, \Omega/\square$ [1b].

Carbon and metal-based coating layer is as common electrostatic dissipation materials. As mentioned in Chapter 1, conducting polymers are as electrostatic dissipation materials are expected, because their conductivity covers semiconductor-metal region, which is enough higher than that of resistance requirements in electrostatic dissipation. However, thin films or layers coated on the surface insulating substrate (e.g. plastics) need in order to make electrostatic dissipation materials. As discussed in Chapters 1 and 2, most conducting polymers in the doped form are infusible and insoluble in common organic solvent. Thus processing into coating and films of conducting polymers on an industrial material has met with severe limitations. To solve processing of conducting polymers is therefore a key to fabricate electrostatic dissipation materials. There are two approaches to process conducting polymers into coatings or films: one is to synthesize soluble conducting polymers in organic solvent by modifying or manipulating the chemistry of the conducting polymers; another is to form composites by dispersing the intractable conducting polymers into the conventional polymers. Detail methods can be found in Chapter 2.

As one knows, PANI is the most possible to be used as the electrostatic dissipation coating or films on the substrate (e.g. plastic) because of its high conductivity, low cost, easy of synthesis and stability in air. In particular, its processability has been basically solved by structural modifying, counter-ion-inducted, secondary doping and self-doping tools [1b]. Among those tools, *m*-cresol acts as "secondary doping" that is particularly valuable where coatings and films with high quality are desired. However, *m*-cresol solvent is disadvantageous, for instance, the application of coatings is firstly limited to glass and other substrates that are resistant to *m*-cresol, and the toxicity of *m*-cresol solvent is very unlikely in practical application. PPy is also reasonable to be used as electrostatic dissipation materials due to its high conductivity and stability in air. Plastic films coated with an antistatic layer of pyrrole have been prepared by polymerizing pyrrole on the surface of the film or by use of PPy grafted onto latex particles [150]. However, PPy is less attractive than PANI because of expensive pyrrole monomer and high absorption at practically all wavelengths in the visible spectrum. A detail review dealing with synthesis, properties and promising applications of the conducting polymer-based electro-static dissipation materials is given in Reference [1b]. Application of the conducting polymer-based electrostatic dissipation as packaged materials is reasonable. However, to reduce cost of

fabrication and to enhance humidity independence for practical applications of conducting polymer-based electrostatic dissipation are still required.

3.6.3　Separated Membrane

Membranes are useful in such far-ranging applications as separating oxygen and nitrogen from air, desalinating seawater, removing organics from waster steams, and separating pure ethanol from its azeotropic mixture with water. Polymers have distinct advantages as membranes for purification of many liquids and gases because they are easily synthesized and processed into flexible thin sheets or high surface area hollow fibers that allow large fluxes of gases or liquids through the membranes. The separation process is divided into three distinct parts of adsorption, diffusion and de-sorption. The adsorption of the constituent feed mixture onto the membrane is called as "adsorption" process. The movement through the membrane and loss out the other side of the membrane are called as "diffusion and se-sorption process", respectively. In principle, the physical process of the permeation is described mathematically in terms of permeability (P), diffusion (D) and solubility (S), which can be calculated using the relationship $P = DS$, assuming the polymer is not plasticized by the penetrate [151]. The slope of the steady-state flux yields permeability (P), while the diffusion coefficient (D) is calculated from the extrapolation of the line at steady-state through the line axis and is described by the equation $\tau = L^2/(6D)$, where τ is the time and L is the thickness of the membrane. Solubility can be determined with the calculated values for P and D from the relationship $P = DS$ [151]. In addition, the separating ability of the membrane for a particular gas is described by the ratio of the individual gases permeability coefficients and is called the separation factor (α), where α is represented by a ratio of P_A to P_B. The separation of gases and liquids depends on the membrane's permeability to each component, which are affected by solubility and diffusion [151]. The diffusivity component is influenced by the physical properties of the polymer, for instance, the glass transition temperature, crystallinity and cross-linking [152]. Solubility is influenced by both chemical and physical factors, such as plasticizing agent and substituent groups that allow more favorable interactions between the permeant and the polymer. Surface area of the membrane also affects the efficacy of a polymer membrane for separations.

As mentioned in Chapter 2, since molecular structure and physical properties of PANI can be changed by adjusting oxidation and protonation state, PANI is an excellent example of a conjugated polymer that can be tailored to specific separation applications through the doping process [153]. It is found that doping and de-doping PANI results in increased permeability's relative to as-cast films owing to localized morphological changes from the addition and removal of the

dopant counter-ions. This indicated that the doing process can be used to modify after membrane formation, opening up new possibilities for enhancing selectivity. Especially re-doping with small amounts of dopants can lead to very high selectivity from important gas pairs, such as O_2/N_2, H_2/N_2, and CO_2/CH_4 [154]. Moreover, the highest current O_2/N_2 selectivity was reported by three independent research teams [154, 155]. Author [156] also found that the permeability was strongly affected by the dopant structure and degree as well as the oxidation state of PANI. In addition, the doping process can be used to control hydrophilicity for liquid separations. However, a future challenge is to develop pinhole-free ultrathin membranes to achieve high flues.

3.6.4 Conducting Textiles

Textiles provide an ideal substrate because of their high surface area, wide range of mechanical properties, high flexibility and large-scale availability. With the rapid development of the electronic industry, conducting textiles have found wide application in the fields of EMI shielding material and static dissipation [1b]. Blending or filling tools have been widely used to fabricate conducting textiles [1b]. Although the blending or filling is a simple method for fabricating conductive textiles, high incorporation of conducting materials (e.g. carbon or metal powders) in the composites reduces mechanical properties of the blends, resulting in considerable processing problems in the production of textile fibers [157]. Another route to conductive textiles is coating with metals. The metal coating on the textiles can be fabricated by vapor deposition, sputtering, reduction of copper salts and electro-deposition using Nobel metal catalysts [158]. Compared to blending or filling route, coating approach with metals is more expensive because some expensive instruments are required.

Conducting polymers offer an interesting alternative to filling or coating plastic or nature textiles. The surface resistance of conductive textiles is usually below $1 \, \Omega/\square$ for metal-coated fibers and above $10^3 \, \Omega/\square$ for carbon-based blend, respectively. Surface resistances of the PPy or PANI-based conductive textiles is about $10 - 10^3 \, \Omega/\square$ [158]. Moreover, conducting polymer-based conductive textiles are advantageous of their excellent adhesion and non-corrosive character compared to metal-coating textiles. However, those conducting polymers are of disadvantageous of brittle, expensive to produce and difficult to manufacture on a large scale.

Conducting polymer-based conductive textiles can be fabricated by *in-situ* polymerization, two-step and dispersion processes. *In-situ* polymerization consists of adsorption of monomer on the surface of the textiles and consequently oxidation polymerization process. Thus the *in-situ* adsorption process of monomer on the surface of the textiles is very important for preparing homogenous and uniform coating layer of conducting polymers on the textiles [159]. The maximum surface

resistance of the conducting polymer-based conductive textiles is as low as 5 $\Omega/\square$. Two-step process is that textiles impregnated with oxidant (e.g. ferric chloride) and then exposed to a solution of monomer (e. g. aniline or pyrrole) [160]. *In-situ* polymerization is normally conducted in aqueous media, whereas a two-step process can be accomplished using a variety of solvents, which influence on the properties of the resultant conductive textiles. Aqueous emulsions of conductive polymers have been also used to fabricate conductive textiles in the presence of fibers [161]. Among those conducting polymers, PPy and PANI are generally used to prepare conductive textiles by above tools. It is found that research of PPy-based conductive textiles is more active than that of PANI-based conductive textiles. The reasons for that may be due to concerns that the highly toxic benzidine moiety formed during the oxidative polymerization of aniline under acidic conditions and incorporated in the polymeric structure.

The mechanical and electrical properties, adhesion of coating layer to the textiles as well as stabilities of the conducting polymer-based conductive textiles are considered for their application in technology. In general, the mechanical properties of conducting polymer-based conductive textiles are rather poor because of their cross-linked nature and aromatic character of the backbone. Textiles coated with a thin layer of conducting polymer might essentially have the same mechanical properties as the textiles. It is expected that the intermolecular forces leads to strong adhesion at the conducting polymer/textile interface. However, a few papers have addressed the adhesion of polypyrrole-coated fabrics with epoxy resins. In addition, the electrical properties of conducting textiles depends on the mass of the substrate, the diameter of the individual textile fibers, the thickness of the adsorbed layer, and the intrinsic volume conductivity of the conducting polymers. The conductivity of those conducting textiles can be also measured by four-probe method as in measurements of conducting films or pressed pellets. However, the resistance of conducting textiles is normally expressed as a sheet resistance in ohms per square ($\Omega/\square$) rather than a volume resistivity or conductivity because of the coating being much thinner than the textile materials.

The stability of conducting textiles is an important concern for their application. It has been demonstrated that the stability of conducting textile is affected by the degradation of the textiles resulted from interruptions in the percolation network of the textiles, and feature of blending or filling and coating conductive materials. The stability of metal-based conductive textiles is mainly limited by corrosion of metals. Although conducting polymer-based conductive textiles are without corrosion problem, relatively high reactivity of conducting polymer with a variety of atmospheric chemicals (e.g. oxygen) results in much less stability in air. Isolation from the environment with a protective coating or laminate has been used to improve the stability of conducting polymer-based conductive textiles in air [162].

In summary, conducting polymers as functional materials become a major field in material sciences and technologies at the present time because of their unique properties and promising applications in electro- and optic as well as

electro-chemical devices. Although many offers on fundamental and application research for development of their applications in technology have been done, their commercial applications are still not realized. As one knows, commercial application for a material actually is difficult and needs long time to solve all problems associated with materials and technologies. Moreover, commercial application for a material also considers low cost, fabrication easy, friendly environment, long life and highly competition with other materials. Up to date, properties of conducting polymers and their devices obtained at the present time are not well comparable with inorganic materials and their devices. Based on above analysis, thus, idea of the conducting polymers replaying inorganic materials is not reasonable. On the contrary, the conducting polymers are used to solve some problems, which inorganic materials are not able doping, might a good way to realize application of conducting polymers in technology.

References

[1] a) *An Introduction to Molecular Electronic* (Eds. M. C. Petty, M. R. Bryce, D. Bloor, E. Arnold). Edward Arnold: London, 1995; b) *Handbook of Conducting Polymer* (Ed. T. A. Skotheim). Marcel Dekker: New York, 1986 and 1998; c) *Conductive Electroactive Polymers* (Ed. G.G. Wallace; G. M. Spinks ; P. R. Teasdale). Technomic Publishing Co.: Lancaster, MI, 1997; d) *One-Dimensional Metals: Physics and Material Science* (Ed. S. Roth). VCH: Weinheim, Germany, 1995; e) In *Advanced Membrane Technology* (Ed. Li, N. N., E., Ho Drioli, W. S. W., Lipscomb, G. G.). Ann. NY Acad. Sci.: New York, 2003

[2] M. F. Hundley, P. N. Adams, B. R. Mattes. Synth. Met., 2002, 129: 291

[3] J. H. Burroughes, D. D. C. Bradley, A. R. Brown, R. H. Marks, K. Mackay, R. H. Friend, P. L. Burns, A. B. Holmes. Nature, 1990, 347: 539

[4] a) G. Grem and G. Leising. Synth. Met., 1993, 57: 4105; b) J. Gruner, H. F. Wittmann, P. J. Hamer, R. H. Frien, J. Huber, U. Scherf, K. Mullen, S. C. Moratti, and A. B. Holmes. Synth. Met., 1994, 67: 181; c) M. Hamaguchi and K. Yoshino. Jpn. Appl. Phys. Lett., 1995, 34: L587

[5] C. Zhang, H. von Seggern, K. Pakbaz, B. Kraabel, H. W. Schmidt, and A. J. Heeger. Synth. Mett.; 1994, 62: 35

[6] V. Ohmori, M. Uchida, K. Muro, and K. Yoshino. Jpn. Appl. Phys. Lett., 1991, 30: L1941

[7] M. Berggren, O. Inganas, G. Gustafsson, J. Rasmusson, M. R. Andersson, T. Hjecberg, and O. Wennerstrom. Nature, 1994, 372: 444

[8] M. S. Sze. Physics of Semiconductor Devices. Wiley-Interscience, New York, 1981; B. L. Sharma (Ed.), Metal-Semiconductor Schottky Barrier Junctions and Their Applications. Plenum, New York, 1984

[9] T. Tsutsui and S. Saito, NATOASI Ser. E. Appl.Sci., 1993, 246: 123

[10] P. Kay. Phys. World, P. 52, March 1995

[11] C. H. Lee, G. Yu, D.Moses, A. J. Heeger. Appl. Phys. Lett., 1994, 65: 664

[12] D. Adarm et al. Nature, 1994, 371: 141

[13] a) B. A. Gregg, M. A. Fox, A. J. Bard. J. Phys. Chem., 1990, 94: 1586; b) C. Y. Liu, H. L. Pan, H. Tang, M. A. Fox, A. J. Bard. ibid., 1995, 99: 7632

[14] R. N. Marks, J. J. M. Halls, D. D. D. C. Bradley, R. H. Frield, A. B. Holmes. J. Phys. Condens. Mater., 1994, 6: 1379

[15] a) P. T. Landsberg, T. Markvart. Solid-State Electron, 1998, 42: 657; b) T. Markvart, P. T. Landsberg. Polysica E., 2002, 14: 71

[16] a) C. J. Brabec, N. S. Sariciftci, J. C. Hummelen. Adv. Funct. Mater., 2001, 11: 15; b) N. S. Sariciftci, L. Smilowitz, A. J. Heeger, F. Wuldl. Science, 1992, 258: 1474; c) C. W. Tang, Appl. Phys. Lett., 1986, 48: 183; d) C. J. Brabec, F. Padinger, N. S. Sariciftcil. J. Appl. Phys., 1999, 85: 6866; e) M. GranstrÖm, K. Petritsch, A. C. Arias, A. Lux, M. R. Andersson, R. H. Friend. Nature, 1998, 395: 257

[17] G. Yu, J. Gao, J. C. Hummelen, F. Wudl, A. J. Heeger. Science, 1995, 270: 1789

[18] J. Bisquert, D. Cahen, G. Hodes, S. Rühle, and A. Zaban. J. Phys. B., 2004, 108: 8106

[19] F. Padinger, R. S. Rittberger, and Niyazi S. Sariciftci. Adv. Funct. Mater., 2003, 13: 85

[20] S. E. Shaheen, C. J. Brabec, N. S. Sariciftci, F. Padinger, T. Fromherz, J. C. Hummelen. Appl. Phys. Lett., 2001, 78: 841

[21] N. S. Sariciftci, and A. J. Heeger. U.S. Patent 5,3,1,183 (1994), U.S. Patent 5,454, 880 (1995); G. Yu and A. J. Heeger. J. Appl. Pyhs., 1995, 78: 4510

[22] a) S. E. Shaheen, C. J. Brabec, N. S. Sariciftci, F. Padinger, T. Fromberz, J. C. Hummelen. Appl. Phys. Lett., 2001, 78: 841; b) M. T. Rispens, A. Meetsma, R. Rittberger, C. J. Brabec, N. S. Sariciftci, J. C. Hummelen. Chem. Commun., 2003, 2116

[23] a) M. Prato. J. Mater. Chem., 1997, 7: 1097; b) M..T. Rispens, L. Sanchez, J. Knol, J. C. Hummelen. Chem. Commun., 2001, 161; c) L. Sanchez, M. T. Rispens, J. C. Hummelen. Angew. Chem., 2002, 41: 838

[24] N. C. Greenham, X..G. Peng, A. P. Alivisatos. Phys. Rev. B., 1996, 54: 17628

[25] W. U. Huynh, J. J. Dittmer, W. C. Libby, G. L. Whiting, A. P. Alivisatos. Adv. Funct. Mater., 2003, 13: 73

[26] J. Liu, T. Tanaka, K. Sivula, A. P. Alivisatos, and J. M. J. Fre'chet. J. Am. Chem. Soc., 2004, 126: 6550

[27] B. A. Gregg, F. Pichot, S. Ferrere, and Clark L. Fields. J. Phys. Chem. B., 2001, 103: 1422-1429

[28] J. Bisquert, D. Cahen, G. Hodes, S. Rühle, and A. Zaban. J. Phys. B., 2004, 108: 8106

[29] O'Regan B., Grätzel, M. Nature, 1991, 353: 737

[30] S. Tan, J. Zhai, B. Xue, M. Wan, Q. Meng, Y. L, L. Jiang and D. Zhu. Langmuir, 2004, 2934

[31] F. Padinger, R. S. Rittberger, and Niyazi, S. Sariciftci. Adv. Funct. Mater., 2003, 13: 85

[32] J. L. N. Violette, D. R. J. White, M. F. Violette. Electromagnetic Compatibility Handbook, Van Nostrand Reinhold Company: New York, 1987.

[33] a) C. Y. Lee, H. G. Song, K. S. Jang, E. J. Oh. Synth. Met., 1999, 102, 1346; b) X. C. Luo, D. D. L. Chuan. Composites: Part B, 1999, 30: 227

[34] a) J. Joo, A. J. Epstein. Appl. Phys. Lett., 1994, 65: 2278; b) A. J. Epstein, M.G. Roe, J. M. Ginder, H. H. S. Javadi, J. Joo. Electromagnetic Radiation Absorbersand Modulators Comprising Polyaniline, US Patent No.5,563,182, 1996; c) N. F. Colaneri, L. W. Shacklette. IEEE Trans. Instrum. Meas., 1992, 41: 291

[35] S. K. Dhawan, N. Singh, S. Venkatachalam. Synth. Met., 2002, 129: 261

[36] Y. Y. Wang and X. L. Jing. Poly. Adv. Tech., 2005, 16: 344

[37] J. Joo, C. Y. Lee. J. Appl. Phys,.2000, 88: 513

[38] Y.-P. Duan, S. H. Liu, and H. T. Guan. Sci. Tech. Adv. Mater., 2005, 6: 513

[39] J. A. Pomposo, J. Rodriguez, H. Grande. Synthetic Met., 1999, 104: 107

[40] A. Kaynak. Materials Research Bulletin, 1996, 31: 845

[41] E. F. Knott, J. F. Schaeffer, M. T. Radar. Cross Section Handbook. Artech House: New York, 1993, p. 237.

[42] International Encyclopedia of Composites, VHC:, New York, 1991, vol.6.

[43] P. Annadurai, A. K. Mallick, D. K. Tripathy. J. Appl. Polym. Sci., 2002, 83: 145

[44] H. S. Nalwa (ed.). Handbook of Organic Conductive Molecules and Polymers (four volumes), Wiley, New York, 1997

[45] P. Chandrasekhar. Conducting Polymers: fundamental and Applications, A Practical Approach. Kluwer Academic Publishers, 1999

[46] A. Kaynak. Mater. Res. Bull., 1996, 845: 8609

[47] R. Faez, I. M. Martin, M. -A. De Paoli, M. C. Rezende. Synth. Met., 2001, 119: 435

[48] H. H. S. Javadi, K. R. Cromack, A. G. MacDiarmid, J. A. Epstein. Phys. Rev. B: Condens. Matter, 1989, 39: 3579

[49] S. M. Abbas, A. K. Dixit, R.Chatterjee, and T. C. Goel. Mater. Sci. Eng. B, 2005, 123: 167

[50] P. M. Jayan. Chem. Rev., 1999, 99: 1787

[51] E. T. Thostenson, Z. Ren, T.-W.Chou. Compos. Sc. Technol., 2001, 61: 1899

[52] D. A. Makeiff, T. Huber. Synth. Met., 2006, 156: 597

[53] R. Faez, I. M. Artin, M. De. Paoli, M. C. Rezende. J. Appl. Polym. Sci., 2002, 83: 1568

[54] a) Y. Cao, M. X. Wan, S. Z. Li, J. C. Li. Chinese Patent No.891005956, 1990. 9. 6; b) M. X. Wan, W. X. Zhou and J. C. Li. Chinese Patent No. 95124933.9, 1996. 7. 7; c) M. X. Wan, S. Z. Li and J. C. Li. Chinese Patent No. 95124945.2, 2000.1.12

[55] L. N. Zakharev, A. A. Lemanskii. Wave Scattering by Black Bodies. Moscow, Sovetskoe Radio, 1972

[56] S. E. Lindsey, G. B. Street. Synth. Met., 1984, 10: 67; UK Patent 2192756, 1988

[57] a) A. F. Diaz, J. I. Castillo. J. Chem. Soc. Chem. Commun., 1980, 397; b) A. J. Heeger. J. Phys. Chem. B, 2001, 105: 8475

[58] T. Ito, H. Shirakawa, S. Ikeda. J. Polym. Sci.(Polym. Chem.Ed), 1974, 12: 11

[59] G. Mengoli, M. M. Musiani, D. Pletcher, S. Valcher. J. Appl. Electrochem., 1987, 17: 515

[60] J. Roncali. J. Chem. Rev., 1992, 92: 711

[61] L. W. Shacklette, R. L. Elsenbaumer, R. R. Chance, J. M. Sowa, D. M. Ivory, G. G. Miller G. G, R. H. Baugman. J. Chem. Soc. Chem. Commun., 1982, 361

[62] a) P. Novak, K. Muller, K. S. V. Santhanam, O. Haas. Chem. Rev., 1997, 97: 207; b) M. D. Levi, Y. Gofe and D. Aurbach. Polym. Adv. Mater., 2002, 13: 697

[63] S. C. Ng, and P. Miao. Macromolecules, 1999, 32: 5313

[64] K. S. Ryu, S. K. Jeong, J. Joo, and K. M. Kim. J. Phys. Chem. B.(published on web01/05/2007]

[65] Q. C. Gu, H. S. Xu. J. Appl. Polym. Sci., 1997, 66: 537

[66] M. A. Ratner, D. F. Shriver. Chem. Rev., 1988, 88: 109; J. Plocharski, H. Wycislik. Solid State Ionics, 1994, 69: 309

[67] N. Costantini, G. Wegner, M. Mierzwa, T. Pakula. Macromol. Chem. Phys., 2005, 206: 1345

[68] G. R. Pedro. Adv. Mater., 2001, 13,163; G. R. Pedro and T. G. Gloria. Adv. Mater., 2000, 12: 1454

[69] T. G. Gloria, M. T. R. Eva, G. R. Pedro. Chem. Mater., 2001, 13: 3693

[70] P. Gomez-Romero, M.Lira-Cantu. Adv. Mater., 1997, 9: 144

[71] M. Lira-Cantu, P. Gomez-Romero. Chem. Matyer., 1998, 10: 698

[72] S. Ye, and D. Be'langer. J. Phys. Chem., 1996, 100: 15848

[73] M. Liu, S. J. Visco, L.C. A. DeJonghe. J. Electrochem. Soc., 1990, 137: 750

[74] a) E. M. Genie's, S. Picart. Synth. Met., 1995, 69: 165; b) N. Oyama, T. Tatsuma, T. Sato, T. Sotomura. Nature, 1995, 373: 598

[75] B. E. Conway. Electrochemical Suppercapacitors: Scientific Fundamentals and Technological Application. Kluwer Academic /Plenum: Dordrecht, 1999

[76] M. Winter, and R. J. Brodd. Chem. Rev., 2004, 104: 4245

[77] S. A. Hashmi, R. J. Latham, R. G. Linford, and W. S. Schlindwein. Poly. International, 1998, 47: 28

[78] a) A. Nishino; J. Power, Sources, 1996, 60,137; b) J.P. Zheng, T.R. Jow ; J. Electrochem. Soc. 1995, 142: L6

[79] F. Marchioni, J. Yang, W. Walker, and F. Wudl. J. Phys. Chem. B, 2006, 110: 22202

[80] a) A. Rudge, J. Davey, I. Raistrick, S. Gottesfeld. J. Power Sources, 1994, 47: 89; b) A. Rudge, J. Davey, I. Raistrick, S. Gottesfeld. Electrochim. Acta, 1994, 37: 273

[81] Y. G. Wang, H. Q. Li, and Y. Y. Xia. Adv. Mater., 2006, 18: 2619

[82] a) G. S. Attard, P. N. Barltett, N. R. B. Coleman, J. M. Elliott, J. R. Owen, J. H. Wang. Science, 1997, 278: 838; b) G. Niu, K. Sichel, R. Hoch, D. Moy, H. Tennent. Appl. Phys. Lett., 1997, 70: 1480; c) S. Ghosh and O. Inganäs. Adv. Mater., 1999, 11: 1214

[83] A. G. McDiarmid, J. C. Chiang, M. Halpern, W. Huang, S. Mu, N. L. D. Somasiri, W. Wu, S. T. Yaniger. Mol. Crst. Liq. Cryst., 1985, 121: 173

[84] Y. Sato, K. Yomogida, T. Nanaumi, K. Kobayakawa, O. Yasuhiko, M. Kawai. Electrochem. Solid-State Lett., 2000, 3: 113

[85] V. Gupta, N. Miura. Electrochem. Sold-State Lett., 2005, 8: A630

[86] Y. Y. Wang, H. Q. Li and Y. Y. Xia. Adv. Mater., 2006, 18: 2619

[87] C. Zhou, and S. Kum. Chem. Mater., 2005, 17: 1997

[88] E. Frackowiak, K. Jurewica, S. Delpeux, F. Beguin. J. Power Sources, 2001, 97 – 98: 822

[89] a) J. N. Barisci, G. G. Wallance, D. R. MacFarlane, R. H. Baughman. Electrochem. Commun., 2004, 6: 22; b) J. N. Barisci, G. G. Wallance, D. Chattopadhyay, F. Papadimitrakopoulos, R. H. J. Baughman. J. Electrochem. Soc., 2003, 150: E409

[90] a) K. Juewicz, S. Delpeux, V. Bertagna, F. Beguin, E. Frackowiak. Chem. Phys. Lett., 2001, 347: 36; b) K. H. An, K. K. Jeon, J. K. Heo, S. C. Lim, D. J. Bae, Y. H. Lee. J. Elctrochem. Soc., 2002, 149: A1058; c) M. Hughes, M. S. P. Shaffer, A.C. Renouf, C. Singh, G. Z. Chen, D. J. Fray, A. H. Windle. Adv. Mater., 1999, 11: 1028

[91] R. M. Dell, D. A. J. Rand. J. Power Sources, 2001, 100: 2

[92] A. Karina Cuentas-Gallegos, Monica Lira-Cantu', Nieves Casañ-Pastor, and Pedro Gómez-Romero. Adv. Funct. Mater., 2005, 15: 1125

[93] A. J. Heeger. Angew. Chem. Let. Edn., 2001, 40: 2591

[94] A.G. MacDiamid, A. J. Epstein. Synth. Met., 1995, 69: 85

[95] J. Janata and M. Josowicz. Nature, 2003, 2: 19

[96] M. Angelopoulos. IBM J. Res. De., 2001, 45: 57

[97] Handbook of Advanced Electronic and Photonic Materials and Devices Vol.10 (ed. H.S. Nalwa), New York, 2001

[98] Polymer Sensors and Actuators (eds Y. Osada and E. D. de Rossi), Springer, Berlin, 2000

[99] K. H. An, S. Y. Jeong, H. R. Hwang, and Y. H. Lee. Adv. Mater., 2004, 16: 1005

[100] W. Zheng et al. Synth. Met., 1997, 84: 63

[101] D. K. Leng, Y. Williams, C. C. Janata, D. Petelenz. Appl. Phys. Lett., 1993, 63: 1413

[102] P. C. Wang, Z. Huang, A. G. MacDiarmid. Synth. Met., 1999, 101: 852

[103] E. Stussi, R. Stella, D. De Rossi. Sens. Actuators B, 1997, 43: 180

[104] C. P. De Melo, C. G. Dos Santos, A. M. S. Silva, F. L. Dos Santos, J. E. De Souza. Mol. Cryst. Liq. Cryst., 2002, 374: 543

[105] a) P. T. Sotomayor, I. M. Raimundo, J. G. Zarbin, J. J. R. Rohwedder, G. O. Neto, O. L. Alves. Sens. Actuators B, 2001, 74: 157; b) M. Kanugno, A. kumar, A. Q. Contractor. J. Electroanal. Chem., 2002, 528: 46; c) M. Matsuguchi, J. Io, G. Sugiyama, Y. Sakai. Synth. Met., 2002, 128: 15; d) Y. B. Wang, G. A. Sotzing, R. A. Weiss. Chem. Mater., 2003, 15: 375

[106] U. Kang, K. D. Wise. IEEE Trans. Electron. Devices, 2000, 47: 702

[107] J. Huang, S. Virji, B. H. Weiller, and R. B. Kaner. Chem. Eur. J., 2004, 10: 1414

[108] a) J. Liu, Y. H. Lin, L. Liang, J. A. Voigt, D. L. Huber, Z. R. Tian, E. Coker, B. Mckenzie, M. J. Mcdermott. Chem. Eur. J., 2003, 9: 605; b) J. Huang, S. Virji, B. H. Weiller, R. B. Kaner. J. Am. Chem. Soc., 2003, 125: 314

[109] H. -A. Ho, M. B-Aberem, and Leclerc. Chem. Eur. J., 2005, 11: 1718

[110] a) H. S. White, G. P. Kittlesen, M. S. Wrighton. J. Am. Chem. Soc., 1984, 106: 5375; b) G. P. Kittlesen, H. S. White, M. S. Wrighton. J. Am. Chem. Soc., 1984, 106: 7389

[111] R. M. Hernadez, L. Richter, S. Semanick, S. Stranik, T. E. Mallouk. Chem. Mater., 2004, 16: 3431

[112] K. Ramanathan, M. A. Bangar, M. Y. Yun, W. Chen, N. V. Myung and A. Mulchandani. J. Am. Chem. Soc., 2005, 127: 498

[113] a) G. Fasol. Science, 1996, 272: 1751; b) S. Nakamura, M. Senoh, N. Iwasa, S. Nagahama. Jpn. J. Appl. Phys., 1995, 34: L797; c) S. Nakamura, M. Senoh, S. Nagahama, N. Iwasa, T. Yamada, T. Matsushita, H. Kiyoku, Y. Sugimoto. Jpn. J. Appl. Phys., 1996, 35: L74

[114] J. R. Platt. J. Chem. Phys., 1961, 34: 826

[115] a) S. K. Deb. Appl. Optics.(Suppl), 1969, 3: 192; b) G. V. Granqvist. Phys. Thin Films, 1993, 17: 301

[116] a) L. Michaelis, E. S. Hill. J. Gen. Physiol., 1993, 16: 859; b) C. L. Bird, A. T. Kühn. Chem. Soc. Rev., 1981, 10: 49

[117] a) M. Green. Chem. Ind., 1996, 641; b) R. A. Batchelov, M. S. Burdis, J. R. Siddle. J. Electrochem. Soc., 1996, 143: 1050

[118] H. W. Heuer, R. Wehrmann, and S. Kirchmeyer. Adv. Funct. Mater., 2002, 12: 8994

[119] a) C. W. Tang, S. A. Van Slyke. Appl. Phys. Lett., 1987, 51: 913; b) J. S. Sheats, H. Antoniadis, M. Hueschen, W. Leonard, J. Miller, R. Moon, D. Roitman, A. Stocking. Science, 1996, 273: 884

[120] a) H. W. Heuer, R. Wehrmann, S. Kirshmeyer. Adv. Funct. Mater., 2002, 12: 89; b) P. Chandrasekhar, T. Dooley. J. Proc. SPIE, 1995, 169: 2528; c) P. Topart, P. Hourquebie. Thin Slid. Films, 1999, 352: 243; d) G. A. Sotzing, J. R. Reynolds. Chem. Mater., 1996, 8: 882

[121] a) N. Tessler. Adv. Mater., 1999, 11: 363; b) N. Tessler, G. J. Denton, R. H. Friend. Nature, 1996, 382: 695; c) M. D. McGehee, M. A. Diaz-Garcia, F. Hide, R. Gupta, E. K. Miler, D. Moses, A. J. Heeger. Appl. Phys. Lett., 1998, 72: 1536; d) N. Suganuma, C. Adachi, T. Koyama, Y. Taniguchi, H. Shiraishi. Appl. Phys. Lett., 1999, 74: 1

[122] A. G. MacDiarmid. Angew. Chem. Int. Ed., 2001, 40: 2581

[123] a) T. K. Obayashi, H. Yoneyama, T. Tamura. J. Electroanal. Chem., 1984, 161: 419; b) T. Kobayashi, H. Yoneyama, T. Tamura. J. Electroanal. Chem., 1984, 177: 281; c) J. E. Dubois, F. Garnier, G. Tourillon, M. Gazard. J. Electroanal. Chem., 1983, 148: 299; d) E. W. Tsai, S. Basok, J. P. Ruiz, Reynolds, K. Rajeshwar. J. Electroanal. Chem., 1989, 136: 3683

[124] H. W. Heuer, R. Wehrmann, and S. Kirchmeyer. Adv. Funct. Mater., 2002, 12: 89

[125] I. Schwendeman, R. Hickman, G. Sönmez, P. Schottland, K. Zong, D. M. Welsch, J. R. Reynolds. Chem. Mater., 2002, 14: 3118

[126] P. H. Aubert, A. A. Argun, A. Cirpan, D. B. Tanner, and J. R. Reynolds. Chem. Mater., 2004, 16: 2386

[127] S. F. Frolov, Fujii, D. Chinn, Z. V. Vardeny, K.Yoshino, R. V. Gregory. Appl. Phys. Lett., 1998, 72: 2811

[128] D. M. Delongchamp, and P. T. Hammond. Chem. Mater., 2004, 16: 4799

[129] G. Decher, J. D. Hong, J. Schmitt. Thin Solid Films, 1992, 210: 831

[130] D. D. Longchamp, and P. T. Hammond. Adv. Mater., 2001, 13: 1455

[131] D. M. Delongchamp, and P. T. Hammond. Chem. Mater., 2004, 16: 4799

[132] F. Huguenin, M. Ferreira, V. Zucolotto, F. C. Nart, R. M. Torresi, and O. N. O. Jr. Chem. Mater., 2004, 16: 2293

[133] E. Kim, and S. Jung. Chem. Mater., 2005, 17: 6381

[134] a) G. Horanyi and G. Inzelt. Electrochim. Acta, 1988, 33: 947; b) G. Tourillon and F. Garnier. J. Electroanal. Chem., 1984, 161: 51; c) T. Yeu, K. -M. Yin, J. Carbajal, and R. E. White. J. Electrochem. Soc., 1991, 138: 2869; d) Y. Qiu and J. R. Reynolds. Polym. Eng. Sci., 1991, 31: 6; e) R. M. Penner, L. S. Van Dyke and C. R. Martin. J. Phys. Chem., 1988, 92: 5274; f) A. Talaie and G. G. Wallance. Synth. Met., 1994, 63: 83

[135] a) T. F. Otero, J. M. Sansinena. Biolectrochem. Bioenerg., 1995, 38: 411; b) R. H. Baughman. Synth. Met., 1996, 78: 339

[136] a) E. Smela, O. Inganäs, I. LundstrÖm. Science, 1995, 268: 1735; b) Q. Pei, O. Inganäs, I. LundstrÖm. Smart Mater. Sruct., 1993, 2: 1; c) Q. Pei, O. Inganäs, I. LundstrÖm. Adv. Mater., 1992, 4: 277; d) K. Akaaneto, Y. Min, A. G. MacDiarmid. U.S. Patent 5,556.700, 1996

[137] R. H. Baughman, L. W. Shacklette, R. L. Elsenbaume, E. J. Plichta and C. Becht. in Molecular Electronics (P. I. Lazarev, ed). Kluwer, Dordrecht, Netherland, 1991

[138] a) T. F. Otero, and J. Rodriguez. in Intrinsically Conducting Polymers, An Emerging Technology (M. Aldissi, ed.). Kluwer, Doddrecht, 1993, p.179; b) Q. Pei and O. Inganas. Synth. Met., 1993, 55 – 57: 3718; c) T. F. Otero and J. M. Sansinena. Bioelectrochemi. Bioenerg., 1995, 38: 411; d) T. F. Otero and M. T. Cortes. Adv. Mater., 2003, 15: 279

[139] a) K. Kaneto, M. Kaneko, Y. Min and A. G. MacDiarmid. Synth. Met., 1995, 71: 2211; b) W. Takashima, M. Kaneko, K. Kaneto, A. G. MacDiarmid. Synth. Met., 1995, 71: 2265; c) W. Takashima, M. Fukui, M. Kaneko, and K. Kaneto. Jpn. J. Appl. Phys., 1995, 34: 3786

[140] a) X. Chen and O. Inganas. Synth. Met., 1995, 74: 159; b) S. Morita, S. Shakuda, T. Kawai and K. Yoshino. Synth. Met., 1995, 71: 2231

[141] L. Bay, K. West, N. Vlachopoulos, S. Skaarup. Presented at Proc. SPIE Int. Soc. Opt. Eng., Newport Beach, CA, 2001, 5 – 8: 54

[142] M. Satoh, K. Kaneto, K. Yoshino. Synth. Met., 1998, 14: 289

[143] W. Lu, E. Smela, P. Adams, G. Zuccarello, and B. R. Mattes. Chem. Mater., 2004, 16: 1615

[144] a) A. M. Fennimore, T. D. Yuzvinsky, W.-Q. Han, M. S. Fuhrer, J. Cumings, A. Zettl. Nature, 2003, 424: 408; b) H. G. Craighead. Science, 2000, 290: 1532; c) A. Requicha. Proc. IEEE, 2003, 91: 1922; d) Yevgeny Berdichevsky and Yu-Hwa Lo. Adv. Mater., 2006, 18: 122

[145] a) M. G. Fontana. Corrosion Engineering. McGraw-Hill, New York, 1986; b) D. A. Jones. Principle and Prevention of Corrosion. Prentice Hall, New York, 1996; c) H. H. Uhlig and R. W. Reive. Corrosion and Corrosion Control. Wiley, New York, 1985

[146] R. M. Hudson and C. J. Warning. Matal. Finish, 1996, 64: 63

[147] D. W. DeBerry. J. Electrochem. Soc., 1985, 132: 1022

[148] A. G. MacDiarmid. Short Course on Conductive Polymers. SUNY, New Paltz, N.Y. 1985

[149] a) C. C. Abdel-Aal and F. H. Assaf. Trans. SAEST, 1980, 15: 107; b) C. C. Nathan. Corrosion, 1953, 9: 199

[150] S. Jasne and C. Chiklis. Synth. Met., 1986, 15: 175

[151] W. J. Koros and G. K. Fleming. J. Membrane Sci., 1993, 83: 1

[152] J. Henis and M. K. Tripoli. Science, 1983, 200: 11

[153] a) M. G. Kanadthidis. Chem. Eng. News, 1990, 68: 36; b) M. R. Aderson, B. R. Mattes, H. Reiss and R. B. Kaner. Synth. Met., 1991, 41 – 43: 1151; c) R. B. Kaner, M. R. Anderson, B. R. Mattes, and H. Reiss. U.S.Patents 5,095,586 (Mar.17, 1992) and 5,358,556 (Oct.24, 1994)

[154] M. R. Anderson, B. R. Mattes, H. Reiss and R. B. Kaner. Science, 1991, 252: 1412

[155] a) S. Kuwabata and C. R. Martin, J. Membrane. Science, 1994, 91: 1; b) L. Rebattet, M. Escoubes, E. Genies, and M. Pineri. J. Appl. Polym. Sci., 1995, 57: 1595

[156] J. P. Yang, Q. S. Sun, X. H. Hou and M. X. Wan. Chinese J. Polym. Sci., 1993, 11: 121

[157] a) W. LÖbel. Mater. Sci., 1990, 16: 73; b) E. K. Sichel (ed). Carbon Black Polymer Composites. Marcel Dekker, New York, 1982

[158] a) H. Ebneth. Melli and Textilber, 1981, 62: 297；b) W. C. Smith. J. Coated Fabr., 1988, 17: 242

[159] a) R. V. Gregory, W. C. Kimbrell, and H. H. Kuhn. Synth. Met., 1998, 28: C623; b) E. M. Genies, C. Petrescu, and L. Olemedo. Synth. Met., 1991, 41: 665; c) H. H. Kuhn, and W. C. Kimbrell. U.S.Patents 4,803,096 (1989) and 4,975,317 (1990)

[160] R. B. Bjorklund and I. LundstrÖm. J. Electron. Mater., 1984, 13: 211

[161] A. E. Wiersma and L. M. A. Van de Steeg. Patent 0,589, 529 A1 (1994)

[162] H. H. Kuhn, W. C. Kimbrell, G. Worrell, and C. S. Chen. Tech. Pap.-Soc. Plast. Eng., 1991, 37: 760

Chapter 4　Conducting Polymer Nanostructures

Nowadays, functionalized nanomaterials, which size is $1-100$ nm, have been received great attention in nanosciences and nanotechnology because of their large surface area. Compared with their bulk materials, moreover, nanomaterials are advantageous of hollow structures. Therefore, the nanotubes or hollow nanospheres can be served as "nanoreactors", allowing chemical reaction carries out inside of the nanotubes or hollow spheres. Furthermore, multi-functionalized composite nanostructures are easily fabricated by coating other materials on the surface of the nanotubes or filling metal nanoparticles inside of the nanotubes. As demonstrated in Chapters $1-3$, conducting polymer nanostructures have unique properties such as π-conjugation polymeric chain, metal-like conductivity, reversible physical properties by a novel doping/de-doping process that can be used as molecule wires and nanodevices, resulting in attracting attention in nanosciences and nanotechnology. For the conducting polymer nanostructures, however, some basic issues are necessary to be solved:

(1) To search simple and efficient methods to synthesize or prepare conducting polymer nanostructures and to understand formation mechanism of various methods.

(2) To character molecular structure and to measure physical properties of the conducting polymer nanostructures, especially finding difference from their bulk materials and understanding their origin.

(3) Since the size of nanomaterials is in a range of $1-100$ nm, influence of size on the physical properties must be considered, which is called as size effect.

(4) To search fabrication technology and to improve properties of nanodevices made of conducting polymer nanostructures.

(5) To realize commercial application of conducting polymer-based nanodevices in technology. Discussions of this chapter are dealing with above-mentioned issues and following an order of synthetic method and formation mechanism, composite nanostructures, as well as physical properties and applications.

4.1　Synthetic Method and Formation Mechanism

Searching facile and efficient synthetic method is a basic and an important object for the conducting polymer nanostructures. Up to date, hard template and soft template method as well as physical methodologies (e.g. electro-spinning technique) have been employed to synthesize conducting polymer nanostructures and their

composite nanostructures. In the hard template method, porous membrane is required as a hard template that guides growth of the nanostructures within the pore in the membranes, leading to completely controlling nanostructures in morphology and diameter dominated by morphology and size of the pores. Since the hard template is often removed after polymerization in order to obtain pure nanostructures, resulting in complex preparation procedure. In the soft template method, super-molecule self-assembled via hydrogen bonds, $\pi - \pi$ stacking interactions, Van der Waals force and electrostatic interaction as the driving forces instead of the hard-template to grow the nanostructures. Therefore, the soft-template method is simpler than that of the hard template method owing to omitting the membrane as a hard template and post-treatment of removing template. Since the formation super-molecule as a soft-template is often affected by the reaction conditions, thus controllability of the soft-template synthesized nanostructures is lack compared with hard-template method. On the contrary, the less controllability of soft-template method might properly provide a great chance to prepare complex three-dimensional (3D) micro/nanostructures self-assembled from one-dimensional (1D) nanostructures, which is unable for the hard template method, because only cylindrical pores are available in the commercial membrane as a hard template. Besides, electro-spinning technique as a physical method has been used to fabricate conducting polymer nanofibers. However, it is difficult to prepare pure conducting polymer nanofibers due to their low viscosity dissolved in organic solvent. Thereby this method is generally used to fabricate composite nanofibers of conducting polymers. In this section, different synthesis methods and formation mechanism for resultant conducting polymer nanostructures and their composite nanostructures are reviewed in detail.

4.1.1   Hard Template Method

Martin explored template-synthesis method, for the first time, to prepare nanofibers or nanotubes and nanowires of conducting polymers [1]. As shown schematic template-synthesis method in Fig. 4.1, this method entails synthesizing the desired material within the pores of a nanoporous membrane as a template or "nano-reactor". In other words, each of the pores is served as a "beaker" that allows a piece of the desired material synthesized. Based on above definition of template method, obviously, the hard template method is of advantages as follows:

(1) It is general tool to prepare material nanostructures including metal, semiconductor and conducting polymers, even their multi-functional composite nanostructures. By using this method, various nanomaterials, such as semiconductors [2], carbons [3] and conducting polymers [1,4] have been prepared.

(2) The diameter of the nanostructures is controlled by size of the pores in the membrane as a template whereas the length and thickness of the nanostructures is usually adjusted by changing polymerization time. That is why the hard template
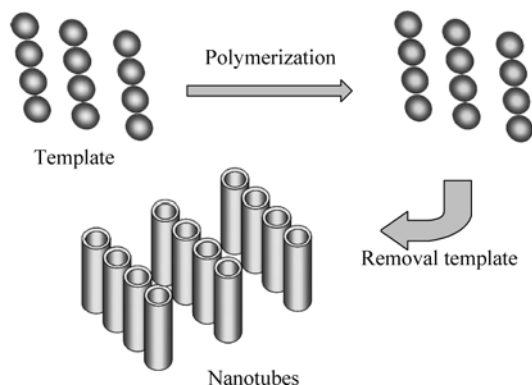
Figure 4.1   Scheme of template-synthesis method to prepare nanostructures

method is the most common and efficient approach to prepare well-controlling and oriented nanostructures; especially the diameter of nano-wires of conducting polymers can be achieved as 3 nm [5].

(3) The nanostructures can be chemically or electrochemically prepared by hard template method. This is particularly useful for the conducting polymer nanostructures because all conducting polymers can be synthesized by either chemical or electrochemical polymerization in the presence of dopants.

(4) The nanostructures (e.g. nanofibers or nanotubes) synthesized within the pores can be freed from the template membrane and collected. Compared to other methods, on the other hand, disadvantages of the hard template method are obviously, which are also summarized as follows:

(1) A membrane as a template and post-treatment of removing template is required that results in complicity of the preparing process, especially the post-treatments often destroy the nanostructures, leading to disorder of the nanostructures. To overcome this problem, Martin et al. [6] recently reported a new approach of oxygen plasma etch to effectively expose ends of gold nanowire template-synthesized by using polycarbonate membranes as a hard template. They observed that when these gold nanowire-containing membranes are exposed to O_2 plasma, the polymer at the membrane surface is selectively removed, exposing the ends of the Au nanowires. The length of the exposed nanowire is therefore controlled by varying the plasma etching time [6].

(2) Quantum of the resultant nanostructures is limited by the size of membrane as a hard template that limits its applications in large mass of the nanostructures required.

In general, hard template method is divided into chemical and electrochemical methods. Chemical synthesis of the hard template is accomplished by simply immersing the membrane into a solution of the desired monomer and its oxidizing agent, and then allows monomer polymerization within the pores reserving as "nano-reactor" [7]. By controlling the polymerization time, tubules with thin walls for short polymerization times or thick walls even fibers for long polymerization

times can be produced [7a]. However, entrance of monomer and oxidant into insides of those pores in the membrane is generally limited by capillary phenomenon produced by nano-scaled diameter of the pores. In the case of conductive polymers, on the other hand, above-problem can be solved by interaction between the nascent conducting polymer and the pore wall, because the polymers are cationic whereas the pore wall is anionic [1]. In order to overcome capillary phenomenon, a "molecular anchor", which interacts with the material being pre-deposited on the pore wall, is used [8]. For an electrochemical hard template synthesis, a metal film coated on one surface of the membrane is required in order to carry out electrochemical polymerization of the desired polymer within the pores of the membrane [4c]. Compared to chemical hard template method, although the electrochemical hard template method is more complex and expensive, it is controllable by changing current density, applied voltage and polymerization time. Like chemical template method, however, disadvantages of complex synthesis process and limited quantum by electrochemical hard template method still exist. So far a large number of conducting polymer nanostructures prepared by a chemical hard template method [1, 4f, 7a, 9] or by an electrochemical hard template method [4c, 10] have been reported.

Figure 4.2 shows typical nanofibers of PTH prepared by electrochemical hard template method [11]. Generally, hard template method is used to prepare nanofibers or nanotubes due to special cylindrical morphology of the pore in the membranes. However, recently nano-cones of PEDOT on commercially available carbon cloth were prepared by using nano-porous alumina membranes as templates [12]. Typical SEM images of the resultant nano-cones are shown in Fig. 4.3. Since the carbon cloth serves as the gas diffusion electrode, the nano-cone morphology results in remarkable fast charge transport, leading to superior electrochemical properties in comparison to the template-free synthesized PEDOT [12]. The low impedance of the nano-cones is promising for their application in polymer electrolyte membrane fuel cells [13].
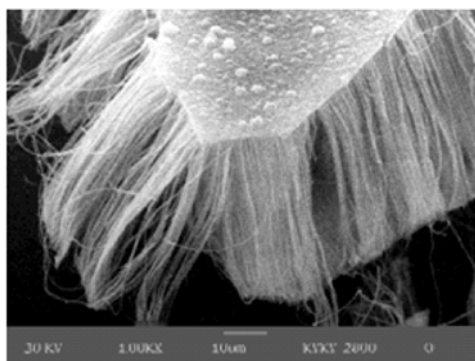

Figure 4.2   SEM images of polythiophene nanofibers prepared by electrochemical template synthesis method [11]
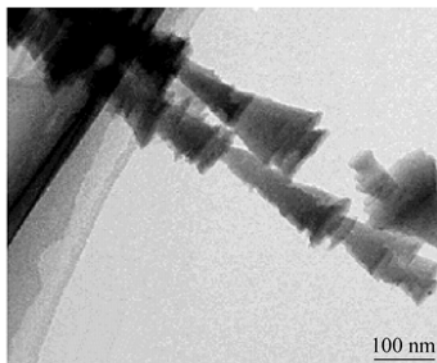
Figure 4.3 Nano-cones of poly (3-methyl) thiophene (PEDOT) using nano- porous alumina membranes as templates on commercially available carbon cloth [12]

According to definition of hard template method, membrane used as a hard template plays an important role in preparation of the nanostructures. Porous alumina membranes (Al_2O_3) and polycarbonate (PC) membranes are widely used as the commercial membranes. Porous alumina membranes are electrochemically prepared from aluminum metal and their pores are arranged in a regular hexagonal lattice and with a pore densities as high as 10^{11} pores/cm^2 [14]. Nowadays, membranes with a broad range of pore diameters even as small as 5 nm are available [15]. PC membrane prepared by "track-etch" method is another conventional hard template [16]. These membranes contain cylindrical pores across the membrane surface with a wide range of a pore diameters (down to 10 nm) and with a pore densities approaching 10^9 pores/cm^2. The PC membranes are also available commercially and a number of companies sell them with micro- and nanoporous [16]. Although these membranes are sold commercially, only a limited number of pore diameters are available [17].

Besides, other new type of membranes, such as a nano-channel array glass membrane [18], porous alumina silicate MCM-41 [5], mesoporous zeolites [19], micro-porous polymeric filtration membranes [11], carbon nanotubes [20], lipid tubule edges [21], electro-spun polymer fibers [22], highly oriented pyrolytic graphite (HOPG) [23] and DNA [24], have been also employed as the hard templates. Herein only DNA and seed as new hard-template are briefly reviewed.

1. DNA as A Hard Template

There are two reasons for DNA serving as hard-template:

(1) DNA templates are capable of directing chemical reactions without obvious structural requirements or functional group adjacency [25].

(2) The chiral nature of DNA raises a possibility that DNA-template synthesis can proceed stereo-selectively without the assistance of chiral groups [26]. On the other hand, poor conductivity in native DNA molecules prevents their direct use in electrical circuits [27]. One strategy to confer electrical conductivity to

DNA molecules is to deposit metals along the DNA strands [28], but their conductance is not controllable. Since metal-like conductivity of conducting polymers, a strategy for fabrication of conducting PANI nanowires on thermally oxidized Si surfaces by use of DNA templates has been reported [24]. The method avoided the agglomeration of DNA when complexes of conducting polymer (e.g. PANI) with DNA formed in solution.

Moreover, the conductivity of the PANI nanowires prepared by DNA as a template is sensitive to acid-base doping and un-doping processes, showing a potential application as sensors [24]. However, the pH value of the reaction solution must be controlled around 4.0, because a low pH value will destroy the DNA template.

2. Seed as A Hard-Template

Manohar et al. [29] firstly described a direct, one-step bulk chemical synthetic route to nanofibers of the conducting polymers by using seed as a hard template, which is also called as a seed method. Compared with above-mentioned traditional commercial membranes as the hard templates, the seed method is advantageous of:

(1) The seed template itself is capable of oxidative reacting with the monomer (e.g. aniline and pyrrole). In other words, the seed is served as both hard template and oxidant at the same time. As a result, the seed template method omits a post-treatment of removing template.

(2) The seed method is one-step to synthesize bulk quantities of nanofibers of the conducting polymers [30], for instance, $1-4$ mg of the seeds could be to synthesize PANI nanofibers of about 200 mg [29]. It therefore is a simple and inexpensive hard-template method to conducting polymer nanofibers.

(3) The seed method has been widely used to prepare various nanostructures including PPy, PEDOT and single-walled carbon nanotube bundles [29], PANI nanofibers [31], nano-fibrous hex peptide [32] and V_2O_5 nanofibers [33].

Although hard template is a universal and controllable approach to prepare conducting polymer nanostructures, in summary, development of new method and simplication of the preparation process for the hard template method is still challenge in realizing its practice application of conducting polymer nanostructures. Above-requirements promised author to search facial and efficient hard-template to special conducting polymer micro/nanostructures such as PANI nanostructures with many convolutions ($140-170$ nm in average diameter) that resemble the cerebral cortex of the brain using aniline/citric acid (CA) salts as the template and hollow octahedrons of PANI by using octahedral cuprous oxide (Cu_2O) crystal as the hard template. Above-samples will be discussed in detail in Chapter 5.

4.1.2   Soft Template Method

Self-assembly based on selective control of non-covalent interactions, such as

hydrogen bonds, Van der Waals forces, $\pi - \pi$ stacking interaction, metal coordination and dispersive forces provides a powerful tool for the creation of well-defined structures at a molecular level [34]. However, direct fabrication of complex nanostructures with controlled morphology, orientation, and surface architectures remains a significant challenge [35]. Among above-mentioned driving forces, hydrogen bonds is regarded as a main driving force in forming render nano-scaled conducting polymer nanostructures by self-organization [36]. The simplest materials through hydrogen bonds are block copolymers with spherical, cylindrical, and lamellar structures via a self-assembly process [37]. For the conjugated polymers, lamellar self-organization in PPy alkyl sulfates [38] and PANI-DBSA [39] were also observed. In particular, Monkman et al. [40] reported that hexagonal cylindrical structures can be prepared by super-molecular self-assembly of CSA doped PANI and hydrogen bonded with 4-hexylresorcinol (Hres). The method was simple just by mixing the components together. They also showed the conductivity of PANI-$(CSA)_{0.5}(Hres)_y$ complexes is increased when the cylindrical structures are formed due to a more extended conformation of PANI chains upon confinement in the cylinders. Another sample via hydrogen bonding to prepare conducting polymer nanostructures is polydiacetylene nanowires (40 – 100 nm in diameter) reported by Zhu et al. [41]. Interesting, the resulting nanowires might be a candidate for field emitters with a low turn-on field (~ 8.2 V/m) and a high current density (>5 mA/cm^2) at an applied field of 15 V/m can be achieved. However, two key conditions are required for the direct formation of the nanostructures via a hydrogen bonding approach: one is that the monomer is able to self-polymerization by irradiation of UV light and another is the self-polymerization polymer can be accured through non-covalent forces.

So far, new type of soft-templates, such as surface micelles [42], liquid-crystalline phases [43] and "soap bubble" [44] has been reported to prepare conducting polymer nanostructures via a self-assembly process. Various conducting polymer nanostructures, such as PANI nanotube junctions and dendrites [45], helical poly (ethylenedioxythiophene) [46], ribbon-like poly (p-phenylene vinylene) [47], wire-, ribbon-, and sphere-like PPy nanostructures synthesized by various surfactants (anionic, cationic, or nonionic surfactant) [48] have been reported. Although these results showed that the morphology and diameter of the self-assembled nanostructures are affected by the preparation conditions, controlling synthesis of the soft-template methods still challenge for material sciences. In the next, concept and typical conducting polymer nanostructures prepared by various soft-templates will be briefly reviewing.

1. Surfactant as Soft-Template

Surfactant is a class of molecules that form thermodynamically stable aggregates of inherently nano-scale dimensions both in solution and at interfaces. Surfactant self-assembly in a solution has been theoretically and experimentally investigated

owing to its importance in the synthesis of materials to micron scale structures with controlled dimensions. For a surfactant-only system, aggregation of the surfactant appears at a critical aggregation concentration that is called as a critical micelle concentration represented by CMC [49]. Moreover, the equilibrium size and shape of surfactant aggregates are controlled by a formula as [49]

$$V_0 / (al_0)$$

where V_0 and l_0 are the volume and length of the surfactant tail within the hydrophobic core of the aggregate and a is the effective area occupied by each surfactant head group at the surface of the aggregate. When a value of the above-parameter lies within the ranges $0-1/3$, $1/3-1/2$, or $1/2-1$, the favored aggregate morphology of the surfactant in a solution is spherical, cylindrical, or a flat bi-layer, respectively [49]. Self-assembly of surfactants at solid-liquid interfaces are also occurred and have been investigated by using *in-situ* atomic force microscopy (AFM) [50]. Phase transitions between morphologies are affected by electrolyte concentration [51], hydrophobic length or counterion type [52], surface chemistry [53] or the addition of co-adsorbing molecules [54]. The self-assembly ability of surfactants in a bulk solution therefore offers potential to fabricate micro- or nanometers as soft-templates whereas micellar polymerization can be used as the surface analogue to form thin polymer films on various surfaces by using adsorbed bi-layered surfactant aggregates as soft-templates [55]. For instance nonionic surfactants have been shown to act as soft-templates for preparing PEDOT orientation films [56]. Wire-, ribbon-, and sphere-like PPy nanostructures reported by Zhang et al. [48] are typical samples for the conducting polymer nanostructures produced by surfactants as the soft-templates. They reported that surfactants and oxidizing agents used in this study played a key role in tailoring the resultant conducting PPy nanostructures and their morphologies are greatly dependent on the monomer concentration, surfactant concentration, and surfactant chain length [48]. Author also directly synthesized PANI and PPy nanotubes or nanofibers in bulk by using amphiphilic molecules (e.g. β-naphthalene sulfonic acid (β-NSA)), which serves as surfactant and dopant at the same time [57]. The method, formation mechanism, structural characteristics and electrical properties of the nanostructures will be discussed in Chapter 5.

Among surfactants as soft-templates, reverse micro-emulsion is also a common route to prepare micro- or nano-structures of conducting polymers [58]. Reverse micelle is defined as an aggregate of surfactant molecules containing a nanometer-sized water pool in the oil phase. The most widely used surfactant to form reverse micelles is sodium bis (2-ethylhexyl) sulfosuccinate (AOT), which is an anionic surfactant with two hydrophobic tail-groups. AOT molecules favorably form reverse micelles in the oil phase because of their bulky hydrophobic tail-groups compared with the hydrophilic head-groups [59]. Several research groups have reported the chemical polymerization of PPy in the presence of AOT [58a]. By

using AOT reverse cylindrical micelles as the soft-templates, PPy nanotubes with about 94 nm in diameter and 2 mm in length has been synthesized [59]. Jang et al. [59] proposed that the reverse cylindrical micelle phase was developed through a cooperative interaction between aqueous $FeCl_3$ solution and AOT in a polar solvent. It means that iron cations were adsorbed to the AOT head-groups and led to the chemical oxidation polymerization of the corresponding monomer on the surface of the reverse cylindrical micelles.

They also pointed out that the aqueous $FeCl_3$ solution played a role in increasing the ionic strength and decreasing the second critical micelle concentration of AOT. Thus the AOT reverse cylindrical micelle phase is controlled by the experimental parameters including the weight ratio of aqueous $FeCl_3$ solution to AOT, type of solvent, and temperature. With increasing weight ratio of aqueous $FeCl_3$ solution to AOT, for instance, the nanotube diameter increased. On the other hand, the nanotube diameter increased when the hydrocarbon chain length of the polar solvents increased and the polymerization temperature was raised, respectively. When the technique was extended to PEDOT system by using same AOT (e.g. 2-ethylhexyl) and oxidant (e.g. $FeCl_3$) as PPy used [58a], interestingly, only nano-rods rather than nanotubes of PEDOT was obtained. Recently Manohar et al. [60] reported PEDOT nanotubes with $50 - 100$ nm in diameter and with a conductivity of $3 - 6$ S/cm could be synthesized by using a hexane/water reverse micro-emulsion consisting of AOT cylindrical micelles as the soft template and $FeCl_3$ as the oxidant, respectively. Besides, Li et al. [61] reported that dendritic PANI nanofibers with diameters of $60 - 90$ nm can be prepared by chemical oxidative polymerization of aniline in a special surfactant gel, which was formed by a mixture of hexadecyltrimethylammonium chloride ($C_{16}TMA$), acetic acid, aniline, and water at $-7\,℃$. These nanofibers are interconnected to form dendritic or network structures, rather than isolated nanofibers or bundles [62].

2. Colloidal Particles as Soft Templates

Colloids of the conducting polymers generally consists of an inner core of conducting polymer (e.g. PPy) and an outer layer of adsorbed stabilizer [63]. The stability of the dispersions arises from steric repulsion between the stabilizer molecules, leading to process of colloids. Several reports have recently demonstrated that macro-porous of conductive polymers, such as PPy [64], PANI [65] and PHT [66] can be formed with the colloidal particle arrays as the soft templates. Among those conducting polymers, the synthesis of PANI colloidal particles is commonly carried out by either chemical [67] or electrochemical [68] in the presence of a steric stabilizer. During the formation of the polymer, the stabilizer is usually adsorbed on the surface of the growing polymer particles, avoiding their aggregation and macroscopic precipitation. Therefore water dispersible colloids provide an easy way to overcome problems of conducting polymer (e.g.

PANI) processability, because they can be cast as films or blended with other water-soluble polymers.

Zhou et al. [69] reported well-ordered PANI honeycomb films polyelectrolyte-coated nano-sphere lithography by an electro-polymerization. Although colloids are advantageous of process, their disadvantages are also obviously as follows: ① Colloids are normally washed by dialysis that normally takes several days, even several hours by washing with an ultrahigh-speed centrifuge. However, PPy particles (from 1 nm to 1 μm) chemically prepared by using poly (styrenesulfonate) as a molecular template can be easily and quickly separated from the reaction medium and washed using either filtration or centrifuging due to their insolubility [70]. ② The colloids dispersion in aqueous media will not be acceptable for applications that require the polymer particles to stay in the solid state. Besides, the enzymatic polymerization of aniline in dispersed media as an environmentally friendly alternative to preparing stabilized PANI colloids [71], and colloids (50 – 350 nm in diameter) prepared by enzymatic polymerization using chitosan and poly (N-isopropylacrylamide) as steric stabilizers [72] have been recently resported

3. Structure-Directing Molecule as Soft-Template

Molecular template-guided synthesis is a common and efficient approach to prepare well-controlled diameter of the nano-materials, because the guest conducting polymers are synthesized within the channels or pores of a molecular template [73]. Poly (acrylic acid) (PAA) or poly (styrenesulfonic acid, SA) has been used to prepare PANI nanostructures as a molecular template [74]. The synthetic process consists of dissolving aniline monomer in a large amount of poly-acid, followed by oxidative polymerization of the monomer. When APS was added as the oxidant, such polymer-monomer complexes could be polymerized. The PANI-SA nanofibers are easily controlled by the concentration of aniline and SA. Up to date, various micro- or nanostructures, such as globule-like conglomerates [75], fibrillar network [76] and hollow micro-spheres [77] of PANI have been prepared by structure-directing molecules (e.g. poly (acylic acid)). Moreover, biopolymer-monomer complexes formed between a biopolymer (SA) with carboxylic groups and an organic monomer (e.g. aniline) with an amino group also play a role of the template for forming conducting polymer nanostructures [78]. Based on this idea, Xue et al. [78] have successfully prepared PANI-sodium alginate nanofibers with 40 – 100 nm in diameter by a template-guided process in a dilute solution of sodium alginate. They reported that the formation of the nanofibers depends on the reaction conditions, for instance, only spherical nano-particles were formed in the absence of SA or $FeCl_3$ was used as the oxidant [78]. Moreover, the oriented PANI nano-rods (80 – 400 nm in diameter and 8 – 15 mm in length) have been also prepared by hydrophilic Allura Red AC (ARAC) as the structure-directing agent [79]. It is proposed that the rod-like micellar arrays (i.e. ARAC/AN)

are responsible for directing the formation of the oriented PANI nano-rods. In addition, a family of self-assembling tri-block molecules with generation one 3,5-dihydroxy-benzoic ester dendritic segments, rigid rod-like segments, and various flexible coil-like segments, which referred to as dendron rod coil (DRC) molecules, has been reported [80].

4. Other Soft-Templates

Except for above mentioned soft-templates, oligomers, "soup bubbles", porous copolymer and phospholipid tubules have been also employed as the soft-templates to prepare conducting polymer nanostructures that will be briefly discussed as below.

(1) Aniline Oligomer as A Soft-Template

As one knows, there has been increased interest in synthesizing chiral conducting polymers or their nanostructures mainly because of their potential applications in chiral separations [81], surface-modified electrodes [81, 82] as well as chemical and biological sensors [83]. Chiral PANI nanofibers doped with CSA was a typical sample of using oligomer as a soft-template [84]. Besides, chiral PANI and its derivatives synthesized by either co-dissolving PANI or a chiral acid in common solvents [85] or by polymerizing aniline in the presence of a chiral acid [86] were also reported. However, the chirality of most of the chiral PANI synthesized from the above method was low. To achieve highly efficient chemical separations using chiral PANI as the chiral stationary phase, it is essential to have both high chirality and high surface area. Li et al. [84] recently reported a novel approach to synthesize chiral PANI nanofibers doped with CSA in an aqueous solution by using aniline oligomer as the template. They found that formation of high chirality of the chiral PANI nanofibers required following reaction conditions: ① High concentration of CSA in solution. ② Aniline oligomer [87] is not only regarded as soft-template in forming chiral nanofibers, but also acceleration polymerization reaction.

(2) "Soap Bubble" as Soft-Template

Electro-chemical polymerization is common, efficient and controlling method to prepare conducting polymers and their nano-structures. In general, it is found that small gas bubbles release from the surface of work electrode due to water decomposition when conducting polymers was prepared by electrochemical polymerization in an aqueous solution [44a]. Actually, the gas bubble associated with an aqueous solution containing monomer and surfactant functionalized dopant results in as called "soap bubble". Shi et al. [44a], for the first time, successfully obtained various α-NSA doped PPy microstructures including bowls, cups, and bottles by using "soap bubbles" as the soft-templates. Typical SEM images of the resultant nanostructures are shown in Fig. 4.4. They found that "soap bubble" size and the growth rate of PPy micro/nanostructures depend on the experimental conditions [44a].
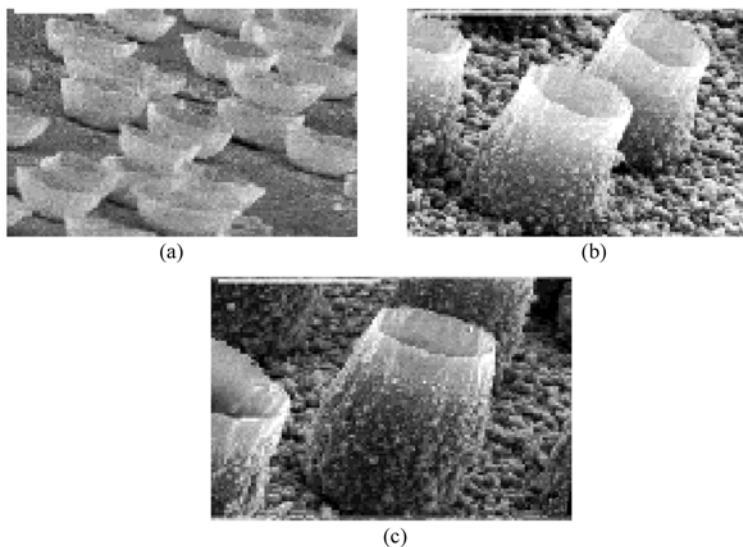
Figure 4.4   SEM images of the NSA doped PPy micro/nanostructures electro-chemically polymerized by using "soap-bubbles" as the templates [44a]

(3) Phospholipid Tubule as A Soft-Template

Phospholipid tubules with about 0.5 μm in diameter and 5 – 200 μm formed from diacetylenic phosphorylcholine have been reported [88]. Goren et al. [89] recently observed a highly selective, non-conformal growth of PPy on the edges, rather than on the surface of the phospholipid tubules. Figure 4.5 shows typical TEM images of the PPy nanostructures prepared by phospholipid tubules as the templates. They reported that once nucleation centers are deposited on the tubule edges, the propagation process occurs by diffusion of pyrrole or pyrrole radical cation into these growing nucleation centers either from solution, or from the tubule surface, and continue to grow there to form special morphology as shown in Fig. 4.5. Moreover, they also found that the nature of the oxidant (i.e. APS or $FeCl_3$) and the oxidant/monomer ratio are crucial in determining the eventual polymer morphology. A possible template mechanism was also discussed [89].

(4) Self-Assembly Process Associated with Gamma Rays

Pillalamarri et al.[90] recently reported PANI nanofibers with 50 – 100 nm in diameter and 1 – 3 μm in length can be produced in a "template-less" fashion in a single stage by irradiating aqueous solutions of aniline, APS, and HCl with gamma rays. It was reported that ionizing radiation affected the morphology of the polymer, but the morphology is unaffected by the polymerization reaction. They also found that ionizing radiation play an important role in formation of self-assembled nanofibers, because non-fibers of PANI were formed without ionizing radiation. In particular, they observed that when aniline was polymerized without irradiation, spheres with 20 – 40 nm in diameters were formed. During irradiation, on other hand, hollow spheres are aggregated to form nanofibers via diffusion-limited colloidal aggregation [91].
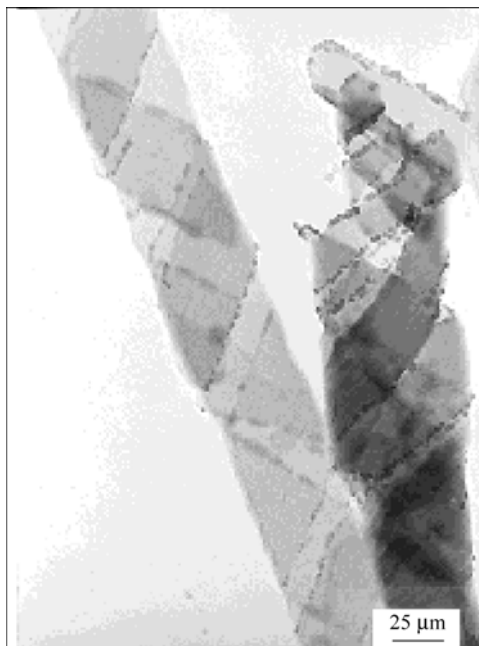
25 μm

Figure 4.5   Typical TEM images of PPy nanostructures prepared by phospholipid tubules as the templates [89]

(5) Super-Molecular Self-Assembly

Nandan et al. [92] recently report a super-molecular self-assembly approach for preparing highly oriented PANI nanowires (30 nm in diameter and several micrometers in length). The nanowires are formed by a unique hierarchical self-assembly in the complexes of the emeraldine base form of PANI with a phosphoric acid-terminated poly (ethylene oxide) (PEO) [93]. They proposed that the driving force for self-assembling such oriented nanowires may be due to strong repulsion between the ionic PANI backbone and nonionic PEO [93]. In general, amphiphilic organic dopants are very promising for preparing PANI nanostructures via a self-assembly process, because it might play a role of both dopant and soft-template at the same time. However, homogeneity in morphology for these self-assembled nanostructures is lack, because amphiphilic dopant molecules form thermodynamically stable aggregates of inherent nano-scale dimensions both in solution and at interfaces, which act as soft-template, affect overall morphology of the PANI [94]. Therefore, to understand the properties of these soft-templates in the synthesis of nanometer to micron scale APNI structures is very important. The emission property of the organic molecules is a powerful tool to identify the super-molecular aggregates such as micelles; the fluorescent tagged renewable dopant was utilized to understand the mechanism of PANI nano-materials [95], because the CMC of the dopant can be obtained from the emission studied.

Based on above idea, self-assembled nanostructured PANI by using new amphi-

philic dopant 4-[4-hydroxy-2((Z)-pentadec-8-enyl) phenylazo]-benzenesulfonicacid, which has fluorescing in water due to its hydrophilic polar head and hydrophobic alkyl chain, has been reported [96]. The new dopant possess unique amphiphilic geometry to form stable aggregates like bi-layers or micelles in water, and its emission behavior either alone or in complex with aniline showed a nonlinear trend with respect to concentration. Especially the amphiphilic dopant forms stable emulsion at a wider composition of dopant: aniline ratio (e.g. from 1:1 to 1:1,500 in moles) [96].

(6) De-Block Copolymer as Template

De-block copolymers compose of two different polymers, which are spontaneously self assemble into periodic nanostructures can be controlled by the molecular weight and composition of copolymers [97]. In a selective solvent for one of the blocks of de-block copolymers, for example, nanometer-sized micelles consisting of a soluble corona and an insoluble core are spontaneously formed [97, 98]. These micelles can be transferred onto solid substrates by Longmuir-Blodgett (LB) technology, dip-coating, or spin-coating methods to form a variety of nanostructures, which have been used as nanostructured templates to synthesize nano-particles or a lithographic mask to fabricate nano-pattern [98, 99]. The de-block copolymer approach for fabricating nano-structures is particularly advantageous for the functional materials difficult to be patterned with a conventional method [100]. Moreover, the approach is also possible to incorporate conducting polymers in nanometer-sized domains by their selective synthesis within the periodic nanostructure of de-block copolymers [101]. Yoo et al. [102] recently reported that a hexagonal array of polystyrene-block-poly (4-vinylpyridine) (PS-PVP) micelles containing $FeCl_3$ fabricated by spin coating was employed as a soft-template for synthesis of nanometer-sized domains of PPy. By exposing the micellar film to pyrrole vapor, the synthesis was directly carried out in the nanometer-sized pattern of the micellar film and the spherical domain turned to the wormlike domain as shown in Fig. 4.6.
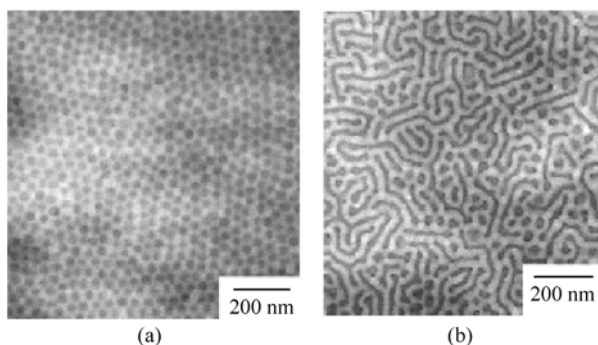

(a)   (b)

Figure 4.6   Plane-view TEM image of a spin-coated monolayer film of PS-PVP micelles containing $FeCl_3$ in the PVP core (b) and plane-view TEM images after exposure of a monolayer film of PS-PVP micelles containing $FeCl_3$ to pyrrole vapor for 20 min (a) [102]

Compared with hard-template method, in summary, soft-template methods are of advantageous as follows: ① The soft-templates are long range ordered and self-assembled structure from that provides well-defined rooms or channels for conducting polymer chains to grow into micro/nanometer-sized products. ② Those soft-template materials are easy to remove after the synthesis, and in the meantime, the micro/nanostructures of the resulting polymers can remain. ③ Morphology and formation of the soft-template is strongly affected by the reaction conditions, resulting in complex micro/nanostructures prepared by soft-template method. On the contrary, more complex micro/nanostructures prepared by hard-template method are difficult because of only membranes with cylindrical ropes being available. Soft-template method is therefore more simple and inexpensive because of omitting hard-template and post-treatment of removal template. However, controllability in morphology and diameter as well as orientation of the nanostructures still remains challenge in fabricating the nanostructures by a soft-template method. Further understanding self-assembly formation mechanism of various soft-template methods in preparing nanostructures might provide an efficient way to solve above-mentioned issues.

4.1.3   Other Methods

Except for above-mentioned hard and soft-template method, other routs, such as electro-spinning technique, interfacial polymerization, current-sensing atomic force microscopy (CS-AFM) and scanning probe microscopes (SPM) or scanning electrochemical microscope (SECM) as well as ordered mesoporous carbons as a precursor, have been also employed to prepare conducting polymer nanostructures. In the next, some of them will be briefly discussed.

1. Electro-Spinning Technique

Electro-spinning technique patented in the 1930s [103] has recently received intense interest in the preparation of polymer fibers with length larger than 100 m and diameters in the range of 30 – 2,000 nm [104]. In the electrospinning method to prepare fibers, in general, a high electrical field is applied between a polymer fluid contained in a glass syringe with a capillary tip and a metallic collection screen. When the applied field reaches a critical value, the charge overcomes the surface tension of the deformed drop of the suspended polymer solution from the tip of the syringe and a jet is produced. The electrically charged jet resulting in the hyperstrectching of the jet undergoes a series of electrically induced bending instabilities during its passage to the collection screen that results in the hyperstretching of the jet. These strectching processes accompanied by the rapid evaporation of the solvent molecules reduce the diameter of the jet. The dry fibers are accumulated on the surface of the collection screen, resuling in a nonwoven mesh of nano- to microdiameter fibers. The morphology and diameter

of the fibers are influenced by preparation parameters [105], such as the applied voltage, solution concentration, polymer molecular weight, solution surface tension, dielectric constant of the solvent, and solution conductivity. The electrospinning method is advantageous of fabricating long fibers and non woven meshes of polymers compared with hard and soft-template method. In electrospinning method, however, a soluble polymer with a high viscosity is required. Generally, it is difficult to prepare pure conducting polymer nanofibers by electro-spinning due to a low viscosity of the conducting polymers dissolved in organic solvent. Only composite nanofibers of conducting polymers are fabricated by using electro-spinning method [106]. In order to overcome this problem, electro-spun polymer fibers are used as templates to prepare tubular materials with controlled dimensions [107]. In this method, the electro-spun polymer nanofibers are used as the template and conducting polymers are then coated on the surface of the core fibers by *in-situ* deposition polymerization from solution containing monomer and oxidant. By this method, it not only can be prepared coaxial conducting polymer composite nanofibers, but also resulting in tubular conducting polymers after dissolving the core polymer. Therefore the selection of the core polymer to be used as the fiber template is critical to the process of the tubular materials. Another key requirement is that the decomposition temperature of the core fibers should not exceed the threshold to cause structural damage to the outer shell material. Dong et al. [108] successfully prepared PANI nanotubes by using this method in the presence of the electro-spun poly (*L*-lactide) (PLA) nanofibers as the template as shown in Fig. 4.7.
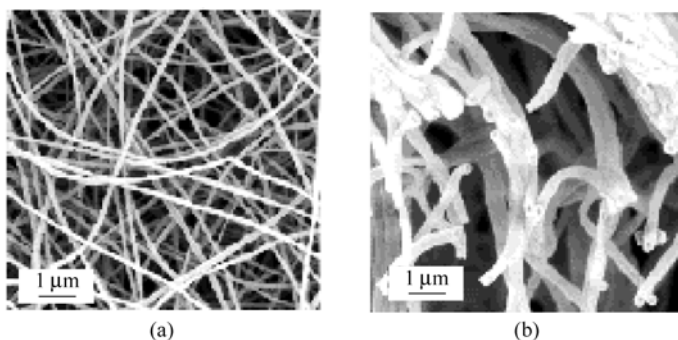

(a)   (b)

Figure 4.7   SEM images of PANI-EB/PLA coaxial fibers (a) and PANI nanotubes (b) after thermal removal of core fibers [108]

2. Interfacial Polymerization

Synthesis of large mass of conducting polymer nanostructures is required for realizing their application in technology. Obviously, template method is unsatisfied owing to limiting size of the template. Although electrochemical polymerization [109] and some physical methods, such as electro-spinning [106] and mechanical stretching [110], can also produce conducting polymer nanofibers without templates,

these nanostructured materials have also been made on a very limited scale. Recently, Kaner and coworkers [111] explored a facile chemical route to high-quality PANI nanofibers under ambient conditions using aqueous/organic interfacial polymerization. The method is called as "interfacial polymerization" that allows oxidative polymerization of aniline only takes place at the interface of organic/water phase, where organic phase consists of aniline whereas oxidant is in water phase, and the product is entered into water phase. The interfacial polymerization method is advantageous of as follows: ① Both the synthesis and purification are simple without template and no template-removing steps needed. ② The synthesis with a formation yield as high as 95% is easily scalable and re-producible, and ③ the nanofibers are readily dispersed in water, which could facilitate environmentally friendly processing and biological applications. Figure 4.8 shows interfacial polymerization of aniline in a water/chloroform system at different reaction times [111b].
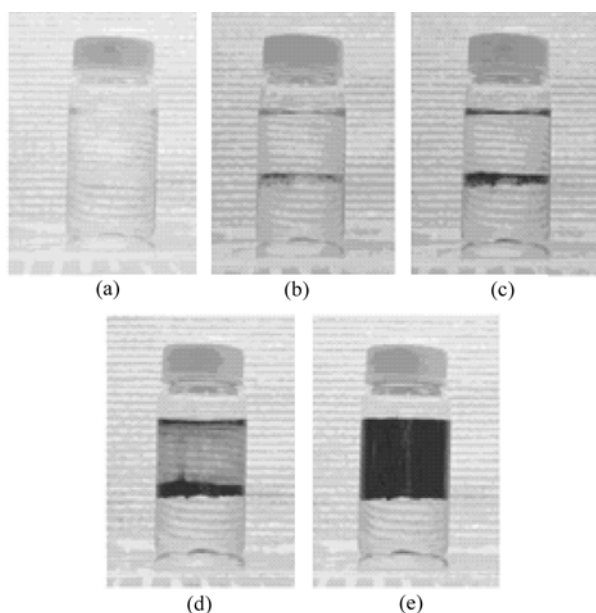
Figure 4.8   Snapshots show interfacial polymerization of aniline in a water/ chloroform system (From (a) to (d), the reaction time is 0, 1.5, 2.5, 4, and 10 min, respectively) [111b]

3. Ultrasonic Irradiation

Ultrasonic irradiation, in the frequency range from 20 kHz to 1 MHz, has been widely used in chemical synthesis, because it leads to an increase in the rate of many chemical reactions (e.g. organic, inorganic and polymerization) [112]. As well known, an ultrasonic wave can generate a very extreme reaction environment that is not only in its ability to accelerate reactions, but also in its ability to generate new chemistry which is not available using other methodologies [113].

Compared with other synthesis methods, some striking results have been reported [114]. For instance, Wang et al. [115] recently reported the PANI powder synthesized by using the ultrasonic method that typical synthesis procedure reported is as follows: a quantity of *p*-toluenensulfonic acid (e.g. 2.113 g) was dissolved in pre-cooled 200 mL of water solution ($\sim 0\,℃$). Aniline (e.g.4.0 g) was then added to the solution and dispersed by an ultrasonic disperser to form an emulsion followed by 16.9 g of APS dissolved in 50 mL of water slowly dropped into the emulsion for over 1 h, and the reaction then continued in the ultrasonic disperser at $0\,℃$ for 20 h [115].

Interestingly, they found that most particles synthesized by using ultrasonic method are thin hexagonal plates with $250-300$ nm in diameter as shown in Fig. 4.9. They also found that the conductivity and thermopower of PANI synthesized by the method are lower than that of samples synthesized by the conventional method. The poor conductivity of the PANI synthesized by the method may be due to the presence of non-conjugated units in the polymer resulted from ultrasonic irradiation during polymerization [115].
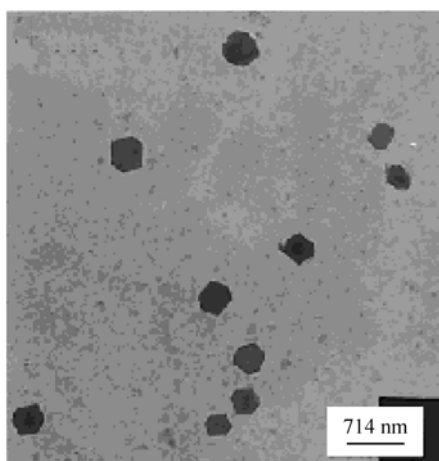
Figure 4.9   TEM images of PANI powders synthesized by ultrasonic irradiation [115]

Moreover, Gedanken et al. [116] reported nano-crystalline Cu_4O_3 embedded in PANI can be prepared in an aqueous solution of cupper (Ⅱ) acetate and aniline (1:10 molar ratio) by ultrasonic irradiation. They also reported that method can be used to prepare other metal oxides (e.g.Fe_3O_4) embedded in PANI to form multi-functionalized composites [116].

Above results showed that although large number of conducting polymer nanostructures including nanofibers or nanotubes and oriented nanostructures have been prepared by different methods, to search facile, high yield and controlling approachs for preparation of the conducting polymer nanostructures is still a basic and academicals object in the field of conducting polymer nanomaterials.

Author offered some novel approaches including hard and soft-template methods to prepare conducting polymer micro/nanostructures that will be discussed in Chapter 5 in detail.

4.1.4 PEDOT Nanostructures

Compared with studies on PANI and PPy nanostructures, as above-described, only a few reports of PEDOT nanostructures, such as nano-particles, nanocomposite particles, and colloidal core-shell particles, were presented [117]. However, a great progess of PEDOT nanostructures associated with applications in technology is achieved. Compared with other conducting polymers (e.g. PANI and PPy), moreover, PEDOT has some advantages as follows:

(1) It is unique conducting polymer with a small band gap, which confers high optical transparency in the doped state [118].

(2) It has a very high conductivity and stability in the doped films [118a, 119].

(3) PEDOT films show wide applications for antistatic layers in photographic films, conducting layers in electroluminescent devices, organic field effect transistors, hole injecting layers in polymeric LEDs and polymer photovoltaic cells [118a, 119a, 120]. Therefore, PEDOT nanostructures as typical sample of conducting polymer nanostructures emphasized on synthesis method will be briefly reviewed below.

1. Electrochemical Template Method

Like PANI or PPy, chemical or electrochemical template method is a conventional approach to prepare PEDOT micro/nanostructures. For instance, Kim et al. [122] reported PEDOT nanotubes electrochemically synthesized in the pores of aluminum oxide template. Moreover, Foulger et al. [123] reported that nanostructures of PEDOT (e.g., tubes, belts, rods, and thimbles) prepared in an aqueous solution by a chemical template-method using an Al_2O_3 membrane as a template. However, they faced difficulty in controlling the reaction rate due to lack of an interaction between the PEDOT and Al_2O_3 and the poor solubility of the 3, 4-ethylenedioxy-thiophene (EDOT) monomer in water. Therefore the synthesis process was changed by the Al_2O_3 membrane being first filled with EDOT monomer under negative pressure, and then the EDOT-filled Al_2O_3 membrane being quickly transferred to an aqueous oxidant solution to initiate the polymerization. Moreover, it reported that the solvophobic properties of the PEDOT polymer led to its preferential growth on the pore wall [123].

As above-mentioned, track-etched porous polycarbonate (PC) membrane is a good candidate for the flexible template. Compared with Al_2O_3 as a common hard-template, PC membrane is very flexible, commercially available with various pore diameters (0.01 – 20 μm), and quite transparent due to the thin film thickness (6 – 10 μm). Lee et al. [124] recently reported PEDOT nanotubes electrochemically

prepared by using PC as the template. They noted that the key parameters for controlling synthesis of the PEDOT nanotubes are applied potential, monomer concentration, and electro-polymerization time, in particular, electro-polymerization time controlled the length of the nanotubes [124].

2. Micelles as The Templates

Like PANI and PPy, PEDOT nanostructures can be also prepared by surfactant as a soft-template or synthesized in micellar solution. For instance, PEDOT particles in micellar solution templates have been prepared by using DBSA as a surfactant and $FeCl_3$ or APS as an oxidant in aqueous media [125]. Moreover, PEDOT nano-particles synthesized by emulsion polymerization in cyclohexane using polyisoprene-block-poly-(methyl methacrylate) (PI-b-PMMA) as the stabilizer and iron (Ⅲ) chloride as the oxidant have been also reported [126]. Interestingly, Zhang et al. [127] described the synthesis of PEDOT nanotubes using sodium bis (2-ethylhexyl) sulfosuccinate (AOT) cylindrical micelles as the templates. More recently, Mumtaz et al. [128] reported spheres of PEDOT synthesized in the presence of poly (ethylene oxide) (PEO) end-functionalized with a (3, 4-ethylenedioxythiophene) moiety using ammonium persulfate or iron (Ⅲ) p-toluenesulfonate hexahydrate as oxidizing agents.

3. Reverse Emulsion

Manohar et al. [127] reported PEDOT nanotubes with $50 - 100$ nm in diameter and with a conductivity of $3 - 6$ S/cm synthesized using a hexane/water reverse micro-emulsion consisting of sodium bis (2-ethylhexyl) sulfosuccinate (AOT) cylindrical micelles as the template and $FeCl_3$ as the oxidant. Besides, composite nanotubes of PEDOT nanotubes with noble metals (e.g. Ag), metal oxides (e.g. iron oxide) were also synthesized using post-synthesis or *in-situ* polymerization methods [127]. The dramatic change in morphology from granules to tubes was observed when the condition of AOT/hexane reverse micro-emulsion was changed. Interestingly, the as-synthesized and doped PEDOT nanotubes can be readily dispersed in common organic solvents and films cast on a variety of substrates [127].

4. Seed Method

Manohar et al. [129] recently reported conductive PEDOT nanotubes (~ 16 S/cm) with $100 - 180$ nm in diameter can be chemically synthesized by using V_2O_5 as a seed. Unlike of PANI or PPy nanostructures prepared in aqueous solution by V_2O_5 as a seed [130], a direct application of this method to the PEDOT polymer yields only granular powders due to a combination of low solubility of EDOT in aqueous mineral acids and dissolution of V_2O_5 seeds before onset of polymerization. This suggested that the polymerization rate of PEDOT should be faster than the rate of dissolution of V_2O_5 seeds. They therefore used organic acids, such as *DL*-camphorsulfonic acid (CSA), instead of aqueous solution, resulting in slow

dissolving V_2O_5 and the EDOT monomer dissolving completely. Figure 4.10 shows SEM images of PEDOT nanofibers synthesized by using V_2O_5 seeds.
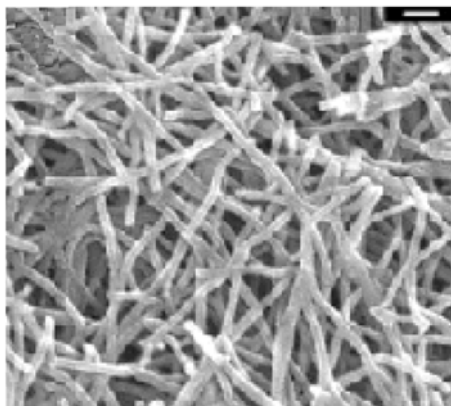

Figure 4.10   Scanning electron microscopy (SEM) images of PEDOT powder synthesized by using V_2O_5 seeds [129]

In summary, large number of conducting polymer nanostructures (e.g. PANI, PPy and PEDOT), their derivative and composite nanostructures has been prepared by different methods. High quality and controllability in morphology and diameter for the conducting polymer nanostructures synthesized by facile methods is still critical for their practical application in nano-devices.

4.2   Composite Nanostructures

Multifunctional nano-composites are a special class of materials, which origin from suitable combinations of two or more nano-particles have been received great attention because of their unique physical properties and wide application potential in diverse areas. Novel properties of nano-composites can be derived from the successful combination of the characteristics of parent constituents into a single material. One-component nanostructures (e.g. nano-rods) are now quite common, but there are relatively few examples of methods for synthesizing multi-component 1D or 3D materials made from both organic and inorganic materials [131]. Template-guided method is commonly used to generate such 1D-conducting polymer composite nanostructures. The method generally divides into two-step: conducting polymers are firstly synthesized within micro-porous Al_2O_3 membrane using a chemical polymerization method. Then the array of conducting polymer tubules in an Al_2O_3 matrix is subjected to electro-deposition of different metals (e.g. Fe, Co, Ni) covering one side by silver and using the Al_2O_3-conducting polymer array as the working electrode to fabricate the metallic nanowires grown within the conducting polymer nano-tubules confined in the

Al₂O₃ membrane. After dissolution of the outer membrane, metallic nanowires encapsulated in a conducting polymer envelope are obtained. Electrochemical polymerization of the monomer within the template at the metal block-solution interface is another common method to fabricate such 1D-composite nanostructures [132]. The latter approach provides excellent control over the block length of the metal and organic regions of the structure, simply by controlling the number of coulombs passed in the experiment. The limitation of the electrochemical approach is that only conducting materials can be deposited within the pores. Based upon above-described synthetic strategy, large number of papers dealing with 1D- and 3D-composite nanostructures of conducting polymers by different methods have been reported in the literature. Herein method and properties of different conducting polymer nano-composites are reviewed based on following orders: metal-conducting polymer composite nanostructures, conducting polymer/carbon nanotube composites; core-shelled composites, chiral and biological composite nanostructures and inorganic oxide nano-crystals.

4.2.1   Metal-Conducting Polymer Composite Nanostructures

Nano-particles of noble metals have attracted steadily growing attention due to their interesting optical [133], electrochemical [134], electronic, [135] and photo-electrochemical properties [136]. For instance gold nano-particles deposited on solid supports exhibit useful catalytic and electro-catalytic properties that are significantly dependent upon their size [137]. Kamat [138] reviewed importance of metal nano-particles, especially emphasized the photo-physical, photochemical, and photo-catalytic of metal nano-particles that would open these materials in the development of a new generation of nano-devices. As mentioned in Chapter 1, conducting polymers are one type of the most perspective materials because of their unique properties and promising application in technology [139]. Moreover, conducting polymers can be easily synthesized by both chemical and electro-chemical routes and preparation of various conducting polymers in both aqueous and nonaqueous solutions [139, 140]. As expected, combination of conducting polymer nanostructures with noble metals will become new composite nanostructures that remain the properties of each component in the composite nanostructures. For instance it has been demonstrated that the sensing and catalytic capabilities of PANI-metal nano-particle composites are enhanced compared to those of pure PANI [141]. Typical samples of nobel-PANI and PPy composite nanostructures will discussed as below.

1. Metal-PPy Composite Nanostructures

Electrochemical deposition is a promising technique for preparing nano-particles due to its easy-to-use procedure and low cost of implementation. Deposition of metal nano-particles in electrically conducting polymers has attracted considerable

attention due to the possibilities of creating suitable materials for electro-catalysis, chemical sensors, and microelectronic devices [142]. Different metal nanostructures on a variety of substrates including metals [143] semiconductors [144] and polymer surfaces [145] has been prepared by reduction of metal ions from an electrolyte solution [146] and the chemical and physical properties of the resultant nano-particles strongly depend on their size and spatial distribution [147]. Among those inorganic materials, gold nano-particles have received a great deal of attention because of their unique electrical and optical properties as well as extensive applications in diverse areas [148]. Shi et al. [149] recently reported electrochemical deposition of gold nano-particles on a thin dodecylbenzene sulfonate (DBS) doped PPy film coated ITO electrode. Various morphologies of the gold nano-particles, such as dendrite rod, nano-sheet, flower-like, and pinecone-like in shape, were obtained. They also found that the electro-catalysis activity and surface property of the films made of these nano-particles are affected by their morphology.

For the electrochemical methods, conductive substrates are generally required. However, photo-polymerization provides a means by which insulating substrates may be employed. Usually, photochemical preparation of conducting polymer films uses mixtures of monomer, electron acceptor, and photoactive species exposed to UV/visible light [150]. Sadik and coworkers studied [151] the role and rate of metal nano-particles incorporated into photo-chemically produced PPy films. They reported that the rate of film formation was found to be dependent upon the metal salt utilized. Moreover, the structural and morphologies incorporated metal nano-particles are a function of synthesis conditions such as metals ions, nature of substrates, exposure time, and monomer counterion ratios [151].

Copper nanostructured particles and clusters on different substrates using a variety of different methods have been also reported [152]. Although several recent studies have been demonstrated the fractal growth of copper on PPy and the plausible chemical interactions between copper and PPy [152, 153], Leung et al. [154] reported the near-perfect cubic copper nano-crystals on thin PPy film substrates by electrochemical method. They reported that PPy thin films were firstly deposited on a gold electrode by electrochemical polymerization at an applied potential of 0.8 V (versus AgCl/Ag standard potential) in a solution pyrrole (0.05 mol/L) and $NaClO_4$ (1.0 mol/L), and copper was then deposited electrochemically on the PPy films in a solution of 0.01 mol/L $CuSO_4$ and 0.1 mol/L $NaClO_4$ under different applied potentials from -0.4 V to -1.4 V (versus AgCl/Ag standard potential) [154]. It was reported that the morphology of final product is affected by fashion of electrochemical polymerization. In the galvanostatic mode, for instance, variety of nanostructures including nanowires, micro-wires, and fractals, as well as cubic nano-crystals, were observed. On the contrary, near-perfect cubic copper nano-crystals with a narrow size distribution are observed in the potentiostatic method [154]. The SEM image of the resultant cubic copper nano-crystals is shown in Fig. 4.11. In addition, Leung et al. [155]

found that both the Cu^{2+} and electrolyte concentrations play an important role in controlling the electro-deposition of copper nano-crystal growth. They further studied the growth mechanism of copper nano structured particles on a thin PPy film electrochemically deposited on polished gold cylinder electrodes [154], showing an instantaneous nucleation mechanism.
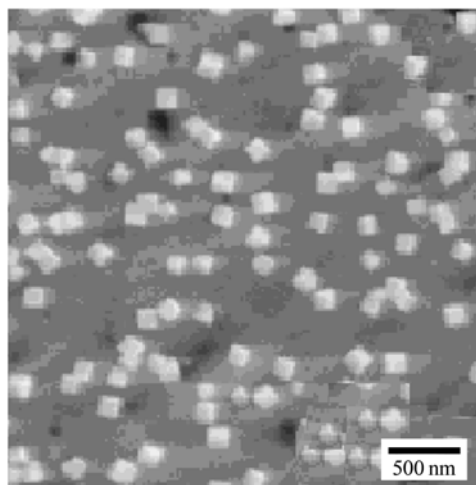

500 nm

Figure 4.11   SEM micrographs for copper deposition obtained in potentiostatic mode at over peak potential (-0.9 V) [154b]

Preparation of metal quantum dots has been recently received considerable attention in the field of nano-science and nano-technology owing to their interesting optical, electrical, and catalytic properties. Block copolymer micelles provide an excellent method for such dispersions, by which the particles of a definite size can be formed and stabilized within the core. Thus the nano-sized compartments formed in this way can serve as nano-reactors for the stabilization of inorganic crystallites or clusters, and the particle size and inter-particle distance can be controlled by the choice of a block copolymer [155]. As a result, the block copolymer technique provides an efficient template and allows facile formation of transparent, homogeneous nano-dispersions. Moreover the block copolymer technique is able to prepare thin films of colloidal polymer stabilized metal dispersions that allow one to prepare the novel functional materials with unique optical and electrical properties. The block copolymer approach has been used for the preparation of conducting polymer nanostructures containing metal nano-particles, for instance, gold-PPy core-shell particles or nanostructures of Au-PPy composites were prepared by using block copolymer micelles as the template [156]. Moreover, polystyrene-*block*-poly (2-vinylpyridine) with different block lengths have been employed to prepare mono-disperse Au nano-particles ($7-13$ nm), dispersed in a PPy matrix by changing the length of block copolymers [157]. Different shapes of Au particles, such as spherical, cubic,

tetrahedral and octahedral were observed, especially elegant dendritic nanostructures of Au-PPy by employing vapor phase polymerization of pyrrole onto solution-cast films of block copolymer ionomers have been also observed as shown in Fig. 4.12.
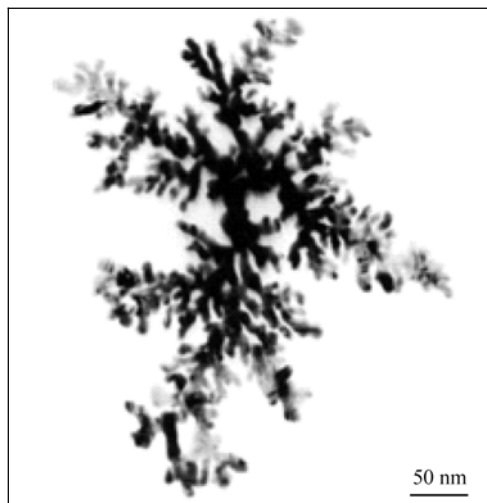

Figure 4.12   TEM images depicting dendritic nanostructures of thin films cast from block copolymer ionomers after vapor phase polymerization of PPy overnight [157]

A conductor/insulator/conductor composite nanostructure, which is an insulating tubule sandwiched between a metal tubule and conducting polymer tubule, to form a coaxial composite nano-structures. Martin et al. [158] reported Au/poly (2,6-dimethylphenol) (PPO)/PPy composite microstructures synthesized in the rather large (3 μm in diameter) pores of a polyester template membrane. The outer gold tubes were prepared using an electro-less deposition method [159]. These Au tubules were then used to electro-polymerize tubules of the insulating polymer poly (2, 6-dimethylphenol) (PPO) [160]. An inner micro-wire of conducting PPy was finally deposited down the center of each PPO tubule by using electro-polymerization method [161]. It is reasonable that this method can be used to prepare various composite microstructures with different conducting, insulating, semiconducting, and photo-conducting and electro-active materials.

2. Metal-PANI Composite Nanostructures

Composites of PANI and noble metal nano-particles (such as Au, Pt, and Pd) are also currently of great research interest due to PANI numerous applications arising from its good environmental stability and tunable electrical and optical properties [139] as well as the unique optical and catalytic properties of metal nano-particles [162]. PANI/Au composite with a significantly higher electrical conductivity prepared from monomer vapor by one-step process [163], PANI/Au multilayer films synthesized by electrochemically catalyze the oxidation of NADH

and detect DNA [164], and PANI/Au nano-particles capped with 2-mercaptoethane acid prepared in the form of thin films on an Au electrode [165] have been reported. In the chemical synthesis of PANI-metal composites, metal ions are often reduced in the presence of preformed PANI.

However, metal nano-particles in the resultant composites are often not effectively dispersed into the polymer matrix, because metal ions and nano-particles interact strongly with the imine groups of the polymer [166]. A procedure, where a gold salt acts both as an oxidizing agent to polymerize aniline and as a source of metal atoms, has been therefore used to overcome this problem [167], resulting in well-dispersed metal nano-particles in bulk PANI. Based on PANI nanofibers formed by exposing aqueous solutions of aniline and an oxidant to γ-irradiation [168], moreover, composite materials consisting of PANI nanofibers decorated with noble-metal (Ag or Au) nano-particles were synthesized with γ-radiolysis [169]. The γ-radiolysis method is advantagous of over previous techniques as follows: ① Fiber or seed [170] as a template, and large amounts of organic solvents are not required [171]. ② Well dispersed fiber-metal composites are produced in a single reaction setup, and the morphology of the metal nano-particles can be controlled by varying the aniline/metal salt ratio. ③ The electrical conductivity of the composites is up to 50 times higher than that of pure PANI nanofibers.

In general, oxidant for polymerization of aniline is a basic reagent for preparing nanostructured conducting polymers (e.g. PANI and PPy) by a chemical polymerization method. Various oxidants including APS [57a, 170], potassium bichromate [172] and hydrogen peroxide [173] have been employed for the oxidative polymerization of aniline in the presence of acids as the dopants. Recently, it has been demonstrated $AuCl_4^-$ could be reduced by amine-containing molecules including hexadecylaniline, diamine-containing oxyethylene linkage, resulting in metallic gold particles accompanied with the formation of corresponding polymers [174, 175]. PANI nanostructures prepared by $AuCl_4^-$ as the oxidant were reported [176, 177]. In the electrochemical polymerization, the metal complex ions (such as $AuCl_4^-$ and $PtCl_6^-$) act as counter-ions in the pre-deposited PANI film via an ion exchange procedure [178]. In the chemical polymerization, on the other hand, chemical preparation of PANI-metal nano-particle composites was often chemically polymerization of PANI around the preformed particles [179] or the aniline monomers act as reductant for the metal ions [180].

As above-mentioned, the preparation of colloidal PANI is one of the attractive alternatives to overcome its poor processability due to its insolubility in common organic solvents and water. This method has some advantages: ① The particle size of the resultant polymer particles was determined by the micellar "reactor" sizes [181]. ② The high local concentration of the monomer in the micellar reaction system enhances growth rate. ③ The resultant PANI is soluble in water or organic solvents [182]. By taking advantage of the micellar reaction,

Kleinermanns et al. [183] reported a micelle-based method to synthesize dispersed PANI-Au composite particles by the direct oxidation of aniline using $AuCl_4^-$ as the oxidant in the presence of micelles of sodium dodecyl sulfate (SDS). The PANI-Au composite particles disperse well in water and have a well-defined tetrahedron shape with an average edge length of about 150 nm as shown in Fig. 4.13. PANI-Au composites and electrodes modified with this material may find interesting applications in electrochemical sensors and conducting polymer coatings [184].

(a)   (b)
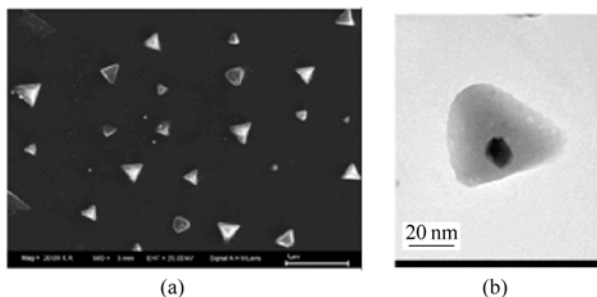
Figure 4.13   (a) SEM micrograph of tetrahedron-shaped PANI-Au composite particles on an evaporated gold film. (b) TEM bright-field micrograph of an isolated PANI-Au particle at higher magnification [183]

In addition, PANI-Au composite hollow spheres were synthesized by using polystyrene/sulfonated polystyrene core/shell gel particle as the template [185], which SEM and TEM images are shown in Fig. 4.14. It was found that the PANI shell thickness and the number of Au nano-particles decorating the PANI could be effectively controlled by adjusting the experimental conditions. Compared to pure PANI modified electrode, the bio-electro-catalytic activity of PANI-Au modified electrode was not only enhanced, but also their electrical conductivity being increased by 3 times [185].

(a)   (b)
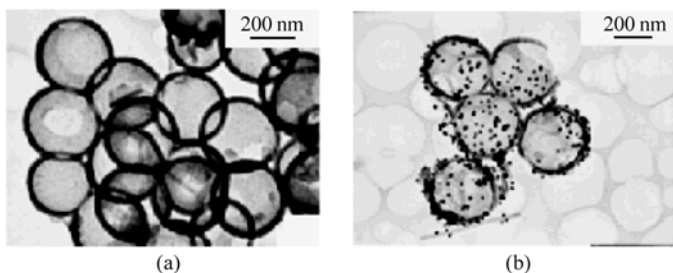
Figure 4.14   TEM images of PANI (a) and PANI-Au composite hollow spheres (b) [185]

Similar results on enhancements of sensing and catalytic capabilities for PANI-metal nano-particle composites compared to those of pure PANI were also reported [186]. In the synthesis of PANI-metal composites, as above-mentioned, metal nano-particles in the composites are often not effectively dispersed into the polymer matrix due to metal ions and nano-particles interact strongly with the imino groups of the PANI polymer [187]. To counteract this problem, Bertino et al. [188] reported a technique to synthesize composites containing PANI nanofibers decorated with metal nano-particles.

Sastry's group recently demonstrated that chloroaurate ions ($AuCl_4^-$) could be reduced by amine-containing molecules including hexadecyl-aniline, diamine-containing oxyethylene linkage, resulting in metallic gold particles accompanied with the formation of corresponding polymers[189]. In previous reported works, much more emphasis was focused on the structure and properties of gold nano-particles, and few efforts were made to investigate the morphology and properties of polymers simultaneously generated with the gold nano-particles. Although so many aniline derivates can react with $HAuCl_4$ and give interesting gold nano-particles or polymer structures, a few works is carried out on the reaction of $AuCl_4^-$ with aniline. For instance Au nano-particle-PANI composite using H_2O_2 as both oxidizing and reducing agent has been reported [190]. Wang et al. [176] reported a facile synthesis route to prepare PANI nanofibers (~35 nm in diameter) using $HAuCl_4$ as oxidant in the polymerization of aniline at room temperature. Except for the nanofibers, micro-scale gold clusters capped with a thin layer of PANI are also obtained [176].

Nano-scale devices such as chemical or electrochemical vapor sensors are usually required to polymerize nanostructures directly on metallic substrates. Nanometer-sized PANI tubes on modified Au electrodes have been previously achieved by using electrochemical and LB methods [191]. However, current methods for synthesizing nanostructured PANI covalently bound to metal surfaces require templates and utilize electrochemical or time-consuming lithography methods produce low yields. Russell el al. [192] provided a simple, two-step process for the synthesis of conductive nano-sized PANI fibers bound directly to the surface of an Au substrate. The process uses an interfacial polymerization technique to form a 2D- mesh of PANI fibers that are grafted to the Au surface using self-assembled monolayer of 4-aminothiolphenol (4-ATP) [192]. The most important aspect of this novel procedure is the remarkable durability of the covalently bonded nanofibers to the Au interface. However, it is not clear whether the PANI grows directly off the 4-ATP-modified gold surface or the PANI is synthesized in solution at the interface and then diffuses to the gold surface where it "links" with the self-assembled monolayer of gold [192].

3. Other Metal-Conducting Polymer Composites

Substitution of aluminum for magnesium will create an overall negative charge, and this negative charge is compensated by exchangeable metal cations such as

Na^+, K^+, Ca^{2+}, and Mg^{2+} [193]. Recently, nano-composites of conducting polymers containing such metal cations have greed of attention because of its large surface area and feature of ion exchange. PANI [194] and PPy [195] nanostructures comtaining montmorillonite (MMT), which belongs to the general family of 2:1 phyllosilicates composed of stacked layers of aluminum octahedron and silicon tetrahedrons, have been reported. Hoang et al. [197] recently also reported a novel approach to the synthesis of PANI-MMT nano-composites by *in-situ* electro-polymerization of anilinium-montmorillonite in 0.3 mol/L sulfuric acid on a gold substrate.

In addition, titanium nitride (TiN) is well-known for its oxidative stability, corrosion resistance, and good electrical conductivity that makes TiN an excellent candidate for electrodes in electrochemical capacitors in highly corrosive electrolytes and in semiconductor devices [198]. Thus, entrapping of nitride nano-particles may bring new electrical, optical, and magnetic properties to conducting polymers (e.g. PANI). Gao et al. [199] recently reported a novel composite of PANI containing TiN nano-particles (~ 20 nm in diameter) produced by *in-situ* polymerization. It was reported that the specific capacity of the PANI-TiN nano-composites is as high as 40 mAh/g under a current density of 125 mA/g.

4.2.2 Conducting Polymer/Carbon Nanotube Composites

CNTs received great attention owing to their extraordinary properties such as excellent Young's modulus, good flexibility, and high electrical and thermal conductivity [200, 201]. On the other hand, as described in Chapters 1 – 3, conducting polymers have been also received great attention owing to their high conjugated length and metal-like conductivity as well reversible chemical and physical properties by doping/dedoping process [139]. Therefore, combination of conducting polymers with CNTs is of great interesting to fabricate conducting polymer (CP) composites (CNT-CP) fabricated by using different methods are briefly reviewed [202].

1. CNT-CP Composites

Generally speaking, functional CNT-PANI composites are expected to exhibit useful electrical and optical properties and superior mechanical strength compared to pure PANI [203] due to its mechanical flexibility, environmental stability, and controllable conductivity with acid/base modification (doping/un-doping) and potential applications in many fields such as lightweight battery electrodes, electromagnetic shielding devices, anticorrosion coatings, sensors [204]. CNTs/PANI composites usually prepared by a mixing method containing PANI as leucoemeraldine-base and emeraldine-salt with the structure of polymer-functionalized carbon nanotubes and nanotube-doped polymers. On the other

hand, the chemical polymerization of aniline in the presence of CNTs leads to composites of fullerene-doped PANI salt [205]. Although functional CNT/PANI composites exhibited useful electrical and optical properties and superior mechanical strength compared to pure PANI, functionality including effective aspect ratio and processability (e.g. adhesion between CNT and conducting polymer) for application in actual devices are required at the same time [206]. Good interfacial bonding therefore is essential to ensure efficient transfer (charge or stress) from the conducting polymer matrix to CNT lattice that is one of the critical issues related to the functionality of CNT/PANI composites. Up to date, two efficient methods for CNT/PANI composites have recently been reported. One is directly mixing the EB form of PANI dissolved in *N*-methylpyrrolidone (NMP) with CNTs [207]. Another is *in-situ* polymerization of aniline monomer in the presence of CNTs [203, 204]. Obviously, the *in-situ* polymerization is much better than the direct mixing route owing to the existence of effective site-selective interactions between the quinoid rings of the PANI and the CNTs facilitating transfer processes between the two components [208]. In addition, stable and positively charged PANI nano-fiber aqueous colloids made by interfacial polymerization have been recently reported [209]. This method might provide new possibilities for solving processability of the CNT/conducting polymer nano-structures. Based on above idea, CNT-PANI nanostructures with strong electrostatic interaction between the C—N$^+$ species of the PANI nanofibers and the COO— species of the multi-functional CNT (MWNT) have been prepared by simply mixing a positively charged PANI nano-fiber aqueous colloid and a negatively charged MWNT aqueous dispersion [210].

Except for CNT-PANI composites, CNT-PPy composites have been also reported [211]. Wang et al. [212] recently reported CNT-PPy composite nanowires prepared by a template-directed electro-polymerization of PPy in the presence of a CNT dopant. Such preparation route offers a conventional reproducible preparation of high-quality conducting-polymer/CNT nanowires of a variety of sizes or compositions. The resulting high-quality nanowires display different voltammetry profiles and electronic properties compared to PPy wires prepared with small anionic dopants [212].

As well known, per-chlorate ion poses significant health concern since it can block the uptake of iodine in the thyroid gland and thereby affect the production of thyroid hormones [213].

Moreover, per-chlorate contamination is now recognized as a widespread concern affecting many water utilities, because per-chlorate salts are extensively used in various chemical productions such as those of leather, rubber, fabrics, paints, and aluminum. Therefore the removal of per-chlorate and the treatment of per-chlorate contaminated groundwater [214] and the determination of per-chlorate ion [215] are of special importance. However, per-chlorate is difficult to remove because it is a very stable substance in aquatic systems due to its solubility and non-reactivity. Several approaches such as ion exchange based on culture [214a],

selective anion exchange [216], microbial and biological reduction [217], and electro-chemical and chemical reduction [218] have been used for evaluation of the treatment of per-chlorate-contaminated waste-waters. However, all those technologies for the treatment of per-chlorate preformed in water that not only result in secondary pollution, but also cost. It is therefore necessary to develop an innovative, cost-effective, and green technology for the treatment of per-chlorate. PPy is a particularly interesting ion exchange material in the development of electrochemically controlled delivery devices and separation systems for charged species [139], because the oxidation and reduction of pyrrole monomer at an electrode surface is accompanied by the elution and uptake of dopant anions for charge balance in the polymer films [219], while when it is reduced the dopant will be released from the polymer. It implies that PPy could be used as an electrically switched ion exchanger. In fact, it has been successfully used in solid-phase micro-extraction of inorganic anions, especially the motilities of these anions have a well-defined order: $ClO_4^- < Br^- < Cl^- < NO_3^-$ [219]. Although the natural ion exchange property of PPy has been realized, its capacity is limited since there is only one positive charge per three pyrrole units [220]. Besides, it is difficult for the dopant anions to diffuse in and out of the polymer due to the poor mass transfer properties of the PPy films. Thus it is expected that one possible way to improve the mass transfer properties of the PPy deposits is to increase the surface area of electrode by depositing PPy on a porous matrix. CNTs are one of the novel nano-structure forms of carbon materials with very high surface area and good conductivity that provide an idea matrix for depositing PPy film. Based on above idea, Lin et al. [221] prepared nanostructured composite thin films of CNT-PPy by electrochemical polymerization and evaluated the composite as an electrically switched ion exchanger for removing per-chlorate ion from aqueous solution. It was reported that the process of electrically switched anion exchange could be finished within 10 s that provided a green process for removing ClO_4^- from wastewater using a novel nanostructured PPy/CNT composite thin film through an electrically switched anion exchange [221].

2. Coaxial CNT-CP Nanostructures

Coaxial CNT-CP nanostructures as nano-cables have received considerable attention because of their cable-like structure favoring charge transfer between conducting polymers (e.g. PANI or PPy) and carbon nanotubes, resulting in enhancement of the electrical properties of the composites. In preparation of co-axial CNT-conducting polymers, surfactant was usually applied to overcome the difficulty of carbon nanotubes dispersing into insoluble and infusible polymer matrix, and aniline or pyrrole monomer is then polymerized *in-situ* at the surface of the carbon nanotubes as the core layer to form nano-cables. Liu et al. [222] synthesized coaxial nanowires of PANI and PPy with single carbon nanotube in aqueous solutions containing cationic surfactant cetyltrimethylammonium bromide

(CTAB) or nonionic surfactant poly (ethylene glycol) mono-*p*-nonyl phenyl ether. It demonstrated that each individual carbon nanotube was encased in its own micelle-like envelope with hydrophobic surfactant groups orientated toward the carbon nanotube and hydrophilic groups orientated toward the solution [222]. The micelle/single carbon nanotube, called as a micelle/single carbon nanotube hybrid template, was form in a hydrophobic region, and insertion and growth of pyrrole or aniline monomers occurs in hybrid template. Upon removal of the surfactant, coaxial carbon/conducting polymer nanowires are produced. They also revealed that the micellar molecules used could affect the surface morphologies of the final coaxial nanowires and single carbon nanotubes played a key role in the conducting polymer/carbon nanotube composites during electron transfer in the temperature range 77 K to room temperature [222].

3. Optically Active CNT-CP Composites

Electro-active polymers, so-called "intelligent materials", have been actively investigated for applications such as electrochromic devices, rechargeable batteries, and chemical and biological sensors [223]. Among those electro-active polymers, PANI is a candidate to become optically active through the addition of chiral dopants such as CSA [224]. The optical activity is thought to arise from adoption of either a helical conformation [225] or a helical packing of polymer chains [226]. Panhuis et al. [227] reported optically active CNT composites induced by chairal PANI using *in-situ* polymerization showed the chiral optical properties of PANI are retained in the presence of carbon nanotubes, as measured by circular dichroism (CD). Moreover, optical microscopy analysis showed significant difference between the morphology of composite films in emeraldine base and salt forms, especially only dendritic structures are mediated by the presence of nanotubes. Sainz et al. [228] also reported optically active PANI emeraldine salt multi-walled carbon nanotubes (MWNT) composites via *in-situ* polymerization of aniline in the presence of MWNT and (*S*)-(+)-10-camphorsulfonic acid (SCA).

4.2.3   Core-Shell Composites

One of the current interests is the preparation of "core-shell" nanostructure composites, where the inorganic core particles are homogeneously covered with ultra-thin films of conducting polymers. Method and properties of the "core-shell" composites of conducting polymers have been reviewed [229]. One approach is chemical synthesis of conducting polymer-coated "core-shell" particles, where the "core" consists of a non-conducting material [230]. Conducting polymer-coated "core-shell" nano-particles, such as PPy [231], PANI [232] and PEDOT [233] have been reported by using poly(*N*-vinylpyrrolidone) (PVP)-stabilized polystyrene (PS) latex particles as core templates, where the oxidant and monomer were introduced via an aqueous dispersion. This approach demonstrated that better

processability and relatively high conductivity can be achieved even with low conducting polymer loading. Another approach to improve processability of conducting polymers (e.g. PANI) is monomer polymerization in the presence of poly (4-styrenesulfonic acid) (PSS) to form PANI-PSS composites by polymerization of aniline in the presence of PSS [234] or thermal post-polymerization of *p*-styrenesulfonic acid (SAA) in a PANI-SSA composite [235]. Park et al. [236] reported mono-dispersed PSS/PANI-coated PS particles and hollow capsules were prepared by a layer-by-layer assembly technique. PSS in this method was used as a polymeric counter-ion for fabrication of the multi-layers as well as a stabilizer and co-dopant. On the other hand, all of above nano-composites of conducting polymers (e.g. PPy) was normal conducting polymers without any degree of molecular orientation.

Therefore, many studies have been carried out to attain a high molecular orientation of conducting polymer (e.g. PPy) using templates such as the nano-pores of zeolites [237], membranes [238], LB films [239] and liquid crystalline media [240]. Generally, to obtain colloidal stability of the nano-composites of conducting polymers while maintaining the order of their molecular orientation, ultra-thin conducting polymer films (>30 nm) should be deposited on the surface of nano-particles to avoid overgrowth to form amorphous conducting polymers and precipitation by gravity.

Nowadays self-assembled mono-layers and adsorbed amphiphilic molecular layers on the surface have been used as the template for growth of ultra-thin film of the conducting polymers. Such templates can afford ordered molecular arrays on the surfaces and be widely used as 2D reaction media to produce ultra-thin polymer films. The method consists of three processes as follows:

(1) Amphiphilic molecules are first adsorbed from aqueous solutions as self-assembled arrays onto a solid surface, which depends on the adsorption behavior (e.g. surface charge for ionic surfactants), the self-assembled arrays can be mono-layers or bi-layers.

(2) Monomer is allowed to partition from water into the self-assembled arrays. Rate of the process is controlled by the nature of the surface and interior properties of the self-assembled arrays.

(3) Polymerization on the solid surface is initiated by adding chemical oxidants and free monomer is generally washed away with water after polymerization, leaving thin conducting polymer coatings on substrates. Chao et al. [241] prepared a stable core-shell PPy nano-composites with a zeolite, titanium silicate-1 (TS-1) nano-particles as the templates by this technique.

As described in Chapter 3, the utility of conducting polymers as photoactive materials in LEDs and solar cells [242] depends largely on following parameters:

(1) The directional mobility of charge carriers through the polymer.

(2) Amount of surface area exposed to light, or is available to form an interface between the polymer and other photoactive materials.

(3) The resistance and the surface area of the contacts between the polymer

and a metal electrode. Conducting polymers basically satisfied above-addressed issues, for instance, a higher ratio of surface area to volume and their polymer chains aligned within nanotubes provides an anisotropic pathway for electrons [243], which are addess issues (1) and (2). Moreover, conducting polymer-metal nanotubes are address issues (3) because they provide a geometry and chemical structure of the polymer-metal interface. Whitesides et al. [244] recently proposed convenient and adjustable procedures for the preparation of metal-polymer core-shell and segmented nanostructures. Figure 4.15 shows typical SEM images of the Ni/Au-thioaniline/PANI segmented structure after dissolution of the Al_2O_3 membrane as the template [244]. The self-assembly provided a good chemisorbed contact between the metal and polymer segments. In addition, they also pointed out that array of aligned, free-standing gold nanotubes could be prepared when the PANI was removed by plasma oxidation [244].
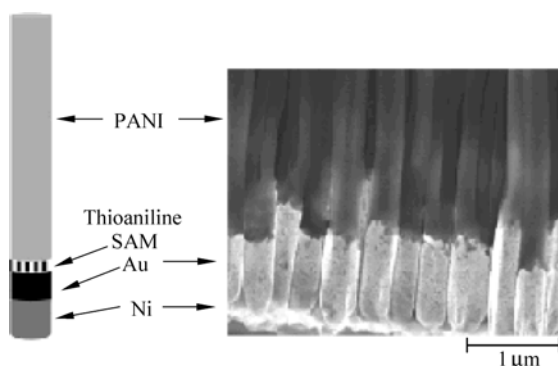
Figure 4.15   SEM images of the Ni/Au-thioaniline/PANI segmented structure after dissolution of the anodized aluminum oxide (AAO) membrane [244]

Surface modification of nanowire or nano-rod arrays with conducting polymers is another type of "core-shell" composites that expected to add more functionality to the system and may lead to completely new nanocomposite materials [245]. The ability to control the thickness of conducting polymer coated on each nanowire and the size of the inter-tubular pores is crucial for applications in optoelectronic nano-devices and sensors [246].

Recently, single crystalline Cu_2S nanowire arrays on a copper surface have been grown by gas-solid reaction under ambient conditions [247]. Since the nanowires are isolated, straight, and phase pure, those nanowires can be regarded as the templates for synthesis conducting polymer nanostructures. However, the previous results showed that grow large area arrays with a uniform density, diameter, and length of Cu_2S nanowires is more difficult. Recently, they successfully synthesized isolated and uniform Cu_2S nano-rods in well-aligned large arrays on a pre-treated copper surface and the homogeneous PPy layers coated Cu_2S nano-rods by interfacial polymerization of chloroform and water in

the presence of Cu_2S nano-rods as the templates [247]. The PPy film growth could be controlled at the interfacial of chloroform and water by the polymerization time, the pyrrole concentration, and the pyrrole-to-oxidant ratio [247].

4.2.4   Chiral and Biological Composite Nanostructures

Recently, nanowires and nanotubes modified with biological molecules are interesting building blocks for self-assembling nanostructures, because very specific bio-molecular interactions can be used to program their assembly [248]. Nanowires and nanotubes modified with different proteins [249], oligo-nucleotides [250], and nanowire field effect transistor (FET) prepared by aligning amine modified silicon nanowires onto electrodes patterned on a silicon wafer [251] have been reported. Among these conducting polymers, PPy is an interesting material for incorporation into nanowire-based sensors and nanostructures because of its high environmental stability, electronic conductivity, ion exchange capacity, and biocompatibility [139, 252]. These properties have made PPy a popular constituent of planar electrochemical biosensors [253]. Mallouk et al. [254] reported recently segmented Au/(PPy)/Au nanowires (300 nm in diameter and a few micrometers long) loaded with proteins in the polymer component. They found that the parameters, such as pH and monomer concentration affected the growth of PPy nanowires in a biocompatible environment. They also observed influence of the electro-deposition method (constant potential or potential cycling) on the morphology and electrochemical properties of the protein-modified conducting polymer segments as well as on the rate of equilibration of the nanowires with biotin [254].

As discussed in Chapters 2 and 3, the functionalized dopant such as CSA or DBSA allows producing soluble PANI in various solvents [255], which is also called as counterion-induced processability. Moreover, there has been increased interest in synthesizing chiral conducting polymers because of their potential applications as surface-modified electrodes [256], and separation materials [257]. Various chiral PANI guided by chiral dopant have been reported [258]. Furthermore the template-guided synthesis of water-soluble non-chiral PANI nano-composites by polymerizing aniline monomer in the presence of a polyelectrolyte has been also reported [259]. The final product is a double-stranded inter-polymeric complex where PANI and the template (polyelectrolyte) are bound by electrostatic interaction [260]. These PANI nano-composites render PANI soluble in water due to the hydrophilic nature of the polyelectrolyte. Recently Wang et al. [261] reported a water-soluble chiral PANI nano-composite template-guided in the presence of poly (acrylic acid) (PAA) as the electrolyte. The synthetic strategy involves three steps [261] as follows: ① Physically adsorb aniline molecules

onto PAA to form the adduct $(An)_x$/PAA in aqueous solution through electrostatic and/or hydrogen bonding interaction. ② Add chirality-inducing agent $(+)$ - or $(-)$ - CSA to adduct $(An)_x$/PAA solution, and ③ add an oxidant to polymerize the adsorbed aniline monomers to form a doped inter-polymer complex. During the synthesis, the inter-polymer complexes aggregate to form PAA/PANI/CSA nano-composites. This novel chiral PANI nanocomposite has advantageous of over conventional chiral materials, for instance, the chiral PANI nanocomposite is water-soluble, long-term stability and can easily be synthesized in large quantity [261]. However, formation of the composites requires careful control of experimental parameters including acid concentration, monomer/template ratio, total reagent concentration, ionic strength, order of reagent addition, timing of reagent addition, and temperature [261].

4.2.5   Inorganic Oxide Nano-Crystals and CP Composites

Inorganic semiconductor such as nano-crystalline titanium dioxide (TiO_2) has unique physical and chemical properties and it can be used in advanced coating [262], cosmetic [263], sensor [264], solar cell [265] and photocatalyst [266]. Therefore TiO_2 and conducting polymer composites has received particular attention in recent years because of their unique properties and promising applications in electrochromic devices, nonlinear optical systems and photoelectrochemical devices [267]. However, it is difficult to prepare conducting polymer/inorganic nano-particle composites by conventional blending or mixing in solution or melt form, because conducting polymers are not molten in nature and generally are insoluble in common solvents, and the nano-particles are easily aggregated due to their high surface energy. A brilliant sol technique has been used to prepare colloidal dispersions of conducting polymers/inorganic nano-particles (~ 20 nm in diameter) [268]. Moreover, Zarbin and coworkers reported the nano-composites of mixed oxide (e.g. TiO_2 and SnO_2) nano-particles and PANI prepared by a sol-gel technique using titanium tetra-isopropoxide and tin tetrachloride as oxide precursors [269]. However, the sol approach encounters some difficulties in preparing such nano-composites, because inorganic oxide nano-crystals are usually obtained by calcinations at a high temperature, and the polymer will decompose at such a high temperature [269]. As well knows that when ultrasonic wave through a liquid medium effect of ultrasonic cavitations, which means that a large number of micro-bubbles, grow, and collapse is produced in a very short time, take place [269]. Thereby the effect of ultrasound cavitations has been extensively applied in dispersion, emulsifying, crushing, and activation of particles. Suslick's theory calculations and the corresponding experiments suggested that ultrasonic cavitations can generate local temperatures as high as 5,000 K and local pressures as high as 500 atm, with heating and cooling rates greater than

109 K/s, a very rigorous environment [270]. Wang and coworkers [271] previously reported that the aggregates of nano silica could be broken apart and be re-dispersed in the aqueous medium, resulting in long-term stable polymer/ nano silica composite latex by ultrasonic irradiation. Based on above results, $0-3$ dimensional PANI/nano-crystalline TiO_2 shell-core composite particles have been prepared by using ultrasound irradiation [271]. It was reported that the aggregation of nano TiO_2 in the aqueous solution can be broken down under ultrasonic irradiation, and the formed PANI deposits on the surface of the nano-particle leading to a core-shell structure. Measurements of FTIR, UV-visible and XPS analyses showed that the interaction between PANI and nano-crystalline TiO_2 is strong [271].

Besides, TiO_2/conducting polymer hybrids have been also prepared by the electrochemical polymerization of the monomer on a film of the oxide [272] or by chemical polymerization of the monomer in a dispersion which contains the oxide nano-particles [273].

In summary, although various conducting polymer nanocomposites prepared by different approaches have been reported, facial, efficient and controlling synthesis of such nano-composites is still challenge. The previous papers only showed physical properties of the nanostructured composites, but lack analysis of those properties, especially size effect on physical properties of those composite nanostructures.

4.3 Physical Properties and Potential Application

As described in Chapters $1-3$, conducting polymers exhibit unique electronic, magnetic, and optical properties similar to semiconductors or metal while retain their flexibility, ease of processing, and lightweight. The conducting polymer nanostructures not only remain all physical properties of conducting polymers, but also large special surface areas, small size and more lightweight caused by hollow structure. These unique properties lead to promising application of the nanostructure conducting polymers as nanodevices. The physical properties and potential applications as well as nanoarrays or nano-patterns of the conducting polymer nanostructures will be discussed in this section.

4.3.1 Electrical and Transport Properties

Since applications of conducting polymers are associated with their electrical and transport properties, studies on the electrical and transport properties of the conducting polymer nanostructures are of an important role in fundamental academic research and technical application of the conducting polymers. As

described in Chapter 1, the electrical conductivity of conducting polymers can vary from an insulator to the metallic state, and can be reversibly modulated over orders of magnitude by changing dopant nature and doping degree [274]. Moreover, the temperature dependence of conductivity of the conducting polymers exhibits a semiconductor behavior and followed by a VRH model proposed by Mott [275] due to polymeric chain and/or particle intercontact resistance. At current time, however, the conductivity of the conducting polymer nanostructures at room temperature and temperature dependence of the conductivity are also presented by pelleted sample, as measured by four-probe method. Obviously the measured room-temperature conductivity for the conducting polymer nanostructures, especially the temperature dependence of the conductivity is not intrinsic because of involving the chain- or fiber-interresistance. Thereby, to measure electrical properties of a single nanotube or nanowire of conducting polymers is critical key for understanding conducting mechanism and transport properties of the conducting polymers. Nowadays, various methods for measuring electrical and transport properties of a single nanotube or nanowire have been reported. Some of them will be briefly discussed as below.

1. Conductivity of A Single Nanotube Measured by Four Probe Method

Martin and coworkers [4b, f, g, 276] firstly observed that the conductivity of template-guided grown nanotubes of conducting polymers (e.g. PANI and PPy) was enhanced compared with the conventional forms (e.g., thin films). The results on polarized infrared absorption spectroscopy (PIRAS) revealed that the polymer chains are oriented in a direction perpendicular to the tubule axis and the extent of orientation decreases as the walls of the tubules become thicker [276]. Based on above results, they further proposed a simple bi-layer model that the conducting polymer (e.g. PPy) initially deposited on the pore walls is highly oriented by the template [276]. Martin and coworkers therefore explained why the conductivity of the nanostructures is higher than that of the bulk form by using above assumption [4b, 4f]. Moreover, they were further found that conductivity of poly (3-methylth-iophene) nanotubes or nanofibers synthesized by template method is a function of the diameter, i.e. the conductivity increases with decrease of the diameter, showing a size effect on conductivity. Similar size effect on conductivity of PPy [277] and PA [4d] nanostructures prepared by template method were also obsereved. These results indicated that measurement of the electrical properties for a single nanofiber or nanotube is necessary in order to understand a difference of the nanostructures from the bulk-materials. Up to date, some papers dealing with the electrical properties of a single conducting polymer nanofiber or nanotube have been reported [278]. As shown in Chapter 1, the doped PA is the model conducting polymer with an extremely high conductivity [279]. In particular, novel helical PA nanofibers with right hand and left hand have been synthesized by using chiral nematic liquid crystals (LCs) as a solvent of Ziegler-Natta catalyst [280]. Park et al. [281] successfully prepared well-dispersed

helical PA single fiber by using hexaethylene glycol mono-*n*-dodecyl ether ($C_{12}E_6$) as a nonionic surfactant in *N*, *N*-dimethylformamide (DMF) solution. PEDOT is another typical conducting polymer and already used in many applications as a hole injector in OLEDs [282] or in plastic memory [283] owing to its long period stability in the *p*-doped state [284]. Like PA and PPy nanostructures, a size effect on conductivity for the PEDOT single nanotube has been also observed [4b, 285]. In contrast with the results generally reported on PPy and PANI nanotubes, however, the room temperature conductivity of PEDOT nanowires seems to be only weakly dependent on the nanowire diameter [286] as shown in Fig. 4.16. Moreover, the electrical transport properties of their nanowires or films were also measured at temperature down to 1.5 K, showing the transport properties of the nanowires differed from the films, for instance, the nanowires with 35 nm in diameter showed a 2D-VRH hopping, while the films close to the
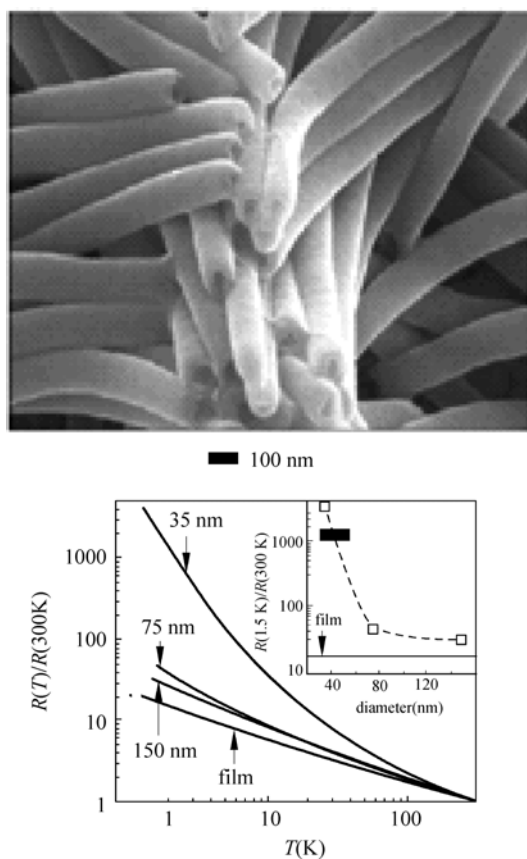
Figure 4.16 SEM images of 150 nm PEDOT nanowires after polycarbonate template removal (upper) and temperature dependence of the resistance $R(T)$ normalized by $R(300 K)$ for PEDOT nanowires and film (below) [286]

metal-insulator transition [286]. Author also studied electrical properties of a single nanotube, nanofiber, even hollow microsphere of conducting polymers (e.g. PANI and PPy) by means of two or four probe method. It is found that the conductivity of a single nanotube or nanowire is enhanced by one or two orders of magnitude and the room temperature conductivity increases with decrease of diameter of the nanotubes or nanowires, exhibiting a size effect on conductivity. Although room temperature conductivity of the single nanotube or nanowire is metal-like, the temperature dependence of the conductivity still exhibits semiconductor behaviour and obeys VRH model [275]. Measuring method, electrical and transport properties of a single nanotube or nanowire, as measured by four probe method, will be discussed in Chapter 5 in detail.

2. Current Sensing Atomic Force Microscopy (CS-AFM)

Distribution of counter-ions in a film or an electron transfer across the interface for the conducting polymers is key factors in determining the performances of the devices. It is therefore necessary to understand the interfacial electronic states of the electron transport properties in conducting polymer nanostructures. Scanning tunneling microscopy (STM) is a technique to measure the electrical characteristics of single molecules [287]. Some disadvantages of STM are obviously, for instance, it firstly can't use non-conducting materials due to the restriction of the typical tunneling distances ($1 - 10$ nm). Moreover, the STM results usually include the vacuum gap between the tip and molecules probed that can cause complexity and materials or very thin ambiguity in the interpretation of intrinsic properties of molecules [288]. Although the Kelvin probe method [289] has been employed to measure the electronic state of a few conducting polymers, it is used only for mapping the surface potential, not for direct quantitative studies [288]. Current-sensing atomic force microscopy (CS-AFM) with a conducting tip has been therefore employed. The CS-AFM approach has some advantageous as follows:

(1) It is excellent approach to measure the electrical characteristics of single molecules, because it not only obtains simultaneously the topographical and current images, but also current-voltage (*I-V*) traces recorded on selected spots of the image on a nanometer scale [290]. In other words, topographical and current images for CS-AFM technique can be obtained simultaneously from different locations that provide important information on the distribution of conducting islands surrounded by insulating areas.

(2) The current-voltage (*I-V*) traces measured by CS-AFM provide a relationshipe between structural features and electrical properties of the materials on the nanometer scale. Thereby CS-AFM provides valuble information for understanding conductance mechanism of the nanostructures [291].

(3) The CS-AFM technique allows easy and reproducible contacts with various substances compared with lithographic processes. Park and other investigators used this technique for studying nano-scale electrical properties of the conducting polymers by measuring *I-V* characteristics [288, 292]. For instance electrical and

morphological properties of PEDOT thin films electrodeposited on gold-on-silicon electrodes by galvanostatic, potentiostatic, and potentiodynamic methods were determined using CS-AFM technique [293]. It was found the average band gap obtained from I-V curves are in excellent agreement with those obtained from the absorption spectra, and morphological and electrical properties of PEDOT films are affected by the type of the preparation methods. In addition, heterogeneous electronic conductivity of PANI films with various thicknesses and degree of doping on ITO substrates by atomic force microscope current image tunneling spectroscopy (AFM-CITS) and transmission electron microscopy (TEM) were recently reported [288]. It was reported that the conductivity of the highest conducting regions of fully doped film is at least 100 times higher than that of the lowest conducting regions. The large spatial variations in the film conductivity on topographically featureless regions are tentatively attributed to the presence of nano-scale crystallites of polaron lattice, which is consistent with previous reported "conducting islands" observed in doped PANI films [288]. Various types of I-V curves representing metallic, semi-conducting, and insulating states are observed depending on the aggregation of polymer chains and doping level of the polymer film. The band gap energies estimated from the I-V or dI/dV-V curves is consistent with UV-visible absorption spectrum and theoretic calculations [294]. In addition, the modification of surfaces on either the atomic or nanometer scale using scanning probe microscopes (SPM) has been widely reported [295]. Localization polymerization of pyrrole on graphite substrate using scanning tunneling microscope (STM) [296] and scanning electrochemical microscope (SECM) [297] has been reported. For instance the platinum tip of a scanning tunneling microscope has been employed to direct the electro-polymerization of aniline on nanometer-scale regions of a graphite surface immersed in an aqueous and aniline-containing electrolyte [298].

3. Electrical Transport Properties

Measuring electrical transport in well-defined submicron or nanometer scale provides important information for understanding transport mechanisms of the conducting polymers and their nanostructures. Many papers regarding electronic transport for conducting polymers (e.g. poly (3-hexylthiophene)) on the submicron scale have been reported [299]. Frisbie et al. [300], for instance, reported the electrical characterization of field effect transistors based on PEDOT nanofibers fabricated using nano-stencil shadow masks. They reported the mobility values were 0.02 cm^2/(V·s) and on/off current ratios of 10^6, especially current densities of about 700 A/cm^2 were achieved in single nanofibers. Kima et al. [301] also reported the field emitting (EF) characteristics of doped and de-doped PPy, PANI, and PEDOT nanotubes and nanowires prepared by electrochemical polymerization using Al$_2$O$_3$ nanoporous templates [302]. The field emitting diode (FED) consisted of ITO for the anode, and the conducting polymer nanotubes or nanowires for the cathode. The distance between the anode and the nano-materials was about

150 nm, and the diode was kept in vacuum, under 10^{-6} torr [303]. It was reported that the nanostructure of PANI were transformed from a conducting state to a semiconducting (or insulating) state via the de-doping process with NaOH solvents. Moreover, the charge carriers of the PANI nanostructures are p-type, as measured by the gate dependence of *I-V* characteristic curves [303]. The field emission characteristics were also observed from the doped PANI-HClO$_4$ nanotubes and PPy-TBAPF$_6$ nanowires, suggesting the potential for use in FED nano-tip emitters [303].

CNTs have been intensively studied as FE materials owing to their electrical and mechanical advantages [303, 304]. However there is a real need to develop cheaper and simpler alternative FED materials. Kim et al. [305] reported a FED of PEDOT nanowires synthesized by an electrochemical polymerization method with a nanoporous template. *J-F* characteristic curves of a FE diode made from PEDOT-DBSA nanowires as nano-tips showed that the field enhancement factor was about 1,200, which is comparable to those of CNTs [305]. Obviously, PEDOT-DBSA as FE materials is much cheaper than that of CNTs.

4. Wettability

The surface wettability is a very important property to the solid materials. The surface wettability is generally related to both the surface free energy and the surface geometric structure [306]. Water contact angle (CA) is used to measure a surface wettability of materials, in general, the surface with CA larger than 150° and lower than 5° is defined as superhydrophobic and superhydrophilic surface, respectively. Nowadays materials with super-hydrophobic surface or super-hydrophilic surface have been extensively investigated due to both fundamental research and practical applications [307]. The applications include micro-fluidic devices [308], controlled-drug delivery [307a], bio-separation [309] and self-cleaning surface [310]. However, permitting a simple and rapid transition in wettability, especially between superhydrophilicity and superhydrophobicity, remains challenge.

Super-hydrophobic or superhydrophilic conducting polymers and their nanostructures have been attracted due to their potential applications in sensors [311], biomedicines [312] and actuators [313]. Few papers dealing with wettability of conducting polymers has been recently reported, for instance, it was reported that CA of PPy doped with various amount of fluorinated counterion changed from 12° to 96° [314]. Super-hydrophobic PPy nanowire networks with $60-90$ nm in diameter were also synthesized by employing an organic diacids (oxalic acid, tartaric acid, or glutaric acid) or triacid (citric acid) and cationic surfactant (hexadecyl-trimethyl-ammonium bromide (HTAB)) [315]. The wettability of PPy film could switch from super-hydrophobic to super-hydrophilic by changing the electrical potential [316]. Moreover, the dual-responsive wettability switching based on the superhydrophobic PANI coaxial nanofibers triggered by changing the pH value and oxidant/reducer concentration of probe solutions has been also reported [317]. Especially, author proposed a new type of conducting

polymer-based gas and pH sensors guided by reversible wettability resulted from doping/de-doping process, which will introduce in Chapter 5 in detail.

4.3.2 Potential Applications

With the development of Si-based nanotechnology, π-conjugated organic materials have been applied to many nano-scale devices and microelectronic devices [318]. So far, PPy, PANI, and PEDOT nanotubes or nanowires electrochemically prepared by using Al_2O_3 as a template [319] have been used to fabricate nano-devices such as biosensors [320], electrochemical devices, and single electron transistors [321] as well as nano-tips in field emission displays (FED) [322]. The next discussion will emphasize on application of the nanostructure conducting polymers as gas sensors, chemical sensors and biologic sensors, while other applications will be briefly discussed.

1. Sensors

Conducting polymer nanowires have become prime candidates for replacing conventional bulk materials in micro- and nano-electronic devices [5, 323]. As described in Chapters 1 and 2, conducting polymers show electrical and optical property change after chemical or electrochemical doping with oxidizing or reducing agents that can change from an initial insulating state to an electrically conducting state [139]. This transition can be used in such applications as optical sensors [324], chemical sensors [325], and biosensors [326]. The PANI, PPy and PTH nanostructure based-sensors have attracted considerable attention, because high surface area allows for fast diffusion of gas molecules into the structures [327]. Reasrch dealing with this object has been reviewed by Wolfbeis [328]. Herein some advantageous of the conducting polymer nanostructures as sensors are summariezed as follows:

(1) Like the bulk mateials of conducting polymers, the properties of conducting polymer nanostructures can be tailored to detect a wide range of chemical compounds [329], because the conductivity is sentive to dopant typer and doping degree.

(2) The sensitivity of the conducting polymer nanostructure-based sensors is enhanced compared with the bulk material-based sensors due to a high surface area of the conducting polymer nanostructures.

(3) Response time of the nanostructure-based sensors is shorter than non-nanostructured sensors, because the porous nature of the nanostructures enables gas molecules to diffuse in and out of the nanostructures rapidly, leading to a much greater extent of doping or dedoping over short times.

(4) The conducting polymer nanostructures remain characteristics of the conventional conducting polymers including reversible conductivity controlled by doping/de-doping process, flexibilities and easy processing. Progress of the

conducting polymer nanostructures as sensors including gas and chemical sensors, biosensors and artificial sensors are briefly reviewed as below.

(1) Gas and Chemical Sensors

Gas or chemical sensor is the simplest sensors. Huang et al. [330] reported a gas sensor of PANI nanofibers (30 – 50 nm in diameter and 500 nm – several micrometers in length) prepared by an interfacial polymerization method. The method is based on the well known chemical oxidative polymerization of aniline in a strongly acidic environment in the presence of APS as the oxidant, but is performed in an immiscible organic/aqueous biphasic system to separate the byproducts (inorganic salts, oligomers, etc.) according to their solubility in the organic and aqueous phases [331]. They found that the nano-fiber thin film responds much faster than the conventional film for both acid doping and de-doping. Interestingly, the nano-fiber films show essentially no thickness (0.2 – 2.5 μm) dependence on their performance [330]. Moreover, PANI nanofibers used as sensing materials for acids, bases, reducing agents, organic vapors, and alcohols has been also reported [332]. Those results sugguest that the conducting polymer nanostructures (e.g. nanofibers or nanotubes) might become a superior gas or chemical sensor material in high sensitivity and short response time owing to their high surface area, small nano-fiber diameter, and porous nature.

In fact, the simplest configuration of an electronic sensor is a resistive junction that is composed of a conducting material sandwiched between two solid-state electrodes [333]. The transport properties of the sensor change upon exposure of the junction to analytes due to doping/dedoping interactions of the analyst molecules with the chemical building blocks of the conducting material. By applying a constant bias across this junction, the presence of analytes can be detected simply by monitoring the conducting current. For example, PANI nanowires prepared by faciel synthesis [334] or by electro-spinning technique [335] have been incorporated into inter-digitized electrodes to prepare gas sensors with an excellent sensitivity. Although many examples, as above-described, have been demonstrated by workable devices and sensors based on the nanostructure conducting polymers, it remains a challenge to discover efficient, scalable, and site-specific approaches for incorporating these nanostructures into lithographically patterned electrode junctions. PANI nano-framework-electrode junctions (PNEJs) have been therefore prepared by electrochemical polymerization at low and constant current [336]. This method develops a highly efficient electrochemical process for the simultaneous and parallel fabrication of PNEJs in an array. In addition, the gas sensors of PEDOT nano-rods (conductivity ~ 72 S/cm) synthesized by interfacial polymerization using a reverse micelle as a soft-template response to NH_3 and HCl vapor concentration were as low as 10 ppm and 5 ppm, respectively also reported, which sensors display good reproducibility and reversibility in response [337].

(2) Hydrogen Sensor

It is well known that hydrogen is a dangerous gas, because it easily ignites in

air. Thereby sensors are required to detect hydrogen leaks to warn of explosion hazards. Palladium metal [338] and palladium alloys [339] are usually used as hydrogen sensors that are advantageous of the suppression of the phase transition vary fast and reversible. However, palladium metal and palladium alloys are required to work at high temperature and inhabitation by oxygen. Janata et al. [340] have shown that a field effect transistor with two layers, palladium and PANI, can be used as a good sensor for hydrogen, which can be operated at 90℃ and displays fast response times. In particular, Ahabnam et al. [341] reported hydrogen sensors of CSA doped PANI nanofibers that might be a good room-temperature hydrogen sensor in a dry atmosphere and its response is not inhibited by oxygen because of a significant interaction between hydrogen and PANI [341].

(3) Hydrazine Sensor

Previous work on conducting-polymer based hydrazine sensors was using PPy or PTH as a detecting material. PTH sensors can measure very low concentrations of hydrazine, but it is air sensitive and subject to degradation if stored at room temperature [342]. PPy sensors are air stable, but have unreasonably high detection limits of about 1% [343]. Since hydrazine is a strong deducing agent, both doped and de-doped the emeraldine oxidation state of PANI changes to its fully reduced leucoemeraldine oxidation state by hydrazine and accompanied with a decrease of the conductivity [344]. Thereby the decrease in conductivity associated with change in oxidation state can be used to develop PANI hydrazine sensors. Previous work showed that direct detection of hydrazine with PANI is possible, but the response is relatively small [332, 345]. Interestingly, incorporation of an additive, including glucose [346], urea [347], oxygen [348] and chloride [349] into PANI increases the response of PANI to hydrazine. Virji et al. [350] also observed that PANI films with fluorinated alcohol (e.g. hexafluoroisopropanol, HFIP) additives showed highly sensitive to hydrazine. They found the enhancement of sensitive to hydrazine is due to strong acid HF produced by a reaction between hydrazine and HFIP, resulting in conductivity enhanced by 4 orders of magnitude [350].

(4) Acetic Acid Sensors

Acetic acid is a component of fermentation products (wines, vinegar and soy sauces) and the tast and flavor of the fermented products are affected by the concentration of acetic acid. In addition, acetic acid molecules have been focused on in disease diagnostics and used as a biomarker in the breath analysis of patients due to its noninvasive and rapid detection [351]. The accurate and rapid determination of acetic acid concentrations is therefore necessary in industrial food laboratories [352] and disease diagnostics [353]. Conducting polymers can be used acetic acid sensing materials because of their conductivity and physical properties of being influenced by factors such as polaron number and charge transfer to adjacent molecules [354]. Jang et al. [355] reported PANI-modified conducting PPy nanotubes as chemiresistive vapor sensors for acetic acid

detection. They found that sensitivity and response of the sensors are as a function of the number of amine spacers and the analytes concentration.

(5) Biosensors

Early reports dealing with application of conducting polymers as biosensors were concerned with PPy for the amperometric detection of glucose, which idea essentially was to provide an electronically conducting polymer matrix for the immobilization of enzyme glucose oxidize [356]. Since the conductivity of the conducting polymers (e.g. PANI) is very sensitive to the chemical potential and pH of the microenvironment of the polymer matrix [357], a new generic concept based on the conductivity of the conducting polymers sensited to the chemical potential and pH of the microenvironment of the polymer matrix was also used for making biosensors [357, 358]. Moreover, PANI micro-tubular biosensors and sensor arrays, which response is enhanced by 10^3 compared with the bulk materials, have been used for glucose, urea, and triglycerides [359].

Since nano-particles or nanotubes have similar dimensions to those of biomolecules (e.g. proteins or DNA), combination of conducting polymer nanostructures with bio-molecules might fabricate new nanoarchitectures that offer promise for numerous applications in the nanosaled-bioelectronics. Tao group [360] fabricated a novel glucose nano-sensor based on conducting polymer/ enzyme nano-junctions by bridging a pair of nano-electrodes separated with a small gap (20 – 60 nm) with PANI/glucose oxidant. The signal transduction mechanism of the sensor was based on the change in the nano-junction conductance as a result of glucose oxidation induced change in the polymer redox state [360]. Due to the small size of the nano-junction sensor, the enzyme was regenerated naturally without the need of redox mediators, which consumed a minimal amount of oxygen and at the same time gaves very fast response (<200 ms)[360]. These features make the nano-junction sensor potentially useful for in vivo detection of glucose.

Since the conductivity of conducting polymers are very sensitive to the chemical potential of the microenvironment within the polymer matrix, recently, there has been considerable interest in the development of probes for the detection of biologically significant molecules using conducting polymers or their nanos-tructures [371]. However, there are two principal challenges in the fabrication of such a biosensor array. One is miniaturization of the single-substrate sensor, and another is preventing cross-talk between neighboring sensors on an array. Meyer et al. [362] have recently described an array of 400 sensors, each independently addressable to obtain a two-dimensional concentration profile of glucose by immobilizing glucose oxidant on all the sensor elements. Moreover, Sangodkar et al. [363] described the fabrication of PANI-based micro-sensors and micro-sensor arrays for the detection of glucose, urea, and triglycerides.

Among those conducting polymers, PANI has been explored in fabrication of sensors for the determination of various biomolecules/ions [364]. However there are two problems for PANI required to be solved as the biosonsrs. One is PANI

loses its electrochemical activity in solutions of pH greater than 4 [365], and another is most of the enzymes are unstable in acidic conditions. Therefore, adaptation of PANI to neutral pH is a key for its application as biosensors. Up to date, great attempts have been made to modify the properties of PANI in order to extend its conductivity to neutral pH. As mentioned in Chapter 2, the self-doped PANI (SPAN) synthesized by sulfonation of the emeraldine and leucoemeraldine form of PANI [366] is one way to extend the PANI conductivity to neutral pH. Self-doped PANI could be also electrochemically synthesized by copolymerization of aniline and metanilic acid where the redox activities of the polymers was maintained up to pH 9 [367]. Another strategy for extending to natural pH is to synthesize the polymer in the presence of anionic polyelectrolyte with a sulfonate group [368].

Several modified self-doped PANI sensors for responsive to glucose and urea could be operated in pH 7 buffer solution [369]. In particular, a novel strategy for enzymatic synthesis of conducting PANI in the presence of a strong acidic polyelectrolyte (e.g. poly-(styrene sulfonate)) at phosphate buffer with a pH of 4.3 and 5.5 has been also reported [370]. The reason is that the pH at the acidic polyelectrolyte surfaces is much lower than that of bulk aqueous medium due to acidic poly-electrolytes attract hydrogen ions electro-statically [371], which provides a suitable microenvironment for the formation of conducting PANI. Chattopadhyay et al. [372] recently report the synthesis of Au nano-particles and PANI on the same cation-exchange resin beads. It showed that the Au nano-particles present in the beads catalyze the oxidation of glucose to gluconic acid, resulting in the change of color of the beads from blue (emeraldine base) to green (emeraldine salt) and the presence of glucose of a minimum 1.0 mM concentration in water can be measured by using the method.

(6) Artificial Sensors

As one knows, the human tongue is able to distinguish four basic types of tastes (e.g. sweet, salty, sour, and bitter) [373]. Although the human tongue and nose can sufficiently respond to chemical substances, they cannot directly contact with chemical substances. Artificial sensors, such as electronic tongue or electronic nose, are the possibility of use in toxic and unpleasant substances. Therefore, the use of artificial sensors for evaluating gustation has been attracted attention, because it is an important tool to improve quality control in the food and beverage industry. Conducting polymers and mixtures with stearic acid as artificial sensors have been reported, for instance, a microtubule sensor array prepared in the presence of poly(styene sulfonate)(PSS) can be used for glucose, urea, and triglyceride [374].These electronic tongues respond to the substances responsible for the basic tastes in the same way as the biological system. Some of them can distinguish between different brands of mineral water or between brands of wine, in addition to detecting ionic metals in water [374]. In addition, Ferreira et al. [375] also reported a sensor array made up of nanostructured LB films is used as an electronic tongue.

However, one key requirement for electronic tongues is the need to have a good performance for the different basic tastes. Regarding this issue, Contractor et al. [376] described the fabrication of micro-tubular biosensors and sensor arrays of PANI as an "electronic tongue" for glucose, urea, and triglycerides. They reported that the response of the micro-tubular sensor for glucose is higher by a factor of more than 10^3. Moreover, an artificial tongue composed of four sensors (e.g. salty, sour, sweet, and bitter) made from ultra-thin films deposited onto gold inter-digitized electrodes has been also reported by Mattoso et al. [377].

2. Electrochemical Actuators and Electrochromic Devices

As mentioned in Chapter 3, the electrochemical doping/de-doping process of the conducting polymers are often companied counterion enter/exit into or out from polymeric chains, resulting in expansion/contraction of volume of conducting polymers [378]. The expansion/contraction produced by electrochemical doping/ de-doping process usually depends on the number and size of ions exchanged [379]. Based on this principle, conducting polymer-based electrochemical actuators have been developed [380]. Moreover, chemical or electrochemical doping/de-doping process for the conducting polymers is also companied color change that can be used to fabricate electrochromic devices. As a result, conducting polymer nanostructure-based electrochemical actuators and electrochromic devices have received great attention due to their nanosize and large surface area. PEDOT and its derivatives are especially one of the most attractive electrochromic materials of conducting polymers due to the high contrast ratios as well as an availability of diverse colors [381]. The color-switching rate and the color contrast are most important properties of conducting polymer-based electrochromic devices [381a]. The fast electrochromic response, in general, can be achieved by reducing the film thickness, because the color-switching rate is determined by the diffusion rate of counter-ions into the film during the redox process. However, this leads to insufficient coloration and color contrast of the electrochromic device. Recently, the electrochromics of PEDOT nanotubes electrochemically synthesized by using pores of the alumina template achieved the extremely fast electrochromic response (less than 10 ms) without sacrificing the color contrast [382]. However, there is a problem in fabricating a flexible electrochromic device using the alumina template due to its fragility. Thereby track-etched porous PC membrane is a good candidate for the flexible template because of its flexible, commercially available with various pore diameters (0.01 – 20 mm), and quite transparent [383]. Therefore, PEDOT nanotubes electrochemically synthesized by using PC as the flexible template could be constructed a fast color change of a nanotube-based electrochromic device. As predicted, the switching rate of PEDOT nanotube-based electrochromic devices was improved by 30 – 50 times compared to the conventional thin film of PEDOT in the flexible electrochromic device [384].

Ultra-thin film conducting polymer layer is a key for fabrication of electro-chromic devices. As mentioned in Chapter 3, the layer-by-layer polyelectrolyte (such as poly-anion and poly-cation) deposition route has been developed for the fabrication of ultra-thin layers of the conducting polymers [385]. Poly-cations and poly-anions are alternately adsorbed from their respective solutions onto the substrate to form a multilayer film by an electrostatic attraction between a charged surface and oppositely charged molecule in solution. More recently, Yang et al. [386] used copolymerization combined with a self-assembly technique to build up a self-doped SPAN ultra-thin film on an indium tin oxide (ITO) substrate. The deposition process was very simple, for instance, aniline (AN) was first dissolved in an aqueous solution of o-aminobenzenesulfonic acid (OSAN) to form micelles, and then APS was added as the oxidant. OSAN in the deposition process played two functions of surfactant and self-dopant at same time. They found that both factors of AN/OSAN ratio and reaction temperature significantly influenced the film formation behavior in the film deposition process [386]. They also fabricated a total solid electrochromic device as ITO/SPANI//LiClO$_4$-WPU//PEDOT: PSS/ITO, where PEDOT: PSS is poly (3,4-ethylenedioxythiophene)/poly(4-styrenesulfonate) as the counter electrode that possesses perceptible color changes from gray to dark blue with switching potentials from -1.5 to 1.5 V [386].

3. As Carbon Precursor

Nanostructured carbon materials attract much attention due to their uses as adsorbents, catalyst supports, and electrode materials [387]. A new class of nanostructured carbons, ordered mesoporous carbons (OMCs), has been recently synthesized by using ordered mesoporous silica as a template [388]. The preparation of OMCs generally involves incorporation of a carbon precursor (such as sucrose, furfuryl alcohol, and acetylene, acenaphthene, or phenol resin) through either a solution-phase or a vapor-phase reaction to mesoporous silica hosts in the presence of a catalyst, followed by the hydrolysis of the carbon precursor. Another synthetic route by catalytic chemical vapor deposition has also been described [389]. It has been demonstrated that morphology and properties of CMCs largely depend on the nature of the carbon precursor and the hydrolysis conditions [390]. In principle, it is expected that conducting polymer can be used as a carbon precursor via a thermo-pyrolysis process because of their polymer chain containing C, N, S and O elements. Yang et al. [391] recently reported that a hexagonally structured carbon replica was obtained, which TEM images of OMC prepared by silicon-guided (SBA-15) PPy as carbon precursor is shown in Fig. 4.17. The quantitative analysis reveals that except for carbon, the resultant OMC material contains nitrogen (~ 5.5%), iron (less than 1%), but no silicon was detected. The iron contained can be removed by HCl solution, indicating iron species produced during the pyrolysis of PPy are not embedded or coated with carbon [391].
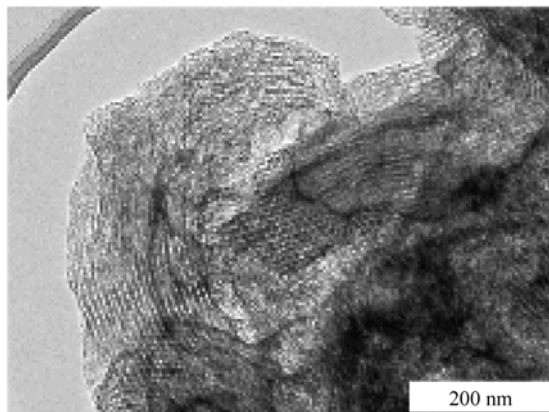
Figure 4.17   TEM images of OMC prepared by silicon-guided (SBA-15) PPy as carbon precursor [401]

4.3.3   Nano-arrays or Nano-patents

As above-mentioned, conducting polymer nanowires and nanotubes are promising materials for a variety of applications including optical and electronic nano-devices and chemical and biological sensors [392]. However, successful application of these nanostructured materials into functional nano-devices requires controlled patterning at micro- and nanometer scale. Various methods, such as photolithography [393], micro-contact printing [394], template assisted synthesis [395], scanning electrochemical microlithography [396], mechanical stretching [397], electro-chemical dip-pen lithography techniques [398] and electro-deposition within channels between two electrodes on the surface of silicon wafers [399] have been used for fabricating micro- and nano-scale arrays from conducting polymers. However, these methods still have limitations in terms of yield, resolution, material multiplicity, positioning, production of high-density arrays, and most of all cost. Herein above-methoned methods are briefly reviewed.

1. Electro-Deposition within Channels

Since electrochemical polymerization is a common and controlling method for preparing conducting polymers and their nanostructures, electro-deposition within channels between two electrodes has been received attention in fabricating molecule devices. For instance, conducting polymer nanowires prepared by an electro-deposition within channels between two electrodes on the surface of silicon wafers have been reported [400]. The deposition and growth of the nanowire chains are based on well-known electrochemical oxidative polymerization. Multiple channels can be etched between gold electrode pairs in the form of arrays to provide formation of any number of individual nanowires. The procedure

is a single-step deposition process for each nanowire, and multiple-nanowire arrays of different materials can be deposited on the same wafer sequentially. In addition, Mulchandani et al. [400] also demonstrated the ability to create scalable high density "arrays" by site-specific positioning of conducting polymer nanowires of same and different composition on the same chip.

2. Electrochemical Dip-Pen Nanolithography

Electrochemical dip-pen nanolithography (E-DPN) is a new atom force morphology (AFM) lithography technique [401]. Like other DPN techniques, E-DPN relies on spontaneous condensation to facilitate transport of material from the AFM tip to the surface [401, 402]. It consists of a chemical/physical process (e.g. covalent bonding or electrochemical reaction), then immobilizes the material on the surface. Since the reaction occurs at the AFM tip, material deposition localizes on the patterns traced by the tip, the E-DPN technique provides a method for depositing polymer and oxidizing the Si surface simultaneously that opens the possibility of a one step nano-electronic device fabrication [403]. Maynor et al. [403] used E-DPN to fabricate PTH nanowires on semiconducting and insulating surfaces in the regime of more than 100 nm. They reported that the nanostructure morphology is dependent on the humidity, applied voltage, and translation speed of the tip.

3. Inkjet Printing

Inkjet printing is attractive for the electronics industry because of its low-cost fabrication. Since many conducting polymers in their conducting states tend to be insoluble and intractable soluble, therefore direct application of inkjet printing in conducting polymers is impossible. Functionalization of conducting polymers with moieties to increase solubility is effective for achieving processability, but the substituent often alter poor and un-desirable conductivity. Liu et al. [404] recently presented a method to pattern conducting polymer (e.g. PPy) nanostructure devices using a grow-in-place vapor-phase procedure that guides growth of polymer by selective condensation on a chemically patterned substrate.

4. Scanning Electrochemical Microscopy

Scanning electrochemical microscopy (SECM) is a surface analysis and modification technique. SECM successfully combines features of scanning tunneling microscopy (STM) and ultra-microelectrodes (UMEs), which is moved in an electrolyte above the surface [405]. Usually, the Faradic current measured at the tip originates from oxidation or reduction of the electrochemical species in the solution depends on both the chemical nature of the substrate and the tip-sample distance. Thereby, the SECM has been shown to be a valuable analytical tool and scanning the UME at a constant height provides valuable information about local surface conductivity, morphology, concentration profiles, and maps of reactive sites [406]. Since high-resolution surface etching and deposition, thus

the novel SECM method can be used to micro-modify surface using deposition and etching processes [407]. Some successful examples of the polymerization of conducting polymers using the SECM have been reported in the literature [408]. Marck et al. [409] recently proposed a new concept of micro-deposition of conducting polymers using the SECM and an immobilized oxidant-coated sample. This new approach is suitable for monomers with high solubility in water. As an application of this new method, the local polymerization of thiophene was performed on a manganese dioxide surface locally activated by tip-generated protons [409].

5. Hydrophilic/Hydrophobic Patterns

Nowadays hydrophilic patterning [410] and even selective condensation [411] to pattern a final conducting polymer patterning has been used to directly fabricate devices in the submicrometer range. Dendritic structures of conducting polymers electrochemically grown between micro-patterned electrodes from a monomer vapor [412] and patterning the hydrophobic/hydrophilic structures on a surface have been reported [413]. Moreover, both ultrahigh-resolution techniques such as e-beam or AFM lithography (<10 nm feature size) and photolithography can be used to prepare conducting nano-scaled patents. Woodson et al. [404] reported an electrochemical method of directly growing conducting PPy nanostructures between metal electrodes with the geometry controlled by hydrophilic/hydrophobic patterns. Moreover, PPy field effect transistors have been produced using this method, showing conductivity strongly dependent on the presence of anionic dopant species during growth, for instance, devices grown with a high concentration of dopant show metallic behavior; while those with less doping behave as *p*-type semiconductors [404].

6. Photolithography Technique Associated with Photo-Acid Generation Process

As mentioned in Chapter 2, PANI can be doped by photo-generated proton. Moreover, photolithography technique is a common tool to fabricate patents of conducting polymers. Therefore photolithography technique associated with photo-acid generation process can be used to prepare micro-structural patent of PANI. PANI with a thermo-labile and acid-labile *tert*-butoxycarbonyl (t-BOC) group, PANI-(t-BOC), is a typical sample for above-described photolithography associated with photo-acid generation process [414]. The PANI-(t-BOC) is highly soluble and thermodynamically stable in low-boiling solvents (e.g. THF, dioxane, and $CHCl_3$), especially which is converted to the insoluble and electrically conductive emeraldine salts upon photodoping with photo-acid generators (e.g. *N*-(tosyloxy) - or camphorsulfonyloxy) norborneneimide or onium salts. The solubility difference leads to producing conducting patterns of high resolution by conventional photolithography process. Upon removal of the t-BOC groups in PANI-(t-BOC) by acid doping, moreover, no obvious morphology change of the films was observed, and such conversion recovered the original conductivity level of the

doped PANI [414]. Since the t-BOC protecting groups are easily removed in doping or acid-catalyzed reaction by chemical amplification or thermal bake, the PANI-(t-BOC) can be used as conductive matrix polymers for negative type photo-imaging or printing materials or for novel solution-processed applications in various microelectronic devices.

In summary, although conducting polymer nanostructures have attracted considerable attention in molecular or nanoelectronic devices owing to their unique properties, scientific research on releaving nano-scaled properties, structure-size and structure-property relationship as well as fabrication technique of the nanodevices are still challenge for realization of commercial applications of the conducting polymer nanostructures.

References

[1] R. Parthasarathy, C. R. Martin. Nature, 1994, 369: 298

[2] J. D. Klein, R. D. I. Herrick, R. D. Palmer, M. J. Sailor, C. J. Brumlik, C. R. Martin. Chem. Mater., 1993, 5: 902

[3] R. V. Parthasarathy, C. R. Martin. Adv. Mater., 1995, 7: 896

[4] a) P. M. Penner, C. R. Martin. J. Electrochem. Soc., 1986, 133, 2206; b) Z. Cai, C. R. Martin. J. Am. Chem. Soc., 1989, 111: 4138; c) L. S. Van Dyke, C. R. Martin. Langmuir, 1990, 6: 1123 – 1132; d) W. Liang, C. R. Martin. J. Am. Chem. Soc., 1990, 112: 9666; e) C. R. Martin. Adv. Mater., 1991, 3: 457; f) Z. Cai, J. Lei, W. Liang, V. Menon, C. R. Martin. Chem. Mater., 1991, 3: 960; g) C. R. Martin, R. Parthasarathy, V. Menon. Synth. Met., 1993, 55: 1165; h) R. M. Penner, C. R. Martin. Anal. Chem., 1987, 59: 2625; i) C. J. Brumlik, V. P. Menon, C. R. Martin. J. Mater. Res., 1994, 9: 1174

[5] C. G. Wu, T. Bein. Science, 1994, 264: 1757

[6] S. F. Yu, N. C. Li, J. Wharton, and C. R. Martin. Nano. Letter, 2003, 3: 815

[7] R. V. Parthasarathy, C. R. Martin. Chem. Mater., 1994, 6: 1627; G. A. Ozin. Adv. Mater., 1992, 4: 612

[8] C. J. Brumlik, C. R. Martin. J. Am. Chem. Soc., 1991, 113: 3174

[9] J. Lei, Z. Cai, C. R. Martin. Synth. Met., 1992, 46: 53

[10] R. M. Penner, C. R. Martin. J. Electrochem. Soc., 1986, 133

[11] M. X. Fu, Y. F. Zhu, R. Q. Tan, and G. Q. Shi. Adv. Mater., 2001, 13: 1874

[12] B. Rajesh, K. R. Thampi, J. M. Bonard, N. Xanthopoulos, H. J. Mathieu, B. Viswanathan. J. Phys. Chem. B, 2004, 108: 10640

[13] X. Ren, P. Zelenay, S. Thomas, J. Davey, S. Gottesfeld. J. Power Sources, 2000, 86: 111

[14] D. AlMawiawi, N. Coombs, M. Moskovits. J. Appl. Phys., 1991, 70: 4421

[15] a) C. A. J. Foss, G. L. Hornyak, J. A. Stockert, C. R. Martin. J. Phys. Chem., 1992, 96: 7497 – 7499; b) C. A. J. Foss, G. L. Hornyak, J. A. Stockert, C. R. Martin. Adv. Mater., 1993, 5: 135; c) C. A. J. Foss, G. L. Hornyak, J. A. Stockert, C. R. Martin. J. Phys. Chem., 1994, 98: 2963

[16] R. L. leischer, P. B. Price, R. M. Walker. Nuclear tracks in University of California Press: Berkeley, 1975

[17] A. Despic, V. P. Parkhutik. In: Modern Aspects of Electrochemistry. J. O. Bockris, R. E. White, B. E. Conway, Eds. Plenum Press: New York, 1989, Vol. 20

[18] R. J. Tonucci, B. L.Justus, A. J. Campillo, C. E. Ford. Science, 1992, 258: 783

[19] J. S. Beck, J. C. Vartuli, W. J. Roth, M. E. Leonowicz, C. T. Kresge, K. D. Schmitt, C. T.W.Chu, D. H. Olson, E. W. Sheppard, S. B. McCullen, J. B. Higgins, J. L. Schlenker. J. Am. Chem. Soc., 1992, 114: 10834

[20] L. Cao, H. Z. Chen, H. B. Zhou, L. Zhu, J. Z. Sun, X. B. Zhang, J. M. Xu, M. Wang. Adv. Mater., 2003, 15: 909

[21] M. Goren, Z. G. Qi, R. B. Lennox. Chem. Mater., 2000, 12: 1222

[22] H. Dong, S. Prasad, V. Nyame, W. E. Jr. Jones. Chem. Mater., 2004, 16: 371

[23] J. D. Noll, M. A. Nicholson, P. G. Vanpatten, C. W. Chung, M. L.Myrick. J. Electrochem. Soc., 1998, 145: 3320

[24] Y. F. Ma, J. M. Zhang, G. J. Zhang, and H. X. He. J. Am. Chem. Soc., 2004, 126: 7097; J. Am. Chem. Soc., 2004, 126: 7097

[25] a) Z. J. Gartner, D. R. Liu. J. Am. Chem. Soc., 2001, 123: 6961；b) Z. J. Gartner, M. W. Kanan, D. R. Liu. Angew. Chem., Int. Ed., 2002, 41: 1796；c) Z. J. Gartner, M. W. Kanan, D. R. Liu. J. Am. Chem.Soc., 2002, 124: 10304；d) C. T. Calderone, J. W. Puckett, Z. J. Gartner, D. R. Liu. Angew. Chem., Int. Ed., 2002, 41: 4104；e) Z. J. Gartner, R. Grubina, C. T. Calderone, D. R. Liu. Angew. Chem., Int. Ed., 2003, 42: 1370

[26] X. Y. Li and D. R. Liu. J. Am. Chem. Soc., 2003, 125: 10188

[27] a) A. Y. Kasumov, M. Kociak, S. Gueron, B. Reulet, V. T. Volkov, D. V. Klinov, H. Bouchiat. Science, 2001, 291: 280; b) H. W. Fink, C. Schonenberger. Nature, 1999, 398: 407; c) D. Porath, A. Bezryadin, S. De Vries, C. Dekker. Nature, 2000, 403: 635

[28] a) K. Keren, M. Krueger, R. Gilad, G. Ben-Yoseph, U. Sivan, E. Braun. Science, 2002, 297: 72; b) W. E. Ford, O. Harnack, A. Yasuda, J. M. Wessels. Adv. Mater., 2001, 13: 1793; c) C. F. Monson, A. Woolley. Nano Lett., 2003, 3: 359; d) M. G. Warner, J. E. Hutchison. Nat. Mater., 2003, 2: 272; e) M. Mertig, L. C. Ciacchi, W. Pompe. Nano Lett., 2002, 2: 841

[29] X. Y. Zhang, W. J. Goux, and S. K. Manohar. J. Am. Chem. Soc., 2004, 126: 4502

[30] H. Coelfen, S. Mann. Angew. Chem., Int. Ed., 2003, 42: 2350

[31] J. Huang, S. Virji, B. H. Weiller, R. B. Kaner. J. Am. Chem. Soc., 2003, 125: 314

[32] M. Von Bergen, P. Friedhoff, J. Biernat, J. Heberle, E. M. Mandelkow, E. Mandelkow. Proc. Natl. Acad. Sci.(U.S.A.), 2000, 97: 5129

[33] H. Coelfen, S. Mann. Angew. Chem., Int. Ed., 2003, 42: 2350

[34] A. K. Boal, F. Ilhan, J. E. DeRouchey, T. T. Albrecht, T. P. Russell, V. M. Rotello. Nature, 2000, 404: 746

[35] Z. R. Tian, J. A. Voigt, J. Liu, B. Mckenzie, M. J. Mcderott, M. A. Rodriguze, H. Konishi, H. F. Xu. Nat. Mater., 2004, 2: 821

[36] M. Muthukumar, C. K. Ober, E. L. Thomas. Science, 1997, 277: 1225

[37] F. S. Bates, G. H. Fredrickson. Annu. Rev. Phys. Chem., 1990, 41: 525

[38] W. Wernet, M. Monkenbusch, G. Wegner. Makromol. Chem., Rapid Commun., 1984, 5: 157

[39] W. Y. Zheng, R. H. Wang, K. Levon, Z. Y. Rong, T. Taka, W. Pan. Makromol. Chem. Phys., 1995, 196: 2443

[40] H. Kosonen, J. Ruokolainen, M. Knaapila, M. Torkkeli, K. Jokela, R. Serimaa, G. T. Brinke, W. Bras, A. P. Monkman, O. Ikkala. Macromolecules, 2000, 33: 8671

[41] H. Y. Gan, H. B. Liu, Y. J. Li, Q. Zhao, Y. L. Li, S. Wang, T. G. Jiu, N. Wang, X. R. He, D. P. Yu, D. B. Zhu. J. Am. Chem. Soc., 2005, 127: 12452

[42] A. D. W. Carswell, E. A. O'Rear, B. P. Grady. J. Am. Chem. Soc., 2003, 125: 14793

[43] a) J. F. Hulvat, S. I. Stupp. Angew. Chem., Int. Ed., 2003, 42: 778; b) L. M. Huang, Z. B. Wang, H. T. Wang, X. L. Cheng, A. Mitra, Y. S. Yan. J. Mater. Chem., 2002, 12: 388

[44] a) L. T. Qu, G. Q. Shi, F. E. Chen, J. X. Zhang. Macromolecules, 2003, 36: 1063; b) L. T. Qu, G. Q. Shi. Chem. Commun., 2003, 2: 206

[45] Z. X. Wei, L. J. Zhang, M. Yu, Y. S. Yang, M. X. Wan. Adv. Mater., 2003, 15: 1382

[46] T. Hatano, A. H. Bae, M. Takeuchi, N. Fujita, K. Kaneko, H. Ihara, M.Takafuji, S. Shinkai. Angew. Chem. Int. Ed., 2004, 43: 465

[47] Y. H. Luo, H. W. Liu, F. Xi, L. Li, X. G. Jin, C. C. Han, Z. M. Cha. J. Am. Chem. Soc., 2003, 125: 6447

[48] X. T. Zhang, J. Zhang, W. B. Song, Z. F. Liu. J. Phys. Chem. B, 2006, 110: 1158

[49] J. Israelachvili, D. J. Mitchell, B. W. Ninham. J. Chem. Soc., Faraday Trans. 2, 1976, 72: 1525

[50] S. Manne, H. E. Gaub. Science, 1995, 270: 1480

[51] R. E. Lamont，W. A. Ducker. J. Am. Chem. Soc., 1998, 120: 7602

[52] a) H. N. Patrick, G. G. Warr, S. Manne, I. A. Aksay. Langmuir, 1999, 15: 1685; b) S. B. Velegol, B. D. Fleming, S. Biggs, E. Wanless, R. D. Tilton. Langmuir, 2000, 16: 2548

[53] L. M. Grant, T. Ederth, F. Tiberg. Langmuir, 2002, 16: 2285

[54] L. Kovacs, G. G. Warr. Langmuir, 2002, 18: 4790

[55] a) G. Cho, D. T. Glatzhofer, B. M. Fung, W. L. Yuan, E. A. O'Rear. Langmuir, 2000, 16: 4424; b) G. Cho, D. T. Glatzhofer, B. M. Fung, W. L. Yuan, E. A. O'Rear. Langmuir, 2000, 16: 4424; c) W. L. Yuan, E. A. O'Rear, B. P. Grady, D. T. Glatzhofer. Langmuir, 2002, 18: 3343

[56] J. F. Hulvat, S. I. Stupp. Angew. Chem., Int. Ed., 2003, 42: 778

[57] a) Z. Wei, Z. M. Zhang, M. X. Wan. Langmuir, 2002, 18: 917; b) L. J. Zhang, M. X. Wan. Nanotechnology, 2002, 13: 750; c) H. J. Qiu, M. X. Wan, B. Matthews, L. M. Dai. Macromolecules, 2001, 34: 675

[58] a) J. Jang, H. Yoon. Chem. Commun., 2003, 6: 720; b) M. Cao, Y. Wang, C. Guo, Y. Qi, C. Hu. Langmuir, 2004, 20: 4784; c) S. I. Yoo, B. H. Sohn, W. C. Zin, J. C. Jung. Langmuir, 2004, 20: 10734; d) H. Shi, L. Qi, J. Ma, H. Cheng. J. Am. Chem. Soc., 2003, 125: 3450; e) S. Xu, H. Zhou, J. Xu, Y. Li. Langmuir, 2002, 18: 10503; f) M. Goren, R. B. Lennox. Nano Lett., 2001, 1: 735; g) J. Jang, M. Chang, H. Yoon. Adv. Mater., 2005, 17: 1616

[59] J. Jang, H. Yoon. Langmuir, 2005, 21: 11484

[60] X. Y. Zhang, J. S. Lee, G. S. Lee, D. K. Cha, M. J. Kim, D. J. Yang, S. K. Manohar. Macromolecules, 2006, 39: 470

[61] G. C. Li, Z. K. Zhang. Macromolecules, 2004, 37: 2683

[62] L. Huang, Z. Wang, H. Wang, X. Cheng, A. Mitra, Y. Yan. J. Mater. Chem., 2002, 12: 388

[63] S. P. Armes, M. Aldissi, G. C. Idzorek, P. W. Keaton, L. J. Rowton, G. L. Stradling, M. T. Collopy, D. B. McColl. J. Colloid Interface Sci., 1991, 141: 119

[64] a) T. Sumida, Y. Wada, T. Kitamura, S. Yanagida. Chem. Commun., 2000, 1613; b) T. Cassagneau, F. Caruso. Adv. Mater., 2002, 14: 34

[65] D. Wang, F. Caruso. Adv. Mater., 2001, 13: 350

[66] P. N. Bartlett, P. R. Birkin, M. A. Ghanem, C. S. Toh. J. Mater.Chem., 2001, 11: 849

[67] a) J. Stejskal, M. Spirkova, A. Riede, M. Helmstedt, P. Mokreva, J. Prokes. Polymer, 1999, 40: 2487; b) D. Chattopadhyay, B. M. Mandal. Langmuir, 1996, 12: 1585

[68] P. C. Innis, I. D. Norris, L. A. P. Kane-Maguire, G. G. Wallace. Macromolecules, 1998, 31: 6521

[69] S. B. Han, A. L. Briseno, X. Y. Shi, A. D. Mah, F. M. Zhou. J. Phys. Chem. B, 2002, 106: 6465

[70] Z. G. Qi, P. G. Pickup. Chem. Mater., 1997, 9: 2934

[71] R. Cruz-Silva, C. Ruiz-Flores, L. Arizmendi, J. Romero-Garcia, E. Arias-Marin, I. Moggio, F. F. Castillon, M. H. Farias. Polymer, 2006, 47: 1563

[72] R. Cruz-Silva. Langmuir, 2007, 23: 8

[73] G. A. Ozin. Adv. Mater., 1992, 4: 612

[74] X. F. Lu, Y. H. Yu, L. Chen, H. P. Mao, L. F. Wang, W. J. Zhang, Y. Wei. Polymer, 2005, 46: 5329

[75] H. L. Hu, J. M. Saniger, J. G. Banuelos. Thin Solid Films, 1999, 347: 241

[76] S. A. Chen, H. T. Lee. Marcromolecules, 1995, 28: 2858

[77] X. Wang, N. Liu, X. Yan, W. J. Zhang, Y. Wei. Chem. Lett., 2005, 34: 42

[78] Y. Yu, S. Zhihuai, S. Chen, C. Bian, W. Chen, G. Xue. Langmuir, 2006, 22: 3899

[79] H. B. Xia, J. Narayanan, D. Cheng, C. Y. Xiao, X. Y. Liu, H. S. O. Chan. J. Phys. Chem. B, 2005, 109: 12677

[80] a) E. R. Zubarev, M. U. Pralle, E. D. Sone, S. I. Stupp. J. Am. Chem. Soc., 2001, 123: 4105; b) E. R. Zubarev, M. U. Pralle, S. E. Sone, S. I. Stupp. Adv. Mater., 2002, 14: 198

[81] H. L. Guo, C. M. Knobler, R. B. Kaner. Synth. Met., 1999, 101: 1

[82] J. C. Moutet, E. Saintaman, F. Tranvan, P. Angibeaud, J. P. Utille. Adv. Mater., 1992, 4: 7

[83] P. A. Bross, U. Schoberl, J. Daub. Adv. Mater., 1991, 3: 198

[84] W. G. Li and H. L. Wang. J. Am. Chem. Soc., 2004, 126: 2278

[85] S. A. Ashraf, L. A. P. Kanemaguire, M. R. Majidi, S. G. Pyne, G. G. Wallace. Polymer, 1997, 38: 2627

[86] L. A. P. Kane-Maguire, A. G. MacDiarmid, I. D. Norris, G. G. Wallace, W. G. Zheng. Synth. Met., 1999, 29: 171

[87] a) J. B. Gao, W. J. Zhang, K. Li, C. Wang, Z. W. Wu, Y. P. Ji. Macromol. Rapid Commun., 1999, 20: 463; b) R. A. Singer, J. P. Sadighi, S. L. Buchwald. J. Am. Chem. Soc., 1998, 120: 213

[88] a) M. S. Spector, J. V. Selinger, A. Singh, J. M. Rodriguez, R. R. Price, J. M.Schnur. Langmuir, 1998, 14: 3493; b) B. R. Ratna, S. Baral-Tosh, B. Kahn, J. M. Schnur, A. S. Rudolph. Chem. Phys. Lipids, 1992, 63: 47

[89] M. Goren, Z. Qi, R. B. Lennox. Chem. Mater., 2000, 12: 1222

[90] S. K. Pillalamarri, F. D. Blum, A. T. Tokuhiro, J. G. Story, M. F. Bertino. Chem. Mater., 2005, 17: 227

[91] a) D. A. Weitz, M. Oliveria. Phys. Rev. Lett., 1984, 52: 1433; b) B. V. Enustun, J. Turkevich. J. Am. Chem. Soc., 1963, 85: 3317

[92] B. Nandan, J. Y. Hsu, A. Chiba, H. L. Chen, C. S. Liao, S. A. Chen, H. Hasegawa. Macromolecules, 2007, 40: 395

[93] B. Nandan, H. L. Chen, C. S. Liao, S. A. Chen. Macromolecules, 2004, 37: 9561

[94] X. Zhang, H. S. Kolla, X. Wang, K. Raja, S. K. Manohar. Adv. Funct. Mater., 2006, 16: 1145

[95] M. Shimomura, T. Kunitake. J. Am. Chem. Soc., 1987, 109: 5175

[96] P. Anilkumar, M. Jayakannan. J. Phys. Chem. C, 2007, 111: 3591

[97] I. W. Hamley. The Physics of Block Copolymers. Oxford University Press: New York, 1998

[98] S. Förster, M. Antonietti. Adv. Mater., 1998, 10: 195

[99] a) L. Bronstein, M. Antonietti, P. Valetsky. In: Nanoparticles and Nanostructured Films. J. H. Fendler Ed. Wiley-VCH: Weinheim, Germany, 1998; b) M. Moffitt, A. Eisenberg. Chem. Mater., 1995, 7: 1178

[100] a) I. W. Hamley. Nanotechnology, 2003, 14: 39; b) R. Glass, M. Möller, J. P. Spatz. Nanotechnology, 2003, 14: 1153

[101] a) M. Goren, R. B. Lennox. Nano Lett., 2001, 1: 735; b) B. H. Sohn, S. I. Yoo, B. W. Seo, S. H. Yun, S. M. Park. J. Am.Chem. Soc., 2001, 123: 12734; c) B. H. Sohn, J. M. Choi, S. I. Yoo, S. H. Yun, W. C. Zin, J. C. Jung, M. Kanehara, T. Hirata, T. Teranishi. J. Am. Chem. Soc., 2003, 125: 6368

[102] S. I. Yoo, B. H. Sohn, W. C. Zin, J. C. Jung. Langmuir, 2004, 20: 10734

[103] A. Formhals. U.S. Patent 1,975,504, 1934

[104] D. H. Reneker, I. Chun. Nanotechnology, 1996, 7: 216

[105] H. Fong, I. Chun, D. H. Reneker. Polymer, 1999, 40: 4585

[106] A. G. MacDiarmid, W. E. Jr. Jones, I. D. Norris, J. Gao, A. T. Johnson, N. J. Pinto, J. Hone, B. Han, F. K. Ko, H. Okuzaki, M. Llaguno. Synth. Met., 2001, 119: 27

[107] a) M. Bognitzki, H. Hou, M. Ishaque, T. Frese, M. Hellwig, C. Schwarte, A. Schaper, J. H. Wendorff; A. Greiner. Adv. Mater., 2000, 12: 637; b) H. Hou, Z. Jun, A. Reuning, A. Schaper, J. H. Wendorff, A. Greiner. Macromolecules, 2002, 35: 2429; c) R. A. Caruso, J. H. Schattka, A. Greiner. Adv. Mater., 2001, 13: 1577

[108] D. Hong, P. Sudhindra, N. Verrad, E. J. Jr. Wayne. Chem. Mater., 2004, 16: 371

[109] a) J. Liu, Y. Lin, L. Liang, J. A. Voigt, D. L. Huber, Z. R. Tian, E. Coker, B. Mckenzie, M. J. Mcdermott. Chem. Eur. J., 2003, 9, 605; b) L. Liang, J. Liu, C. F. Windisch, G. J. Exarhos, Y. H. Lin. Angew. Chem., Int. Ed., 2002, 41: 3665

[110] H. X. He, C. Z. Li, N. Tao. J. Appl. Phys. Lett., 2001, 78: 811

[111] a) J. Huang, S. Virji, B. H. Weiller, R. B. Kaner. J. Am. Chem. Soc., 2003, 125: 314; b) J. Huang and R. B. Kaner. J. Am. Chem. Soc., 2004, 126: 851

[112] a) Mason, Ed. Advances in Sonochemistry. JAI Press: London, 1990, Vol. 1; b) Mason, Ed. Advances in Sonochemistry. JAI Press: London, 1991, Vol. 2

[113] E. B. Flink, K. S. Suslick. Science, 1990, 3: 1439

[114] a) A. Koshio, M. Yudasaka, M. Zhang, S. Iijima. Nano Lett., 2001, 1: 361; b) H. Xia, Q. Wang. Chem. Mater., 2002, 14: 2158; c) M. Bradley, F.Grieser. J. Colloid Interface Sci., 2002, 251: 78; d) Y. Kojima, S. Koda, H. Nomura. Ultrason. Sonochem., 2001, 8: 75

[115] H. Liu, X. B. Hu, J. Y. Wang, R. I. Boughton. Macromolecules, 2002, 35: 9414

[116] R. Vijaya Kumar, Y. Mastai, A. Gedanken. Chem. Mater., 2000, 12: 3892

[117] a) M. G. Han, S. P. Armes. Langmuir, 2003, 19: 4523.23; b) J. W. Choi, M. G. Han, S. G. Oh, S. S. Im. Synth. Met., 2004, 141:293. 24; c) M. G. Han, S. H. Foulger. Adv. Mater., 2004, 16: 231. 25; d) M. G. Han and S. H. Foulger. Chem. Commun., 2004, 2154

[118] a) L. B. Groenendaal, F. Jonas, D. Freitag, H. Pielartzik, J. R. Reynolds. Adv. Mater., 2000, 12: 481; b) L. B. Groenendaal, G. Zotti, P. H. Aubert, S. M. Waybright, J. R. Reynolds. Adv. Mater., 2003, 15: 855; c) Y. H. Ha, N. Nikolov, S. K. Pollack, J. Mastrangelo, B. D. Martin, R. Shashidhar. Adv. Funct. Mater., 2004, 14: 615

[119] a) S. Kirchmeyer, K. Reuter. J. Mater. Chem., 2005, 15: 2077; b) S. Garreau, G. Louarn, J. P. Buisson, G. Froyer, S. Lefrant. Macromolecules, 1999, 32: 6807

[120] a) D. Hohnholz, H. Okuzaki, A. G. MacDiarmid. Adv. Funct. Mater., 2005, 15: 51; b) K. H. Hong, K. W. Oh, T. J. Kang. J. Appl. Polym. Sci., 2005, 97: 1326.19

[121] a) B. H. Kim, M. S. Kim, K. T. Park, J. K. Lee, D. H. Park, J. Joo, S. G. Yu, S. H. Lee. Appl. Phys. Lett., 2003, 83: 539; b) J. L. Duvail, P. Retho, S. Garreau, G. Louarn, C. Godon, S. Demoustier-Champagne. Synth. Met., 2002, 131: 123

[122] B. H. Kim, D. H. Park, J. Joo, S. G. Yu, S. H. Lee. Synth. Met., 2005, 150: 279

[123] M. G. Han, S. H. Foulger. Chem. Commun., 2005, 3092

[124] S. I. Cho, D. H. Choi, S. H. Kim, S. B. Lee. Chem. Mater., 2005, 17: 4564

[125] S. G. Oh, S. S. Im. Curr. Appl. Phys., 2002, 2: 273

[126] K. M. Ller, M. Klapper, K. Müllen. Macromol. Rapid Commun., 2006, 27: 586

[127] X. Zhang, J. S. Lee, G. S. Lee, D. K. Cha, M. J. Kim, D. J. Yang, S. K. Manohar. Macromolecules, 2006, 39: 470

[128] M. Mumtaz, A. de Cuendias, J. L. Putaux, E. Cloutet, H. C. Macromol. Rapid Commun., 2006, 27: 1446

[129] X. Zhang, A. G. MacDiarmid, S. K. Manohar. Chem. Commun., 2005, 5328–5330

[130] X. Zhang, S. K. Manohar. J. Am. Chem. Soc., 2004, 126: 12714

[131] a) M. S. Gudiksen, L. J. Lauhon, J. Wang, D. C. Smith, C. M. Lieber. Nature, 2002, 415: 617; b) K. B. Lee, S. Park, C. A. Mirkin. Angew. Chem., Int. Ed., 2004, 43: 3048; c) N. I. Kovtyukhova, B. R. Martin, J. K. N. Mbindyo, P. A. Smith, B. Razavi, T. S. Mayer, T. E. Mallouk. J. Phys. Chem. B, 2001, 105: 8762; d) D. J. Pena, J. K. N. Mbindyo, A. J. Carado, T. E. Mallouk, C. D. Keating, B. Razavi, T. S. Mayer. J. Phys. Chem. B, 2002, 106: 7458; e) S. Park, J. H. Lim, S. W. Chung, C. A. Mirkin. Science, 2004, 303: 348; f) S. R. Nicewarner-Pena, R. G. Freeman, B. D. Reiss, L. He, D. J. Pena, I. D. Walton, R.Cromer, C. D. Keating, M. J. Natan. Science, 2001, 294: 137

[132] S. Park, J. H. Lim, S. W. Chung, C. A. Mirkin. Science, 2004, 303: 348

[133] A. C. Templeton, J. J. Pietron, R. W. Murray, R. P. Mulvaney. J. Phys. Chem. B, 2000, 104: 564

[134] C. Demaille, M. Brust, M. Tsionsky, A. Bard. J. Anal. Chem., 1997, 69: 2323

[135] G. Peto, G. L. Molnar, Z. Paszti, O. Geszti, A. Beck, L. Guczi. Mater. Sci. Eng. C, 2002, 19: 95

[136] N. Chandrasekharan, P. V. Kamat. J. Phys. Chem. B, 2000, 104: 10851

[137] O. V. Cherstiouk, P. A. Simonov, E. R. Savinova. Electrochim. Acta, 2003, 48: 3851

[138] P. V. Kamat. J. Phys. Chem. B, 2002, 106: 7729

[139] Handbook of Conducting polymers. T. A. Skotheim Ed. Marcel Dekker: New York, 1986 and 1998

[140] E. Kriván, C. Visy, J. Kankare. J. Phys. Chem. B, 2003, 107: 1302

[141] a) A. Kitani, T. Akashi, K. Sugimoto, S. Ito. Synth. Met., 2001, 121: 1301; b) A. Relinkiewicz, M. Hasik, M. Kloc. Catal. Lett., 2000, 64: 41.357; c) P. T. Radford, S. E. Creager. Anal. Chem. Acta, 2001, 449: 199

[142] a) A. Sargent, T. Loi, S. Gal, O. A. Sadik. J. Electroanal. Chem., 1999, 470: 144; b) A. Sargent, O. A. Sadik. Electrochim. Acta, 1999, 44: 4667; c) M. J. Croissant, T. Napporn, J. Leger, C. Lamy. Electrochim. Acta, 1998, 43: 2447

[143] a) R. J. Nichols, D. Schröer, H. Meyer. Electrochim. Acta, 1995, 40: 1479; b) R. J. Tremont, G. Cruz, C. R. Cabrera. J. Electroanal. Chem., 2003, 558: 65

[144] a) R. Stiger, B. Craft, R. M. Penner. Langumir, 1999, 15: 790; b) S. Gorer, J. A. Ganske, J. C. Hemminger, R. M. Penner. J. Am. Chem. Soc., 1998, 120: 9584

[145] J. M. Ortega. Thin Solid Films, 2000, 360: 159

[146] S. Strbac, O. M. Magnussen, R. Behm. J. Phys. Rev. Lett., 1999, 83: 3246

[147] R. Schuster, G. Ertl. In: Catalysis and Electrocatalysis at Nanoparticle Surface. A. Wieckowski, E. R. Savinova, C. G. Vayenas Eds. Marcel Dekker: New York, 2003, p.211

[148] Y. C. Liu, L. Y. Jang. J. Phys. Chem. B, 2002, 106: 6748

[149] Y. Li, G. Q. Shi. J. Phys. Chem. B, 2005, 109: 23787

[150] a) J. M. Kern, J. P. Sauvage. J. Chem. Soc., Chem. Commun., 1989, 657; b) H. Segawa, T. Shimidzu, K. Honda. J. Chem. Soc., Chem. Commun., 1989, 132

[151] M. A. Breimer, G. Yevgeny, S. Sy, and O. A. Sadik. Nano Letter, 2001, 6: 305

[152] a) N. Cioffi, L.Torsi, I. Losito, C. D. Franco, I. D. Bari, L. Chiavarone, G. Scamarcio, V. Tsakova, L. Sabbatini, P. Zambonin. J. Mater. Chem., 2001, 11: 1434; b) V. Tsakova, D. Borissov, B. Ranguelov, C. Stromberg, J. W. Schultze. Electrochim. Acta, 2001, 46: 4213; c) D. K. Sarkar, X. J. Zhou, A. Tannous, K. T. Leung. J. Phys.Chem. B, 2003, 107: 2879

[153] Y. C. Liu, K. H. Yang, M. D. Ger. Synth. Met., 2002, 126: 337

[154] D. K. Sarkar, X. J. Zhou, A. Tannous, K. T. Leung. J. Phys. Chem. B, 2003, 107: 2879 – 2881

[155] a) Y. N. C. Chan, R. R. Schrock, R. E. Cohen. J. Am. Chem. Soc., 1992, 114: 7295; b) M. Antonietti, S. Foerster, J. Hartmann, S. Ostreich. Macromolecules, 1996, 29: 3800

[156] S. T. Selvan, J. P. Spatz, H. A. Klok, M. Moeller. Adv. Mater., 1998, 10: 132; S. T. Selvan. J. Chem. Soc., Chem. Commun., 1998, 351

[157] S. T. Selvan, T. Hayakawa, M. Nogami, M. Moller. J. Phys. Chem. B, 1999, 103: 7441

[158] V. M. Cepak, J. C. Hulteen, G. Che, K. B. Jirage, B. B. Lakshmi, E. R. Fisher, C. R. Martin. Chem. Mater., 1997, 9: 1065

[159] a) M. Nishizawa, V. P. Menon, C. R. Martin. Science, 1995, 268: 700; b) V. P. Menon, C. R. Martin. Anal. Chem., 1995, 67: 1920

[160] N. Oyama, T. Ohsaka, Y. Ohnuki, T. Suzuki. J. Electrochem. Soc., 1987, 134: 3068

[161] R. V. Parthasarathy, C. R. Martin. J. Polym. Sci., 1996, 62: 875

[162] Metal Nanoparticles: Synthesis, Characterization and Applications. D. L. Feldheim, A. F. Jr. Colby Eds. Marcel Dekker: New York, 2002

[163] T. K. Sarma, D. Chowdhury; A. Paul, A. Chattopadhyay. Chem.Commun., 2002, 1048

[164] S. Tian, J. Liu, T. Zhu, W. Knoll. Chem. Mater., 2004, 16: 4103

[165] E. Granot, E. Katz, B. Basnar, I. Willner. Chem. Mater., 2005, 17: 4600

[166] J. A. Smith. M. Josowicz, J. Janata. J. Electrochem. Soc., 2003, 150: E384

[167] J. M. Kinyanjui, D. W. Hatchett, J. A. Smith, M. Josowicz. Chem. Mater., 2004, 16: 3390

[168] S. K. Pillalamarri, F. D. Blum, A. F. Tokuhiro, J. G. Story, M. F. Bertino. Chem. Mater., 2005, 17: 227

[169] S. K. Pillalamarri, F. D. Blum, A. T. Tokuhiro, M. F. Bertino. Chem. Mater., 2005, 17: 5941

[170] X. Y. Zhang, W. J. Goux, S. K. Manohar. J. Am. Chem. Soc., 2004, 126: 4502

[171] J. X. Huang, S. Virji, B. H. Weiller, R. B. Kaner. J. Am. Chem Soc., 2003, 125: 314

[172] E. M. Genie´s, C. Tsintavis, A. A. Syed. Mol. Cryst. Liq. Cryst.,1985, 121: 181

[173] Z. Sun, Y. Geng, J. Li, X. Jing, F. Wang. Synth. Met., 1997, 84: 99

[174] P. R. Selvakannan, P. S. Kumar, A. S. More, R. D. Shingte, P. P. Wadgaonkar, M. Sastry. Langmuir, 2004, 20: 295

[175] P. R. Selvakannan, P. S. Kumar, A. S. More, R. D. Shingte, P. P. Wadgaonkar, M. Sastry. Adv. Mater., 2004, 16: 966

[176] Y. Wang, Z. M. Liu, B. X.Han, Z. Y. Sun, Y. Huang, G. Y. Yang. Langmuir, 2005, 21: 833

[177] R. R. Bhattacharjee, M. Chakraborty, T. K. Mandal. J. Nanosci. Nanotechnol., 2003, 3: 487

[178] D. W. Hatchett, M. Josowicz, J. Janata, D. R. Baer. Chem. Mater., 1999, 11: 2989

[179] T. K. Sarma, A. Chattopadhyay. J. Phys. Chem. A, 2004, 108: 7837

[180] X. Dai, Y. Tan, J. Xu. Langmuir, 2002, 18: 9010

[181] P. J. Kinlen, J. Liu, Y. Ding, C. R. Graham, E. E. Remsen. Macromolecules, 1998, 31: 1735

[182] N. Kuramoto, A. Tomita. Polymer, 1997, 38: 3055

[183] Z. Peng, L. Guo, Z. Zhang, B. Tesche, T. Wilke, D. Ogermann, S. Hu and K. Kleinermanns. Langmuir, 2006, 22: 10915

[184] E. Granot, E. Katz, B. Basnar, I. Willner. Chem. Mater., 2005, 17: 4660

[185] X. Feng, C. Mao, G. Yang, W. Hou, J. J. Zhu. Langmuir, 2006, 22: 4384

[186] a) A. Relinkiewicz, M. Hasik, M. Kloc. Catal. Lett., 2000, 64: 41; b) P. T. Radford, S. E. Creager. Anal. Chem. Acta, 2001, 449: 199

[187] J. A. Smith, M. Josowicz, J. Janata. J. Electrochem. Soc., 2003, 150: E384

[188] S. K. Pillalamarri, F. D. Blum, A. T. Tokuhiro, M. F. Bertino. Chem. Mater., 2005, 17: 5941

[189] a) P. R. Selvakannan, P. S. Kumar, A. S. More, R. D. Shingte, P. P. Wadgaonkar, M. Sastry. Langmuir, 2004, 20: 295; b) P. R. Selvakannan, P. S. Kumar, A. S. More, R. D. Shingte, P. P. Wadgaonkar, M. Sastry. Adv. Mater., 2004, 16: 966

[190] T. K. Sarma, D. Chowdhury, A. Paul, A. Chattopadhyay. Chem. Commun., 2002, 10: 1048

[191] a) W. A. Hayes, C. Shannon. Langmuir, 1998, 14: 1099; b) L. A. Jr. Porter, A. E. Ribbe, J. M. Buriak. Nano Lett., 2003, 3: 81043

[192] R. A. Lipeles, A. R. Hopkins. Chem. Mater., 2004, 16: 1606

[193] a) Q. H. Zeng, D. Z. Wang, A. B. Yu, G. Q. Lu. Nanotechnology, 2002,13: 549; b) B. Feng, Y. Su, J. Song, K. Kong. J. Mater. Sci. Lett., 2001, 20: 293

[194] a) B. H. Kim, J. H. Jung, S. H. Hong, J. Joo. Macromolecules, 2002, 35: 1419; b) D. Lee, K. Char, S. W. Lee, Y. W. Park. J. Mater. Chem., 2003, 13: 2942

[195] J. W. Kim, F. Liu, H. J. Choi, S. H. Hong, J. Joo. Polymer, 2003, 44: 289

[196] N. Ballav, M. Biswas. Synth. Met., 2004, 142: 309

[197] H. V. Hoang, R. Holze. Chem. Mater., 2006, 18: 1976

[198] a) S. Kaskel, K. Schlichte, G. Chaplais, M. Khanna. J. Mater. Chem., 2003, 13: 1496; b) N. Jiang, H. J. Zhang, S. N. Bao, Y. G. Shen, Z. F. Zhou. Phys. B, 2004, 352: 118; c) J. Li, L. Gao, J. Sun, Q. Zhang, J. Guo, D. J. Yan. J. Am. Ceram. Soc., 2001, 84: 3045

[199] Y. Qiu, L. Gao. J. Phys. Chem. B, 2005, 109: 19732

[200] S. Iijima. Nature, 1991, 354: 56

[201] R. H. Baughman, A. A. Zakhidov, W. A. de Heer. Science, 2002, 297: 787

[202] a) S. Jonghwan, K. Nikhil, K. K. Pawel, A. Pulickel. Nat. Mater., 2005, 4: 134; b) N. I. Kovtyukhova, T. E. Mallouk. J. Phys. Chem. B, 2005, 109: 2540; c) B. Pradhan, S. K. Batabyal, A. J. Pal. J. Phys. Chem. B, 2006, 110: 8274

[203] a) T. M. Wu, Y. W. Lin, C. S. Liao. Carbon, 2005, 43: 734; b) R. Sainz, A. M. Benito, M. T. Martinez, J. F. Galindo, J. Sotres, A. M. Barl, B. Coraze, O. Chauvet, W. K. Maser. Adv. Mater., 2005, 17: 278; c) R. Sainz, A. M. Benito, M. T. Martinez, J. F. Galindo, J. Sotres, A. M. Barl, B. Coraze, O. Chauvet, A. B. Dalton, R. H. Baughman, W. K. Maser. Nanotechnology, 2005, 16: S150

[204] A. G. MacDiarmid. Angew. Chem., Int. Ed., 2001, 40: 2581

[205] S. Lefrant, I. Baltog, M. Baibarac, J. Y. Mevellec, O. Chauvet. Carbon, 2002, 40: 2201

[206] C. Y. Zhi, Y. Bando, C. C. Tang, S. Honda, K. Sato, H. Kuwahara, D. Golberg. Angew. Chem., Int. Ed., 2005, 44: 7929

[207] M. Baibarac, I. Baltog, S. Lefrant, J. Y. Mevellec, O. Chauvet. Chem. Mater., 2003, 15: 4149

[208] M. Cochet, W. K. Maser, A. M. Benito, M. A. Callejas, M. T. Martínez, J. M. Benoit, J. Schreiber, O. Chauvet. Chem. Commun., 2001, 1450

[209] a) J. Huang, R. B. Kaner. J. Am. Chem. Soc., 2004, 126: 851; b) J. Huang, R. B. Kaner. Angew. Chem., Int. Ed., 2004, 43: 5817; c) J. Huang, S. Virji, B. H. Weiller, R. B. Kaner. J. Am. Chem. Soc., 2003, 125: 314; d) D. Li, R. B. Kaner. Chem. Commun., 2005, 3286; e) J. Huang, R. B. Kaner. Chem. Commun., 2006, 367

[210] X. B. Yan, Z. J. Han, Y. Yang, B. K. Tay. J. Phys. Chem. C (Published on Web 02/23/2007)

[211] G. Z. Chen, M. S. P. Shaffer, D. Coleby, G. Dixon, W. Zhou, D. J. Fray, A. H. Windle. Adv. Mater., 2000, 12: 522

[212] J. Wang, J. Dai, and T. Yarlagadda. Langmuir, 2005, 21: 9

[213] Y. Xiaolicui, I. Jaganbontha. Environ. Sci. Technol., 2006, 40: 4004

[214] a) Y. Cang, D. J. Roberts, D. A. Clifford. Water Res., 2004, 38: 3322; b) K. Kim, M. D. Gurol. Environ. Sci. Technol., 2004, 38: 1918; c) B. Gu, W. Dong, G. Brown, D. Cole. Environ. Sci. Technol., 2003, 37: 2291

[215] a) A. J. Krynitsky, R. A. Niemann, D. A. Nortrup. Anal. Chem., 2004, 76: 5518; b) J. Lizondo-Sabater, M. J. Seguli, J. M. Lloris, R. Martinez-Manez, T. Pardo, F. Sancenon, J. Soto. Sens. Actuators B, 2004, 101: 20

[216] a) B. Gu, Y. Ku, G. M. Brown. Remediation, 2002, 12: 51; b) B. Gu, Y. Ku, G. M. Brown. Environ. Sci. Technol., 2005, 39: 901

[217] N. C. Sturchio, P. B. Hatzinger, M. D. Arkins, C. Suh, L. J. Heraty. Environ. Sci. Technol., 2003, 37: 3859

[218] C. M. V. B. Almeida, B. F. Giannetti, T. Rabockai. J. Electroanal. Chem., 1997, 422: 185

[219] U. Johanson, M. Marandi, T. Tamm, J. Tamm. Electrochem. Acta, 2005, 50: 1523

[220] A. J. Fernández Romero, J. J. López Cascales, T. Fernández Otero. J. Phys. Chem. B, 2005, 109: 907

[221] Yuehelin, Xiaolicui, Jaganbotha. Environ. Sci. Technol., 2006, 40: 4004

[222] X. T. Zhang, Z. Lu, M. T. Wen, H. L. Liang, J. Zhang, Z. F. Liu. J. Phys. Chem. B, 2005, 109: 1101

[223] L. A. P. Kane-Maguire, S. E. Moulton, P. C. Innis, G. G. Wallace. J. Nanosci. Nanotech., 2004, 4: 976

[224] N. A. Young, W. Henry, J. Hjelm, J. G. Vos. J. Phys. Chem. B, 2005, 109: 13205

[225] M. Cochet, W. K. Maser, A. M. Benito, M. A. Callejas, M. T. Martinez, J. M. Benoit, J. Schreiber, O. Chauvet. Chem. Commun., 2001, 1850

[226] W. K. Maser, A. M. Benito, M. A. Callejas, T. Seeger, M. T. Martinez, J. Schreiber, J. Muszynski, O. Chauvet, Z. Osvath, A. A. Koos, L. P. Biro. Mater. Sci. Eng. C, 2003, 23: 87

[227] Marc in het Panhuis, Raquel Sainz, Peter C. Innis, Leon A. P. Kane-Maguire, Ana M. Benito, M. Teresa Martínez, Simon E. Moulton, Gordon G. Wallace, Wolfgang K. Maser. J. Phys. Chem. B, 2005, 109: 22725

[228] R. Sainz, W. R. Small, N. A. Young, C. Vallés, A. M. Benito, W. K. Maser, Marc in het Panhuis. Macromolecules, 2006, 39: 7324

[229] R. Gangopadhyay, A. De. Chem. Mater., 2000, 12: 608

[230] M. A. Khan, S. P. Armes. Adv. Mater., 2000, 12: 671

[231] D. B. Cairns, S. P. Armes, L. G. B. Bremer. Langmuir, 1999, 15: 8052

[232] C. Barther, S. P. Armes, M. M. Chehimi, C. Bilem, M. Omastova. Langmuir, 1998, 14: 5032

[233] a) M. A. Khan, S. P. Armes. Langmuir, 1999, 15: 3469; b) M. A. Khan, S. P. Armes, C. Perruchot, H. Ouamara; M.M. Chehimi; S.J. Greaves; J.F. Watts; Langmuir 2000, 16, 4171

[234] a) W. Liu; J. Kumar, S. Tripathy, K. J. Senecal, L. Samuelson. J. Am. Chem. Soc., 1999, 121: 71; b) P. C. Innis, I. D. Norris, L. A. P. Kane-Maguire, G. G. Wallace. Macromolecules, 1998, 31: 6521

[235] H. Tsutsumi, S. Yamashita, T. Oishi. J. Appl. Electrochem., 1997, 27: 477

[236] M. K. Park, K. Onishi, J. Locklin, F. Caruso, R. C. Advincula. Langmuir, 2003, 19: 8550

[237] a) G. L. Haller, M. Marquez. J. Phys. Chem., 1992, 96: 4145; b) G. J. Miller, A. M. Lewis, G. A. Browmake, R. P. Cooney. J. Mater. Chem., 1993, 3: 867

[238] a) M. Goren, Z. Qi, R. B. Lennox. Chem. Mater., 1995, 7: 171; b) H. P. Wong, B. C. Dave, F. Leroux, J. Harreld, B. Dunn, L. F. Nazar. J. Mater. Chem., 1998, 8: 1019

[239] T. A. Skotheim, X. Q. Yang, J. Chen, P. D. Hale, T. Inagaki, L. Samelson, S. Tripathy, K. Hong, M. F. Rubner. Synth. Met., 1989, 28: 229

[240] W. Torres, M. A. Fox. Chem. Mater., 1992, 4: 583

[241] C. Cho, B. M. Fung, D. T. Glatzhofer, J. S. Lee, Y. G. Shul. Langmuir, 2001, 17: 456 – 461

[242] a) Q. Huang, J. Li, G. A. Evmenenko, P. Dutta, T. Marks. J. Chem. Mater., 2006, 18: 2431; b) G. Koller, R. I. R. Blyth, S. A. Sardar, F. P. Netzer, M. G. Ramsey. Appl. Phys. Lett., 2000, 76: 927; c) M. Paulose, K. Shankar, O. K. Varghese, G. K. Mor, B. Hardin, C. A. Grimes. Nanotechnology, 2006, 17: 1446

[243] J. Wang, J. Dai, T. Yarlagadda. Langmuir, 2005, 21: 9

[244] M. Lahav, E. A. Weiss, Q. B. Xu, G. M. Whitesides. Nano Letter, 2006, 6: 2166

[245] a) R. Gangopadhyay, A. De. Chem. Mater., 2000, 12: 608; b) R. Czerw, Z. Guo, P. M. Ajayan, Y. P. Sun, D. L. Carroll. Nano Lett., 2001, 1: 423

[246] W. X. Zhang, X. G. Wen, S. H. Yang. Langmuir, 2003, 19: 4420

[247] a) S. Wang, S. Yang. Chem. Mater., 2001, 13: 4794; b) X. Wen, S. Yang. Nano Lett., 2002, 2: 451

[248] C. E. Flynn, S. W. Lee, B. R. Peelle, A. M. Belcher. Acta Mater., 2003, 51: 5867

[249] a) A. Star, J. P. Gabriel, K. Bradley, G. Gruner. Nano Lett., 2003, 3: 639; b) K. Besteman, J. Lee, F. G. M. Wiertz, H. A. Heering, C. Dekker. Nano Lett., 2003, 3: 727; c) I. A. Banerjee, L.Yu, H. Matsui. Nano Lett., 2003, 3: 283

[250] J. Li, H. T. Ng, A. Cassell, W. Fan, H. Chen, Q. Ye, J. Koehne, J. Han, M. Meyyappan. Nano Lett., 2003, 3: 597

[251] Y. Cui, Q. Wei, H. Park, C. M. Lieber. Science, 2001, 293: 1289

[252] a) J. Joo, J. K. Lee, S. Y. Lee, K. S. Jang, E. J. Oh, A. J. Epstein. Macromolecules, 2000, 33: 5131; b) S. Sadki, P. Schottland, N. Brodie, G. Sabouraud. Chem. Soc. Rev., 2000, 29: 283

[253] Z. Zhong, F. Qian, D. Wang, C. M. Lieber. Nano Lett., 2003, 3: 343

[254] Rose M. Hernández, Lee Richter, Steve Semancik, Stephan Stranick, Thomas E. Mallouk. Chem. Mater., 2004, 16: 3431

[255] a) Y. Cao, P. Smith, A. J. Heeger. Synth. Met., 1992, 48: 91; b) Y. Cao, P. Smith, A. J. Heeger. Synth. Met., 1993, 57: 3514

[256] J. C. Moutet, E. Saintaman, F. Tranvan, P. Angibeaud, J. P. Utille. Adv. Mater., 1992, 4 (7 – 8): 511

[257] H. Guo, C. M. Knobler, R. B. Kaner. Synth. Met., 1999, 101: 44

[258] a) M. R.Majidi, L. A. P. Kane-Maguire, G. G. Wallace. Polymer, 1995, 36: 3597; b) R. Nagarajan, W. Liu, J. Kumar, S. K. Tripathy, F. F. Bruno, L. A. Samuelson. Macromolecules, 2001, 34: 3921

[259] J. M. Liu, L. Sun, S. C.Yang. U. S. Patent 5,489,400, 1996

[260] L. Sun, H. Liu, R. Clark, S. C. Yang. Synth. Met., 1997, 84: 67

[261] P. A. McCarthy, J. Huang, S. C. Yang, H. L. Wang. Langmuir, 2002, 18: 259

[262] X. Wang, Y. Zu, X. Li. Adv. Chem. Technol., 2000, 1: 67

[263] Y. Zu, Y. Lei, X. Yu. New Mater. Chem. Technol., 1998, 6: 26

[264] W. Zhou, C. W. Sun, Z. Z. Yang. Acta Inorg. Mater., 1998, 13: 275

[265] B. O'Regan, M. Gratzel. Nature, 1991, 353: 737

[266] M. Machida, K. Norimoto, T. Watanabe, K. Hashimoto, A. Fujishima. J. Mater. Sci., 1999, 34: 2569

[267] a) Y. Hao, M. Yang, C. Yu, S. Cai, M. Liu, L.Fan, Y. Li. Sol. Energy Mater. Sol. Cells, 1998, 56: 75; b) K. Murakoshi, R. Kogure, Y. Wada, S. Yanagida. Sol. Energy Mater. Sol. Cells, 1998, 55: 113; c) N. Kobayashi, K.Teshima, R. Hirohashi. J. Mater. Chem., 1998, 8: 497

[268] a) R. Flitton, J. Johal, S. Maeda, S. P. Armes. J. Colloid Interface Sci., 1995, 173: 135; b) M. D. Butterworth, R. Corradl, J. Johal, S. F. Lascelles, S. Maeda, S. P. Armes. J. Colloid Interface Sci., 1995, 174: 510

[269] D. C. Schnitzler, M. S. Meruvia, I. A. Hümmelgen, A. J. G. Zarbin. Chem. Mater., 2003, 15: 4658

[270] K. S. Suslick. Science, 1990, 3: 1439

[271] Q. Wang, H. S. Xia, C. H. Zhang. J. Appl. Polym. Sci., 2001, 80: 1478

[272] a) K. Murakoshi, R. Kogure, Y. Wada, S. Yanagida. Sol. Energy Mater. Sol. Cells, 1998, 55: 113; b) G. Wang, H. Chen, H. Zhang, C. Yuan, Z. Lu, G. Wang, W. Yang. Appl. Surf. Sci., 1998, 135: 97

[273] a) W. Feng, E. Sun, A. Fujii, H. Wu, K. Nihara, K. Yoshino. Bull. Chem. Soc. Jpn., 2000, 73: 2627; b) H. Xia, Q. Wang. Chem. Mater., 2002, 14: 2158

[274] a) A. G. MacDiarmid. Synth. Met., 2002, 125: 11；b) A. J. Heeger. Synth. Met., 2002, 125: 23；c) H. Shirakawa. Synth. Met., 2002, 125: 3; d) C. Marck, K.Borgwarth, J. Heinze. Chem. Mater., 2001, 13: 747

[275] N. F. Mott, E. A. Davis. Electronic Processes in Non-crystalline Materials (2nd Edition). Oxford: Clarendon Press, 1979

[276] R.V. Parthasarathy, C. R. Martin. Chem. Mater., 1994, 6: 1627

[277] C. R. Martin, L. S. Van Dyke, Z. Cai, W. Liang. J . Am .Chem. Soc., 1990, 112: 8976

[278] a) J. Huang, S. Virji, B. H. Weiller, R. B. Kaner. J. Am. Chem. Soc., 2003, 125: 314 ; b) J. Huang, R. B. Kaner. J. Am. Chem. Soc., 2004, 126: 851; c) Y. Zhou, M. Freitag, J. Hone, C. Stail, A. T. Jr. Jonson, N. J. Pinto, A. G. MacDiarmid. Appl. Phys. Lett., 2003, 83: 3800

[279] a) A. G. MacDiarmid. Rev. Mod. Phys., 2001, 73: 713; b) A. J. Heeger. Rev. Mod. Phys., 2001, 73: 701; c) J. G. Park, B. Kim, S. H. Lee, A. B. Kaiser, S. Roth, Y. W. Park. Synth. Met., 2003, 299: 135; d) A. B. Kaiser, Y. W. Park. Synth. Met., 2003, 245: 135

[280] K. Akagi, G. Piao, S. Kaneko, K. Sakamaki, H. Shirakawa, M. Kyotani. Science, 1998, 282: 1683

[281] H. J. Lee, Z. X. Jin, A. N. Aleshin, J. Y. Lee, M. J. Goh, K. Akagi, Y. S. Kim, D. W. Kim, Y. W. Park. J. Am. Chem. Soc., 2004, 126, 16722

[282] M. P. de Jong, L. J. van Ijzendoorn, M. J. A. de Voigt. Appl. Phys. Lett., 2000, 77: 2255

[283] S. Möller, C. Perlov, W. Jackson, C. Taussig, S. Forrest. Nature, 2003, 426: 166

[284] L. Groenendaal, F. Jonas, D. Freitag, H. Pielartzik, J.,R. Reynolds. Adv. Mater., 2000, 12: 481

[285] a) V. P. Menon, J. Lei, C. R. Martin. Chem. Mater., 1996, 8: 2382; b) S. Demoustier-Champagne, P. Y. Stavaux. Chem. Mater., 1999, 11: 829

[286] J. L. Duvail, P. Rétho, V. Fernandez, G. Louarn, P. Molinié, O. Chauvet. J. Phys. Chem. B, 2004, 108: 18552

[287] a) F. R. F. Fan, J. Yang, S. M. Dirk, D. W. Price, D. V. Kosynkin, J. M. Tour, A. J. Bard. J. Am. Chem. Soc., 2001, 123: 2454; b) F. R. F. Fan, J. Yang, L. Cai, D. W. Price, S. M. Dirk, D. V. Kosynkin,Y. Yao, A. M. Rawlett, J. M. Tour, A. J. Bard. J. Am. Chem. Soc., 2002, 124: 5550

[288] C. G. Wu, S. S. Chang. J. Phys. Chem. B, 2005, 109: 825

[289] a) O. A. Semenikhin, L. Jiang, T. Iyoda, K. Hashimoto, A. Fujishima. J. Phys. Chem., 1996, 100: 18603; b) O. A. Semenikhin, L. Jiang, T. Iyoda, K. Hashimoto,A. Fujishima. Electrochim. Acta, 1997, 42: 3321; c) J. N. Barisci, R. Stella, G. M. Spinks, G. G. Wallace. Electrochim. Acta, 2000, 46: 519

[290] T. W. Kelley, E. T. Granstrom, C. D. Frisbie. Adv. Mater., 1999, 11: 261; b) C. E. Gardner, J. V. Macpherson. Anal. Chem., 2002, 74: 576A

[291] a) Y. H. Liau, N. F. Scherer; K. Rhodes. J. Phys. Chem. B, 2001, 105: 3282; b) J. Planes, F. Houze, P. Chretien, O. Schneegans. Appl. Phys. Lett., 2001, 79: 2993; c) J. V. Macpherson, J. P. G. de Mussy, J. L.Delplancke. J. Electrochem. Soc., 2002, 149: B306

[292] a) H. J. Lee, S. M. Park. J. Phys. Chem. B, 2004, 108: 1590; b) D. H. Han, S. M. Park. J. Phys. Chem. B, 2004, 108: 13921; c) S. M. Park. J. Phys. Chem. B, 2005, 109: 13247; d) S. Y. Hong, Y. M. Jung, S. B. Kim, S. M. Park. J. Phys. Chem. B, 2005, 109: 3844; e) J. G. Park, S. H. Lee, B. Kim, S. K. Saha, Y. K. Su, C. L. Lin, D. W. Jaw. Nanotechnology, 2004, 15: 66; f) C. Ionescu-Zanetti, A. Mechler, S. A. Carter, R. Lal. Adv. Mater., 2004, 16: 385

[293] D. H. Han, J. W. Kim, S. M. Park. J. Phys. Chem. B, 2006, 110: 14874

[294] D. S. Boudreaux, R. R. Chance, J. F. Wolf, L. W. Schacklette, J. L. Bredas, B. Themans, J. M. Andre, R. Silby. J. Chem. Phys., 1986, 85: 4584

[295] R. Wiesendanger. Jpn. J. Appl. Phys., Part 1, 1995, 34: 3388

[296] K. Sasano, K. Nakamura, K. Kaneto. Jpn. J. Appl. Phys., Part 2, 1993, 32: L863

[297] C. Kranz, M. Ludwig, H. E. Gaub, W. Schuhmann. Adv. Mater., 1995, 7: 38

[298] R. M. Nyffenegger and R. M. Penner. J. Phys. Chem., 1996, 100: 17041

[299] N. Kiriy, E. Jahne, H. J. Adler, M. Schneider, A. Kiriy, G. Gorodyska, S. Minko, D. Jehnichen, P. Simon, A. A. Fokin, M. Stamm. Nano Lett., 2003, 3: 707

[300] J. A. Merlo, C. D. Frisbie. J. Phys. Chem. B, 2004, 108: 19169

[301] B. H. Kima, D. H. Park, J. Joo, S. G. Yu, S. H. Lee. Synthetic Metals, 2005, 150: 279

[302] a) J. Joo, K. T. Park, B. H. Kim, M. S. Kim, S. Y. Lee, C. K. Jeong, J. K.Lee, D. H. Park, W. K. Yi, S. H. Lee, K. S. Ryu. Synth. Met., 2003, 135/136: 13; b) K. Kim, J. I. Jin. Nano Lett., 2001, 11: 631

[303] W. K. Yi, T. W. Jeong, S. G. Yu, J. N. Heo, C. S. Lee, J. H. Lee, W. S. Kim, J. B. Yoo, J. M. Kim. Adv. Mater., 2002, 14: 1464

[304] M. A. Guillorn, A. V. Melechko, F. K. Hensley, M. L. Simpson, D. H. Lowndes. Appl. Phys. Lett., 2002, 81: 3660

[305] B. H. Kim, M. S. Kim, K. T. Park, J. K. Lee, D. H. Park, J. Joo. Appl. Phys. Lett., 2003, 83: 539

[306] a) G. De Crevoisier, P. Fabre, J. M. Corpart, L. Leibler. Science, 1999, 285: 1246; b) K. Ichimura, S. K. Oh, M. Nakagawa. Science, 2000, 288: 1624

[307] a) J. Lahann, S. Mitragotri, T. Tran, H. Kaido, J. Sundaram, I. Choi, S. Hoffer, G. Somorjai, R. Langer. Science, 2003, 299: 371; b) S. Minko, M. Müller, M. Motornnov, M. Nitschke, K. Grundke, M. Stamm. J. Am. Chem. Soc., 2003, 125: 3896; c) X. Gao, L. Jiang, Nature, 2004, 432: 36; d) T. Sun, L. Feng, X. Gao, L. Jiang. Acc. Chem. Res., 2005, 38: 644

[308] B. Zhao, J. S. Moore, D. J. Beebe. Science, 2001, 291: 1023

[309] S. C. D'Andrea, A. Y. Fadeev. Langmuir, 2006, 22: 3962

[310] R. Blossey. Nat. Mater., 2003, 2: 301

[311] A. Kros, R. J. M. Nolte, N. A. J. M. Sommerdijk. Adv. Mater., 2002, 14: 1779

[312] E. Smela. Adv. Mater., 2003, 15: 481

[313] Y. Berdichevsky, Y. H. Lo. Adv. Mater., 2006, 18: 122

[314] D. Mecerreyes, V. Alvaro, I. Cantero, M. Bengoetxea, P. A. Calvo, H. Grande, J. Rodriguez, J. A. Pomposo. Adv. Mater., 2002, 14: 749

[315] W. B. Zhong, S. M. Liu, X. H. Chen, Y. X. Wang, W. T. Yang. Macromolecules, 2006, 39: 3224

[316] L. Xu, W. Chen, A. Mulchandani, Y. Yan. Angew. Chem., Int. Ed., 2005, 44: 6009

[317] Y. Zhu, L. Feng, F. Xia, J. Zhai, M. Wan, L. Jiang. Macromol. Rapid Commun., 2007, 28: 1135

[318] a) K. Hagen, H. Marcus, Z. Ute, E. Florian, S. Gunter, D. Christine. Appl. Phys. Lett., 2003, 82: 4175; b) A. Bachtold, P. Hadley, T. Nakanishi, C. Dekker. Science, 2001, 294: 1317

[319] K. Kim, J. I. Jin. Nano Lett., 2001, 11: 631

[320] S. A. Sana, C. Gabrielli, H. Perrot. J. Electrochem. Soc., 2003, 150: E444

[321] a) S. K. Saha. Appl. Phys. Lett., 2002, 81: 3645; b) H. W. C. Postma, T. Teepen, Z. Yao, M. Grifoni, C. Dekker. Science, 2001, 293: 76

[322] a) B. H. Kim, M. S. Kim, K. T. Park, J. K. Lee, D. H. Park, J. Joo, S. G. Yu, S. H. Lee. Appl. Phys. Lett., 2003, 83: 539; b) M. Granström, M. Berggren, O. Inganäs. Science, 1995, 267: 1479

[323] a) A. R. Hopkins, P. G. Rasmussen, R. A. Basheer. Macromolecules, 1996, 29: 7838; b) J. Liu, Y. Lin, L. Liang, J. A. Voigt, D. L. Huber, Z. R. Tian, E. Coker, B. Mckenzie, M. Mcdermott. J. Chem. Eur. J., 2003, 9: 604

[324] E. Pringsheim, D. Zimin, O. S. Wolfbeis. Adv. Mater., 2001, 13: 819

[325] a) A. Bossi, S. A. Piletsky, E. V. Piletska, P. G. Righetti, A. P. F. Turner. Anal. Chem., 2000, 72: 4296; b) J. Janata, M. Josowicz. Nature Mater., 2003, 2: 19

[326] M. Gao, L. Dai, G. G. Wallace. Eletroanalysis, 2003, 15: 1089

[327] a) J. Liu, Y. Lin, L. Liang, J. A. Voigt, D. L. Huber, Z. R. Tian, E. Coker, B. Mckenzie, M. Mcdermott. J. Chem. Eur. J., 2003, 9: 604; b) S. Wu, F. Zeng, F. Li, Y. Zhu. Eur. Polym. J., 2000, 36: 679; c) U. Kang, K. D. Wise. IEEE Trans. Electron Devices, 2000, 47: 702

[328] O. S. Wolfbeis. Anal. Chem., 2002, 74: 2663

[329] L. Dai, P. Soundarrajan, T. Kim. Pure Appl. Chem., 2002, 74: 1753

[330] J. X. Huang, S. Virji, B. H. Weiller, R. B. Kaner. J. Am. Chem. Soc., 2003, 125: 314 – 315

[331] W. S. Huang, B. D. Humphrey, A. G. MacDiarmid. J. Chem. Soc., Faraday Trans., 1986, 82: 2385

[332] S. Virji, J. X. Huang, R. B. Kaner, H. Weiller. Nano Letter, 2004, 4: 491

[333] A. L. Kukla, Y. M. Shirshov, S. A. Piletsky. Sens. Actuators B, 1996, 37: 135

[334] S. Sharma, C. Nirke, S. Pethkar, A. A. Athawale. Sens. Actuators B, 2002, 85: 131

[335] M. R. Anderson, B. R. Mattes, H. Reiss, R. B. Kaner. Science, 1991, 252: 1412

[336] J. Wang, S. Chan, R. R. Carlson, Y. Luo, G. Ge, R. S. Ries, J. R. Heath, H. R. Tseng. Nano Letters, 2004, 4: 1693

[337] J. Jang, M. Chang, H. Yoon. Adv. Mater., 2005, 17: 1616

[338] N. Watari, S. Ohnish, T. Ishi. J. Phys.: Condens. Matter, 2000, 12: 6799

[339] R. C. Hughes, W. K. Schubert. J. Appl. Phys., 1992, 71: 542

[340] K. Domansky, D. L. Baldwin, J. W. Grate, T. B. Hall, M. Josowicz, J. Janata. Anal. Chem., 1998, 70: 473

[341] S. Virji, R. B. Kaner, B. H. Weiller. J. Phys. Chem. B, 2006, 110: 22266

[342] D. L. Ellis, M. R. Zakin, L. S. Bernstein, M. F. Rubner. Anal. Chem., 1996, 68: 817

[343] N. M. Ratcliffe. Anal. Chim. Acta, 1990, 239: 257

[344] a) C. H. Hsu, P. M. Peacock, R. B. Flippen, S. K. Manohar, A. G. MacDiarmid. Synth. Met., 1993, 60: 233; b) J. Yano, K. Terayama, S. Yamasaki, K. Aoki. Electrochim. Acta, 1998, 44: 337

[345] J. Huang, S. Virji, B. H. Weiller, R. B. Kaner. Chem. Eur. J., 2004, 10: 1314

[346] V. Volotovsky, A. P. Soldatkin, A. A. Shul'ga, V. K. Rossokhaty, V. I. Strikha, A. V. El'skaya. Anal. Chim. Acta, 1996, 322: 77

[347] A. P. Soldatkin, V. Volotovsky, A. V. El'skaya, N. Jaffrezic-Renault, C. Martelet. Anal. Chim. Acta, 2000, 403: 25

[348] W. Xu, R. C. McDonough, B. Langsdorf, J. N. Demas, B. A. DeGraff. Anal. Chem., 1994, 66: 4133

[349] H. Shin Jae, L. Lee Hyo, H. Cho Sung, J. Ha, H. Nam, S. Cha Geun. Anal. Chem., 2004, 76: 4217

[350] S. Virji, R. B. Kaner, B. H. Weiller. Chem. Mater., 2005, 17: 1256

[351] M. Phillips, J. Herrera, S. Krishnan, M. Zain, J. Greenberg, R. N. Cataneo. J. Chromatogr. B, 1999, 75: 729

[352] F. Mizutani, T. Sawaguchi, Y. Sato, S. Yabuki, S. Iijima. Anal. Chem., 2001, 73: 5738

[353] a) E. S. Tillman, M. E. Koscho, R. H. Grubbs, N. S. Lewis. Anal. Chem., 2003, 75: 1748; b) T. Gao, E. S. Tillman, N. S. Lewis. Chem. Mater., 2005, 17: 2904

[354] a) J. Jang. Adv. Polym. Sci., 2006, 199: 189; b) H. Yoon, M. Chang, J. Jang. J. Phys. Chem. B, 2006, 110: 14074

[355] S. Ko, J. Jang. Biomacromolecules, 2007, 8: 182

[356] M. Umana, J. Waller. Anal. Chem., 1986, 58: 2980

[357] a) D. T. Hoa, T. N. Suresh Kumar, R. S. Srinivasa, R. Lal, N. S. Punekar, A. Q. Contractor. Anal. Chem., 1992, 64: 2645; b) A. Q. Contractor, R. S. Srinivasa, T. N. Suresh Kumar, R. Narayanan, S. Sukeerthi, R. Lal. Electrochim. Acta, 1994, 39: 1321; c) H. Sangodkar, S. Sukeerthi, R. Lal, R. S. Srinivasa, A. Q. Contractor. Anal. Chem., 1996, 68: 779

[358] a) J. Ochmanska, P. G. Pickup. J. Electroanal. Chem. Interfacial Electrochem., 1991, 297: 211; b) J. P. Travers, M. Nechtschein. Mol. Cryst. Liq. Cryst., 1987, 21: 135; c) A. G. MacDiarmid, J. C. Chiang, W. Huang, B. D. Humphrey, N. L. D. Somasiri. Mol. Cryst. Liq. Cryst., 1985, 125: 30

[359] S. Sukeerthi, A. Q. Contractor. Anal. Chem., 1999, 71: 2231

[360] E. S. Forzani, H. Zhang, L. A. Nagahara, I. Amlani, R. Tsui, N. Tao. Nano Lett., 2004, 4: 1785

[361] a) T. D. Hoa, T. N. Suresh Kumar, N. S. Punekar, R. S. Srinivasa, R. Lal, A. G. Contractor. Anal. Chem., 1992, 64: 2645; b) M. Nishizawa, T. Matsue, I. Uchida. Anal. Chem., 1992, 64: 2642; c) P. N. Bartlett, P. R. Birkin. Anal. Chem., 1994, 66: 1552

[362] H. Meyer, H. Drewer, B. Grundig, K. Camman, R. Kakerow, Y. Manoli, W. Mokowa, M. Rospert. Anal. Chem., 1995, 67: 1164

[363] H. Sangodkar, S. Sukeerthi, R. S. Srinivasa, R. Lal, A. Q. Contractor. Anal. Chem., 1996, 68: 779

[364] a) H. Sangodhkar, S. Sukeerthi, R. Lal, R. S. Srinivasa, A. Q. Contractor. Anal. Chem., 1996, 68: 779; b) S. Sukeerthi, A. Q. Contractor. Anal. Chem., 1999, 71: 2231; c) R. D. Dabke, G. D. Singh, A. Dhanabalan, R. Lal, A. Q. Contractor. Anal. Chem., 1997, 69: 724

[365] a) N. Gospodinova, L. Terlemyzyan, P. Mokreva, K. Kossev. Polymer, 1993, 34: 2434; b) N. Gospodinova, P. Mokreva, L. Terlemezyan. Polymer, 1994, 35: 3102

[366] a) J. W. Yue, H. Jhao, K. R. Cromack, A. J. Epstein, A. G. MacDiarmid. J.Am. Chem. Soc., 1991, 113: 2265; b) X. Wei, Y. Z. Wang, S. M. Lang, C. Bobeczcko, A. J. Epstein. J. Am. Chem. Soc., 1996, 118: 2545

[367] A. A. Karyakin, A. K. Strakhova, A. K. Yatimirsky. J. Electroanal. Chem., 1994, 371: 259

[368] G. Austria, G. W. Jang, A. G. MacDiarmid, K. Doblhofer, C. Zhang Ber.Bunsen-Ges. Phys. Chem., 1991, 95: 1381

[369] a) M. M. Castillo-Ortega, D. E. Rodriguez, J. C. Encinas, M. Plascencia, F. A. Mendez-Velarde, R. Olayo. Sens. Actuators B, 2002, B85: 19; b) T. Tatsuma, T. Ogawa, R. Sato, N. Oyama. J. Electroanal. Chem., 2001, 501: 180; c) O. A. Raitman, E. Katz, A. F. Bueckmann, I. Willner. J. Am. Chem. Soc., 2002, 124 (22): 6487

[370] a) W. Liu, A. L. Cholli, R. Nagarajan, J. Kumar, S. Tripathy, F. F. Bruno, L. Samuelson. J. Am. Chem. Soc., 1999, 121: 11345; b) R. Nagarajan, S. Tripathy, J. Kumar, F. F. Bruno, L. Samuelson. Macromolecules, 2000, 33: 9542

[371] G. S. Manning. J. Chem. Phys., 1988, 89: 3722

[372] G. Majumdar, M. Goswami, T. K. Sarma, A. Paul, A. Chattopadhyay. Langmuir, 2005, 21: 1663

[373] L. Durán, E. Costell. Food Sci. Technol. Int., 1999, 299

[374] M. Kanungo, A. Kumar, A. Q. Contractor. Anal. Chem., 2003, 75: 5673

[375] F. Marystela, R. Jr. Antonio, W. Karen, J. F. Fernando, N. O. Jr. Osvaldo, H. C. M. Luiz. Anal. Chem., 2003, 75: 953

[376] S. Sukeerthi, A. Q. Contractor. Anal. Chem., 1999, 71: 2231

[377] A. Jr. Riul, D. S. Jr. dos Santos, K. Wohnrath, R. Di Tommazo, A. C. P. L. F. Carvalho, F. J. Fonseca, O. N. Jr. Oliveira, D. M. Taylor, L. H. C. Mattoso. Langmuir, 2002, 18: 239

[378] E. Smela, O. Inganas, I. Lundstrom. Science, 1995, 268: 1735

[379] M. R. Gandhi, P. Murray, G. M. Spinks, G. G. Wallace. Synth. Met., 1995, 73: 247

[380] Q. B. Pei, O. Inganas. Adv. Mater., 1992, 4, 277; b) T. F. Otero, M. T. Cortes. Adv. Mater., 2003, 15: 279

[381] a) P. H. Aubert, A. A. Argun, A. Cirpan, D. B. Tanner, J. R. Reynolds. Chem. Mater., 2004, 16: 2386 – 2393; b) L. B. Groenendaal, G. Zotti, P. H. Aubert, S. M. Waybright, J. R. Reynolds. Adv. Mater., 2003, 15: 855

[382] S. I. Cho, W. J. Kwon, S. J. Choi, P. Kim, S. A. Park, J. Kim, S. J. Son, R. Xiao, S. H. Kim, S. B. Lee. Adv. Mater., 2005, 17: 171

[383] S. I. Cho, D. H. Choi, S. H. Kim, S. B. Lee. Chem. Mater., 2005, 17: 4564

[384] P. H. Aubert, A. A. Argun, A. Cirpan, D. B. Tanner, J. R. Reynolds. Chem. Mater., 2004, 16: 2386

[385] a) G. Decher. Science, 1997, 277: 1232; b) D. Laurent, J. B. Schlenoff. Langmuir, 1997, 13: 1552; c) V. E. Campbell, P. A. Chiarelli, S. Kaur, M. S. Johal. Chem. Mater., 2005, 17: 186

[386] C. H. Yang, L. R. Huang, Y. K. Chih, S. L. Chung. J. Phys. Chem. C (Published on Web 02/14/2007)

[387] a) J. Lee, S. Yoon, S. M. Oh, C. H. Shin, T. Hyeon. Adv. Mater., 2000, 12: 359; b) S. H. Joo, S. J. Choi, I. Oh, J. Kwak, Z. Liu, O. Terasaki, R. Ryoo. Nature, 2001, 412: 169; c) L. Schlapbach, A. Züttel. Nature, 2001, 414: 353; d) M. R. Smith, E. W. Bittner, W. Shi, J. K. Johnson, B. C. Bockrath. J. Phys. Chem. B, 2003, 107: 3752; e) P. X. Hou, S. T. Xu, Z. Ying, Q. H. Yang, C. Liu, H. M. Cheng. Carbon, 2003, 41: 2471

[388] a) S. Jun, S. H. Joo, R. Ryoo, M. Kruk, M. Jaroniec, Z. Liu, T. Ohsuna, O. Terasaki. J. Am. Chem. Soc., 2000, 122: 10712; b) J. S. Lee, S. H. Joo, R. Ryoo. J. Am. Chem. Soc., 2002, 124: 1156; c) M. Kruk, M. Jaroniec, T. W. Kim, R. Ryoo. Chem. Mater., 2003, 15: 2815; d) C. Yu, J. Fan, B.Tian, D. Zhao, G. D. Stucky. Adv. Mater., 2002, 14: 1742; e) S. B. Yoon, A. H. Lu, B. Schmidt, B. Spliethoff, F. Schüth. Adv. Mater., 2003, 15: 1602

[389] W. H. Zhang, C. Liang, H. Sun, Z. Shen, Y. Guan, P. Ying, C. Li. Adv. Mater., 2002, 14: 1776

[390] T. W. Kim, I. S. Park, R. Ryoo. Angew. Chem., Int. Ed., 2003, 42: 4375

[391] C. M. Yang, C. Weidenthaler, B. Spliethoff, M. Mayanna, F. Schüth. Chem. Mater., 2005, 17: 355

[392] H. He, N. J. Tao. In: Encyclopedia of Nanoscience and Nanotechnology. H. S. Nalwa Ed. New York: American Scientific Publishers, 2003, Vol. X, p.1 – 18

[393] E. W. H. Jager, E. Smela, O. Inganas. Science, 2000, 290: 1540

[394] J. F. Yu, S. Holdcroft. Chem. Commun., 2001, 1274

[395] C. Marck, K. Borgwarth, J. Heinze. Chem. Mater., 2001, 13: 747

[396] C. R. Martin. Chem. Mater., 1996, 8: 1739

[397] H. X. He, C. Z. Li, N. J. Tao. Appl. Phys. Lett., 2004, 84: 828

[398] B. W. Maynor, S. F. Filocamo, M. W. Grinstaff, J. Liu. J. Am.Chem. Soc., 2002, 124: 522

[399] M. Yun, N. V. Myung, R. P. Vasquez, C. Lee, E. Menke, R. M. Pender. Nano Lett., 2004, 4: 419

[400] a) K. Ramanathan, M. A. Bangar, M. Yun, W. Chen, A. Mulchandani and N. V. Myung. Nano Letter, 2004, 4: 1237; b) M. Yun, N. V. Myung, R. P. Vasquez, C. Lee, E. Menke, R. M. Pender. Nano Lett., 2004, 4: 419

[401] Y. Li, B. W. Maynor, J. Liu. J. Am. Chem. Soc., 2001, 123: 2105

[402] a) S. H. Hong, J. Zhu, C. M. Mirkin. Science, 1999, 286: 523; b) B. W. Maynor, Y. Li, J. Liu. Langmuir, 2001, 17: 2575; c) A. Ivanisevic, C. A. Mirkin. J. Am. Chem. Soc., 2001, 123: 7887

[403] B. W. Maynor, S. F. Filocamo, M. W. Grinstaff; J. Liu. J. Am. Chem. Soc., 2002, 124: 522

[404] M. Woodson, J. Liu. J. Am. Chem. Soc., 2006, 128: 3760

[405] a) A. J. Bard, F. R. Fan, J. Kwak, O. Lev. Anal. Chem., 1989, 61: 132; b) R. C. Engstrom, M. Weber, D. J. Wunder, R. Burgess, S. Winquist. Anal. Chem., 1986, 58: 844

[406] a) A. J. Bard, F. R. Fan. Anal. Sci. Technol., 1995, 8: 69A; b) G. Wittstock, K. J. Yu, H. B. Halsall, T. H. Ridgway, W. R. Heineman. Anal. Chem., 1995, 67: 3578; c) K. Borgwarth, D. Ebling, J. Heinze. Electrochim. Acta, 1995, 40: 1455

[407] a) C. Hess, K. Borgwarth, C. Ricken, D. G. Ebling, J. Heinze. Electrochim. Acta, 1997, 42: 3065; b) D. Mandler, S. Meltzer, I. Shohat, Isr. J. Chem., 1996, 36: 73; c) J. W. Schultze, T. Morgenstern, D. Schattka, S. Winkels. Electrochim. Acta, 1999, 44: 1847

[408] a) C. Kranz, M. Ludwig, H. E. Gaub, W. Schuhmann. Adv. Mater., 1995, 7: 38; b) J. Zhou, D. O. Wipf. J. Electrochem. Soc., 1997, 144: 1202; c) K. Borgwarth, N. Rohde, C. Ricken, M. L. Hallensleben, D. Mandler, J. Heinze. Adv. Mater., 1999, 11: 1221

[409] C. Marck, K. Borgwarth, J. Heinze. Chem. Mater., 2001, 13: 747

[410] J. Z. Wang, Z. H. Zheng, H. W. Li, W. T. S. Huck, H. Sirringhaus. Nat. Mater., 2004, 3: 171

[411] S. Natarajan, S. H. Kim. Langmuir, 2005, 21: 7052

[412] M. Su, L. Fu, N. Q. Wu, M. Aslam, V. P. Dravid. Appl. Phys. Lett., 2004, 84: 828

[413] a) K. Critchley, J. P. Jeyadevan, H. Fukushima, M. Ishida, T. Shimoda, R. J. Bushby, S. D. Evans. Langmuir, 2005, 21: 4554; b) H. Sugimura, K. Ushiyama, A. Hozumi, O. Takai. Langmuir, 2000, 16: 885

[414] a) C. W. Lee, Y. H. Seo, S. H. Lee. Macromolecules, 2004, 37: 4070; b) X. Zhang, J. P. Sadighi, T. W. Mackewitz, S. L. Buchwald. J. Am. Chem. Soc., 2000, 122: 7606

Chapter 5   Template-Free Method to Conducting Polymer Micro/Nanostructures

As mentioned in preface, in 1998, author accidentally discovered that PANI nanotubes could be prepared by conventional *in-situ* doping polymerization in the presence of β-NSA as the dopant without using any membrane as the template. The created method was latterly called as "template-free method" due to omitting membrane as the template. At that time, however, author's knowledge on nanomaterials, especially conducting polymer nanostructures, was very lack that results in my interesting in systematically studying synthesis method, structural characteristics, physical properties and potential applications of the conducting polymer nanostructures by the method. This chapter will therefore mainly introduce author's work on template-free synthesized conducting polymers dealing with the method and formation mechanism, structure characteristic and electrical and transport properties as well as multifunctionality and application. The chapter consists of six sections, where the first three sections mainly introduce results of template-free synthesized conducting polymers whereas the later three sections focus on other methods created by author to unusual micro/nanostructured conducting polymers and application of nanostructured conducting polymers as microwave absorbing materials and sensors guided by reversible wettability, respectively.

5.1   Template-Free Method

Actually, template-free method to conducting polymer nanostructures was accidentally found in studying soluble PANI and PPy prepared by *in-situ* doping polymerization in the presence of sulfonic acids as the dopants. By chance, author found that PANI and PPy microtubes could be prepared by *in-situ* doping polymerization in the presence of β-nanphilene sulfonic acid (β-NSA) as the dopant without using any membrane as the hard-template [1]. Due to without using any membrane as a template, the new method was latterly called as template-free method. Compared with hard-template method [2], the new method is simple and inexpensive because of omitting template and post-treatment of removal template. As a new method, however, a lot of issues dealing with this method were completely un-understood at that time. For instance, how about the universality of the method for preparing conducting polymer nanostructures?

What is formation mechanism of the self-assembled nanostructures by template-free method? How to control the morphology and size of the self-assembled nanostructures? It is possible to realize multi-functionalized nanostructures based on template-free method? Dose the physical properties, especially electrical properties of the nanotubes differ from their bulk materials? What are intrinsic properties of the template-free synthesized nanostructures? How about size effect on the physical properties of the nanostructures? Can we find some promising potential applications for the self-assembled nanostructures? All above described issues promised author to systematically investigatior. Fortunately, most of above issues were basically solved and athour would like to share these achievements with readers.

5.1.1   Discovery of Template-Free Method

Since intractable polymer chain conducting polymers, soluble conducting polymers becomes one of major objects in the field of conducting polymers in order to satisfy requirements in technology [3]. As mentioned in Chapters 1 and 2, PPy and PANI are typical and useful conducting polymers. Like other conducting polymers, the doped PANI or PPy is generally insoluble in common solvent. Cao et al. [4] first reported that highly conductive PANI doped with CSA or DBSA is soluble in organic solvents. This find provided a simple and efficient approach, which was called as dopant-induced method, to prepare soluble conducting polymers. Therefore, author studied soluble PPy and PANI by *in-situ* doping polymerization method in the presence of diffent sulfonic acids as the dopants. By chance, author found that microtubes of PPy and PANI could be synthesized by *in-situ* doping polymerization in the presence of β-NSA as the dopant [1] without using any membrane as the template. The new method latterly was called as template-free method because without using template. Finding and conforming process of the new method are showing as below.

1. Soluble PPy Induced by Sulfonic Acids

Of conducting polymers, PPy stands out as an excellent one due to its high conductivity and good environmental stability and a large variety of application potential [5]. Several kinds of soluble PPy, such as soluble poly (3-alkyl pyrrole) with an alkyl group in common solvents [6] or soluble PPy substituted with hydrophilic groups (e.g. —SO_3H) [7] in water have been reported. However, synthesis of 3-substituted pyrrole monomer is more complex, and the substituted PPy on nitrogen not only has poor conductivity [8], but also partly soluble in some organic solvents even with long alkyl groups on the nitrogen of pyrrole rings. After report of soluble and conductive PANI-CSA and PANI-DBSA [4], Lee et al. [9] also reported that the DBSA doped PPy is soluble with a conductivity
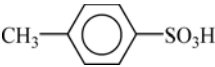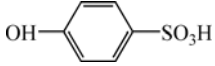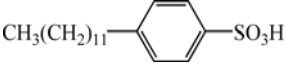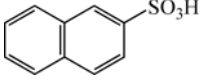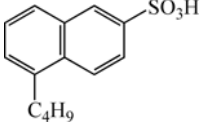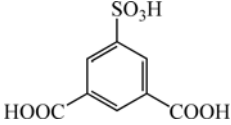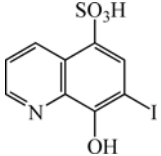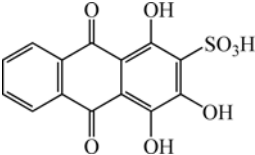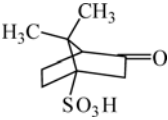
of 2S/cm in *m*-cresol or chloroform in the presence of an extra amount of DBSA. These results suggested that soluble PPy maybe induced by sulfonic acids as the dopants. Author thus selected some sulfonic acids such as CSA, DBSA, *p*-methylbenzene sulfonic acid (MBSA) and 5-*n*-butyl naphthalene sulfonic acid (BNSA) as the dopants to synthesize PPy by *in-situ* doping polymerization. It is found that nature of the sulfonic acids not only affects the solubility of the PPy, but also conductivity, morphology and thermo-stability of Ppy [10] as shown in Table 5.1. The resultant results are summarized as follows: ① Only β-NSA doped PPy is nanotubes whereas other sulfonic acids doped PPy is typically granular, as measured by SEM and TEM images [10]. This was, for the first time, to synthesize PPy nanotubes without using hard-templates. ② The conductivity of the doped PPy, as measured by four probe method, is affected by nature of the sulfonic acids as shown in Table 5.1. Moreover, the conductivity increases with increase of the molar ratio of dopant to pyrrole due to enhancement of doping degree [10]. ③ Solubility of the doped PPy can be generally induced by a long alkyl group of the sulfonic acids. However, β-NSA without long alkyl group also renders PPy soluble that may be due to strong interaction between the naphthalene ring and the phenyl ring of *m*-cresol, suggesting the strong interaction (e.g. hydrogen bonding) between sulfonic acids and solvent also results in enhancement of the PPy solubility in solvent. In addition, solubility of PPy-β-NSA in *m*-cresol increases with increasing concentration of β-NSA and reaches a maximum value of about 1.2 g/100 mL at a β-NSA concentration of 0.57 mol/L [10]. These results indicated that influence of dopant nature on the solubility of the doped PPy is very complex, in other words, the coordination role of molecular size, hydrogen bonds and long alkyl group on the solubility of the doped PPy should be considered. ④ The thermo-stability of the doped PPy is also affected by sulfonic acids as the dopants, especially the doped PPy with β-NSA or BNSA are more thermo-stable with a weight loss at 317℃, showing that doped PPy with naphthalene sulfonic acid possesses a good thermo-stability. Above-results indicated that β-NSA is a good dopant to dope PPy by *in-situ* doping polymerization.

2. PANI Doped with Sulfonic Acids As Dopants

Above-described results indicated that the doped PPy with β-NSA is not only soluble in organic solvent and high thermo-stability, but also having tubular morphology. The discovery of the PPy-β-NSA microtubes promised author to further study effect of nature of the sulfonated acids on the PANI prepared by *in-situ* doping polymerization. Six sulfonic acids, such as methanesulfonic acid (MSA), MBSA, β-NSA, α-naphthalenesulfonic acid (α-NSA), 1,5-naphthalene-disulfonic acid (1,5-NSA), and 2,4-dinitronaphol-7-sulfonate acid (NONSA), were chosen as the dopants, which molecular structure is given in Table 5.2. In fact, the selected dopants were divided into three groups: the first group includes MSA, MBSA, β-NSA and NONSA, using for understanding effect of naphthalene ring on the formation of the tubes. The second group (e.g. α-NSA and 1,5-NSA
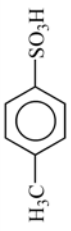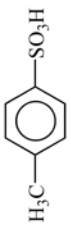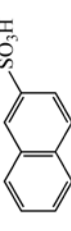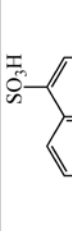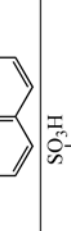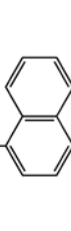
Table 5.1　Effect of sulfonated acids on morphology, solubility and conductive of PPy prepared by *in-situ* doping polymerization [10]

Sulfonic acids	Structure	Solubility in *m*-cresol	a_{RT} (S/cm)	Charge carrier
p-methyl benzene sulfonic acid (MBSA)	CH$_3$—〇—SO$_3$H	×	16.0	polaron and bipolaron
p-hydroxy benzene sulfonic acid (HBSA)	OH—〇—SO$_3$H	○	11.0	polaron and bipolaron
p-dodecyl benzene sulfonic acid (DBSA)	CH$_3$(CH$_2$)$_{11}$—〇—SO$_3$H	⊙	2.0	polaron and bipolaron
β-naphthalene sulfonic acid (NSA)	SO$_3$H	⊙	18.0	polaron and bipolaron
5-*n*-butyl naphthalene sulfonic acid (BNSA)	SO$_3$H ... C$_4$H$_9$	⊙	0.5	polaron and bipolaron
5-sulfo-isophthalic acid (SIA)	SO$_3$H ... HOOC ... COOH	○	3.0	polaron and bipolaron
8-hydroxy-7-iodo-5-quinoline sulfonic acid (QSA)	SO$_3$H ... N ... I ... OH	○	3.0	bipolaron
Alizarin red acid (ARA)	O OH ... SO$_3$H ... OH ... O OH	○	8	bipolaron
Camphor sulfonic acid (CSA)	CH$_3$ ... H$_3$C ... =O ... SO$_3$H	×	18	polaron and bipolaron

×:insoluble;　⊙:soluble;　○: slightly soluble

Table 5.2 Effect of molecular structure of the sulfonic acids on morphology, conductivity, solubility of the PANI prepared by *in-situ* doping polymerization [11]

Sulfonic acids	Structure	Polaron peak (nm)	ESR signals		σ_{RT} (S/cm)	Doping Level	T_0(K)	Solubility in m-cresol (wt %)	Morphology
			ΔH(G)	g Factor					
Methane sulfonic acid (MSA)	CH_3SO_3H	800	1.9	2.0032	0.26	0.22	6799	<0.10	Granule
p-methyl benzene sulfonic acid (MBSA)	H_3C—⟨⟩—SO_3H	900	2.8	2.0032	0.21	0.33	5168	0.29	Granule
β-naphathalene sulfonic acid (β-NSA)	naphthalene-SO_3H	>900 with long tail	2.8	2.0032	4.0	0.41	3674	0.45	Tubule
α-naphthalene sulfonic acid (α-NSA)	naphthalene-SO_3H	918 with long tail	3.9	2.0032	1.5	0.38	4073	0.17	Oriented bar
1,5-naphthalene disulfonic acid (1,5-NSA)	naphthalene SO_3H, SO_3H	1118	4.1	2.0032	2.2	0.25	7491	0.23	Blocks
2,4-dinitronaphol-7-sulfonic acid (NONSA)	naphthalene OH, NO_2, NO_2, SO_3H	1060	3.9	2.0032	0.73	0.53	4252	>0.50	Thin tubule

or NONSA) was used to investigate effect of the number of the sulfonic groups (—SO₃H) attached on the naphthalene ring on the formation of the nanotubes, while the third group including α-NSA and β-NSA was used to measure influence of the locations of the sulfonic group (—SO₃H) attached on naphthalene ring on the tubular morphology. It is fount that granular morphology is formed when PANI is doped with MSA and MBSA without naphthalene ring. Moreover, the granular morphology changed to flakes and blocks when the size of the dopants increases. Interestingly, only PANI-β-NSA is found to have regular tubular morphology [11] that was the first PANI nanotubes synthesized by template-free method. It indicated that the naphthalene ring in the selected dopants is necessary in forming tubular PANI, while the number and the location of sulfonic-groups (—SO₃H) attached on the naphthalene ring only modify the morphology of the PANI. In addition, all PANI doped with the selected sulfonic acids have certain solubility in solvents such as NMP, *m*-cresol, DMF, and DMSO. The solubility is affected by structure of the sulfonic acids as given in Table 5.2 [11]. However, there is no significant difference in room temperature conductivity; for instance, room-temperature conductivity of all doped PANI is in the range of 10^{-1} and 1 S/cm and their temperature dependence of conductivity exhibits semiconductor behavior, following 1D-VRH model [12].

3. Validity of Template-Free Method

Above-results indicated that PANI-β-NSA or PPy-β-NSA micro- or nanotubes were accidentally found by *in-situ* doping polymerization without using membrane as the template. Moreover, it suggested that β-NSA as the dopant and *in-situ* doping polymerization might play an important role in forming PANI and PPy microtubes. In order to check its validity, PANI and PPy were synthesized by different methods in the presence of different sulfonic acids. Four methods, such as *in-situ* doping polymerization, two-step method, immerse method and grind-doping method, were used to synthesize PANI or PPy. The schematic processes of these methods are shown in Fig. 5.1. MBSA, DBSA, β-NSA, BNSA, 5-sulfo-isophthalic acid (SIA) and alizarin red acid (ARA) were chosen as the dopants, which molecular structures are given in Table 5.3. For a given dopant, interestingly, the tubular morphology was only obtained by *in-situ* doping polymerization. Typical SEM and TEM images of PANI-β-NSA microtubes prepared by *in-situ* doping polymerization are shown in Fig. 5.2. At the case of β-NSA as the dopant, by using other methods, such as two-step doping for PPy as well as grind-doping and immerse-doping method for PANI, only granular morphology was obtained [13]. These results indicate that *in-situ* doping polymerization is one of the prerequisites to synthesize tubular PANI and PPy by using the new method. Moreover, only β-NSA as dopant could obtain tubular morphology for both PANI and PPy by *in-situ* doping polymerization, indicating β-NSA dopant is another prerequisite to obtain tubular morphology by the new method. These results further proved that cooperative effect of β-NSA dopant with *in-situ* doping polymerization plays an
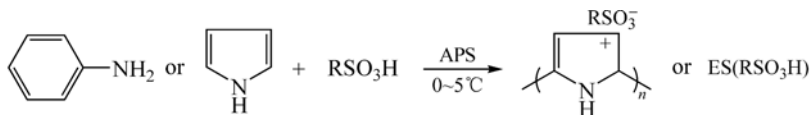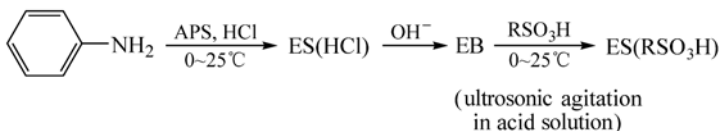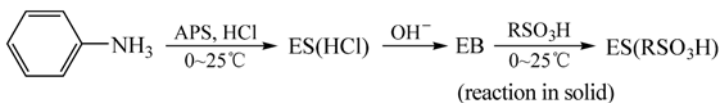
(a) two steps method
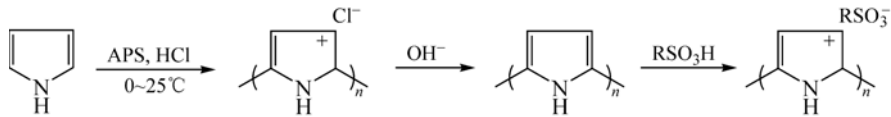
(b) immerse method

(c) grind-doping method

(d)

EB form of PANI:

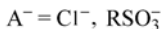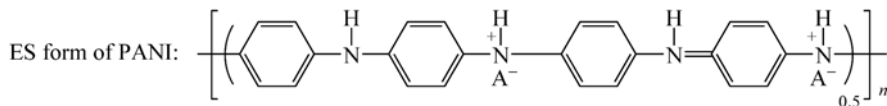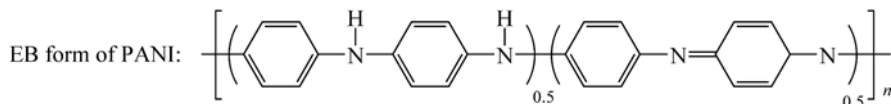ES form of PANI:

$A^- = Cl^-$, RSO_3^-

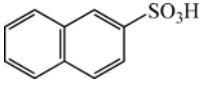**Figure 5.1**   Schematic processes of different doping method used for PANI and PPy [13]

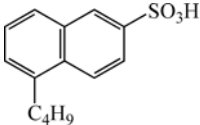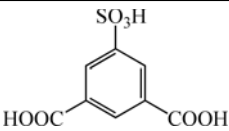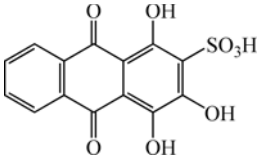(a)   (b)
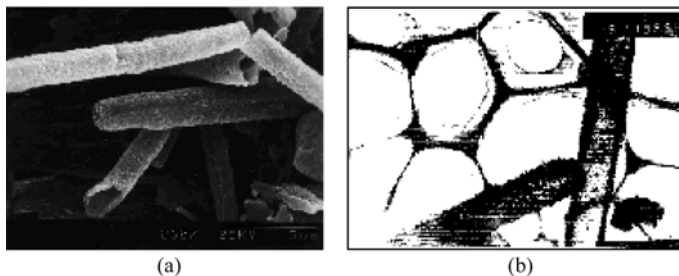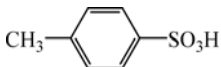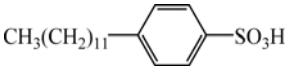
Figure 5.2   (a) Typical SEM and (b) TEM images of PANI-β-NSA microtubes prepared by *in-situ* doping polymerization [13, 14]

Table 5.3   Molecular structure of the selected sulfonic acids as dopants [13]

Sulfonic acids	Structure
p-methyl benzene sulfonic acid (MBSA)	CH₃——⟨benzene ring⟩——SO₃H
p-dodecyl benzene sulfonic acid (DBSA)	CH₃(CH₂)₁₁——⟨benzene ring⟩——SO₃H
β-naphthalene sulfonic acid (NSA)	⟨naphthalene⟩—SO₃H
5-*n*-butyl naphthalene sulfonic acid (BNSA)	⟨naphthalene with C₄H₉⟩—SO₃H
5-sulfo-isophthalic acid (SIA)	⟨benzene ring with SO₃H, HOOC, COOH⟩
Alizarin red acid (ARA)	⟨anthraquinone structure with OH, SO₃H, OH, O⟩

important role in synthesizing tubular morphology for both PANI and PPy [13]. Above-results strongly supported that the accident discovery of the tubular PANI-β-NSA and PPy-β-NSA by template-free method is inevitable!

5.1.2   Universality of Template-Free Method

After discovery of template-free method, the first question in author mind was how about universality of the new method in synthesizing or preparing conducting polymer nanostructures? In order to answer the question, universality of the new method to conducting polymer nanostructures was proved by changing polymer chain, polymerization method (chemical and electrochemical polymerization) and dopant nature. Up to date, all results provided strong and positive evidences for supporting that template-free method is a facile and universal approach to conducting polymer nanostructures. These supporting evidences are discussed as below.

1. By Changing Polymeric Chain and Polymerization Method

It is well known that the polymeric chain, nature of the substitution group along the

polymeric chain or as a side chain will affect morphology and physical properties of the conducting polymers [3]. In addition, chemical and electrochemical polymerization is conventional and main method to prepare conducting polymers [3]. Therefore it is firstly necessary to confirm universality of template-free method by changing polymeric chain and polymerization method. The next discussion will emphasis on two parts: one is the substituted and copolymerized PANI by chemical template-free method in the presence of β-NSA as the dopant, and another is PPy-β-NSA prepared by chemical and electrochemical template-free method.

(1) POT-β-NSA Microtubes

Poly (ortho-toluidine) (POT) is one of derivatives of PANI, in which a methyl group (—CH$_3$) is introduced into the benzene ring on the polymer chain of PANI [15]. So POT was excellent candidate to understand effect of the methyl group on the tubular morphology of PANI by the template-free method in the presence of β-NSA as the dopant. Interestingly, the POT-β-NSA microtubes with 0.8 and 6.0 μm in diameter were obtained [16], indicating the template-free method [1] is a reliable and practical method of synthesizing tubular PANI and its derivatives. It noted that the wall thickness of the POT-β-NSA microtubes is about 50 to 100 nm, which was much thinner than that of PANI-β-NSA microtubes [11]. Like PANI-β-NSA microtubes, the completeness and size of POT-β-NSA microtubes depend upon the concentration of β-NSA, for instance, the average diameter of POT-β-NSA tubules increases with an increase in the concentration of β-NSA as shown in Fig. 5.3.
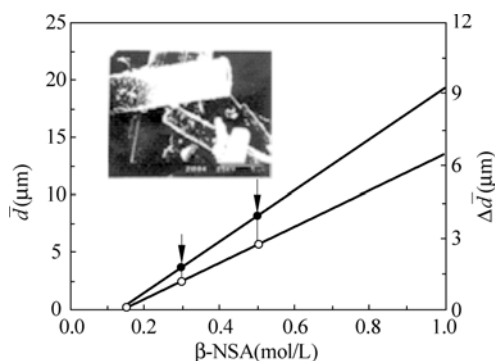

Figure 5.3 Effect of the concentration of β-NSA on the average diameter of POT-β-NSA microtubes prepared by template-free method and inset is SEM images of POT-β-NSA [16]

However, the lower concentration of β-NSA favored the formation of complete tubules, which is different from PANI-β-NSA microtubes where a high concentration of β-NSA is required to form complete PANI-β-NSA tubules [11]. The POT microtubes are also conductive with a room-temperature conductivity of 10^{-4} to 10^{-2} S/cm, depending upon doping degree [16]. The maximum conductivity at room temperature is about 3.0×10^{-2} S/cm, which is consistent with that of the

POT-HCl grains synthesized by a common method [17]. However, it is one or two orders of magnitude lower than that of PANI-β-NSA (4.0 S/cm) [11] due to an increase of torsion in neighboring benzene rings on the polymer chain resulted from the introduction of the —CH$_3$ groups into the benzene ring on the polymer chain, as measurement by UV-visible spectra [16].

(2) Self-Doped PANI-ANSA Copolymer Nanotubes

As above-mentioned, only micro/nanotubes of PANI or PPy were synthesized by template-free method in the presence of β-NSA as a dopant [11, 18]. It suggested that β-NSA plays an important role in the formation of PANI or PPy micro/nanotubes [11, 18, 19]. Atkinson et al. [20] synthesized a completely sulfonated PANI derivative, poly (5-aminonaphthalene-2-sulfonic acid) (ANSA), by the oxidization of sodium 5-aminonaphthalene-2-sulfonate, which is typical self-doped PANI although its conductivity ($10^{-3} - 10^{-5}$ S/cm) is much lower than that of the doped PANI. Author found that ANSA could be co-soluble with aniline in water when the aniline/ANSA molar ratio was higher than 2 at 0℃ [21], suggesting self-doped copolymer of PANI-ANSA might be chemically prepared by APS as the oxidant. As predicted, a dark green precipitate was produced after addition of APS for about 24 h, indicating PANI-NASA copolymer maybe used to prove universality of template-free method by co-polymeric chain. As a result, influence of the molar ratio of aniline to NASA on morphology, solubility, thermal and electrical properties of the PANI-NASA copolymers was investigated. It is found that the polymer chain of the PANI-ANSA is similar to PANI [22] and its self-doping character was conformed by FTIR measurements [21]. However, the molar ratio of aniline to ANSA had a strong influence on the morphologies of PANI-ANSA. At a high molar ratio (aniline/ANSA ~ 50), for example, fibrous and granular morphologies coexisted. Typical SEM and TEM images of self-doped PANI-NASA nanotubes (60 – 100 nm in outer diameter) are shown in Fig. 5.4, which further proved template-free method is a universal way to prepare conducting polymer nanostructures [21]. Although the conductivity of the self-doped PANI-NASA nanotubes is lower than that of the PANI-HCl [22], the solubility and thermal properties are better than that of PANI-HCl due to the —OSO$_3$H group linked with the polymer backbone by a covalent bond [21].

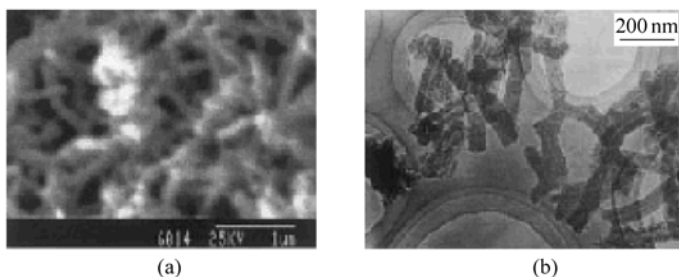(a)   (b)

Figure 5.4   Morphology the self-doped PANI-NASA nanotubes prepared by template-free method: (a) SEM; (b) TEM [21]

(3) PPy-β-NSA Micro/Nanotubes by Chemical and Electrochemical Method

In general, electrochemical polymerization is not only a common method for preparing large-scaled free standing films of PPy, but also controlling synthesis by changing current density, applied based voltage and polymerization time [3]. PPy is therefore a good candidate as a conducting polymer prepared by both chemical and electrochemical polymerization. In addition, above-results demonstrated that β-NSA plays an important role in forming PPy or PANI nanotubes by template-free method, which might be due to its hydrophilic group (—SO$_3$H) and the hydrophobic lipophilic group (—OC$_{10}$H$_7$), showing amphiphilic behavior. Based on above-idea, therefore, author tried to synthesize PPy nanotubes by electrochemical [23a] and chemical [23b] template-free method in the presence of β-NSA as the dopant. Universality of template-free method was further conformed by PPy-β-NSA prepared by chemical and electrochemical template-free method, which main results are discussed as below.

(a) PPy-β-NSA Microtubes by Chemical Template-Free Method

As shown in Fig. 5.5, the PPy-β-NSA microtubes not only were successfully prepared by electrochemical template-free method [23a], but also by chemical template-free method [23b]. In particular, the morphology of as-synthesized PPy-β-NSA nanostructures prepared by electrochemical template-free method is unaffected by a de-doping and re-doping process as shown in Fig. 5.6. In other words, the tubular morphology is more stable although counter-ions withdraw from or entrance into polymeric chain of the PPy-β-NSA nanostructures undergone de-doping or re-doping process. Like PANI-β-NSA nanotubes synthesized by chemical template-free method, the PPy-β-NSA nanostructures synthesized by chemical template-free method could be also dissolved in *m*-cresol [23b]. Interestingly, the morphology of PPy-β-NSA undergone a change from grain-short tube-long tube with increasing polymerization time [23b]. In addition, the rate of oxidant addition affects on formation of the tubules [23b], for instance, granular PPy-β-NSA was obtained when the the rate of adding oxidant is quick (e.g. about 10 s/drop), but, the tubular PPy-β-NSA with 150 nm in diameter was prepared when the rate was slow (e.g. about 1 min/drop), indicating growth of the PPy-β-NSA nanotubes prepared by a chemical template-free method is a slow self-assembly process. This is different from the PANI-β-NSA nanotubes prepared by chemical template-free method [24]. Moreover, it noted that morphology of the PPy-β-NSA microtubes is modified by adding the inorganic salts, showing addition of the electrolyte leads to enhancement of the diameter of the microtubes due to increase the aggregation number of the surfactant and decrease the CMC [23b]. Results on effect of electrolyte additions on morphology of the PPy-β-NSA microtubes further proved that surfactant characteristic of β-NSA dopant plays an important role in the formation of the self-assembled PPy-β-NSA microtubes by template-free method.
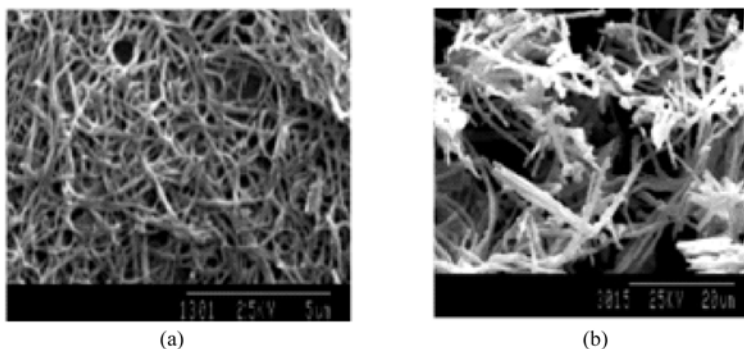
(a)

(b)

Figure 5.5   Typical SEM images of PPy-β-NSA prepared by chemical method (a) [23b] and electrochemical method (b) [23a]
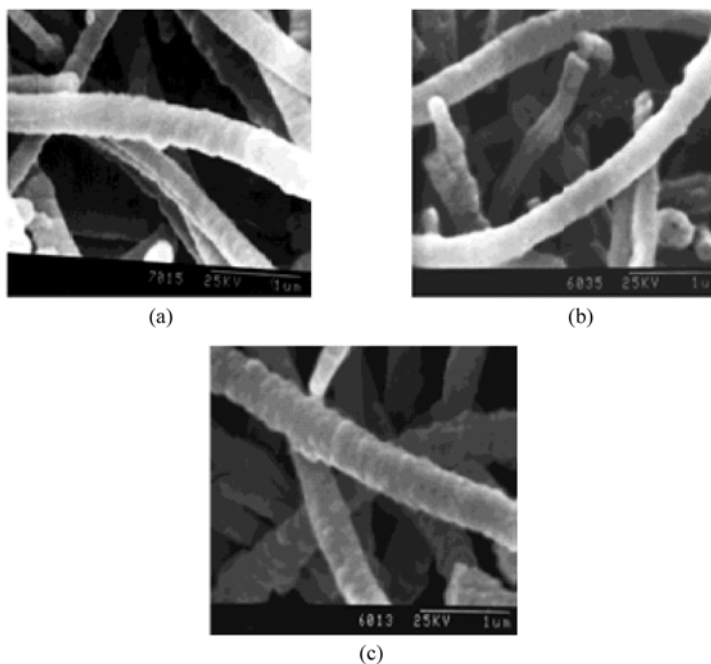

(a)

(b)

(c)

Figure 5.6   The SEM images of PPy-β-NSA nanostructures prepared by chemical template-free method: (a) as-synthesized, (b) de-doped in 2 mol/L aqueous NH₄OH for 12 h; and (c) sample b was re-doped in 0.57 mol/L aqueous solution for 24 h [23a]

(b) PPy-β-NSA Microtubes by Electrochemical Template-Free Method

It was reported that large-scale free standing films of PPy with high conductivity could be synthesized by electrochemical polymerization [25]. Compared with chemical polymerization, the electrochemical method is easily controlled by adjusting the applied potential, current density and polymerization time. Therefore it is necessary to further prepare PPy nanostructures by using electrochemical

template-free method in the presence of β-NSA as the dopant. The PPy-β-NSA nanotubes with $0.8 - 2\,\mu m$ diameter and $15 - 30\,\mu m$ length are successfully prepared by using electrochemical template-free method [26]. However, it is found that the formation of the nanotubes is affected by the electrochemical polymerization conditions, such as nature of work electrode, current density, concentration of β-NSA and pyrrole monomer as well as polymerization time [26]. Especially, it showed that non-corrosive steel as the work electrode is an important parameter in forming PPy-β-NSA tubules by electrochemical template-free method, while other parameters only change the diameter of the tubules. As increasing polymerization time, moreover, the diameter of the nanotubes is increased whereas the tubular morphology does not change [26], suggesting the formation of the nanotubes prepared by electrochemical template-free method is a fast self-assembly process that differs from that of the nanotubes prepared by chemical template-free method, in which is slow growth process [23b].

Above results suggested that there are some similarities in PPy-β-NSA nanotubes prepared by chemical and electrochemical template-free method [27]. For instance, the PPy-β-NSA nanotubes prepared by either chemical or electrochemical template-free method are identical to the doped PPy synthesized in a common method [28]. Elemental analysis suggested that the doping level, assigned as [S]/[N], is about $0.3 - 0.33$, indicating for each three pyrrole rings doping by one counter ion, which is consistent with the previous report [29]. Although room-temperature conductivity of the PPy-β-NSA nanotubes is strongly affected by the synthesis method and conditions, their temperature dependence of the conductivity is independent upon the polymerization method, showing a semiconductor behavior and following a 3D-VRH model proposed by Mott [12]. However, the growth process of the PPy-β-NSA nanotubes self-assembled by a chemical and electrochemical template-free method is different; for instance, the formation of the nanotubes by a chemical template-free method is a slow process whereas it is a fast process for the formation of the PPy nanotubes by electrochemical template-free method [23b, 26, 27].

2. By Changing Dopant Nature

As well known, dopant structure plays an important role in determining morphology, electrical and other properties of conducting polymers prepared by both chemical and electrochemical method [3]. Therefore it is necessary to prove universality of template-free method in preparing nanostructured conducting polymers by changing dopant structure. In order to do so, various dopants including organic sulfonated acids, inorganic acids and special sulfonated carbon 60 (C_{60}) and CNTs were used as the dopants to prepare PANI nanostructures by a chemical template-free method. Moreover, author also tried to prepare nanotube or nanofiber junctions or dendrites of PANI doped with some organic sulfonated acids by chemical template-free method in order to further prove the universality of template-free method.

(1) Organic Sulfonated Acids as the Dopants

As above-mentioned, β-NSA is a key in formation of PANI nanotubes by a chemical template-free method and is served as dopant and soft-template at the same time due to the surfactant and dopant behavior of —SO$_3$H group attached on the naphthalene ring [3, 11]. So it is necessary to test possibility in preparing PANI nanostructures by a chemical template-free method in the presence of other organic sulfonated acids as the dopants. In order to check that, various organic sulfonated acids, such as self-designed and synthesized 4-{n-[4-(4-nitrophenylazo) phenyloxy] alkyl} aminobenzene sulfonic acid (Cn-ABSA), D-10-camphorsulfonic acid (D-CSA), and dicarboxylic acids were selected as the dopants. The main results are discussed as below.

(a) Cn-ABSA (n = 2, 4, 6, 8 and 10) as the Dopants

p-nitrophenylazobenzene group with cis-$trans$ isomerization is often considered a mesogen for synthesizing side-chain liquid-crystal polymers [30] because of its typical characteristics of a large π-flowing field consisting of donor and acceptor electricity groups in the backbone [31]. The asymmetric electricity backbone with a charge-transferring character can easily be induced to polarize and orient in the extra field [32]. Such sulfonated acids might be used as dopants for PANI, resulting in special morphologies and new physical properties [22]. Based on this idea, author designed and synthesized 4-{3-[4-(4-nitrophenylazo) phenyloxy]propyl} aminobenzene sulfonic acid (C$_3$-ABSA) as a novel dopant to dope PANI by a chemical template-free method. It is interested that nano-cylindrical PANI was successfully obtained [33] that prompted us to further design and synthesize a series of sulfonic acids, 4-{n-[4-(4-nitrophenylazo) phenyloxy]alkyl} aminobenzene sulfonic acid (Cn-ABSA, where n = 2, 4, 6, 8, or 10), as novel dopants to check the universality of template-free method [34]. UV-visible spectra of Cn-ABSA dissolved in NMP show two peaks at 260 and 380 nm that are assigned as the π − π* transition of the benzene ring of Cn-ABSA and the π − π* transition of the $Trans$ isomer of the azobenzene moiety [32a; 35]. Morphology of the resultant PANI-Cn-ABSA is affected by the synthesis conditions, such as the ratio and concentration of reagents (aniline, Cn-ABSA, and APS), especially the addition of water before polymerization. Nano-cylinders of PANI-Cn-ABSA (n = 2, 4, 6, 8 and 10) with 100 − 300 nm in diameter are successfully synthesized by chemical template-free method under suitable conditions [34].

However, SEM images discovered some of the nano-cylinders are hollow (i.e., tubules) and others are solid (i.e., nano-fibers) even nanofibers with branched structures are observed. In particular, the addition of water before polymerization significantly reduces by several orders of magnitude the diameter from micrometers to nanometers (e.g., 4.0 mm to 100 nm) and makes the cylinders partial in branched shapes associated with the amount of water added [34]. The emulsion of aniline/Cn-ABSA/water was measured by dynamic light scattering (DLS). It indicated that the average size and number dispersion of the micelles could be

adjusted through the control of the number of alkyl groups (*n*) of C*n*-ABSA as shown in Fig. 5.7, indicating micelles are formed in the reaction solution. This is a positive evidence for supporting the micelles can be served as the soft-templates in forming nanostructures by template-free method. Above results provided another strong evidence to support template-free method is an universal method to conducting polymer nanotubes.
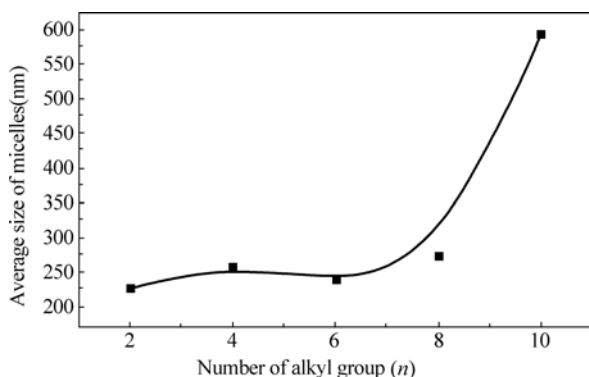

Figure 5.7 Dependence of the average size on the number of alkyl groups (*n*) of C*n*-ABSA, and inset is SEM images of the nanowires at C*n* = 2 – 8 [34]

(b) *D*-CSA as the Dopant

As mentioned before, CSA is an excellent dopant for PANI because CSA doped PANI not only has high conductivity (~ 400 S/cm) [4], but also improving solubility in organic solvent [36]. Moreover, PANI doped with *D*-10-camphorsulfonic acid (*D*-CSA) or *L*-10-camphorsulfonic acid (*L*-CSA) showed optical activity and electrical properties [37], indicating electro-optical activity nanostructures of PANI might be synthesized by template-free method associated with introduced effect of optical activity dopants. Based upon above idea, author successfully synthesized the chiral PANI-*D*-CSA nanotubes with 80 – 180 nm in diameter and conductivity in a range of $3.4\times10^{-3} - 3.5\times10^{-1}$ S/cm by a chemical template-free method [38]. It is found that morphology, size and conductivity of the nanostructures are affected by the reaction conditions. Especially, the conductivity increases with increase of the molar ratio of *D*-CSA to aniline [38]. The self-assembled chiral PANI-*D*-CSA nanotubes again provided another evidence for supporting universality of the template-free method to nanostructures of conducting polymers.

(c) Dicarboxylic Acids as the Dopants

It is well known that conducting polymers are composed of π-conjugated polymer chains and counter-ions produced by a doping process [3]. The total conductivity of the conducting polymers, as measured by a four-probe method, is therefore a result of intra-molecular and inter-molecular factors [39]. The intra-molecular factors include the localization length, which can be altered by controlling the

defect rates in the polymer (sp^3 defects) or head-head coupling [40] while the inter-chain distances, inter-chain cross-linking, degree of chain orientation, and fraction of crystallinity comprise the intermolecular factors [39]. The inter-chain distance can be modified by using ring-substituted monomers [41] or counter-ions of different sizes [42]. In addition, dopant size and crystallinity contribute to the delocalization of chains within three-dimensional regions play an important role in influencing the electrical properties of the conducting polymers [43]. So far a series of papers dealing with the effect of crystallinity and dopant size on the electrical properties of conducting polymers have been published [44]. However, systematic studies on influence of dopant size on morphology and size as well as crystallinity and conductivity of the nanostructured conducting polymers by either hard-template or soft-template method are lacking. Dicarboxylic acids (HOOC (CH$_2$)$_n$ COOH), such as oxalic acid ($n = 0$, OA), malonic acid ($n = 1$, MA), succinic acid ($n = 2$, SA), glutaric acid ($n = 3$, GA), and adipic acid ($n = 4$, AA), have an alkyl chain (i.e., —CH$_2$ groups) of varying length ($n = 0 - 4$) and double —COOH groups.

Obviously, the length of the alkyl chain dominated the size of the dopant, while the —COOH groups served as proton dopants, which allow each acid molecule to dope two adjacent chains at the same time, resulting in inter-chain orientation. Based on above analysis, author thought that the dicarboxylic acids might be a good candidate for investigating influence of dopant nature on morphology, crystallinity and electrical properties of the conducting polymer nanostructures. As predicted, highly crystalline PANI nanostructures (nanotubes or nanofibers) with $80 - 170$ nm in diameter were prepared by a chemical template-free method in the presence of dicarboxylic acids as the dopants [45]. The diameter of the nanostructures is affected by the length of —CH$_2$ groups, showing the average diameter increased from 100 to 170 nm accompanied by an enhancement in the aspect ratio of the nanostructures [45] as shown in Fig. 5.8. Interestingly, XRD measurements showed that the inter-chain distance perpendicular to the polymer-chain direction increases with increase of the length of —CH$_2$ group, while the inter-chain distance parallel to the polymer-chain direction remained constant as shown in Fig. 5.8. This is consistent with the inter-chain distance is dominated by size of the dopants, because the size of dopants is controlled by the length of —CH$_2$ group. In particular, a sharp peak at $2\theta = 6.50°$, attributed to the separating aliphatic chains [46], is observed in the XRD spectrum of nanostructured PANI, showing the orientation of the dicarboxylic acids in the polymeric chain. XRD measurements indicate that high crystallinity results from orientation arrange of the dicarboxylic acids along the polymer chain of the nanostructures.

According to micelles proposed by author [19], micelles composed of dicarboxylic acids are formed in the reaction solution due to the hydrophilic —COOH group. In addition, the room-temperature conductivity of the nanostructures increased when the length of —CH$_2$ group decreased [45]. This might be the result of two
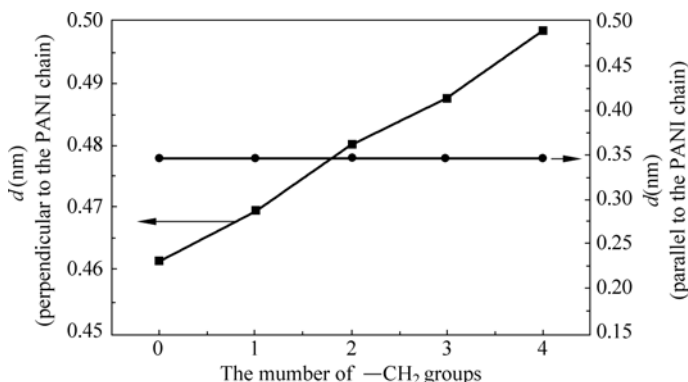
Figure 5.8   Effect of the number of —CH_2 groups in the dopant on the inter-chain distances perpendicular and parallel to the PANI chain direction in the resulting PANI nanostructures [45]

factors: one is decreasing the inter-chain distance, as confirmed by XRD, and the other may be size effects, as proven by the fact that the diameter decreases when n decreases, which is consistent with the results obtained from electrical measurements on single nanotubes [47]. Moreover, the conductivity increased with increasing [dopant]/[An] ratio that results of enhancement of the doping degree, as measured by XPS [45]. The results on dicarboxylic acids doped PANI nanotubes not only further support the universality of template-free method to prepare nanostructure of conducting polymers, but also proving an approach for enhancement of crystallinity of the conducting polymers.

(2) Special Sulfonated Acids as the Dopants

As well known, carbon 60 (C_{60}) is typical carbon materials. Moreover, dendrimer is novel materials with controlling size and functionalized group. The sulfonated C_{60} or dendrimer can be used to dope PANI because of its proton doping characteristic. Author tried to synthesize PANI nanotubes by using chemical template-free method in the presence of hydrogensulfated fullerenol with six —(O)SO_3H groups (C_{60}-(O$SO_3H)_6$) [48] and sulfonated dendrimer containing 24 terminal groups of 3,6-disulfonaphthylthiourea (PAMAM$_{4.0}$) [49] as the dopants. It is found that uniform PANI-C_{60}-(O$SO_3H)_6$ and PANI-PAMAM$_4$ nanotubes with about $100 - 300$ nm in diameter and several micrometers in length were successfully obtained as shown in Fig. 5.9. Unlike other dopants, addition of water in the reaction solution before oxidation polymerization of aniline is critical in forming these nanotubes because granular PANI is obtained in the absence of H_2O [48]. Although it was not clear at that time for the self-assembly mechanism of these nanotubes, the addition of H_2O at this stage maybe caused the aniline/PAMAM$_{4.0}$ or aniline/C_{60} (O$SO_3H)_6$ acting as a soft-template to form self-assembled nanostructures [50]. This was also supported by the non-tubular morphology produced by prolonged powerful ultra-sonication during the template-free polymerization.
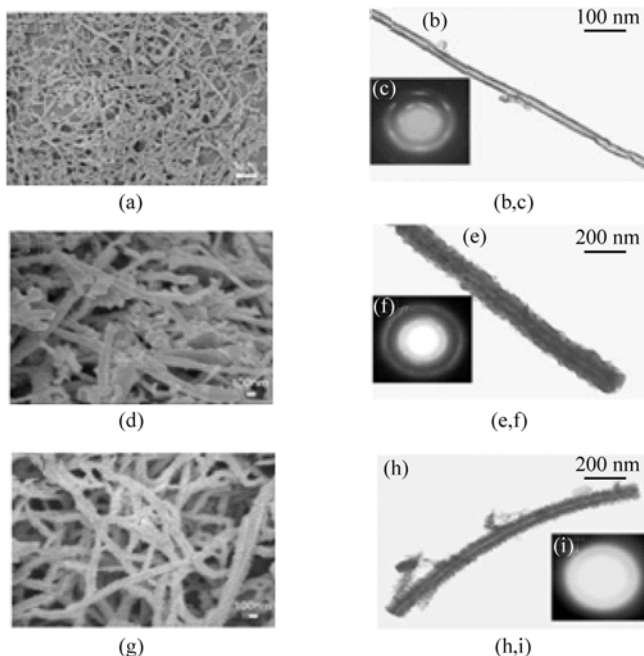
Figure 5.9   SEM images (a, d, g), TEM images (b, e, h) and electron diffraction patterns (c, f, i) ((a – c) MWNT-(OSO$_3$H$_n$); (d – f) PANI-c-MWNT-(OSO$_3$H$_n$); (g – i) PANI-d-MWNT-(OSO$_3$H$_n$) nanotubes) [60]

According to micelle model proposed by author [19], now, it is reasonable to accepted that addition of water during polymerization results in formation of micelles composed of PAMAM$_{4.0}$ or C$_{60}$(OSO$_3$H)$_6$ dopant due to hydrophilic —SO$_3$H group of the PAMAM$_{4.0}$ or C$_{60}$(OSO$_3$H)$_6$ that is served as the soft-template. As a result, the diameter decreased from micro- to nano-scale as increase of water addition is expected that was also consistent with the observations [51]. The conductivity for a PANI-C$_{60}$(OSO$_3$H)$_6$ nanotube pellet, as measured by four-probe method was ca. 0.1 S/cm that is slightly lower than the conductivity reported for doped PANI films previously reported [48] due to a relatively low doping level of 0.25 (represented by of [S]/[N]), as determined by X-ray photoelectron spectroscopy. Temperature-dependent measurements revealed a $\ln \sigma(T) - T^{-1/4}$ relationship for PANI-C$_{60}$(OSO$_3$H)$_6$, consistent with 3D-VRH model [12].

CNTs have been investigated for use in a wide range of devices, including nanoelectronic and biomedical devices [52]. In particular, the mass production of CNTs and their soluble derivatives have promoted a great deal of interest in developing multifunctional carbon nanotube composites with other materials [53]. CNTs have been used to impart electrical properties to non-conducting materials (e.g. polymers) for electronic applications [54]. As well known, conducting

polymers (CPs) have also been used for similar application [3]. It is therefore expected that combination of CNTs and CPs leads to composite materials processing the properties of each of the constituent components [55]. Examples include highly efficient photovoltaic cells based on the composite materials of CNTs with PPV [56] or poly (3-octylthiophene)[57], conjugated polymer/CNT composite LEDs with low current densities and good thermal stabilities[58], and aligned CNT/CP coaxial nanowires of high surface and interface areas[59]. It is expected that the sulfonated CNTs might be used as a dopant due to proton doping characteristic of PANI [22]. Author and professor Liming Dai reported PANI nanostructures prepared by a chemical template-free method in the presence of the sulfonated multi-walled carbon nanotubes designed as MWNT-(OSO_3H_n) as the dopant [60] for the first time. It is found two kinds of composite nanostructures are prepared, depending upon the aniline to MWNT-(OSO_3H_n) ratio. Only PANI-coated MWNT-(OSO_3H_n), represented as PANI-c-MWNT-(OSO_3H_n), is obtained when the ratio aniline to MWNT-(OSO_3H_n) is less than 1. At the ratio aniline to MWNT-(OSO_3H_n) larger than 2, on the other hand, MWNT-(OSO_3H_n) doped PANI nanotubes, represented as PANI-d-MWNT-(OSO_3H_n), are obtained [60]. Typical SEM images of PANI nanostructures are shown in Fig. 5.10. The formation of PANI-c-MWNT-(OSO_3H_n) actually raised the polymerization of aniline on the surface of MWNT-(OSO_3H_n) nanotubes acting as the dopant and template at the same time, while PANI-d-MWNT-(OSO_3H_n) is derived from a self-assembly process induced by the interaction between MWNT-(OSO_3H_n) and
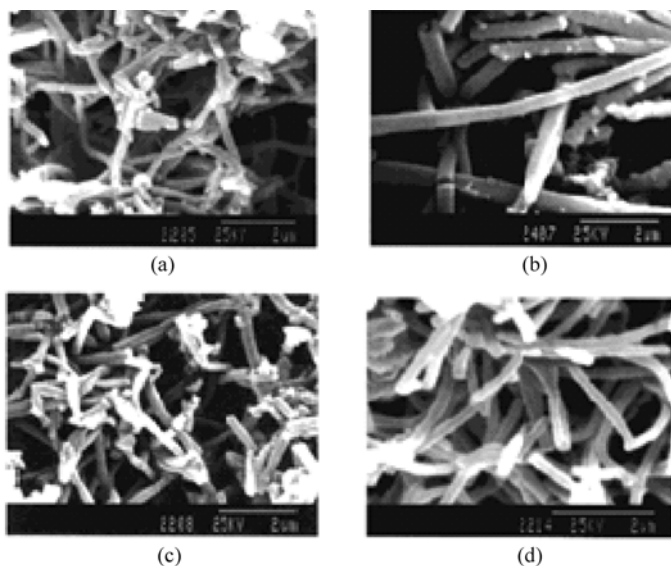

(a) (b) (c) (d)

Figure 5.10 SEM images of PANI nanostructures doped with different inorganic acids: (a) HCl, (b) H_2SO_4, (c) HBF_4, (d) H_3PO_4 ([An]/[acid]) [61]

PANI [60]. Raman spectra indicated that PANI chains in both PANI-c-MWNT-(OSO$_3$H$_n$) and PANI-d-MWNT-(OSO$_3$H$_n$) nanotubes are in doped state, but with different chain conformation. For instance, the PANI chains in the PANI-d-MWNT-(OSO$_3$H$_n$) nanotubes are more extended conformation due to its nano-tubular structure [60]. Room temperature conductivity, as measured by four-probe method, is estimated to be 1.4×10^{-2} S/cm and 2.2×10^{-2} S/cm for PANI-c-MWNT-(OSO$_3$H$_n$) and PANI-d-MWNT-(OSO$_3$H$_n$), respectively. The temperature dependence of conductivity for both composite nanostructures exhibits a typical semiconductor behavior, and fits 1D-VRH model [12]. However, the hopping barrier of the PANI-d-MWNT-(OSO$_3$H$_n$) nanotubes deduced from the slope of $\ln \sigma(T)$ vs. $T^{-1/2}$ lines is 2.7×10^4 K, which is one order of magnitude higher than that of PANI-c-MWNT-(OSO$_3$H$_n$) [60].

(3) Inorganic Acids as The Dopants

Since above-discussed organic sulfonated acids have a —SO$_3$H group, micelles composed of these dopants are easily formed in the reaction solution due to its surfactant function. In general, however, inorganic acids such as HCl, H$_2$SO$_4$ and H$_3$PO$_4$, which are without surfactant function, are used as the common dopants for synthesis conductive PANI [3]. Therefore, it is necessary to prove the universality of template-free method by using inorganic acids without surfactant function. Fortunately, self-assembled PANI nanotubes or nano-wires with an average diameter of 150 – 340 nm and a conductivity of $10^{-1} – 1$ S/cm were successfully prepared by template-free method in the presence of inorganic acids (e.g. HCl, H$_2$SO$_4$, H$_3$PO$_4$, and HBF$_4$) as dopants [61]. Typical SEM images are shown in Fig. 5.10, further proving universality of template-free method for preparing PANI nanostructures although the dopants are without surfactant function.

In order to understand if the surfactant is an essential condition for formation of the PANI nanostructures by template-free method, effect of addition of surfactant on the formation of the PANI nanostructures doped with inorganic acids as the dopants was investigated. It is found that addition of surfactant during poly-merization does not affect formation of the nanostructures by template-free method, but the diameter is slightly changed [61]. Obviously, the self-assembly mechanism of the PANI nanostructures doped with inorganic acids is different form that of the PANI nanostructures doped with organic surfactant organic dopants, which will be discussed in formation mechanism of the nanostructures prepared by template-free method. The self-assembled PANI nanotubes by template-free method in the presence of inorganic acids as the dopants not only provided strong evidence for supporting universality of the template-free method, but also information for understanding self-seembly mechanism.

3. Nanotube Junctions and Dendrites

It is well known that the vessels in the bodies of animals and in plants are composed of tubes, and their junctions often exist in a dendritic morphology [62]. Nanotube

junctions, as well as individual nanotubes, play a key role in nanoelectronic devices [63]. Carbon nanotube junctions have been prepared by chemical vapor deposition (CVD), template and by joining two individual nanotubes [64]. Although micro- and nanotubes of conducting polymers have been prepared by hard template [2] and self-assembly [1, 19, 61 and 65], few publications concern micro- or nanotube junctions of the conducting polymers, especially complicated junctions with dendritic morphology are seldom reported. Interestingly, nanotube or nanofiber junctions or dendrites of PANI and PPy doped with sulfonated acids were prepared by template-free method [66]. Typical SEM and TEM images of the self-assembled sub-micrometer-sized tube junctions and their aggregated dendrites of PANI-D-CSA and PPy-p-TSA nanotube junctions are shown in Fig. 5.11.
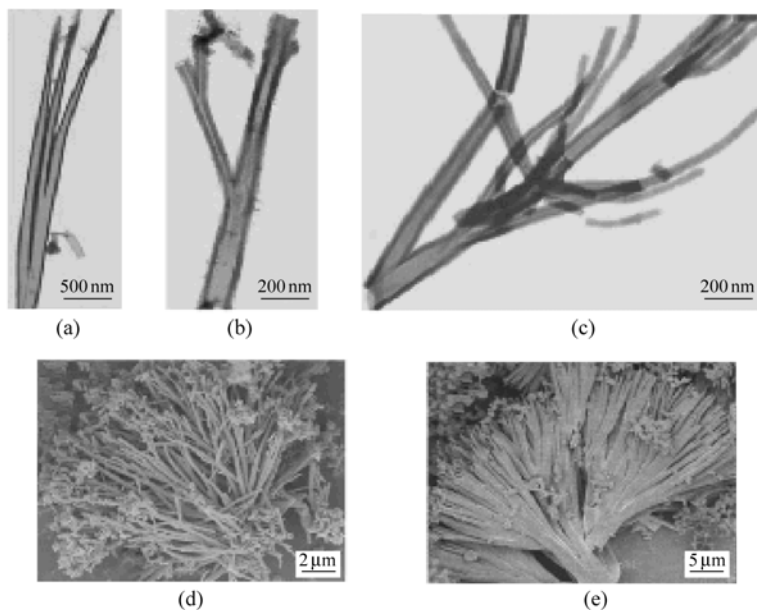

Figure 5.11   Self-assembled sub-micrometer-sized tube junctions and their aggregated dendrites: a-c) TEM images of PANI-D-CSA; d) SEM images of PANI-D-CSA; e) SEM images of PPy-p-TSA [66]

Similarly, the nanotube junctions and dendrites of PANI are also obtained when β-NSA and 1,5-NDSA is used as the dopants, indicating the formation of such nanotube junctions and dendrites of the conducting polymers prepared by template-free method is a common phenomenon under satiation synthesis conditions. The diameter of nanotubes and aggregated dendritic morphology can be adjusted by varying the synthesis conditions such as dopant nature, the monomer concentration and the molar ratio of monomer to dopant [67]. It was proposed that the strong interactions among the polymer chains, including the π – π interactions, hydrogen

bonds, and even ionic bonds are as the driving forces for formation of such nanotube junctions and dendrites of PANI or PPy via a self-assembly process [67]. It noted that a stationary environment without ultrasonic stirring is required for information of such nanotube junctions and dendrites [66].

In fact, the nanotube junction and dendrite is a kind of non-uniform fractal structure. According to fractal theory [62], the fractal dimension, D, is described by an expression: $D = \ln N \left[\ln(r^{-1})\right]^{-1}$, where N is the number of branches of the trunk, and r is the self-similarity ratio. By analyzing SEM and TEM measurements, the value of r to be in the range of 0.5 to 0.6, depending on the synthesis conditions. Therefore, when $N = 2$ was used, the fractal dimension D was estimated to be between 1 and 1.4, which is consistent with the value of nature fractals [62]. The junctional nanotubes are more difficult to be fabricated by a hard-template method due to only cylideric pores in membrane is avariable as a template, further proving the universality of the template-free method to conducting polymer nanostructures.

By changing polymer chain, polymerization method and dopant structure, in summary, it has been demonstrated that template-free method is a universal and facile approach to prepare conducting polymer micro/nanostructures, even nanotube or nanofiber junctions.

5.1.3   Controllability of Morphology and Diameter by Template-Free Method

Unlike hard-template method, morphology and size controllability of the micro/ nanostructures prepared by template-free method is lack because of omitting hard membrane as the templates. However, it is found that morphology and diameter of the template-free synthesized micro/nanotubes are strongly affected by dopant structure and polymerization conditions. Therefore, morphology and diameter of the template-free synthesized micro/nanostructures can be controlled by changing polymerization conditions such as dopant and monomer nature as well as conditions including the concentration of dopant, monomer and oxidant, the molar ratio of dopant and oxidant to monomer and reaction temperature etc. These reaction parameters can be served as efficient ways to control morphology and size of the template-free synthesized micro/nanostructures. The following discussion will show how to control morphology and diameter of the template-free synthesized micro/nanostructures by above-parameters through some typical samples.

1. Morphology Controllability

3D hollow spheres of function materials are interesting in the field of medicine, material science, and catalysis due to their hollow structure, which makes them

particularity applications for drug delivery, medical imaging, protein and enzyme transplantation, encapsulation of products (cosmetics, inks, and dyes), and contaminated waste removal [68]. So far, metal, semiconductor, and polymer nanotubes [69] have been synthesized by either hard- or soft-template method. Based on previous studies of PANI-β-NSA nanotubes prepared by template-free method [11], author successfully synthesized hollow microspheres of PANI-β-NSA prepared at a low temperature (−10 ℃) by template-free method [65] or synthesized at a room temperature using ortho-hydroxybenzoic acid (SA) as the dopant [70]. These results further demonstrated that template-free method not only is a universal method for preparing nanotubes or nanofibers, but also hollow microspheres. In particular, it is found that the hollow spheres change from 3D microspheres to 1D nanotubes by adjusting reaction conditions. For PANI-β-NSA sample, for instance, the hollow spheres changed to nanotubes when the reaction temperature is increased from −10℃ to room temperature [65]. For PANI-SA sample, on the other hand, the hollow spheres changed to nanotubes as the molar ratio of SA to aniline decreases from 1.0 to 0.1[70]. Change in morphology from hollow 3D-microspheres to 1D-nanotubes for PANI-β-NSA and PANI-SA is shown in Fig. 5.12. Above two samples provided strong evidences to support template-free method is not only a universal approach to prepare micro/nanostructured conducting polymers, but also controlling morphology by changing the reaction conditions.
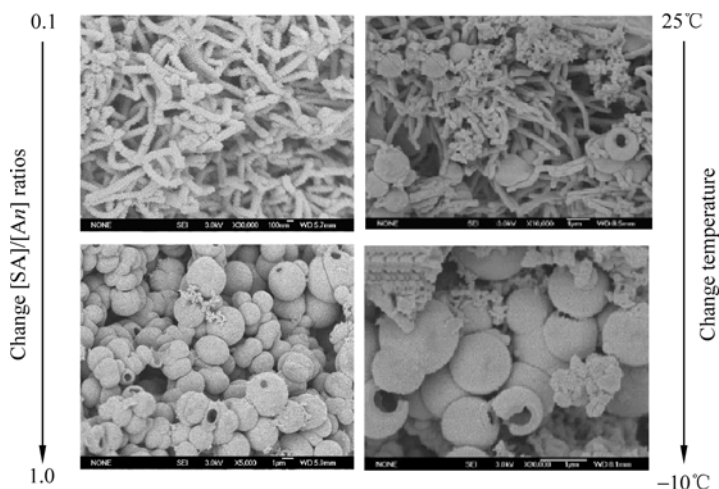

Figure 5.12 Change in morphology from 1D nanotubes to 3D hollow spheres of PANI-SA (left) by changing the molar ratio of SA to aniline [70] and PANI-β-NSA (right) by changing polymerization temperature [65]

Change in morphology of the PANI-β-NSA and PANI-SA from hollow spheres to nanotubes with variation of reaction conditions might be related to their self-assembled mechanism. It has been demonstrated that the self-assembly mechanism of the PANI-β-NSA hollow microspheres [65] differs from that of

the PANI-SA microspheres [70] although micelle model proposed by author [19] is satisfied them. In case of PANI-β-NSA hollow microspheres, for instance, aniline droplets are served as the soft-template in the information of the hollow spheres at $-10^{\circ}\mathrm{C}$ because of hydrophilic aniline, while micelles formed by β-NSA/aniline salt are regarded as soft-templates of the nanotubes synthesized at room temperature because of amphiphilic structure of β-NSA, which consists of hydrophilic $-SO_3H$ and lipophilic $-C_{10}H_7$ [65]. For the PANI-SA hollow microspheres, on the other hand, spherical micelles consisted of SA are served as soft-templates in forming either nanotubes or hollow spheres of the PANI-SA though a self-assembly process. However, the hydrogen bond of the $-OH$ group of SA with the amine of PANI might be a driving force results in change of the PANI-SA morphology from hollow spheres to nanotubes as increase of the molar ratio of SA to aniline from 1.0 to 0.1[70]. This result indicates that the self-assembly mechanism of the micro/nanostructured PANI conducting polymers prepared by template-free method are depending on the dopant structure and reaction concentrations.

2. Diameter Controllability

In review articles in the literature, it has been demonstrated that the physical properties of the conducting polymer nanostructures are strongly affected by their diameter, which sometimes is called as a size effect. For instance, the conductivity of the nanostructured conducting polymers usually increases with decrease of their diameter [2]. Therefore synthesis of well-controlling diameter of the conducting polymer nanostructures is very important in application as the nano-devices. Although synthesis of well-controlling nanostructures by template-free method is difficult due to omitting membrane as the template, it is found that the diameter of the template-free synthesized nanostructures is strongly affected by the reaction conditions, which include structure, size and concentration of dopant, molar ratio of dopant to monomer or oxidant to monomer as well as the concentration of each reagents, polymerization temperature, even stirring fashion so on. Author found some efficient ways to control the diameter of the template-free synthesized nanostructures of conducting polymers through systematic studies. How to control the diameter of the template-free synthesized nanostructures by above-parameters is discussed one by one as follows:

(1) By Changing Dopant Structure

It has been demonstrated that molecular structure of dopant and doping degree strongly affect the physical properties of conducting polymers and their nanos-tructures [3, 71]. Since micelles composed of dopant or salt of dopant/monomer are served as the templates in forming nanostructures by template-free method [19], influence of molecular structure and concentration of dopants on the diameter of the nanostructures by template-free method is expected. Some typical samples dealing with influence of dopants on the diameter of the template-free synthesized nanostructures are given below.

(a) By Changing Number and Position of —SO$_3$H Group of Naphthalene Sulfonic Acids

As above-mentioned, β-NSA was the first dopant to be used for synthesizing PANI microtubes by a template-free method due to its —SO$_3$H group attached to the naphthalene ring that plays a dopant and soft-template at the same time [11]. In fact, naphthalene sulfuric acid has various derivatives, such as α-NSA, β-NSA and 1,5-NDSA. Each of those derivatives has —SO$_3$H group attached on the naphthalene ring, but their number and position of the —SO$_3$H group attached on the naphthalene ring is different. Therefore, these derivatives are excellent candidates to understand effect of molecular structure of the dopants on the diameter, morphology and electrical properties of PANI synthesized by template-free method [67]. Some interesting results were obtained as follows: ① All PANI doped with naphthalene derivatives are nanotubes when PANI is synthesized at low concentration of dopants (e. g. $1.3 \times 10^{-2} - 5.0 \times 10^{-3}$ mol/L) as shown in Fig. 5.13. On the other hand, solid fibers are synthesized at high concentration of the dopants (e.g. 0.1 mol/L) [67]. ② The formation yield of the nanotubes is affected by the molar ratio of dopant to aniline (represented as [dopant]/[An]). Formation yield of PANI-(α-NSA) nanotubes, for example, is achieved as high as 95% at some [dopant]/[An] ratios (e.g. 0.5 and 0.25). However, it decreases with reducing the
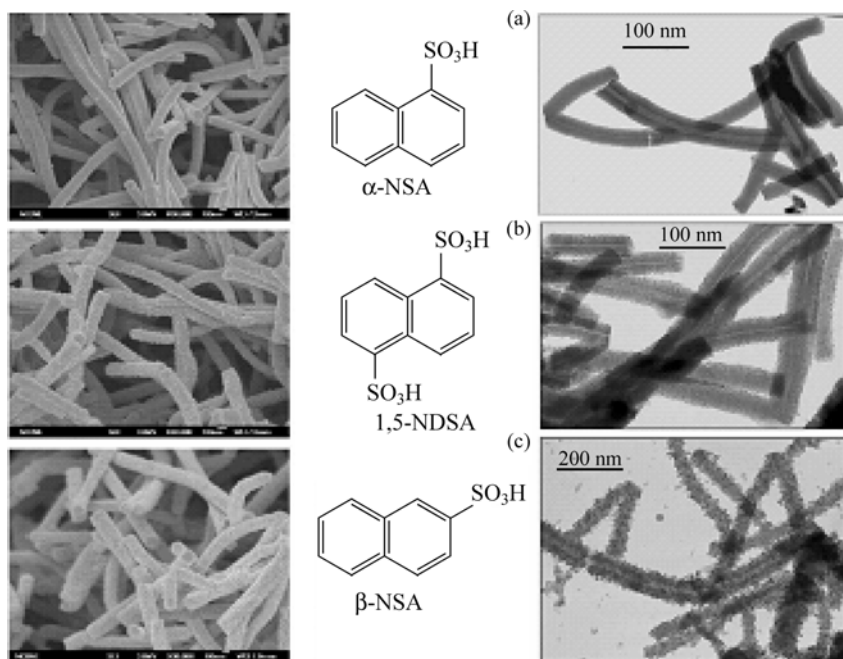

Figure 5.13   SEM and TEM images of PANI nanotubes doped with different naphthalene sulfuric acid at [dopant] = 0.0125 mol/L: (a) PANI-(α-NSA); (b) PANI-(β-NSA) and (c) PANI-(1,5-NDSA) [67]

[dopant]/[An] ratio; only grains could be obtained when the [dopant]/[An] ratio reached 0.0125 [67]. Similar results were also observed from PANI-(β-NSA) and PANI-(1,5-NDSA) samples. In addition, the formation yield of the nanotubes is also affected by the dopant structure and the dopant concentration. For example, fibrous PANI is obtained when the concentration of the dopants ranged from 5×10^{-1} to 5×10^{-3} mol/L. However, the tubular formation yield decreased slightly with the decrease of the dopant concentration. At low concentration of dopant (e.g. at 5×10^{-3} mol/L), however, the formation yield of the nanotubes slightly depended on the dopant structure, for instance, the formation yield of PANI-(α-NSA) and PANI-(β-NSA) nanotubes synthesized at this condition is high as 75%, while the yield for PANI-(1,5-NDSA) is only 25% [67]. ③ In particular, changing the dopant structure and the dopant concentration can control the diameter of the PANI nanotubes as shown in Fig. 5.14. The average diameter of the nanotubes was independent of the dopant concentration when the dopant concentration is less than 2.5×10^{-2} mol/L, however, it increases with the increase in dopant concentration when the dopant concentration is larger than 2.5×10^{-2} mol/L. At the same dopant concentration, moreover, the average diameter of the nanotubes is different, following an order of PANI-(α-NSA)<PANI-(β-NSA)< PANI-(1,5-NDSA). Above results indicate that influence of dopant structure and reaction conditions on the formation yield, morphology and diameter of the PANI nanostructures is very complete when the template-free method is used.
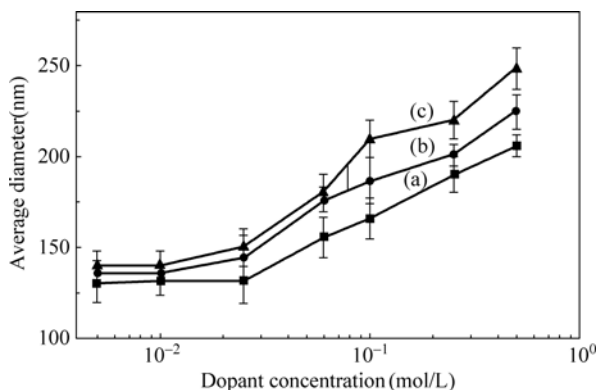

Figure 5.14   Effect of the dopant concentration on the average diameters of PANI nanostructures: (a) PANI-(α-NSA); (b) PANI-(β-NSA) and (c) PANI-(1,5-NDSA) [67]

(b) By Changing Alkyl Group of Sulfonic Acids

Sulfonic acid with controlling number of alkyl group is a good candidate to study influence of dopant size on the diameter of the template-free synthesized nanostructures. There are three samples to show how influence of the number of alkyl group on the diameter of the nanostructures. The first sample is saturated fatty acids as the dopants [72]. As well known, acetic acid (CH_3COOH, $n = 1$, AA), hexanoic acid ($CH_3(CH_2)_4COOH$, $n = 5$, HA), lauric acid ($CH_3(CH_2)_{10}COOH$,

$n = 11$, LA) and stearic acid ($CH_3 (CH_2)_{16} COOH$, $n = 17$, SA) belong to unitary saturated fatty acids. These acids are typical amphiphilic molecules that the —COOH group acts as doping and surfactant function at the same time, while the number of —CH_2 group of the alkyl chain is related to the size of the fatty acids. Therefore, these saturated fatty acids with different number of CH_2 group of the alkyl chain are good candidates to investigate the size effect of dopants on the formation, morphology and diameter of the self-assembled nanostructures prepared by template-free method. Thus above-mentioned four fatty acids (i.e. AA, HA, LA and SA) were used as the dopants to understand their influence on morphology and diameter of the PANI nanostructures by template-free method [72]. It is found that uniform and smooth nanofibers of the PANI doped with saturated fatty acids are obtained as shown in Fig. 5.15 (bottom), indicating the morphology did not affected by the number of —CH_2 group of the alkyl chain.

As predicted, however, the diameter of the nanofibers is controllable, showing the diameter increases with increase of the number of —CH_2 group of alkyl chain [72] as shown in Fig. 5.15 (upper). The secondary sample is dicarboxylic acids as the dopants, which are also typical sulfonic acids [45]. Dicarboxylic acids ($HOOC (CH_2)_n COOH$) include oxalic acid ($n = 0$, OA), malonic acid ($n = 1$, MA), succinic acid ($n = 2$, SA), glutaric acid ($n = 3$, GA), and adipic acid ($n = 4$, AA). These acids have an alkyl chain (i.e., —CH_2 groups) with varying length ($n = 0 - 4$) and double —COOH groups. The length of the alkyl chain is dominated by the size of the dopant, while the —COOH groups are served as proton dopants that allow each acid molecule to dope two adjacent chains of PANI at the same time, resulting in inter-chain orientation. Based on above analysis, the dicarboxylic acids were good candidates for investigating influence of the length of the alkyl chain on the diameter of the PANI nanostructures by template-free method. As predicted, the PANI nanofibers were not only synthesized by template-free method in the presences of those dicarboxylic acids as the dopants, but also the diameter increasing as increase of the length of the alkyl chain [45]. The third sample is designed and synthesized a series of 4-{n-[4-(4-nitrophenylazo) phenyloxy] alkyl} aminobenzene sulfonic acid (Cn-ABSA, where $n = 2$, 4, 6, 8, or 10), as novel dopants, in which the size of the dopants can be controlled by changing the number of alkyl group ($n = 2$, 4, 6, 8 and 10) [33].

It is found that the PANI-Cn-ABSA nano-cylinders were obtained by template-free method [34]. Similarly, the diameter is also increases with increase of the number of alkyl group of Cn-ABSA [34]. Above-three samples strongly show that to change size of dopants (e.g. the length of alkyl group) is an efficient way to control the diameter of the template-free synthesized PANI nano-structures.

(2) By Changing Reaction Conditions

For a given monomer and dopant, it is found that the diameter of the conducting polymers by template-free method is affected by the reaction conditions. The reaction conditions include the concentration of dopant, monomer and oxidant, molar ratio of dopant and oxidant to monomer, redox potential of oxidants, as well
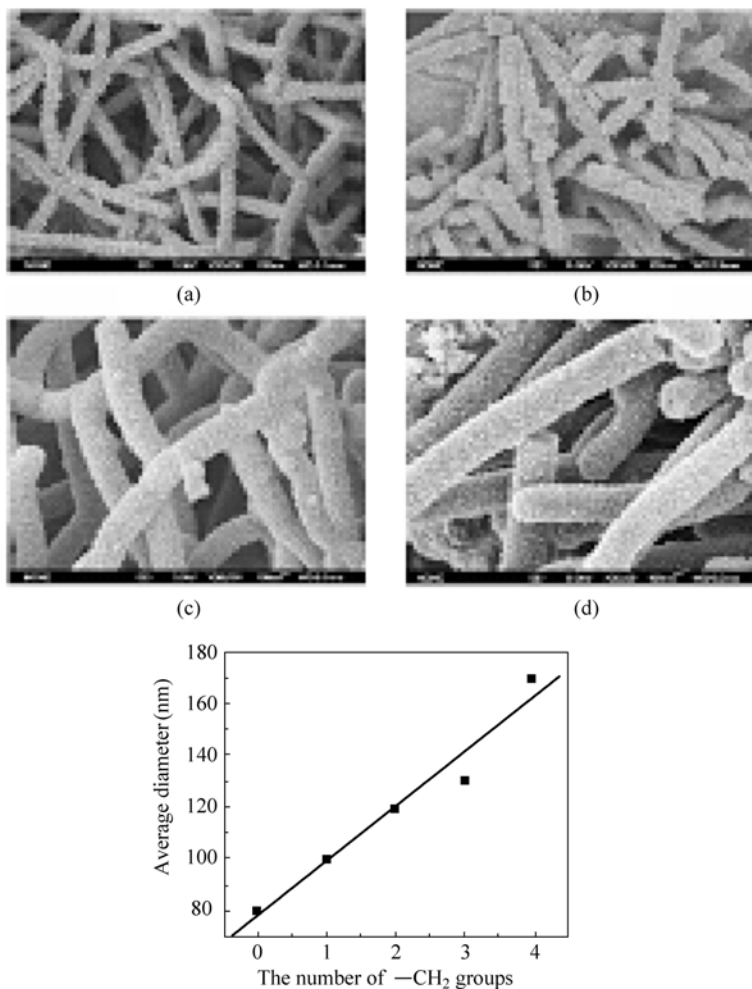
(a)   (b)

(c)   (d)

Figure 5.15   Influence of the number of —CH$_2$ group of alkyl chain of the fatty acids on morphology as well as the outer diameter of the PANI nanofibers by template-free method：(a) PANI-AA; (b) PANI-HA; (c) PANI-LA; and (d) PANI-SA [72]

as polymerization temperature and stirring fashion so on [71]. Influence of these parameters on the diameter of the template-free synthesized PANI nanostructures will be discussed, especially emphases on effect of the molar ratio of dopant to monomer on the diameter of the PANI nanostructures by template- free method.

The chiral PANI doped with *D*-CSA is a good sample to show how influence of the reaction conditions on the formation, morphology and diameter of the PANI-*D*-CSA nanostructures by template-free method [73]. When the molar ration of *D*-CSA to aniline, represented by *D*-CSA/A*n*, changed from 0.01 to 1, for instance, the formation probability of the nanotubes is enhanced from 40% to 90% [73]. When the *D*-CSA/A*n* ratio reached 2, but, granular PANI-(*D*-CSA) is

instead of the tubes. For a given D-CSA/An ratio, moreover, the concentration of D-CSA in the reaction media was also important in the formation of PANI-(D-CSA) nanotubes, showing both lower concentration (0.03 mol/L) and higher concentration (0.5 mol/L) of D-CSA are unfavorable for synthesizing PANI-(D-CSA) nanotubes. But the concentrations of D-CSA in between 0.07 and 0.2 mol/L are favorable to the formation of PANI-(D-CSA) nanotubes [73].

In particular, it is found that the diameter of the PANI nanostructures can be controlled by changing the molar ratio to aniline, as represented by [dopant]/[An]. There are three samples to show how influence of the [dopant]/[An] ratios on the diameter of the PANI nanostructures by template-free method. The first sample is the chiral PANI-D-CSA nanotubes [73] that show the diameter increases with increase of the [D-CSA]/[An] ratios. When the [D-CSA]/[An] ratio changed from 0.01 to 1, for instance, the diameter of PANI-(D-CSA) nanotubes increased from 85 to 180 nm as shown in Fig. 5.16(a). The second sample is PANI nanotubes prepared by template-free method in the presence of inorganic acids (e.g. HCl, H_2SO_4, H_3PO_4 and HBF_4) as the dopants [61]. Taking PANI-H_3PO_4 nanotube as a sample, it is found that the diameter decreases with increase of the [An]/[H_3PO_4] ratio as shown in Fig. 5.16(b). The third sample is the chiral PANI doped with $(1R)$-($-$)-10-camphorsulfonic acid (L-CSA) and $(1S)$-(+)-10- camphorsulfonic acid (D-CSA) as the chiral dopants [74]. The diameter of the chiral nanotubes doped by either L-CSA or D-CSA increases with increase of the [CSA]/[An] ratio as shown in Fig. 5.16(c). Above results suggested that the diameter of the PANI nanostructures generally increases with increase of the [dopant]/[An] ratios, indicating change of the [dopant]/[monomer] ratios is an efficient approach to control the diameter of the conducting polymer nanostructures prepared by template-free method. According to micelle model proposed by author [19], the diameter of the micelles formed in the reaction is dominated by the dopant structure and the molar ratio of the dopant to monomer. For a given dopant, the diameter of the micelles is obviously increasing as increase of the [dopant]/[monomer] ratios. That is why the diameter can be adjusted by changing the molar ratio of dopant to monomer when the dopant structure is fixed.

(3) By Changing Redox Potential of Oxidants

Although above results suggest that the diameter of the PANI nanostructures prepared by template-free method can be adjusted by the polymer and dopant structure as well as the polymerization conditions, particularly the molar ratio of dopant to monomer [33, 34, 61], simple and quantitative approach to prepare nanostructured conducting polymers with well-controlled diameters via a soft-template method is necessary. As mentioned in Chapter 2, the molecular structure of PANI is complex, which composes of alternated reduced (—B—NH—B—NH—) and oxidized (—B—N Q N—) repeated units where B and Q denote C_6H_4 rings in the benzenoid and quinoid states, respectively [75]. The terms of "leucoemeraldine", "emeraldine" and "pernigraniline" refer to the
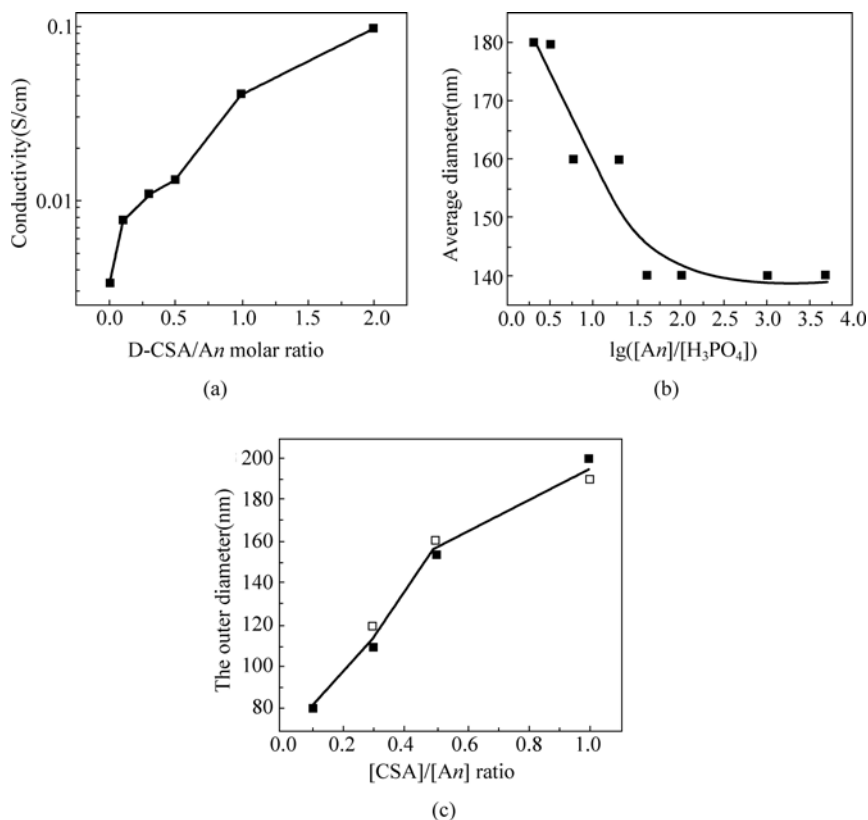
(a)

(b)

(c)

Figure 5.16   Influence of the molar ratio of dopant to aniline on the diameter of the PANI nanostructures prepared by template-free method: PANI-*D*-CSA nanotubes (a) [73], PANI-H_3PO_4 nanotubes (b) [61] and PANI-(*L*-CSA) and PANI-(*D*-CSA) nanotube (c) [74]

different oxidation state of PANI [76]. Thus, the redox potential of oxidants has an important role in controlling the structure and physical properties of PANI.

Usually, PANI is polymerized in a strong acidic medium by using APS as the oxidant [22]. Based on previous proposed micelle formation mechanism proposed by author [19], moreover, it is expected that the redox potential will affect the morphology and size of the micelles as the soft-templates, resulting in changing the morphology and size of the nanostructures. In addition, the diameter of the template-free synthesized nanostructures by using APS as the oxidant is in the range of 150 – 200 nm, which is not in the nano-scaled (1 – 100 nm) [75]. These promised author to template-free synthesize micro/nanostructured PANI by using another oxidant instead of APS. Interestingly, the self-assembled PANI nanofibers with 17 – 30 nm in average diameter were successfully prepared by using ferric chloride ($FeCl_3 \cdot 6H_2O$) as an oxidant in the presence of *p*-toluenesulfonic acid (*p*-TSA), β-NSA, and CSA as the dopant [75] as shown in Fig. 5.17. The diameter

of nanofibers oxidized by $FeCl_3 \cdot 6H_2O$ as the oxidant is reduced by 10 times compared with that of the nanotubes oxidized by APS [75]. The conductivity of the nanofibers oxidized by $FeCl_3 \cdot 6H_2O$ is also larger approximately ten times as compared with that of PANI nanofibers oxidized by APS [75].
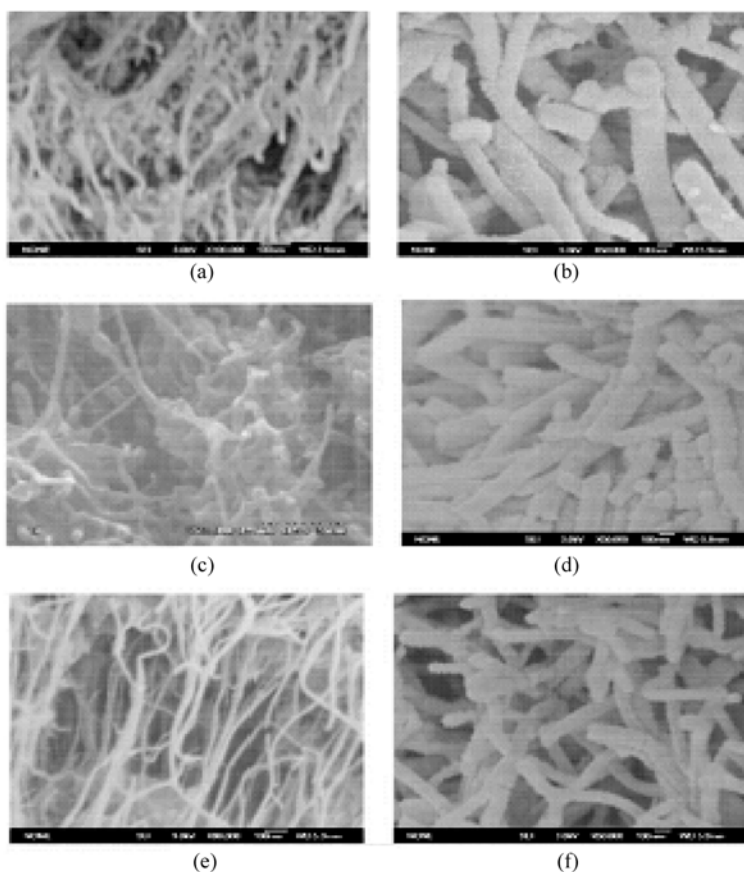

Figure 5.17 SEM images of the PANI nanofibers doped with different sulfonic acids: (a, b) CSA, (c, d) β-NSA, and (e, f) p-TSA oxidized by $FeCl_3$ (a, c, e) [75]

These results show a size effect on the conductivity, which means the conductivity increases with decrease of the diameter observed by Martin et al. [77] and our studies on the conductivity of a single nanotube or fiber, as measured by four-probe method [78]. Moreover, it is found that FTIR spectra of the PANI nanofibers oxidized by either APS or $FeCl_3$ are in good agreement with the emeraldine salt form of PANI [79], indicating the redox potential of the oxidants un-affect the main polymeric structures. However, the crystalline of the nanofiber oxidized by $FeCl_3$ is higher than that of the nanotubes oxidized by APS [75], as

measured by XRD. The XRD pattern of CSA, β-NSA, and *p*-TSA doped PANI nanofibers oxidized by FeCl$_3$, for instance, show some sharp peaks at $2\theta = 8.98°$, 14.78°, 20.48°, 25.8°, and 26.78°, which are in the monoclinic space group P21 [80]. On the other hand, the XRD of the PANI-*p*-TSA nanofibers oxidized by APS only have two peaks centered at $2\theta = 20.18°$ and 25.28°, showing amourphous which is in agreement with our previous results [61]. The higher crystalline might be another reason for the conductivity of the nanofibers oxidized by FeCl$_3$ larger than that of the nanotubes oxidized by APS.

According to micelle model proposed by author [19], it is reasonable to accept that micelles composed of dopant and aniline, formed in the reaction due to hydrophilic —SO$_3$H group of the dopants are served as the soft-templates in the formation of the nanofibers. Since the redox potential of FeCl$_3$ (0.77) is lower than that of APS (2.0) [81], the accretion [82] or elongation process [83] process for the PANI nanofibers oxidized by FeCl$_3$ might be much slower compared with that of the PANI nanofibers oxidized by APS, resulting in the diameter of the nanofibers oxidized by FeCl$_3$ being smaller than that of the nanofibers oxidized by APS [75]. Highlight of above-described results is found that the oxidant with a low redox potential might be an efficient way to reduce and control the diameter of the diameter of the conducting polymer nanostructures by template-free method.

So far, APS [84], tetrabutylammonium persulfate (TBAP) [85], hydrogen peroxide benzoy [86], peroxide [87], ferric chloride [88] and chloroaurate acid [89] have been used to synthesize PANI as the oxidants. Previously reported results mainly emphasize the effect of oxidants on the polymerization yield, and APS is regarded as the optimal oxidant for PANI because of its high yield [90].

However, the effect of the oxidant on the size of the PANI nanostructures has seldom been reported. As APS used as the oxidant, moreover, it is found that the pH value in the reaction solution decreases with increase of the polymerization time, indicating the protons are formed due to oxidation polymerization of aniline with APS [91]. This finding suggests template-free method created [11] might simplify by omitting acids as the dopants. These thought promised author to try synthesize PANI nanotubes by template-free method in the absent of acids as the dopants, which was called as simplified template-free method (STFM). As predicted, the PANI nanofibers were successfully prepared by using STFM through chemically oxidative polymerization in the presence of APS, Ce (SO$_4$)$_2$, FeCl$_3$, Fe$_2$ (SO$_4$)$_3$, and CuCl$_2$ as the oxidants [92]. Typical SEM images of these nanofibers are shown in Fig. 5.18. In this approach, the oxidant serves as both oxidant and dopant at the same time because of protons (H$^+$) generated during the polymerization that was supported by following two evidences: ① The pH value in the reaction solution decreases with decrease of the polymerization, indicating the protons are produced during polymerization. ② Structural characterization of the resultant nanofibers, as measured by FTIR, UV-visible and XPS spectra and conductivity measured by four-probe method, are identical to the emeraldine salt
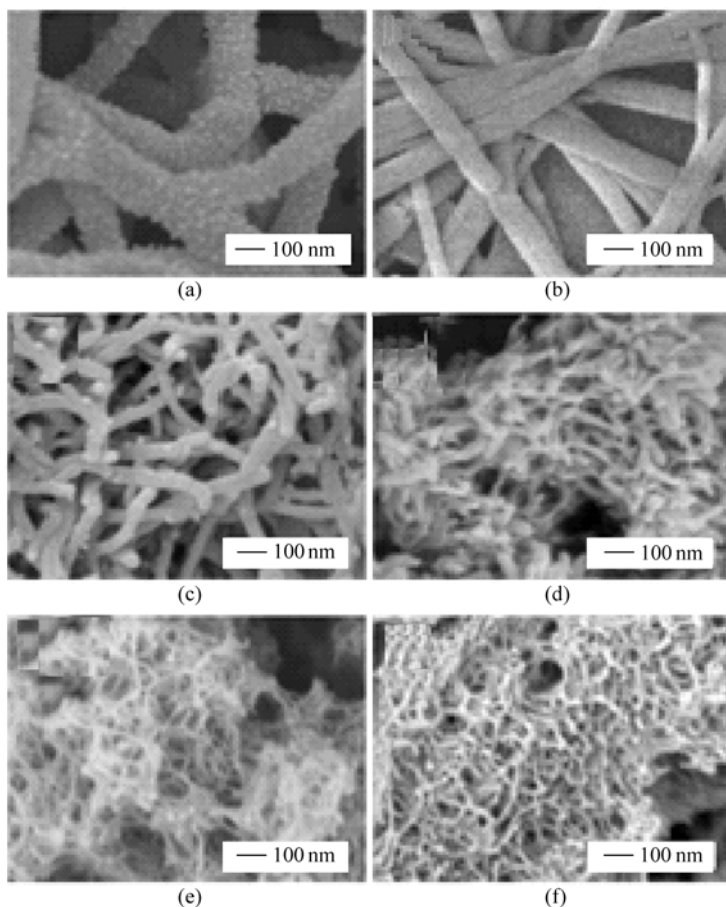
Figure 5.18 SEM images of the PANI nanofibers prepared by using the DFTFM in the presence of different oxidants through chemically oxidative polymerization: (a) APS; (b) H_2O_2; (c) $Ce(SO_4)_2$; (d) $FeCl_3$; (e) $Fe_2(SO_4)_3$; (f) $CuCl_2$ [92]

form (i.e. conducting state) [92], further proving the PANI has been doped by protons. In particular, it is found that the diameter of the nanofibers decreases with decrease of the redox potential of the oxidants used, for instance, the average outer diameter decreased from ca. 130 nm at a redox potential of $E_{ox} = 2.05$ V (i.e., APS) to ca. 12 nm at $E_{ox} = 0.56$ V (i.e., $CuCl_2$). In particular, there is a well-fitting linear correlation between the standard redox potential of the oxidants and the logarithm of the average outer diameter, as shown in Fig. 5.19 (solid squares) [92], which can be expressed as

$$\lg d = 0.69 + 0.71 \, E_{ox} \tag{5.1}$$

where d is the average outer diameter of the nanofibers and E_{ox} is the standard redox potential of the oxidants.
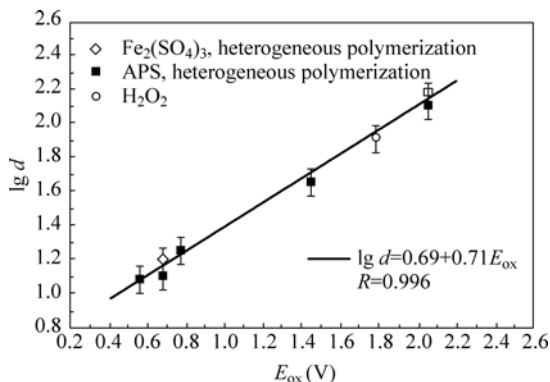
Figure 5.19   The diameter of the PANI nanofibers prepared by DFIFM through chemically oxidation polymerization as a function of the redox potential of the oxidants used [92]

The Equation (5.1) indicates that a well-controlled diameter of the PANI nanofibers can be realized by only changing the redox potential of the oxidants used. Universality of above equation has been further demonstrated by following evidences: ① The PANI oxidized by H_2O_2 as the dopant is not only fibrous in morphology, but also its diameter of about 90 nm, as measured by SEM, is good agreement with the 87 nm calculated from equation. ② The nanofibers oxidized using APS as the oxidant by interfacial polymerization in the absent of acids as the dopants were also obtained and their diameter, as measured by SEM, was estimated to be about ca. 150 nm for APS (Fig. 5.19, open square), which are also fitted the formula. ③ In particular, all diameters of the PANI nanofibers prepared by using the template-free method with various organic functionalized acids as the dopants [75], for instance, $17-30$ nm for $FeCl_3$ and ca. 150 nm for APS as the oxidant, are in good agreement with the equation. Based on the equation, a well-controlled diameter of the PANI nanofibers is able to be obtained by only changing the redox potential of the oxidant used, but also predicting the size range in advance. Highlight of this work is that the method not only provides a quantitative way of controlling the diameter of the PANI nanofibers, but also simplifies the reagents.

In principle, the aniline monomer can be regarded as an amphiphilic molecule because of its hydrophobic benzene ring and hydrophilic —NH_2 group. As a result, micelles composed of aniline monomers are expected to exist in either homogeneous or heterogeneous polymerization. The micelles can serve as soft templates in the formation of PANI nanofibers prepared by using the STFM. Once the oxidant is added, the polymerization takes place at the micelle/water interface because of hydrophilic oxidants [93] and the growth of the nanofibers is controlled through polymerization and elongation process [94]. Since the amount of aniline in this study was kept a constant, whereas the oxidant/aniline ratios were changed according to the redox potential of the oxidants. Based on the

standard redox potential of the selected oxidants [95], the optimum molar the oxidant/aniline ratio was established to be 1:1, 2:1, 3:1, 4:1, and 6:1 for APS/An, Ce(SO$_4$)$_2$/An, FeCl$_3$/An, Fe$_2$(SO$_4$)$_3$/An, and CuCl$_2$/An, respectively [95]. Thereby the size of the micelles (the soft templates) is expected to be constant, in other words, it is independent of the redox potential of the oxidants. However, the redox potential of the oxidants will affect the polymerization or elongation process, which controls the growth of the nanofibers. This means that higher redox potential leads to higher polymerization or elongation rate, resulting in a larger diameter of the nanofibers for a given polymerization time. This might be why the diameter increased with increasing redox potential of the oxidants [92]. The results suggest that the standard potential of the oxidant is a key parameter in controlling the diameter of PANI nanofibers.

In summary, although template-free method is without using membrane as the template, the formation yield, morphology and diameter of the resultant PANI micro/nanostructures could be controlled by changing dopant structure and reaction conditions. In particular, it is found that well-controlling diameter of PANI nanofibers can be synthesized by adjusting redox potential of the oxidants.

5.1.4 Self-Assembly Mechanism of Micro/Nanostructures by A Template-Free Method

It is well known that the growth of the hard-template synthesized nanostructures is guided by the membrane as the hard-template. When template-free method is employed to prepare nanostructures of the conducting polymers, on the other hand, formation and growth of the nanostructures is a self-assembly process because of omitting hard-template. Molecular interactions, such as hydrogen bonds, Van der Waals forces, $\pi - \pi$ stacked interaction, are usually served as powerful driving forces for self-assembly of the nanostructures in the absence of hard-template [96].

Moreover, an iterm of "soft-template" is often employed to interpret the formation of the nanostructures prepared by a self-assembly process. The "soft-template" includes surfactants, colloidal particles, structure-directing molecules, oligomers, "soup bubbles", porous and copolymers as well as phospholipid tubules have been discussed in Chapter 4 in detail. Author proposed that a micelle formed in the reaction solution is served as a "soft-template" in the formation of the micro/nanostructures of conducting polymers by template-free method [19], which is called as a "micelle model". The micelle model is based on two facts: ① Surfactant is a common "soft-template" because it is easy to form thermodynamically stable and controllable nano-scale dimensions in solution or at interfaces. As mentioned in Chapter 4, the equilibrium size and shape of surfactant aggregates are controlled by a formula of $\dfrac{V_0}{al_0}$ [97], where V_0

and l_0 are the volume and length of the surfactant tail within the hydrophobic core of the aggregate and a is the effective area occupied by each surfactant head group at the surface of the aggregate. Moreover, the favored aggregate morphology of the surfactant in solution, such as spherical, cylindrical, or a flat bi-layer, is formed depending on the value of α [97]. ② The reagents in a chemical synthesis of PANI or PPy generally include monomer, dopant and oxidant. In principle, micelles in aqueous solution can be formed by dopant, dopant/monomer salt or super-molecule and monomer itself due to hydrophilic dopant (—SO$_3$H group) and dopant/monomer salt or amphiphilic molecule of monomer (e.g. aniline). Once the micelle model is employed, one should be considered as follows: ① It is expected that formation, morphology and diameter of those micelles are affected by structure of dopant, monomer and oxidant as well as reaction conditions including the concentration of the reagents, molar ratio of dopant and oxidant to monomer, reaction temperature and polymerization time even stirring fashion, leading to influence of above parameters on morphology and diameter of the resultant nanostructures. ② The micelles formed by dopant, dopant/monomer salt or super-molecule and monomer itself might co-exist in the reaction solution, depending on the reaction conditions. As a result, competition between those micelles, which is driven by the reaction conditions, might result in variation of morphology and diameter of the template-free synthesized nanostructures with polymerization process and reaction conditions. ③ Coordination effect of those micelles with above-mentioned molecular interactions as the driving forces for self-assembly process should be considered that maybe resulting in formation of complex 3D-microstructures assembled from 1D-nanostructures. The concept and intrinsic of the micelle model, formation mechanism and self-assembly process of various micro/nanostructures of the conducting polymers prepared by template-free method are discussed one by one.

1. Micelle as A "Soft-Template"

In general, spherical micelles are formed at the initial stage due to the low surface energy. These spherical micelles can be aggregated to form cylindrical or flat bi-layer [97], depending on the reaction conditions. At the same time, monomer can be also diffused into those spheric and cylindrical or junction micelles to form monomer filled micelles. These micelles with or without monomer are reserved as the "soft-templates" in forming micro/nanostructures prepared by template-free method. Once oxidant is added, polymerization only takes place at water/micelle interface because of hydrophilic oxidant. Growth of the micro / nanostructures is controlled by accretion [82] and elongation process [98]. As above-mentioned, the reaction system is complex including micelles formed by dopant, dopant/monomer salt or super-molecule and monomer itself, competition between these micelles and molecular interactions (e.g. hydrogen bonds, $\pi-\pi$ staked and hydrophobic interactions) that will result in various micro/nanostructures, such as hollow spheres, nanotubes or nanofibers, nanotube or nanofiber junctions

even 3D hollow spheres self-assembled from 1D-nanofibers. The scheme of self-assembly process of the micro/nanostructures prepared by template-free method is proposed based on above-described micelles as the "soft-templates" as shown in Fig. 5.20. Now it is necessary to provide authority of the micelles formed in the solution of PANI or PPy when template-free method is used. There are three positive evidences for supporting existence of the micelles: ① When PANI-β-NSA nanotubes were synthesized by template-free method, it is demonstrated that exsistance of micelles in reaction solution by dynamic light scattering (DLS), showing the average diameters of the micelles is ca. 89.2, 53.4, and 16.7 nm at [NSA]/[An] rato of 1, 0.5, and 0.25 [19], respectively. A comparison of diameter as a function of [NSA]/[An] ratios between nanotubes and micelles are given in Fig. 5.21. It shows the diameter of both nanotubes and micelles increases with increase of the [NSA]/[An] ratios, however, the average diameter of the micelles is smaller than the outer diameter and bigger than the inner diameter of the nanotubes/nanofibers as-synthesized at different ratios of [NSA]/[An], indicating the micelles existing in the reaction solution [19]. ② In general, the micelle size can be adjusted by changing the ionic strength of solution or the polarity of the solvent [99]. It is noted that the diameter of PANI-β-NSA synthesized at [NSA]/[An] of 0.5 increased from 92 to 148 nm when 0.1 mol/L KCl aqueous solution was added as the solvent. Similarly, the diameter of the nanotubes synthesized at [NSA]/[An] of 0.5 enhanced the diameter from 92 to 165 nm when a mixed solvent (alcohol/water = 1:4 in volume) was used [19], further proving the micelles are formed in the reaction solution. ③ Usually the cylindrical micelles with and without monomer are regarded as the "soft-templates" in the formation of the nanotubes or nanofibers by template-free method that were supported by two evidences: one was the static and dynamic light scattering measurements on the template-free synthesized PPy nanofibers doped with p-hydroxyl-azobenzene sulfonic acid (p-OH-ABSA) as a dopant [100], which showed the hydrodynamic radius, R_h, and the radius of gyration, R_g, were
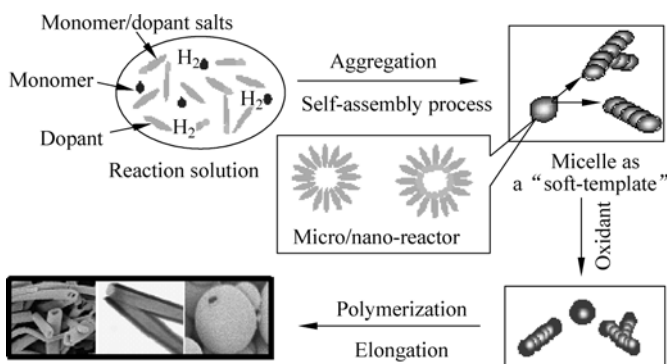

Figure 5.20   Scheme of self-assembly process proposed based on micelles as the "soft-templates" in forming micro/nanostructures prepared by template-free method
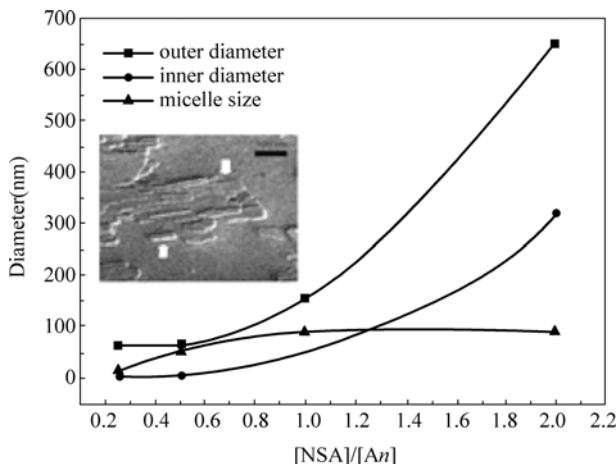
Figure 5.21   Comparison of diameter as a function of [NSA]/[An] ratios between nanotubes and micelles [19], and the inset is freeze-fracture transmission electronic microscopy (FFTEM) image of PPy/p-OH-ABSA mixture [100]

calculated to be 22.7 and 42.4 nm, respectively. Thereby the ratio of R_g to R_h was about 1.9 which is in agreement with the model of flexible cylindrical micelles [101]. Another was the cylindrical shape of the micelles are directly measured by freeze-fracture transmission electronic microscopy (FFTEM) image [100] as shown in Fig. 5.21. Up to date, self-assembly mechanism of various micro/nanostructures prepared by template-free method can be explanation based on above-described micelle model [19].

2. Intrinsic of The Micelles as The "Soft-Templates"

In principle, as above-mentioned, micelle formed by dopant, dopant/monomer salt and monomer itself can be form in the reaction solution. However, their formation is affected by the reaction conditions. In other words, intrinsic of the micelles formed in the reaction solution is different, depending on the reaction conditions that include nature of dopant, monomer and oxidant, the concentration of dopant, monomer and oxidant, the molar ratio of dopant and oxidant to monomer, polymerization temperature and time even stirring fashion. One should therefore understand intrinsic of the micelles formed in the reaction solution in order to rightly interpret the self-assembly mechanism of the micro/nanostructures by using the micelle as the "soft-template". Analysis of intrinsic of different micelles is discussed as follows:

(1) Micelle Formed by Sulfonated Acids

Typical sample that micelles composed of dopant serves as a soft-template in forming conducting polymer nanostructure by template-free method is the template-free synthesized PANI-β-NSA nanotubes due to hydrophilic group of —SO$_3$H and lipophilic group is —C$_{10}$H$_7$ of β-NSA. At the same time, aniline monomer can diffuse into these micelles to form aniline filled micelles. Both

micelles with or without aniline monomer are served as the "soft-templates", resulting in formation of the nanotubes or nanofibers, depending on the molar ratio of β-NSA to aniline (represented as [NSA]/[An] ratio). This is consistent with observations from PANI-β-NSA nanostructures prepared by template-free method [19].

(2) Micelle Composed of Dopant/Monomer Salt

In fact, dopant/monomer salt is easily formed in the reaction through an acid/base reaction due to basic monomer and acidic dopant. Thereby the dopant/monomer salt can be also served as the "soft" or "hard" templates. However, the "hard" template is usually formed at a high [dopant]/[monomer] ratios, for instance, the [NSA]/[An] salt is served as "hard-template" in the formation of PANI-β-NSA microtubes at [NSA]/[An] ratios of 2.0 [102]. There are two supporting evidences: ① As measured by SEM, the aniline salt is needle-like in shape whereas the PANI-β-NSA is tubular morphology in shape as shown in Fig. 5.22, indicating there is somewhat similarity in morphology between the [NSA]/[An] salt and the PANI-β-NSA tubes. ② As measured by XRD, all shape peaks observed from XRD of the aniline salt could be found in the microtubes except for a shape peak assigned as the repeat unit of polyemeraldine chain [103]. Same results from PANI-β-NSA nanotubes prepared at a low temperature ($-10℃$) by template-free method was also observed [19] as shown in Fig. 5.22. These results indicated either XRD of the PANI-β-NSA microtubes prepared at a high [NSA]/[An] ratio [102] or the PANI-β-NSA nanotubes prepared at a low temperature ($-10℃$) [19] covers the characteristic peaks of the aniline salt, proving the aniline salt exists in the micro/nanostructures. ③ Based on above evidences and the proton doping taking only place on the imine segment of the polyemeraldine chine [104], a model assumed a tight interconnect of polymer chain in the microtubes was proposed based on the aniline salt as the template. The calculated values based on the model
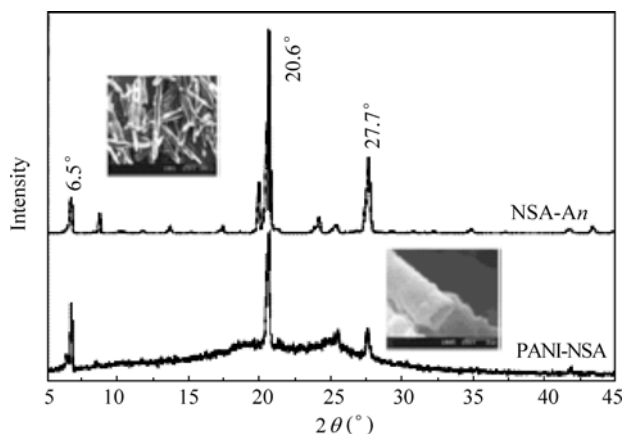

Figure 5.22 SEM images and XRD patterns of β-NSA/An salt and PANI-β-NSA microtubes prepared by template-free method at [NSA]/[An] at 2 [102]

are in agreement with that of dates measured by XRD [102]. Above-described results indicate that dopant/monomer salt or super-molecule could be served as a "hard-template" to prepare micro/nanotubes of the conducting polymers by template-free method.

On the other hand, sometimes aniline salt can be also served as a "soft-template" in forming PANI-β-NSA nanotubes at a low [dopant]/[aniline] ratios. As above-mentioned, a typical sample is PANI-β-NSA nanotubes prepared at a low temperature ($-10\,^{\circ}\!\mathrm{C}$) and a low [$p$-NSA]/[A$n$] ratio [65]. These results indicated that aniline salt can be served as either "hard-template" or "soft-template", depending upon the ratio of dopant to aniline. When the ratio is high, in general, the aniline salt is served as a hart-template, whereas it is regarded as a soft-template when a low ratio of dopant to anilie is used.

(3) Micelles Formed by Anilinium Cation

As above-mentioned, the PANI nanotubes can be also prepared by template-free method in the presence of inorganic acids (e.g. HCl, H_2SO_4 and H_3PO_4) as the dopants [61]. Since those dopants without surfactant function, there are no long micelles composted of surfactants. Therefore to examine whether the surfactant is the prerequisite to form self-assembled PANI nanostructures by template-free method was very important. In order to do so, the influence of the surfactant structure and concentration on the morphology of the PANI nanostructures prepared by template-free method in the presence of inorganic acids was studied [61]. When sodium dodecylbenzenesulfonate (SDBS) was used as the surfactant, it showed that surfactant function of the dopant is not the prerequisite for the formation of self-assembled PANI nanostructures by template-free method, however, addition of the surfactant and its concentration affect the diameter of PANI nanostructures [61].

In fact, aniline may exist in the form of anilinium cations or free aniline in the reaction solution. Spherical micelles composed of anilinium cations may be formed as the soft-templates [105]. Anilinium cations can be absorbed in the micelle/water interface to form micelle (represented by A), or a part of free aniline diffuses into micelles to form micelle (represented by B) [106]. Micelles A and B are assumed as the "soft-templates" to form PANI nanostructures in the presence of a surfactant. On the other hand, it is expected that micelles formed by anilinium cations, which are represnted by C and D, might be the "soft-templates" to form PANI nanostructures in the absence of a surfactant. The reaction takes place mainly in the micelle/water interface adjacent to the surfactant head-groups because hydrated APS molecules cannot penetrate into the micelle surface [107]. With the polymerization proceeding, the micelles become big spheres through accretion [82] or tubes/rods through elongation [98], depending on the local conditions. The size of the micelles may greatly affect the size of the resulting nanostructures; therefore, PANI nanotubes or nanofibers doped with different inorganic acids have different diameters [61]. The results are reasonable to

conclude that the PANI nanostructures can be synthesized by a template-free method in the presence of inorganic dopants without surfactant function, because the micelles formed by anilinium cation are served as the "soft-templates". However, the diameter of the resultant nanostructures could be adjusted by changing nature and concentration of the added surfactants.

(4) Aniline Droplet as A "Soft-Template"

It has been mentioned that morphology change from nanotubes to nanotubes and hollow microspheres coexisted in the PANI-β-NSA prepared at a low temperature ($-10\,^{\circ}\text{C}$) by template-free method when the molar ratio of NSA to aniline is increased [65]. Obviously, the formation of the hollow spheres and nanotubes results from different micelle as the "soft-template". For instance formation of the hollow microspheres of PANI-β-NSA prepared at a high [NSA]/[An] ratio (e.g. 2:1 or 4:1) [65] are interpreted by an aniline droplet serving as a "soft-template", which is also a typical sample to show aniline droplets acting as the soft-templates in the formation of the micro/nanostructures of the conducting polymers by template-free method. In case of a high [NSA]/[An] ratios (e.g. 2:1 or 4:1) and a low temperature ($-10\,^{\circ}\text{C}$), NSA and its anilinium salt is expected to form two kinds of particles in the emulsion: micelles and aniline droplets [65]. Because NSA is acidic and aniline basic, it is therefore reasonable to understand that the micelle was composed of NSA/anilinium salt while the aniline droplets in the emulsion was composed of free aniline and NSA/aniline salt, which act as the core and the shell respectively. Because the oxidant APS is water soluble, it is almost impossible for it to diffuse into the droplets to oxidize the aniline [107].

Therefore, when APS was added, the polymerization would proceed on the surface of micelles and droplets respectively. Because the polymerization was carried out at $-10\,^{\circ}\text{C}$, the micelles and droplets were confined in ice. The reaction proceeded on the surfaces of the aniline droplets and micelles, respectively, producing hollow microspheres and nanotubes simultaneously. According to the SEM observations, the inner surface of the hollow spheres is smoother than that of the outer surface, which indicates the oxidation reaction occurred on the side of water phase of aniline/water interface of the droplets, further proposing that aniline droplets play a "soft-template" in the formation of PANI-β-NSA microspheres by template-free method [65].

In summary, micelle model proposed by author [19] can interpret the formation of various micro/nanostructures of the conducting polymers prepared by template-free method. Once the model is used, influence of the reaction conditions on formation and morphology of the micelles, competition of different micelles and coordination effect of the micelles with molecular interactions including hydrogen bands, $\pi-\pi$ staked, Van der Waals force, and hydrophobic interactions should be considered. In particular, cooperative of micelles as the "soft-templates" with above-described molecular interactions provides a facile and efficient approach

to prepare 3D-microstructures self-assembled 1D-nanostructures of the conducting polymers. On the contrary, hard-template method can't prepare such completed 3D-micro/nanostructures because morphology of the pores in membrane is limited. The concept and intrinsic of the micelles serving as the soft-templates in the formation of template-free synthesized conducting polymer nanostructures will be further understood through following discussions on multi-functional nanostructures synthesized by template-free method associated with other approaches and 3D-nanostructures assembled from 1D-nanostructures.

5.2   Multi-Functionality of Micro/Nanostructures Based on Template-Free Method

Nowadays multi-functionalized micro/nanostructures of conducting polymers have received great attention because of their unique properties and technological applications in electrical, optical, and magnetic materials and devices [71, 108]. Design and synthesis of multi-functionalized nanostructures of conducting polymers are necessary for realizing their practice applications in nano-devices. Compared with hard-template method, multi-functional micro/nanostructures are easier to be prepared via a self-assembly process.

   As above-mentioned, the intrinsic of template free method is self-assembly process because of the micelles composed of dopant or dopant/monomer salt even monomer itself serving as the templates in the formation of the micro- or nanostructures. This suggests that it is possible to synthesize or prepare multi-functional micro/nanostructures of conducting polymers by template-free method associated with other approaches. So far, author successfully prepared a variality of multi-functionalized composite micro/nanostructures of conducting polymers such as soluble composite nanotubes, carbon nanotube-conducting polymer composite nanostructures, electro-magnetic, electro-optic and electro-superhydrophobic composite micro/nanostructures, by template-free method associated other approaches. Synthesis method, morphology, formation mechanism, structure characteristic, and physical properties of these multi-functional micro/nanostructures of the conducting polymers are discussed one by one.

5.2.1   Processing Composite Nanostructures

As above-mentioned, the PANI-β-NSA nanotubes are slightly dissolved in some organic solvent (e.g. *m*-cresol) [11]. However, the novel tubular morphology disappears after dissolving, limiting their application in technology. Up to date, various methods such as covalent substitution [109], doping with functional acids [110] and blending with soluble polymers [111] have been developed for

improving the processability of PANI prepared by conventional method. However, those methods are difficult to directly synthesize soluble nanostructures of conducting polymers of PANI.

Obviously pre-synthesized nanostructures prepared by either hard or soft-template method blend with soluble polymers might be a suitable approach for improving the processability of the conducting polymer nanostructures. Based on above idea, free standing composite films of the PANI-β-NSA nanotubes blended with water-soluble poly (vinyl alcohol) (PVA) as a matrix were prepared [112]. As shown in Fig. 5.23(a) the uniform composite film containing 16% of PANI-β-NSA
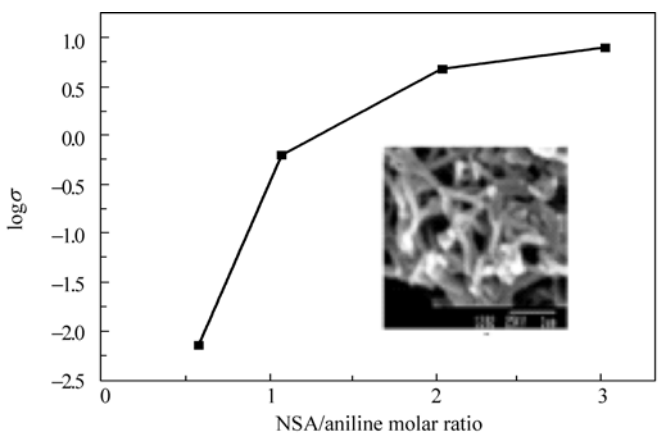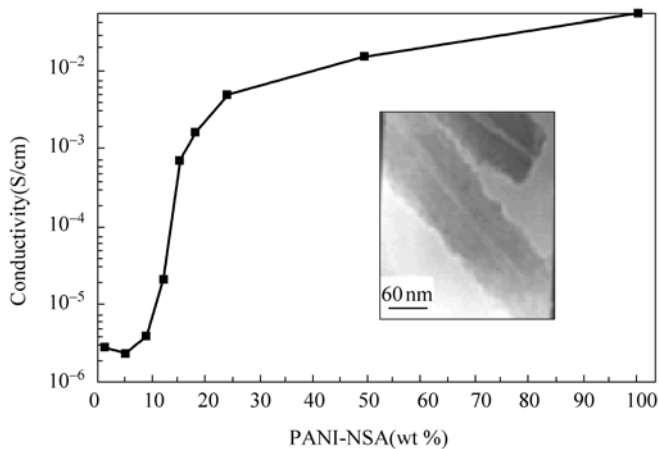
Figure 5.23 Room temperature conductivity of PANI-β-NSA nanostructures as a function of β-NSA/aniline ratio (a) and PANI-β-NSA/PVA composite films as a function of the content of the PANI-β-NSA nanotubes (b), and the inset is SEM and TEM images of the PANI-β-NSA/PVA composite nanotubes (b) [112]

nanotubes, which has a conductivity of 10^{-2} S/cm, a tensile strength of 603 kg/cm^2, a tensile modulus of 4.36×10^5 kg/cm^2 and an ultimate elongation of about 80%, has been obtained [112]. It is found that the conductivity of the PANI-β-NSA/PVC composite nanotubes is enhanced by increasing the content of PANI-β-NSA nanotubes in the composites as shown in Fig. 5.23 that is contributed to the conductive PANI-β-NSA nanotubes.

5.2.2   PPy-CNT Composite Nanostructures

Carbon nanotubes [113] and its bulk synthesis [114] have been stimulated for their potential applications in nano-scale devices and materials [115], field emission [116] and scanning probe microscopy [117]. Various approaches have been developed for opening up [118], the CNT ends and encapsulating material [118, 119] to form a nanocomposite, which might be used in catalyst, separation, and storage technology and in the development of materials with new magnetic and electrical properties [120].

As mentioned in Chapter 1, conducting polymers not only have semiconductor and metal behaviors, but also retaining characteristics of conventional polymers. Combination of conducting polymers with CNTs therefore opens a new way to prepare new type of functional nanomaterials which have features of either conducting polymers and CNTs. Author [121] successfully synthesized PPy coated CNTs by *in-situ* doping polymerization in the CNTs as the hard-templates. Typical SEM and TEM images of PPy-CNT composite nanotubes are shown in Fig. 5.24. The structural characterizations, as measured by elemental analysis, X-ray photoelectron spectroscopy (XPS), Raman spectra, and X-ray diffraction, showed there is no chemical reaction between CNTs and PPy taking place; indicating the CNTs only serve as the templates in the polymerization of PPy. However, the electrical, magnetic, and thermal properties of the CNTs are modified by PPy [121].
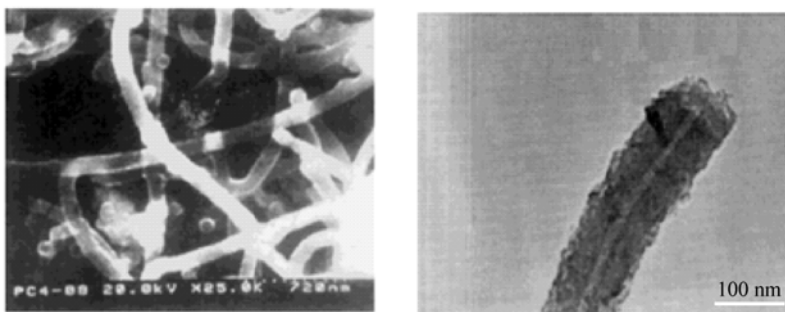

Figure 5.24   Typical SEM and TEM images of PPy-CNT composite nanotubes [121]

As described in Chapter 1, the delocalization of π-electrons is a major contributor to the third-order optical susceptibility [122]. Similar to fullerenes (C_{60}), a CNT also possesses a highly delocalized π-conjugated electron system that results in fast nonlinear optical response due to the large polarizability arising from the $\pi - \pi^*$ virtual transitions [123]. The nonlinear optical properties of the C_{60} have been intensively studied [124]. However, few papers dealing with nonlinear optical properties of CNTs were reported [125] due to their poor solubility in solution. During investigation of PPy-CNTs nanotubes, by chance, author found the solubility of CNTs in solution can be enhanced by using a mixing PPy and m-cresol with ethanol as the solvent. The new finding promised author to cooperate with Prof. Peixiang Ye, Institute of Physics, Chinese Academy of Sciences to directly measure the nonlinear optical properties of CNTs. The third nonlinear optical properties of CNTs were measured by DFWM method at $\lambda = 1064$ and 532 nm using a light source of Nd: YAG laser with a 30 ps wide single pulse output or Nd: YAG laser with an 8 ns wide, respectively [123]. Usually it is impossible to calculate the third-order optical nonlinearity of a single nanotube because of unknown the exact number of CNTs solved in solution. However, the average contribution of one carbon atom to the third-order optical nonlinearity can be evaluated by the mass of CNTs dissolved in the solution. By using this method, the third-order nonlinearity ($\chi^{(3)}$) of one carbon atom in CNTs was calculated, for the first time, to be 5.921×10^{-36} esu at $\lambda = 1064$ nm, while for C_{60} whose is about 3.000×10^{-34} esu at $\lambda = 1064$ nm [126], indicating the contribution of one carbon atom in the CNTs is higher than that in the C_{60} [123].

5.2.3 Electro-Magnetic Functional Micro/Nanostructures

Among those multi-functionalized micro/nanostructures, electro-magnetic functionalized micro/nanostructures of conducting polymers are of special interesting due to their potential applications in EMI shielding and microwave absorbing materials [127]. Although a series of PANI and PPy composites containing nano-magnets have been reported [128], few papers of the electromagnetic functional micro/nanostructures of conducting polymers are seldom reported. Author was done a lot of workers on the electromagnetic functionalized nanostructures of PANI and PPy by template-free method associated with different approaches. Synthesis methods, effect of the main parameters, such as molecular structure of conducting polymer, nature of dopant and magnet as well as the content of the magnetic nano-particles in composites on the electro-magnetic properties of the composite micro/nanostructures are discussed as below.

1. PANI-β-NSA/Fe₃O₄ Nanotubes or Nanofibers

Since the β-NSA dopant has surfactant function due to its hydrophilic —SO_3H

group attached to the naphthalene ring [11], micelles containing magnet nano-particles, formed by β-NSA, might be regarded as soft-templates in the formation of electromagnetic functionalized PANI nanostructures according to self-assembly mechanism of the nanostructures prepared by template-free method [19]. Therefore, author tried to prepare electromagnetic functional PANI-β-NSA nanostructures by template-free method associated with magnetic Fe_3O_4 nano-particles (~ 10 nm in diameter) as the additives. It is found that PANI-β-NSA /Fe_3O_4 nanofibers or nanotubes with a diameter of 80 – 100nm were successfully synthesized [129]. Figure 5.25 shows typical SEM and TEM images of Fe_3O_4, PANI-β-NSA nanotubes and PANI-β-NSA/Fe_3O_4 composites.
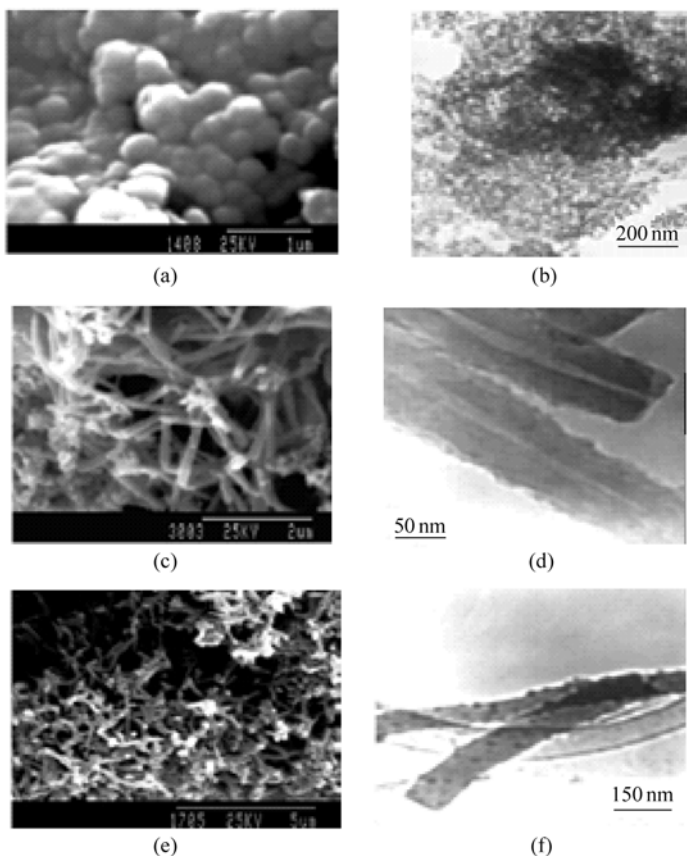

Figure 5.25   SEM and TEM images of Fe_3O_4 (a, b), PANI-β-NSA nanotubes (c, b) and PANI-β-NSA/Fe_3O_4 nanostructures (e, f) [129]

As one can see, Fe_3O_4 particles are ball-like in shape with a diameter of 100 – 150 nm which consist of some smaller balls with an average diameter of about 10 nm, as measured by TEM, indicating the small Fe_3O_4 balls are aggregated to

form Fe_3O_4 clusters through the magnetic interactions or intermolecular interactions. The PANI-β-NSA nanotubes with 60 – 80 nm in diameter are mostly obtained, but a small quantity of nanofibers are observed [129]. Most of the PANI-β-NSA/Fe_3O_4 composites are fibers with 80 – 100 nm in diameter, on the other hand, only a small quantity of hollow fibers can be found. TEM images discovered some black dots with about 10 nm in diameter embedded in the composite nanofibers. Those black dotes are regarded as Fe_3O_4 nano-particles because these dots are absent from the PANI-β-NSA nanotubes or nanofibers. In addition, the formation of the composite nanostructures is affected by the Fe_3O_4/ aniline mass ratios, showing a low mass ratio is favorable for forming smoother composite nanostructures.

Since Fe_3O_4 nano-particles are dispersed in aniline monomer before polymerization, a "core-shell" structural mixture, in which Fe_3O_4 nanoparticles are as a "core" and aniline as a "shell", might be formed. According to micelles model [19], aniline/NSA micelles containing Fe_3O_4 nanoparticles might form due to hydrophobic aniline and hydrophilic —SO_3H group attached to naphthalene ring of β-NSA. Thus the micelle with "head-tail" structure, in which β-NSA is assigned as a "head" whereas aniline containing Fe_3O_4 nanoparticles as a "tail", might be formed. In general, spherical micelles are expected to form through aggregation process [130] due to the lowest surface energy, and they have a fluid surface since the repulsive interactions of "head" group of the micelles. At the same time, a part of free aniline existing in the reaction solution can be diffused into the micelles to form aniline filled micelles. The micelles filled with or without free aniline are served as the soft-templates in the formation of composite nanotubes and nanofibers, respectively. Since the oxidant (e.g. APS) is hydrophilic, the polymerization mainly takes place in the micelle/water interface [131]. With the polymerization proceeding, the micelles become big spheres by accretion [132] or tubes/fibers by elongation [133], depending on the local conditions.

It is found that the conductivity of the composite nanostructures decreases with increase of the content of Fe_3O_4 in the composites due to partial blockage of the conductive path by Fe_3O_4 nanoparticles embedded in the PANI-β-NSA matrix, and the maximum conductivity is as high as 10^{-2} S/cm as shown in Fig. 5.26(a). Temperature dependence of the conductivity exhibits semiconductor behavior and follows 1D-VRH model [12]. Besides, the PANI-β-NSA/Fe_3O_4 nanostructures also have magnetic properties as shown in Fig. 5.26(b). The dependence of the magnetization of the PANI-β-NSA/Fe_3O_4 nanostructures on the applied magnetic fields exhibits super-paramagnetic behavior, in which saturated magnetization (M_s), remnant magnetization (M_r) and coercive force (H_c) were estimated to be ca. 6 emu/g, zero and zero respectively when 20wt% of Fe_3O_4 was added in the composites. Obviously Fe_3O_4 nanoparticles in the composite nanostructures contribute to the super-paramagnetic behavior, because Fe_3O_4 nanoparticles also show supper-paramagnetic feature although its saturated magnetization is high (e.g. $M_s = 65$ emu/g).
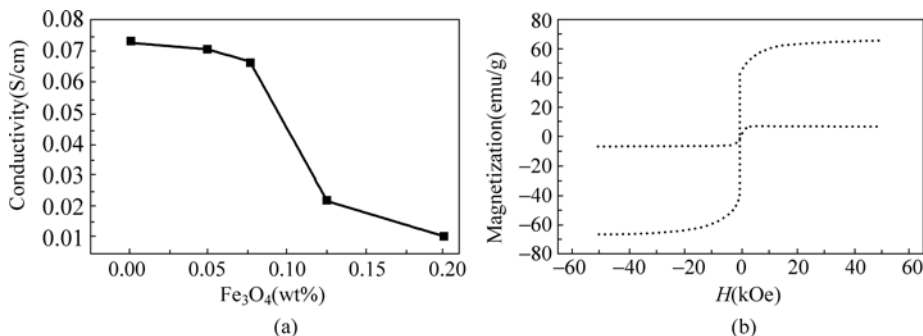
Figure 5.26 The electrical (a) and magnetic (b) properties of the PANI-β-NSA/Fe$_3$O$_4$ nanostructures as a function of the content of Fe$_3$O$_4$ in the composites [129]

2. PANI-H$_3$PO$_4$ /Fe$_3$O$_4$ Nanotubes or PANI-H$_3$PO$_4$/γ-Fe$_2$O$_3$ Coaxed Nanofibers

Although the PANI-β-NSA /Fe$_3$O$_4$ nanostructures have both electrical and magnetic properties, their conductivity at room temperature was poor (~ 10^{-2} S/cm). So it is necessary to improve the electrical properties of the electromagnetic function nanostructures of conducting polymers. Since electromagnetic composite nanostructures are composed of conducting polymers and magnetic materials, their molecular structure, morphology and electromagnetic properties are basically affected by their molecular structures and content of the electrical and magnetic component in the composites.

Regarding conducting polymers, the molecular structure of the dopant used strongly affects the electrical properties of the conducting polymers [3]. For instance a conductivity of PANI nanotubes doped with inorganic acids (e.g. HCl, H$_2$SO$_4$, H$_3$PO$_4$ and HBF$_4$) by template-free method could be achieved as high as $10^{-1}-1$ S/cm [61], indicating enhancement of the electrical properties of PANI composite nanostructures is possible. Moreover, Fe$_3$O$_4$ or γ-Fe$_2$O$_3$ is a common magnet that of different morphology and size is variable. Therefore author tried to prepare electromagnetic functional nanostructures of PANI doped with inorganic acids as the dopant in the presence of spherical Fe$_3$O$_4$ or needle-like γ-Fe$_2$O$_3$ as the magnets. Electrical and magnetic functionalized PANI composite nanostructures containing magnetic nano-particles, which are spherical Fe$_3$O$_4$ (10 nm in diameter) or γ-Fe$_2$O$_3$ nano-needles (30 – 60 nm in diameter and 500 – 600 nm in length), were prepared by template-free method in the presence of H$_3$PO$_4$ as a dopant [134]. Typical SEM and TEM images of these PANI-H$_3$PO$_4$ electromagnetic functionalized composite nanostructures and pure PANI-H$_3$PO$_4$ as well as Fe$_3$O$_4$ and γ-Fe$_2$O$_3$ magnet are shown in Fig. 5.27. As one can see, PANI-H$_3$PO$_4$ /γ-Fe$_2$O$_3$ are co-axed nanofibers, where γ-Fe$_2$O$_3$ is served as a hard-template.

On the other hand, the PANI-H$_3$PO$_4$/Fe$_3$O$_4$ nanofibers are self-assembled by anilinium salt containing Fe$_3$O$_4$ nano-particles as the soft-templates via a self-assembly process [134], as mentioned before. As predicted, the maximum conductivity of the PANI-H$_3$PO$_4$ nanotubes is as high as 4.9×10^{-1} S/cm, which is
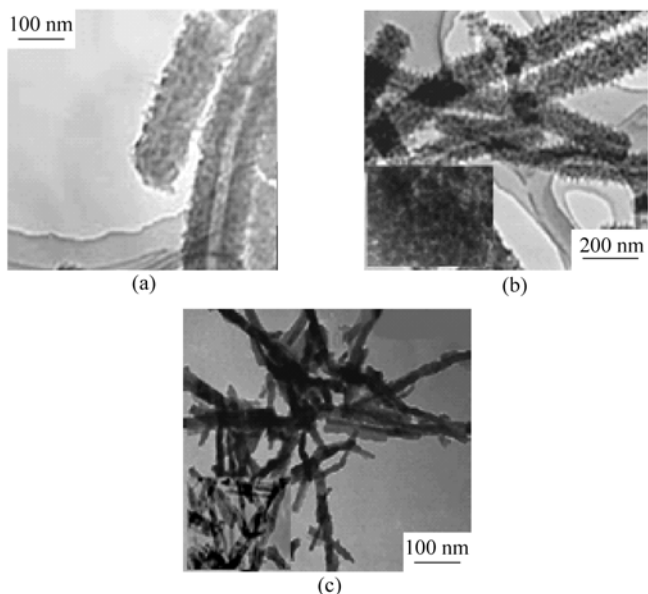
Figure 5.27   SEM and TEM images of (a) PANI-H$_3$PO$_4$ nanotubes, (b) PANI-H$_3$PO$_4$/Fe$_3$O$_4$ nanotubes and (c) PANI-H$_3$PO$_4$/γ-Fe$_2$O$_3$ nanofibers, the insert in (b) and (c) is TEM of Fe$_3$O$_4$ and γ-Fe$_2$O$_3$, respectively [134]

one order of magnitude higher than that of PANI-β-NSA nanotubes (~10^{-2} S/cm) [129]. Both composite nanostructures have electrical and magnetic properties, for instance, the conductivity of the PANI-H$_3$PO$_4$/γ-Fe$_2$O$_3$ coaxed nanofibers and PANI-H$_3$PO$_4$/Fe$_3$O$_4$ nanofibers at room temperature decreases with increasing the content of magnetic nano-particles due to partial blockage of the conductive path by magnetic particles embedded in the composites as shown in Fig. 5.28(a). Moreover, the conductivity of both PANI-H$_3$PO$_4$/Fe$_3$O$_4$ and PANI-H$_3$PO$_4$/γ-Fe$_2$O$_3$ nanostructures decreased with decreasing temperature, exhibiting a semiconductor behavior and following 1D-VRH model as shown in Fig. 5.28(b). Except for electrical properties, both composite nanostructures also show magnetic properties, depending on the nature of magnet in the composites as shown in Fig. 5.29. The spherical Fe$_3$O$_4$ nano-particles magnet exhibits super-paramagnetic behavior (no hysteresis loop), leading to similar super-paramagnetic feature of the PANI-H$_3$PO$_4$/Fe$_3$O$_4$ nanofibers [134]. However, PANI-H$_3$PO$_4$/γ-Fe$_2$O$_3$ exhibits a ferromagnetic behavior contributed to ferromagnetic γ-Fe$_2$O$_3$ nano-needles. Compared with γ-Fe$_2$O$_3$ nano-needles, interestingly, the coercive force of the composite nanostructures is larger than that of the γ-Fe$_2$O$_3$ nano-needles, which might result from magnetic interaction between γ-Fe$_2$O$_3$ needles and polaron of PANI-H$_3$PO$_4$ [135].

3. Electromagnetic Functionalized Core-Shell Micro/Nanostructures

Usually, room-temperature conductivity of PPy is higher than that of PANI, for

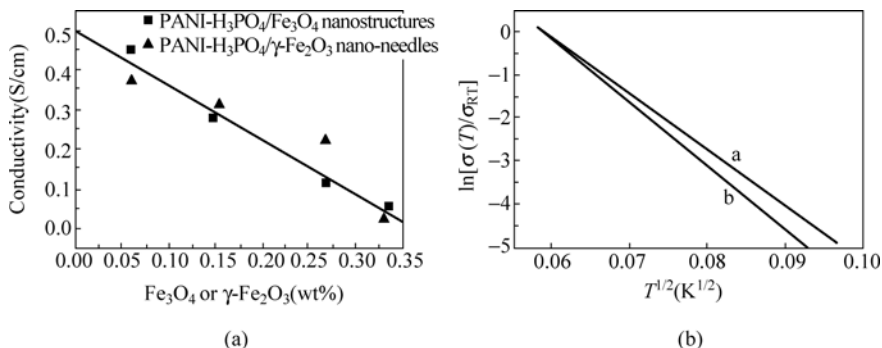(a)   (b)

Figure 5.28   Room temperature of the composite nanostructures of PANI-H$_3$PO$_4$ as a function of the content of magnet (Fe$_3$O$_4$ and γ-Fe$_2$O$_3$) in the composites (a) and their temperature dependence of the conductivity (b) [134]

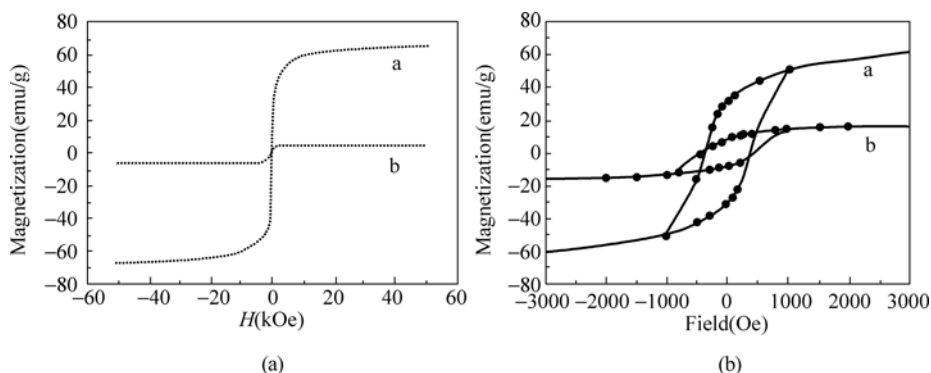(a)   (b)

Figure 5.29   Dependence of magnetization on the applied magnetic field at room temperature: Fe$_3$O$_4$ nano-particles and PANI-H$_3$PO$_4$/Fe$_3$O$_4$ nanotubes (a) as well as γ-Fe$_2$O$_3$ and PANI-H$_3$PO$_4$/γ-Fe$_2$O$_3$ nanofibers (b) [134]

instance, the room conductivity of PPy doped with *p*-TSA by an electrochemical method could reach 200 S/cm [136]. It is therefore interesting in chosen PPy as a conducting polymer to prepare electromagnetic micro/nanostructures via a self-assembly process. The electromagnetic functional composites of PPy were synthesized by template-free method associated with spherical carbonyl ion (Fe(OH)) magnet as the hard-template in the presence of *p*-TSA as the dopant [137]. Scheme of synthesis of the electromagnetic PPy-*p*-TSA/FeOH composites is shown in Fig. 5.30.

Typical SEM and TEM images of the spherical Fe(OH), self-assembled PPy-*p*-TSA nanotubes prepared in the absence of Fe(OH) and PPy-*p*-TSA/Fe(OH) composites are shown in Fig. 5.31. In the presence of Fe(OH) as a hard template, the self-assembled PPy-*p*-TSA nanofibers (20 – 30 nm in diameter) are coated on the surface of spherical Fe(OH) to form typical core-shell micro/nanostructures where Fe(OH) is as a "core" whereas PPy-*p*-TSA nanofibers are as a "shell" [137],
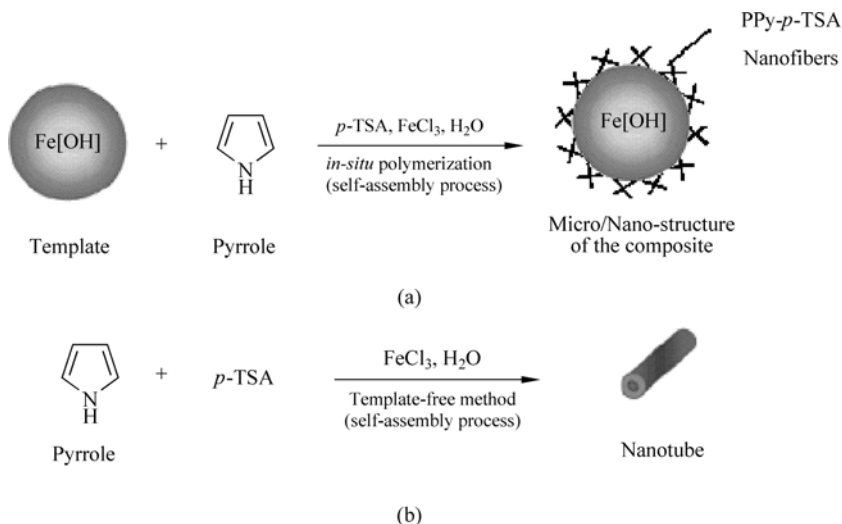
Figure 5.30 Scheme of core-shell micro/nanostructures of PPy-*p*-TSA/Fe (OH) composites [137]

indicating coordination effect of Fe(OH) as a hard-template (i.e. "core") and micelles composed of pyrrole super-molecules as the soft-templates in forming PPy nanofibers (i.e. shell) drives to form the core-shell composite micro/ nanostructures. Importantly, the core-shell composites show controllable electro-magnetic properties by changing the content of Fe(OH) magnet in the composites as shown in Fig. 5.32. As one can see, the maximum conductivity of the composites at [Fe(OH)]/[PPy] of 1:1 is as high as 53.6 S/cm, which is increased by more than two times compared with that of PPy-*p*-TSA nanotubes and is consistent with our previous results [138].

However, it is noted that the variation tendency of the conductivity of the micro/nanostructures versus the content of the magnetic materials is significantly different from previous results obtained from PANI-Fe_3O_4 nanotubes [129] or PANI-γ-Fe_2O_3 nano-needles [134], in which the conductivity of the composites decreases with the increase of the content of magnetic nano-particles in the composites due to the insulating magnetic particle. As shown in Fig. 5.32, the conductive PPy-*p*-TSA nanofibers formed on the Fe(OH) magnetic spheres results in decrease of the inter-contact resistance between composites that leads to enhancement of the conductivity at a lower [Fe(OH)]/[PPy] ratio. On the other hand, the conductivity is then decreased due to the large quantum of insulating magnet in the composites disrupting the PPy polymer chain. This was further supported by a fact of no maximum conductivity being observed in composites of PPy nanofibers mixed with Fe(OH) magnets as shown in Fig. 5.32. Magnetic measurements showed that Fe(OH) magnetic spheres are super-paramagnetic and which M_s, M_r, and H_c are estimated to be 180.4 emu/g, 0, and 0, respectively. On the other hand, the PPy nanotubes are antimagnetic.
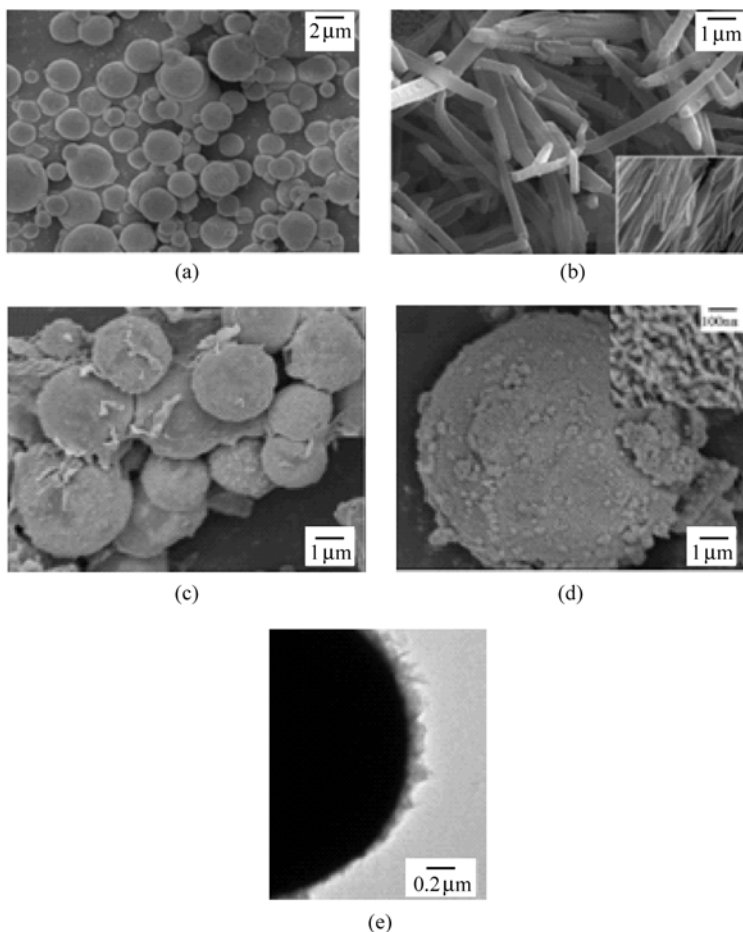
Figure 5.31   SEM images of (a, b) pure FeOH spheres and self-assembled PPy-*p*-TSA nanofibers by template-free method and (c, d, e) SEM and TEM images of core-shell PPy-*p*-TSA/FeOH [137]

Obviously, the super-paramagnetic behavior observed in PPy-*p*-TSA/Fe(OH) composites is induced by the super-paramagnetic Fe(OH) spheres. Like dependence of the conductivity on the [Fe(OH)]/[PPy] ratio, the M_s of the composite is also dependent on the [Fe(OH)]/[PPy] ratios, and the maximum M_s of the composite is observed at [Fe(OH)]/[PPy] = 1:1. This also differs from conducting polymers mixed with magnets which their magnetization increases with increase of the magnet in the composites. Thus the conductive PPy nanofibers coated on the surface of Fe(OH) spheres provides an excellent electrical and magnetic interaction between micro/nanostructures.

In order to further prove above phenomena, electro-magnetic functionalized PANI-Fe(OH) micro/nanostructures were also prepared by template-free method associated with spherical Fe(OH) magnet as the hard-template in the presence of
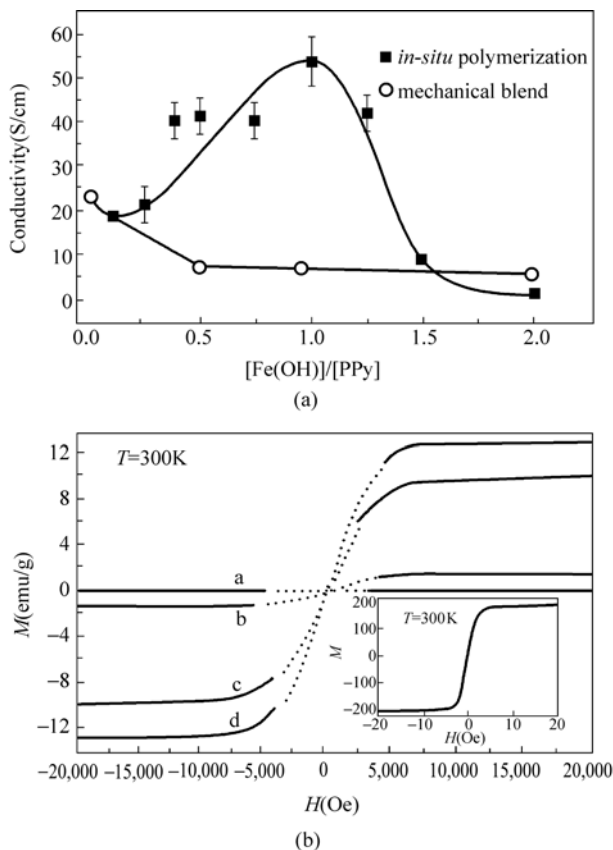
Figure 5.32 Electro-magnetic properties of the PPy-*p*-TSA/Fe(OH) composites as a function of the content of Fe(OH) in the composites [137, 140]

β-NSA as the dopant [139]. Similarly, the PANI-β-NSA nanofibers are also coated on the surface of the Fe(OH) microspheres to form novel core-shelled composite and which have both electrical and magnetic properties, in particular, a maximum conductivity of the composites also observed. Above-results suggested that the conductive PPy-*p*-TSA or PANI-β-NSA nanotubes coated on the surface of magnetic Fe(OH) spheres result in a maximum of conductivity at room temperature observed from the core-shelled micro/nanostructures. This is different from previous reports, which the conductivity decreases with increase of the content of the magnetic particles in the composites due to insulating behavior of the magnetic materials [129, 134].

4. PANI-γ-Fe₂O₃ Nanofibers by A "Chemical One Step Method"

Although electromagnetic micro/nanostructures with different morphology and electromagnetic functions have been prepared, as above-mentioned, a simple route is still required for preparing nano-scaled electromagnetic functionalized conducting

polymer micro- or nanostructures. Fe_3O_4 or γ-Fe_2O_3 is a common inorganic magnet, which is generally prepared by chemical reaction of $FeCl_3$ with $FeCl_2$ in a basic solution [141], where $FeCl_3$ is used as the oxidant. As well known, the doped PANI (i.e., the emeraldine salt form) is chemically polymerized in a strong acidic medium (e.g., 1.0 mol/L HCl) using APS as the oxidant [142]. Moreover, highly crystalline PANI nanofibers doped with different sulfonic acids, which their diameter is less than 30nm, were prepared by using $FeCl_3$ as the oxidant [75].

Actually, $FeCl_3$ is an acidic salt that is able to produce protons (H^+) in aqueous solution through hydrolysis. Therefore it is expected that aniline monomer would be directly oxidized and doped by $FeCl_3$ to form the conducting PANI (i.e., emeraldine salt form) without adding acidic dopant. This hypothesis has been provided that a series well-controlling nanostructures were prepared by changing redox potation of the oxidants without using acidic dopants [92]. Although the formation of magnets needs an alkaline medium whereas the synthesis of the conducting PANI is carried out in an acidic medium, $FeCl_3$ in both cases is used as the oxidant. Therefore, the two reactions for preparing γ-Fe_2O_3 and doped PANI could be combined to prepare electromagnetic PANI composites by adjusting the procedure and amount of $FeCl_3$ and $FeCl_2$ reagent added. Thus, a "chemical one step method" (COSM) is proposed to prepare electro-magnetic functional PANI
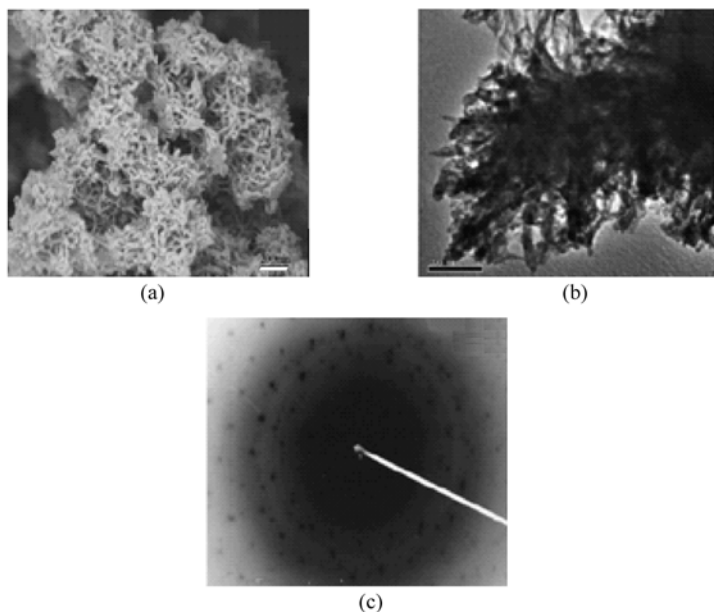

Figure 5.33   SEM (a), TEM (b) and electronic diffraction patterns (c) of PANI-γ-Fe_2O_3 nanofibers prepared by "chemical one step method" [140]

composite nanofibers (~ 20 nm in diameter) containing γ-Fe$_2$O$_3$ magnets via a self-assembly process [140]. The SEM and TEM images of PANI-γ-Fe$_2$O$_3$ nanofibers prepared by COSM are shown in Fig. 5.33. Compared with previous methods, the COSM is simpler, because only one step is required. In this method, FeCl$_3$ not only acts as the oxidant for aniline to form PANI or FeCl$_2$ for the magnets, but also provides protons for doping PANI via hydrolysis. It is reasonable to believe that this method offers a simple approach to prepare electromagnetic nanostructures of conducting polymers on a large scale. In particular, the electrical and magnetic properties of the composite nanofibers are controllable, where the conductivity is adjusted by the ratio of FeCl$_3$ to aniline monomer whereas the magnetic properties are mainly dominated by the amount of FeCl$_2$ as shown in Fig. 5.34 and Fig. 5.35, respectively.
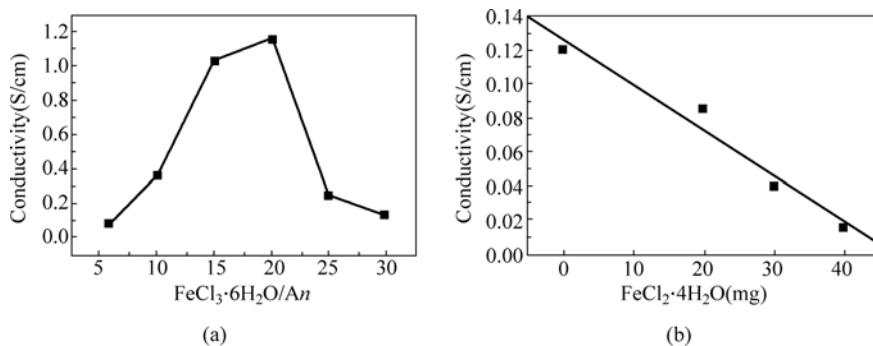

(a)   (b)

Figure 5.34 Influence of the [FeCl$_3$]/[An] ratios (a) and the amount of FeCl$_2$; (b) room temperature conductivity of the PANI-γ-Fe$_2$O$_3$ nanofibers [140]

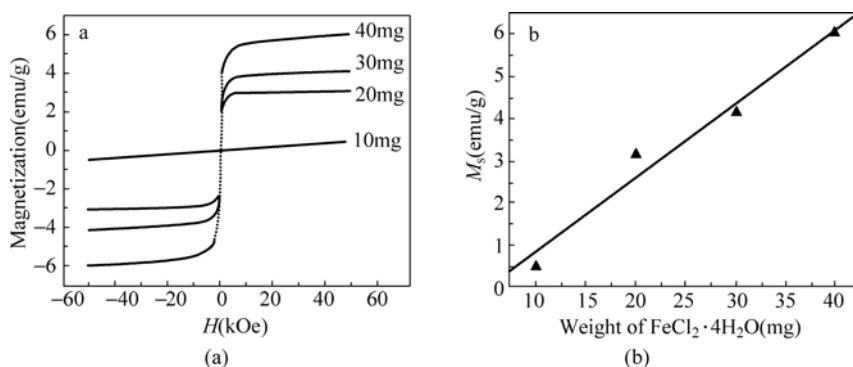(a)   (b)

Figure 5.35 Dependence of magnetization on the applied magnetic field at room temperature for the PANI-γ-Fe$_2$O$_3$ nanofibers synthesized with different amounts of FeCl$_2$ (a) and effect of the amount of FeCl$_2$ on the saturated magnetization of PANI composites (b) [140]

5.2.4   Electro-Optic Micro/Nanostructures

Electro-optic composite nanostructures or chiral nanostructures of the conducting polymers have been received great attention in application in electro-optic nano-devices [71]. Author also studied electro-optic PANI or PPy micro/ nanostructures or their composites prepared by template-free method associated with some approaches. The photoisomerization, chiral and optic nanostructures or composite nanostructures of conducting polymers are prepared by template-free method associated with other routs. The main results will be discussed as below.

1. PANI and PPy Nanostructures with A Photo-Isomerization Function

Azobenzene and its derivatives are generally characterized by reversible transformations from the more stable *trans* state to the less stable *cis* form upon irradiation with UV light [143]. The photoiduced isomerization of the azobenzene moiety is accompanied by a structural change, as reflected by changes in the dipole moment and geometry [144]. Since azobenzene can be selectively attached to the side chains, main chains, cross-links, or chain ends of a polymer, it is used as a "photochromic" probe to construct new polymers with photochromic characteristics. Azobenzene-functionalized polymers have promising applications as reversible optical storage media [145], holographic gratings [146], opticals [147] and electro-optic modulators [148] because of the photochromic characteristic providing light control of the chemical functions through an "on-off light switch". Recently, Chen et al. [149] reported that copolymers of 3-hexylthiophene and azobenzene-modified 3-hexylthiophene showed photo-controlled conductivity switching behavior attributed to the generation of a photo-excitation in the azobenzene moiety upon irradiation by UV light. Moreover, PPV and PA derivatives including azobenzene moieties as side chains, which showed optical anisotropy accompanied by *trans-cis* isomerization of azobenzene upon irradiation by linearly polarized light, have been also reported [150]. Therefore, studies on conducting polymers and their nanostructures with a photoisomerization function are interesting object in the field of conducting polymers and nanomaterials.

(1) PAPNPAPOA Copolymer with A Photo-Isomerization Function

Author designed and synthesized 1-bromo-3-(4-(4-nitrophenylazo) phenyloxy) propane, which was represented by B_3, by the Williams etherification method as described in Ref. [151].

A PANI derivative containing B_3 segment, which is called as poly (aniline-*co-N*-propane [4-(4-nitrophenylazo)-phenyloxy] aniline) (PAPNPAPOA), was synthesized by the fully reduced LEB form of PANI as a starting material [152]. It is found the freestanding thin film of PAPNPAPOA doped with 1.0 mol/L HCl has a conductivity of 1.2 S/cm at room temperature, which is higher than that of other *N*-alkylsubstituted PANI ($10^{-2} - 10^{-7}$ S/cm) [153]. The molecular structure of the PAPNPAPOA copolymer was characterized by FTIR, UV-visible and 1H NMR spectrum as well as elemental analysis [152]. The FTIR spectrum of the

PAPNPAPOA shows that all characteristic bands of PANI, indicating the structure of PAPNPAPOA is identical to that of the main chain of PANI [154]. However, the presence of absorption peaks at 1105 cm^{-1}, 1150 cm^{-1} (characteristic of C—O—C stretching mode) and 1236 cm^{-1} (characteristic of C—O—Ar stretching mode) also observed [155], suggesting alkaneoxynitroazobenzene side groups are linked on the PANI. The 1H NMR spectrum also demonstrated that the protons of methylene group directly bonded to nitrogen and which are consistent with the FTIR results as mentioned before. [152]. The graft concentration of the copolymers was estimated to be 0.42 based on O/N atomic ratio of 0.56, as measured by elemental analysis. The UV-visible spectrum of the PAPNPAPOA dissolved in NMP solution has two absorption peaks at 338 and 638 nm, which is identical to the emeraldine base form of PANI [156]. However, the thin film of the PAPNPAPOA doped by 1.0 mol/L HCl is identical to the ES form of PANI [22b]. In particular, the photoisomerization of PAPNPAPOA dissolved in NMP solution upon irradiation with UV light ($\lambda = 365$ nm) is observed. Interestingly, the absorption peak at 338 nm, attributed to the $\pi - \pi^*$ transition of the *trans*-azobenzene units, rapidly decreased. However, the weak absorption peak at 480 nm, attributed to the $n - \pi^*$ transition of the *cis*-azobenzene units, increased, which is more obvious compared with that of azobenzene moiety [157]. Meanwhile, the absorption peak at 640 nm, attributed to the exciton absorption of the quinoid rings of PANI, is largely blue-shifted to 605 nm upon irradiation with UV light due to effect of photoisomerization of the azobenzene units [158].

(2) PANI-ABSA Nanotubes with A Photo-Isomerization Function

Based on self-assembly mechanism of the template-free method for preparing conducting polymer nanostructures [19], the photoisomerization function of the conducting polymer nanostructures might be induced by using dopant with a photo-isomerization function via a self-assembly process. The photo-isomerization dopant will be serving as dopant, soft-template and bring about photo-isomerization functions at the same time. Based on above idea, the electro-photo-isomerization PANI nanotubes with a diameter of 110 – 130 nm and a conductivity of $2.5 – 10^{-2}$ S/cm were synthesized by template-free method in the presence of azobenzenesulfonic acid (ABSA) [159]. The formation and size of the PANI-ABSA nanotubes could be adjusted by changing the aniline-to-ABSA ratio and the concentration of ABSA [159].

Typical SEM and TEM images of the PANI-ABSA nanotubes with electro-photo-isomerization are shown in Fig. 5.36 (a). In particular, the PANI-ABSA nanotubes exhibited *trans-cis* photo-isomerization upon irradiation with UV light ($\lambda = 365$ nm) as shown in Fig. 5.36 (b), which is attributed to the azobenzene moiety of the ABSA dopant [159]. Two bands at about 330 and 440 nm are observed in the UV-visible absorption spectrum of ABSA, where the first absorption band corresponds to the $\pi - \pi^*$ transition of the azobenzene moiety, while the latter is assigned as the $n - \pi^*$ transition of the azobenzene moiety [160]. The absorption intensity at about 330 nm significantly decreased, while the

intensity of the peak at 440 nm increased upon irradiation with ultraviolet light ($\lambda = 365$ nm) that are identical to those of *trans-cis* isomerization of the azobenzene moiety [157], indicating the ABSA dopant has photo-isomization behaviour as same as azobenzene moiety. For PANI-ABSA nanotubes, on the other hand, three bands at about 330, 430, and 800 nm are observed, where the band around 330 nm is attributed to the overlap of the $\pi - \pi^*$ transition of the benzoid rings of PANI and the azobenzene moiety [156], whereas the band at about 430 nm is related to the $n - \pi^*$ transition of the azobenzene moiety [160] that is a piece of evidence supporting the PANI-ABSA nanotubes having photo-isomerization character, because the peak is absent although a band at 420 nm is often observed in the spectrum of doped PANI [156]. The band at about 800 nm with a long tail is assigned to the polaron transition of PANI [22], indicating ABSA acts as a dopant. Especially, a similar isomerization for PANI-ABSA nanotubes is also observed.
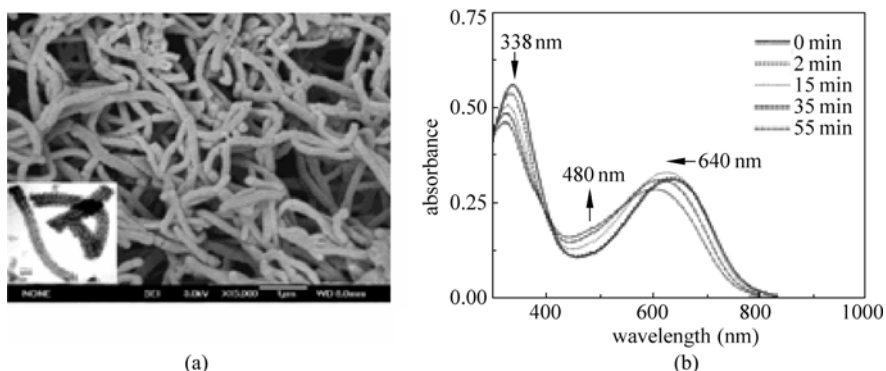

Figure 5.36   SEM and TEM images (a) of the PANI-ABS nanotubes and their UV-visible spectra (b) dissolved in *m*-cresol solution upon UV irradiation ($\lambda = 365$ nm) [159]

Obviously, the photo-isomerization of PANI-ABSA nanotubes is attributed to the isomerization characteristics of the azobenzene moiety, indicating ABSA bring about a photo-isomerization to the nanotubes. Studies on the kinetics of the photo-isomerization of PANI-ABSA dissolved in *m*-cresol suggest that although a similar photo-isomerization process is observed from PANI-ABSA nanotubes, the rate of photo-isomerization of PANI-ABSA is reduced in comparison to that of ABSA [159]. The recovery of PANI-ABSA exhibits a synchronization process with ABSA, suggesting the doped *trans* azobenzene moieties along the backbone, probably owing to steric hindrance, are more resistant to the photo-isomerization process.

(3) PPy-(*p*-OH-ABSA) Nanofibers with A Photo-Isomerization Function

Above results indicate dopant with a photo-isomerization function is an efficient way to prepare PANI nanotubes with an electro-photo-isomerization function by

template-free method. However, the conductivity of the PANI-ABSA nanotubes is only in the range of $2.5 - 10^{-2}$ S/cm [159]. In order to improving conductivity of the electro-photoisomerization nanostructures, PANI was replaced by PPy due to its higher conductivity compared with PANI. Therefore the PPy nanofibers (60 – 120 nm in average diameter) with an electro-photoisomerization function were prepared in the presence of p-hydroxyl-azobenzene sulfonic acid (p-OH-ABSA) as a functionalized dopant [161].

The micelle model proposed by author [19] is also satisfied the self-assembly of the PPy nanofibers. In particular, cylindrical micelles act as "soft-templates" were directly conformed by means of DLS and FFRTEM [161]. Interestingly, when ABSA without —OH group was used as a dopant, the resulting PPy-ABSA was granule, indicating the —OH group plays a stabilizing effect on the integrity of the micelle to allow the formation of the nanofibers. As predicted, the conductivity of the PPy nanofiber is as high as 120 – 130 S/cm, which was enhanced by $10^2 - 10^4$ times compared with that of PANI-ABSA nanotubes [159]. Although the nanofibers have metal-like conductivity at room temperature, temperature dependence of the conductivity still exhibits semiconductor behavior and follows 3D-VRH model [12]. Like PANI-ABSA nanotubes [159], a photoisomerization function was also observed, definitely resulting form isomerization of azobenzene moiety of p-OH-ABSA [161].

2. PANI-TiO$_2$ Composite Micro/Nanostructures

Titanium dioxide (TiO$_2$) nano-particles have received great attention because of their unique electrical and optic properties as well as extensive application in diverse areas [162]. Many papers on conducting polymer composites containing TiO$_2$ nano-particles (e.g. PANI/TiO$_2$) were published [163]. Based on synthesis method of the electromagnetic composite nanostructures of PANI containing magnetic nano-particles (e.g. Fe$_3$O$_4$) mentioned above, it suggested that combination of template-free method with co-structure of inorganic nanoparticles might be used to prepare electro-optic composite micro/nanostructured conducting polymers. Therefore it was interested to prepare PANI composite micro/nanostructures by template-free method in the presence of TiO$_2$ nano-particles as the optic materials.

(1) PANI-β-NSA/TiO$_2$ Composite Nanotubes

The PANI-β-NSA/TiO$_2$ composite nanotubes with an average diameter of 90 – 130 nm were prepared by template-free method associated with inorganic nano-particle co-construction tool [164]. It is found that the morphology, size, molecular structure, electrical properties, and wettability of the composite nanotubes are strongly affected by the content of TiO$_2$ in the composites, which are summarized as follows: ① It shows a low content of TiO$_2$ is favorable for information of the composite nanotubes [164]. ② The diameter of the composite nanotubes is a function of the content of TiO$_2$ in the composites as shown in Fig. 5.37(a). This
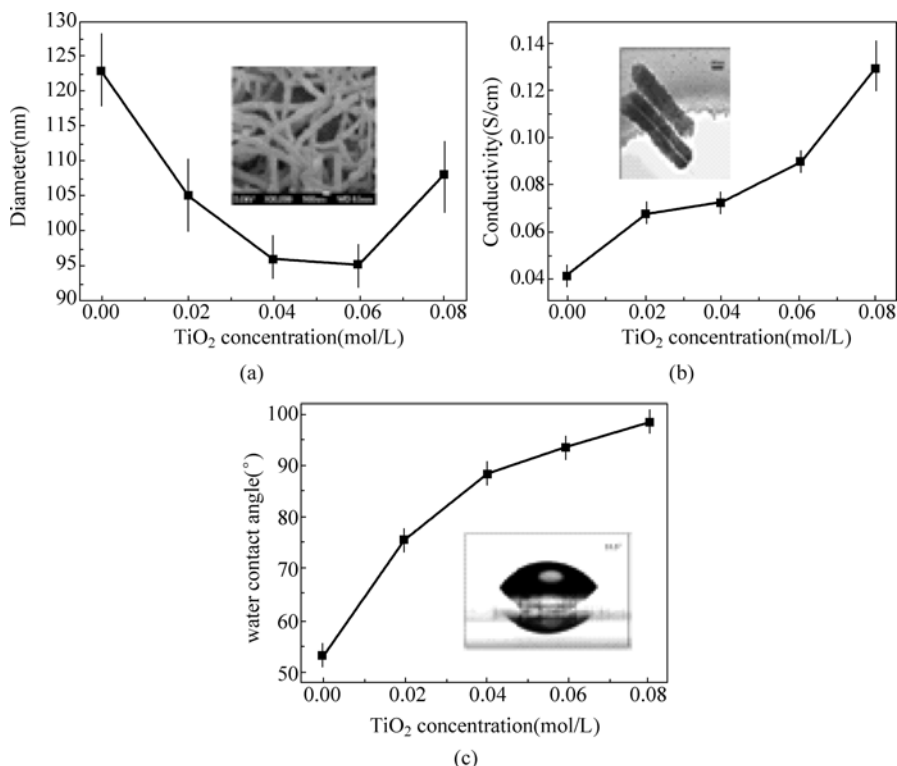
(a)

(b)

(c)

Figure 5.37   Effect of the content of TiO$_2$ on the diameter (a), the conductivity (b) and water contact angle (c) of the composite nanotubes of PANI-β-NSA nanotubes by template-free method, and the inset is SEM and TEM images of the composite nanostructures [164]

can be explained by model of core-shell micelles [19], where TiO$_2$ nano-particles are assigned as the "core" of the micelles due to hydrophobic behavior of the TiO$_2$ nano-particles, while β-NSA is regarded as the "shell" of the micelles due to its hydrophilic —SO$_3$H group, leading to the diameter of the composite nanotubes is as a function of the content of TiO$_2$ in the composites. ③ The morphology of the composite nanotubes affects their conductivity at room temperature, for instance, the conductivity of the granular composites is dropped two orders of magnitude compared with that of the tubular composites. The higher conductivity of the composite nanotubes may be caused by their tubular morphologies, resulting from some alignment of the polymer chain along the nanotubes. The conductivity of the composite nanotubes is increases with increase of the content of TiO$_2$ in the composites, as shown in Fig. 5.37(b), which might be due to two reasons. One may be resulting from interaction between PANI and TiO$_2$ nano-particles, which is consistent with previous results [163b], and another might be due to decrease of the diameter, which is called as size effect suggested by Martin et

217

al. [77]. Temperature dependence of the conductivity for the composite nanotubes is semiconductor behavior and follows the 1D-VRH models [12]. ④ In general, water contact angle, CA, is usually used to evaluate the wettability of the surface, and a hydrophobic surface is defined as the CA larger than 90˚, whereas the CA less than 90˚ are called as hydrophilic surface [165]. The CA value for the PANI-β-NSA nanotubes was measured to be 53.4˚, exhibiting hydrophilicity due to the hydrophilic —SO_3H. The CA value of the composite nanotubes is increased with increasing the content of the TiO_2 in the composites due to hydrophobic TiO_2 as shown in Fig. 5.37(c), indicating the wettability of the composite nanotubes can be changed by adjusting content of TiO_2 nano-particles in the composites. ⑤ The molecular structure of the composite nanotubes was characterized by synchronous energy-dispersive X-ray spectrum, Raman spectrum and XRD to prove the existence of TiO_2 in the composites. Synchronous energy-dispersive X-ray spectrum measurements revealed that the titanium element is clearly seen to be in the wall of the composite nanotubes, which is absent in the PANI-β-NSA nanotubes.

Moreover, the four characteristic modes at 146, 398, 515, and 640 cm^{-1}, which are assigned as assigned as B_{1g}, A_{1g}, and E_g modes of the anatase phase [166] respectively, are also observed in the composite nanotubes. Besides, the characteristic peak of the TiO_2 particles [167] are also observed from the XRD of the composite nanotubes except for two broad peaks centred at $2\theta = 21˚$ and $25˚$ ascribed to the periodicity parallel and perpendicular to the polymer chain [168].
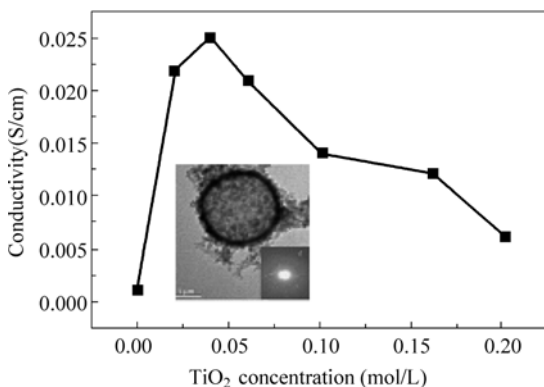
(2) PANI-SA/TiO_2 Composite Microspheres

Since microspheres with hollow interiors have drawn a number of interests due to their applications including stationary phases for separation science, biomedical devices, coating additives, controlled release reservoirs and as small containers for micro-encapsulation [169]. Moreover, hollow microspheres of PANI doped with SA and their composites were successfully prepared by a template-free method [70]. Therefore it is interested in synthesizing PANI-SA/TiO_2 composite microspheres by using same method as the PANI-β-NSA/TiO_2 composite nanotubes for further proving valid of co-construction tool as the association approach. The composite microspheres of PANI-SA/TiO_2 with $2.5 - 3.6$ μm in average diameter were successfully prepared by a template-free method associated with co-construction tool [70b].

Typical SEM and TEM images of the PANI-SA hollow spheres and PANI-SA/TiO_2 composite spheres are shown in Fig. 5.38. Like PANI-β-NSA/TiO_2 composite nanotubes, the morphology, diameter, hydrophobic and electrical properties of the PANI-SA/TiO_2 composite microspheres are affected by the content of TiO_2 nano-particles in the composites. There are some similarity and difference between the PANI-SA/TiO_2 spheres and PANI-β-NSA/TiO_2 nanotubes. Like the PANI-β-NSA nanotubes, for instance, the hydrophobic behavior of the

PANI-SA/TiO$_2$ microspheres are increased with increase of the content of TiO$_2$ in the composites as shown in Fig. 5.38(a), however, the influence of the content of TiO$_2$ in the composites on the hydrophobic properties of the PANI-SA/TiO$_2$ microspheres is weaker than that of the PANI-β-NSA/TiO$_2$ nanotubes [70]. Moreover, dependence of conductivity with content of TiO$_2$ in the composites of the PANI-SA/TiO$_2$ composite microspheres differs from that of the PANI-SA/TiO$_2$ composite nanotubes, for instance, a maximum conductivity for the PANI-SA/TiO$_2$ composite microspheres is observed [70], while the conductivity of the PANI-β-NSA/TiO$_2$ composite nanotubes are increased with increasing the content of TiO$_2$ nano-particles as shown in Fig. 5.38(b), which is consistent with previous results [170].
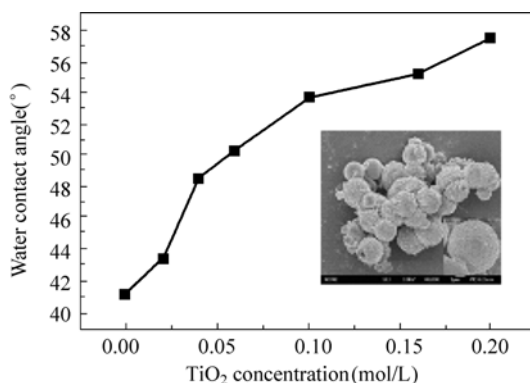
(a)

(b)

Figure 5.38   Effect of the content of TiO$_2$ on the water contact angle of the PANI-SA/TiO$_2$ films deposited on the glass substrate (a) and the room temperature conductivity (b) of PANI-SA/TiO$_2$ microspheres, and the inset is SEM and TEM images of the composite microspheres [70b]

According to formation mechanism of the PANI-SA microspheres [19], the micelles containing TiO_2 nano-particles having a "core-shell" structure, where TiO_2 nano-particles are assigned as a "core" of the micelles due to its hydrophobic feature, while SA and anilinium cations as a "shell" of the micelles due to hydrophilicity of SA dopant caused by ─COOH group attached on the benzene ring, maybe served as soft-templates in the formation of PANI-SA hollow microspheres and the hydrogen bond between ─OH group of SA and amine group of polymer chain is a driving force to form self-assembled microspheres [170]. Based on above proposal, it is not only easy to understand the morphology, diameter, hydrophobic and electrical properties are affected by the content of the TiO_2 nano-particles in the composites, but also suggesting that PANI-SA is co-structured with TiO_2 nano-particles to form composite microspheres through a self-assembly process.

Above-described results on the PANI-β-NSA/TiO_2 nanotubes or PANI-SA/TiO_2 microspheres suggested that template-free method associated with co-construction tool is a facile and efficient method to prepare electro-optic composite micro/ nanostructures of conducting polymers (e.g. PANI) and their morphology, diameter, electrical and hydrophobic properties can be adjusted by changing the content of nano-particles as the guest materials.

(3) PANI-SA Hollow Microspheres with Fluorescent Function

Study on the multi-functionality of hollow micro-spheres of conducting polymers is an important subject in the field of material science. Various approaches have been designed to realize the multi-functionality of micro/nanostructured conducting polymers in order to match the requirements of applications in optics, electronics, mechanics, membranes, protective coatings, catalysis, sensors, biology, and others [171].

As above mentioned, however, only PANI-SA/TiO_2 solid composite microspheres were obtained [70], rather than hollow composite microspheres. Author therefore prepared PANI-SA hollow micro-spheres (1.9 ─ 3.3 mm in average diameter) with a high conductivity (~ 10^{-1} S/cm) and a strong fluorescence by template-free method in the presence of rhodamine B (RhB) as the fluorescent material [172]. Typical SEM and TEM images of the PANI-SA/RhB hollow spheres are shown in Fig. 5.39. Like PANI-β-NSA/TiO_2 composite nanotubes [164] and PANI-SA/TiO_2 composite microspheres [70], the content of RhB in the composite affects the morphology, diameter and electrical properties of the hollow composite spheres.

In summary, combination of template-free method with other association approaches, such as hard-template, construction with inorganic functional nano-particles and functional dopant guide, can be used to prepare electro-magnetic, electro-optic and electro-hydrophobic micro/nanostructures of the conducting polymers. The morphology, diameter and physical properties of the multi-functional micro/nanostructures can be adjusted by changing the component of the composites and polymerization conditions.
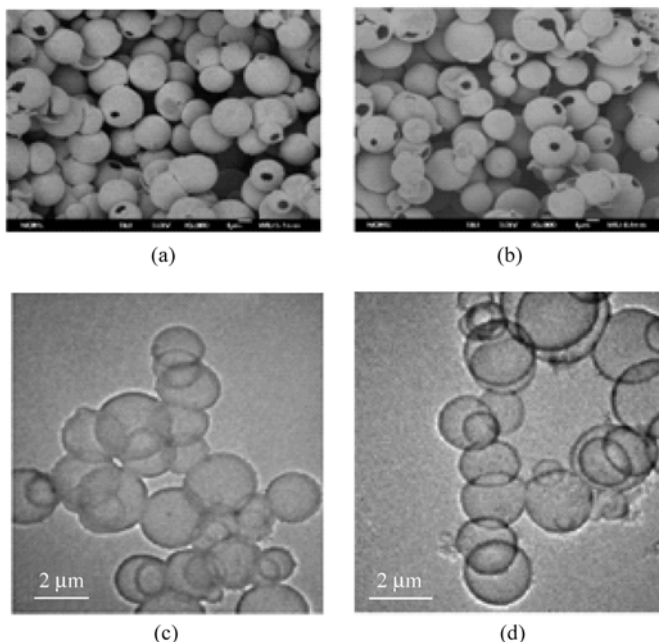
(a) (b)

(c) (d)

Figure 5.39   SEM and TEM images of PANI-SA/RhB hollow spheres synthesized at different concentrations of RhB: (a, c) 0 mol/L, (b, d) 1×10^{-3} mol/L [172]

5.2.5   Super-Hydrophobic 3D-Microstructures Assembled from 1D-Nanofibers

Nowadays various micro/nanostructures of conducting polymers, such as nano-particles [173], nanofibers [174], nanotubes [19], nanowires [175], spheres [67, 73] even dendrites [66, 176] are easily prepared by "hard" or "soft" templates. However, 3D-microstructures assembled from 1D-nanotubes or nanofibers are actually needed because they provide high functionality and performance for their applications in technology. However, synthesis of such novel 3D-microstructures assembled from 1D-nanostructures is challenge object in the field of nanostructured conducting polymers.

In addition, superhydrophobic surfaces, characterized by a water contact angle (CA) higher than $150°$, are arousing much interest because of their high water repellency and practical applications such as in the prevention of adhesion of snow to antennas and windows, self-cleaning traffic indicators, metal refining, stain-resistant textiles [177]. Combination of micro- and nanostructured conducting polymers with a superhydrophobic function is therefore an interesting object in nanomaterial and nanotechnology. In fact, few papers dealing with superhydrophobic conducting polymers have been reported [178]. However, the previous results on

superhydrophobicity mainly focus on films rather than the micro/nanostructures. Thereby design and synthesis of conductive and superhydrophobic 3D-microstructures assembled from 1D-nanotubes or nanofibers are challenge. Compared with other conducting polymers, PANI is advantageous of good environmental stability, and unique physical properties controlled by its oxidation states and protonation states [71]. There is possible to prepare above-mentioned 3D-microstructure assembled from 1D-nanostructures by some evidences as follows: ① It is well known that dopant plays an important role in self-assembly of micro/nanostructures by template-free method. If functionalized acid (e.g. optic or superhydrophobic feature) with surfactant feature (e.g. with —SO$_3$H group) is used as a dopant, it would simultaneously provide three functions: doping, "soft-template", and bring about corresponding feature of dopant. Moreover, morphology of the micro/nanostructures is strongly affected by reaction parameters including dopant and monomer nature as well as reaction conditions. ② Intrinsic of template-free method to the micro/nanostructures is a self-assembly process, because dopant, dopant/monomer salt or super-molecule even monomer itself can be served as "soft-templates" in the formation of micro/nanostructures. Thus the morphology of the resulting micro/nanostructures are affected by the reaction condition and competition of those "soft-templates". ③ Multifunctional micro/nanostructures can be induced by a functional dopant without using template. ④ Molecular interactions such as hydrogen bonds, π – π stacked interactions and Van der Waals forces are powerful driving forces for self-assembly of the micro/nanostructures without using hard-template. Besides, hydrophobic and hydrophilic interaction is also regarded as driving force for self-assembly process. Therefore, superhydrophobic and conductive 3D-microstructures whould be assembled from 1D-nanotubes or nanowires of PANI through a cooperative effect of "soft-templates" as well as above-mentioned molecular interactions. Based on above-designed idea, author recently synthesized some conductive and superhydrophobic 3D-microstructures assembled from 1D-nanofibes of PANI including superhydrophobic hollow rambutan-like spheres [179], hollow dandelion-like 3D-microstructures [180] and hollow cubebox-like 3D-microstructures of PANI [181] by template-free method in the presence of low surface energy sulfonic acids as the dopants. Synthesis method, structural characteristic, formation mechanism, physical properties of these 3D-micro/nanostructures assembled from 1D-nanofibers of PANI are discussed as below.

1. Super-Hydrophobic Rambutan-like Hollow Spheres

Although hard-template method is common and controlling method to prepare nanostructures of the conducting polymers, it is difficult to fabricate hollow spheres, because the pore of the most membranes as the hard-templates is cylindrical morphology in shape. On the other hand, hollow microspheres of conducting polymers are easily synthesized by soft-template method. For instance hollow PPy capsules in the presence of chitosan have been prepared by using one-step

pathway [182]. Moreover, author also reported hollow micro-spheres of PANI prepared by a template-free method using a dopant of either SA [70] or β-NSA at −10℃ [65].

However, synthesis of the multifunctional and 3D hollow spheres assembled from one dimensional 1D-nanostructures of PANI are seldom reported. Since perfluorooctane sulfonic acid (PFOSA) consists of hydrophilic —SO_3H group and hydrophobic lipophilic C_8F_{17} perfluorinated carbon chain, it is therefore expected that combination of its —SO_3H group and surfactant feature might be served as both dopant and "soft-template", while its hydrophobic lipophilic C_8F_{17} perfluorinated carbon chain will be contributed to hydrophobic properties of the micro/ nanostructures. Based on above-analysis, PFOSA was firstly chosen as a dopant to prepare micro/nanostructures of PANI by template-free method. Interestingly, conductive and superhydrophobic rambutan-like hollow spheres of PANI-PFOSA were obtained [179].
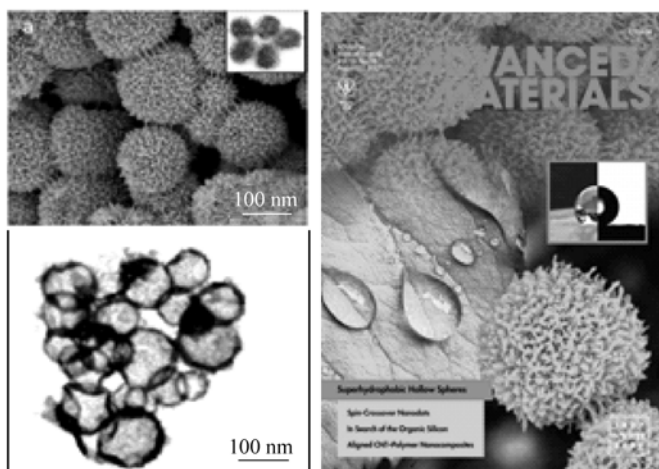

Figure 5.40   SEM and TEM image (left) of the rambutan-like hollow PANI spheres and the cover (right) of *Advanced Materials* published in Vol. 19, 2007[179]

As shown in Fig. 5.40(left), the rambutan-like hollow spheres are with an average diameter of 600 – 940 nm and with a shell thickness in 30nm, which is assembled by nanofibers (– 20 nm in diameter and 120 nm in length). It shows the water sphere formed has a CA as high as 164.5°, revealing the superhydrophobic nature of the rambutan-like hollow spheres. The novel conductive and superhy-drophobic rambutan-like hollow spheres were therefore chosen as the cover of *Advanced Materials* published in Vol. 19 in 2007 as shown in Fig. 5.40(right). Importantly, the hollow spheres float on the surface of the water, and remain floating for several months because of their hollow and superhydrophobic characteristics, exhibiting a high stability of the super-hydrophilicity. Room-temperature conductivity of the hollow spheres, as measured by the four-probe

method, is 9.6×10^{-1} S/cm and decreases with decreasing temperature, showing typical semiconductor behavior [179].

Above-results indicate that the rambutan-like hollow spheres are not only conductive, but also superhydrophobic. Structural characterizations by FTIR, UV-visible and XPS spectra demonstrated that the electrical properties of the hollow spheres results from the —SO_3H group of PFOSA serves as the counterion, while the lipophilic C_8F_{17} perfluorinated carbon chain and the hierarchical micro- and nano-scale structure on the surface of the rambutan-like hollow sphere leads to the superhydrophobic feature [179].

It is reasonable to accept that the micelles composed of PFOSA are easily formed in aqueous solution because of the amphiphilic properties of PFOSA due to its hydrophilic —SO_3H group and hydrophobic lipophilic C_8F_{17} perfluorinated carbon chain. The aniline monomer can also diffuse to the inside of the spherical PFOSA micelles to form spherical micelles filled with aniline monomer due to hydrophobic aniline. These aniline-filled spherical micelles can serve as a "micro-reactor" for aniline polymerization. At the same time, aniline-PFOSA salt is also formed in the spherical PFOSA micelles through an acid-base reaction, which serves as the "soft template" to form nanotubes or nanofibers of PANI. Once $FeCl_3$ is added as the oxidant, oxidation polymerization only takes place at the water/micelle interface on the surface of the spherical micelles, because $FeCl_3$ is hydrophilic. This is supported by a fact that the inside surface of the hollow spheres is very smooth, as measured by TEM.

Based on the above discussions, it is proposed that the rambutan-like hollow spheres are formed by the co-operative effect of two self-assembly processes: one is the PFOSA spherical micelles, "micro-reactors", are regarded as the "soft templates" of the hollow spheres, and the second is the aniline-PFOSA salt micelles act as the "soft template" for nanofiber formation on the hollow spheres [179]. Based on above-proposal growth process of the hollow spheres, it is expected that the completed hollow rambutan-like spheres undergo a growth process of crescent-shaped to open hemisphere shape to completed sphere, which in agree with the observations [179]. According to the above proposal, moreover, the morphology of the hollow spheres prepared at a given concentration of aniline would be affected by increasing the PFOSA/aniline molar ratio, which is also consistent with observations [179].

2. Super-Hydrophobic Hollow Dandelion-like 3D-Microstructures

Above results indicated that sulfonated dopants with low surface energy plays an important role in formation of superhydrophobic 3D-microstructurs assembled from 1D-nanostructures by template-free method. In order to further conform it, the PANI micro/nanostructures were again prepared by template-free method in the presence of perfluorosebacic acid (PFSEA) as the dopant, because PFSEA is bola-amphiphilic molecule, which contains a perfluorinated carbon chain and two hydrophilic —COOH end groups. In other words, the PFSEA dopant is

simultaneously satisfied doping, "soft-template" and hydrophobic function. By using PFSEA as the dopant, large-scaled superhydrophobic dandelion-like 3D-microstructures assembled from 1D-nanofibers of PANI were successfully synthesized by template-free method [180].
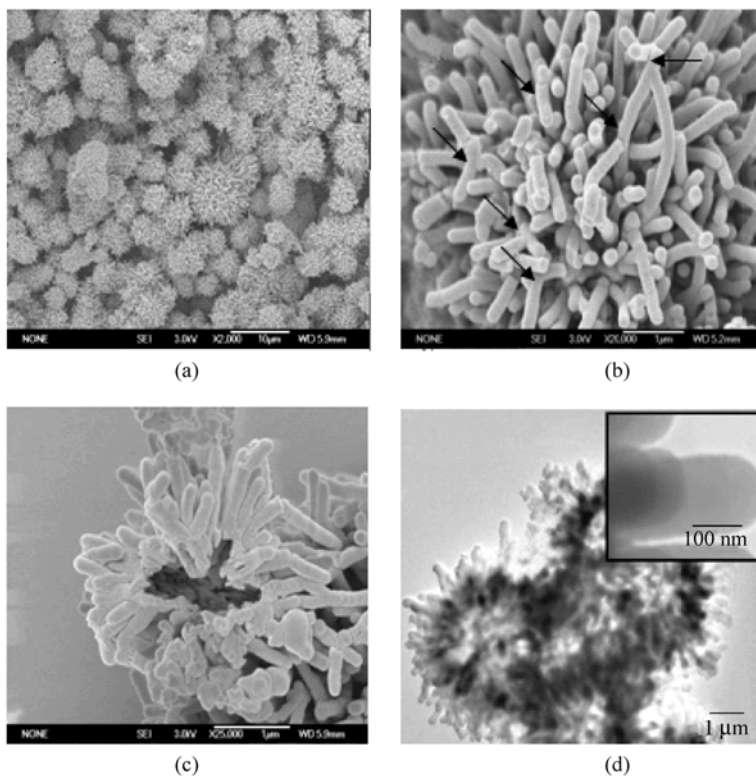

Figure 5.41   (a) SEM image of the dandelion-like PANI 3D-microstructures; (b) high-magnification SEM image of one dandelion-like PANI 3D-microstructures; arrows show the Y-shaped junctions; (c) SEM image of broken dandelion-like PANI 3D-microstructures; (d) TEM image of the dandelion-like PANI 3D-microstructures; Inset shows high-magnification TEM image of nanofibers [180]

As shown in Fig. 5.41, dandelion-like PANI-PFSEA microstructures (~ 5 μm in diameter), as measured by SEM and TEM, were observed when aniline of 0.1 mol/L and the molar ratio of PFSEA and oxidant to aniline were 0.25:1 and 1:1, respectively. Interestingly, the highly magnified SEM images futher revealed that the dandelion-like microspheres are composed of uniform Y-shaped junction nanofibers with about 210 nm in an average diameter and several micrometers in length. Such Y-shaped junction nanofibers are also demonstrated from the half-sphere broken by supersonic for 4 h (Fig. 5.41(c)), indicating the Y-shaped junction nanofiber might be regarded as a self-assembly unit for the dandelion-like

microspheres assembled from 1D-nanofibers.

Moreover, TEM images also further reveal the dandelion-like microstructure is hollow [180]. FTIR and UV-visible spectra of the dandelion-like microstructures of the dandelion-like microstructure are identical to the emeraldine salt form of PANI [22, 76]. Besides, there are two evidences for further conforming above-concludes: one is that two vibration bands at 1155 and 1248 cm^{-1} ascribed to the symmetric and asymmetric CF_2 stretches [183] are observed from FTIR of the dandelion-like microstructures; another is room-temperature conductivity, as measured by four-probe method, is about 3.8×10^{-3} S/cm [180].

Since PFESA is bola-amphiphilic molecule, which contains a perfluorinated carbon chain and two hydrophilic —COOH end groups, cylindrical micelles composed of PFESA and aniline cations might be formed through acid/base reaction and hydrophobic/hydrophilic interactions. FTIR measurements showed a strong and broad band at 3234 cm^{-1} assigned as the hydrogen-bonded N—H vibration [184], and a weak intense carbonyl absorption of the carboxylic acid end groups in PFESA at 1679 cm^{-1}, as assigned to a hydrogen-bonded C=O stretch [185], respectively, indicating hydrogen bonds are formed in the dandelion-like microstructures. Thereby these cylindrical micelles can be further aggregated to form branched micelles through those hydrogen bonds. These branched micelles might be served as the templates to form nanofiber junctions and dendrites, which are consistent with across-type nanofibers observed in the dandelion-like microstructures. Once adding APS as the oxidant, similarly, the polymerization only takes place at the water/micelle interface. As the polymerization proceeds, the growth of the nanofibers occurs by accretion, or an elongation process [61]. According to above-analysis, cooperative effect of molecular interactions, such as hydrogen bonds and hydrophobic interactions might drive 1D-nanofibers forming 3D-dandelion-like microstructures via a self-assembly process. Obviously, the formation mechanism of the superhydrophobic dandelion-like microstructures differs from above-described superhydrophobic rambutan-like hollow spheres [179] due to different molecular structure of dopant used.

Since PFESA has hydrophobic behavior, the surface wettability of the 3D microstructures was also evaluated by means of CA measurements. The water CA was estimated to be ca. 152.3° for the surfaces of the dandelion-like microstructures, showing superhydrophobic properties [186]. Moreover, the dandelion-like PANI microstructures float on the surface of the water for server weeks, indicating the superhydrophobic properties is stable. The superhydrophobic properties result from two reasons: one is a low surface energy of the PFESA dopant due to F element, as conformed by XPS [180], and another is enough rough surfaces produced by the micro- and nano-scale hierarchical structure, leading to air fill in the vacancy between individual microspheres so that the contact area between water and PANI microspheres can be minimized [186b].

226

3. Super-Hydrophobic Hollow Cubebox-like 3D-Microstructures

For a given dopant and oxidant and polymeric chain, the competition of above-mentioned molecular interactions is affected by reaction conditions such as the concentration of monomer and dopant as well as the molar ratios of dopant and oxidant to monomer. In order to conform it, effect of the concentration of aniline and molar ratio of PFESA to aniline on morphology of the dandelion-like 3D-microstructures of PANI-PFESA was further investigated. At the same molar ratio of APS to aniline (1:1), it was superiors that the hollow dandelion-like 3D-microstructures assembled from 1D-nanotubes are changed to the hollow cubebox-like 3D-microstructures assembled from 1D-nanotubes when the concentration of aniline decreased from 0.1 to 0.02 mol/L and the molar ratio of PFSEA to aniline reduced from 0.25 to 0.05:1, respectively [181]. The higher-magnification SEM image conformed that the cubebox-like 3D-microstructures assembled from 1D-nanotubes are assembled from cross-junction nanofibers with 40 nm in an average diameter that is completely different from the dandelion-like nanostructures, in which Y-shaped nanofiber junctions are served as the self-assembly units. Both SEM images of the broken cubebox-like 3D-microstructures assembled from 1D-nanotubes by supersonic for 4 h and TEM images of sample of hollow structure with about 120 nm in shell thickness are shown in Fig. 5.42.
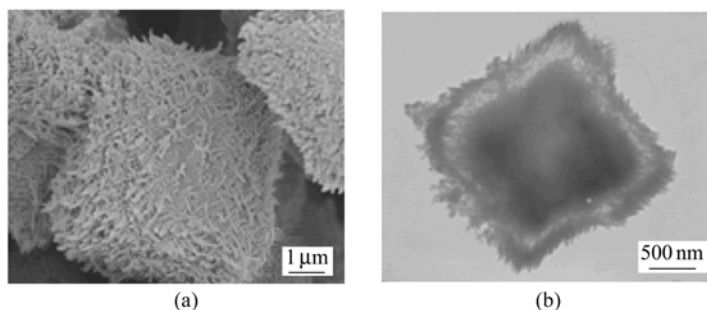

(a)   (b)

Figure 5.42   Morphology of the cubebox-like PANI microstructures: (a) SEM and (b) TEM images [181]

In addition, above-mentioned reaction conditions also affect the molecular structure and electrical properties of the cubebox-like 3D-microstructures assembled from 1D-nanotubes, as measured by FTIR and UV-visible spectra as well as conductivity measured by four-probe method. Although two strong peaks centered at $2\theta = 18.6°$ and $25.4°$, as ascribed to periodicity parallel, and perpendicular to the polymer chain [187] respectively, are observed from XRD of both hollow 3D-cubebox-like and dandelion-like 3D-microstructures, a strong peak at $\theta = 6.4°$, assigned as the periodicity along the polymer chain [188], is observed in the cubebox-like 3D-microstructures, which is absence in the dandelion-like 3D-microstructures, indicating crystalline of the cubebox-like 3D-microstructures is

higher than that of the dandelion-like 3D-nanostructures due to different 3D-microstructures assembled from 1D-nanofibers. Moreover, molecular structure and room temperature conductivity of 3D-microstructures assembled from 1D-nanofibers is also affected by above-mentioned reaction conditions. For instance structural characterizations by FTIR and UV-visible spectra showed that the cubebox-like 3D-microstructures are the emeraldine base form of PANI [22, 76], which is consistent with a poor conductivity (10^{-8} S/cm), as measured by four-probe method. This might results in low concentration of aniline and doping degree compared with that of the dandelion-like nanostructures.

Similarly, micelles formed by PFSEA and aniline cations can be regarded as "soft-templates" in forming nanofibers of PANI. Moreover, hydrogen bonds are observed in the cubebox-like 3D-microstructures, because a strong and broad band at 3234 cm^{-1} assigned as the hydrogen bonded N—H vibration [184] and a hydrogen bonded C=O stretch [189] at 1679 cm^{-1} assigned a carbonyl absorption of the carboxylic acid end groups in PFSEA are observed, as measured by FTIR. Above-results suggest that micelles as soft-templates and molecular interactions including hydrogen bonds and hydrophobic interactions exist in the reaction system of the cubebox-like 3D-microstructures assembled from 1D-nanotubes. Since low concentration of aniline and molar ratios of PFSEA to aniline was used in synthesizing the cubebox-like microstructures, the competition of above-mentioned molecular interactions (e.g. hydrogen bonds and hydrophobic interactions during polymerization of the cubebox-like microstructures differs from that of the dandelion-like microstructures. In other words, diffrence in reaction conditions results in different driving forces, leading to different morphology of 3D-microstructures assembled from 1D-nanofibers.

Similar to the dandelion-like microstructures, the cubebox-like microstructures also exhibit superhydrophobic characteristics with CA as high as 151.7°, as measured by water contact angle, and float on the surface of the water for several weeks, exhibiting high stability [181].

In summary, above-three samples addressed some very important results: ① Sulfonated acids with a low surface energy plays an important role in formation of superhydrophobic 3D-microstructures assembled from 1D-nanostructures of PANI, because it has dopant, soft-template and superhydrophobic functions at the same time. ②The superhydrophobic surface of 3D-microstructures assembled from 1D-nanofibers may protect their conductive properties as well as the materials encapsulated within, especially combination of conductive and superhy-drophobic properties might find potential applications in biosensors, drug delivery without loss of drug, controllable separation, and controlled drug release [190]. ③ Cooperative effect of the micelles as "soft-templates" and the molecular interactions including hydrogen bonds, $\pi - \pi$ stacking interactions and Van der Waals forces, as well as hydrophobic/hydrophilic interactions provides a facile and efficient approach to prepare multi-functional and 3D-microstructures assembled from 1D-nanostructures of conducting polymers. Change of polymerization

conditions results in competition between the soft-templates and the molecular interactions, leading to different morphology of 3D-microstructures assembled from 1D-nanostructures.

5.3   Mono-Dispersed and Oriented Micro/Nanostructures

Mono-dispersed and/or oriented conducting polymer micro/nanostructures have attracted considerable attention due to their broad range of applications ranging from chemical and biological sensors and medical diagnosis to energy conversion and storage, light-emitting display devices, catalysis, drug delivery, separation, microelectronics, and optical storage [191]. Synthesis of highly oriented arrays of the micro/nanostructured conducting polymer is a challenge to chemists and materials scientists because they are prerequisites for fabricating micro/nano-devices. Although chemical vapor deposition is a widely used method for carbon nanotube [192], it is not suitable for conducting polymers. So far, several methods such as template synthesis [2, 193], surfactant-assisted polymerization [194], interfacial polymerization [195], "seeding" [196], electro-spinning [197] and dilute polymerization [198] have been used to prepare conducting polymer micro/nanostructures.

Among these methods, only template synthesis is an effective and controllable approach to fabricate oriented arrays of the conducting polymer micro/nanostructures because of growth of the nanotubes or nanofibers are guided inside of pores of the membrane as the hard-templates [193], but it is difficult to prepare oriented hollow microspheres, because most templates only have cylindrical pores, rather than spherical pores. Although various micro/nanostructures including nanotubes, nanofibers, junctional nanotubes or nanofibers, hollow spheres even 3D-nanostructures assembled from 1D-nanofibers can be synthesized by template-free method, it is difficult to fabricate mono-dispersed or oriented micro/nanostructure arrays. Based on self-assembly mechanism of the template-free method, author searched some simple template-free method associated with a deposition process [199] and combined with Al_2O_3 template [200] to successfully prepare mono-dispersed or oriented arrays of PANI micro/nanostructures.

5.3.1   Template-Free Method Combined with Al_2O_3 Template for Oriented Nanowires

As well known, unique and oriented nanostructures of the conducting polymers can be directly built by using the template-synthesis method, but post-processing is required in order to remove the template. On the other hand, a myriad of nano-scale morphologies can be constructed through self-assembly, but controlling the orientation and size is difficult. Liu et al. [201] directly synthesized uniform

and oriented PANI nanowires on various substrates by an electrochemical method without using a hard-template. This provides a new approach for fabrication of microelectronic and optical devices on the basis of electro-polymerization.

As above-mentioned, template-free method [1] provided an attractive and alternative route to nanotubes or fibers, even microspheres, but obtaining oriented arrays is quite difficult. Author demonstrated a simple and novel template-free method combined with a porous template (Al_2O_3) and hard-template to prepare highly oriented arrays of PANI nanowires doped with 4-(3-(4-((4-nitrophenyl)azo) phenyloxy)propyl) aminobenzene sulfonic acid (C_3-ABSA) as the dopant [200]. It is found that the nanowires grow out of the template and aggregate to form bunches on the micrometer scale with surface crack, which maybe caused by shrinkage of the polymer during drying. The top of these bunches are uniformly flat, indicating the even growth rate of the nanowires at the initial step. The high resolution image (Fig. 5.43(upper)) shows these nanowires protruded vertically from the surface of the porous Al_2O_3 template to form a 1D highly ordered arrays [200]. With increasing polymerization time, the morphology of the nanowires changed from the 1D ordered of vertical alignment to flower-like aggregated bunches as shown in Fig. 5.43(upper) that might be attributed to the different growth rates of the wires, resulting in different length of the nanowires. Actually, formation of the PANI-C_3-ABSA nanotubes is a self-assembly process through
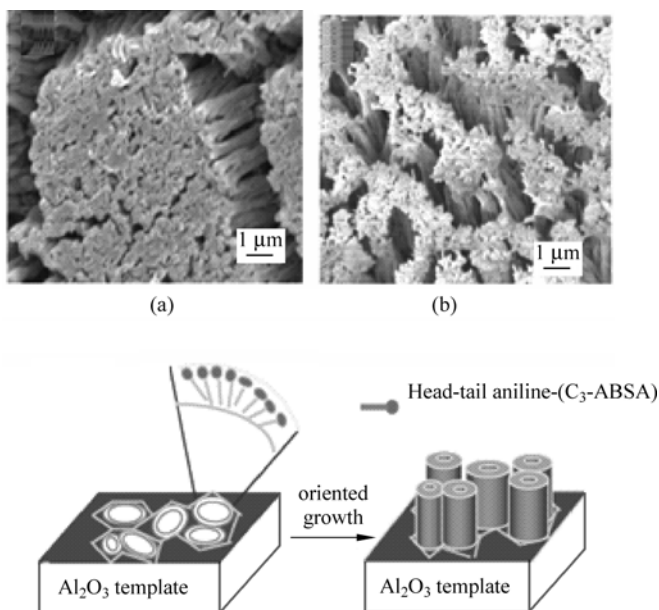

Figure 5.43 SEM images of PANI-(C_3-ABSA) nanowires prepared by template method combined with self-assembly process (a) and after polymerization for 90 h (b), and scheme of formation mechanism of the self-assembled oriented arrays of the nanowires is shown (bottom) [200]

the micelles of aniline/C_3-ABSA salt as the soft-templates due to hydrophlilic
—SO_3H group of the C_3-ABSA and hydrophobic aniline [202]. The micelles are
easily introduced into the hydrophilic pore through the driving force of
interfacial attraction depending on the curvature and interfacial hydrophilic
properties of the pore. It noted that no oriented arrays are grown when the Al_2O_3
is treated to be hydrophobic. These results suggest that the oriented nanowire
arrays are controlled by a co-ordination effect of the orientation of the nanowires
guided by the pores of Al_2O_3 template and the formation and growth of the
nanowires controlled via a self-assembly process. Scheme of the formation
mechanism of the oriented arrays of the nanowires prepared by combination of
template-free method with Al_2O_3 porous template is shown in Fig. 5.43(lower).

5.3.2   Template-Free Method Associated with A Deposition to Mono-Dispersed and Oriented Microspheres

Although oriented nanowires of PANI-C_3-ABSA nanowires were prepared by
using a template-free method cominated with a hydrophilic porous Al_2O_3
template [200], some times, the hard-template needs subsequently removing to
leave the desired the nanostructures that often destroy the desired product structure.
Although template-free method is another way to nanostructures, the resultant
nanostructures are disorder due to lacking hard-templates. Therefore, to search
for a simple and effective method, especially template-free method, to fabricate
mono-dispersed and/or oriented arrays of the micro/nano-structures of conducting
polymers still remains a scientific challenge. Author found that mono-dispersed
PANI micro-spheres deposited on glass substrates [199a] or highly oriented arrays
on silicon wafers [199b] could be prepared by template-free method associated
with a deposition process.

   Compared with other methods, obviously, the method is simple and inexpensive.
Setup used for the deposition of PANI micro/nano-spheres doped with SA as the
dopant by template-free method associated with a deposition process is shown in
Fig. 5.44. The typical preparation process is as follows [199a]: A pre-cleaned
glass substrate and treated with a piranha solution is dipped perpendicularly into
mixture solution of aniline and SA for a predetermined time. Oxidant (e.g. APS)
dissolved in an aqueous solution is then added into above mixture. The
polymerization takes place immediately after adding oxidant, and a thin layer of
the doped PANI (e.g. PANI-SA) was formed on the surface of the substrate. The
coated PANI substrate is then withdrawn vertically from the suspension at a
constant rate. Finally the PANI coated substrate is washed with ethanol and copious
amount of water several times and dried with N_2 gas at room temperature. The
aggregated morphology and size of the PANI-SA deposed on the substrate are
affected by the nature of the substrate, deposition rate and polymerization times
[199a]. By using this method, mono-dispersed and oriented PANI-SA microspheres
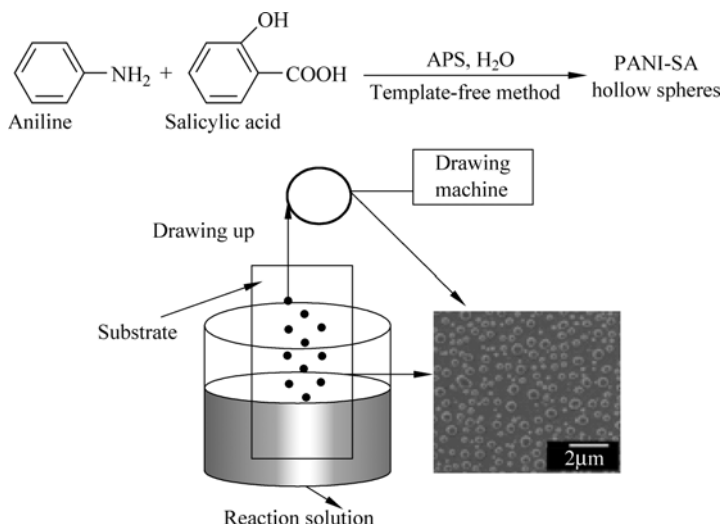deposed on the substrate were obtained.

Figure 5.44 Setup used for the deposition of PANI-SA micro/nano-spheres by template-free method associated with a deposition process; and inset is SEM images of the mono-dispersed spheres deposited on glass substrates [199a]

1. Mono-Dispersed Microspheres

Mono-dispersed PANI-SA micro-spheres (300 – 400 nm in average diameter), as measured by SEM, deposed on the glass substrate were successfully prepared [199b] as shown in Fig. 5.44. It is found that the morphology of the PANI-SA spheres deposited on the glass substrate is unchanged with deposition time, however, the diameter and aggregated structures of the spheres are affected by the deposition time [199a]. According to micelle models [19], spherical micelles composed of SA might act as a "soft template" in the formation of PANI-SA spheres because of the hydrophilic —OH and —NH groups and the hydrophobic benzene ring. When the substrate is immersed in the solution, the micelles might adsorb onto the surface of the substrate, which can be regarded as the "soft templates" in the formation of the spheres deposited on the substrate. Since APS is hydrophilic, the polymerization takes place only at the micelle/water interface. The diameter of the spheres initially deposited on the substrate is unaffected by the polymerization time [203].

However, the micelles which remain in the solution can couple with the aniline monomer to grow larger by polymerization and accretion process [61] under the driving force caused by the hydrogen bond between the —OH group of SA with the amine of PANI [70]. During the initial stage, the micelles with a small diameter first adsorb onto the surface from the suspension prior to the larger micelles because the heavy mass of the large micelles retards their movement in the solution and hence their adsorption at the interface. With increasing polymerization time, large spheres are gradually adsorbed onto the surface. That

232

is why the polymerization time influences the topographic structure aggregated by the spheres on the substrate [199a].

　　It is well known that the hydrophobicity of a surface is enhanced by modifying the surface with low-surface-energy materials (e.g., fluorinated or silicon compounds) [204]. For a given material, the hydrophobicity of a surface is dominated by its surface topographic structure assigned as surface roughness [205]. Jiang and co-workers [206] recently revealed that the superhydrophobic surface of the lotus leaf results from micro- and nano-scale hierarchical structures on their surface. As above-mentioned, the aggregated morphology and size of the PANI-SA spheres deposited on the glass substrate is affected by the polymerization time [199a].

　　These results encouraged the author to measure wettability of the surface of the PANI-SA spheres deposited on the glass substrate by means of CA. It is found that the CA value is a function of the polymerization time as shown in Fig. 5.45. It shows that when the micro-and nanometer scaled PANI-SA spheres deposited on the glass substrate are coexisted the maximum CA estimated to be 148.0°, exhibiting superhydrophobic behavior [199a]. This is significantly different from a surface of the PANI-SA spheres prepared from a bulk solution, which displays hydrophilic behavior with a CA of 41° [70]. The hydrophobicity originates from the contribution of the air trapped in the interior spaces of the rough surface [207]. Compared with CVD techniques [208], "template-synthesis" methods [209] and electro-hydrodynamic techniques [210] to create superhydrophobic surfaces, this method is simpler and cheaper.
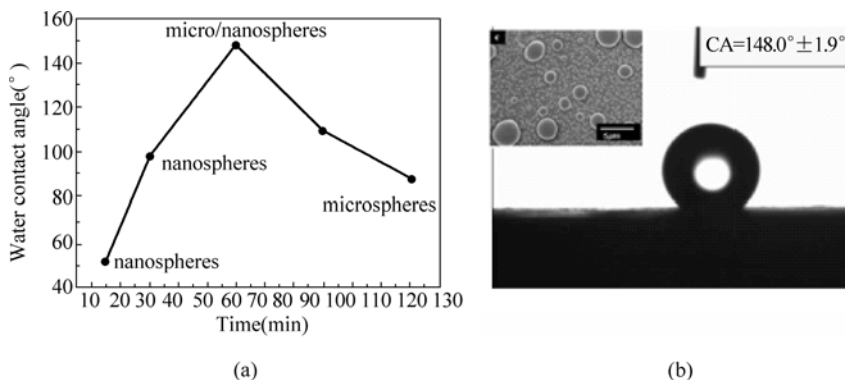

(a)　　　　　　　　　　　　　　　　　(b)

Figure 5.45　CA value of the PANI-SA spheres deposited on the glass substrate as a function of the polymerization time (a) and morphology and corresponding a water contact angle of 148.08° (b)[199a]

2. Mono-Dispersed and Oriented Microspheres

Based on above results, it is expected that mono-dispersed and oriented PANI-SA spheres on an orientating substrate might be prepared by the same method. As

predicted, mono-dispersed and highly oriented arrays of the PANI-SA spheres with a diameter of 300 – 600 nm deposited on silicon wafers or on the glass slice modified with polytetrafluoroethylene (PTFE) were successfully obtained [199b] as shown in Fig. 5.46.
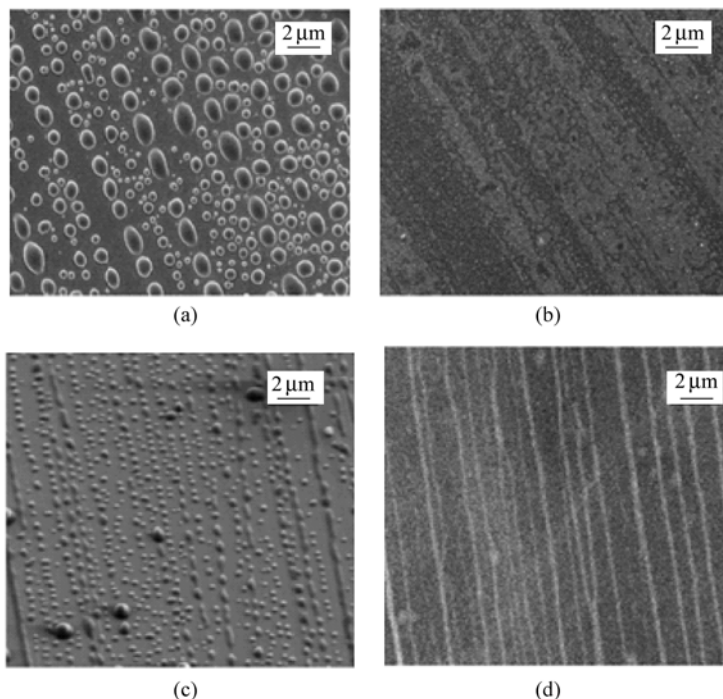

Figure 5.46   SEM images (a) of PANI-SA spheres deposited on the silicon wafer (b) and silicon wafer and PANI-SA spheres deposited on the PTFE modified glass substrate (c) and PTFE modified glass substrate (d) [199a]

As one can see, the self-assembled oriented arrays of the microspheres on the substrates are induced by the oriented surface structure of the substrates. Based on above discussed on self-assembly mechanism of mono-dispersed PANI-SA spheres deposited on the substrate, it is expected that the micelles deposed on the channels of the surface of the substrates might be served as the soft-templates in the formation of oriented arrays on the substrate due to low energy in these channels [199a]. The structural characterizations by FTIR, UV-visible spectrum and XRD indicate the main chain of the oriented arrays is similar to that of the typical PANI structure [76], but their crystalline is higher than that of the spheres produced in a bulk solution, which might be due to orientation of the spheres deposited on the substrate. Above results suggest that although micro/nanostructures of the conducting polymers prepared by template-free method are disorder, mono-dispersed or oriented nanowire arrays [199] of the PANI microspheres could be

prepared by template-free method associated with deposition polymerization that is simple and cheap compared with other approaches.

5.4   Electrical and Transport Properties of Conducting Polymer Nanostructures

Like bulk conducting polymers prepared by a common method [3], the electrical and transport properties are one of important properties of the micro/nanostructured conducting polymers. In general, the reagents in a chemical template-free method are simple, including only monomer, dopant and oxidant. However, influence of the polymerization parameters such as the nature of dopant, monomer and oxidant, the concentration of these reagents (e.g. the molar ratios of dopant and oxidant to monomer), polymerization temperature and time even stirring fashion on morphology and diameter of the micro/nanostructures are observed. Obviously, an effect of these parameters on the electrical and transport properties of the template-free synthesized micro/nanostructures is expected. As a result, influence of these parameters on the electrical and transport properties of the micro/nanostructures is discussed by using some micro/nanostructures as the typical samples. In particular, electrical properties of a single nanotube or nanowire even micro-sphere is discussed, as measured by four-probe method. In addition, magneto-resistance of the nanostructures is also briefly discussed.

5.4.1   Room Temperature Conductivity

Like bulk conducting polymers, the electrical properties of the nanostructured conducting polymers prepared by either "hard-template" or "soft-template" are affected by nature of dopant and monomer as well as the polymerization conditions, especially doping degree related to the molar ratio of dopant to monomer and the concentration of the dopants [71]. Effect of above-mentioned parameters on the electrical properties of the micro/nanostructured conducting polymers by template-free method will be discussed as follows:

1. Monomer Structure

Since conducting polymers constructed of π-conjugation length and counterion induced by doping process, influence of molecular structure of the monomer on the electrical properties of the template-free synthesized micro/nanostructures should be firstly considered. Influence of monomer structure on room temperature conductivity of the template-free synthesized PANI is therefore discussed by choosing PANI-β-NSA, POT-β-NSA and PPy-β-NSA micro/nanotubes as the typical samples. For the PANI-β-NSA micro/nanotubes, the maximum room temperature conductivity is about 1 S/cm and one order magnitude higher than that

of the granules [211]. POT is one of derivatives of PANI, in which a methyl group (—CH$_3$) is introduced into the benzene ring on the polymer chain of PANI [15]. The maximum room temperature conductivity of the POT-β-NSA microtubes is only about 10^{-2} S/cm that is one or two orders of magnitude lower than that of PANI-β-NSA microtubes (4.0 S/cm) [11] due to an increase of torsion in neighboring benzene rings on the polymer chain resulting from the introduction of the —CH$_3$ groups into the benzene ring on the polymer chain. Interestingly, the maximum room temperature conductivity of the PPy-β-NSA micro/nanotubes is as high as 27 S/cm [23a] that is enhanced by two orders of magnitudes compared with that of the PANI-β-NSA nanotubes [24].

Moreover, the nature of the charge carries of these micro/nanostructures is different, for instance, the polaron and bipolaron are regarded as the charge carriers for either chemical or electrochemical template-free synthesized PPy-β-NSA nanostructures, as measured by UV-visible and ESR spectra [23], while the polaron is regarded as the charge carries for both of PANI-β-NSA nanotubes and POT-β-NSA microtubes [24]. Thus influence of the monomer structure on room temperature conductivity of the nanostructures of the conducting polymers might be related to nature and transport of the charge carrieres produced by a doping process along the polymeric chain produced [71].

2. Doping Degree

The conductivity of the conducting polymers is strongly dependent upon the doping degree, which is related to the molar ratio of dopant to monomer and the concentration of dopant in the reaction solution [3]. Effect of the concentration of the dopants and the molar ratio of dopant to monomer on room temperature conductivity of the template-free synthesized micro/nanostructures is expected. For instance room temperature conductivity of PANI-D-CSA nanotubes [73] increases with increase of the molar ratio of D-CSA to aniline as shown in Fig. 5.47(a).

Similar results were also observed from POT-β-NSA micro/nanotubes [16] and PPy-β-NSA nanotubes [23a] as shown in Fig. 5.47(b, c). The conductivity of POT-β-NSA microtubes was increased from 10^{-4} to 10^{-2} S/cm as the concentration of β-NSA varied from 0.1 to 0.5 mol/L, which corresponds to the doping degree of 0.55 and 0.65, as measured by XPS [16] (see Fig. 5.47(b)). Similarly, room temperature conductivity of PPy-β-NSA nanotubes also increases with increase of the concentration of β-NSA used [23a] (see Fig. 5.47(c)). These results are consistent with observations from bulk materials prepared by a conventional method [3].

3. Dopant Structure

As mentioned in Chapter 1, a unique characteristic of the conducting polymers is that the insulating state of conducting polymers can become a conducting state through a doping process [3]. The doping process is always companied with inserting counterion in the polymeric chain [3]. Effect of nature of the dopants
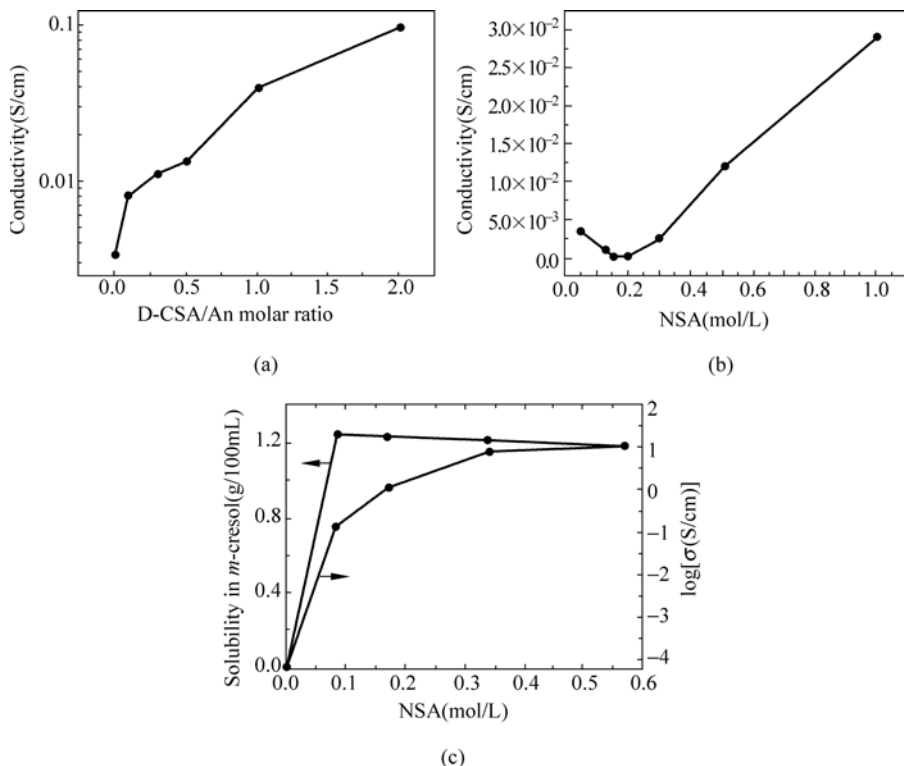
(a)

(b)

(c)

Figure 5.47   Effect of the concentration of dopant on room temperature conductivity
of PANI-D-CSA (a) [73], POT-β-NSA (b) [16] and PPy-β-NSA (c) [23a] nanotubes

on the electrical properties of the template-free synthesized micro/nanostructures
is therefore expected. Some typical samples are discussed as follows:

(1) PANI-Cn-ABSA Nanotubes

A series of sulfonic acids, 4-{n-[4-(4-nitrophenylazo) phenyloxy]alkyl} amino-
benzene sulfonic acid (Cn-ABSA, where $n = 2, 4, 6, 8$ and 10) is firstly chosen as
the samples to show influence of the dopant structure on the electrical properties of
the PANI nanostructures because size of the dopants is controlled by the number
of alkyl group of Cn-ABSA ($n = 2, 4, 6, 8$ and 10) [33]. It is found that the
conductivity is a function of the number of alkyl group of Cn-ABSA, especially
where a maximum conductivity is observed at $n = 6$ [34] as shown in Fig. 5.48.

As one knows, conducting polymers are composed of π-conjugated polymer
chains and counter ions produced by a doping process [3]. The total conductivity
of conducting polymers, as measured by a four-probe method, is determined by
the intra-molecular and inter-molecular factors [212]. The intra-molecular factors
include the localization length, which can be altered by controlling the defect
rates in the polymer (sp^3 defects) or head-head coupling [213], while the inter-
chain distances, inter-chain cross-linking, degree of chain orientation, and fraction

of crystallinity comprise the intermolecular factors [212]. The inter-chain distance can be modified by using ring-substituted monomers [214] or counter ions of different sizes [215].
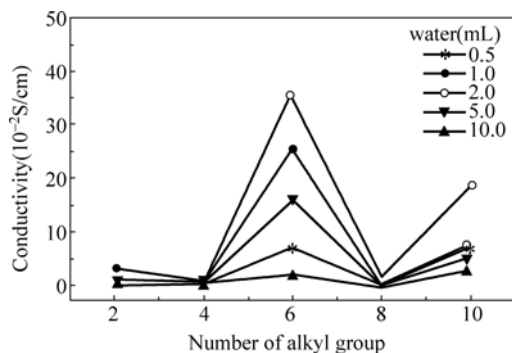

Figure 5.48 Influence of the number of alkyl group of Cn-ABSA on the room temperature conductivity of the PANI-Cn-ABSA nano-cylinders [34]

In addition, dopant size and crystallinity contribute to the delocalization of chains within three-dimensional regions and play an important role in influencing the electrical properties of the polymers [168]. Since dicarboxylic acids (HOOC (CH$_2$)$_n$ COOH), such as oxalic acid ($n = 0$, OA), malonic acid ($n = 1$, MA), succinic acid ($n = 2$, SA), glutaric acid ($n = 3$, GA) and adipic acid ($n = 4$, AA), have an alkyl chain (i.e., —CH$_2$ groups) of varying length ($n = 0 - 4$) and double —COOH groups. Obviously, the length of the alkyl chain dominated the size of the dopant, while the —COOH groups served as proton dopants, which will allow each acid molecule to dope two adjacent chains at the same time, resulting in inter-chain orientation.

Based on above analysis, the dicarboxylic acids (HOOC (CH$_2$)$_n$ COOH) were also good samples to show influence of the dopant structures on the electrical properties of the PANI nanostructures by template-free method. As predicted, room temperature conductivity of the resultant PANI nanostructures increased when the length of —CH$_2$ group of the dopants decreased [45] as shown in Fig. 5.49(a). This might be the result of two factors: one is decreasing the inter-chain distance, as confirmed by XRD and the other may be size effects when the diameter decreases with the decrease of the length of —CH$_2$ group, which is consistent with the results obtained from electrical measurements on single nanotubes [216]. Moreover, room temperature of conductivity of the template-free synthesized nanostructures is affected by the molar ratio of dopant to monomer (represented by [dopant]/[monomer] ratios). In general, the conductivity at room temperature is increased as increasing the [dopant]/[monomer] ratios due to enhancement of the doping degree, as measured by XPS. A typical sample is shown in Fig. 5.49(b).
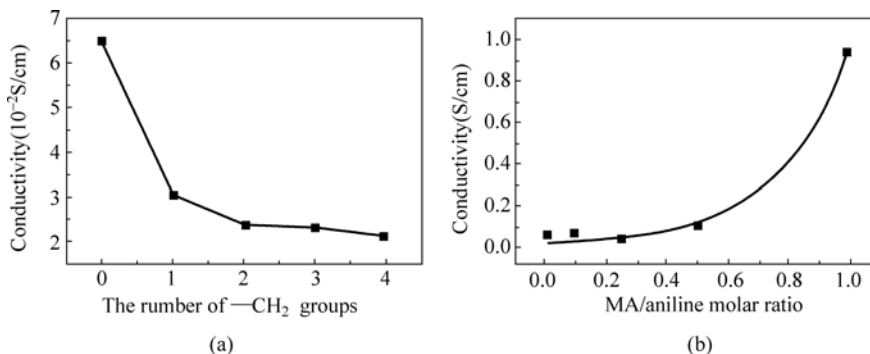
Figure 5.49 Room temperature conductivity of the PANI nanostructures as a function of the number of —CH$_2$ group of dicarboxylic acids as the dopants (a) and the molar ratios of dopants to aniline (e.g. MA/aniline) (b) [45]

(2) Morphology Effect

It is found that the morphology of the PANI-β-NSA prepared by the template-free method changes to granule-mixed granule and tubules-regale tubules when the molar ratio of aniline to NSA is increased [217]. The room temperature conductivity of the tubules is one order magnitude higher than that of the granules [217]. As above-mentioned, two kinds of the nanotubes of PANI doped with sulfonated carbon nanotubes as the dopants, such as PANI-c-MWNT-(OSO$_3$H$_n$) and PANI-d-MWNT-(OSO$_3$H$_n$), were observed when the molar ratio of dopant to monomer is changed [60]. Room temperature conductivity, as measured by four-probe method, is estimated to be 1.4×10^{-1} S/cm and 2.2×10^{-2} S/cm for PANI-c-MWNT-(OSO$_3$H$_n$) and PANI-d-MWNT-(OSO$_3$H$_n$), respectively. This is consistent with results that the hopping barrier of the PANI-d-MWNT-(OSO$_3$H$_n$) nanotubes deduced from the slope of $\ln\sigma(T)$ vs. $T^{-1/2}$ lines is 2.7×10^4 K, which is one order of magnitude higher than that of PANI-c-MWNT-(OSO$_3$H$_n$) [60], showing that the conductivity is affected by the morphology of the nanostructures.

5.4.2   Temperature Dependence of Conductivity

Temperature dependence of conductivity measured by four-probe method is a basic and important approach to understand transport properties of the conducting polymers and their nanostructures. As a result, temperature dependence of conductivity of the PANI nanotubes prepared by template-free method in the presence of various protonic acids including NSA, 1,5-NSA, HCl, H$_2$SO$_4$ and H$_3$PO$_4$ and HBF$_4$ as the dopants was measured by four-probe method [218]. It is found that temperature dependence of the conductivity of the PANI nanotubes is affected by the dopant structure and the molar ratio of dopant to aniline. However, all conductivity versus temperature exhibits a semiconductor behavior, i.e. the conductivity decreases with decrease of temperature, and follows 1D-VRH

model [12] independent of the dopant structure as shown in Fig. 5.50. Similarly, temperature dependence of conductivity for β-NSA [11], sulfonated carbon nanotubes [60] and sulfonated carbon 60 (e.g. C_{60} $(OS_3H)_6$) [51] doped PANI nanotubes as well as POT-β-NSA microtubes [16] also exhibit 1D-VRH model [12]. However, temperature dependence of the conductivity for template-free synthesized PPy-β-NSA nanotubes [23a] obeys 3D-VRH [23a]. Figure 5.51 shows temperature dependence of the conductivity of the PPy-β-NSA nanotubes prepared at different concentration of β-NSA.
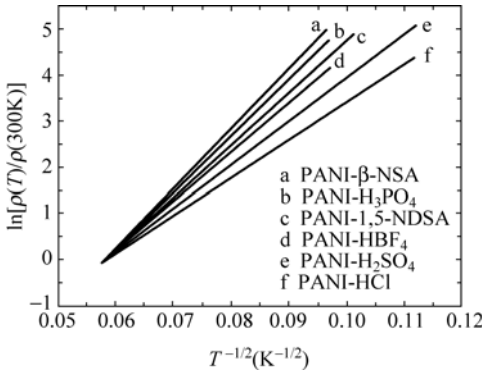

Figure 5.50 The temperature dependence of resistivity of PANI nanotubes doped with various dopants at the same doping concentration (the molar ratio of An/protonic acid=1: 0.5) [218a]
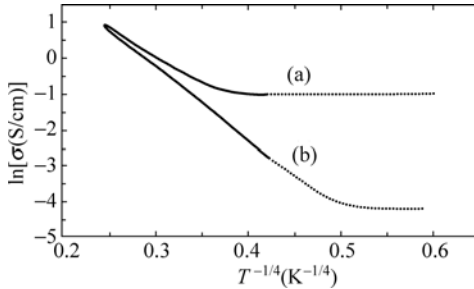

Figure 5.51 Temperature dependence of the conductivity of the PPy-β-NSA prepared at different NSA concentrations: (a) 0.085 mol/L and (b) 0.57 mol/L [23a]

In general, the VRH model can be described as follows:

$$\begin{cases} \sigma(T) = \sigma_0 \exp(T_0 / T)^{-1/(n+1)} \\ T_0 = 288 \dfrac{\alpha^3}{\pi K_B N(E_F)} \\ n = 1, 2, 3 \end{cases} \qquad (5.2)$$

where α^{-1} is the localization length, $N(E_F)$ is the density of states at the Fermi level and T_0 is the energy needed for charge carriers' hopping conduction. The value of T_0 can be calculated from the plots of $\ln\sigma(T)$ versus $T^{-1/(n+1)}$, defined as the energy needed for charge carriers' hopping conduction. Therefore, a low T_0 value implies a low energy for charge carriers' hopping conduction is required, leading to high conductivity that actually results from high doping degree related to the molar ratio of dopant to monomer. It is found that the T_0 value decreases with increase of the molar ratio of dopant to monomer. On the contrary, the diameter increases with increase of the molar ratio of dopant to monomer [218a]. This can be interpreted using a micelle model [19], because the diameter of the micelles is enhanced by the increase of the molar ratio of dopant to monomer, which leads to the diameter increases with increase of the ratios.

Although four-probe method is widely employed for measuring room temperature conductivity and temperature dependence of conductivity of the nanostructured conducting polymers, in fact, the measured electrical properties are not intrinsic because of large interresistance between fibers or tubes even polymer chains. In addition, since the transverse localization length (~ 2 nm) in conducting polymers [219] is much larger than the inter-chain separation (~ 0.35 nm) [168], resulting in a strong interaction of inter-chain in the conducting polymers.

Moreover, it has been demonstrated that the conductivity of a single nanotube or nanowire of the conducting polymers synthesized by hard-template method is enhanced by one or two orders compared with pellet nanotubes or nanowires [2], indicating the nanotubes can be regarded as a "metallic" bundle of coupled curled chains where the electronic wave functions are completely delocalized over the entire bundle [218b].

According to above discussions and the fact of the nanostructures surround by amorphous insulating regions, as measured by SEM, it is reasonable to propost that transport properties of the PANI micro/nanostructures are controlled by conduction along the chain and between the chains through hopping and tunneling mechanisms. If inter-chain coupling is weak, tunneling conduction is possible in between the chains. If the inter-chain coupling is sufficiently strong, on the other hand, the three-dimensional delocalization of the charge carriers is dominant [219].

In addition, current-voltage (*I-V*) curve, as measured by four-probe method, is also important tool to understand conducting mechanism of the conducting polymers and their nanostructures [71]. The *I-V* curve of the PANI-β-NSA microspheres measured at different temperature [220] showed that the *I-V* curves are non-ohmic at a high applied voltage whereas an ohmic behavior at a low applied voltage is observed that is independent upon the temperature. The electric field strength corresponding to non-ohmic region was estimated to be ca. 10^2 V/cm [221], which is small compared with that of PANI or other conjugated polymer films ($10^4 - 10^5$ V/cm) [222]. The temperature dependence of the resistivity of PANI micro-spheres measured [220] can be explained by the charging-energy-limited

tunneling model [223] due to its microscopic in-homogeneity. Such a variation was widely obtained from protonic acids doped PANI [222b, 224].

5.4.3 Electrical Properties of A Single Micro/Nanostructure

Up to date, pellet conductivity, as measured by two or four-probe method, is generally presented as the electrical properties of the conducting polymer nanostructures. Obviously, the electrical properties, as measured by the method, are not intrinsic properties of the conducting polymer nanostructures, because the measured resistances involvs large inter-resistance of the inter-chains and inter-fibers or inter-tubes. Martin et al. [2], for the first time, reported the conductivity of a single template-synthesized nanotube by measuring the bulk resistance across the host membrane using two-probe method. Few papers dealing with electrical properties of the single nanotube or nanofiber of PANI and PPy measured by using same method have been reported [225].

For instance, the conductivity of a single PPy nanotube is enhanced by one or two orders of magnitude compared with pellet samples of the nanotubes [226]. In this method, actually, the conductivity of a single nanotube or nanofiber is calculated by assuming that the number and diameter of tubes known and the resistance of the membrane as the template is neglected. Obviously, the conductivity measured by this method is not precise due to unkown for the number and diameter of tubes or fibers in membrane. Thereby direct measurement of the electrical properties for a single nanotube or nanowire of the conducting polymers is critical for understanding conductance mechanism of the conducting polymer nanostructures. However, this is challenge in the field of conducting polymer nanomaterials.

Fortunately, author cooperated with Prof. Zhaojia Cheng and Dr. Yunzhe Long at Institute of Physics, Chinese Academy of China to measure electrical properties of a single template-free synthesized nanotube or hollow micro-sphere of PANI by four-probe method. The first sample for measuring electrical properties of a single nanotube was carried out on the template-free synthesized PANI-CSA nanotubes [218b] by using four-platinum (Pt) microelectrode fabricated by focused ion beam deposition [227]. Typical preparation processes of the Pt electrodes are as follows: the nanotubes (e.g. PANI-CSA) pre-ultrasonically dispersed in ethanol were placed onto an insulating SiO_2 substrate, and the Pt electrodes (with 0.5 mm breadth and 0.5 mm thickness) were then fabricated by focused ion beam deposition. The SEM images of PANI-CSA nanotubes and the SEM images of a single PANI-CSA nanotube attached on the Pt microelectrodes with a length of 80 mm and cross section of 0.5 mm^2 is shown in Fig. 5.52(a).

In order for comparison, the pellet PANI-CSA nanotubes were also measured by four-probe method. It showed that the room-temperature conductivity of a
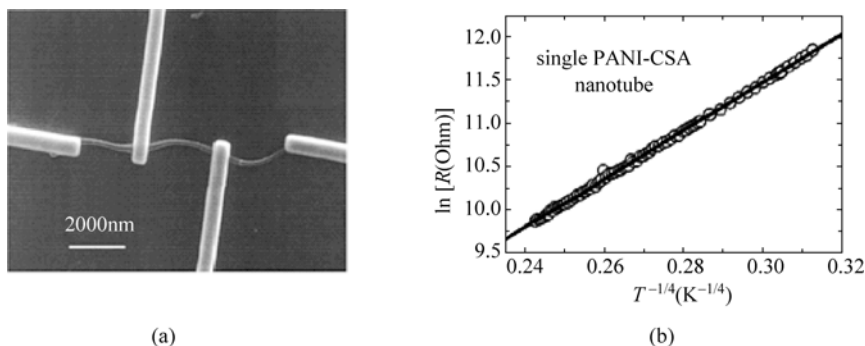
(a)   (b)

Figure 5.52   SEM images of a single PANI-CSA nanotube attached on four-Pt electrodes (a) and temperature dependence of conductivity (b) of the single nanotube, as measured by four-probe method [218b]

single PANI-CSA nanotube is enhanced by two orders of magnitude compared with the pellet nanotubes [218b], which is consistent with results reported by Martin el al. [226]. To further prove above-results, room temperature conductivity of a single PANI-SA micro-sphere was also measured by four-probe method [220]. Like single PANI-SCA nanotube, the room temperature conductivity of the individual PANI-SA micro-sphere is also two orders of magnitude higher than that of the pellet of PANI-SA micro-spheres, further proving the conductivity of a single micro- or nanostructure of conducting polymers is higher than that of their pellet samples [220]. Enhancement of the conductivity of a single nanotube compared with the pellet samples might be due to chain orientation along the nanotubes [2].

On the other hand, temperature dependence of the conductivity for a single nanotube is similar to that of the pellet nanotubes, exhibiting a semiconductor behavior and obeying a 1D-VRH model [12] as shown in Fig. 5.52(b). It indicates that although room temperature conductivity of a single nanotube or micro-sphere is one or two orders of magnitude higher than that of pellet micro/nanostructures, transport properties of the charge carriers in a single nanotube or microsphere are both dominated by contact-resistance between inter-chain and inter-tube or inter-fiber.

Above results suggest that large inter-resistance exists in the pellet sample. So contact resistance crossed PANI-CSA nanotubes, as resistance of nano-junction A-E-B and A-E-D resistance as a function of temperature, were measured by two-probe method as shown in Fig. 5.53. The contact resistance of the inter-tubes is very large, about 500 kΩ at room temperature, which is nearly 16 times larger than the intra-tube resistance of an individual PANI-CSA nanotube (A-C, 30 kΩ) [228], indicating the resistance of the bulk sample is dominated by the contact resistance [218a]. This is a reason why the early reported conductivities of compressed samples of nanostructures were small.
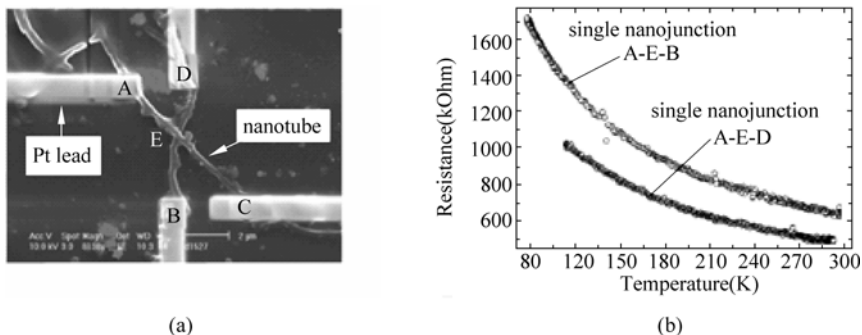
(a)   (b)

Figure 5.53 SEM images of two crossed PANI-CSA nanotubes A-C and B-D and their Pt leads (a) and resistances of junctions A-E-B and A-E-D as a function of temperature (b) [228]

5.4.4 Magneto-Resistance

Magneto-resistance (MR) is one of important physical propertiers for conducting polymers and their nanostructures. MR of PANI [229] and its composites [230], Ppy [231] as well as PEDOT [232] reported usually exhibited a positive magneto-resistance at low temperatures ($T < 10$ K) and MR $\propto H^2$ due to shrinkage of the localized wave functions of electrons in the presence of a magnetic field [233].

However, highly conductive conducting PA films [235] usually show a negative magneto-resistance at a low temperature due to the weak localization effects [236]. Except for above resultes, some new results on electrical properties of the nanostructured conducting polymers have been recently also reported in the literature [237 – 240]. Although the MR of bulk polymer films have been extensively studied, only a few papers have reported the MR of conducting polymer nanostructures [241], especially more comprehensive studies on the MR difference between pellets and single nanotubes/wires of conducting polymers are lacking. Author cooperated with Prof. Zhaojia Cheng and Dr.Yunzhe Long at Institute of Physics, Chinese Academy of Sciences to investigate difference in MR between single and pellets of PANI and PPy nanowires at a temperature range of 250 and 2 K [242]. Some interesting results are obtained that are described as follows: ① The sign of MR in both PANI and PPy nanowire and pellets is changed from negative to positive when the temperature decreased as shown in Fig. 5.54. The positive MR of PANI and PPy nanotube pellet shows H^2 dependence as shown in Fig. 5.55 due to a wave function shrinkage effect and their negative MR is discussed in terms of a quantum interference effect in hopping conduction. ② The MR of a single nanowire at different temperature is very small even at 2 K compared with that of the pellet nanowires. Moreover, no evident and stable negative MR at temperature between 50 and 200 K is observed from the single nanowire. These results suggest that the magneto-resistance in the bulk pellets of the nanowires is controlled by a random network of inter-fibril contacts [242].
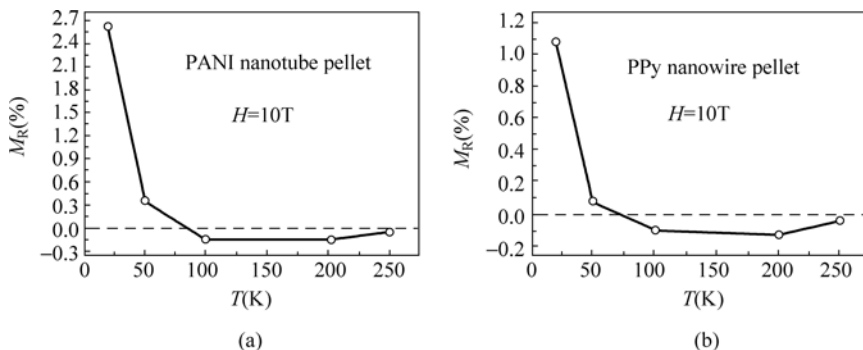
Figure 5.54   Temperature dependence of magneto-resistance of (a) polyaniline nanotube pellet and (b) polypyrrole nanowire pellet at $H = 10$ T [242]
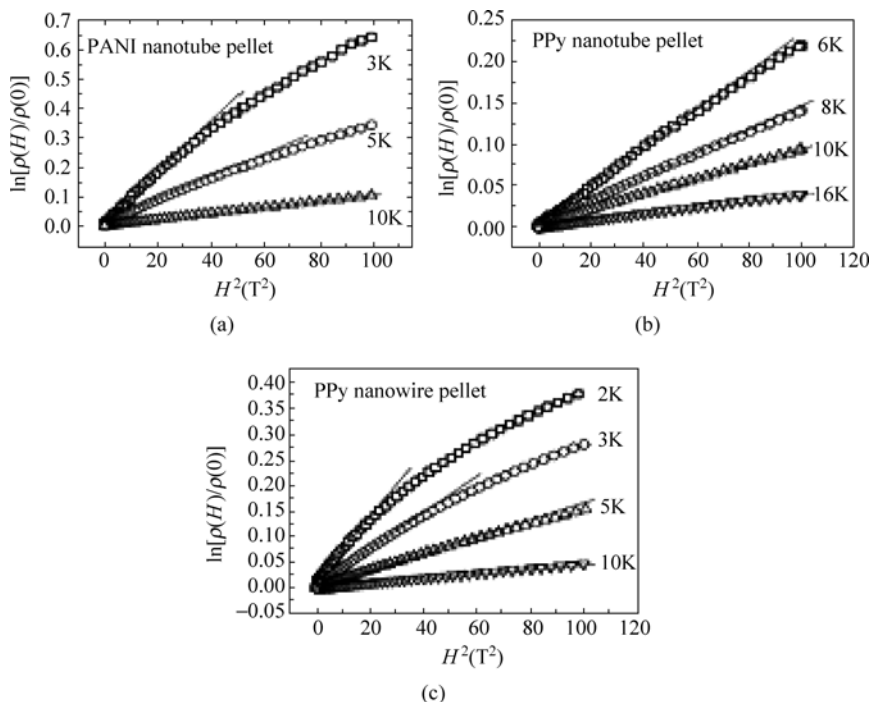

Figure 5.55   ln $[\rho(H)/\rho(0)]$ versus H^2 plots of the positive magneto-resistance data of (a) a polyaniline nanotube pellet, (b) a polypyrrole nanotube pellet and (c) a nanowire pellet [242]

Above results on the electrical and transport properties of nanostructured conducting polymers can be summarized as follows: ① The room temperature conductivity of the pellet micro/nanostructures of the conducting polymers, as measured by four-probe method, is affected by the nature of dopant and monomer as well as dopant degree related to the molar ratio of dopant to monomer and the

concentration of dopant. Temperature dependence of the conductivity of the pellet micro/nanostructures, as measured by four-probe method, exhibits a semiconductor behavior and obeys VRH model due to a large contact resistance crossed nanotubes or nanowires. ② The conductivity of a single nanotube of the conducting polymers, as measured by four-probe method, is one or two orders of magnitude higher than that of the pellet micro/nanostructures due to orientation of the polymeric chain along the nanotubes. ③ Although the single nanotube has metal-like conductivity at room temperature, its temperature dependence of the conductivity still shows a semiconductor behavior and obeys VRH. Moreover, a model of metal-like nanotubes surrounded by amorphous insulating regions is proposed to interpret charge transport in a single nanotube of the conducting polymers. ④ The MR of the single nanotube or macro-sphere is smaller than that of the pellet micro/nanostructures, indicating that the magneto-resistance in the bulk pellets of the nanowires or nanotubes is controlled by a random network of inter-fibril or inter-tubular contacts.

5.5 Special Methods for Micro/Nanostructures of Conducting Polymers

Although micro/nanostructured conducting polymers can be prepared by hard- and soft-template as well as other methods (e.g. electro-spinning technique), which have been described in Chapter 4, novel, facile and control methods for synthesis or fabrication of the micro/nanostructured conducting polymers, especially 3D-microstructures assembled form 1D-nanostructures are still desired. Recently, author search some facial methods to fabricate special brain-like nanostructures by using aniline salt as a template, hollow octahedral and spherical PANI by using Cu_2O as a hard-template, PANI-DBSA honeycomb structure by water-assisted fabrication and hollow 3D-microspheres assembled from 1D-nanofibers of PANI-β-NSA by a reversed micro-emulsion polymerization. In this section, method, and physical properties are discussed one by one.

5.5.1 Aniline/Citric Acid Salts as The "Hard-Templates" for Brain-like Nanostructures

The controlled synthesis of nanometer-scaled materials is a fascinating objective in modern materials sciences. Among these synthesis methods for nanostructured conducting polymers, as discussed in Chapter 4, a great deal of attention has been devoted to template-synthesis, because it is an efficient, controllable, and conventional route to prepare micro/nanostructures of the conducting polymers. Although porous alumina, track-etched polycarbonate, glass membranes, zeolites,

seed nanofibers, and polymer fibers have been used as the templates, new and novel morphology template is still required [71]. Author explored a novel approach, for the first time, to prepare PANI nanostructures with many convolutions (140 – 170 nm in average diameter), which resemble the cerebral cortex of the brain, using aniline/citric acid (CA) salts as the template by a gas/solid reaction using chlorine gas as the oxidant [243].
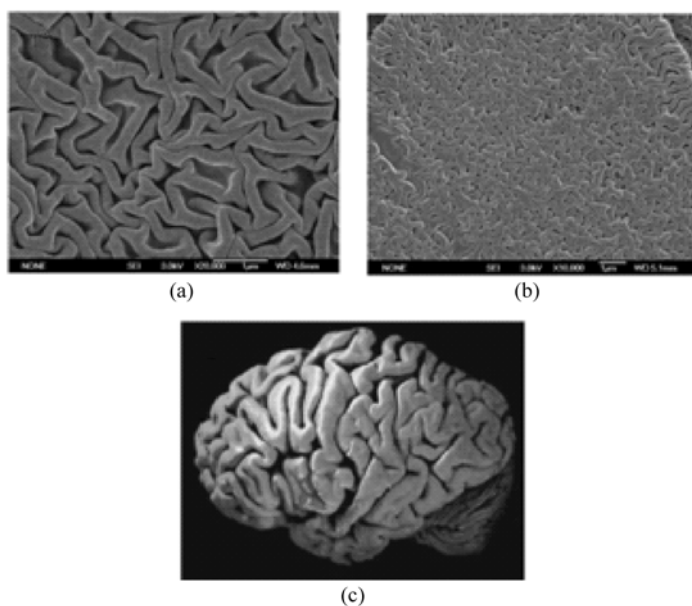

Figure 5.56   SEM images (a) conductive and brain-like PANI nanostructures by using aniline/citric acid salt as the template, (b) brain-like aniline/citric acid salt as the template and (c) photograph of brain [243]

Typical SEM images of the brain-like aniline/citric acid salt as the template and resultant conductive and brain-like PANI nanostructures are shown in Fig. 5.56. It is found that shape of the salt crystals as the templates is affected by the polarity of solvents due to different growth speed of the crystal surface resulted from polarity of the solvents. However, the brain-like structures does not change when the polarity of the solvents are changed, indicating the method is a universal approach to prepare brain-like aniline/citric acid salt. Evolution of the solvents might be a driving force for the formation of the convolutions on the surface of the salt crystal, as supported by following evidences: ① The reaction system of the salt only includes three reagents of aniline monomer, CA dopant, and organic solvent, in which only the solvent in the reaction system should be considered, because the salt formed through acid/basic reaction is insoluble. ② It is found that a relatively quick evaporation of the solvent is favorable to form novel convolutions on the surface of the salt crystal. Although the conductivity of the

barin-like PANI, as measured by surface resistance, is poor, structural characterizations by FTIR and UV-visible spectra showed the brain-like PANI is identical to the emeraldine salt form of PANI [22, 76]. The typical FTIR and UV-visible spectra of the brain-like nanostructures are shown in Fig. 5.57. Like conventional PANI [22], in particular, a reversible doping/de-doping process was observed in the brain-like nanostructures as shown in curve 3 in Fig. 5.57. Above results indicate that the method provided a novel, universal, and efficient approach to prepare brain-like nanostructures of PANI, and is completely different from the traditional chemical method that utilizes an acidic aqueous solution. The special brain-like nanostructures are identical to the emeraldine salt form of PANI; especially a reversible doping/dedoping process (i.e., conducting state/insulating state) for the brain-like nanostructures is realized by using hydrochloric acid gas/ammonia gas. The novel brain-like nanostructures with a reversible conducting/ insulating state realized by hydrochloric acid gas/ammonia gas may have a potential application in memory information devices.
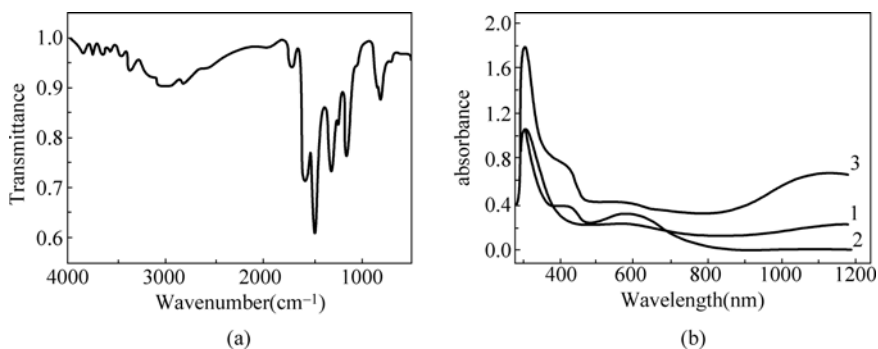

Figure 5.57 Characterization of the brain-like nanostructured PANI: (a) FTIR spectrum, and (b) UV-visible spectrum [243]

5.5.2 Cu₂O Crystal as A Hard Template

Cuprous oxide (Cu_2O) is a *p*-type inorganic semiconductor [244], which has attracted attention for the conversion of solar energy into electrical or chemical energy [245], and also use in catalyst [246] as well as antifouling coating [247]. In general, conductive PANI is synthesized from acidic solution in the presence of APS as the oxidant [22]. By chance, author found that Cu_2O in an acidic solution can react with APS to form a soluble Cu^{2+} salt. The new finding indicated that APS might be regarded as an oxidant for either aniline or Cu_2O crystal in an acidic solution, suggesting the conducting polymers can be not only imitated Cu_2O morphologies by using corresponding Cu_2O crystal as a template, but also omitting post-treatment for removal template. Based on above idea, author, for

the first time, synthesized hollow octahedrons of PANI by using Cu_2O crystal as the hard template in the presence of H_3PO_4 and APS as a dopant and an oxidant, respectively [248]. The reality of the resultant hollow PANI octahedrons were proved by positive evidences as follows: ① The hollow octahedrons are mainly composed of C, N and O, as measured by synchronous energy depressive and X-ray (EDX) analysis, indicating the octahedron is PANI instead of an octahedral Cu_2O crystal. ② Electronic diffraction measurements showed that the hollow octahedrons are amorphous rather than Cu_2O crystals, further proving that the observed octahedrons were real PANI. Compared with the common hard template, Cu_2O crystal is not only a new type of hard template in both shape and quality, but also omits its post-treatment due to soluble Cu^{2+} salt formed by the reaction of Cu_2O with APS during polymerization process.

The universality of Cu_2O as a hard template to micro-structured PANI was also proved by using corresponding morphology of Cu_2O crystal as a hard template. Typical SEM and TEM images of the resultant hollow octahedrons and micro-spheres of PANI by using corresponding morphology of Cu_2O crystal as the hard-templates are shown in Fig. 5.58. It noted that the morphology, oxidation and protonation state of the hollow microstructures of PANI prepared by octahedral Cu_2O as the "hard template" is affected by the $[Cu_2O]/[An]$ and $[APS]/[An]$ molar ratio [249]. For instance, the hollow octahedrons in the reduced form with a conductivity of $<10^{-8}$ S/cm could transform to conductive hollow micro-spheres in the emeraldine salt form with a conductivity of 10^{-2} S/cm when the $[APS]/[An]$ ratio changed from 1:1 to 2:1[249] as shown as Fig. 5.59(b). Since Cu_2O is able to react with APS to form soluble Cu^{2+} salt during the polymerization that was conformed by blue color of the reaction solution after Cu_2O reacted with APS in an acidic solution (e.g. H_3PO_4) [249], therefore, it is reasonable to accept that Cu_2O as a template does not need removing after polymerization.

Moreover, it is expected that the reaction of aniline or Cu_2O with APS in the reaction solution is competitive that was conformed by comparison of the pH value in the reaction as a function of polymerization time (Fig. 5.59(b)). The pH value decreased with increasing polymerization time in the absence of Cu_2O due to the H_2SO_4 produced during polymerization [191c]. On the other hand, the variation of pH value with reaction time in the presence of the Cu_2O template is smoother compared with that in the absence of the Cu_2O template, suggesting oxidation of aniline with APS is more easily than Cu_2O that results in either maintaining the template or dissolving the Cu_2O crystal at the same time. Based on above assumption, it is easy to understand the ability to omit post-treatment of the template is due to soluble Cu^{2+} formed by the reaction of Cu_2O with APS during the polymerization, while the competitive reaction of aniline and Cu_2O with APS results in the morphology, oxidation and protonation state of the PANI micro/nanostructures affected by the Cu_2O/An and APS/An ratio when octahedral Cu_2O crystal was used as a template to prepare microstructures [249]. It is therefore

expected that other metallic oxidants can be also used as hard-template to fabricate the conducting polymer microstructures. However the metallic oxides are required to react with the oxidant (e.g. APS or FeCl$_3$) in order to form soluble metal ions.
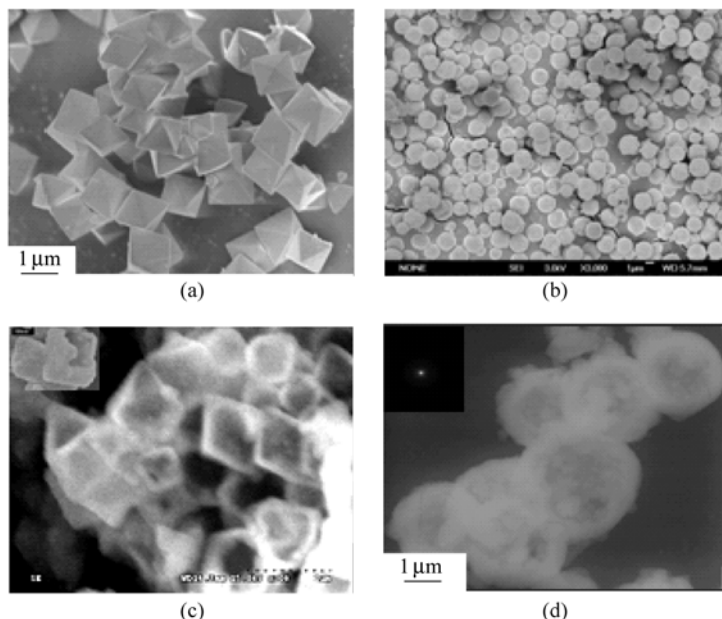

(a)　(b)

(c)　(d)

Figure 5.58 SEM and TEM images of hollow micro-structures of PANI template-synthesized by using cuprous oxide (Cu$_2$O) crystal as a template: (a) and (b) SEM images of octahedral [248] and spherical Cu$_2$O [249] as the template, respectively; (c) and (d) TEM images of hollow octahedral and spherical PANI prepared by Cu$_2$O as a template

(a)　(b)
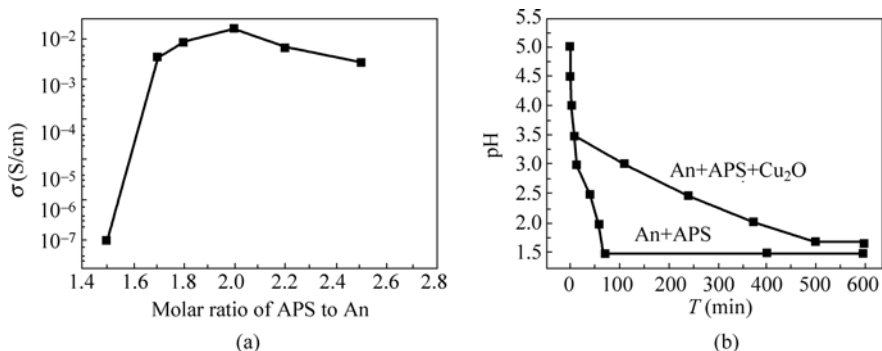
Figure 5.59 Effect of the [APS]/[An] ratio on the conductivity of the PANI microstructures prepared at [Cu$_2$O]/[An] = 1:2 with octahedral Cu$_2$O as a template (a), and comparison of variation of pH value with polymerization time in the absence and presence of Cu$_2$O (b) [249]

5.5.3   Water-Assisted Fabrication of PANI-DBSA Honeycomb Structure

The 3D-ordered network of PANI has been fabricated by template synthesis method [250]. Author cooperated with Professor Lei Jiang and Jing Zhai, Institute of Chemistry, Chinese Academy of Sciences to fabricate the honeycomb structure film of DBSA doped PANI by a simple water-assisted method in a moist atmosphere [251]. It is found that the formation of such special honeycomb structure is affected by parameters including the concentration of the PANI-DBSA solution, the relative humidity in the atmosphere, the film formation temperature and the wettability of the substrates [251].

Among those parameters, the concentration of PANI-DBSA and the relative humidity in the atmosphere are a key to form the honeycomb structures. Fig. 5.60 shows typical AFM images of the honeycomb structures of PANI-DBSA as-fabricated by a simple water-assisted method in a moist atmosphere [251]. It is found that the lower concentration of PANI-DBSA solution and higher humidity are favor for formation of the honeycomb structures. However no such honeycomb structure was observed when the same experiments were conducted at a much lower relative humidity (55%). Although the honeycomb structure is identical to the emeraldine salt form of PANI [22], as measurement of UV-visible spectra, the conductivity was difficult measured by four-probe method because of the limitation of the film thickness.
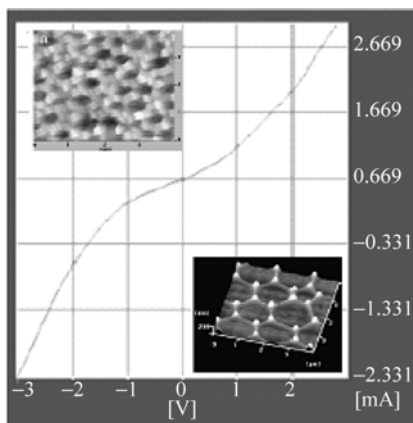
Figure 5.60   Typical AFM images of honeycomb structures (inset) and the current-voltage (*I-V*) curve of the thin films (right) [251]

Therefore, the conductivity of the honeycomb-structured film deposited on ITO glass with the diluted solution was measured by AFM, using a conductive cantilever under the application of bias voltages [251]. As shown in Fig. 5.60, the *I-V* curve not only proves the honeycomb structures being conductive, but also

exhibiting Schottky effect [252]. In addition, it is suggested that the "fast nucleation and slow growth" are necessary for the formation of the uniform size of the water droplet [253]. Self-assembly of the honeycomb structure results from the surface tension between water and organic solvent and the impulsive force of the water droplet as the driving forces. Obviously the two driving forces are competition, depending on the concentration of PANI-DBSA solution and the relative humidity used. The formation mechanism of such honeycomb structures has been also discussed elsewhere [254].

5.5.4 Reversed Micro-Emulsion Polymerization

In general, PANI is synthesized in an acidic aqueous solution [22, 76]. As mentioned before, β-NSA is a typical dopant with surfactant function due to its —SO$_3$H group. However, the reaction system of aniline polymerization trout to a typical reversed micro-emulsion polymerization when 1,2-dichloroethane is used as the reaction solvent retained at same condition. The reversed micro-emulsion consists of water as a "core" and aniline/NSA micelle as a "shell" that is regarded as a "micro-reactor", allowing the aniline polymerization carried out in its inner sides due to the hydrophilic APS as the oxidant. Based on above idea, author reported hollow micro-spheres of PANI-β-NSA assembled from its nanofibers by using a novel a reversed micro-emulsion polymerization in the presence of 1,2-dichloroethane as reaction solvent and water-soluble APS as the oxidant under ultra-sonic irradiation[255].
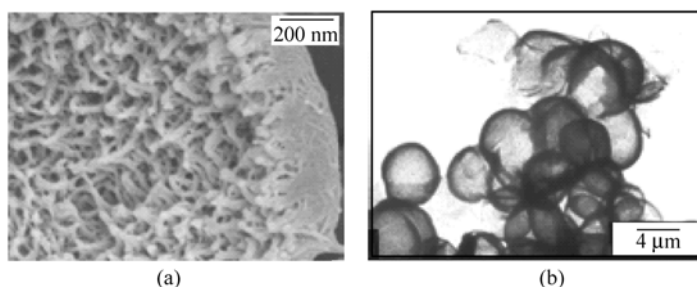

(a)   (b)

Figure 5.61 SEM images of the PANI-β-NSA hollow spheres prepared by a novel reversed micro-emulsion polymerization associated with a self-assembly process under ultra-sonic irradiation: SEM images of the broken spheres (a) and TEM images of complete hollow spheres (b) [255]

Typical SEM and TEM images of the hollow microspheres are shown in Fig. 5.61. As TEM shown, the microspheres are hollow with $150-250$ nm in shell thickness, which are constructed with final fibers $20-30$ nm in average diameter and $150-250$ nm in average length. Moreover, the insides of the hollow microspheres were rougher than that the outsides, suggesting the oxidation reaction took place

within the reversed emulsion [255]. It noted that stirring fashion affects on the formation of such hollow micro-spheres assembled from the nanofibers, for instance, enough emulsified by using ultra-sonic irradiation before oxidation is required in order to form uniform reversed micro-emulsion. Once the polymerization took place, however, ultra-sonic irradiation during initial polymerization was performed for a short time (e.g. 10 min). After that, the polymerization process was carried out without ultra-sonic irradiation in order to obtain completed micro-spheres because high energies of ultra-sonic will destroy the resulting micro-spheres [255], indicating fashion and time of the ultra-sonic irradiation during different polymerization stages plays a critical role in forming completed micro-spheres.

As well known, β-NSA is an amphiphilic molecule due to its lipophilic $OC_{10}H_7$ and hydrophilic OSO_3H groups, which is also a counterion for the doped PANI. As a result, the β-NSA dopant plays doping and surfactant functions at the same time. Moreover, aniline/NSA micelles are formed in an aqueous solution through an acid/base reaction.

Therefore, the reversed microemulsion with a core–shell structure is regarded as a "microreactor", where water (the core) is a soft template in the formation of the microspheres whereas the aniline/NSA micelle (the shell) acts as a soft template in the formation of the nanotubes or nanofibers. Once APS is added as the oxidant, aniline oxidation polymerization only took place inside close to the water phase of the "microreactor" because of its hydrophilicity. This is consistent with the outside surface of the microspheres is smoother than the inside surface [255]. According to above-discussions, coordination effect of the reversed-emulsion polymerization with micelles as the the nanofiber soft-templates might be a driving force in the formation of 3D-microspheres assembled from 1D-nanofibers. Moreover, it seems that water plays a critical role in controlling the diameter and formation yield of the hollow microspheres, for instance, the hollow microspheres are only obtained in a narrow range of the [water]/[aniline/NSA] ratios, and the diameter increased to $5.0 - 8.0 \, \mu m$ as increasing the ratio [255]. The hollow microspheres are identical to the emeraldine salt form of PANI, as characterized by FTIR, which is also consistent with conductivity $(6.2 \times 10^{-2} - 1.5 \times 10^{-1} \, S/cm)$, as measured by four-probe method [255].

5.6   Potential Applications of Conducting Polymer with Micro/Nanostructures

In principle, applications of the nanostructure conducting polymers are similar to that of their bulk materials. Since conducting polymer nanostructures are advantageous of light-weight, large surface areas and high conductivity compared with their bulk materials, performance of the micro/nanostructure conducting polymers better than that of the bulk materials is expected, as described in

Chapter 4. Moreover, it has been demonstrated that template-free method is facile, low-cost and controlling approach to conducting polymer micro/nanostructures that provides a basic prerequisite for studying potential application of the conducting polymer micro/nanostructures. Since conducting polymer-based microwave absorbing and EMI materials as well as sensors are active objects in the field of conducting polymers, therefore, author tried to investigate possibility of the template-free synthesized conducting polymer nanostructures as microwave absorbing and SMI materials as well as sensors guided by wettability.

5.6.1 Microwave Absorbing Materials

From discussion of Chapter 3, it is well known that conducting polymer-based microwave absorbing materials have received great attention in the field of the conducting polymers. Compared with traditional inorganic microwave absorbing materials, the conducting polymer-based microwave absorbing materials are advantageous of lower surface mass, easy complex and processing as well as adjustable electromagnetic parameters by changing the doping degree, dopant nature, main polymer chain, synthetic method and conditions [3].

So far, a series of papers concerning conducting polymer-based microwave absorbing materials have been reported in the literature [256]. Among these conducting polymer-based microwave absorbing materials, PANI or PPy is regarded as a promising conducting polymer-based microwave absorbing materials because of high conductivity, easy synthesis of large-mass by chemical polymerization, and controlling electromagnetic parameters by adjusting both oxidation and protonation state [3]. For instance, influence of dopant nature and protonation state on the dielectric properties of PANI at the microwave frequency ($f = 8 - 18\,\text{GHz}$) have been reported [256a and c]. However, most results reported in the literature showed the conducting polymer-based microwave materials belong to typical dielectrical loss materials at the microwave frequency, which can't satisfy the application requirements, because both dielectrical and magnetic loss at the microwave frequency region is required for practice application of microwave absorbing materials.

It is necessary to improve the magnetic losses of the conducting polymer-based microwave absorbing materials in order to enhance its absorbing efficiency and to expand the absorbing band at the microwave frequency. There are three ways to solve above issues. One is blending conducting polymers with inorganic magnetic materials to prepare hybrid composites with both dielectrical and magnetic loss. This is a common approach; however, the surface mass of the hybrid composites is limited by adding magnetic loss materials. The second way is to synthesize tubular conducting polymers, because theoretical calculations reveal that the tubular materials exhibit a unique absorption character [257]. However, synthesis of large-scaled mass and low-cost for the micro/nanostructure conducting polymers

is challenge, because hard-template, as main method, is unsatisfied due to size limitation of the membrane as the hard-templates. Since the absorbing properties and working frequency of the chiral materials can be adjusted by changing their real and ideal dielectric constant [258], recently, chiral materiers have therefore received great attention as new type of microwave absorbing materials.

   As above-mentioned, conducting polymers even their nanostructures with chiral structure can be synthesized by template-free method. Therefore conducting polymers blended with chiral materials or direct synthesis of chiral conducting polymer nanostructures maybe prove the third way to improve dielectrical and magnetic loss of the conducting polymers at microwave frequency. Author tried above-three approaches to improve feature of the conducting polymer-based microwave absorbing materials at the microwave frequency.

1. Chiral PANI Microtubes Doped with β-NSA/D-Glucose as The Co-Dopant

Template-free synthesized and doped with β-NSA/D-glucose as the co-dopant chiral PANI microtubes were chosen to study their microwave absorbing properties at microwave frequency (1 – 18 GHz), which were basically considerations as follows: ① Template-free method, a self-assembly process, is a universal and controllable approach to synthesize conducting polymer micro/nanostructures. ② PANI-β-NSA microtubes with high formation yield and unique properties [11]. ③ D-glucose is not only has chiral feature, but also doping function. When β-NSA and D-glucose are used as the co-dopant, it is found that β-NSA is served as either the soft-template or dopant at the same time while D-glucose is contributed to chiral characteristic of the microtubes [16]. Both PANI-β-NSA and PANI-β-NSA/D-glucose are tubular morphology in shape with 1 – 3 μm in diameter as shown in Fig. 5.62, indicating the addition of D-glucose as the co-dopant does not change the morphology of the microtubes.
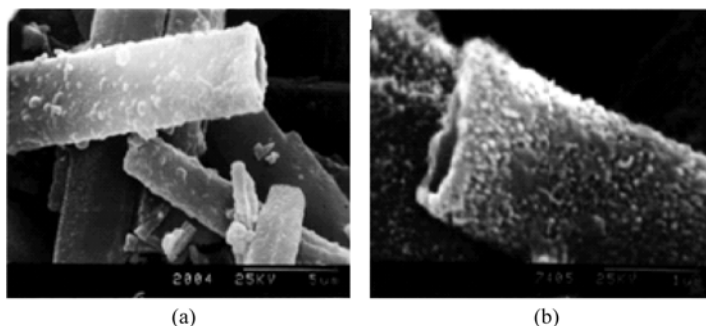

(a)   (b)

Figure 5.62   SEM images of the microtubes of PANI-β-NSA (a) and PANI-β-NSA/D-glucose (b) prepared by template-free method [16]

   Moreover, both microtubes are identical with the emeraldine salt form of PANI, as measured by FTIR and UV-visible spectra [16] that is also consistent with the

conductivity of 3.5 S/cm for PANI-β-NSA and 2.6 S/cm for PANI-β-NSA/D-glucose, as measured by four-probe method [16].

As shown in Fig. 5.63, both dielectrical and magnetic losses at $f = 1-18\,\text{GHz}$ are observed in both microtubes. However, the magnetic loss of PANI-β-NSA/D-glucose microtubes is higher than that of PANI-β-NSA microtubes, which is contributed to chiral feature of D-glucose dopant [258]. The magnetic losses observed in the PANI-β-NSA/D-glucose nanotubes was intrinsic, which was proved by some positive evidences as follows: ① The granular PANI-β-NSA only shows dielectrical loss without magnetic loss at the microwave frequency, while tubular PANI-β-NSA/D-glucose exhibited unusual high magnetic loss at the microwave frequency as shown in Fig. 5.64(a). ② There was no magnetic loss in the β-NSA dopant and the aniline/β-NSA salt as shown in Fig. 5.64(b). Based on above evidences, thus, high magnetic loss at $f = 1-18\,\text{GHz}$ region observed from the PANI-β-NSA/D-glucose nanotubes is reasonable, which probably arose from partial order of the polarons, as charge carries, along the tubes [259].

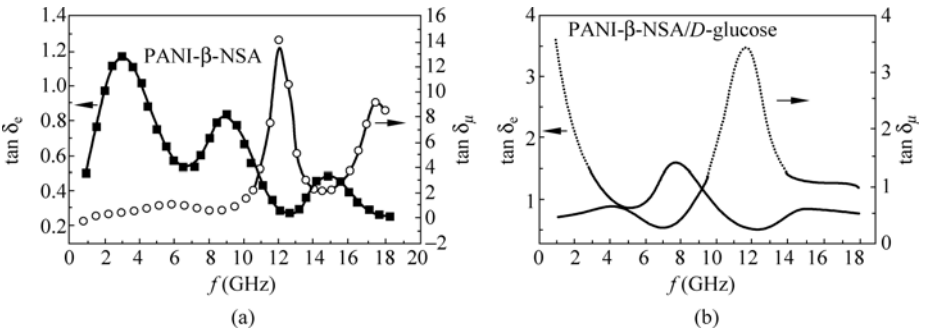
Figure 5.63 Dependence of the microwave frequency on the dielectrical and magnetic electromagnetic loss of the microtubes of PANI-β-NSA (a) and PANI-β-NSA/D-glucose (b) [16]
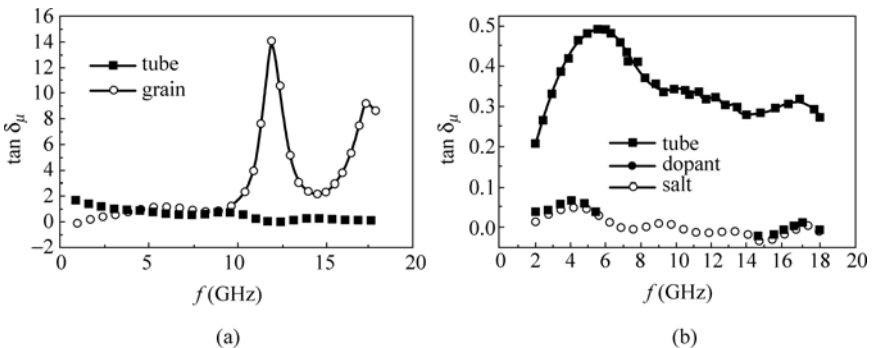

Figure 5.64 Influence of morphology of PANI-β-NSA on the magnetic loss at $f = 1-18$ GHz (a) and dependence of the microwave on the magnetic loss at $f = 1-18$ GHz for tube, dopant and salt respectively (b) [16]

2. PPy-*p*-TSA Nanotubes as New Microwave Absorbing Materials

Theoretical calculation on microwave materials revealed that absorption properties of a material at a microwave frequency (1 – 18 GHz) predicted that the tubular materials exhibited novel microwave absorption characters [257]. This is consistent with our observations, for instance, the template-free synthesized PANI-DBSA micro/nanotubes exhibited both dielectric and magnetic loss in the frequency region of 1 – 18 GHz [16, 260], while the bulk PANI-DBSA synthesized by a conventional method only shows dielectric loss at microwave frequency without magnetic losses.

In general, the dielectrical loss of the microwave absorbing is related to their conductivity at room temperature [3]. Among these conducting polymers, PPy is outstanding owing to its high conductivity at room-temperature and stability in air. Moreover, its room-temperature conductivity is generally higher than that of PANI when the same dopant is used [3].

Therefore, the template-free synthesized PPy nanostructures might be used as excellent microwave absorbing materials. Along this line, large-scaled mass of the PPy-*p*-TSA nanotubes with a room-temperature conductivity as high as 27 S/cm have been synthesized by template-free method [23a]. Typical SEM and TEM images of PPy-*p*-TSA nanotubes as well as photograph of large-mass sample and sample of single coated for measurement of absorbing efficiency are shown in Fig. 5.65.
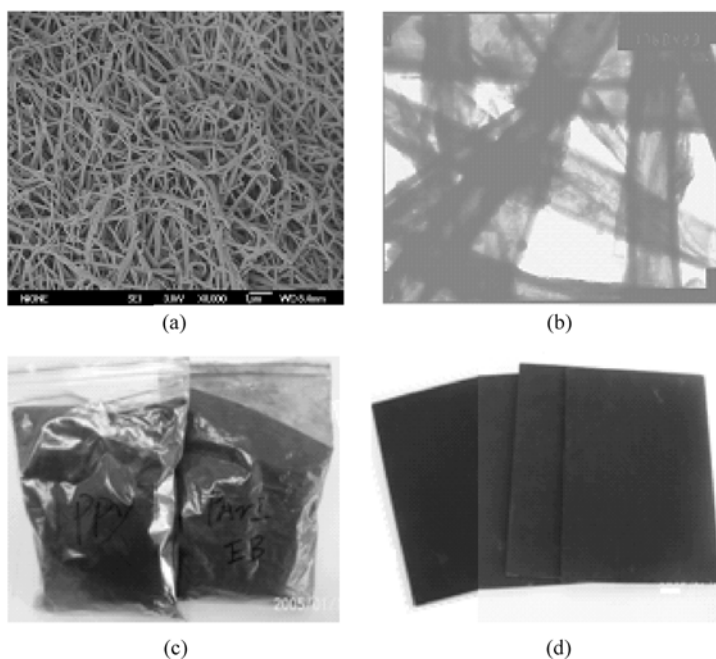

(a)

(b)

(c)

(d)

Figure 5.65   PPy-*p*-TSA nanotubes prepared by template-free method: SEM images (a), TEM images (b) and powder samples (c) [23a]

Large-scaled mass of the PPy-p-TSA nanotubes provided a possibility to measure the absorbing efficiency (R) at $f = 8 - 18$ GHz for a single layer coated on aluminum substrate (180 mm × 180 mm). The relative permittivity (ε_r) and permeability (μ_r) of the PPy-p-TSA nanotubes is a function of the microwave frequency (f) as shown in Fig. 5.66(a). Like PANI-β-NSA/D-glucose nanotubes [260], both dielectrical and magnetic losses are observed in the PPy-p-TSA nanotubes. According to "conductive-island" proposed by author [261], the dielectric loss of conducting polymer micro/nanostructures mainly results from interface polarity caused by polaron produced through a doping process.
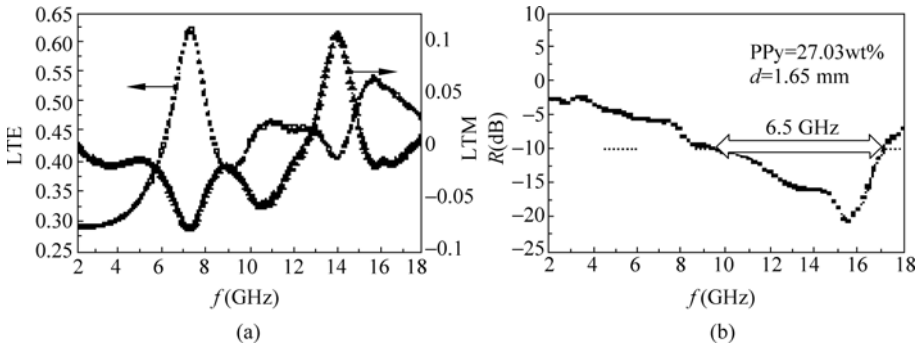

Figure 5.66 Dielectric and magnetic loss as a function of frequency at $1 - 18$ GHz PPy-p-TSA nanotubes (a) and reflection efficiency of single layer of PPy-p-TSA coated on aluminum sheet (180 mm × 180 mm × 1.68 mm) at $f = 8 - 18$ GHz (b) [260]

Although the magnetic losses observed in the micro/nanotubes is not clearly understood at the present time, it might result from a co-ordination effect of spin-polaron (i.e. charge carrier) and orientation of polymeric chain along the tubes. Dependence of absorbing efficiency, R, with microwave frequency ($f = 8 - 18$ GHz) for a single layer (e.g. 1.68 mm in thickness) of the PPy-p-TSA nanotubes coated on aluminum substrate (180 mm × 180 mm) and a bandwidth as high as 6.5 GHz at an average level of about 10dB was estimated [260], opening a new way to improve feature of conducting polymer-based microwave absorbing materials.

Above results promised author to calculated the relative permittivity and permeability of conducting polymers with different morphology at the microwave frequency region ($f = 1 - 18$ GHz) by using numerical analysis [262]. The calculated results are summaried as follows: ① Both dielectric and magnetic loss are affected by their morphology and obey an order of sheets > tubes > spheres [262] as shown in Fig. 5.67. ② The position corresponding to maximum absorption efficiency is shifted to high frequency as increasing the fraction of the nanostructures in the absorbing layers. In addition, the absorption characters of hollow structured materials are better than that of solid materials, which is also dependent upon the fraction of the hollow structures in composites as shown in Fig. 5.68.
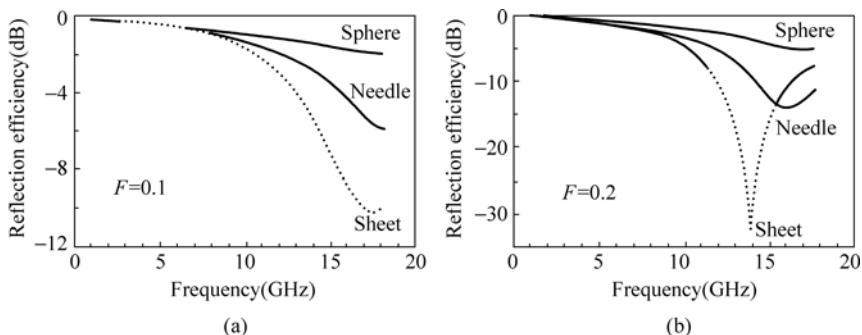
Figure 5.67　Reflection efficiency calculated at $f = 1 - 20$ GHz for different morphology of PANI-NSA as microwave absorbing materials [260]
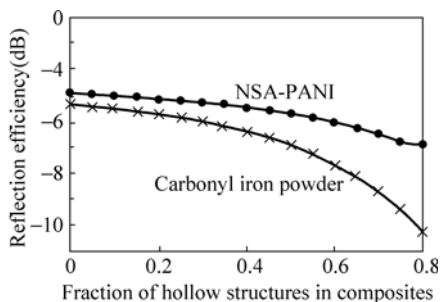

Figure 5.68　Effect of hollow fraction of materials on calculated reflection efficiency for PANI-NSA and carbonyl irons, respectively [260]

Although conducting polymer-based microwave absorbing materials have received great attention in the stealth materials owing to their high conductivity, controlling dielectro-magnetic properties and lightweight, their commercial application at current time is still limited by their narrow bandwidth due to only having dielectric loss and poor strength. Investigations on conducting polymer-based microwave absorbing materials should therefore forward to enhancing the absorbing efficiency, expending bandwidth and improving mechanical properties. Although hybrid composites of the conducting polymers with magnetic losses is a common way for improving magnetic loss of the conducting polymers, addition of the magnetic loss materials in the hybrid is limited because these magnetic materials are usually heaving. Above results on the conducting polymer nanostructures prepared by template-free method open a facile and efficient approach to fabricate conducting polymer-based microwave materials that satisfy requirements for developing new type microwave absorbing materials.

5.6.2　EMI Shielding Materials

From discussion in Chapter 3, it is well known that conducting polymers can be

served as new EMI shielding materials owing to their low density (e.g. 1.1 – 1.3 g/cm^3), metal-like conductivity, good processability and corrosion-less. In order to realize their application as EMI shielding materials, however, their processability must be solved. Like other conducting polymers, although PANI is regarded as excellent EMI shielding materials, it is generally categorized as an intractable material. Therefore melt-processing of PANI is not possible owing to decomposing at temperature below a softening or melting point.

However, discovery of counter-ion induced processability of the doped PANI with CSA [4] opened a feasibility of processing in the conducting form of PANI. Protonated PANI with suitably functionalized acids can be processed from solution to enable the fabrication of thin films, sheets, fibers, transparent conductive films, bulk parts [4]. Moreover, a variety of conducting poly-blends containing PANI can be fabricated that is advantageous of omits post-processing chemical treatment. However, both conducting PANI complex and poly-blends are needed co-soluble in a solvent. In addition, these materials exhibit relatively high levels of electrical conductivity at low volume fractions of the PANI complex, while maintaining excellent mechanical properties, essentially equivalent to those of the host bulk polymer [4]. Among these soluble PANI doped with functionalized protonic acids, CAS is the best functionalized acids for the soluble PANI because their high conductivity (e.g. 100 – 400 S/cm), high mechanical properties and low percolation threshold [263]. In general, m-cresol is used as a good solvent for PANI-CSA, resulting in high conductivity and mechanical properties, but it is a toxicant solvent. The PANI doped with DBSA is soluble in CH$_3$Cl rather than m-cresol, but its conductivity is lower than that of PANI-CSA (1 S/cm) [4a, 264]. Since both of PANI-CSA and PANI-DBSA are soluble although in different solvent, it is possible to fabricate free standing films or coated layers of PANI-CSA and PANI-DBSA through a solution process. By using above-method, author successfully prepared free-standing films of the PANI-DBSA-based blends with different content of PANI-CSA. This method avoids using large aquatitum of toxicant m-cresol solvent. Moreover, the conductivity of the blends increases with increase of the content of the PANI-CSA and the maximum conductivity is achieved as high as about 160 S/cm when the content of PANI-CSA is about 5%. This method not only remains the conductivity of the blends as high as that conductivity of the PANI-CSA films (e.g. 200 S/cm), but also most m-cresol solvent replacing by CH$_3$Cl.

CNTs have received considerable scientific interest as EMI shielding materials due to their low specific mass and excellent electrical, thermal and mechanism properties [265]. Moreover, the high aspect ratio of CNTs allows small amounts to be dispersed in polymer materials to yield composite materials with superior properties [266]. Since large sacaled free-standing films of PANI doped with CSA and DBSA as the co-dopant can be fabricated by a solution process, author tried to prepare composite films of PANI-CSA/DBSA blended with multi-walled carbon nanotubes (MCNTs) as the EMI shielding materials. Room temperature

conductivity of pure MCNTs pellets, as measured by four-probe method, was as 8 S/cm. With addition of MCNTs increasing to 25%, the room temperature conductivity of the composite films accordingly increases from 162 S/cm to a maximum of 212 S/cm followed by sharply declines after the MCNTs fraction of 25% (Fig. 5.69), indicating the conductivity of the composite films is enhanced by adding MCNTS. Based on calculated equation of the *SE* at near-field and far-field, as discussed in Chapter 4, the *SE* value for composite films with different fraction of MCNTs was calculated in the range 1 – 1000 MHz and at room temperature. As shown in Fig. 5.69, the maximum *SE* value as high as 90 – 100 dB was obtained from the composite films with 25% weight fraction of WCNTs [267]. Above-results suggested that the method might open a new way to prepare conducting polymer-based EMI shielding materials, which is advantageous of light-weight, highly conductivity and processability compared with metal-based EMI shielding materials.
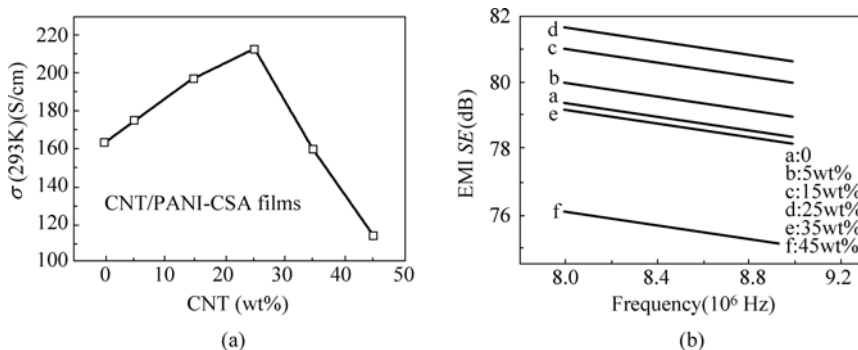

(a)   (b)

Figure 5.69   Room temperature conductivity (a) and *SE* (b) of the PANI-CSA/ DBSA-MCNT composite films as a function of the loading MCNTs. The *SE* was calculated by using equation of $SE\,(dB) = 20\,\lg[cZ_0\sigma d/(2\omega r)]$ and assuming each sample's thickness (*d*) and effective source-shield distance (*r*) is $d = 2.0 \times 10^{-5}$ m and $r = 3.95 \times 10^{-2}$ m, respectively [267]

5.6.3   Conducting Polymer Nanostructure-Based Sensors Guided by Reversible Wettability

As discussed in Chapter 4, conducting polymer as a chemical or electrochemical sensor is one of major applications of the conducting polymers in technologies. In principle, the conducting polymer sensors are based on reversible change of conductivity from insulator to metal by doping/de-doping process. Since nanostructure conducting polymers are advantageous of large surface areas compared with their bulk materials, their nanostructure-based sensors with a high sensitivity and fast responding are expected. Recently, control of the surface wettability has received considerable attention because of their promising applications in intelligent

devices based on reversible switching between superhydrophobicity and super-hydrophilicity [268]. So far, light irradiation [269], thermal [270] and acidic [268c and g] treatment have been used to control the wettability of material surface. In particular, the wettability of conducting polymers has recently received attention because of it being a crucial parameter for controllable separation and application of conducting polymer-based sensors [271].

As discussed in Chapter 2, PANI is an excellent conducting polymer because of its good environmental stability, easy synthesis, and a controlling reversible acid/base doping process [191c]. Especially the reversible insulator/conductor of PANI is controlled by both protonation and oxidation state [191c]. The reversible transition of doping/dedoping process and tuned oxidation states has been employed for applications in such as optical sensors, chemical sensors, and biosensors [272]. However, few papers dealing with *in-situ* wettability transition between superhydrophobicity and super-hydrophilicity for PANI has been reported.

Wettability of surface is governed by both the chemical composition and the geometrical microstructure of a surface [273]. In other words, low surface energy composition and rough surface are basic requirements for a superhydrophobic surface of materials. Based on definition of wettability, therefore conducting polymers with coexisted microstructure and nanostructures and doped with a low surface energy material as a dopant might be developing a new type of reversible switching devices by changing surface wettability. Based on above idea, author recently carried out some studies on sensors based on the reversible wettability of PANI micro/nanostructures and their composites.

1. PANI-PAN Coaxial Nanofibers

Coaxial nanofibers of PANI coated electro-spun polyacrylonitrile (PAN) were prepared by a chemical polymerization [274]. As shown in Fig. 5.70, the electro-spun PAN fibers ($d{\sim}127$ nm) are smooth, but surface of the coaxial PANI-PAN fibers ($d{\sim}273$ nm) are very rough caused by PANI particles (~ 80 nm in diameter) deposited on the surface of the PAN nanofibers. Such rough surface of the coaxial PANI-PAN is advantageous for a superhydrophobic surface. In order to satisfy low surface energy of the PANI-PAN nanofibers, the nanofibers are post-doped with perfluorooctanesulfonic acid (PFOS, $C_8F_{17}SO_3H$). Wettability of the PANI-PAN coaxial nanofibers doped with PFOS was evaluated in terms of water CA.

As shown in Fig. 5.71, the surface of PFOS-doped PANI-PAN coaxial nanofibers is superhydrophobic with a water CA as high as 164.5°, indicating the PFOS is not only reserved as dopant, but also bring about hydrophobic function because of its —SO_3H group and perfluorinated carbon chain [274]. It is well known that the air trapped in the surface is very important to superhydrophobicity because the water CA of air is regarded to be 180°. The hierarchical structures of the PANI-PAN nanofibers doped with PROS increase the surface roughness dramatically so that air can be trapped in the aperture of nanofibers. Based on above discussions, the superhydrophobicity results from a coordinative effect of the superhydrophobic PFOS and hierarchical structures [274].
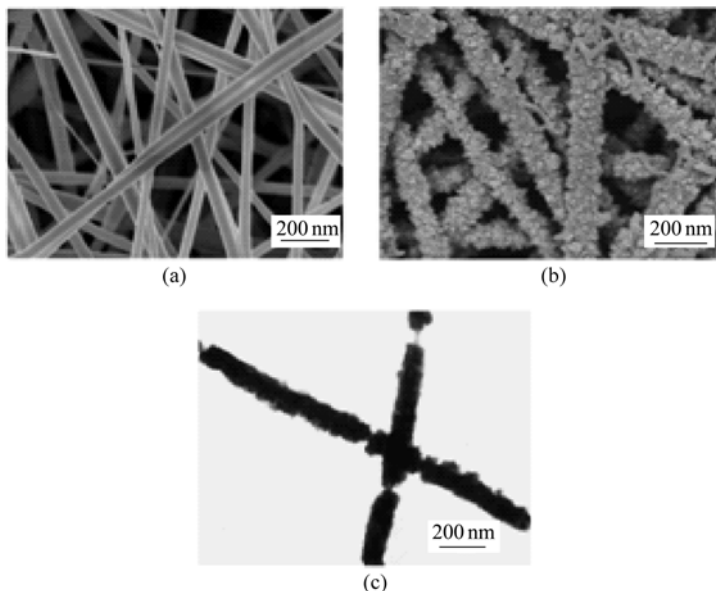
(a)

(b)

(c)

Figure 5.70　(a) SEM image of the electro-spun PAN nanofibers; (b) SEM image of PANI-PAN coaxial nanofibers; (c) TEM image of PANI-PAN coaxial nanofibers [274]
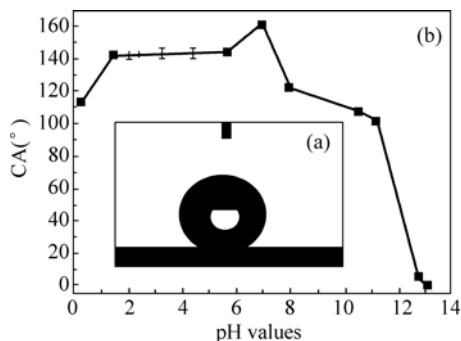
Figure 5.71　(a) Water droplet on the surface of the PANI-PAN coaxial nanofibers; (b) the relationship of the pH values of probe liquid and the CAs on the PFOS-doped PANI-PAN coaxial nanofibers [274]

Since PANI is sensitive to pH due to proton doping mechanism, thus, the CA is as a function of the pH values of probe liquid as shown in Fig. 5.71. Because of the conductivity of PANI is also controlled by its oxidation state [191c], moreover, the wettability is also a function of the redox properties of probe solution [274]. Reversible superhydrophobicity/super-hydrophilicity on the surface of PFOS-doped PANI-PAN coaxial nanofibers for a basic and an acidic droplet is shown in Fig. 5.72. These results demonstrate that sensors made of conducting polymer nanostructures doped with a low surface enegy dopant can be guided by

adjusting wettability through doping/de-doping process, expending sensitive region of conducting polymer-based sensors.

Figure 5.72 Reversible superhydrophobicity/super hydrophilicity on the surface of PFOS-doped PANI-PAN coaxial nanofibers for a basic (a) and an acidic droplet (b) [274]

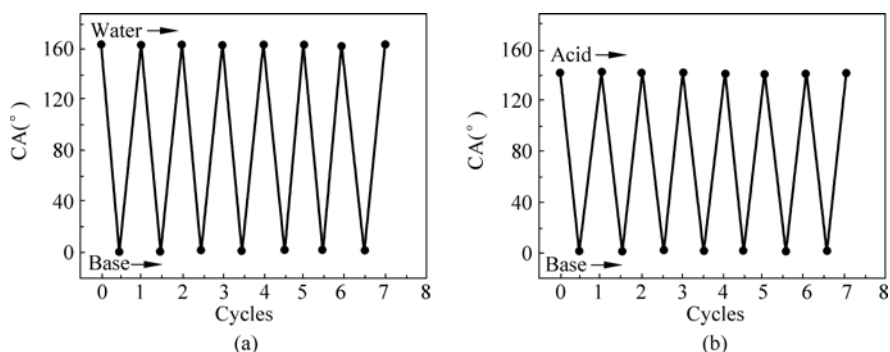## 2. PANI-PFSEA Coated Fabrics as Ammonia Gas Monitor

Fabric is an excellent substrate to be coated conducting polymers as the conductive composites because of synthesis sample, low cost, high strength and flexible. Above-results showed that nanostructure conducting polymer-based sensors could be guided by adjusting wettability that promised author to further fabricate PANI coated on polyester fabrics with high surface area and high strength by using *in-situ* doping polymerization in the presence of perfluorosebacic acid (PFSEA) as the dopant [180]. Since PFSEA is a typical dopant with a low surface energy, it not only has dopant function, but also brings about superhydrophobic properties to the PANI-PAN fibers. Moreover, the PANI-PFSEA nano-particles (~ 180 nm in diameter) are coated on the surface of the fabric, resulting in double-roughness structure which is the favorable structure for superhydrophobic surface.

Thus, coordination effect of reversible doping/dedoping of PANI, large surface area of the polyester fabric and low surface energy of PFSEA results in fast switching from superhydrophobic to superhydrophilic triggered by ammonia gas is reversible [180].

Similar phenomena were observed from all PANI-PFSEA coated on four-different fabrics as the substrates, indicating the method is reproducible. As predicted, the doped fibers are superhydrophobicity with a static CA as high as 160.9° due to a coordination effect of the pore structure of fabric and a low surface energy of the PFSEA dopant. After the doped fabric exposed to dry ammonia gas for 1 min, the water droplets on the surface of fabric spread out in less than 12 s, resulting in a CA of about 0°, exhibiting superhydrophilic behavior as shown in Fig. 5.73.
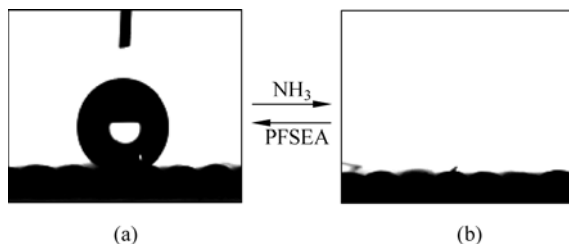
Figure 5.73   Photographs of water droplet shape on the PANI-PFSEA coated S130 fabric before (a) and after (b) treatment by ammonia gas [180]

Obviously doping/de-doping process of PANI results in changing wettability of the PANI-PFSEA coated fabrics from superhydrophobic to superhydrophilic. In particular, the superhydrophobic PANI-PFSEA coated fabric is chemically stable even over several months without any special treatment, and the reversible switching wettability can be repeated several times as shown in Fig. 5.74, exhibiting high reproducibility and stability [180]. To evaluate the properties of PANI-PFSEA coated fabric as the sensors, the normalized contact angle change (θ/θ_0), where θ and θ_0 denote the real-time contact angle and the initial contact angle, was measured, respectively. It is found that change in the normalized contact angle is a function of the concentration of ammonia gas as shown in Fig. 5.74(b), indicating the ammonia-responsive reversible wettability allows PANI-PFSEA coated fabric can be used as sensor to monitor ammonia gas. The fast response, stability, flexible and good reproducibility of the superhydrophobic PANI-PFSEA coated fabrics makes them possess potentially applications for ecology and biotechnology.
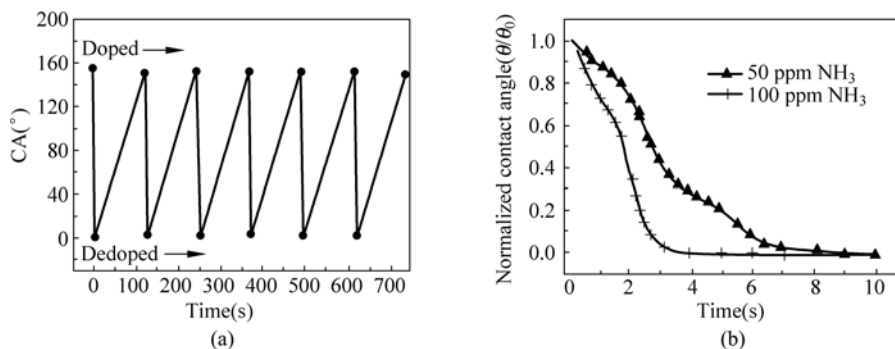
Figure 5.74   (a) Reversible superhydrophobic-superhydrophilic conversion of the PANI-PFSEA coated fabric S130 through doping with PFSEA and de-doping by ammonia gas; (b) Response of PANI-coated fabric S130 with time when it was exposed to 100 and 50 ppm gaseous ammonia of apparent concentration [180]

Above results show promising potential application of the nanostructure conducting polymers as microwave absorbing and EMI materials as well as pH

and gas sensors guided by wettability, however, some basic issues for realizing their applications in technology are still required to be solving. For microwave absorbing materials, for instance, large-scaled mass, low-cost and reproducible synthesis of the nanostructured conducting polymers is firstly solved. Moreover, it needs understanding mechanism of magnetic losses of conducting polymer nanostructures in microwave frequency. In addition, to improve sensitivity, responsibility and reproducibility of the nanostructure conducting polymer-based sensors guided by wettability is still required in order for commercial applications.

References

[1] M. X. Wan, Y. Q. Shen, J. Huang. Chinese Patent No. 98109916.5, 1998

[2] C. R. Martin. Science, 1994, 266: 1961

[3] Handbook of Conducting Polymers (Eds: T. A. Skotheim, R. L. Elsenbaumer, J. R. Reynolds, 2nd ed.). New York: Marcel Dekker, 1998

[4] a) Y. Cao, P. Smith, A. J. Heeger. Synth. Met., 1992, 48: 91; b) Y. Cao, J. Qiu, P. Smith. Synth. Met., 1995, 69 – 71: 187

[5] a) A. F. Diaz, K. K. Kanazawa, G. P. Gardini. J. Chem. Soc.; Chem. Commun., 1979, 635; b) T. A. Skotheim (ed.). Handbook of Conducting Polymers. New York: Marcel Dekker, 1986, Vol. 1

[6] P. Audebert, P. Aldebert, N. Girault. Synth. Met., 1993, 58: 251

[7] E. E. Havinga, L. W. V. Horssen, W. T. Hoeve, H. Wynberg, E. W. Meijer. Polym. Bull., 1987, 18: 277

[8] D. Stanke, M. L. Hallensleben, L. Toppare. Synth. Met., 1995, 73: 267

[9] J. Y. Lee, D. Y. Kim, C. Y. Kim. Synth. Met., 1995, 74: 103

[10] Y. Q. Shen, M. X. Wan. Synth. Met., 1998, 96: 127

[11] J. Huang, M. X. Wan. Journal of Polymer Science, Part A: Polymer Chemistry, 1999, 37: 1277

[12] N. F. Mott, E. A. Davis. Electronic Processes in Non-crystalline Materials (2nd Ed.). Oxford: Clarendon Press, 1979

[13] M. X. Wan, J. Huang, Y. Q. Shen. Synth. Met., 1999, 101: 708

[14] J. Huang, M. X. Wan. Solid State Communications, 1998, 108: 255

[15] M. X. Wan, J. P. Yang. Synth. Met., 1995, 73: 201

[16] M. X. Wan, J. L. Li. Polym. Adv. Tech., 2003, 14: 320

[17] F. R. Diay, C. O. Shanchey, A. M. Del Valle, J. C. Bernede, Y. Tregouet. Bol. Soc. Chil. Quim., 2000, 45: 181

[18] S. Qing, M. X. Wan. J. Polym. Sci. Part A: Polym. Chem., 1999, 37: 1443

[19] Z. X. Wei, Z. Zhang, M. X. Wan. Langmuir, 2002, 18: 917

[20] S. Atkinson, H. S. O. Chan, A. J. Neuendorf, S. C. Ng, T. T. Ong, D. Young. J. Chem. Lett., 2000, 276

[21] Z. X. Wei, M. X. Wan. Journal of Applied Polymer Science, 2003, 87: 1297

[22] A. G. MacDiarmid, J. C. Chang, M. Halpern, W. S. Mu, N. L.Somasiri, W. Wu, S. I. Yaniger. Mol. Cryst. Liq. Cryst., 1985, 121: 187

[23] a) Y. Q. Shen, M. X. Wan. Journal of Polymer Science. Part A: Polymer Chemistry, 1997, 35: 3689; b) J. Liu and M. X. Wan. J. Mater. Chem., 2001, 11: 404

[24] J. Huang and M. X. Wan. J. Polymer. Sci. Part A: Polymer. Chem., 1999, 37: 1443

[25] a) J. Ouyang, Y. Li. Polymer, 1997, 38: 3997; b) J. Ouyang and Y. Li. Synth. Met., 1996, 79: 121

[26] Y. S. Yang, M. X. Wan. J. Mater. Chem., 2001, 11: 2022

[27] Y. S. Yang, J. Liu, M. X. Wan. Nanotechnology, 2002, 13: 771

[28] W. R. Salanak, R. P. J. Erlandsson, I. Lundström, D. Inaganas. Synth. Met., 1983, 5: 125

[29] E. M. Genies, A. A. Syed. Synth. Met., 1984, 21: 10

[30] a) M. Li, E. L. Zhou, J. P. Xu, C. C. Yang, X. Y. Tang. Polym. Bull., 1995, 35: 65; b) H. J. Qiu, M. Li, X. F. Chen. Liq. Cryst., 1998, 25: 419

[31] N. Carr, M. Goodwin. J. Makromol. Chem. Rapid Commun., 1987, 8: 487

[32] a) S. A. Chen, C. S. Liao. Makromol. Chem. Rapid Commun., 1993, 14: 69; b) A. Natansohn, P. Rochon, X. Meng, C. Barrett, T. Buffeteau, S. Bonenfant, M. Pezolet. Macromolecules, 1998, 31: 1155

[33] H. J. Qiu, M. X. Wan. Chin. J. Polym. Sci., 2001, 19: 65

[34] H. J. Qiu, M. X. Wan. Journal of Polymer Science. Part A: Polymer Chemistry, 2001, 39: 3485

[35] G. S. Kumar, D. C. Neckers. Chem. Rev., 1989, 89: 1915

[36] J. R. Jr. Santos, J. A. Malmonge, A. J. G. C. Silva, A. J. Motheo, Y. P. Mascarenhas, L. H. C. Mattoso. Synth. Met., 1995, 69: 141

[37] a) P. C. Innis, I. D. Norris, L. A. P. Kane-Maguire, G. G. Wallace. Macromolecules, 1998, 31: 6521; b) H. Guo, C. M. Knobler, R. B. Kaner. Synth. Met., 1999, 101: 44; c) S. Su, N. Kuramoto. Macromolecules, 2001, 34: 7249

[38] L. J. Zhang, M. X. Wan. Nanotechnology, 2002, 13: 750

[39] L. T. Cai, S. B. Yao, S. M. Zhou. J. Electroanal. Chem., 1997, 421: 45

[40] R. D. McCullough, R. D. Lowe. J. Chem. Soc., Chem. Commun., 1992, 70

[41] a) Z. H. Wang, A. Ray, A. G. MacDiarmid, A. J. Epstein. Phys. Rev. B, 1991, 43: 4373; b) A. Ezquerra, J. Ruhe, G. Wegner. Chem. Phys. Lett., 1987, 144: 194

[42] A. Kobayashi, X. F. Xu, H. Ishikawa. J. Appl. Phys., 1992, 72: 5702

[43] J. P. Pouget, M. E. Jozefowicz, A. J. Epstein, X. Tang, A. G. MacDiarmid. Macromolecules, 1991, 24: 779

[44] a) W. J. Bae, W. H. Jo, Y. H. Park. Synth. Met., 2003, 132: 239; b) A. Gok, H. K. Can, B. Sari, M. Talu. Mater. Lett., 2005, 59: 80; c) H. K. Chaudhari, D. S. Kelkar. J. Appl. Polym. Sci., 1996, 62: 15

[45] Z. M. Zhang, M. X. Wan, Y. Wei. Adv. Funct. Mater., 2006, 16: 1100

[46] J. Laska, D. Djurado, W. Luzny. Eur. Polym. J., 2002, 38: 947

[47] Y. Z. Long, L. J. Zhang, Z. J. Chen, K. Huang, Y. S. Yang, H. M. Xiao, M. X. Wan, A. Z. Jin, C. Z. Gu. Phys. Rev. B, 2005, 71: 165

[48] a) L. Dai, J. Lu, B. Matthews, A. W. H. Mau. J. Phys. Chem. B, 1998, 102: 4049; b) J. Lu, L. Dai, A. W. H. Mau. Acta Polym., 1998, 49: 371

[49] B. R. Mattews, G. Holan. Int. Pat. Appl. WO 95/34595, Dec 21, 1995

[50] a) M. Bockstaller, W. Köhler, G. Wegner, D. Vlassopoulos, G. Fytas. Macromolecules, 2000, 33: 3951; b) O. Karthaus, N. Maruyama, X. Cieren, M. Shimomura, H. Hasegawa, T. Hashimoto. Langmuir, 2000, 16: 6071

[51] H. J. Qiu, M. X. Wan, B. Matthews, L. M. Dai. Macromolecules, 2001, 34: 675

[52] a) A. Bachtold, P. Hadeky, T. Nakanish, C. Dekker. Science, 2001, 294: 1317; b) S. Fan, M. G. Chapline, N. R. Franklin, T. W. Tombler, A. M. Cassell, H. Dai. Science, 1999, 283: 512; c) S. Frank, P. Poncharal, Z. L. Wang, W. A. de Heer. Science, 1998, 280: 1744

[53] J. L. Bahr, E. T. Mickelson, M. J. Bronikowski, R. E. Smally, J. M. Tour. Chem. Commun., 2001, 93

[54] J. Sandler, M. Shaffer, T. Prasse, W. Bauhofer, K. Schulte, A. H. Windle. Polymer, 1999, 40: 5967

[55] a) G. Z. Chen, M. S. P. Shaffer, D. Coleby, G. Dixon, W. Zhou, D. J. Fray, A. H. Windel. Adv. Mater., 2000, 12: 522; b) C. Douns, J. Nugent, P. M. Ajayan, D. J. Duguette, K. S. V. Santhanam. Adv. Mater., 1999, 11: 1028

[56] H. Ago, K. Pertritsch, M. S. P. Shaffer, A. H. Windle, R. H. Friend. Adv. Mater., 1999, 11: 1281

[57] E. Kymakis, G. A. J. Amaratunga. Appl. Phys. Lett., 2002, 80: 112

[58] S. A. Curran, P. M. Ajayan, W. J. Blau, D. L. Carroll, J. N. Coleman, A. B. Dalton, A. P. Davey, A. Drury, B. McCarthy, S. Maier, A. Strevens. Adv. Mater., 1998, 10: 1091

[59] M. Gao, S. Huang, L. Dai, G. Wallance, R. Gao, Z. Wang. Angew. Chem. Int. Ed., 2000, 39: 3664

[60] Z. X. Wei, M. X. Wan. Adv. Mater., 2003, 15: 136

[61] Z. M. Zhang, Z. X. Wei, M. X. Wan. Macromolecules, 2002, 35: 5937

[62] B. B. Mandelbrot. The Fractal Geometry of Nature. Freeman, San Francisco, CA, 1982

[63] a) M. Menon, D. Srivatava. Phys. Rev. Lett., 1997, 79: 4453; b) G. Treboux, P. Lapstun, K. Silverbrool. Chem. Phys. Lett., 1999, 306: 402; c) A. N. Andriotis, M. Menon, D. Srivastava, L. Chernozatonskii. Phys. Rev. Lett., 2001, 87: 066802

[64] J. Li, C. Papadopoulos, J. Xu. Nature, 1999, 402: 253; b) M. Terrones, F. Banhart, N. Grobert, J. C. Charlier, H. Terrones, P. M. Ajayan. Phys. Rev. Lett., 2002, 89: 075505

[65] Z. X. Wei, M. X. Wan. Adv. Mater., 2002, 14: 1314

[66] Z. X. Wei, L. J. Zhang, M. Yu, Y. S. Yang, M. X. Wan. Adv. Mater., 2003, 15: 1382

[67] Z. M. Zhang, Z. X.Wei, L. J. Zhang, M. X. Wan. Acta Materialia, 2005, 53: 1373

[68] a) F. Caruso, R. A. Caruso, H. Möhwald. Science, 1998, 282: 1111; b) Y. Xia, B. Gates, Y. Yin, Y. Lu. Adv. Mater., 2000, 12: 693; c) K. B. Thurmond, T. Kowalewski, K. L.Wooley. J. Am. Chem. Soc., 1997, 119: 6656; d) R. Gref, Y. Minamitake, M. T. Peracchia, V. Trubetskoy, V. Torchilin, R. Langer. Science, 1994, 263: 1600; e) I. Gill, A. Ballesteros. J. Am. Chem. Soc., 1998, 120: 8587; f) F. Caruso, M. Spasova, V. S. Maceira, M. L. Marzan. Adv. Mater., 2001, 13: 1090; g) S. M. Marinakos, J. P. Novak, L. C. Brousseau, A. B. House, E. M. Edeki, J. C. Feldhaus, D. L. Feldheim. J. Am. Chem. Soc., 1999, 121: 8518

[69] a) E. Tosatti, S. Prestipino. Science, 2000, 289: 561; b) P. Kim, C. M. Leiber. Science, 1999, 286: 2148; c) B. H. Hong, S. Bae, C. W. Lee, S. Jeong, K. S. Kim. Science, 2001, 294: 348; d) S. Xu, H. Zhou, J. Xu, Y. Li. Langmuir, 2002, 18: 10503

[70] a) L. Zhang, M. X. Wan. Adv. Funct. Mater., 2003, 13: 815; b) L. J. Zhang, M. X. Wan, Y. Wei. Synthetic Metals, 2005, 151: 1

[71] M. X. Wan. Conducting Polymer Nanofibers. In: Encyclopedia of Nanoscience and Nanotechnology. H. S. Nalwa Ed. Stevenson Ranch: American Scientific Publishers. 2004, Vol. 2, p.153 – 169

[72] L. X. Zhang, L. J. Zhang, M. X. Wan, Y. Wei. Synthetic Metals, 2006, 156: 454

[73] L. J. Zhang, M. X. Wan. Nanotechnology, 2002, 13: 750

[74] L. J. Zhang, M. X. Wan. Thin Solid Films, 2005, 477: 24

[75] L. J. Zhang, M. X. Wan, Y. Wei. Macromol. Rapid Commun., 2006, 27: 366

[76] a) A. G. MacDiarmid, J. C. Chiang, A. F. Richter, A. J. Epstein. Synth. Met., 1987, 18: 285; b) J. C. Chiang, A. G. MacDiarmid. Synth. Met., 1986, 13: 193

[77] Z. Cai, J. Lei, W. Liang, V. Menon, C. R. Martin. Chem. Mater., 1991, 3: 960

[78] Y. Long, Z. Chen, N. Wang, Y. Ma, Z. Zhang, L. Zhang, M. X. Wan. Appl. Phys. Lett., 2003, 83: 1863

[79] a) S. G. Kim, J. W. Kim, H. J. Choi, M. S. Suh, M. J. Shin, M. S. John. Colloid Polym. Sci., 2000, 278: 894; b) I. Sapurina, M. Mokeev, V. Lavrentev, V. Zgonnik, M. Trchová, D. Hlavatá, J. Stejskal. Eur. Polym. J., 2000, 36: 2321

[80] a) M. E. Jozefwicz, R. Laversanne, H. H. S. Javadi, A. J. Epstein, J. P. Pouget, X. Tang, A. G. MacDiarmid. Phys. Rev. B, 1989, 39: 12958; b) J. Stejskal, A. Riede, D. Hlavatá, J. Prokes, M. Helmstedt, P. Holler. Synth. Met., 1998, 96: 55

[81] CRC Handbook of Chemistry and Physics (61st edition). R. C. Weast, M. J. Astle Eds. Boca Raton: CRC Press, Inc. FL 1980 – 1981, p. D155 – D160

[82] B. J. Kim, S. G. Oh, M. G. Han, S. S. Im. Langmuir, 2000, 16: 5841

[83] M. Harada, M. Adachi. Adv. Mater., 2000, 12: 839

[84] Z. Zhang, J. Sui, L. Zhang, M. Wan, Y. Wei, L. Yu. Adv. Mater., 2005, 17: 2854

[85] I. Kogan, L. Fokeeva, I. Shunina, Y. Estrin, L. Kasumova, M. Kaplunov, G. Davidova, E. Knerelman. Synth. Met., 1999, 100: 303

[86] B. K. Kim, Y. H. Kim, K. Won, H. Chang, Y. Choi, K. Kong, B. W. Rhyu, J. J. Kim, J. O. Lee. Nanotechnology, 2005, 16: 1177

[87] a) S. Palaniappan. Polym. Adv. Technol., 2004, 15: 111; b) P. S. Rao, D. N. Sathyanarayana, S. Palaniappan. Macromolecules, 2002, 35: 4988

[88] A. Yasuda, T. Shimidzu. Polym. J., 1993, 4: 329

[89] Y. Wang, Z. Liu, B. Han, Z. Sun, Y. Huang, G. Yang. Langmuir, 2005, 21: 833

[90] a) S. Tan, J. H. Tieu, D. Belanger. J. Phys. Chem. B, 2005, 109: 14 085; b) E. Erdem, M. Karakisla, M. Sacak. Eur. Polym. J., 2004, 40: 785

[91] M. Trchová, I. Sÿedĕnková, E. N. Konyushenko, J. Stejskal, P. Holler, G. CÄ irić-Marjanović. J. Phys. Chem. B, 2006, 110: 9461

[92] H. J. Ding, M. X. Wan, Y. Wei. Adv. Mater., 2007, 19: 465

[93] J. H. Fuhrhop, W. Helfrich. Chem. Rev., 1993, 93: 1565

[94] M. Harada, M. Adachi. Adv. Mater., 2000, 12: 839

[95] a) Handbook of Chemistry and Physics (62nd ed., R. C. Weast Ed.). Boca Raton: CRC Press. FL 1982; b) Inorganic and Analytical Chemistry (W. L. Guo Ed.). Harbin: Harbin Institute of Technology Press, P. R. China, 2004

[96] A. K. Boal, F. Ilhan, J. E. DeRouchey, T. T. Albrecht, T. P. Russell, V. M. Rotello. Nature, 2000, 404: 746

[97] J. Israelachvili, D. J. Mitchell, B. W. Ninham. J. Chem. Soc., Faraday Trans. 2, 1976, 72: 1525

[98] M. Harada, M. Adachi. Adv. Mater., 2000, 12: 839

[99] M. J. Rosen. In: Surfactant and Interfacial Phenomena (2nd ed.). NewYork: John Wiley & Sons, 1989

[100] K. Huang, M. X. Wan, Y. Z. Long, Z. J. Chen, Y. Wei. Synth. Met., 2005, 155: 495

[101] P. Schurtenberger, C. Cavaco. Langmuir, 1994, 10: 100

[102] M. X. Wan, J. C. Li. Journal of Polymer Science. Part A: Polymer Chemistry, 2000, 38: 2359

[103] a) R. H. Baughman, J. F. Wolf, H. Echhardt, L. W. Schacklette. Synth. Met., 1998, 259: 121; b) M. E. Jozefowicz, A. J. Epstein, J. P. Pouget, J. G. Master, A. Ray, Y. Sun, X. Tang, A. G. MacDiarmid. Synth. Met., 1991, 41: 779; c) Y. B. Moon, Y. Cao, P. Smith, A. J. Heeger. Polym. Commun., 1989, 30: 30

[104] M. X. Wan, J. P. Yang. J. Appl. Polym. Sci., 1995, 55: 399

[105] J. H. Funrhop, W. Helfrich. Chem. Rev., 1993, 93: 1565

[106] H. G. Elia. In: Macromolecules 2, Synthesis and Materials. New York: Plenum Press, 1977, p. 73

[107] B. J. Kim, S. G. Oh, M. G. Han, S. S. Im. Synth. Met., 2001, 122: 297

[108] a) E. W. McFarland, J. Tang. Nature, 2003, 421: 616; b) E. Coronado, J. R. Galán-Mascarós, C. J. Gómez-García, V. Laukhin. Nature, 2000, 408: 447

[109] Y. Wei, W. N. Focke, G. E. Wnek, A. Ray, A. G. MacDiarmid. J. Phys. Chem., 1989, 93: 49512

[110] a) Y. Cao, P. Smith, A. J. Heeger. Synth. Met., 1992, 48: 91; b) J. E. Osterholm, Y. Cao, F. Klavetter, P. Smith. Synth. Met., 1993, 55 – 57: 1034; c) Y. Cao, P. Smith. Polymer, 1993, 34: 3139

[111] a) E. Ruckenstein, S. Yang. Synth. Met., 1993, 53: 283; b) N. Kuramoto, K. Teramae. Polym. Adv. Technol., 1998, 9: 222; c) K. Ogura, H. Shiigi, M. Nakayama, A. Fujii. J. Electrochem. Soc., 1998, 145: 3351

[112] Z. M.Zhang, M. X. Wan. Synth. Met., 2002, 128: 83

[113] S. Iijima. Nature, 1991, 354: 56

[114] T. W. Ebbesen, P. M. Ajayan. Nature, 1992, 358: 220

[115] M. M. J. Treay, T. W. Ebbesen, J. M. Gibson. Nature, 1996, 381: 678

[116] W. A. de Heer, A. Chàtelain, D. Ugarte. Science, 1995, 270: 1179

[117] H. Dai, J. H. Hafner, A. G. Rinzler, D. T. Colbert, R. E. Smalley. Nature, 1996, 384: 147

[118] a) R. S. Ruoff, D. C. Lorents, B. Chan, R. Malhotra, S. Subramoney. Science, 1993, 259: 346; b) S. Seraphin, D. Zhou, J. Jiao, J. C. Withers, R. Loufty. Nature, 1993, 362: 503

[119] Y. Saito, T. Yoshikawa, M. Okuda, M. Ohkohchi, Y. Ando, A. Kasuya, Y. Nishina. Chem. Phys. Lett., 1993, 209: 72

[120] S. C. Tsang, Y. K. Chen, P. J. F. Harris, M. L. H. Green. Nature, 1994, 372: 159

[121] J. H. Fan, M. X. Wan, D. B. Zhu, B. H. Chang, Z. W. Pan, S. S. Xie. Journal of Applied Polymer Science, 1999, 74: 2605

[122] J. R. Heflin, K. Y. Wong, O. Zamani-Khamiri, A. F. Garito. Phys. Rev. B, 1988, 38: 1573

[123] X. H. Liu, J. H. Si, B. H. Chang, G. Xu, Q. Yang, Z. W. Pan, S. S. Xie, P. X. Yea, J. H. Fan, M. X. Wan. Appl. Phys. Lett., 1999, 74: 164

[124] a) S. R. Flom, R. G. S. Pong, F. J. Bartoli, Z. H. Kafafi. Phys. Rev. B, 1992, 46: 15598; b) D. Neher, G. I. Stegeman, F. A. Tinker, N. Peyghambarian. Opt. Lett., 1992, 17: 1491; c) Z. Shuai, J. L. Bredas. Phys. Rev. B, 1992, 46: 16135

[125] R. H. Xie, J. Jiang. Appl. Phys. Lett., 1997, 71: 1029

[126] Z. H. Kafafi, J. R. Lindle, R. G. S. Pong, F. J. Bartoli, L. J. Lingg, J. Milliken. Chem. Phys. Lett., 1992, 188: 492

[127] a) Y. Y. Wang, X. L. Jing. Polym. Adv. Technol., 2005, 16: 344; b) C. Y. Lee, D. E. Lee, C. K. Jeong, Y. K. Hong, J. H. Shim, J. Joo, M. S. Kim, J. Y. Lee, S. H. Jeong, S. W. Byun, D. S. Zang, H. G. Yang. Polym. Adv. Technol., 2002, 13: 577; c) S. Koul, R. Chandra, S. K. Dhawan. Polymer, 2000, 41: 9305

[128] a) M. X. Wan, J. C. Li. J. Polym. Sci. A, 1998, 36: 2799; b) M. X. Wan, W. X. Zhou, J. C. Li. Synth. Met., 1996, 78: 27; c) M. X. Wan, J. H. Fan. J. Polym. Sci. A, 1998, 36: 2749; d) M. X. Wan, J. C. Li. Synth. Met., 1999, 101: 844; e) J. Liu, M. X. Wan. J. Polym. Sci. A, 2000, 38: 2734

[129] Z. M. Zhang, M. X. Wan. Synth. Met., 2003, 132: 205

[130] J. H. Funrhop, W. Helfrich. Chem. Rev., 1993, 93: 1565

[131] B. J. Kim, S. G. Oh, M. G. Han, S. S. Im. Synth. Met., 2001, 122: 297

[132] B. J. Kim, S. G. Oh, M. G. Han, S. S. Im. Langmuir, 2000, 16: 5841

[133] M. Harada, M.Adachi. Adv. Mater., 2000, 12: 839

[134] Z. M. Zhang, M. X. Wan, Y.Wei. Nanotechnology, 2006, 16: 2827

[135] A. G. MacDiarmid, A. J. Epstein. Faraday Discuss. Chem. Soc., 1989, 88: 317

[136] a) R. Y. Qian, J. J. Qiu. Polym. J., 1987, 19: 157; b) J. M. Ko, D. Y. Park, N. V. Myung, J. S. Chung, K. Nobe. Synth. Met., 2002, 128: 47; c) K. Suri, S. Annapoorni, R. P. Tandon, C. Rath, V. K. Aggrawal. Curr. Appl. Phys., 2003, 3: 209

[137] X. Li, M. X. Wan, Y. Wei, J. Y. Shen, Z. J. Chen. J. Phys. Chem. B, 2006, 110: 14623

[138] a) M. X. Wan, K. Huang, L. J. Zhang, Z. M. Zhang, Z. X. Wei, Y. S.Yang. Int. J. Nonlinear Sci. Numer. Simul., 2002, 3: 465; b) Y. S. Yang, M. X. Wan. Nanotechnology, 2002, 13: 771

[139] X. Li, J. Y. Shen, M. X. Wan, Z. J. Chen, Y. Wei. Synth. Met., 2007, 157: 575

[140] Z. M. Zhang, J. Y. Deng, J. Y. Shen, M. X. Wan, Z. J. Chen. Macromol. Rapid Commun., 2007, 28: 585

[141] X. Lu, Y. Yu, L. Chen, H. Mao, H. Gao, J. Wang, W. Zhang, Y. Wei. Nanotechnology, 2005, 16: 1660

[142] W. S. Huang, B. D. Humphrey, A. G. MacDiarmid. J. Chem. Soc., Faraday Trans., 1986, 82: 2385

[143] G. S. Humar, D. C. Neckers. Chem. Rev., 1989, 89: 1915

[144] G. Zimmerman, L. Chow, U. Paik. J. Am. Chem. Soc., 1958, 80: 3528

[145] a) M. Eich, J. H. Wendorff. J. Opt. Soc. Am. B, 1990, 7: 1428; b) I. Ikeda, O. Tsutusumi. Science, 1995, 268: 1873

[146] a) P. Rochon, E. Batalla, A. Natanshon. Appl. Phys. Lett., 1995, 66: 136; b) D. Y. Kim, L. Li, J. Kummar, S. K. Tripathy. Appl. Phys. Lett., 1995, 66: 1166

[147] T. Lückemeyer, H. Francke. Appl. Phys. Lett., 1988, 53: 2017

[148] T. Seki, M. Skuragi, Y. Kawanishi, Y. Suzuki, T. Tamiki, R. Fukuda, L. Ichimura. Langmuir, 1993, 9: 211

[149] S. A. Chen, C. S. Liao. Makromol. Chem., Rapid Commun., 1993, 14: 69

[150] T. Matsui, T. Nagata, M. Ozaki, A. Fujii, M. Onoda, M. Teraguchi, T. Masuda, K. Yoshino. Synth. Met., 2001, 119: 599

[151] H. J. Qiu, M. Li, X. F. Chen, F. Y. Jiang, E. L. Zhou. Liq. Cryst., 1998, 25: 419

[152] K. Huang, H. J. Qiu, M. X. Wan. Macromolecules, 2002, 35: 8653

[153] a) S. K. Manohar, A. G. MacDiarmid, K. R. Cromack, J. M. Ginder, A. J. Epstein. Synth. Met., 1989, 29: E349; b) A. Watanabe, K. Mori, A. Iwabuchi, Y. Iwasaki, Y. Nakamura. Macromolecules, 1989, 22: 3521; c) W. Y. Zheng; K. Levon, J. Laakso, J. E. Oesterholm. Macromolecules, 1994, 27: 7754

[154] J. S. Tang, X. B. Jing, B. C. Wang, F. S. Wang. Synth. Met., 1988, 24: 231

[155] S. M. Silverstein, G. C. Bassler, T. Morrill. Spectrometric Idendification of Organic Compounds (4th ed.). New York: John Wiley & Sons, 1981, p.116

[156] S. C. Yang, R. J. Cushman, D. Zhang. Synth. Met., 1992, 48: 24

[157] G. S. Kumar, D. C. Neckers. Chem. Rev., 1989, 89: 1915

[158] a) E. M. Genies, A. Boyle, M. Lapkowski, C. Tsintavis. Synth. Met., 1990, 36: 139; b) A. G. MacDiiarmid, J. C. Chiang, A. J. Epstein. Faraday Discuss. Chem. Soc., 1989, 88: 317

[159] K. Huang, M. X. Wan. Chem. Mater., 2002, 14: 3486

[160] N. Tamai, M. Hiroshi . Chem. Rev., 2000, 100: 1875

[161] K. Huang, M. X. Wan, Y. Z. Long, Z. J. Chen, Y. Wei. Synthetic Metals, 2005, 155: 495

[162] a) T. Matsumoto, Y. Murakami, Y. Takasu. J. Phys. Chem. B, 2000, 104: 1916; b) Y. V. Zubavichus, Y. L. Slovokhotov, M. K. Nazeeruddin, S. M. Zakeeruddin, M. Gratzel, V. Shklover. Chem. Mater., 2002, 14: 3556

[163] a) K. Gurunathan, D. C. Trivedi. Mater. Lett., 2000, 45: 262; b) S. Su, N. Kuramoto. Synth. Met., 2000, 114: 147; c) W. Feng, E. Sun, A. Fujii, H. Wu, K. Niihara, K. Yoshino. Bull. Chem. Soc. Jpn., 2000, 73: 2627; d) H. Xia, Q. Wang. Chem. Mater., 2002, 14: 2158

[164] L. J. Zhang and M. X. Wan. J. Phys. Chem. B, 2003, 107: 6748

[165] T. Onder, S. Shibuichi, N. Satoh, K. Tsujiii. Langmuir, 1996, 12: 2125

[166] C. A. Melendres, A. Narayanasamy, V. A. Maroni, R. W. Siegel. J. Mater. Res., 1989, 4: 1246; M. Zhang, Z. Yin, Q. Chen. Ferroelectrics, 1995, 168: 131

[167] H. Tang, K. Prasad, R. Sanjinés, P. E. Schmid, F. Lévy. J. Appl. Phys., 1994, 75: 2042

[168] J. P. Pouget, M. E. Józefowicz, A. J. Epstein, X. Tang, A. G. MacDiarmid. Macromolecules, 1991, 24: 779

[169] a) Y. Xia, B. Gates, Y. Yin, Y. Lu. Adv. Mater., 2000, 12: 693; b) F. Caruso, M. Spasova, V. S. Maceira, M. L. Marzán. Adv. Mater., 2001, 13: 1090

[170] Lijuan Zhang and Meixiang Wan. J. Phys. Chem. B, 2003, 107: 6748 – 6753

[171] a) J. Xu, X. Li, J. Liu, X. Wang, Q. Peng, Y. Li. J. Polym. Sci. Part A: Polym. Chem., 2005, 43: 2892; b) J. A. Smith, M. Josowicz, J. Janata. J. Electrochem. Soc., 2003, 150: E384; c) H. Cao, C. Tie, Z. Xu, J. Hong, H. Sang. Appl. Phys. Lett., 2001, 78: 1592

[172] Z. J. Zhang, M. X. Wan, Y.Wei. Macromol. Rapid Commun., 2006, 27: 888

[173] D. Li, R. B. Kaner. J. Am. Chem. Soc., 2006, 128: 968

[174] J. Huang, S. Virji, B. H. Weiller, R. B. Kaner. J. Am. Chem. Soc., 2003, 125: 314; J. Huang, R. B. Kaner. J. Am. Chem. Soc., 2004, 126: 851; J. Huang, R. B. Kaner. Angew. Chem. Int. Ed., 2004, 43: 5817; S. Virji, J. Huang, R. B. Kaner, B. H. Weiller. Nano Lett., 2004, 4: 491

[175] a) X. Ma, G. Li, M. Wang, Y. Cheng, R. Bai, H. Chen. Chem. Eur. J., 2006, 12: 3254; b) H. Liu, J. Kameoka, D. A. Czaplewski, H. G. Craighead. Nano Lett., 2004, 4: 671

[176] W. Zhong, X. Chen, S. Liu, Y. Wang, W. Yang. Macromol. Rapid Commun., 2006, 27: 563

[177] a) T. Sun, L. Feng, X. Gao, L. Jiang. Acc. Chem. Res., 2005, 38: 644; b) L. Feng, S. Li, Y. Li, H. Li, L. Zhang, J. Zhai, Y. Song, B. Liu, L. Jiang, D. Zhu. Adv. Mater., 2002, 14: 1857; c) H. Y. Erbil, A. L. Demirel, Y. Avci, O. Mert. Science, 2003, 299: 1377

[178] a) H. Yan, K. Kurogi, H. Mayama, K. Tsujii. Angew. Chem. Int. Ed., 2005, 44: 3453; b) L. Xu, W. Chen, A. Mulchandani, Y. Yan. Angew. Chem. Int. Ed., 2005, 44: 6009; c) M. Nicolas, F. Guittard, S. Géribaldi. Angew. Chem. Int. Ed., 2006, 45: 2251; d) M. Nicolas, F. Guittard, S. Géribaldi. Langmuir, 2006, 22: 3081; e) Y. Zhu, J. Chang, Y. Zheng, Z. Huang, L. Feng, L. Jiang, Adv. Funct. Mater., 2006, 16: 568

[179] Y. Zhu, D. Hu, M. X. Wan, J. Lei, Y. Wei. Adv. Mater., 2007, 19: 2092

[180] Y. Zhu, J. M. Li, M. X. Wan, L. Jiang. Macromol. Rapid Commun., 2007, 28: 2230

[181] unpublished

[182] a) D. Cheng, H. Xia, H. S. O. Chan. Langmuir, 2004, 20: 9909; b) D. Cheng, X. Zhou, H. Xia, H. S. O. Chan. Chem. Mater., 2005, 17: 3578; c) X. Yang, Y. Lu. Polymer, 2005, 46: 5324

[183] K. K. S. Lau, S. K. Murthy, H. G. P. Lewis, J. A. Caulfield, K. K. Gleason. J. Fluorine Chem., 2003, 122: 93

[184] W. Zheng, M. Angelopoulos, A. J. Epstein, A. G. MacDiarmid. Macromolecules, 1997, 30: 2953

[185] J. J. Max, C. Chapados. J. Phys. Chem. A, 2002, 106: 6452

[186] a) R. Blossey. Nature Mater., 2003, 2: 301; b) T. Sun, L. Feng, X. Gao, L. Jiang. Acc. Chem. Res., 2005, 38: 644; c) S. Wang, L. Feng, L. Jiang. Adv. Mater., 2006, 18: 767

[187] Y. B. Moon, Y. Cao, P. Smith, A. J. Heeger. Polymer Commun., 1989, 30: 196

[188] Z. M. Zhang, M. X. Wan, Y. Wei. Adv. Funct. Mater., 2006, 16: 1100

[189] J. J. Max, C. Chapados. J. Phys. Chem. A, 2002, 106: 6452

[190] a) P. Jiang, J. F. Bertone, V. L. Colvin. Science, 2001, 291: 453; b) S. M. Marinakos, M. F. Anderson, J. A. Ryan, L. D. Martin, D. L. Feldheim. J. Phys. Chem. B, 2001, 105: 8872; c) X. Feng, C. Mao, G. Yang, W. Hou, J. J. Zhu. Langmuir, 2006, 22: 4384

[191] a) A. G. MacDiarmid. Rev. Mod. Phys., 2001, 73: 701; b) D. Kumar, R. C. Sharma. Eur. Polym. J., 1998, 34: 1053; c) L. Liang, J. Liu, C. F. Windisch, G. J. Exarhos, Y. Lin. Angew.Chem. Int. Ed., 2002, 41: 3665

[192] a) W. Z. Li, S. S. Xie, L. X. Qian, B. H. Chang, B. S. Zou, W. Y. Zhou, R. A. Zhao, G. Wang. Science, 1996, 274: 1701; b) Z. F. Ren, Z. P. Huang, J. W. Xu, J. H. Wang, P. Bush, M. P. Siegel, P. N. Provencio. Science, 1998, 282: 1150

[193] a) C. G. Wu, T. Bein. Science, 1994, 264: 1757; b) M. A. Khan, S. P. Armes. Adv. Mater., 2000, 12: 671; c) P. Jiang, J. F. Bertone, V. L. Colvin. Science, 2001, 291: 453

[194] X. Zhang, S. K. Manohar. Chem. Commun., 2004, 20: 2360

[195] a) J. Huang, S. Virji, B. H. Weiller, R. B. Kaner. J. Am. Chem. Soc., 2003, 125: 314; b) J. Huang, R. B. Kaner. J. Am. Chem. Soc., 2004, 126: 851; c) X. Zhang, R. Chan-Yu-King, A. Jose, S. K. Manohar. Synth. Met., 2004, 145: 23

[196] X. Zhang, W. J. Goux, S. K. Manohar. J. Am. Chem. Soc., 2004, 126: 4502

[197] I. D. Norries, M. M. Shaker, F. K. Ko, A. G. MacDiarmid. Synth. Met., 2000, 114: 109

[198] N. R. Chiou, A. J. Epstein. Adv. Mater., 2005, 17: 1679

[199] a) H. J. Ding, C. J. Zhu, Z. M. Zhou, M. X. Wan, Y. Wei. Macromol. Rapid Commun., 2006, 27: 1029; b) H. J. Ding, C. J. Zhu, Z. M. Zhou, M. X. Wan, Y. Wei. Macromol. Chem. Phys., 2006, 207: 1259

[200] H. Qiu, J. Zhai, S. Li, L. Jiang, M. X. Wan. Adv. Funct. Mater., 2003, 13: 925

[201] a) L. Liang, J. Liu, C. F. Windisch, G. J. Exarhos, Y. Lin. Angew. Chem. Int. Ed., 2002, 41: 3665; b) J. Liu, Y. Lin, L. Liang, J. A. Voigt, D. L. Huber, Z. R. Tian, E. Coker, B. McKenzie, M. J. McDermott. Chem. Eur. J., 2003, 9: 605

[202] H. J. Qiu, M. X. Wan. Mater. Phys. Mech., 2001, 4: 1

[203] S. Biggs, L. M. Walker, S. R. Kline. Nano Lett., 2002, 2: 1409

[204] a) D. Anton. Adv. Mater., 1998, 10: 1197; b) J. T. Woodward, H. Gwin, D. K. Schwartz, Langmuir, 2000, 16: 2957; c) T. Sun, W. Song, L. Jiang. Chem. Commun., 2005, 13: 1723; d) T. Nishino, M. Meguto, K. Nakamae, M. Matsushita, Y. Ueda. Langmuir, 1999, 15: 4321

[205] R. D. Hazlett. J. Colloid Interface Sci., 1990, 137: 527

[206] a) L. Feng, S. Li, Y. Li, H. Li, L. Zhang, J. Zhai, Y. Song, B. Liu, L. Jiang, D. Zhu. Adv. Mater., 2002, 14: 1857; b) X. Gao, L. Jiang. Nature, 2004, 432: 36

[207] A. B. D. Cassie, S. Baxter. Trans. Faraday Soc., 1944, 40: 546

[208] a) H. Li, X. Wang, Y. Song, Y. Liu, Q. Li, L. Jiang, D. Zhu. Angew. Chem. Int. Ed., 2001, 40: 1743; b) S. Li, H. Li, X. Wang, Y. Song, Y. Liu, L. Jiang, D. Zhu. J. Phys. Chem. B, 2002, 106: 9274; c) H. Liu, S. Li, J. Zhai, H. Li, Q. Zhang, L. Jiang, D. Zhu. Angew. Chem. Int. Ed., 2004, 43: 1146

[209] L. Feng, S. Li, H. Li, J. Zhai, Y. Song, L. Jiang, D. Zhu. Angew. Chem. Int. Ed., 2002, 41: 1221

[210] L. Jiang, Y. Zhao, J. Zhai. Angew. Chem. Int. Ed., 2004, 43: 4338

[211] J. Huang, M. X. Wan. Solid State Communications, 1998, 108: 255

[212] L. T. Cai, S. B. Yao, S. M. Zhou. J. Electroanal. Chem., 1997, 421: 45

[213] R. D. McCullough, R. D. Lowe. J. Chem. Soc., Chem. Commun., 1992, 70

[214] a) Z. H. Wang, A. Ray, A. G. MacDiarmid, A. J. Epstein. Phys. Rev. B, 1991, 43: 4373; b) A. Ezquerra, J. Ruhe, G. Wegner. Chem. Phys. Lett., 1987, 144: 194

[215] A. Kobayashi, X. F. Xu, H. Ishikawa. J. Appl. Phys., 1992, 72: 5702

[216] Y. Z. Long, L. J. Zhang, Z. J. Chen, K. Huang, Y. S. Yang, H. M. Xiao, M. X. Wan, A. Z. Jin, C. Z. Gu. Phys. Rev. B, 2005, 71: 165

[217] J. Huang, M. X. Wan. Solid State Communications, 1998, 108: 255

[218] a) Y. Z. Long, Z. J. Chen, N. L. Wang, Z. M. Zhang, M. X. Wan. Physica B, 2003, 325: 208; b) Y. Z. Long, Z. J. Chen, P. Zheng, N. L. Wang, Z. M. Zhang, M. X. Wan. J. Appl. Phys., 2003, 93: 2962

[219] Z. H. Wang, C. Li, E. M. Scherr, A. G. MacDiarmid, A. J. Epstein. Phys. Rev. Lett., 1991, 66: 1745

[220] Y. Z. Long, Z. J. Chen, Y. J. Ma, Z. Zhang, A. Z. Jin, C. Z. Gu, L. J. Zhang, Z. X. Wei, M. X. Wan. Appl. Phys. Lett., 2004, 84: 22

[221] J. P. Spatz, B. Lorenz, K. Weishaupt, H. D. Hochheimer, V. Menon, R. Parthasarathy, C. R. Martin, J. Bechtold, P. H. Hor. Phys. Rev. B, 1994, 50: 14888

[222] a) Z. H. Wang, E. M. Scherr, A. G. MacDiarmid, A. J. Epstein. Phys. Rev. B, 1992, 45: 4190; b) S. V. Rakhmanova, E. M. Conwell. Appl. Phys. Lett., 2000, 76: 3822

[223] B. Abele, P. Sheng, M. D. Coutts, and Y. Arie. Adv. Phys., 1975, 24: 407

[224] a) F. L. Zuo, M. Angelopoulos, A. G. MacDiarmid, A. J. Epstein. Phys. Rev. B, 1987, 36: 3475; b) J. H. Jung, B. H. Kim, B. W. Moon, J. Joo, S. H. Chang, K. S. Ryu. Phys. Rev. B, 2001, 64: 035101

[225] a) M. Delvaux, J. Duchet, P. Y. Stavaux, R. Legras, S. Demoustier-Champagne. Synth. Met., 2000, 113: 275; b) S. K. Saha. Appl. Phys. Lett., 2002, 81: 3645

[226] J. G. Park, S. H. Lee, B. Kim, Y. W. Park. Appl. Phys. Lett., 2002, 81: 4625

[227] a) T. Tao, J. S. Ro, J. Melngailis, Z. Xue, H. D. Kaesz. J. Vac. Sci.Technol. B, 1990, 8: 1826; b) J. F. Lin, J. P. Bird, L. Rotkina, P. A. Bennett. Appl. Phys. Lett., 2003, 82: 802

[228] Y. Long, L. Zhang, Y. Ma, Z. Chen, N. Wang, Z. Zhang, M. X. Wan. Macromol. Rapid Commun., 2003, 24: 938

[229] a) A. K. Mukherjee, M. Reghu. J. Phys.: Condens. Mater., 2005, 17: 1947 ; b) G. Tzamalis, N. A. Zaidi, A. P. Monkman. Phys. Rev. B, 2003, 68: 245106

[230] a) M. Reghu, C. O. Yoon, D. Moses, P. Smith, A. J. Heeger, Y. Cao. Synth. Met., 1995, 69: 271; b) J. Planés, A. Wolter, Y. Cheguettine, A. Pron, F. Genoud, M. Nechtschein. Phys. Rev. B, 1998, 58: 7774

[231] a) C. O. Yoon, M. Reghu, D. Moses, A. J. Heeger. Phys. Rev. B, 1994, 49: 10851; b) D. Sutar, M. Mithra, M. Reghu, S. V. Subramanyam. Synth. Met., 2001, 119: 455

[232] A. N. Aleshin, R. Kiebooms, M. Reghu, A. J. Heeger. Synth. Met., 1997, 90: 61

[233] B. I. Shklovskii, A. L. Efros. Electronic Properties of Doped Semiconductors. Berlin: Springer, 1984

[234] a) A. Kurobe, H. Kamimura. J. Phys. Soc. Japan, 1982, 51: 1904; b) P. A. Lee, T. V. Ramakrishnan. Rev. Mod. Phys., 1985, 57: 287

[235] a) E. S. Choi, G. T. Kim, D. S. Suh, D. C. Kim, J. G. Park, Y. W. Park. Synth. Met., 1999, 100: 3; b) V. I. Kozub, A. N. Aleshin, D. S. Suh, Y. W. Park. Phys. Rev. B, 2002, 65: 224204

[236] P. A. Lee, T. V. Ramakrishnan. Rev. Mod. Phys., 1985, 57: 287

[237] a) H. Liu, C. H. Reccius, H. G. Craighead. Appl. Phys. Lett., 2005, 87: 253106; b) S. K. Saha, Y. K. Su, C. L. Lin, D. W. Jaw. Nanotechnology, 2004, 15: 66

[238] a) B. K. Kim, Y. H. Kim, K. Won, H. Chang, Y. Choi, K. Kong, B. W. Rhyu, J. J. Kim, J. O. Lee. Nanotechnology, 2005, 16: 1177; b) S. Samitsu, T. Shimomura, K. Ito, M. Fujimori, S. Heike, T. Hashizume. Appl. Phys. Lett., 2005, 86: 233103

[239] a) K. Ramanathan, M. A. Bangar, M. Yun, W. Chen, A. Mulchandani, N. V. Myung. Nano Lett., 2004, 4: 1237; b) A. N. Aleshin, H. J. Lee, S. H. Jhang, H. S. Kim, K. Akagi, Y. W. Park. Phys. Rev. B, 2005, 72: 153202

[240] a) A. N. Aleshin. Adv. Mater., 2006, 18: 17; b) S. Cuenot, S. Demoustier-Champagne, B. Nysten. Phys. Rev. Lett., 2000, 85: 1690

[241] a) J. M. Mativetsky, W. R. Datars. Physica B, 2002, 324: 191; b) J. G. Park, G. T. Kim, V. Krstic, B. Kim, S. H. Lee, S. Roth, M. Burghard, Y. W. Park. Synth. Met., 2001, 119: 53

[242] Y. Z. Long, Z. J. Chen, J. Y. Shen, Z. M. Zhang, L. J. Zhang, K. Huang, M. X. Wan, A. Jin, C. Z. Gu, J. L. Duvail. Nanotechnology, 2006, 17: 1

[243] Y. Zhu, J. M. Li, M. X. Wan, L. Jiang, Y. Wei. Macromol. Rapid Commun., 2007, 28: 1339

[244] a) M. Y. Shen, T. Yokouchi, S. Koyama, T. Goto. Phys. Rev. B, 1997, 56: 13066; b) A. J. Ghijson, L. H. Tjeng, J. V. Elp, H. Eskes, J. Westerrink, G. A. Sawatzky, M. T. Czyzyk. Phy. Rev. B, 1988, 38: 11322

[245] a) R. N. Briskman. Sol. Energy Mater. Sol. Cells, 1992, 27: 361; b) A. O. Musa, T. Akomolafe, M. J. Carter. Sol. Energy Mater. Sol. Cells, 1998, 51: 305; c) L. C. Olsen, F. W. Addis, W. Miller. Sol. Cells, 1982, 7: 247

[246] P. E. de Jongh, D. Vanmaekelbergh, J. J. Kelly. Chem. Commun., 1999, (12): 1069

[247] V. J. D. Rascio. Corros. Rev., 2000, 18: 133

[248] Z. M. Zhang, J. Sui, L. J. Zhang, M. X. Wan, Y. Wei, L. M. Yu. Adv. Mater., 2005, 17: 2854

[249] Z. M. Zhang, J. Y. Deng, J. Sui, L. M. Yu, M. X. Wan, Y. Wei. Macromol. Chem. Phys., 2006, 207: 763

[250] a) P. N. Bartlett, P. R. Birkin, M. A. Ghanem, C. S. Toh. J. Mater. Chem., 2001, 11: 849; b) D. Wang, F. Caruso. Adv. Mater., 2001, 13(5): 350; c) R. Mezzenga, J. Ruokolainen, G. H. Fredrickson, E. J. Kramer, D. Moses, A. L. Heeger, O. Ikkala. Science, 2003, 299: 1872

[251] C. L. Yu, J. Zhai, X. F. Gao, M. X. Wan, L. Jiang, T. J. Li, Z. H. Li. J. Phys. Chem. B, 2004, 108: 4586

[252] F. R. F. Fan, A. J. Bard. J. Phys. Chem., 1993, 97: 1431

[253] N. Maruyama, O. Karthaus, K. Ijiro, M. Shimomura, T. Koito, S. Nishimura, T. Sawadaishi, N. Nishi, S. Tokura. Supramol. Sci., 1998, 5: 331

[254] a) M. Srinivasarao, D. Collings, A. Philips, S. Patel. Science, 2001, 292: 679; b) B. J. Briscoe, K. P. Galvin. J. Phys. D, 1990, 23: 422; c) D. Beysens, C. M. Knobler. Phys. Rev. Lett., 1986, 57: 1433

[255] K. Huang, H. M. Xiao, M. X. Wan. Journal Applied Polymer Science, 2006, 100: 3050

[256] a) L. Olmedo, P. Hourquebie, F. Jouses. Adv. Mater., 1993, 5: 373; b) H. de Chanternac, P. Roduit, N. Belhadz-Tahar, A. Four-rierramer, Y. Djigo, S. Heiyach, P. C. Lacaze. Synth. Met., 1992, 521: 183; c) L. Olmedo, P. Hourquebie, F. Jouses. Synth. Met., 1995, 69: 205; d) A. Kijnak, J. Unsworth, R. Clout, A. S. Mohan, G. E. Beard. J. Appl. Polym. Sci., 1994, 54: 269; e) J. Unsworth, A. Kaynak, B. A. Lunn, G. E. Bread. J. Mater. Soc., 1993, 28: 3307; f) G. Philips, R. Surech, J. Chen, J. Waldman, J. Kumar, S. Tripathy, J. Huang. Solid State Commun., 1990, 76: 963; g) P. T. C. Wong, B. Chambers, A. P. Anderson, P. A. Wright. Elect. Lett., 1992, 28: 1651

[257] F. D. Ge. Ph.D. Thesis. Beijing University of Science and Technique, 1997

[258] V. V. Varadan, R. Ro, V. K. Varadan. Radio Science, 1994, 29: 9

[259] M. X. Wan, W. X. Zhu. Acta Phys. Sinica, 1992, 41: 347

[260] M. X. Wan, S. Z. Li, J. C. Li. Chinese Patent No. 99100651.8，2003

[261] M. X. Wan. Acta Physica Sinica (in Chinese), 1992, 41: 917

[262] Yu Min. Conducting Polymer, the Growth Simulation of Nanotube Dendrites and Theory Discussion of Microwave Absorbability (post-doctor report). Institute of Chemistry, Chinese Academy of Sciences, 2005

[263] R. Zallen. The Physics of Amorphous Solids. New York: John & Wiley, 1983

[264] Y. M. Li, M. X. Wan. Acta Polymerica Sinica, 1998, 2: 177

[265] P. M. Jayan. Chem. Rev., 1999, 99: 1787

[266] E. T. Thostenson, Z. Ren, T. W. Chou. Compos. Soc. Technol., 2001, 61: 1899

[267] Meixiang Wan, Xin Li, Yongshen Yang and Junchao Li. Synthesis method and application of electro-magnetic composite micro/nanostructures. Chinese Patent Application No. 200510000640.3, applied on 25, January, 2005

[268] a) Q. Fu, G. V. Rama Rao, S. B. Basame, D. J. Keller, K. Artyushkova, J. E. Fulghum, G. P. López. J. Am. Chem. Soc., 2004, 126: 8904; b) L. Ionov, N. Houbenov, A. Sidorenko, M. Stamm, I. Luzinov, S. Minko. Langmuir, 2004, 20: 9916; c) X. Yu, Z. Wang, Y. Jiang, F. Shi, X. Zhang. Adv. Mater., 2005, 17: 1289; d) S. Minko, M. Müller, M. Motornov, M. Nitschke, K. Grundke, M. Stamm. J. Am. Chem. Soc., 2003, 125: 3896; e) D. Julthongpiput, Y. H. Lin, J. Teng, E. R. Zubarev, V. V. Tsukruk. Langmuir, 2003, 19: 7832; f) J. Lahann, S. Mitragotri, T. N. Tran, H. Kaido, J. Sundaram, I. S. Choi, S. Hoffer, G. A. Somorjai, R. Langer. Science, 2003, 299: 371; g) T. N. Krupenkin, J. A. Taylor, T. M. Schneider, S. Yang. Langmuir, 2004, 20: 3824

[269] R. Rosario, D. Gust, M. Hayes, F. Jahnke, J. Springer, A. A. Garcia. Langmuir, 2002, 18: 8062

[270] a) T. Sun, G. Wang, L. Feng, B. Liu, Y. Ma, L. Jiang, D. Zhu. Angew. Chem. Int. Ed., 2004, 43: 357; b) Q. Fu, G. V. Rama Rao, S. B. Basame, D. J. Keller, K. Artyushkova, J. E. Fulghum, G. P. López. J. Am. Chem. Soc., 2004, 126: 8904

[271] a) J. Isaksson, C. Tengstedt, M. Fahlman, N. Robinson, M. Berggren. Adv. Mater., 2004, 16: 316; b) L. Xu, W. Chen, A. Mulchandani, Y. Yan. Angew. Chem. Int. Ed., 2005, 44: 6009

[272] a) E. Pringsheim, D. Zimin, O. S. Wolfbers. Adv. Mater., 2003, 13: 819; b) J. Janata, M. Josowicsz. Nat. Mater., 2003, 2: 19; c) Y. Ma, S. R. Ali, A. S. Dodoo, H. He. J. Phys. Chem. B, 2006, 110: 16359

[273] a) G. De Crevoisier, P. Fabre, J. M. Corpart, L. Leibler. Science, 1999, 285: 1246; b) K. Ichimura, S. K. Oh, M. Nakagawa. Science, 2000, 288: 1624; c) B. S. Gallardo, V. K. Gupta, F. D. Eagerton, L. I. Jong, V. S. Craig, R. R. Shah, N. L. Abbott. Science, 1999, 283: 57

[274] Y. Zhu, L. Feng, F. Xia, J. Zhai, M. X. Wan, L. Jiang. Macromol. Rapid Commun., 2007, 28: 1135

Appendix   Term Definitions

Chapter 1

Doping: Doping is a basically tool for π-conjugated polymers from insulator becoming conductor. Like inorganic semiconductors, doping type in the conducting polymers is divided into *p*- and *n*-type of doping. However, intrinsic of the doping item in the conducting polymers is completely different from that of inorganic semiconductors. The concept and essence of doping item are discussed in Chapter 1.

π-conjugated: π-conjugated polymer is a polymer composed of relative localized π-bonds, rather than σ (sigmer). Polyacetylene is typical π-conjugated polymer with an alternating double and single bonds.

Conducting Polymers or Synthetic Metals: Conducting polymers were discovered by three awarders of Nobel Prize of Chemistry in 2000, who were Alan J. Heeger at University of California at Santa Barbara, USA, Alan G. MacDiarmid at University of Pennsylvania, Philadelphia, USA, and Hideki Shirakawa at University of Tsukuba, Japan. Conducting polymers composted of π-conjugated polymeric chain are produced via a doping process to be conductors. Some times conducting polymers are also called as "synthetic metals" due to their metal-like conductivity. The conducting polymers are advantageous of conductivity covering whole insulator-semiconductor-metal region, reversible doping/de-doping process, controllable physical, chemical and electrochemical properties by doping degree and remand flexibility of a conventional polymer. In other words, conducting polymers not only have semiconductor and metal propertied, but also reserving behavior of insulators. These unique properties result in promising potential application in technology, leading to hold an important position in the field of material sciences.

(SN)$_x$: (SN)$_x$ is abbreviation of sulphur nitride and the first metal-like inorganic covalent polymer without metal atoms.

PPy: PPy is abbreviation of polypyrrole.

PTH: PTH is abbreviation of polythiophene.

PPP: PPP is abbreviation of poly (*p*-phenylene).

PPV: PPV is abbreviation of poly (*p*-phenylenevinylene).

PTV: PTV is abbreviation of poly (2, 5-thineylenevinylene)(PTV).

Degenerate and Non-Degenerate: The ground states of conjugated polymers are usually divided into degenerate and non-degenerate. The degenerate polymer has alternating C—C and C=C bonds. The total energy curve of the degenerate polymer has two equal minima, where the alternating C—C and C=C bonds are reversed. The prototype of degenerate polymers is *trans*-polyacetylene. On the other hand, a non-degenerate polymer has no two identical structures in the ground state. Most conjugated polymers, such as PPy and PANI, belong to non-degenerate polymers.

π-conjugation: The polymer backbone in conducting polymers consists of π-conjugated chain, where are the π-electrons of the carbon atoms and the overlap of their wave function. The wave overlap is called conjugation, because it leads to a sequence of alternating double and single bonds, resulting in unpaired electrons delocalized along the polymeric chain. Thus π-conjugation is a basic requirement for a polymer becoming conducting polymer. However, π-conjugation leads to insoluble and poor mechanical properties of conducting polymer, limiting application in technology.

Doping: Doping is an important tool for π-conjugated polymers becoming conducting polymers. Like inorganic semiconductors, doping in conducting polymers consists of *p*- and *n*-doping, but essence of the doping item in conducting polymers completely differs from that of inorganic semiconductors. The difference in doping item between inorganic semiconductors and conducting polymers are as follows: ① Essence of doping in conducting polymers is a oxidation (*p*-doping)/reduction (*n*-doping) process, rather than atom replacement in inorganic semiconductors. ② Doping in conducting polymers is often accompanied with incoppration of couterion, such as cation for *p*-doping or anion for *n*-doping, into polymer chain to satify electrical nature, which is absent inorganic semicondutors. ③ De-doping process not only accurse in conducting polymers, but also reversible doping/de-doping. Both is absent in inorganic semiconductors. ④ Doping degree in conducting polymers can be as high as 50%. This is larger than that of inorganic semiconductors, which doping degree is about tenth of thousand.

Proton Doping: Proton doping is one of doping methods in conducting polymers. The characteristic of proton doping does not inlov a change in the number of electrons associated with the polymer chain. This differs from redox doping (e.g.oxidation or reduction doping) where the partial addition (reduction) or removal (oxidation) of electrons to or from the π system of the polymer backbone take place.

Conductivity: Conductivity, σ, is an important property for evaluation of conducting polymers. Usually σ is measured by a four-probe method and expressed as $ne\mu$, where e is charge of electron, n and μ are density and mobility of charge carriers, respectively.

Energy Gap: Energy gap is defined as energy difference between valence band and conducting band, as presented by E_g (eV). Charge transport in a semiconductor is described by a band model, which the electrical properties are dominated by energy gap.

Solitons, Polarons and Bipolarons: Soliton or polaron and bipolaron is an item for describing charge carriers in conducting polymers. It is different form nether free electron in a metal or electron or hole in a semiconductor. Usually, soliton is served as the charge carrier for a degenerated conducting polymer whereas polaron or bipolaron is used as charge carrier in a non-degenerated conducting polymer.

ESR: ESR is abbreviation of electron spin response and a tool for measuring spin of materials.

CSA: CSA is abbreviation of camphorsulfonic acid and a powerful dopant for preparing soluble conducting polymers. For instance, CSA doped PANI is not only soluble in organic solvent (e.g. *m*-cresol), but also high conductivity at room temperature.

Four-Probe Method: Four-probe method is a common method to measure electrical properties of materials. In this method, four probes with a same distance are required, where two out probes are represented as current terminals whereas two middle probes are assigned as the voltage terminals. In general, when a constant current passes through the current templates, the voltage between two voltage terminals is measured. According to Ohmic law, the conductivity can be calculated by taking current used and voltage measured as well as geometry parameters (e.g. length and cross-section surface for passing current).

Voltage Shorted Compaction (VSC) Method: VSC is abbreviation of voltage shorted compaction and is created by Coleman to simulate pure temperature dependence of conductivity of organic poly-crystals. Construction of VSC method is similar to four-probe method, but two voltage terminates are shorted by a thing layer of silver paste, which can effectively short circuit the inter-crystallinity contact resistance. Therefore the intrinsic properties of temperature dependence of the tested materials can be qualitatively determined by VSC method due to eliminate the inter-crystalline contact resistance. However, the specific conductivity, as measured by VSC method, is meaning-less, because the measured conductivity involves resistance of the silver paste.

Variable Range Hopping (VRH) Model: VRH is abbreviation of variable range hopping and was proposed by Mott. This is a common model to describe electrical transport properties of a semiconductor. According to the model, the conductivity is described as $\ln\sigma(T)$ versus $T^{-1/(n+1)}$, where "n" is defined as the dimensionality of the conduction, and varies from 1 to 3. The value of T_0, which is energy required for transportation of charge carriers, calculated from the plots of $\ln\sigma(T)$ versus $T^{-1/(n+1)}$ is characteristic parameter of VRH model. The lower T_0, the higher conductivity is found.

Chapter 2

APS: APS is abbreviation of ammonium peroxydisulfate and is a common and efficient oxidation for polymerization of aniline in an acidic solution (e.g. 1 mol/L HCl) for synthetic conducting polyaniline.

PANI: PANI is abbreviation of polyaniline and is an older and promising conducting polymer. PANI consists of reduced and oxidized unite, depending on the oxidation state. The completely reduced form and oxidized form are assigned as "leucoemeraldine" base form ($y = 1$, LEB) and "pernigraniline" form ($y = 0$, PEN), respectively. The "half-oxidized" form is called as "emeraldine base" form ($y = 0.5$, EB). Usually only the emeraldine base form (EB) can be protonated by using proton (e.g. 1 mol/L HCl) to form conducting emeraldine salt form (ES). Compared with other conducting polymers, PANI is advantageous of easy synthesis, low-cost, structure complex and special proton doping, as well as physical properties controlled by both oxidation and protonation state.

Photo-Induced Doping: Photo-induced doping is one of common doping methods for conducting polymers, especially for PANI. The photo-induced doping is contributed to protons released when the photon-acid generators under light excitation. Therefore, photon-acid generators are necessary for photo-induced doping.

XRD: XRD is abbreviation of X-ray diffraction and a powerful technique to determine molecular structure and crystalline of materials.

De-Doping: De-doping is an approach to recover origin state of conducting polymers (i.e. insulating state) from the doped state (i.e. conducting state). In case of PANI, for instance, the doped PANI can be recovered to its insulating state (i.e. the emeraldine base form, EB) by de-protonation (e.g. NH_4OH or NH_3).

Self-Catalyzing or Auto-Acceleration: Self-catalyzing or auto-acceleration are the phenomena observed from electrochemical polymerization of aniline monomer

in acidic solution. They mean that the initial formation (or nucleation) of PANI on the surface of the electrode is slow, but the initially formed PANI accelerated the polymer growth greatly and the current increased proportionally with the second power when potentiostatic techniques was used to electrochemically polymerize aniline.

Mechanochemical Route: Mechanochemical route is a solvent-free method by using a solid anilinium salt as the precursor to prepare conductive polyaniline. This method opens a sample and solvent-free method to prepare a large amount of the conducting PANI.

NLO: NLO is abbreviation of nonlinear optical. NLO effect is an optic pheromone and defined that when a light passes through a nonlinear optic-active medium the frequency, phase, amplitude or transmission of the coming out of light are changed.

α, β and γ: α, β and γ is abbreviation of the polarizability, hyperpolarizability and the second hyperpolarizability of the molecules, respectively, and are used to describe molecular characteristics of NLO materials.

$\chi^{(1)}$, $\chi^{(2)}$ and $\chi^{(3)}$: $\chi^{(1)}$, $\chi^{(2)}$ and $\chi^{(3)}$ is abbreviation of the first-, second- and third-order susceptibilities of materials and is used to describe bulk characteristic of NLO materials.

SHG and THG: SHG and THG is abbreviation of second and third harmonic generation, respectively, which are of bulk characteristics of NLO materials.

EFISH and DFWM: EFISH and DFWM are abbreviation of electric-induced second harmonic generation, and degenerate four-wave mixing, respectively that are methods for measuring NLO behavior of materials.

Photovoltaic Effect: Photovoltaic effect is opt-electrical phenomenon that means electrons and holes produced by light irradiation are collected at electrodes when an optical material is illuminated.

C-AFM and CS-AFM: CS-AFM and CS-AFM are abbreviation of atomic force microscopy with a conducting tip or current-sensing atomic force microscopy, respectively, which are an excellent tool for measuring the local conductivity and current-voltage (I-V) characteristics of conducting polymers. The method not only provide topographical and current image information at the same time, but also the current-voltage (I-V) traces giving the relations between structural features and electrical properties of the materials on the nanometer scale.

NMP: NMP is abbreviation of *N*-methylpyrrolidone and a good solvent for formation of a soluble insulating PANI (i.e. the emeraldine base form, EB).

EPR: EPR is abbreviation of electron paramagnetic resonance and tool to measure magnetic properties of materials.

SPAN: SPAN is abbreviation of sulfonated polyaniline and also called self-doped polyaniline. SPAN is a water soluble conducting PANI derivative, which molecular structure with different the degree of sulfonation defined as the sulfur-to-nitrogen (S/N) ratio. The conductivity increases with increase of the S/N ratios. Compared with PANI, the conductivity of SPAN is almost un-dependent upon the pH value.

Emulsion Polymerization: Emulsion polymerization is one of approaches to synthesize soluble PANI. The reagents in this method consist of aniline, a protonic acid and an oxidant combined with a mixture of water, or a non-polar or weakly polar solvents.

Dispersion Polymerization: Dispersion polymerization is one of the methods to synthesize soluble PANI. The method is carried out in an aqueous mixture, which contains aniline monomers, dopant, oxidant and steric stabilizer, to produce soluble PANI colloidal particles. The colloids prepared from dispersion polymerization usually have a "core-shell" structure, where the core is mainly composed of insoluble PANI whereas the shell is constructed with water soluble polymers.

Ionic Liquids: Ionic liquids are organic salts with a low melting point (<100℃) that has chemical stability, low flammability, negligible vapor pressure, high ionic conductivity, and wide electrochemical window. The ionic liquids are stable and excellent electrolyte solutions and are considered as prospective environmentally friendly solvents for chemical or electrochemical reactions.

Layer-by-Layer: Layer-by-layer is a common and controlling self-assembly technique to prepare thin and oriented films through anion /cation or electrostatic and hydrogen bonding interactions. The method is advantageous of simple in procedure, easy to control and friendly to environment.

PEO: PEO is abbreviation of poly (ethylene oxide) and a good ion-conducting polymer.

Chapter 3

LED: LED is abbreviation of light emitting diode and one of important electronic devices. LED is based on photovoltaic effect and fabricated by a suitable optic solid film sandwiched between two electrodes. When an electric field is applied

electromagnetic radiation emits from the optic solid sandwiched between two electrodes.

HOMO and LUMO: HOMO and LUMO are abbreviation of the highest occupied molecular orbital and the lowest unoccupied molecular orbital, respectively. The energetic difference between them affects the emission characteristic of the electroluminescence polymers.

PL and EL: PL and EL are abbreviation of the photoluminescence and electroluminescence emission spectra, respectively. The PL and EL items are used to characterize the electroluminescence properties of the polymers in LEDs.

Work Function: Work function is defended as energetic difference between the valence and conducting band of a material.

Ohmic and Rectifying or Schottky Contact: Ohmic and rectifying or Schottky contact are items to describe electrical contact feature when a semiconductor contacts with a metal. The contact nature between semiconductor and metal depends on work function of semiconductor and metal as well as nature of charges carriers. For a *p*-type semiconductor, in principle, a rectifying or Schottky contact is formed when the work function of semiconductor is larger than that of metal. On the contrary, Ohmic contact between the semiconductor and metal is formed when the work function of the semiconductor is less than that of the metal.

Depletion: The rectifying or Schottky contact results in that electrons flow from the metal into the semiconductor, spontaneously, a build-in potential in between the metal and the semiconductor is created. The electrons (minority carries) in *p*-type semiconductor recombine with the holes (majority carriers) in the semiconductor, resulting in a negative space-charge region created at the semiconductor/metal interface, which is called as depletion region.

Solar Cells: Solar cells are able to directly convent sunlight into electric power so that it is a cheap and friendly-environment energy source. Solar cells are optic specie as optic-absorber is sandwiched between two electrodes, where one electrode is metallic electrode and another electrode is transparence electrode (e.g. indium-tin-oxide, ITO).

ITO: ITO is abbreviation of indium-tin-oxide. In general, the ITO is coated on a glass substrate as a conducting and transparence electrode.

DSSC: DSSC is abbreviation of dye-sensitized solar cell. The dye-sensitive is an efficient approach to enhance conversion efficiencies of the solar cells because of ensuring the interfacial charge recombination after initial charge separation.

The concept of dye-sensitized solar cells is that upon illumination, electrons are injected from the photoexcited dye into the semiconductor and move toward the transparent conductive oxide electrode (e.g. ITO), while the electrolyte reduces the oxidized dye and transports the positive charge to the metallic electrode, resulting in formation of high-surface-area interface between the semiconductor and the electrolyte solution.

EMI: EMI is abbreviation of electromagnetic interference. Shielding of the EMI is of critical issue because of not only concerning its interference with other electronic devices, but also the dangerousness of electromagnetic field on health as exposure to electromagnetic wave.

Skin Effect: Skin effect is one of metal characteristics. It means that the current conducts only along the surface of the metal and described by a skin depth, which is related to the frequency of the electromagnetic wave, the magnetic permeability of the metal and the absolute permeability of free space as well as the conductivity of the metals.

SE: SE is abbreviation of shielding efficiency and definite as the ratio of the power of incoming and outgoing wave in dB unit. The SE value is an important parameter for evaluating feature of EMI shielding materials.

RAM or MAM: RAM or MAM is abbreviation of radar-absorbing material or microwave absorbing material, respectively. MAM or RAM is made with compounds having a high loss energy, which enables them to absorb the incident radiation in synchronized frequencies and dissipate in the form of heat. RAM or MAM materials play an important role in the field of stealth materials and technologies.

CNTs: CNTs is abbreviation of carbon nanotubes, which is not only typical carbon materials, but also unique nanostructures with low specific mass and excellent electrical, thermal and mechanism properties.

DBSA: DBSA is abbreviation of dodecylbenzene sulfonic acid, which is a common dopant to synthesize soluble conducting polyaniline.

Rechargeable Batteries: Rechargeable battery, sometimes called as secondary battery, is a common energy source, can be restored to its original charged condition by an electric current flowing in the direction opposite to the flow of current when the cell was discharged.

PEO: PEO is abbreviation of poly (ethylene oxide) (PEO) and a typical and common solid electrolyte.

Supercapacitor: Supercapacitor is a device of stores electrical energy, which is in the electrical double layer formed at the interface between an electrolytic solution and an electronic conductor. The configuration of supercapacitors is almost similar to that of batteries, but there are some differences in between batteries and supercapacitors. In batteries, for example, energy is generated by conversion of chemical energy via redox reaction at the anode and cathode. On the contrary, the energy-delivering process in supercapacitors is performed via electrical double layers formed and released by orientation of electrolyte ions at the electrolyte/electrolyte interface, resulting in a parallel movement of electrons in the external wire.

Sensor: Sensor is one of electronic devices for detecting gas, chemical or biochemical materials. It can be generally divided into electronic or optoelectronic and electromechanical devices. Conducting polymer-based sensors are based on their reversible change in conductivity caused by doping/de-doping process.

Electrochromic Effect: Electrochromic effect is based on a fact that certain materials change color by means of redox reaction. When doping or de-doping process takes place in conducting polymers, where not only results in change of the conductivity, but also accompanied color variation. This is one of characteristics of conducting polymers and leads to developing conducting polymer-based electrochromic devices such as displays, smart windows, and electronic paper.

PEDOT: PEDOT is abbreviation and a derivative of poly (3, 4-ethylenedioxy-thiophene). It is outstanding and soluble conducting polymer with a small band gap, high conductivity and stability.

LBL: LBL is abbreviation of layer by layer and an excellent assembly technique to fabricate low-roughness thin film grown on a substrate through electrostatic interaction. The method is simple and inexpensive, and allows the incorporation of different functional materials within a single film without phase separation.

Electrochemical Actuators: Electrochemical actuators are promising potential applications of conducting polymers in technology that are based on a volume change of a conducting polymer during its redox process, which results in electrolyte ion transport into/out of the polymer, solvent transport into/out of polymer, polymer chain configuration change, and electrostatic expulsion between polymer chains.

Corrosion: Corrosion, which essentially an electrochemical process is the destructive result of chemical reactions between a metal or metal alloy and its environment.

Electrostatic Dissipation: Charge is easily accumulated on the surface of

insulator materials and accumulation of electrostatic charge on the surface of materials often results in discharge suddenly, which will damage to electronic devices or human health. Protection of electrostatic charge accumulation on the surface of materials is called as electrostatic dissipation.

Secondary Doping: Secondary doping is one of doping methods in conducting polymers. It usually takes place in a primary-doped polymer, resulting in enhancement of conductivity and change of conformation of structures. Detail information can be found in A. G. MacDiarmid, and A. J. Epstein, *Synth. Met.* 1995, 69: 85, 91.

Self-Doping: Self-doping is also one of doping methods in conducting polymers. It is defined that the dopant is an integral part of the polymer backbone attached on polymeric chain (e.g. PANI) and the self-doped polymer displays good resistance to water.

Surface Resistance: Surface resistance is used to evaluate electrical properties of a layer coated on the surface of materials, which is defined as resistance per square in $\Omega/\square$ unit; independent of the size of the square or its dimensional units. The surface resistance sometimes is also called as sheet resistance, which differs from volume resistivity due to the thickness of the coated layers is much thinner than that of substrate.

Chapter 4

Nanomaterials: "Nano" is scale unit, which means 1 nanometer, that is equal to one billionth of a meter (10^{-9}m). Thereby, size of the nanomaterials is defined in range of $1-100$ nm. Nowadays, Nanoscience and Nanotechnology have been received great attention in material sciences and nano-devices due to their large surface area, hollow structures and different properties from the bulk materials.

Size Effect: Size effect is one of characters of nanomaterials and means the physical properties are affected by the size, for instance, the conductivity of conducting polymer nanostructures usually increases with increase of the diameter.

Hard Template Method: Hard method is main approaches to prepare nanostructures of various materials including semiconductor, metal and conducting polymer nanostructures and their composites. For a hard-template method, porous membrane is required as a hard template that guides growth of the nanostructures within the pore in the membranes, leading to completely controlling nanostructures in morphology and diameter dominated by morphology and size of the pores. As a result, hard-template method is a common, universal and controlling method.

However, removing template is also required after polymerization that not only results in complex preparation process, but also in disorder of the nanostructures.

Soft-Template Method: Soft-template is another main approach to synthesize conducting polymer nanostructures. Compared with hard-template method, soft-template method dose not need membrane as a template whereas the soft-template synthesized nanostructures are formed by a self-assembly process through molecular interactions including hydrogen banding, $\pi - \pi$ band stacking, and Van der Waals force as the driving forces. Soft-template-method therefore is simpler and cheaper than that of hard-template method because omits membrane as a template and post-treatment of removing template. On the other hand, controllability in morphology and diameter of the soft-template is less than that of hard-template method due to omitting membrane as the template. On the contrary, the poor controllability of soft-template method might provide a chance for synthesis of three-dimension nanostructures self-assembled from one dimension nanostructures, which is impossible for hard-template method.

Self-Assembly: Self-assembly is a powerful tool for the creation of well-defined structure at a molecular level that is based on selective control of non-covalent interactions, such as hydrogen bonds, Van der Waals forces, $\pi - \pi$ stacking interaction, metal coordination and dispersive forces as the driving forces.

Surfactant: surfactant is a class of molecules that form thermodynamically stable aggregates of inherently nano-scale dimensions both in solution and at interfaces. Amphiphilic character of the surfactant is often served as a soft-template in the formation of nanostructures through a self-assembly process.

CMC: CMC is abbreviation of critical micelle concentration and means that formation of the micelles aggregated by surfactant in aqueous solution only appears at a critical aggregation concentration.

Revered Micelle: Reversed micelle is defined as an aggregate of surfactant molecules containing a nanometer-sized water pool in the oil phase. Reversed micelle is also a common route to prepare micro-or nano-structures of conducting polymers.

Colloids: Colloids are typical core/shell structure, where polymer is used as a core whereas absorbed stabilizer is as shell. The stability of the dispersions arises from stearic repulsion between the stabilizer molecules, leading to process of colloids. The colloids particles are usually used as the soft-templates to prepare nanostructures of conducting polymers. Moreover, water dispersible colloids provide an easy way to overcome problems of conducting polymer (e.g. PANI) processability, because they can be cast as films or blended with other water-soluble polymers.

Molecular Template: Molecular template is a common and efficient approach to prepare well-controlled diameter of the nano-materials, because the guest conducting polymers are synthesized within the channels or pores of a molecular template. Poly (acrylic acid) (PAA) or poly (styrenesulfonic acid, SA) is common molecular template.

Aniline Oligomer: Aniline oligomer is derivatives of PANI with a short chain ($n = 3-18$) and is advantageous of well-desirable molecular structure, high solubility and comparable conductivity with PANI. More recently, it is found that it can be used to prepare high chirality of the chiral PANI nanofibers in the presence of chiral dopant, where not only used as a soft-template in forming chiral nanofibers, but also acceleration polymerization reaction.

Soap Bubble: In general, small gas bubbles release from the surface of work electrode due to water decomposition when conducting polymers was prepared by electrochemical polymerization in an aqueous solution. Actually, the gas bubble associated with an aqueous solution containing monomer and surfactant functionalized dopant results in as called "soap bubble". Recently it is found that the "soap bubble" can be used as a soft-template to electrochemically synthesize conducting polymer nanostructures.

Amphiphilic Dopant: Amphiphilic dopant usually consists of hydrophilic polar head and hydrophobic alkyl chain that is very promising for preparing conducting polymer (e.g. PANI) nanostructures via a self-assembly process because it plays role of both dopant and soft-template at the same time.

LB: LB is abbreviation of Longmuir-Blodgett. LB technology is a technique for preparation of ultra-thin organic film and offers unique control over the thickness and molecular orientation of the films. However, the method not only requires a very particular instrumental setup, but also the polymer needing good solubility and amphiphilic nature.

Electro-Spinning Technique: Electro-spinning technique patented in the 1930s is widely employed to prepare fibers of polymers and composite nanofibers. In the electro-spinning method, in general, a high electrical field is applied between a polymer fluid and a metallic collection screen. When the applied field reaches a critical value, a jet is formed and the dry fibers are accumulated on the surface of the collection screen, forming a non-woven mesh of nano-to micro-diameter fibers on the collection screen. The morphology and diameter of the fibers are affected by preparation parameters, such as the applied voltage, solution concentration, polymer molecular weight, solution surface tension, dielectric constant of the solvent, and solution conductivity. Compared with other methods, the electro-spinning method is advantageous of fabricating long fibers and non-woven meshes of polymers

and composites. However, a soluble polymer with a high viscosity is required. Thereby, pure fibers of conducting polymers are difficult to be fabricated by the electro-spinning method due to poor solubility of the conducting polymer in organic solvents. However, tubular fibers of conducting polymers can be obtained by using electro-spun polymer fibers as the templates and then conducting polymers polymerized on the surface of the templates followed by dissolving polymeric cores as the templates.

Interfacial Polymerization: Interfacial polymerization is recently developed a facial and simple and self-assembly method to synthesize large scaled mass of PANI fibers. The method only allows oxidative polymerization of aniline takes place at the interface of organic/agues phase, where organic phase consists of aniline whereas oxidant is in aqueous phase, and the product is entered into agues phase.

Ultrasonic Irradiation: Ultrasonic irradiation is an electromagnetic wave in the frequency range from 20 kHz to 1 MHz and widely used in chemical synthesis owing increase of the rate of many chemical reactions (e.g. organic, inorganic and polymerization). It is recently employed to prepare nanostructures (e.g. thin hexagonal plates) and composite nanostructures of conducting polymers.

PC: PC is abbreviation of polycarbonate. Track-etched porous PC is widely used as a hard-template for preparation of nanostructured materials. It is advantageous of flexible and transparent template.

CP: CP is abbreviation of conducting polymer.

CD Spectrum: CD is abbreviation of circular dichroism and CD spectrum is a powerful tool for measuring characteristic of chiral materials.

Ultrasonic Irradiation: When ultrasonic wave through a liquid medium effect of ultrasonic cavitations take place, which means that a large number of micro-bubbles, grow, and collapse is produced in a very short time. Thereby the effect of ultrasound cavitations has been extensively applied in dispersion, emulsifying, crushing, and activation of particles.

PIRAS: PIRAS is abbreviation of polarized infrared absorption spectroscopy and is a powerful tool to measure of orientation of the polymeric chains.

CS-AFM: CS-AFM is abbreviation of current-sensing atomic force microscopy. CS-AFM with a conducting tip is powerful tool to simultaneously provide information of topographical and current images form different locations. This method has been employed to measure electrical and transport properties of single nano-tube or nano-fiber of conducting polymers.

AFM-CITS: AFM-CITS is abbreviation of atomic force microscope current image tunneling spectroscopy and is also a tool to measure electrical and transport properties of thin films of conducting polymers.

FE and FED: FE and FED are abbreviation of field emitting and field emitting diode, respectively. FED is based on FE effect. LED made of conducting polymer nanostructures consists of transparent electrode (e.g. ITO) for the anode, and the conducting polymer or its nanostructure for the cathode.

Wettability: Wettability of the surface is a very important property to the solid materials, which is generally related to both the surface free energy and the surface geometric structure of the materials. The wettability of the surface of materials is evaluated by water contact angle (CA). In general, the surface with CA larger than 150° and lower that 5° is definite as superhydrophobic and superhydrophilic surface, respectively.

Sensors: Sensor is one of electronic devices for measuring gas, or chemical and biomaterials. Sensors made of conducting polymers are based on a reversible change in conductivity resulted from doping/de-doping process.

OMC: OMC is abbreviation of ordered mesoporous carbon and usually synthesized by using ordered mesoporous silica as a template or by the hydrolysis of the carbon precursor at high temperature under nitrogen atmosphere. The morphology and properties of OMC largely depend on the nature of the carbon precursor and the hydrolysis conditions.

E-DPN: E-DPN is abbreviation of Electrochemical Dip-Pen Nanolithography and new atom force morphology lithography technique. The E-DPN technique opens the possibility of a one step nano-electronic device fabrication.

SECM: SECM is abbreviation of scanning electrochemical microscopy. It combines features of scanning tunneling microscopy and ultra-microelectrode, which is moved in an electrolyte above the surface, and is a surface analysis and modification technique.

Chapter 5

β-NSA: β-NSA is abbreviation of naphthalene sulfonic acid and widely used as a dopant for conducting polymers, especially polyaniline. In particular, the β-NSA doped polyaniline nanotubers were the first sample of conducting polymer nanostructures synthesized by a template-free method.

POT: POT is abbreviation of poly (ortho-toluidine) and derivative of polyaniline with a methyl group ($—CH_3$) attached on the benzene ring of the polymer chain.

DLS: DLS is abbreviation of dynamic light scattering and a powerful tool for characterization of micelles form in solution.

FFTEM: FFTEM is abbreviation of freeze-fracture transmission electronic microscopy and a powerful method for directly measuring morphology of the micelles formed in solution.

XPS: XPS is abbreviation of X-ray photoelectron spectroscopy and a tool to measure component of materials.

CA: CA is abbreviation of contact angle of water and is evaluated wettability of surface of materials. In general, the surface with CA larger 150° or less 5° are defined as a superhydrophobic and superhydrophilic, respectively.

MR: MR is abbreviation of magneto-resistance and one of important physical properties for the conducting polymers and their nanostructures.

EDX: EDX is abbreviation of energy depressive and X-ray that is powerful tool for elemental analysis in a tiny region.